Synthesis of Ferrocene Nucleic Acid Monomers and Ferrocene Containing Drug Candidates

by

Jonathan L. Kedge



UNIVERSITY OF BIRMINGHAM

A thesis submitted to the
University of Birmingham
For the degree of
DOCTOR OF PHILOSOPHY

School of Chemistry
College of Engineering and Physical Sciences
University of Birmingham
September 2016

UNIVERSITY OF
BIRMINGHAM

University of Birmingham Research Archive

e-theses repository

This unpublished thesis/dissertation is copyright of the author and/or third parties. The intellectual property rights of the author or third parties in respect of this work are as defined by The Copyright Designs and Patents Act 1988 or as modified by any successor legislation.

Any use made of information contained in this thesis/dissertation must be in accordance with that legislation and must be properly acknowledged. Further distribution or reproduction in any format is prohibited without the permission of the copyright holder.

Abstract

The first ferrocene nucleic acid (FcNA) was reported by the Tucker group in 2012. Furnished with two nucleobases and two hydroxyl groups, the tetrasubstituted metallocene assumes the position traditionally occupied by the two sugars of a dinucleotide. This thesis describes the successful synthesis of two FcNA monomers; a tetrasubstituted dithyminyl variation and a disubstituted control compound bearing no nucleobases. These monomers were oligomerised, their binding characteristics assessed by thermal melting studies, and compared to other monomers belonging to the group. Through the study of these compounds the Tucker group has demonstrated that FcNA monomers behave similarly to conventional nucleic acids, displaying selective H-bonding and π-stacking interactions within a hybrid duplex. A preliminary methodology for the production of diguaninyl FcNA monomers was also explored.

As published in 2014, the corresponding disubstituted systems, in which a hydroxyl and a nucleobase are linked through a sugar-like ferrocene unit, are also being investigated as potential nucleoside analogues. Adding to the groups growing library, a number of related compounds were synthesised in which the hydroxyl linker length, the planar chirality, the substitution pattern of the ferrocene and the nucleobase were varied. The compounds were electrochemically characterised and assessed for their biological activity which revealed interesting structure-activity-relationships involving both the redox potentials and chirality.

Following the example of ferroquine and ferrocifen, in which existing pharmaceuticals are modified through the incorporation of ferrocene, the synthesis and preliminary biological activity of novel ferrocenyl β-blockers, in which the metallocene replaces the naphthol unit of the prototypical β-blocker propranolol, is reported herein.

Acknowledgements

Firstly, huge thanks to Prof Jim Tucker for the opportunity to undertake this project, for your guidance, encouragement, and understanding over the last four years; I have learnt lot. Special thanks also to Dr Huy Nguyen for guiding me in the lab, for your invaluable advice and your Zen-like calm. Thank you to Dr Jean-Louis Duprey for the molecular dynamic simulations and Dr James Carr-Smith for the thermal melting studies. Thank you to all other members of the Tucker group, both past and present; the grainger group and all others on the fourth floor, it has been a pleasure and a privilege to work alongside you all. I wish you all the best for the future.

Thanks to Dr Louise Male for her incredible XRD studies which has formed a fascinating aspect of the project. Thanks to Dr Nik Hodges, Dr Zahra Khan and Prof Jan Balzarini for the many biological studies of ferrocenyl nucleoside analogues and Dr Youcef Mehellou, Lily Cao and Migena Tushe for the biological studies of the ferrocenyl β-blockers. Thanks to Dr Sarah Horswell for her generous advice and guidance regarding electrochemistry and more.

Thanks to the members of the analytical department, Dr Chi Tsang, Dr Cécile Le Duff, Dr Allen Bowden, Pete Ashton, Leanne Hill and Dr Neil Spencer, for their diligence, invaluable advice and without who's continuous efforts this thesis would have been impossible. Thanks to the School of Chemistry, the last eight years have gone all too quickly in your company.

Thanks to Lucy Baines, your friendship, loyalty and beauty makes me melt. Thanks also to my house-husband Sam Minnear and house-elf Anna for taking care of me. Thanks to Misty's Big Adventure, thanks to Festival, thanks to Curry Club. Thanks to Hannah Mary Baines and Matthew Gidley for entrusting your lovely home to us.

Finally, thanks to my mom and dad, Valerie and Roland Kedge, for believing in me; for your endless love, nourishment and forbearance.

Table of Contents

Abstract i

Acknowledgements ii

Table of Contents iv

Abbreviations x

1 Introduction 1

1.1 Ferrocene 1

1.1.1 Structure 1

1.1.2 Reactivity and Synthetic Considerations 2

1.1.3 Electrochemistry 9

1.1.4 Applications of Ferrocene 14

1.1.5 Thesis Outline 15

1.2 References 16

2 Synthesis of Novel Tetrasubstituted Ferrocene Nucleic Acid (FcNA) Monomers 18

2.1 Introduction 18

2.1.1 Deoxyribonucleic Acid (DNA) 18

2.1.2 Non-Canonical Bases 20

2.1.3 Metal Base-Pairs 23

2.1.4 Peptide Nucleic Acid (PNA) 25

2.1.5 Fluorescent Oligonucleotides 27

2.1.6 Redox-Active Oligonucleotides 30

2.1.7 Ferrocene Nucleic Acid (FcNA) 32

2.2 Objectives 36

2.3 Results and Discussion 38

2.3.1 Synthesis of Tetrasubstituted FcNA Monomers 38

2.3.2 Attempted Oligomerisation of Tetrasubstituted Diguaninyl FcNA monomer Fcn3c2GG$_{(RRpSpS)}$ 64

2.3.3 Thermal Melting Studies 69

2.4 Conclusions 79

2.5 Future Work 81

2.5.1 Further investigation of Diguaninyl FcNA Monomer 81

2.5.2 G-Quadruplex Formation 82

2.6 References 85

3 Synthesis and Biological Activity of Novel Ferrocenyl Nucleoside Analogues 89

3.1 Introduction 89

3.1.1 Cisplatin 90

3.1.2 Medicinal Bioorganometallic Chemistry 91

3.1.3 Ferrocene and Ferrocenium Compounds 92

3.1.4 Nucleoside Analogues 98

3.1.5 Nucleoside Analogues with a Ferrocenyl Linker 105

3.2 Objectives 108

3.3 Results and Discussion 112

3.3.1 Synthesis of Ferrocene Containing Nucleoside Analogues 112

3.3.2 Electrochemistry and Lipophilicity 135

3.3.3 Biological Activity 143
3.3.4 Discussion 151
3.4 Conclusions 155
3.5 Future Work 158
3.6 References 160
4 Synthesis and Biological Activity of Novel Ferrocenyl β-Blockers 166
4.1 Introduction 166
4.1.1 Adrenergic Receptors 166
4.1.2 Propranolol, the Prototypical β-blocker 167
4.1.3 β-blocker Structure-Activity Relationships 168
4.1.4 β-blockers for Treatment of Infantile Haemangioma 170
4.1.5 β-blockers for Treatment of Malaria 170
4.2 Objectives 172
4.3 Results 173
4.3.1 Synthesis of Novel Ferrocenyl β-Blockers 173
4.3.2 Biological Activity of Novel Ferrocenyl β-Blockers 180
4.4 Discussion 187
4.5 Conclusion 189
4.6 References 190
5 Experimental 193
5.1 Synthesis 193

5.1.1 Experimental Procedures for the Synthesis of Ferrocene Nucleic Acid (FcNA) Monomers 194

5.1.2 Experimental Procedures for the Synthesis of Ferrocenyl Nucleoside Analogues 235

5.1.3 Experimental Procedures for the Synthesis of Ferrocenyl β-Blockers 277

5.2 High-Performance Liquid Chromatography 289

5.3 X-Ray Diffraction 290

5.4 Oligonucleotide Solid-Phase Synthesis 291

5.5 Thermal Melting Experimental 292

5.6 Electrochemistry 293

5.7 Biological Methods 294

5.7.1 Crystal Violet Cell Viability Assay for HOS 294

5.7.2 Crystal Violet Cell Viability Assay for OE21 294

5.7.3 MTS Cell Viability Assay for L1210, CEM and Hela Cells 295

5.7.4 CPE Reduction Assay for Antiviral Activity 296

5.7.5 Western Blot Cells and Chemicals 296

5.7.6 Western Blot Cell Culture and Maintainance 296

5.7.7 Compound Preparation for Western Blot 297

5.7.8 Cell Plating and Cell Lysate Preparation 297

5.7.9 Measurement of Protein Concentration 298

5.7.10 Sodium Dodecyl Sulphate Polyacrylamide Gel Electrophoresis (SDS-PAGE) and Transphoresis 299

5.7.11 Immunolocalisation of Proteins (Western Blot) 300

5.7.12 Data Analysis and Statistics 300

5.8 References 302

6 Appendix 304

6.1 Crystal Data 304

6.1.1 Crystal Data for 2.31 304

6.1.2 Crystal Data for Fcn1c2T$_{(Rp)}$ 306

6.1.3 Crystal Data for Fcn1c2T$_{(Sp)}$ 308

6.1.4 Crystal Data for Fcn2c2T$_{(Rp)}$ 310

6.1.5 Crystal Data for Fcn2c2T$_{(Sp)}$ 312

6.1.6 Crystal Data for Fcn1c2G$_{(Rp)}$ 314

6.1.7 Crystal Data for 4.5 316

6.1.8 Crystal Data for 4.8 318

6.1.9 Crystal Data for 4.10 320

6.1.10 Crystal Data for 4.12 322

6.1.11 Crystal Data for 4.13 324

6.1.12 Crystal Data for 4.15 326

6.2 Electrochemistry 328

6.2.1 Electrochemistry Plots for Fcn3c2T$_{(S,Rp)}$ 328

6.2.2 Electrochemistry Plots for Fcn2c2T$_{(Rp)}$ 329

6.2.3 Electrochemistry Plots for Fcn1c2T$_{(Rp)}$ 330

6.2.4 Electrochemistry Plots for Fcn2c2T 331

6.2.5 Electrochemistry Plots for Fcn2c2G$_{(Sp)}$ 332

6.2.6 Electrochemistry Plots for Fcn1c2G$_{(Rp)}$ 333

6.2.7 Electrochemistry Plots for Fcn2c2G 334

7 Publications, Presentations, Awards and Courses 335

Abbreviations

5-FU	5-Fluorouracil
A	Adenine
Ac	Acetyl
AD	Amylose chiral column
ADP	Adenosine diphosphate
AIDS	Aquired immunodeficiency virus
AMP	Adenosine monophosphate
aq.	Aqueous
AR	Adrenergic receptor
ar	Aryl
atm.	Atmosphere
ATP	Adenosine triphosphate
AZT	Azidothymidine
Bn	Benzyl
Bu	Butyl
Bz	Benzoyl
C	Cytosine
C.E.	Counter electrode
ca.	Circa
cAMP	Cyclic AMP
cat.	Catalytic
CBS	Corey-Bakshi-Shibata
cDNA	Complementary DNA
ClogP	Calculated log P
conc.	Concentrated
Cp	Cyclopentadienyl
CPE	Cytopathic effect
CV	Cyclic voltammogram
d	Doublet
DAP	2,6-Diaminopurine
DCC	*N*,*N*-Dicyclohexylcarbodiimide
DCM	Dichloromethane
DEAD	Diethylazodicarboxylate
DIAD	Diisopropylazodicarboxylate
DIBAL	Diisobutylaluminium hydride
DIPA	Diisopropylamine
DIPEA	Diisopropylethyamine
DMAc	Dimethylacetamide
DMAP	4,4-Dimethylaminopyridine
DMF	Dimethylformamide
dmfc	Decamethylferrocene
DMG	Direct metallation group
dMP	Deoxyribose monophosphate
DMSO	Dimethylsulfoxide
DMT	Dimethoxytrityl
DNA	Deoxyribonucleic acid
DPC	Diphenylcarbamate
e.e.	Enantiomeric excess

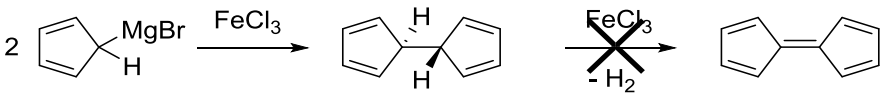
EC	Effective concentration
EI	Electron impact ionisation
ep	Epoxide
eq.	Equivalents
ES	Electrospray ionisation
Et	Ethyl
Fc	Ferrocene
FcNA	Ferrocene nucleic acid
FRET	Förster resonance energy transfer
G	Guanine
H.W.E.	Horner-Wadsworth-Emmons
H-bond	Hydrogen bond
HPLC	High performance liquid chromatography
hr	Hour
HRMS	High-resolution mass spectrometry
HSV1	Herpes simplex virus 1
HSV2	Herpes simplex virus 2
IC	Inhibitory concentration
IPA	Isopropyl alcohol
IR	Infrared
Isop	Isoproterenol
LDA	Lithium diisopropylamide
LKB1	Liver kinase B1
m.p.	Melting point
MALDI	Matrix-assisted laser desorption/ionisation
Me	Methyl
min	Minutes
MS	Mass spectrometry
N.C.	Negative control
n-BuLi	*n*-Butyllithium
NMR	Nuclear magnetic resonance
NOE	Nuclear Overhauser effect
Oligo	Oligonucleotide
Ph	Phenyl
PKA	Protein kinase A
P-LKB1	Phospho-liver kinase B1
PNA	Peptide nucleic acid
ppm	Parts per million
Pr	Propyl
Prop	Propranolol
PTSA	*para*-Toluenesulfonic acid
Py	Pyridine
q	Quartet
qu	Quintet
R.E.	Reference electrode
RNA	Ribonucleic acid
rt	Room temperature
s	Singlet
sat.	Saturated

Ser	Serine
T	Thymine
t	Triplet
TBAF	Tetrabutylammonium fluoride
TBDPS	*tert*-butyldiphenylsilyl
t-BuLi	*tert*-Butyllithium
TDS	(Dimethyl)thexylsilyl
TEA	Triethylamine
TFA	Trifluoroacetic acid
THF	Tetrahydrofuran
TLC	Thin-layer chromatography
TMEDA	Tetramethylethylenediamine
TMS	Trimethylsilyl
TOF	Time-of-flight
U	Uracil
UV	Ultraviolet
VV	Varicella virus
VZV	Varicella zoster virus
W.E	Working electrode
XRD	X-ray diffraction

1 Introduction

1.1 Ferrocene

"Yellow sludge" is how the workers at Union Carbide first described dicyclopentadienyliron (or ferrocene as it is now more widely known); it was blocking the pipes.[1] Within a few years however, this beautiful yellow crystalline solid would inspire an entirely new field of organometallic chemistry and be studied across the world for its unusual structure and unique properties. The first official report was by Pauson who also stumbled inadvertently across the "bright orange crystals" while trying to prepare fulvalene from $FeCl_3$ and a cyclopentadienyl Grignard reagent (**Scheme 1.1**); he characterised the composition of the undesired product as $C_{10}H_{10}Fe$.[2] These unusual findings were independently corroborated the following year when "dicyclopentadienyliron" was reported by Miller who again produced the compound serendipitously.[3]



Scheme 1.1 Pauson's attempted synthesis of fulvalene from a cyclopentadienyl Grignard reagent and $FeCl_3$[2]

1.1.1 Structure

In the early 1950's, there was widespread scepticism regarding the feasibility of forming stable carbon-metal bonds, and therefore this new compound, which showed no decomposition up to its melting point of 173 – 174 ºC, was something of a curiosity.[3,4] Although the bonding and exact structure were not yet understood, Pauson attributed this exceptional stability to an "aromatic tendency", as suggested by the resonance structures he proposed (**Fig. 1.1**).[2]

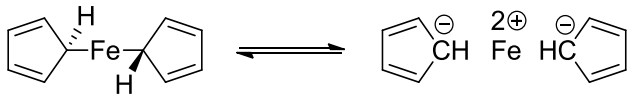


Fig. 1.1 The structure of ferrocene showing the "aromatic tendency" proposed by Pauson[2]

Within a year, examination of its unique properties led Wilkinson to suggest the 'sandwich' structure, consistent with the compound's diamagnetism, lack of dipole moment and single C–H absorption frequency. Although he depicted the molecule in both its staggered and eclipsed conformations, it is known that the rings are in fact very free to rotate (**Fig. 1.2**).[5,6] Each cyclopentadienyl (Cp) ring is anionic, planar, with a total of 6 π-electrons, and is as such aromatic; these D_{5h} symmetric plates 'sandwich' the central Fe^{2+} ion balancing the charge. Upon complexation, the six electrons of each Cp ring combine with the six d-electrons of the central metal ion resulting in a stable 18-electron configuration. Following the discovery of ferrocene, various related compounds with general structure $M(\eta\text{-}C_5H_5)_2$ have been synthesised and constitute a family known as the 'metallocenes'.[7]

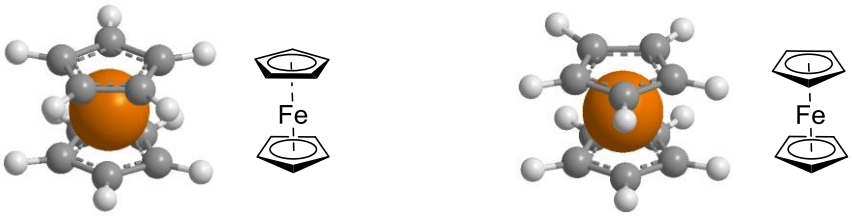
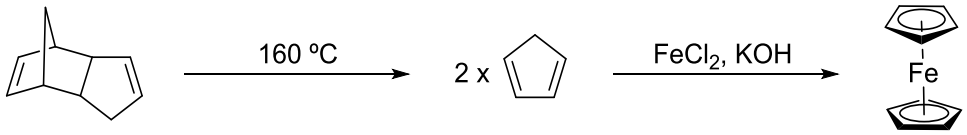


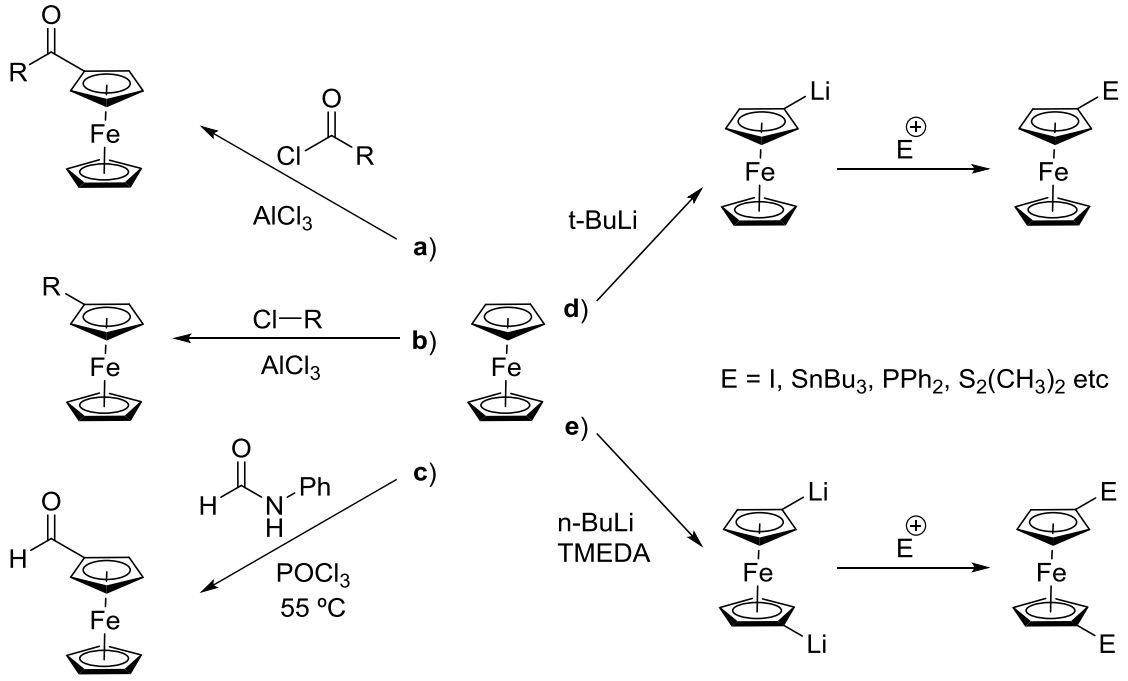
Fig. 1.2 Wilkinson's dicyclopentadienyl 'sandwich' structure $Fe(\eta\text{-}C_5H_5)_2$, showing both the staggered and eclipsed conformations[5]

1.1.2 Reactivity and Synthetic Considerations

Today ferrocene is most often produced using iron(II) chloride and freshly cracked cyclopentadiene, which is deprotonated with potassium hydroxide; the pure compound is usually purified by recrystallization or sublimation from the crude mixture (**Scheme 1.2**).[8]



Scheme 1.2 Modern laboratory synthesis of ferrocene from dicyclopentadiene and iron (II) chloride[8]



Scheme 1.3 Common reactions of ferrocene **a**) Friedel-Crafts acylation, **b**) Friedel-Crafts alkylation, **c**) Vilsmeier-Haack formylation, **d**) mono-lithiation and **e**) di-lithiation

Bearing two negatively charged aromatic rings, the chemistry of ferrocene can be compared to that of an electron-rich benzene, indeed this forms the etymology of the name.[9] Electrophilic substitution reactions such as Friedel-Crafts acylation/alkylation, and Vilsmeier-Haack type formylations are therefore commonly employed to functionalise the metallocene.[9,10] In addition, ferrocene can be deprotonated by butyllithium reagents (BuLi), a particularly useful reaction as the metallated, pseudo-carbanion can be reacted with a variety

of electrophiles to give a range of functionalised products. Whereas *t*-BuLi typically favours the mono-, *n*-BuLi with TMEDA tends to favour the di-lithiated species (**Scheme 1.3**).[11,12]

These organolithium reagents are also often employed in directed-lithiation reactions, a process by which extant substituents bearing direct metalation groups (DMGs) facilitate the selective lithiation of a neighbouring carbon atom. Given the planar geometry of benzene, in simple aryl systems the ortho-positions are often degenerate, and therefore reaction on either side yields an identical product. The corresponding ortho-lithiation of ferrocene however results in a pair of planar chiral enantiomers which may or may not be desirable (**Fig. 1.3**).

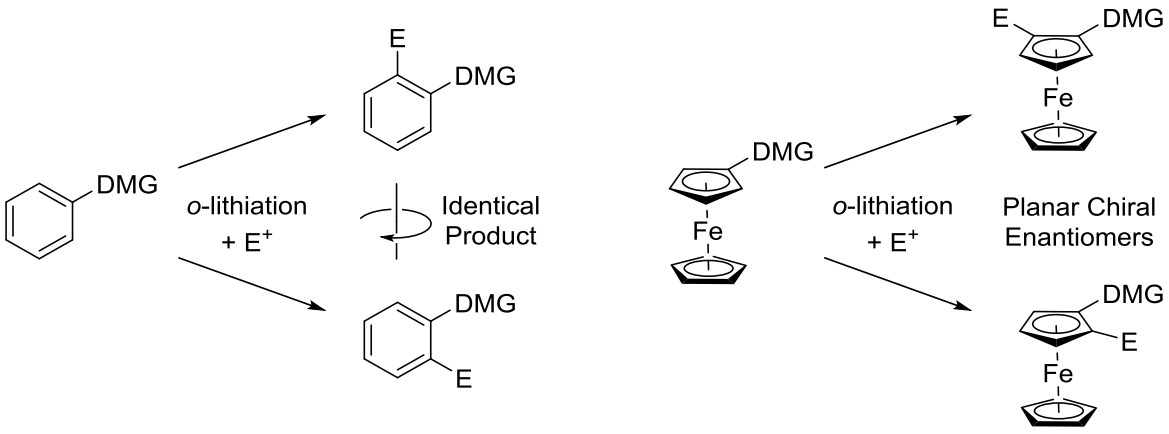


Fig. 1.3 Directed ortho-lithiation reactions of a simple aryl, which produces a single product; and a simple ferrocene, which produces a pair of planar chiral enantiomers

Planar chirality is most often described by assigning priority according to the Cahn-Ingold-Prelog rules, then, looking down on the plane of interest, (R_p) designates the enantiomer with a clockwise increase in priority, whereas (S_p) designates the opposite, anticlockwise enantiomer (**Fig. 1.4**).[13]

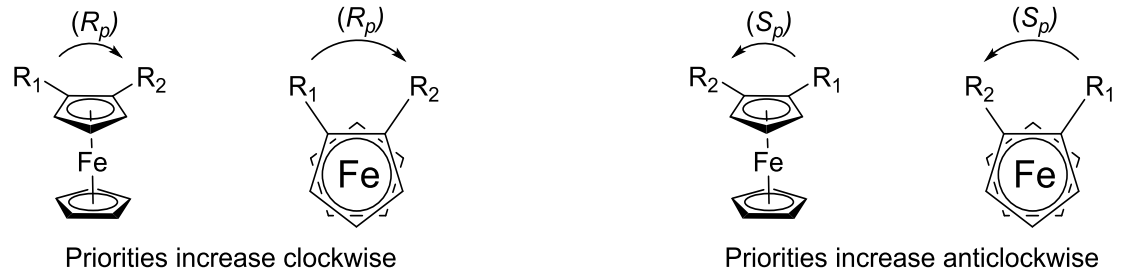
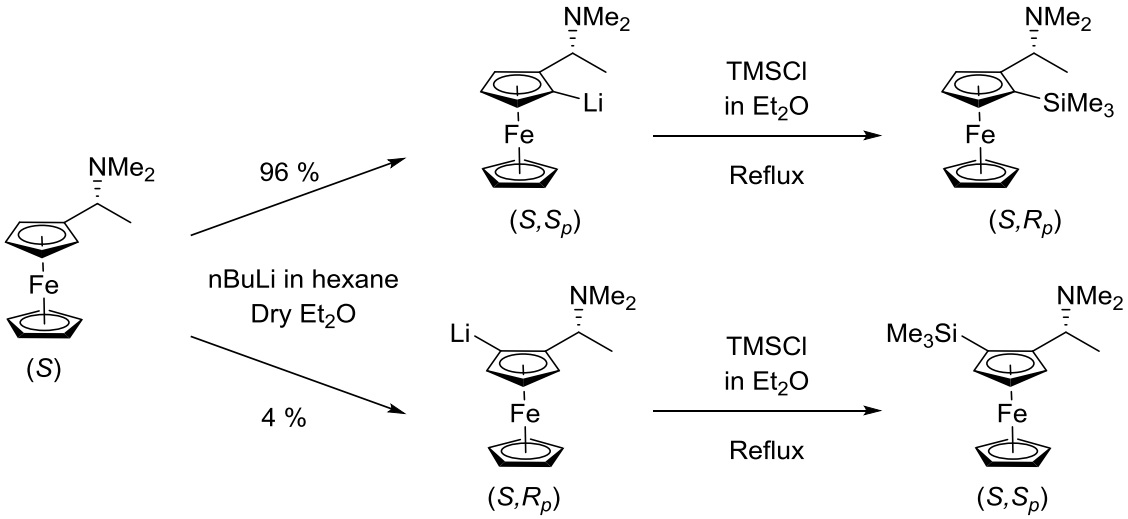


Fig. 1.4 Planar chiral designations (R_p) and (S_p) of ferrocenes both from the side and above

To gain control over this important aspect of metallocene chemistry, various stereoselective, ortho-directing groups have been developed which favour the lithiation of a single carbon atom.[14] Producing a diastereomeric ratio of 96:4, a very successful example of this was developed by Ugi in the early 1970s; the easily accessible chiral amine he used to direct the lithiation now bears his name in honour (**Scheme 1.4**).[15]



Scheme 1.4 Ortholithiation of the 'Ugi amine' to produce a 96:4 diastereomeric ratio of products[15]

NOE experiments have shown that in the lowest energy configuration, the large methyl and dimethylamine groups of the 'Ugi amine' assume positions of minimal steric interference with the iron centre, residing instead beyond the plane of the Cp ring on the periphery of the

molecule.[16] The amine group is thus preferentially placed in the proximity of a single carbon atom, and subsequently, through complexation of the Li^+ ion, stabilises the metal at this position (**Fig. 1.5**). As demonstrated by Knochel, this method works equally well when applied to both rings simultaneously, the high level of enantioselectivity is maintained (e.e. > 98%) (**Scheme 1.5**).[16]

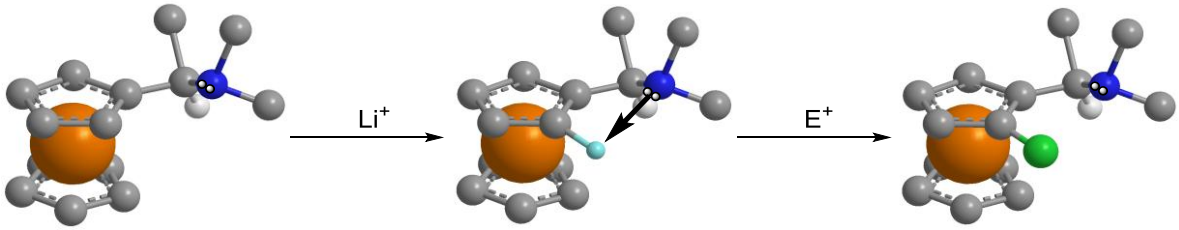
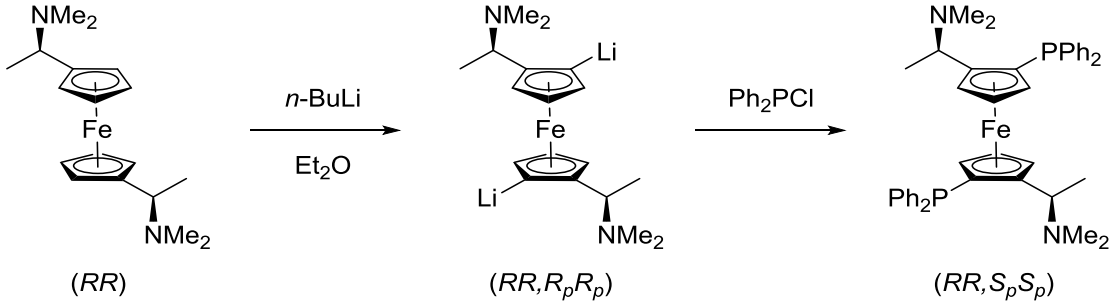
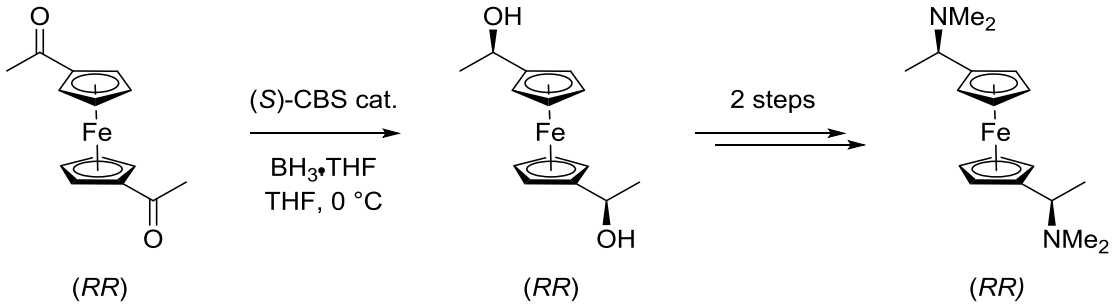


Fig. 1.5 Directed ortho-lithiation using the 'Ugi amine'[16]

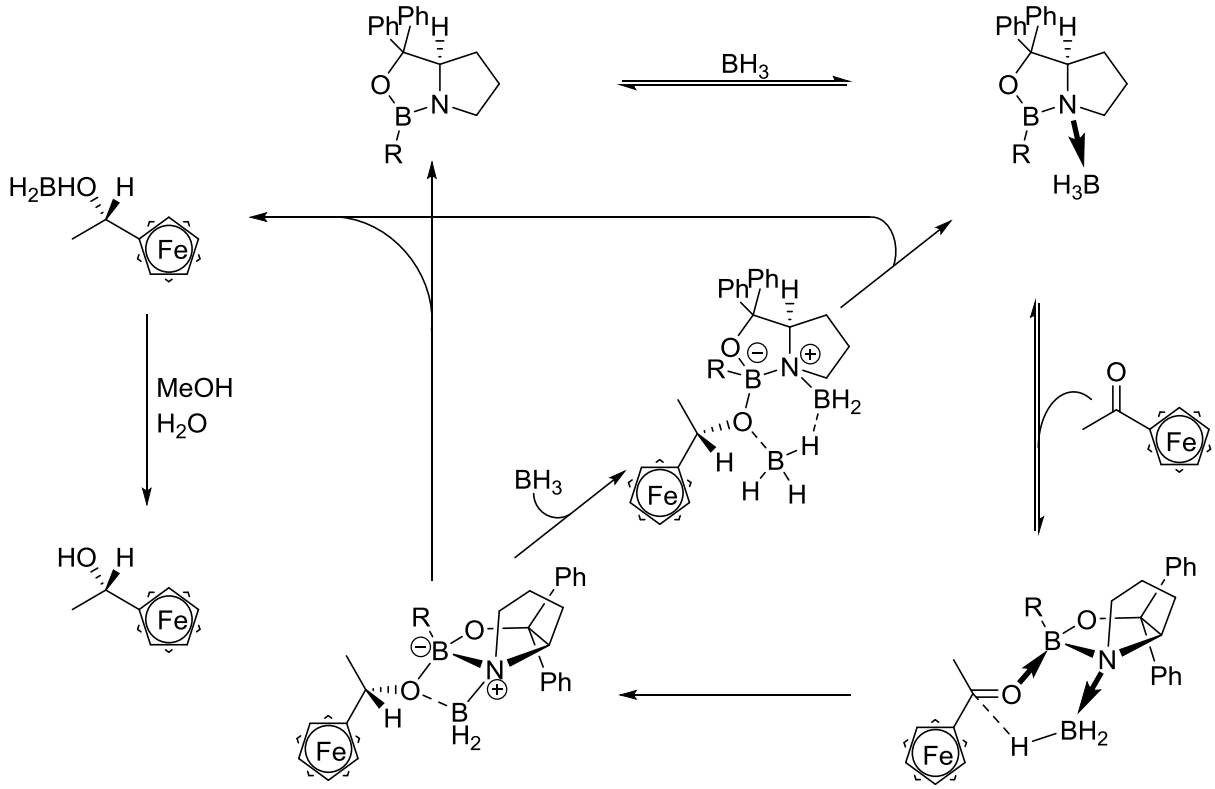


Scheme 1.5 Ortho-lithiation on both Cp rings using the 'bis-Ugi amine' by Knochel[16]

In the 1970s the 'Ugi amine' was prepared as a racemic mixture from ferrocenylethanol and the two enantiomers subsequently resolved by complexation with (*R*)-(+)-tartaric acid.[15] More recent advances in asymmetric catalysis however allow the production of chiral ferrocenes with very high enantioselectivity and relative ease. Knochel for instance used the Corey-Bakshi-Shibata (CBS) catalyst to induce chirality, performing a Corey-Itsuno reduction of diacetylferrocene to the corresponding diol with high yield (98%) and a diastereomeric ratio *dl:meso* of 98.5:1.5. Two facile functional group interconversions then deliver the required 'Ugi-diamine' in high yield (**Scheme 1.6**).[16,17]



Scheme 1.6 Knochel's route to the 'Ugi-diamine' using a CBS reduction of diacetylferrocene to establish the central chirality[16]

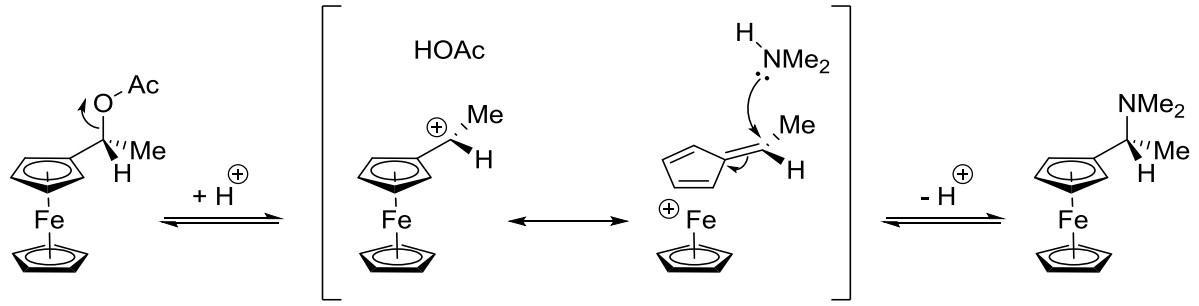


Scheme 1.7 Corey-Itsuno reduction of acetylferrocene using the CBS catalyst[19]

The Corey-Itsuno reaction employs the chiral oxazaborolidine CBS catalyst to stereoselectively reduce ketones to their corresponding chiral alcohols.[18] The BH_3 reducing agent is first coordinated by the nitrogen lone pair enhancing its hydride donor properties (**Scheme 1.7**). The ketone then associates with the activated complex via coordination of the endocyclic boron, the bulky ferrocene unit and phenyl groups of the catalyst dictating a conformation of minimal steric hindrance. The hydride is thus delivered preferentially to one

side of the ketone via a six-membered transition-state, an alkoxyborane is released which yields the corresponding alcohol upon work up.[19] This process works particularly well for acetylferrocene and tolerates a range of other ferrocenyl ketones; it is worth noting however that as the steric bulk of the R group increases, a significant decrease in stereoselectivity is observed.[16]

Following the CBS-reduction, Knochel's route to the Ugi amine highlights another interesting aspect of ferrocene chemistry, demonstrating a highly stereoselective S_N1-type reaction at the α-position. The chiral alcohol is first transformed to a good leaving group by a straightforward esterification to the acetoxy, which is substituted by the dimethylamine nucleophile in the subsequent step.



Scheme 1.8 Highly stereoselective S_N1-type reaction at the α-position of ferrocene[20]

Unusually, although proceeding by an S_N1 mechanism, an uncharacteristic retention of stereochemistry is observed; a number of contributing factors have been cited to account for this phenomenon.[20] It is thought that the leaving group departs from the top face of the Cp ring, away from the sterically demanding iron centre (**Scheme 1.8**). The resulting carbocation is then stabilised by both delocalisation into the aromatic Cp ring, and from orbital contributions from the iron; the rotation of the cationic centre is thus restricted. The incoming nucleophile therefore approaches along the same, least hindered trajectory to assume an identical position.[21,22]

1.1.3 Electrochemistry

Ferrocene is renowned for its well-defined electrochemistry, undergoing a reversible, single-electron redox conversion to the positively charged ferrocenium(III) ion. This process is typically studied by cyclic voltammetry, in which an applied potential is varied in a cyclic fashion and the output current of the electro-active system is recorded. A three-electrode system is usually employed, comprising of a working electrode (W.E.), a counter electrode (C.E.) and a reference electrode (R.E.) (**Fig. 1.6**). All three are connected through a potentiostat which is used to both control and monitor them. A voltage is applied at the W.E. and is controlled relative to the R.E.; current does not flow between the two however due to the high impedance of the voltmeter. Instead, the current flows through the solution between the W.E. and the C.E. and is recorded as a function of the applied voltage.[23,24,25]

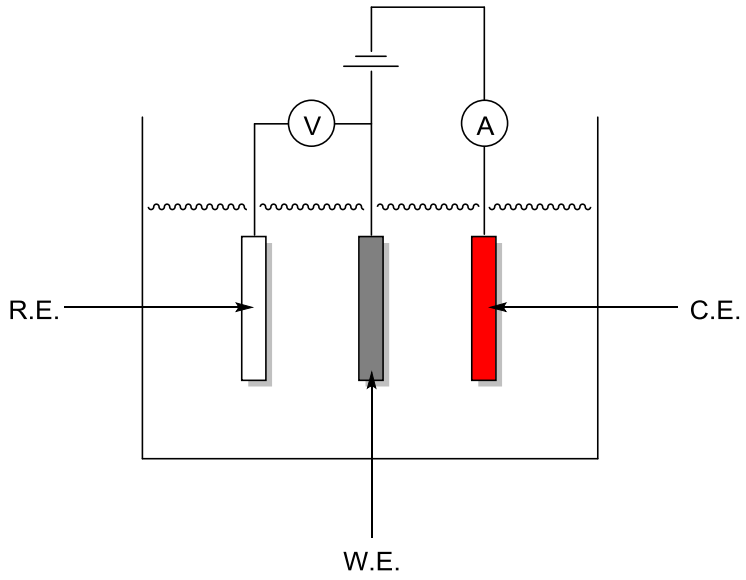


Fig. 1.6 A simplified schematic of the three-electrode system used in cyclic voltammetry showing the reference electrode (R.E.), working electrode (W.E.), counter electrode (C.E.) voltmeter (V) and ammeter (A).

In a cyclic voltammetry experiment, the voltage between the W.E. and R.E. is increased in a linear sweep from an initial value E_i, at which oxidation cannot occur, to second value E_λ (the switching potential) at which electron transfer is strongly induced. At this point the direction of the sweep is reversed and the voltage is returned to its original value, overall tracing a symmetrical, triangular waveform (**Fig. 1.7**). The current between the W.E. and C.E. is monitored throughout this process and plotted against the potential to produce a cyclic voltammogram (CV). Ferrocene produces a very characteristic waveform consisting of two peaks, one on the forward sweep corresponding to oxidation, and one on the reverse sweep due to the reverse process of reduction.[23,24]

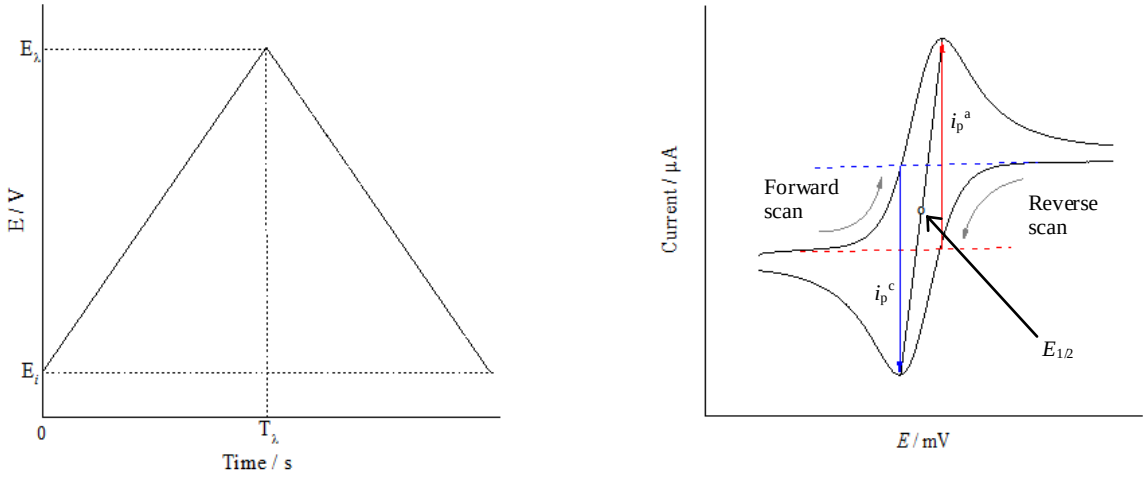


Fig. 1.7 The triangular waveform of a cyclic voltammetry experiment and the resulting CV for ferrocene, showing both oxidation and reduction peaks

Initially, the applied potential is not sufficient to induce electron transfer and hence no current is observed. However, the voltage increases throughout the forward scan and eventually becomes sufficient to oxidise the ferrocene from the Fe(II) to the Fe(III) state, the electrons are transferred to the W.E. and the corresponding current is registered at the C.E.. Initially the current increases exponentially with the potential. However, as the analyte at the surface of the electrode is consumed, and is only partially replenished by fresh material from the bulk solution, a threshold *peak current*, i_{pa} is achieved before a rapid falling off is

observed. The potential sweep is then reversed and the opposite process is induced; the layer of oxidised ferrocenium analyte at the surface of the electrode is reduced resulting in a cathodic current. Again, although initially an exponential response is observed, the current reaches a maximum at i_{pc} before rapidly falling off as material diffuses from the surface.[23,24]

Under these conditions, due to the influence of both mass transfer and kinetic effects, the anodic and cathodic processes occur at slightly different potentials, E_{pa} and E_{pc} respectively. $E_{½}$ is defined as the midpoint between the anodic and cathodic peak potentials relative to the reference electrode and is therefore very useful when comparing the electrochemistry of different species (**Eq. 1.1**).[25]

Eq. 1.1 $$E_{½} = ½ (E_{pa} + E_{p})$$

Typically however, when examining the electrochemistry of ferrocene and its derivatives, decamethylferrocene (dmfc) is employed as an internal standard against which relative $E_{½}$ values can be measured directly. Two separate electron transfer processes are now observed corresponding to the oxidation and reduction of each species, the $E_{½}$ value of dmfc is set to zero and the $E_{½}$ of the analyte is given relative to it (**Fig. 1.8**).

Repeating the cyclic voltammetry experiment at different scan rates provides further information regarding the reversibility of the system and also allows the diffusion coefficient of the analyte to be calculated. Current is defined as the rate of flow of electric charge, and its units are amperes (A) (coulombs per second). It is worth noting therefore, that as the scan rate is increased, larger peak currents are observed due to the increasing rate of electron transfer (**Fig 1.9**).

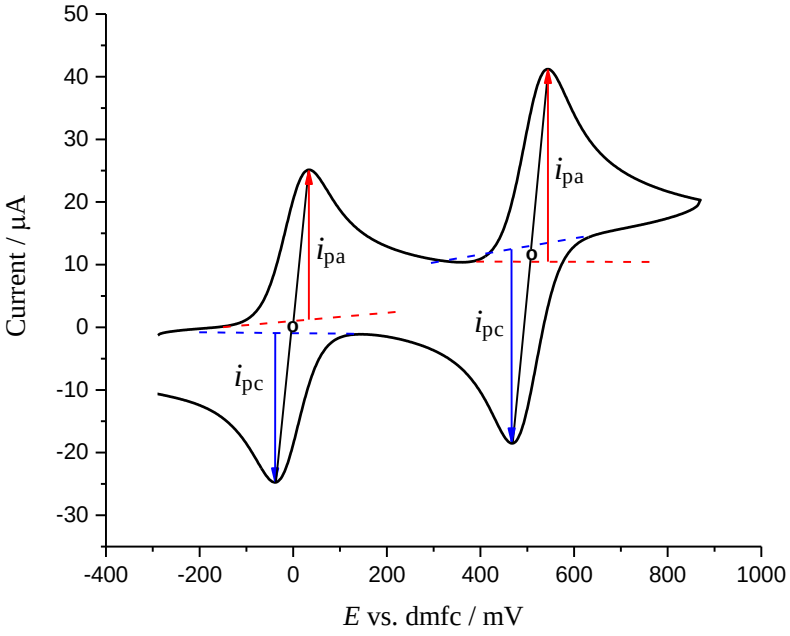


Fig. 1.8 CV of ferrocene using an internal standard of dmfc

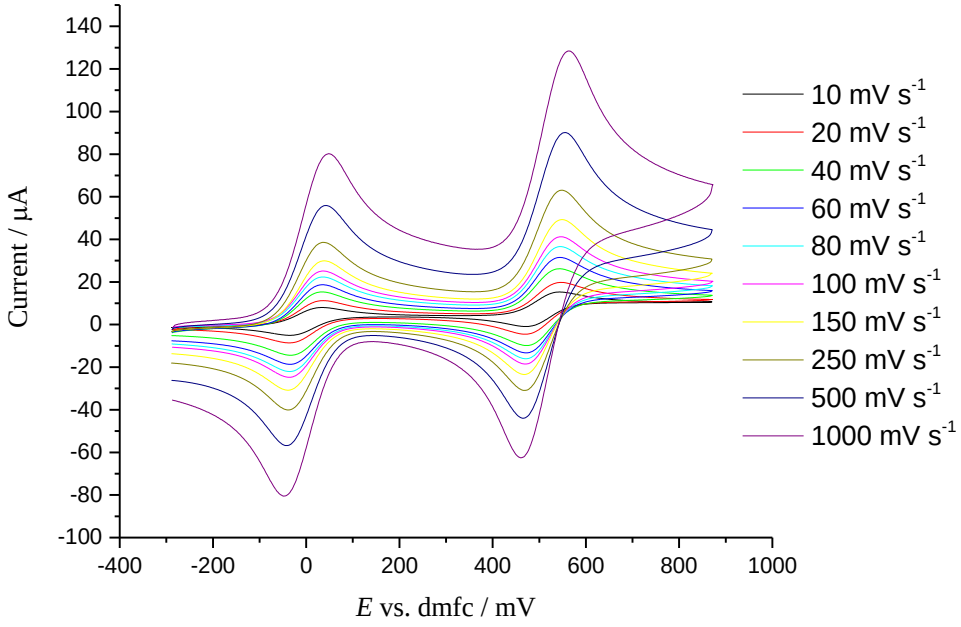


Fig. 1.9 CV of ferrocene at various scan rates using an internal standard of dmfc

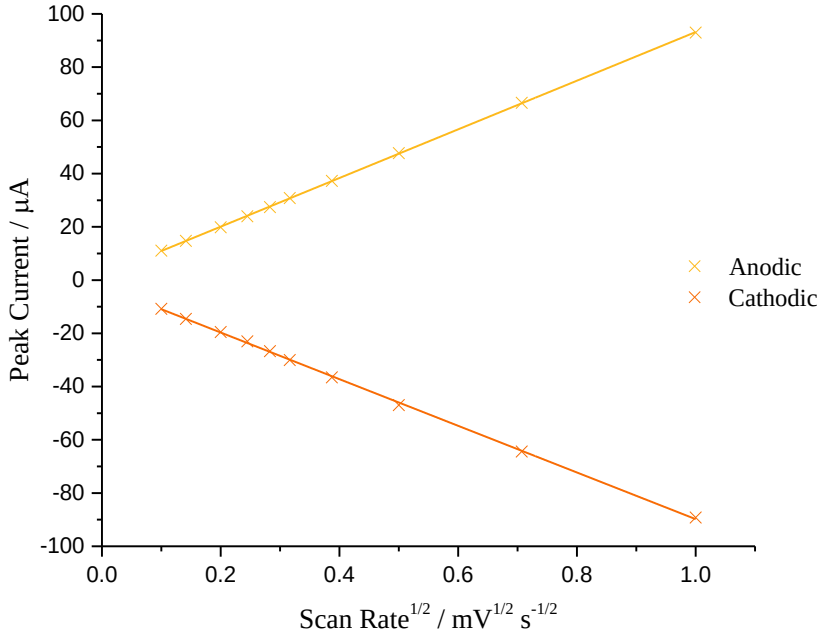


Fig. 1.10 Plot of peak current vs the square root of the scan rate for ferrocene

The diffusion coefficient of the electro-active species can be calculated using the Randles-Sevcik equation (**Eq. 1.2**).[26,27]

Eq. 1.2 $$i_p = 0.4463\ nFAC\left(\frac{nFvD}{RT}\right)^{\frac{1}{2}}$$

Where:

i_p = peak current (A)

v = scan rate (V s^{-1})

n = electron transfer per molecule

D = diffusion coefficient

F = Faraday constant (C mol^{-1})

R = Gas constant (V C K^{-1} mol^{-1})

A = surface area of the electrode (cm^2)

T = temperature (K)

C = bulk concentration of solution (mol cm^{-3})

For a single electron transfer process at 25 ºC this simplifies to give **Eq. 1.3**.

Eq. 1.3 $$i_p = 268{,}600\ AD^{\frac{1}{2}}Cv^{\frac{1}{2}}$$

i_p is therefore plotted against $v^{1/2}$ and the gradient (m) calculated using computer fitting software (**Fig. 1.10**).

Eq. 1.4 $m = 268{,}600\ A D^{\frac{1}{2}} C$

Thus the diffusion coefficient (D) can be calculated according to **Eq. 1.5**

Eq. 1.5 $D = \left(\frac{m}{268{,}600\ A C}\right)^2$

For a system to be considered electrochemically reversible it must fulfil the three criteria of Nernstian behaviour.[23,28] Firstly, the anodic and cathodic peak currents must be of the same magnitude (**Eq. 1.6**).

Eq. 1.6 $i_{pa} / i_{pc} = 1$

Secondly, they must be separated, in the case of a single-electron transfer process, by approximately 59 mV (at 25 ºC) and this should not vary with scan rate (**Eq. 1.7**).

Eq. 1.7 $\Delta E_p = E_{pa} - E_{pc} = 59\ mV$

And lastly, the relationship between the peak current and the square root of the scan rate should be linear, as demonstrated for ferrocene above (**Fig. 1.10**).

1.1.4 Applications of Ferrocene

The stability, structural versatility and unique properties of ferrocene have led to the molecule being investigated in a range of diverse roles and applications. For instance, ferrocene is often employed as an anti-knock agent in combustion engines and derivatives such as 1,3-diferrocenyl-1-butene have been researched as potential burn-rate catalysts in rocket fuel.[29,30] Following the development of the ferrocene based drug candidates ferrocifen and ferroquine, the pharmaceutical properties of the compound are also of great interest, while everyday, ferrocene based electrochemical sensors are used by diabetics to test their blood-sugar levels.[31,32,33] Exploiting the unusual sandwich structure and electronic properties of the

molecule, highly successful ligands such as 1,1'-bis(diphenylphosphino)ferrocene (dppf) and chiral variations which make use of the planar chiral properties of the metallocene have also been developed.[34]

1.1.5 Thesis Outline

This thesis explores the use of ferrocene in three areas of research. **Chapter 2** describes the synthesis of ferrocene nucleic acid (FcNA) monomers, in which a tetrasubstituted ferrocene unit replaces the traditional sugar of deoxyribonucleic acid (DNA). **Chapter 3** describes the synthesis and biological activity of the closely related disubstituted ferrocene nucleoside analogues, in which the hydroxyl and nucleobase functionalities, which typify this class of compound, are linked through a ferrocene unit. **Chapter 4** describes the synthesis and preliminary biological activity of a library of potential ferrocenyl β-blockers in which the metallocene replaces the aryl unit of a typical β-blocker.

1.2 References

[1] H. Werner, *Angew. Chem. Int. Ed.*, **2012**, 51, 2 – 9.

[2] T. J. Kealy, P. L. Pauson, *Nature*, **1951**, 168, 1039 – 1040.

[3] S. A. Miller, J. A. Tebboth, J. F. Tremaine, *J. Chem. Soc.*, **1952**, 632 – 635.

[4] P. L. Pauson, *J. Organomet. Chem.*, **2001**, 637 – 639.

[5] G. Wilkinson, M. Rosenblum, M. C. Whiting, R. B. Woodward, *J. Am. Chem. Soc.*, **1952**, 74, 6148 – 6149.

[6] E. W. Abel, N. J. Long, K. G. Orrell, A. G. Osborne, V. Ŝik, *J. Organomet. Chem.*, **1991**, 403, 195 – 208.

[7] O. E. Fischer, W. Pfab, *Z. Naturforsch. B.*, **1952**, 7, 377 – 379.

[8] G. Wilkinson, *Org. Synth.*, **1963**, 4, 473.

[9] R. B. Woodward, M. Rosenblum, M. C. Whiting, *J. Am. Chem. Soc.*, **1952**, 74, 3458 – 3459.

[10] G. D. Broadhead, J. M. Osgerby, P. L. Pauson, *Chem. and Ind.*, **1957**, 209.

[11] M. Roemer, C. A. Nijhuis, *Dalton Trans.*, **2014**, 43, 11815 – 11818.

[12] F. Rebiere, O. Samuel, H. B. Kagan, *Tetrahedron Lett.*, **1990**, 31, 3121 – 3124.

[13] A. Togni, T. Hayashi, *Ferrocenes: Homogeneous Catalysis, Organic Synthesis, Materials Science*, VCH Verlagsgesellschaft, Weinheim (Federal Republic of Germany), VCH Publishers, New York, NY (USA), **1995**, 173 – 174.

[14] V. Mamane, *Tetrahedron: Asymmetry*, **2010**, 21, 1019 – 1029.

[15] D. Marquarding, H. Klusacek, G. Gokel, P. Hoffmann, I. Ugi, *J. Am. Chem. Soc.*, **1970**, 92, 5389 – 5393.

[16] P. Knochel, L. Schwink, *Chem. Eur, J.*, **1998**, 4, 950 – 968.

[17] J. Wright, L. Frambes, P. Reeves, *J. Organomet. Chem.*, **1994**, 476, 215 – 217.

[18] A. Hirao, S. Itsuno, S. Nakahama, N. Yamazaki, *Chem. Commun.*, **1981**, 315 – 317.

[19] E. J. Corey, C. J. Helal, *Angew. Chem. Int. Ed.*, **1998**, 37, 1986 – 2012.

[20] G. W. Gokel, D. Marquarding, I. K. Ugi, *J. Org. Chem.*, **1972**, 37, 3052 – 3058.

[21] J. J. Dannenberg, M. K. Levenberg, J. H. Richards, *Tetrahedron*, **1973**, 29, 1575 – 1584.

[22] R. L. Sime, R. J. Sime, *J. Am. Chem. Soc.*, **1974**, 96, 892 – 896.

[23] N. Aristov, A. Habekost, *World J. Chem. Edu.*, **2015**, 3, 115 – 119.

[24] G. A. Mabbott, *J. Chem. Educ.*, **1983**, 60, 697 – 702.

[25] F. Scholz, *Electroanalytical Methods*, **2002**, Springer-Verlag BerlinHeidelberg New York.

[26] J. E. B. Randles, *J. Chem. Soc., Faraday, Trans.*, **1948**, 44, 322 – 327.

[27] A. Ševčik, *Collect. Czech. Chem. Commun.*, **1948**, 13, 349 – 377.

[28] A. J. Bard, L. R. Faulkner, *Electrochemical Methods: Fundamentals and Applications*, **2001**, Wiley and Sons.

[29] G. M. Gore, K. R. Tipare, R. G. Bhatewara, U. S. Prasad, M. Gupta, S. R. Mane, *Defence Sci. J.*, **1999**, 49, 151 – 158.

[30] N. D. Marsh, I. Preciado, E. G. Eddings, A. F. Sarofim, *Combust. Sci. and Tech.*, **2007**, 179, 987 – 1001.

[31] S. Top, J. Tang, A. Vessieres, D. Carrez, C. Provote, G. Jaouen, *Chem. Commun.*, **1996**, 8, 955 – 956.

[32] C. Biot, G. Glorian, L. A. Maciejewski, J. S. Brocard, *J. Med. Chem.*, **1997**, 40, 3715 – 3718.

[33] A. E. G. Cass, G. Davis, G. D. Francis, H. A. O. Hill, W. J. Aston, I. J. Higgins, E. V. Plotkin, L. D. L. Scott, A. P. F. Turner, *Anal. Chem.*, **1984**, 56, 667 – 671.

[34] L. –X. Dai, T. Tu, S. –L. You, W. –P. Deng, X. –L. Hou, *Acc. Chem. Res.*, **2003**, 36, 659 – 667.

2 Synthesis of Novel Tetrasubstituted Ferrocene Nucleic Acid (FcNA) Monomers

2.1 Introduction

A hundred years after the publication of Charles Darwin's seminal work, *On the Origin of Species*, Watson and Crick elucidated the general structure of DNA and laid bare the fundamental physical processes of inheritance and evolution.[1,2,3] Since then, our understanding of this remarkable molecule and the associated processes of molecular biology have revolutionised the life sciences. The human genome project was the largest single biological study in the world, sequencing the hundreds of thousands of base-pairs which comprise the human genetic code and mapping the functionality of the genes therein; the implications upon our understanding of health and medicine cannot be overstated.[4] Beyond its primary biological function however, DNA and other nucleic acids also form a group of macromolecules with very interesting and potentially useful chemical characteristics. The supramolecular aspects of recognition and self-assembly are of particular interest, and, while the investigation of customisable synthetic DNA analogues offers great insight into the workings of nature's original building blocks, it also allows us to exploit these unique properties to new and exciting ends.

2.1.1 Deoxyribonucleic Acid (DNA)

Although responsible for all the diversity of the biological world, the basic chemical unit of DNA is remarkably simple; a tripartite monomer consisting of a phosphate, a deoxyribose sugar and one of four nucleobases; adenine (A), cytosine (C), guanine (G) and thymine (T) (**Fig. 2.1**). These nucleotides are oligormerised to form long strands, the alternating phosphate and sugar groups form a backbone from which the bases protrude. It is the

sequence of these bases which forms the genetic code, the all-important blueprint from which proteins are synthesised.

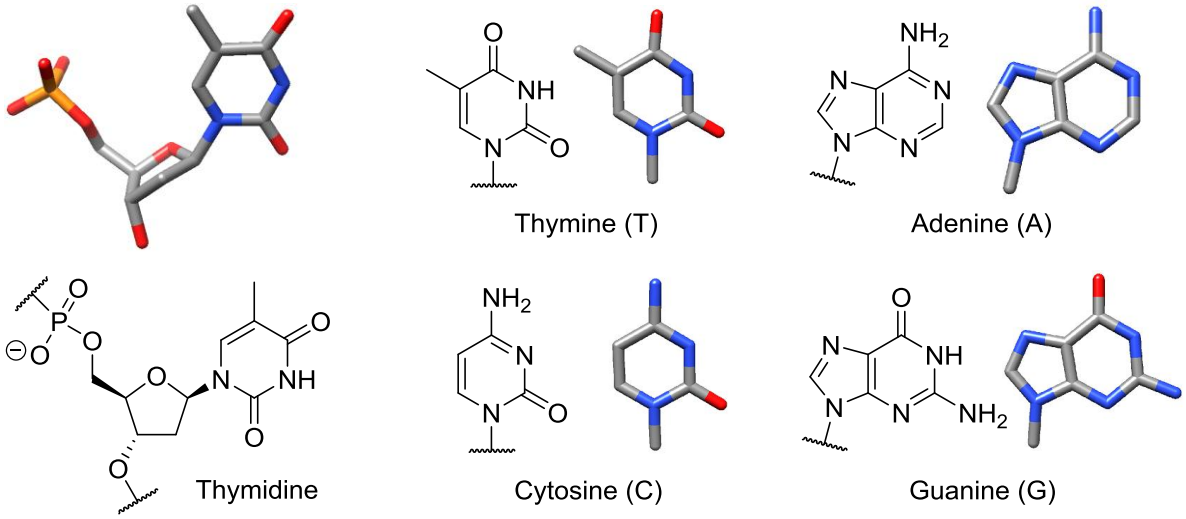


Fig. 2.1 The tripartite DNA monomer (thymidine) and the four canonical DNA nucleobases T, A, C and G

To ensure the safety and integrity of this precious information, DNA is typically stored as a double helix. The 'sense' strand is matched through selective base-pairing to its complementary 'anti-sense' strand, the two wind around each other wrapping the nucleobases in the centre of a tight coil, A matches T and G matches C, forming two and three H-bonds respectively (**Fig. 2.2**).

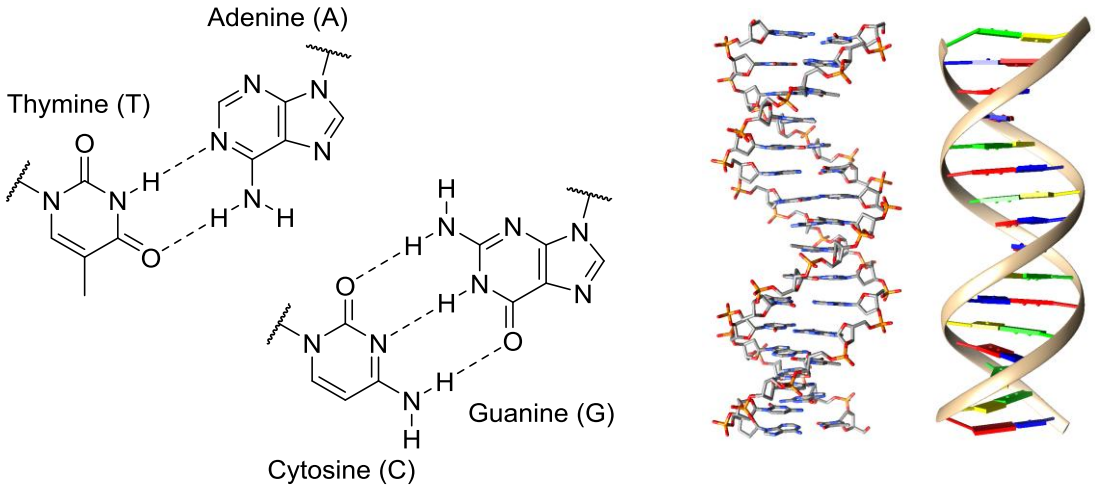


Fig. 2.2 H-bonding between T and A, C and G, and a DNA duplex

2.1.2 Non-Canonical Bases

Although the canonical bases of DNA number just four, it is well established that modifications are implemented within biological systems to regulate the function of nucleic acids and the related cellular machinery.[5,6] Uracil (U), for instance is the RNA equivalent of T and their essential function is the same, both selectively bind A via two hydrogen bonds allowing the transfer of genetic information (**Fig. 2.3**). However, given that C has a tendency to spontaneously deaminate to give U, the presence of an extra methyl group on T allows recognition by repair enzymes which seek to remove the degraded base from DNA.[7] This is an important characteristic for maintaining the integrity of DNA which is extraneous to the relatively short-lived, single-stranded RNA.

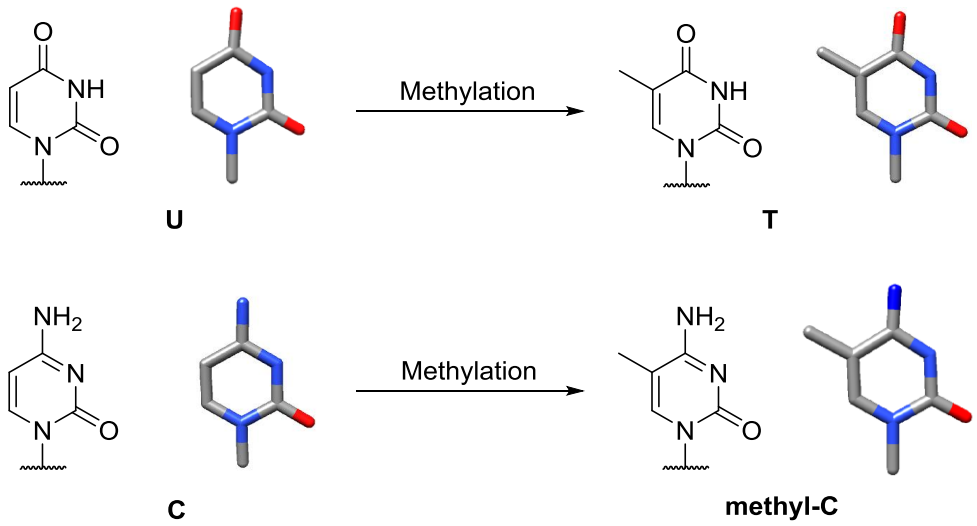


Fig. 2.3 Nucleobases U and C, and the methylated variants T and methyl-C

Methylation of other nucleobases, especially C, has also been implicated in important epigenetic processes; again the effect is subtle and 5-methylcytosine maintains all the essential function of the unmodified nucleobase (**Fig. 2.3**). Although the mechanism is not fully understood, heavily methylated areas of the genome are however less transcriptionally active; the gene expression and protein output is thus correspondingly lower.[8]

Another naturally occurring nucleobase modification is found in the DNA of the S-2L cyanophage (a virus of the Siphoviridae family which infects cyanobacteria), in which A is replaced by 2,6-diaminopurine (DAP).[9] The presence of an additional, exocyclic amine group strengthens the interaction with T through the formation of a third H-bond (**Fig. 2.4**).[10] This confers additional stability upon the duplex, significantly increasing the thermal melting temperature compared to unmodified DNA.[11] It is thought that this protects the genetic material of the virus from attack by the host. DAP-containing duplexes have been shown to resist degradation by certain nucleases; the enzymes typically exploit the weaker base-pairing interaction between canonical A and T to instigate their action.[12]

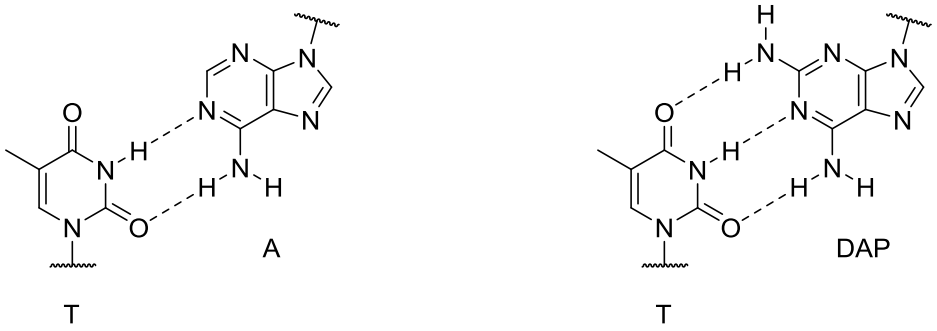
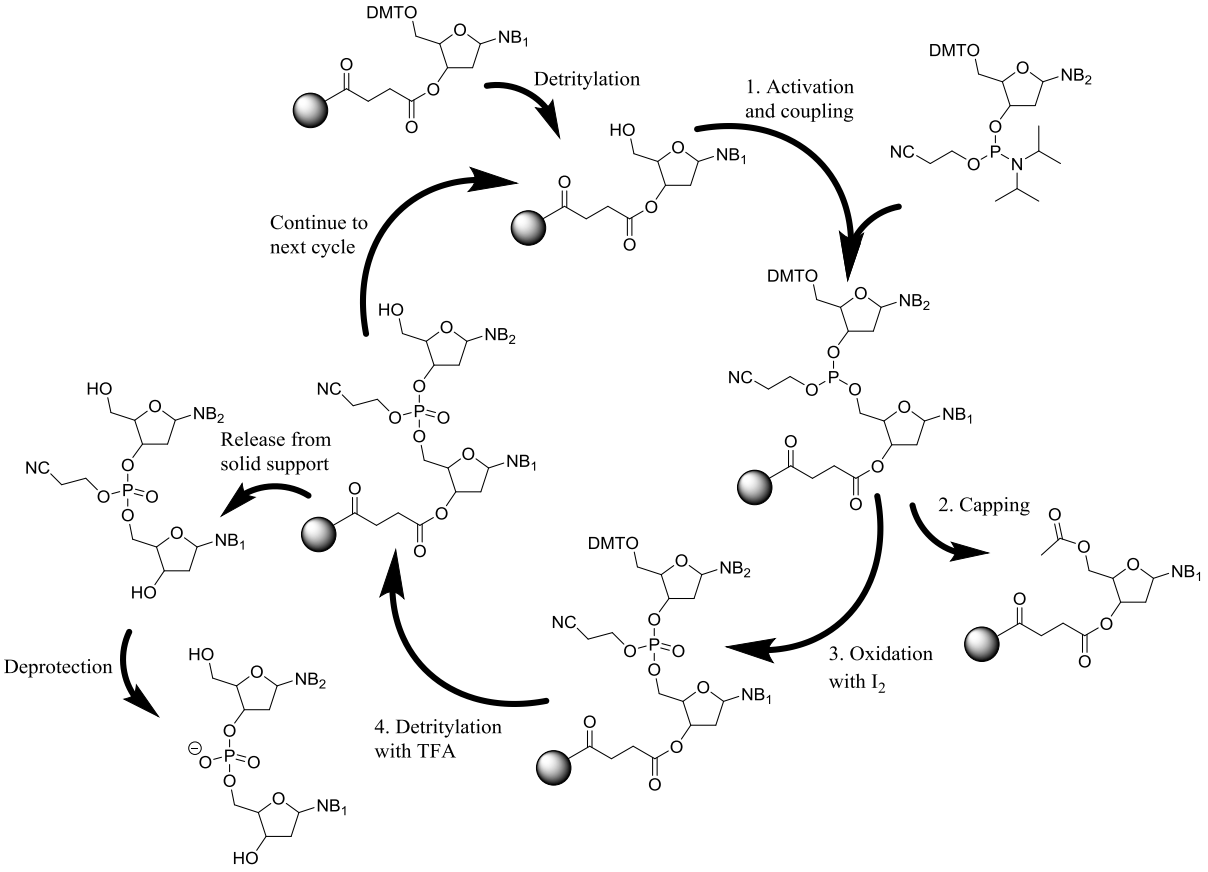


Fig. 2.4 Base pairing of A with T, forming two H-bonds and DAP with T, forming three H-bonds

Having identified the single most important molecule at the heart of all life, chemists have sought to further understand, manipulate and exploit the exquisite properties of this intriguing bioinformatic system. While structural modifications have been applied to both the phosphate-sugar backbone and the nucleobase moieties, culminating today in the availability of totally synthetic analogues; other modifications, such as the inclusion of fluorescent or redox-active units have produced nucleic acids with more exotic and unusual properties.[13,14,15,16]

Crucial to the production of many of these modified oligonucleotides is the automated solid-phase synthesis technology developed by Beaucage and Caruthers in 1981 which allows the production of short oligomers in which the sequence of nucleosides can be programmed (**Scheme 2.1**).[17] Substrates are prepared prior to use through the protection of functional groups; specifically, a dimethoxytrityl (DMT) group must be employed at the 5′-hydroxyl position and a phosphoramidite at the 3′-hydroxyl. The first nucleoside in the sequence is attached separately to a solid support which anchors the growing chain for the duration of the synthesis.



Scheme 2.1 Oligonucleotide synthesis using the solid phase phosphoramidite strategy developed by Beaucage and Caruthers[18]

Detritylation of the anchored nucleoside reveals the 5′-hydroxyl group which, when exposed to the second phosphoramidite, reacts at phosphorous to replace the diisopropylamine group.

Any unreacted 5′-hydroxyl groups are then 'capped' using a mixture of acetic anhydride and *N*-methylimidazole in THF to prevent any further reaction. Using iodine, the growing oligonucleotide is then oxidised from a phosphite-triester to a phospho-triester, which is stable to the acid conditions required for the DMT deprotection. The cycle continues and the various nucleosides are added according to the pre-programmed sequence. The synthesis finishes with deprotection from the solid support and removal of the cyanoethyl protecting group. This method has proven very robust and tolerates a range of modified and even fully artificial monomers; the crucial requirement is that they bear two hydroxyl groups which can be protected in the appropriate manner, with a DMT and phosphoramidite group respectively.

2.1.3 Metal Base-Pairs

With possible application in nano-scale electronic devices, 'metal base-pairs' were originally conceived as potential molecular wires. In these systems the bases act simply as ligands and pair via selective metal complexation.[19,20] In 1962 Katz reported the stabilization of a T/T mismatch by Hg^{2+} demonstrating the first T-Hg^{2+}-T metal-base pair.[21] A similar discovery was made in 2007 by Ono, who employed Ag^{+} ions to stabilize a C/C mismatch to produce the C-Ag^{+}-C metal-base pair (**Fig. 2.5**).[22] In both examples the duplex retains its normal curvature, the linear metal complex being complementary to the planar geometry of conventional Watson-Crick pairing.[19]

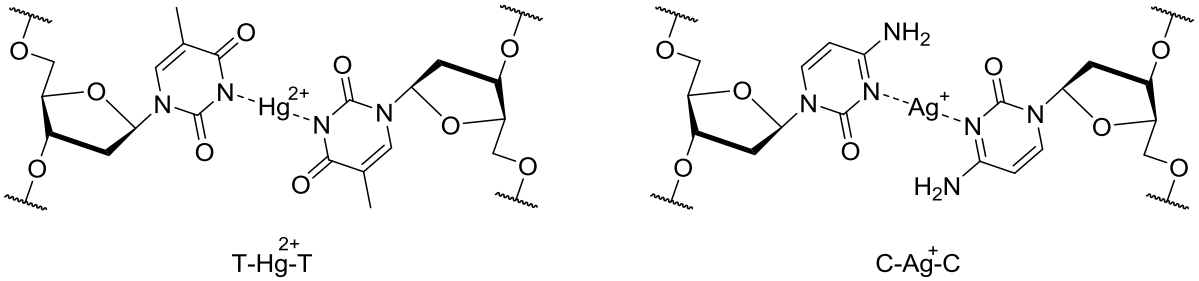


Fig. 2.5 Metal base-pairs consisting of T-Hg^{2+}-T developed by Katz and C-Ag^{+}-C by Ono

Using just the naturally occurring bases these interactions are however very limited, the number of metal-base pairs is very few and interference from normal Watson-Crick type pairing is prevalent.[19] A completely orthogonal system was therefore sought in which the bases are replaced by specifically designed ligands. The metal complexation properties of these artificial bases can thereby be optimised, both in terms of selectivity and strength; the number of metal-base pairs vastly expanded and the interference of Watson-Crick pairing negated. With this in mind, Shionoya developed various chelator-type bases, thus improving and extending the range of these metal-base pairs. Opposing phenylenediamine bases were shown to complex Pd^{2+} in a square planar geometry while pyridine bases were used to complex Ag^{+} in a linear fashion (**Fig. 2.6**).[23,24]

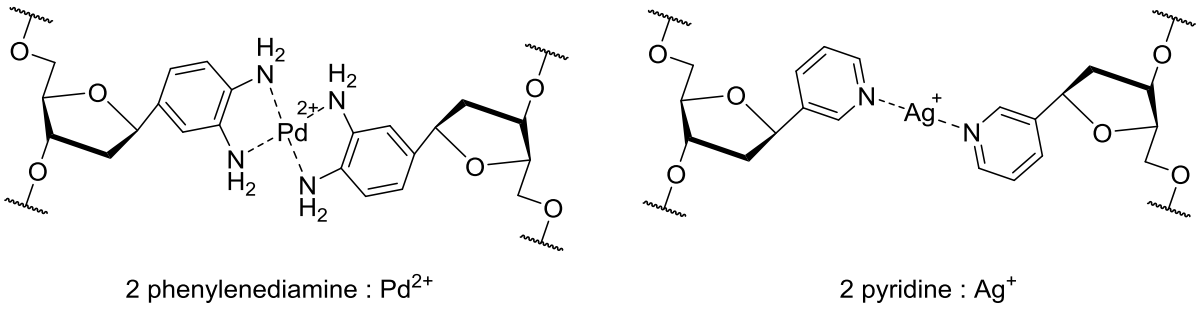


Fig. 2.6 Metal base-pairs consisting of two phenylenediamine ligands with Pd^{2+} and two pyridine ligands with Ag^{+} developed by Shionoya

The use of hydroxypyridone ligands in conjunction with Cu^{2+} is also particularly noteworthy. Incorporated into an oligonucleotide, the motif was repeated at five adjacent positions to chelate a stack of metal ions at the centre of the double helix (**Fig. 2.7**).[25] Subsequently, using a mixture of both hydroxypyridone and pyridine bases, a system of mixed metal stacking was developed which allowed the selective incorporation of both Cu^{2+} and Hg^{+} ions into the DNA duplex (**Fig. 2.8**).[26]

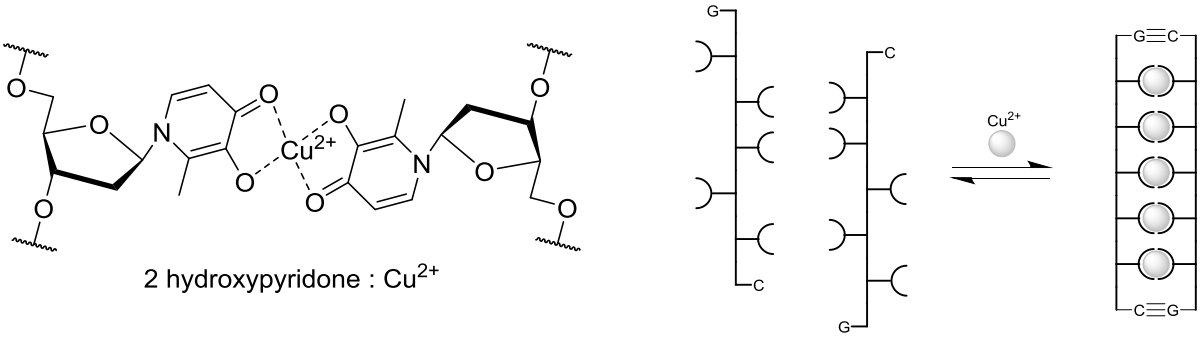


Fig. 2.7 Metal-base pairing and metal stacking, using hydroxypyridone ligands and Cu^{2+} by Shionoya[25]

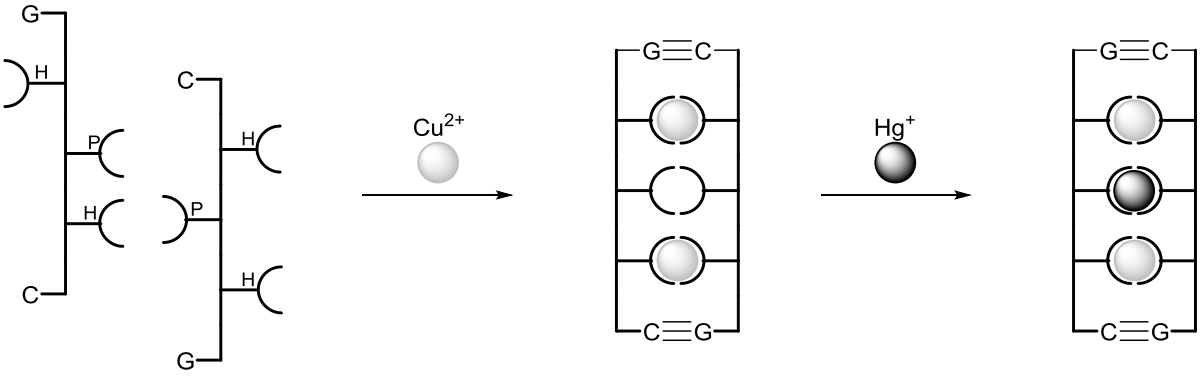


Fig. 2.8 Mixed metal stacking of Cu^{2+} and Hg^{+} at the centre of a modified DNA helix using hydroxypyridone and pyridine ligands by Shinoya[26]

2.1.4 Peptide Nucleic Acid (PNA)

Peptide nucleic acid (PNA) was developed by Nielsen in the 1990s and has become a well-known and widely utilised DNA analogue.[27] In this system, the entire phosphate-sugar backbone is replaced by repeating *N*-(2-aminoethyl)glycine monomers, onto which the various bases are appended via methylene carbonyl linkers.[28] As a DNA mimic, the spatial configuration and conformational flexibility of PNA enables specific hybridisation with natural DNA, complementary base-pairs exhibit conventional hydrogen bonding and a PNA/DNA duplex results (**Fig. 2.9**).[29] Lacking phosphate groups, PNA is uncharged however. With no electrostatic repulsion between the two strands, the stability of the duplex

is increased by approximately 1 °C per base pair compared to DNA. For example, the typical PNA 15-mer H-TGTACGTCACAACTA-NH_2, hybridized in an antiparallel orientation with fully complementary DNA 3′-d(ACATGCAGTGTTGAT) has a thermal melting temperature (T_m) of 69.5 °C; an increase of 16.2 °C compared to the corresponding DNA/DNA system which gives a T_m of 53.3 °C.[30] This neutral character also negates the effect of salt concentration upon binding affinity allowing PNA to successfully bind to its targets at concentrations which would inhibit hybridization of a purely DNA based system.[31] Interestingly, PNA also exhibits enhanced selectivity; mismatched base-pairs typically result in a more profound destabilisation of the PNA/DNA duplex compared to the DNA/DNA equivalent.[30]

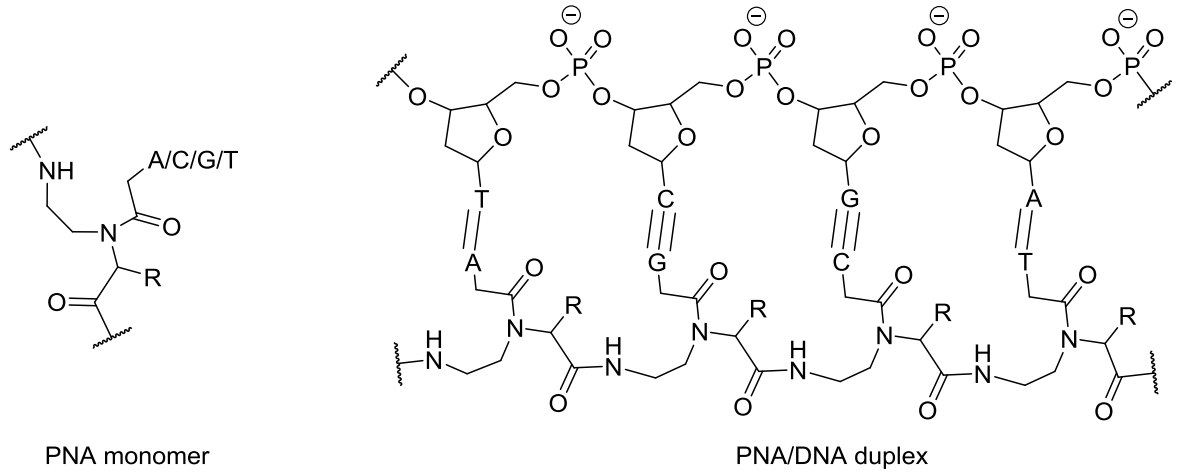


Fig. 2.9 A general PNA monomer and a PNA/DNA hybrid duplex developed by Nielsen

These properties render PNA a very attractive material with potential applications in the biomedical field. Although challenges relating to delivery of these agents are still being overcome, in vitro experiments have demonstrated PNA as a useful antisense agent, binding selectively to both DNA and RNA targets to modulate gene expression.[32] Interestingly, the N-(2-aminoethyl)glycine backbone of PNA has recently been found within cyanobacteria,

leading some to moot PNA as a prototype genetic material, a possible precursor to the popular 'RNA world'. [33,34]

2.1.5 Fluorescent Oligonucleotides

There are many examples in which nucleic acids have been modified through the inclusion of fluorophores. These units are often employed as 'reporter groups', the changes in output of which can be linked to changes in their microenvironment. Ono, for instance modified DNA with both metal binding base-pairs, a fluorophore (fluorescein) and a quencher (dabcyl) group to produce a fluorescent mercury sensor (**Fig. 2.10**).[35]

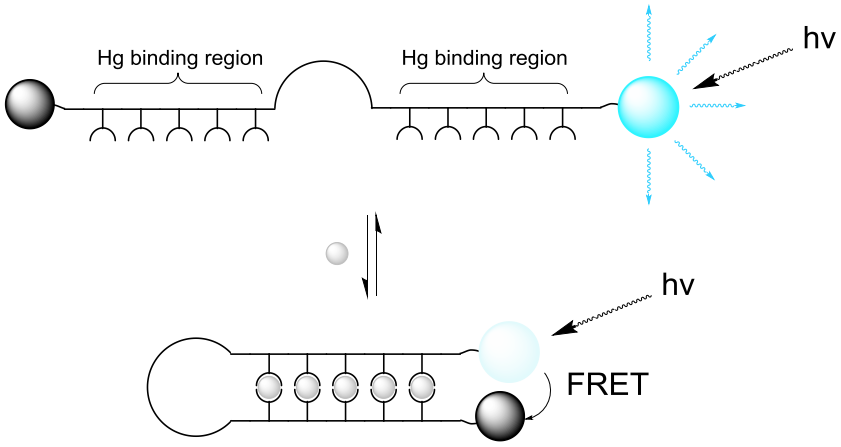


Fig. 2.10 Fluorescent mercury sensor by Ono[35]

In the absence of mercury, located at opposite ends of the oligonucleotide, the quencher unit is held remote from the fluorophore; no FRET (Förster Resonance Energy Transfer) occurs between the two and hence fluorescence is observed. Upon the addition of mercury however, the modified base-pairs complex the metal and the strand forms a hair-pin bringing the fluorophore and the quencher group into close proximity, FRET occurs between the two and hence fluorescence is turned off.

Due to the growing importance of medical diagnostic applications, photo-active oligonucleotides have also been developed as DNA sensors. In 2011 the Tucker group published an anthracene modified oligonucleotide which, through the fluorescent output, could not only be used to distinguish between a fully-matched and singly mis-matched strand, but could also give the identity of the nucleobase in question (**Fig 2.11**).[36]

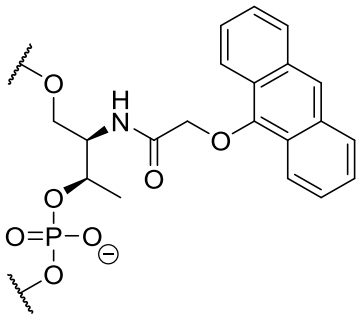


Fig. 2.11 Anthracene bearing L-threoninol monomer developed by Tucker[36]

Table 2.1 Oligonucleotide sequences consisting of the probe – 5′-CLC in which L represents the L-threoninol monomer, and the targets 3′-B–G in which B represents the four canonical nucleobases (G, A, C and T) and '–' represents the 'missing' nucleobase[36]

Oligonucleotide	Sequence
Probe 5′-CLC	5′-TGG-ACT-CLC-TCA-ATG-3′
Target 3′-B–G (B = G, A, C, T)	3′-ACC-TGA-B–G-AGT-TAC-5′

Anthracene was appended onto L-threoninol which was to take the place of the sugar unit, the diastereomerically pure diol was then DMT and phosphoramidite protected and incorporated into an oligonucleotide (5′-CLC) by automated synthesis (**Table 2.1**). Target strands were produced in which the nucleobase directly opposite the anthracene unit was omitted, allowing full intercalation of the fluorophore into the helix 3′-B–G. Four variations were synthesised in

which the adjacent position was occupied by each of the natural nucleobases (B = G, A, C, T).

The probe strand was then titrated against each of the four target oligonucleotides (**Fig. 2.12**) and the fluorescence intensity monitored. With the complementary (G) nucleobase in the adjacent position, an increase in the fluorescent emission intensity was observed. Conversely, the three non-complementary bases (A, T and C) produced a decrease in the fluorescent emission intensity compared to the single stranded probe alone. Interestingly, upon full hybridisation of the probe strand, the four nucleobases produced different percentage changes in the fluorescent emission intensity, thus allowing the presence of each nucleobase to be discriminated.

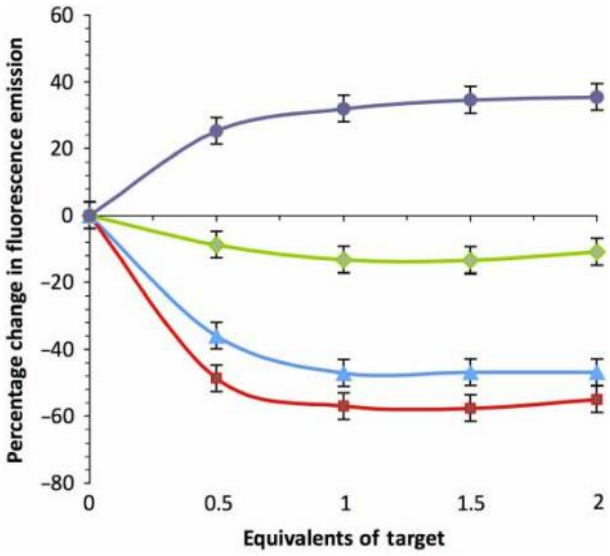
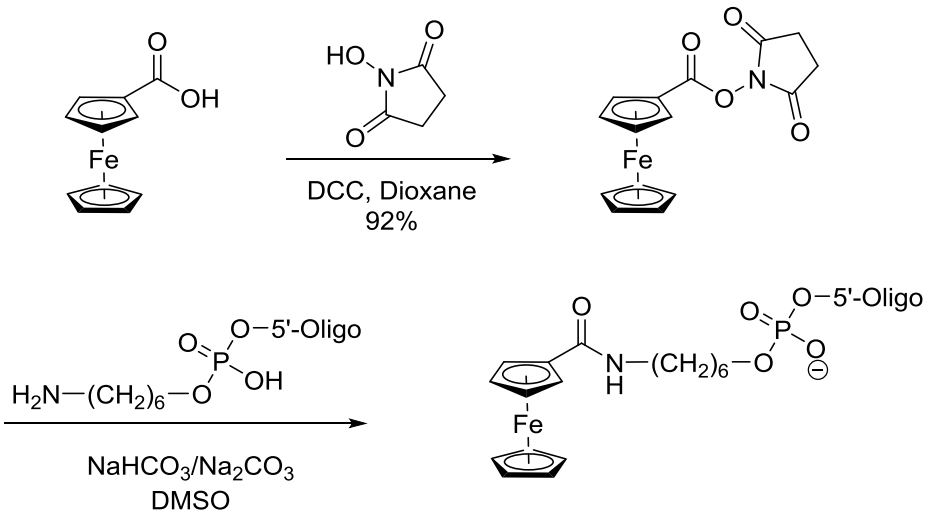


Fig. 2.12 Fluorescence titration plots at 440 nm for probe 5′-CLC with 0.5, 1.0, 1.5 and 2.0 equivalents of fully matching targets 3′-G–G (blue triangles) and mismatched targets 3′-C–G (red squares) 3′-T–G (green diamonds) and 3′-A–G (purple circles), 10 mM (pH 7.0) phosphate buffer, 100 mM NaCl, ca. 298 K.[36]

2.1.6 Redox-Active Oligonucleotides

Through the incorporation of ferrocene, the supramolecular and recognition features of the oligonucleotide are augmented with the electrochemical characteristics of the metallocene. The resulting redox-active oligonucleotides have formed the basis of a number of molecular devices in which hybridisation and denaturation events can be detected electrochemically. One popular method of incorporation is the post-synthetic 'tagging' of oligonucleotides with ferrocene. Ihara, for instance, used the succinimide ester of ferrocene carboxylic acid to tag the 5′-amino terminus of an amino-hexyl-linked oligonucleotide (**Scheme 2.2**).[37]



Scheme 2.2 Synthesis of ferrocene tagged amino-hexyl-linked oligonucleotides by Ihara[37]

Using this strategy, Plaxco developed a surface bound system in which the metallocene acts as an electrochemical molecular beacon (**Fig. 2.13**).[38] The single-stranded oligonucleotide is attached to a gold surface using thiol chemistry and, through partial self-complimentarity forms a 'hair-pin' which brings the ferrocene reporter group into close proximity with the electrode. In this state electron transfer is very efficient and a large current is observed. In the presence of the target however, a conformational shift occurs, the 'stem-loop' is unwound as the probe binds preferentially to the fully complementary strand. The resulting duplex

removes the reporter group from the surface and holds it at a more remote position; the electron transfer efficiency is thus reduced, resulting in a loss of redox current. This "signal off" system is remarkably sensitive with detection levels in the picomolar range.[38]

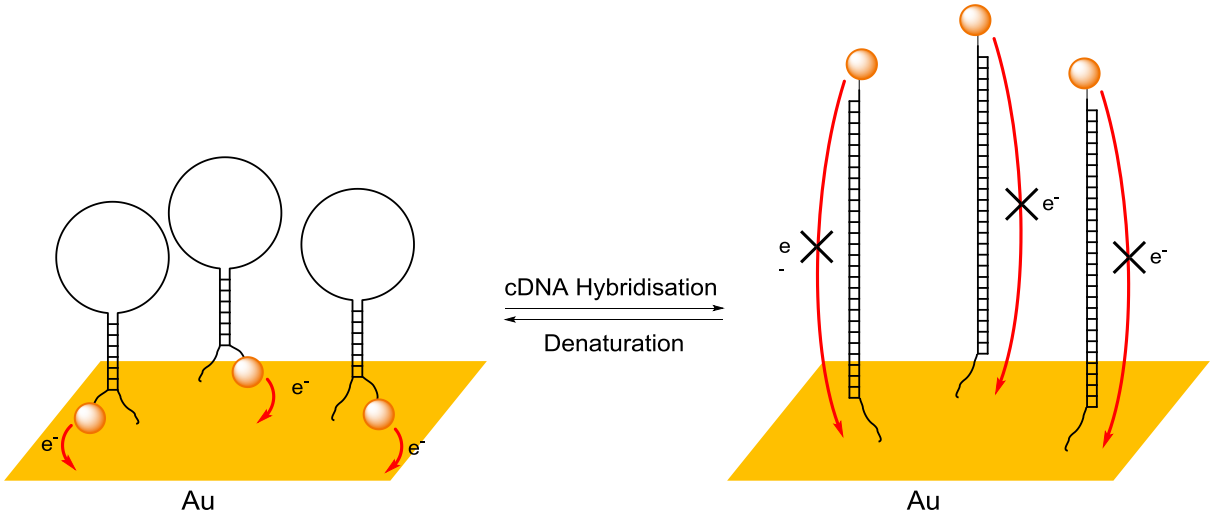


Fig. 2.13 Ferrocene tagged surface-bound molecular beacons by Plaxco[38]

Nakayama employed the same, post-synthetic ferrocene tagging to produce a more selective "signal on" sandwich-type assay (**Fig. 2.14**).[39] In this example, the target is partly complementary to a surface bound sequence and partly complementary to a ferrocene tagged, solution based sequence. Complete hybridization thus results in a ternary complex consisting of the three separate strands, the redox reporter is delivered much closer to the surface and a significant increase in current is observed.

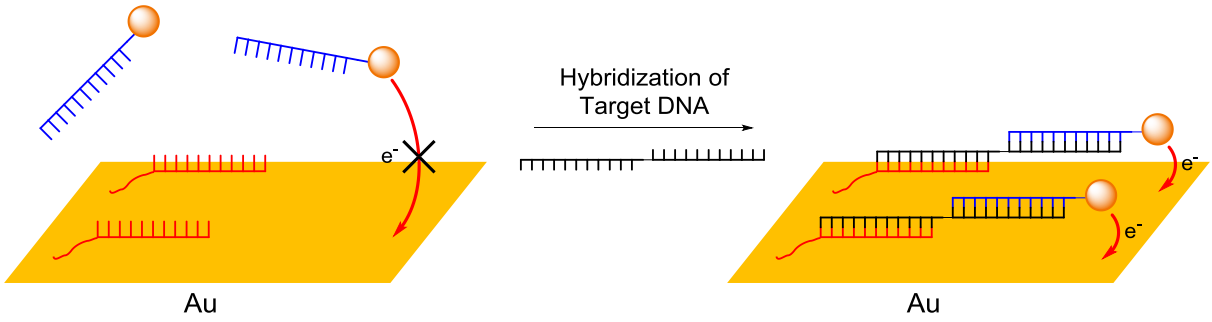


Fig. 2.14 Ferrocene tagged 'signal on' sandwich assay by Nakayama[39]

2.1.7 Ferrocene Nucleic Acid (FcNA)

Recognising that the distance between adjacent base pairs in DNA (3.4 Å) was remarkably similar to the distance between the two cyclopentadienyl rings of ferrocene (3.3 Å) (**Fig. 2.15**), the Tucker group envisaged a tetrasubstituted ferrocene monomer, which, bearing both a nucleobase and a hydroxyl linker on each Cp ring, could be oligomerised using automated synthesis to produce the first functional organometallic DNA analogue.[40]

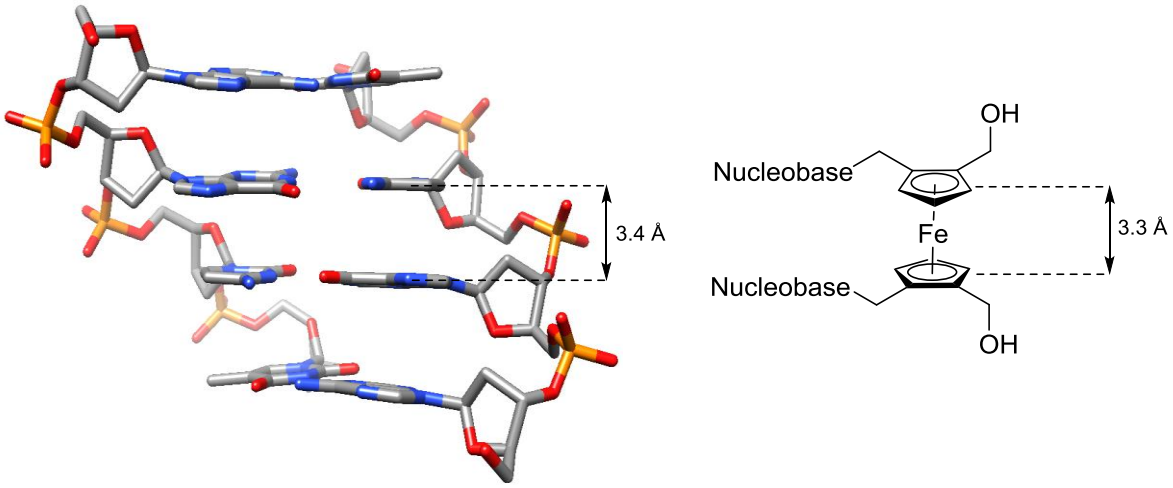
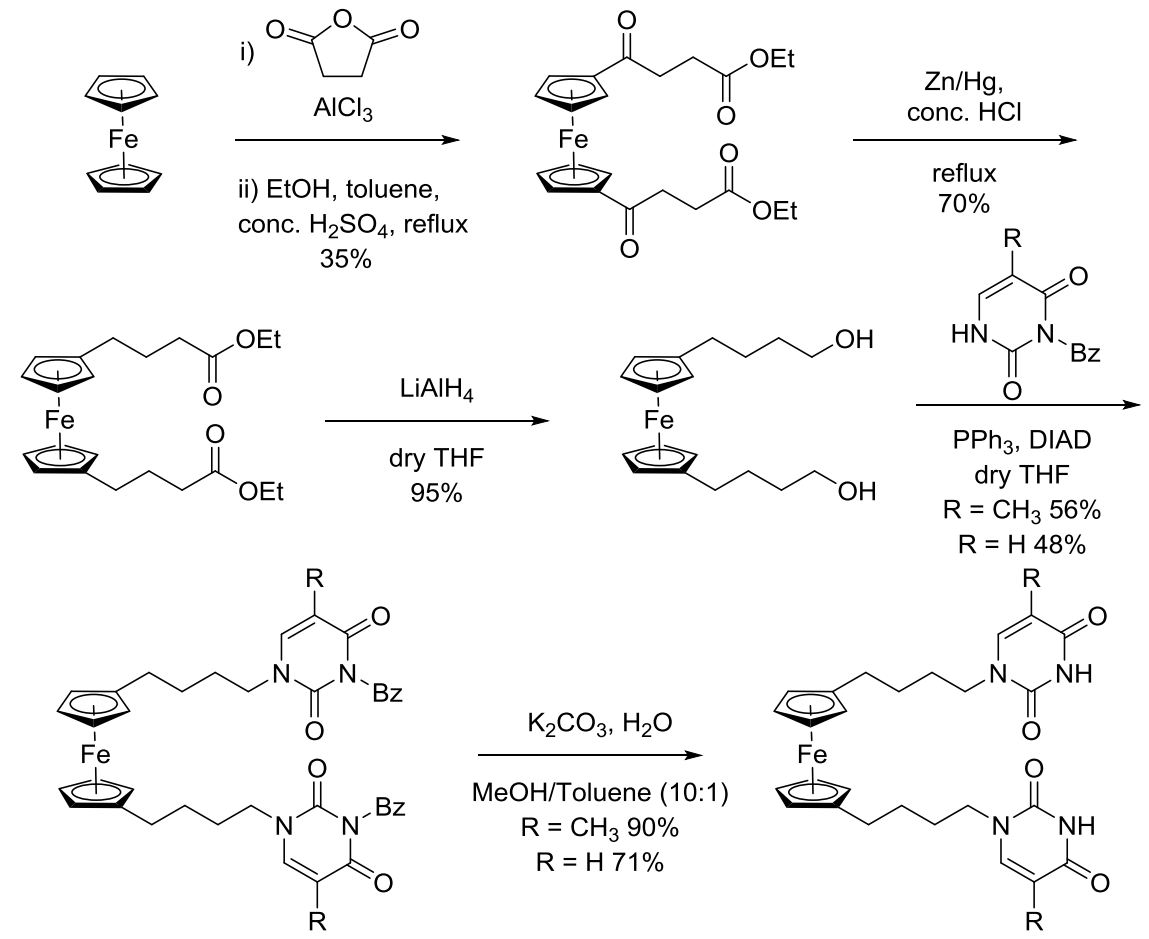


Fig. 2.15 Size comparison of the interbase distance of DNA, and the distance between the Cp rings of a generic ferrocene nucleic acid monomer[40]

Through the use of appropriate protecting groups, Ganesh had demonstrated the coupling of thymine and uracil nucleobases to a ferrocene diol under Mitsunobu reaction conditions (**Scheme 2.3**).[41] Interestingly, these bis-substituted ferrocenes, with one nucleobase attached to each Cp ring, were shown to self-assemble into a supramolecular array via typical Watson-Crick and reverse Watson-Crick H-bonding (**Fig. 2.16**).



Scheme 2.3 Synthesis of dithyminyl and diuricyl ferrocene conjugates by Ganesh[41]

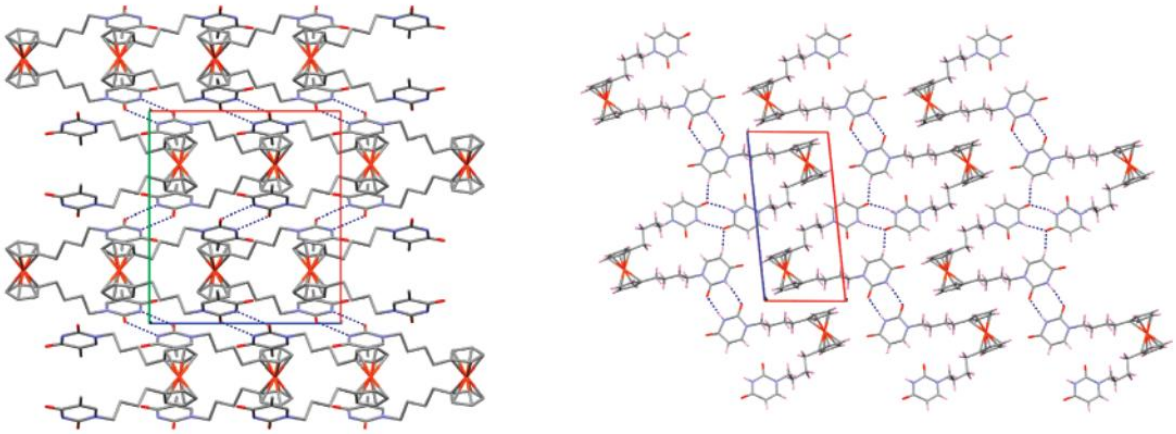
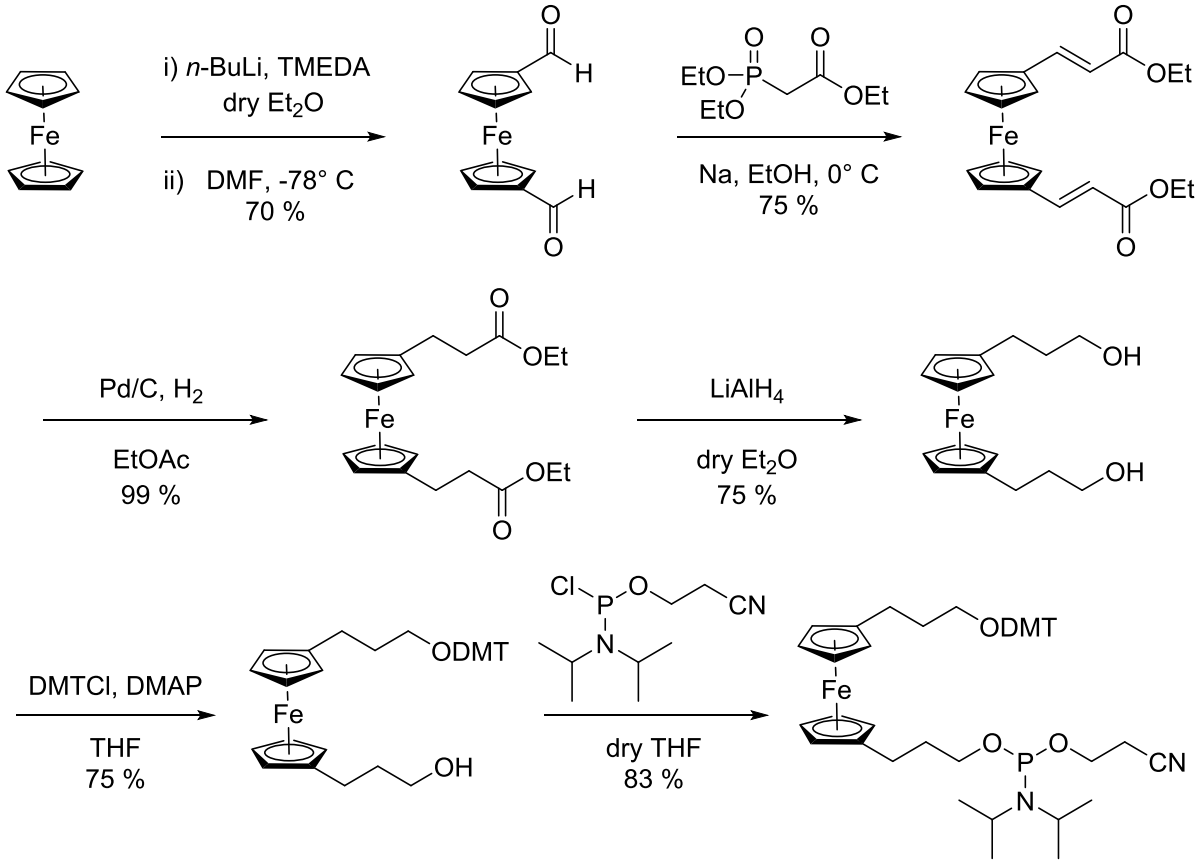


Fig. 2.16 Supramolecular arrays of thyminyl and uracyl ferrocene conjugates by Ganesh[41]

In 2004 Brisset had shown that a similar ferrocene diol could be protected with a DMT and phosphoramidite group and incorporated into an oligonucleotide using the automated

synthesis system of Beaucage and Caruthers (**Scheme 2.4**).[17,42] The coupling yield for the ferrocene monomer was 95% which compares favourably with the value of 98% for typical unmodified oligonucleotides.



Scheme 2.4 Synthesis of a ferrocene phosphoramidite monomer for solid-phase automated oligonucleotide synthesis by Brisset[42]

Bearing an identical, achiral substituent on each Cp ring, the ferrocene derivatives of Ganesh and Brisset pose little synthetic challenge. When the structures are combined however, the architectural complexity of the molecule increases dramatically; issues of both stereo- and regio- control become apparent, not least because of the planar chiral relationship between the ferrocene substituents. However, by carefully exploiting the well-established ferrocene chemistry described in **Chapter 1**, these problems were overcome. Thus, in 2012 the Tucker group reported the first tetrasubstituted dithyminyl FcNA monomer which was successfully

prepared as a DMT-protected phosphoramidite and oligomerised into a 16-mer chain of eight repeating units (**Fig. 2.17**).[40]

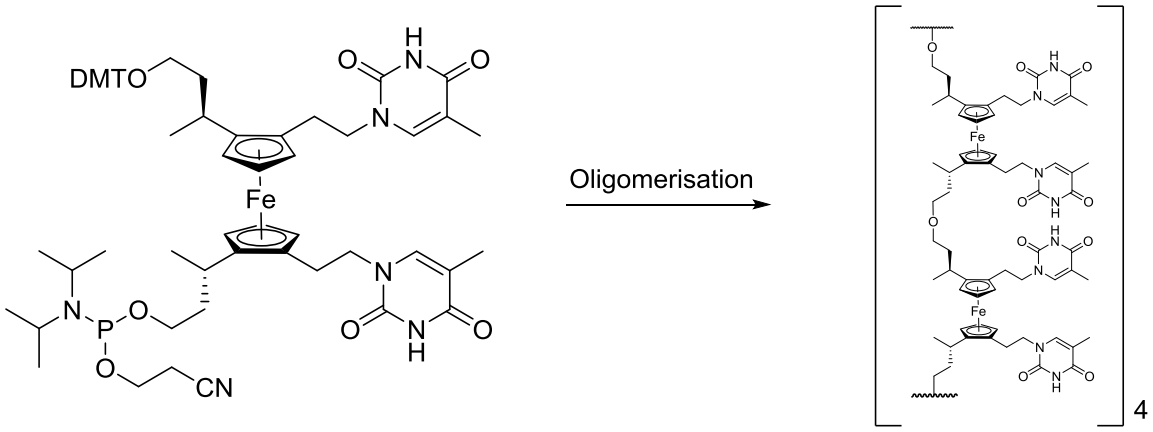


Fig. 2.17 The first tetrasubstituted dithyminyl FcNA monomer by Tucker which was oligomerised using automated solid-phase synthesis to give a 16-mer

2.2 Objectives

Four structural features of FcNA were identified as crucial to the functioning of the monomer: the backbone linker length, the nucleobase linker length, the planar chirality and the identity of the nucleobase. The central chirality was only present in the monomer as an artefact of synthetic strategy, not of design, and could possibly be dispensed with. The next step in the development of FcNA was therefore the optimisation of these structural parameters to ensure the best possible match to DNA and a naming system of the form Fcnc$BB_{(XXpYpY)}$ was developed to describe them (**Fig. 2.18**).

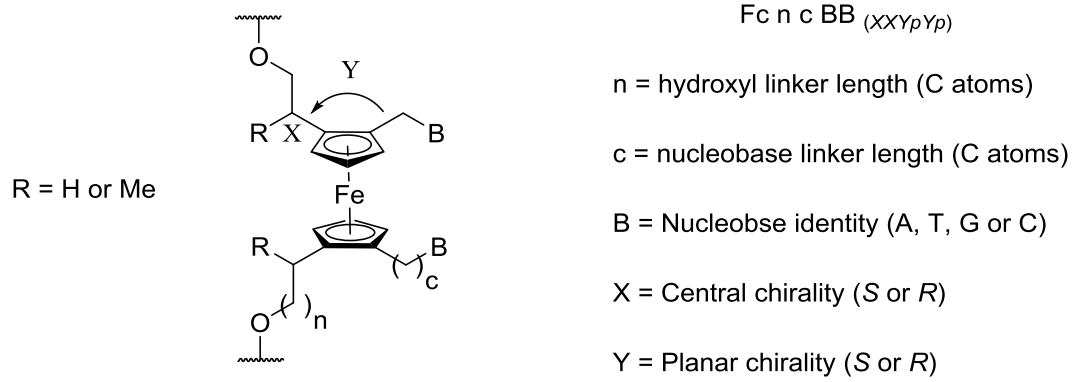


Fig. 2.18 Structural parameters and nomenclature of tetrasubstituted FcNA monomers

The aim of this project therefore was the synthesis of a number of FcNA monomers in which these structural variations are explored. Comparison with other variations made within the group would then provide insight into the binding characteristics of these molecules.

Firstly, planar chirality was to be explored through the comparison of FcNA enantiomers. Given that DNA is itself a chiral molecule, it was expected that one enantiomer would be more conformationally suited to the constraints of the β-helix and would thus stabilise the duplex more than the other. Therefore the **Fcn3c3TT**$_{(RR,SpSp)}$ monomer was synthesised to complement the **Fcn3c3TT**$_{(SS,RpRp)}$ monomer produced by another member of the group and their binding characteristics compared.

Secondly, the effect of nucleobase linker length was explored. Although the distance between Cp rings of ferrocene is a very close match to the inter-base distance of DNA, due to the geometrical differences in bonding, some conformational flexibility is required for the FcNA monomer to fit best within the duplex. The enantiomers with nucleobase linker length of three atoms **Fcn3c3TT**$_{(RR,SpSp)/(SS,RpRp)}$ were therefore compared to the corresponding enantiomers with nucleobase linker length of two carbon atoms **Fcn3c2TT**$_{(RR,SpSp)/(SS,RpRp)}$ to establish which system provides the best stabilisation to the duplex.

Thirdly, a strategy for the incorporation of the guanine nucleobase was to be developed and the binding characteristics of the **Fcn3c2GG**$_{(SSpRpR)}$ monomer assessed. Previous work in the group had explored the incorporation of thymine and adenine nucleobases, which form two hydrogen bonds upon complementary base-pairing. Guanine and cytosine base-pair via the stronger interaction of three hydrogen bonds and therefore provide a greater stabilisation to the duplex. As well as completing the set of canonical bases, incorporation of these two nucleobases into FcNA monomers would also provide valuable information as to the nature of the supramolecular interactions involved in duplex formation and how well the monomer compares to native DNA. With another member of the group already investigating cytosine, this project focussed upon the incorporation of guanine nucleobases.

2.3 Results and Discussion

2.3.1 Synthesis of Tetrasubstituted FcNA Monomers

2.3.1.1 Synthesis of Tetrasubstituted Dithyminyl Ferrocene Diol 2.1-(*RR*,S_pS_p)

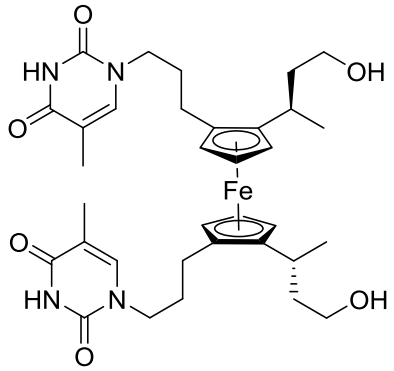
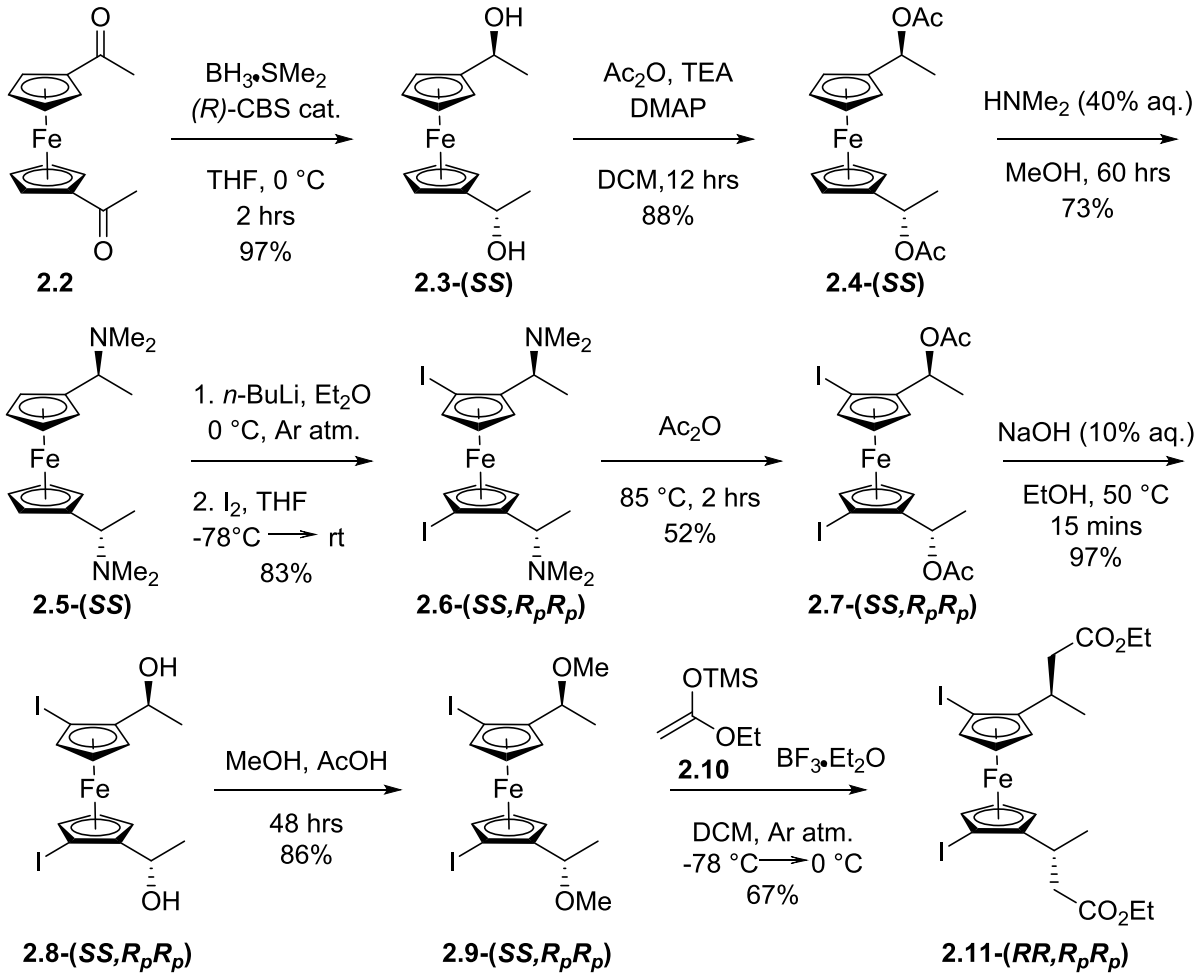


Fig. 2.19 Tetrasubstituted dithyminyl FcNA diol target **2.1-(*RR*,S_pS_p)**

With a synthetic route to the **Fcn3c3TT**$_{(SS,RpRp)}$ monomer already established in the group, the tetrasubstituted dithyminyl ferrocene diol precursor **2.1-(*RR*,S_pS_p)** for the opposite enantiomer **Fcn3c3TT**$_{(RR,SpSp)}$, was produced according to the same method using the opposite enantiomer of the CBS catalyst to establish the central chirality.

Having purified the diacetylferrocene starting material **2.2**, which was obtained from the undergraduate teaching laboratories, the first eight steps proceeded as planned according to the procedure previously published by the Tucker group (**Scheme 2.5**). The central chirality was established using (*R*)-CBS catalyst, reducing the diketone **2.2** to the corresponding chiral diol **2.3-(*SS*)**. The hydroxyl groups were then converted to acetoxy groups **2.4-(*SS*)** using acetic anhydride and successfully substituted with retention of stereochemistry by dimethylamine to give the 'Ugi-diamine' **2.5-(*SS*)**. Ortho-lithiation was then achieved using *n*-BuLi in dry ether, before the carbanion was reacted on with iodine to produce **2.6-(*SS*,R_pR_p)** according to the method of Knochel.[43] A series of three highly stereoselective substitutions were then performed, going via the diacetoxy **2.7-(*SS*,R_pR_p)** and alcohol

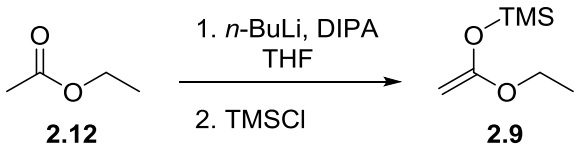
2.8-(*SS,R*$_p$*R*$_p$) functionalities to prepare the methoxy leaving groups of **2.9-(*SS,R*$_p$*R*$_p$)**. It is worth noting that the last of these three steps is very time consuming and inefficient, the reaction typically takes 48 hours and does not go to completion, the starting material therefore has to be recovered and re-reacted to get full conversion to the product. The carbon skeleton was then extended through a reaction with silyl enol ether **2.10** in the presence of the Lewis acid catalyst BF_3 to give the diester **2.11-(*RR,R*$_p$*R*$_p$)**.



Scheme 2.5 The first eight steps of the synthesis of tetrasubstituted dithyminyl ferrocene diol target **2.1-(*RR,S*$_p$*S*$_p$)**

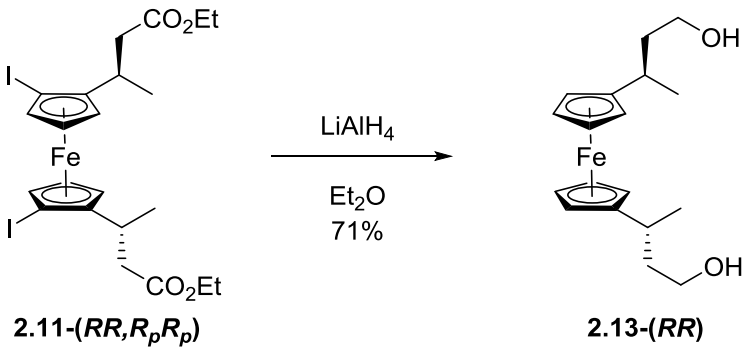
Silyl enol ether **2.10** was in turn freshly prepared from EtOAc **2.12** (**Scheme 2.6**). LDA was first generated in situ from *n*-BuLi and DIPA, before being employed to deprotonate the ester. TMSCl was then added to trap the resulting enolate in the desired silyl enol ether form.

Following the gentle removal of THF on a rotory evaporator, the volatile product was further purified by vacuum distillation. NMR analysis showed the purity to be approximately 70% with residual EtOAc still present.



Scheme 2.6 Synthesis of the silyl enol ether **2.9** from EtOAc **2.12**

The next step required reduction of the diester **2.11-(*RR*,R_pR_p)** to the corresponding diol for which DIBAL would typically be used. The first time this transformation was attempted, very poor turnover was achieved; it was concluded that the reducing agent was old and possibly degraded and therefore new stock was ordered. Keen to progress, and following a route previously utilised by the group, it was decided that $LiAlH_4$ was a perfectly reasonable substitute reagent and practical work continued. Using this reagent, the ester was indeed reduced, however a metal-halogen exchange reaction also removed the iodo groups leaving the disubstituted diol **2.13-(*RR*)**, thus bringing the synthesis to a premature end (**Scheme 2.7**).



Scheme 2.7 Reduction of diester **2.11-(*RR*,R_pR_p)** with inadvertant iodo group removal using $LiAlH_4$ to give disubstituted diol **2.13-(*RR*)**

Diol **2.13-(*RR*)** is, nevertheless a valuable material for investigation as it can be incorporated into DNA as a 'no-nucleobase' control (i.e. **Fcn3HH**$_{(RR)}$) against which tetrasubstituted,

nucleobase bearing systems can be compared. If the hypothesis that FcNA monomers do indeed offer some stabilisation to the duplex through base-pairing and π-stacking interactions, comparison with a system in which these processes are precluded could offer valuable insight into the nature and magnitude of these supramolecular interactions. Having obtained a clean ^{1}H NMR spectra, the (non-chiral) purity of **2.13-(*RR*)** was then confirmed by analytical high-performace chromatography (HPLC). Using a C18 column with isocratic eluent system of 5% H_2O in MeCN, at a flow rate of 1.00 ml min^{-1}, a single sharp peak was produced with retention time of 25.30 mins (**Fig. 2.20**).

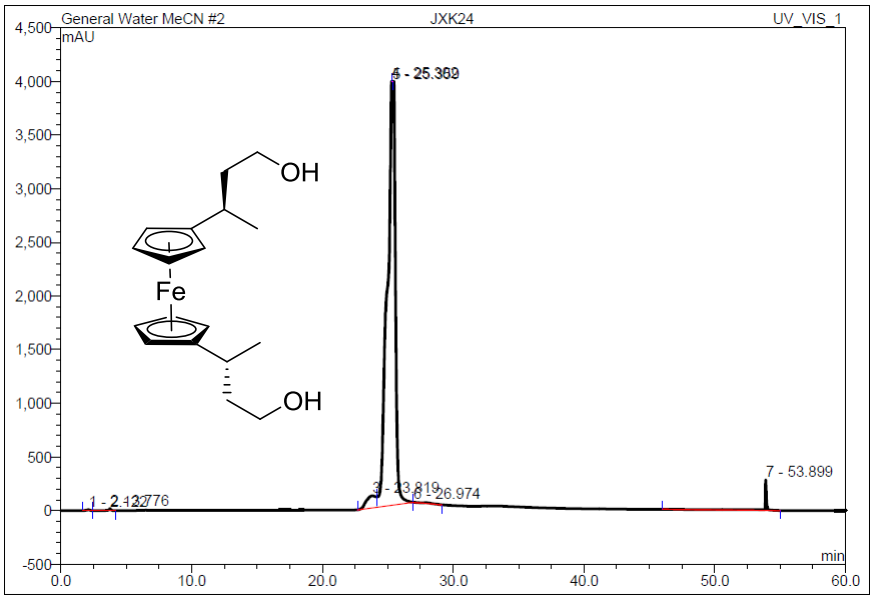


Fig. 2.20 Analytical HPLC trace of diol **2.13-(*RR*)**

The enantiomeric purity of **2.13-(*RR*)** was then assessed by chiral HPLC. Using an amylose (AD) column with isocratic eluent system of 5% IPA in hexane, at a flow rate of 1.00 ml min^{-1}, a single sharp peak was produced at 61.67 mins retention time (**Fig. 2.21**). This sample was then combined with the opposite enantiomer (kindly donated by another member of the group) and the mixture coeluted under identical conditions. Although the resolution was not complete, two distinct peaks were produced, one at 60.79, the other at 65.44 mins retention

time, clearly demonstrating the effective separation of the method and the high enantiomeric purity (100%) of the analyte (**Fig. 2.22**).

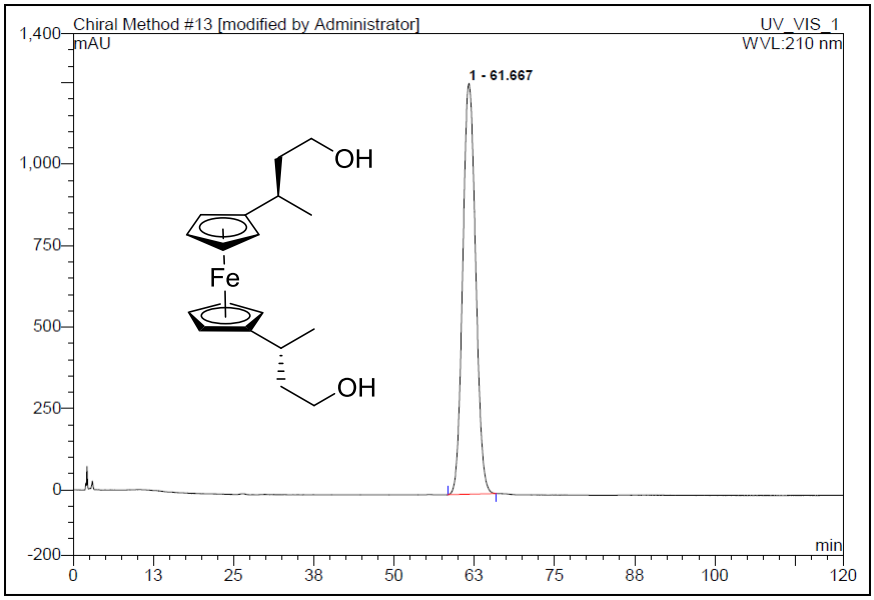


Fig. 2.21 Chiral HPLC trace of **2.13-(*RR*)**

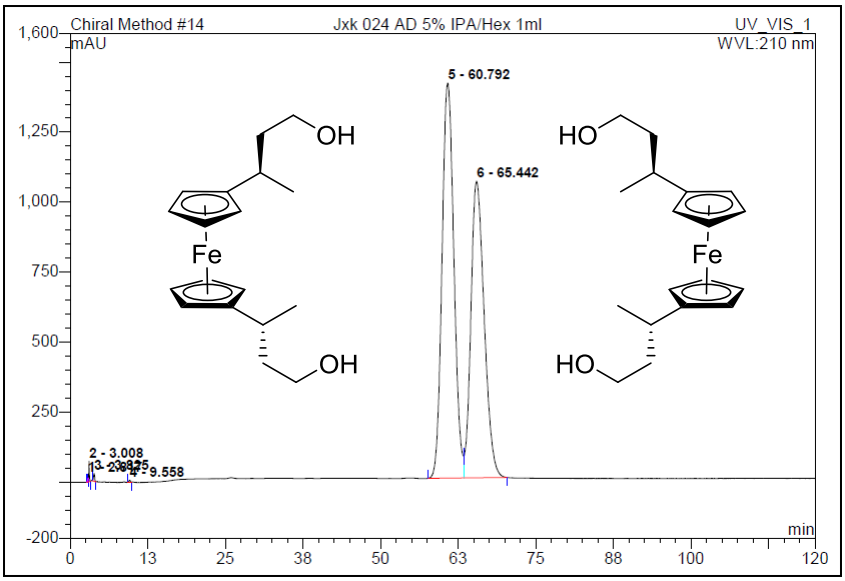
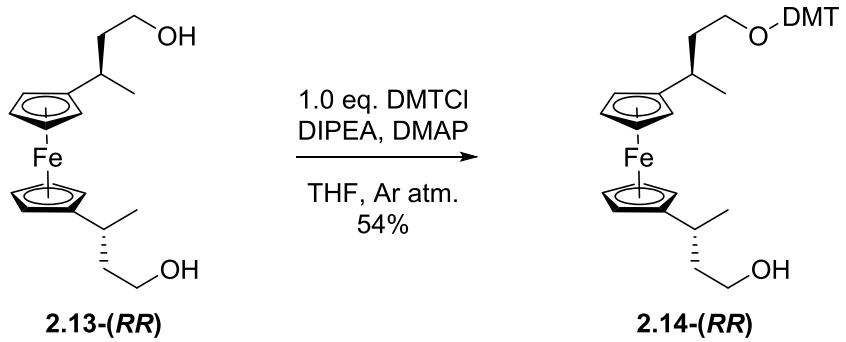


Fig. 2.22 Chiral HPLC trace of a mixture of **2.13-(*RR*)** and the opposite enantiomer **2.13-(*SS*)**

With the chiral purity confirmed, diol **2.13-(*RR*)** was mono-protected with a DMT group to give **2.14-(*RR*)** (**Scheme 2.8**) which was presented to another member of the group for phosphitylation, oligomerisation and binding studies.



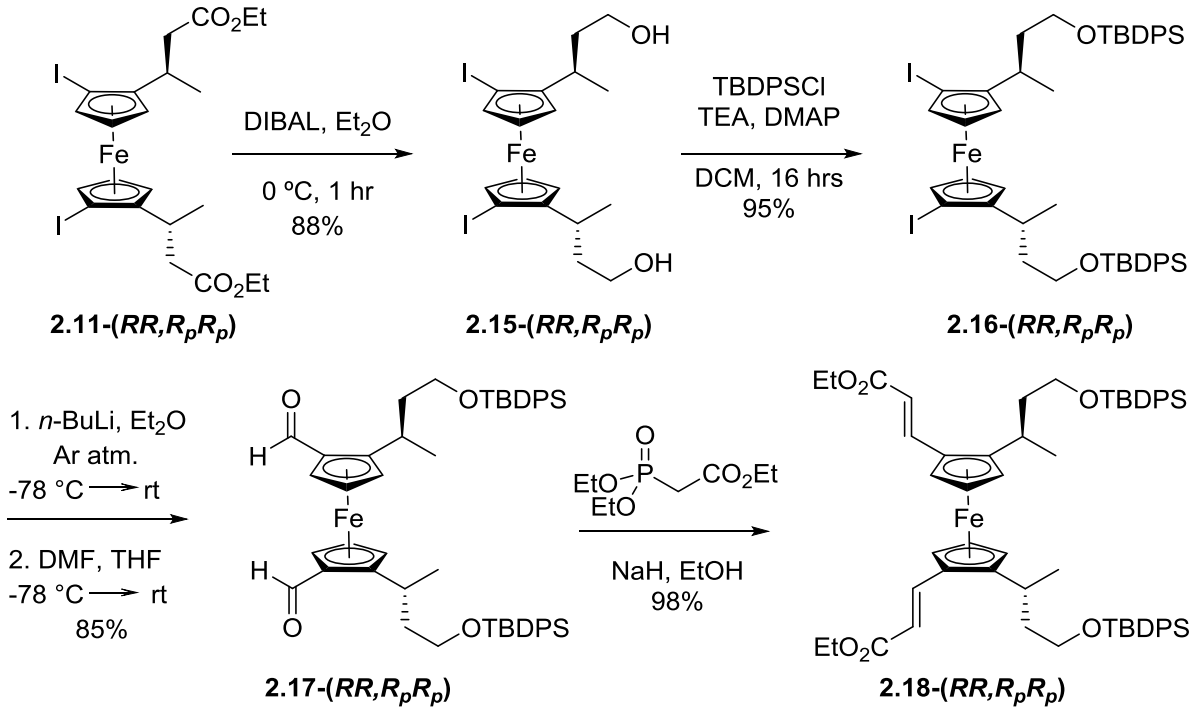
2.13-(*RR*) **2.14-(*RR*)**

Scheme 2.8 DMT mono-protection of the abasic diol **2.13-(*RR*)** to give **2.14-(*RR*)**

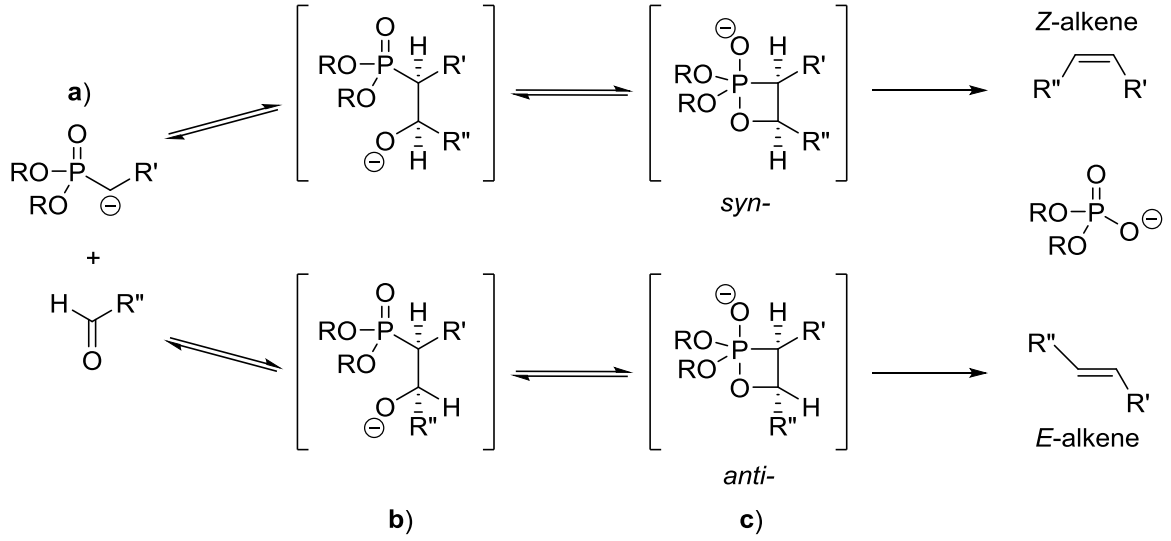
The full synthesis of tetrasubstituted dithyminyl ferrocene diol **2.1-(*RR*,S_pS_p)** was completed following a more cautious second attempt. Fresh DIBAL was used to reduce the diester **2.11-(*RR*,R_pR_p)** to the tetrasubstituted diol **2.15-(*RR*,R_pR_p)**, before the hydroxyls were protected with TBDPS groups to give **2.16-(*RR*,R_pR_p)** **(Scheme 2.9)**. *n*-BuLi was used to effect a halogen-lithium exchange, before reaction with DMF produced the dialdehyde **2.17-(*RR*,R_pR_p)**. The carbon chain was then extended using a Horner-Wadsworth-Emmons reaction (H.W.E.) with triethylphosphonoacetate to give **2.18-(*RR*,R_pR_p)**.

The H.W.E. reaction, a modification of the Wittig-olefination, employs a phosphonate stabilised carbanion to produce a predominance of the *E*-alkene. The generally accepted mechanism firstly sees the formation of an oxyanion, which then progresses through a four-membered intermediate under reversible conditions, before an irreversible step produces the alkene (**Scheme 2.10**). The *E*-selectivity is believed to derive from the relative steric hindrance of the two cyclic intermediates, in which the two bulky R-groups are positioned in a *syn*- or *anti*- relationship.[44] Separation between the R-groups is greater in the *anti*-

arrangement than the *syn*-, the reaction therefore favours progression through this lower energy intermediate to produce the corresponding *E*-alkene.

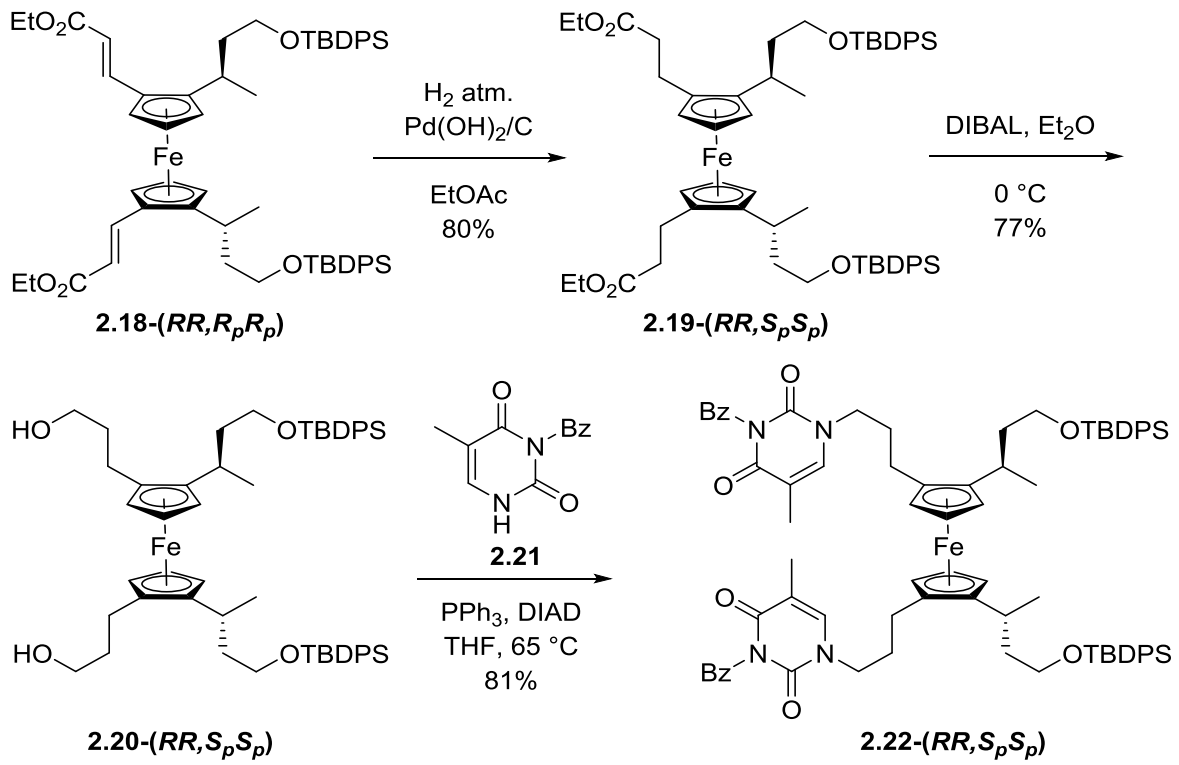


Scheme 2.9 Continued synthesis of tetrasubstituted dithyminyl ferrocene diol **2.01-(*RR*,S_pS_p)**



Scheme 2.10 Mechanism of the Horner-Wadsworth-Emmons reaction showing **a**) the phosphonate stabilised carbanion, **b**) the two oxyanion intermediates, and **c**) both the *syn*- and *anti*- four-membered intermediates[44]

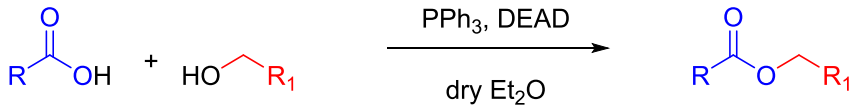
In accordance with theory, very little of the *Z*-alkene was produced. However a small, faint spot was observed by TLC with a very similar R_f value to the product. This impurity was easily removed by column chromatography but was not charactersised. It is important to note that the double bond is removed in the very next step, and therefore, in this specific context, the stereoselective outcome of the H.W.E reaction is of little consequence. The synthesis continued with the hydrogenation of **2.18-(*RR,SpSp*)** using hydrogen over Pearlman's catalyst in EtOAc, before DIBAL was again used to reduce the resulting diester **2.19-(*RR,R_pR_p*)** to the corresponding diol **2.20-(*RR,S_pS_p*)** in preparation for the Mitsunobu coupling of the nucleobase (**Scheme 2.11**).



Scheme 2.11 Continued synthesis of tetrasubstituted dithyminyl ferrocene diol **2.1-(*RR,S_pS_p*)**

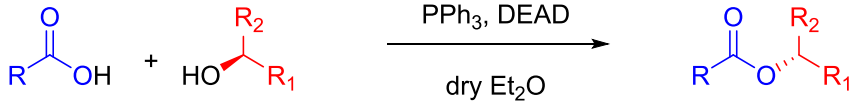
This eponymous reaction was discovered in 1967 by Oyo Mitsunobu who observed that in the presence of PPh_3 and diethyl azodicarboxylate (DEAD), the usual reactivity of

esterification is reversed; the alcohol is effectively converted to an electrophile and is attacked by the deprotonated carboxylic acid (**Scheme 2.12**).[45]



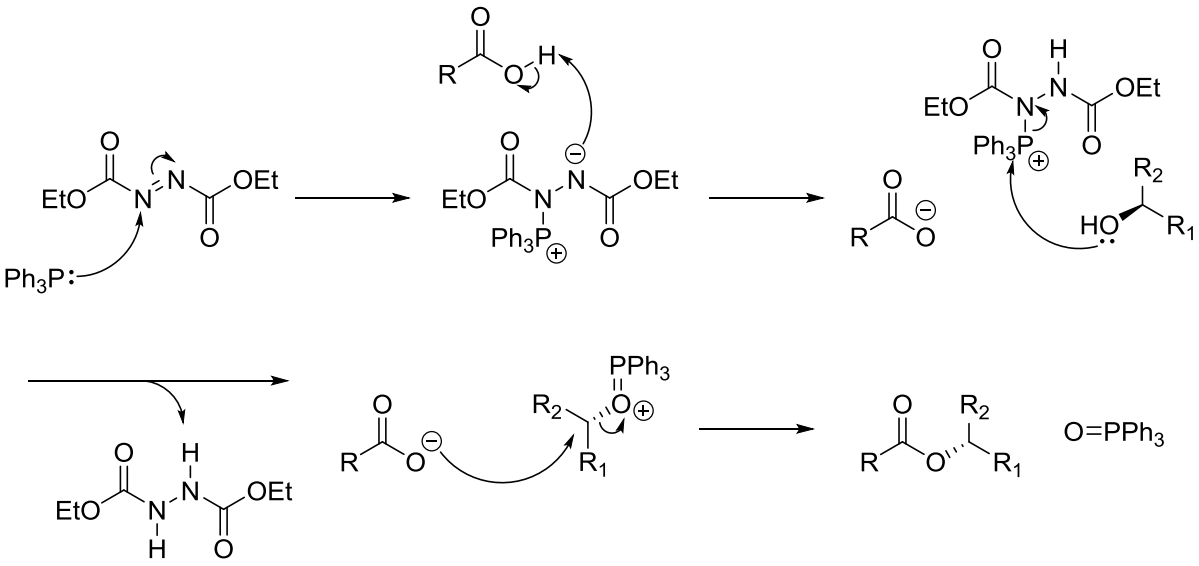
Scheme 2.12 Mitsunobu ester formation showing the reversal of normal reactivity

Using a primary alcohol the result is unspectacular; the product ultimately remains unaffected by the reversal of reactivity. Secondary alcohols however undergo the same process, and in this case the transformation is accompanied by a potentially useful inversion of stereochemistry (**Fig. 2.13**). The greatest contribution of this reaction however lies in its scope; through the dual activation of both reagents, a variety of otherwise unlikely pronucleophiles including phenols, imides and secondary amines can be successfully employed to give a range of functionality.[46]



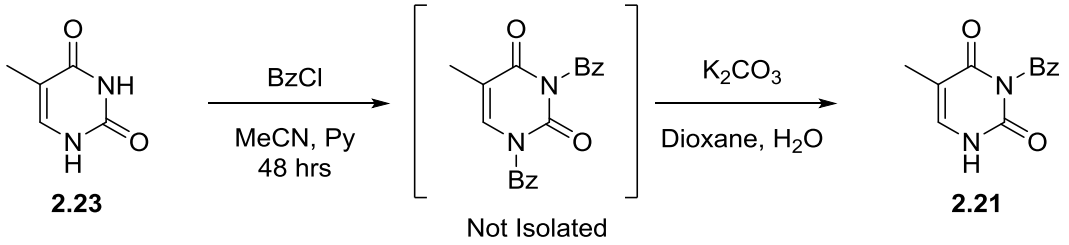
Scheme 2.13 Mitsunobu ester formation demonstrating the inversion of stereochemistry of a secondary alcohol

Although after years of study, the exact mechanism has been refined and modified to account for the many subtleties of outcome that can result from this complex reactivity, the relatively simple scheme originally proposed by Mitsunobu in 1967 still provides a good overview of the most important aspects (**Scheme 2.14**).[45,47]



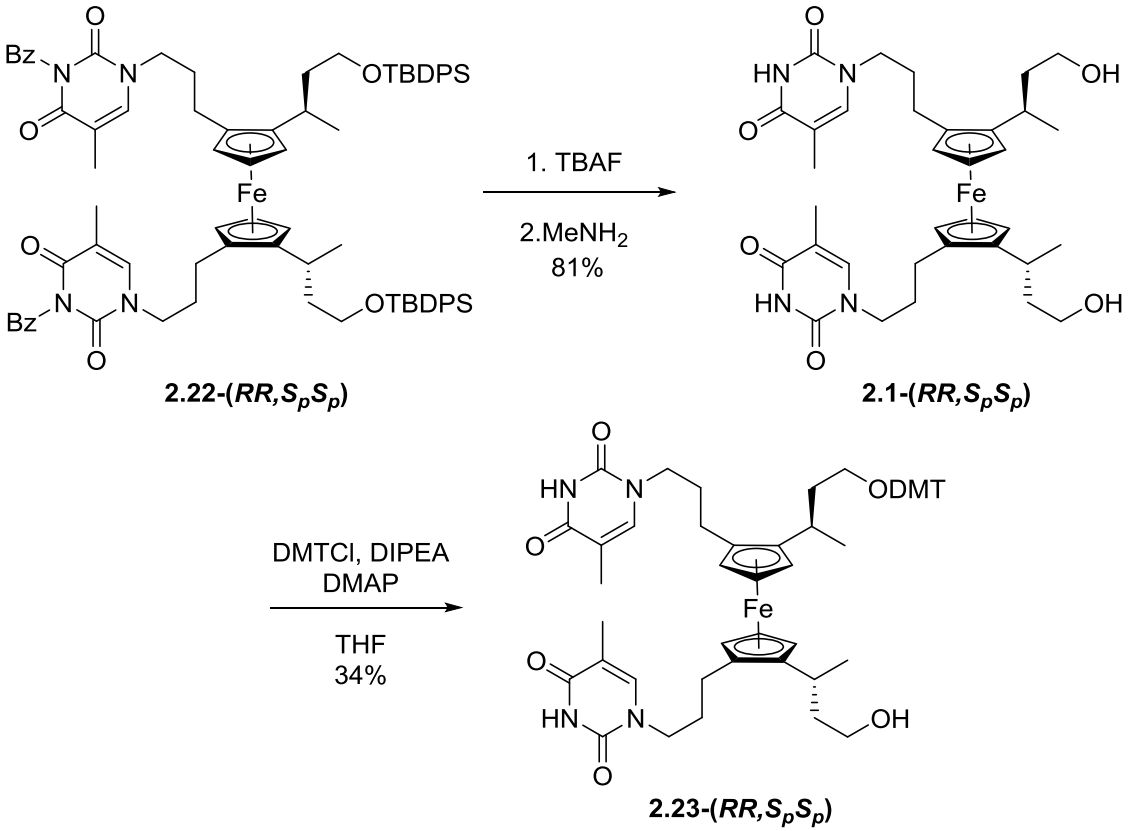
Scheme 2.14 The basic Mitsunobu reaction mechanism proposed in 1967.[45]

The first step involves the formation of a betaine intermediate between the phosphine and the DEAD which in turn primes the pronucleophilic carboxylic acid by deprotonation. As the better nucleophile, the alcohol then attacks the cationic phosphorous, preparing an oxophosphonium leaving group through formation of a strong P–O bond. The nucleophilic carboxylate ion now attacks the electrophilic carbon via an S_N2 mechanism, releasing PPh_3 oxide upon formation of the P=O double bond. As demonstrated by Ganesh, this reaction proved very useful for coupling the secondary amide functionalities of both thymine and uracil to a ferrocenyl alcohol, and had already been successfully employed by the Tucker group in previous FcNA syntheses.[40,41]



Scheme 2.15 Synthesis of *N3*-benzoyl thymine **2.21** from thymine **2.23**

To control the regioselectivity of this reaction while simultaneously improving the solubility of the compound, thymine was selectively protected with a benzoyl group at *N*3 through a two-step process. In the first step, thymine **2.23** is reacted at both *N*1 and *N*3 with benzoyl chloride (BzCl) in pyridine (Py). This was then dissolved in a 1:1 mixture of dioxane and H_2O, and a selective deprotection at *N*1 effected by K_2CO_3 to give **2.21**. This reaction proceeds under relatively mild conditions due to the ester-like quality of the exocyclic amide. The nitrogen lone-pair interacts strongly with the cyclic, co-planar carbonyl system, leaving the benzoyl group, which is non-co-planar and hence has poor orbital overlap, relatively electron deficient. Although both benzoyl groups experience similar 'ester-activation', *N*1 (with one adjacent carbonyl) is sterically more accessible than *N*3 (with two adjacent carbonyls) and hence the hydrolysis proceeds much more readily at this position.



Scheme 2.16 Continued synthesis, of tetrasubstituted dithyminyl diol **2.1-(*RR*,S_pS_p)** including the subsequent DMT protection to give **2.23-(*RR*,S_pS_p)**

Following the Mitsunobu coupling of *N3*-benzoyl thymine **2.21** to give **2.22-(*RR*,S_pS_p)** the TBDPS protecting groups were removed with tetrabutylammonium fluoride (TBAF) before methylamine was used to cleave the benzoyl groups from the thymine residues to yield the target tetrasubstituted dithyminyl ferrocene diol **2.01-(*RR*,S_pS_p) (Scheme 2.16)**. The diol **2.01-(*RR*,S_pS_p)** was mono-protected with a DMT group to give **2.23-(*RR*,S_pS_p)** before being passed on to another member of the group for phosphorylation, oligomerisation and binding studies.

Previous attempts in the group to perform HPLC on the bulky and highly polar dithyminyl diol **2.1-(*RR*,S_pS_p)** had proven problematic, it was therefore suggested that diol **2.20-(*RR*,S_pS_p)** be used to assess the enantiomeric purity. No scrambling of stereochemistry should occur after this point in the synthesis therefore the analysis should also be representative of the final product. The (non-chiral) purity was again assessed by ^{1}H NMR and confirmed by analytical HPLC. Using a C18 column with isocratic eluent of 5% H_2O in MeCN at a flow rate of 0.75 ml min^{-1} a single sharp peak was observed at 32.91 mins retention time (**Fig. 2.23**).

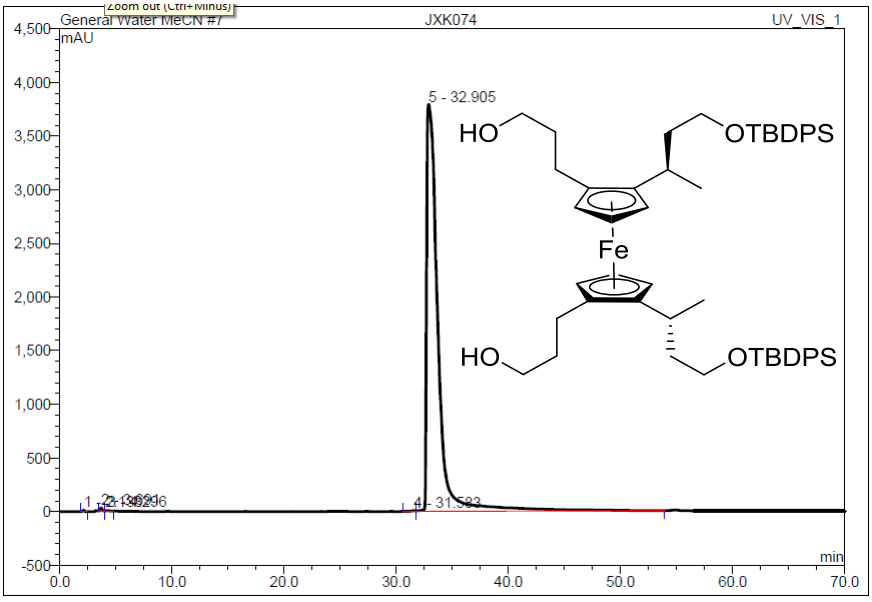


Fig. 2.23 Analytical HPLC trace of tetrasubstituted ferrocene diol **2.20-(*RR*,S_pS_p)**

The enantiomeric purity of **2.20-(*RR*,S_pS_p)** was then assessed by chiral HPLC using an AD column with isocratic eluent system of 1.5% IPA in hexane and a flow rate of 2.5 ml min^{-1}. Two small peaks with relative areas of 1.93% and 0.76% respectively, eluted after 13.87 and 19.45 mins retention time, followed by the major peak with a relative area of 97.31% at 27.23 mins retention time (**Fig. 2.24**).

The sample was combined with the opposite enantiomer (kindly donated by a member of the group) and the mixture co-eluted under identical conditions. Although both peaks are broad and the resolution is quite poor, two distinct peaks are clearly visible, one at 19.33, the other at 26.94 mins retention time (**Fig. 2.25**). The small peak at approximately 14 mins retention time is again obseverd but remains unidentified. Thus the effective separation of the enantiomers was demonstrated and the high enantiomeric purity of **2.20-(*RR*,S_pS_p)** (e.e. = 98%).

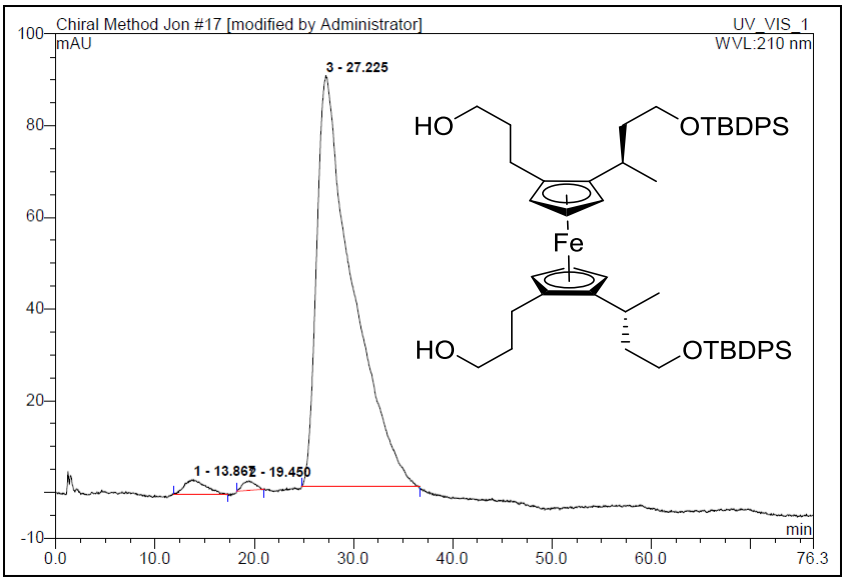


Fig. 2.24 Chiral HPLC trace of tetrasubstituted ferrocene diol **2.20-(*RR*,S_pS_p)**

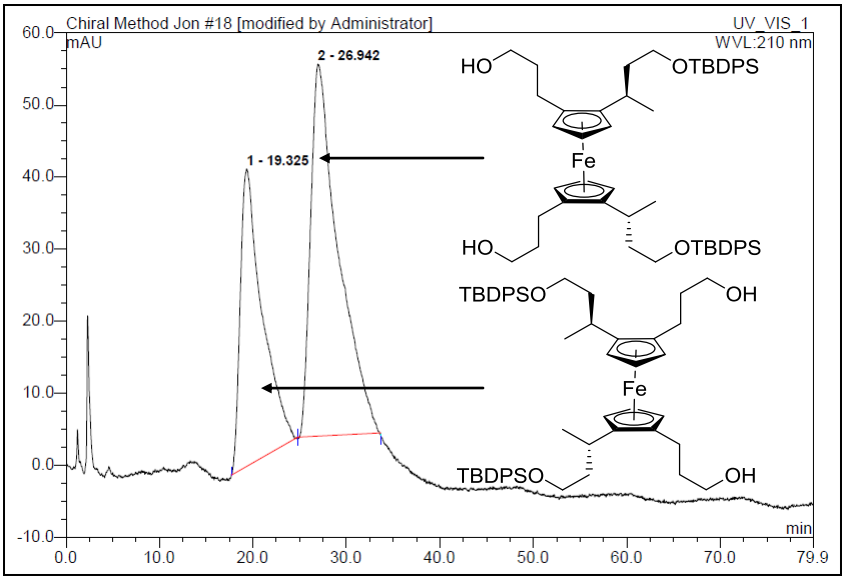


Fig. 2.25 Chiral HPLC trace of a mixture of **2.20-(*RR*,S_pS_p)** and its opposite enantiomer **2.20-(*RR*,S_pS_p)**

2.3.1.2 Synthesis of Ferrocene Guanine Conjugates

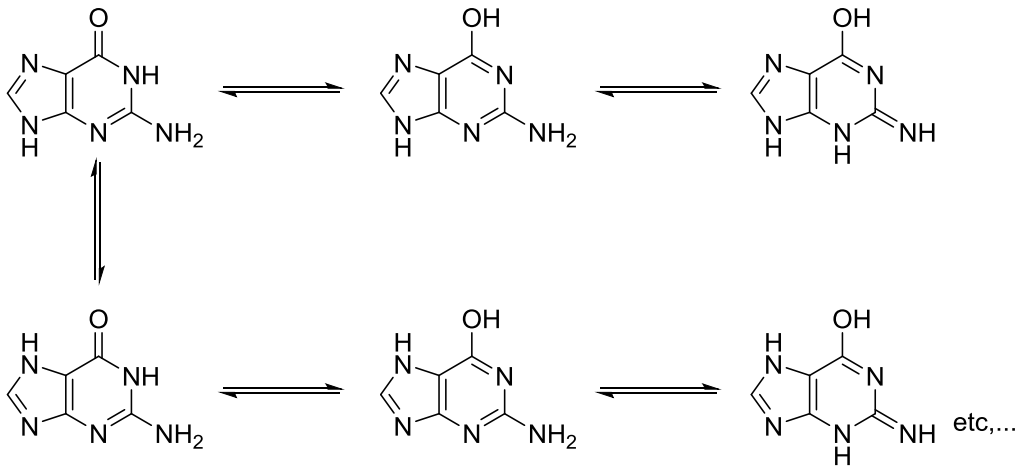
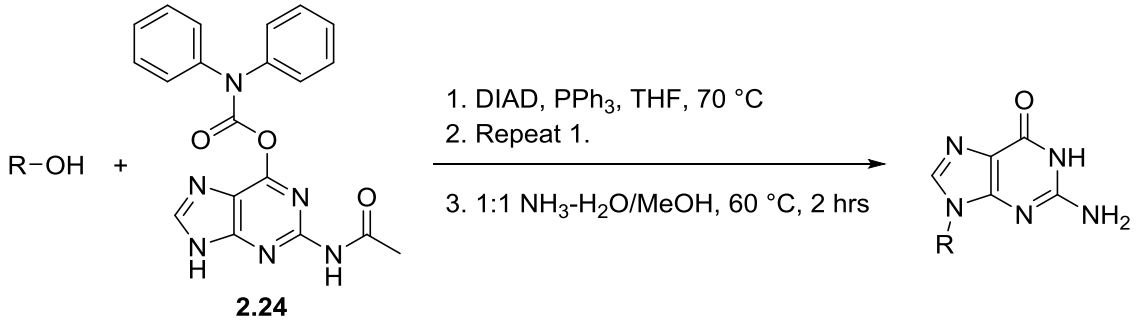


Fig. 2.26 Various tautomeric forms of the guanine nucleobase

With various tautomeric forms (**Fig. 2.26**) and poor solubility, guanine is notorious as the most synthetically demanding nucleobase. A cunning protective strategy is therefore required both to control the regiselectivity of its reactions and to render the compound more synthetically amenable. Previous work by Shi had demonstrated that protected guanine **2.24**, with an acetyl group deactivating the exocyclic amine, and a bulky carbamoyl group blocking

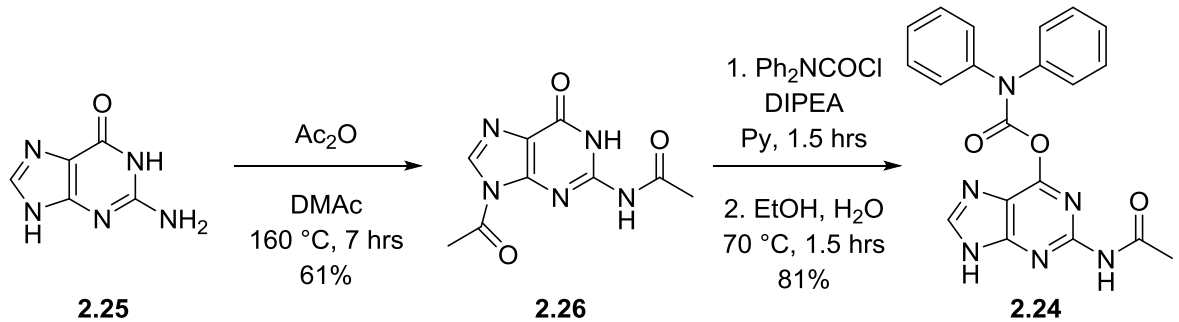
*N*7, could be selectively coupled at *N*9 to a range of primary alcohols using the Mitsunobu reaction (**Scheme 2.17**).[48] Crucially, both of these protecting groups were then removed under typical oligonucleotide deprotection conditions using ammonium hydroxide.



2.24

Scheme 2.17 The *N9* regioselective Mitsunobu coupling of protected guanine **2.24** and a range of alcohols

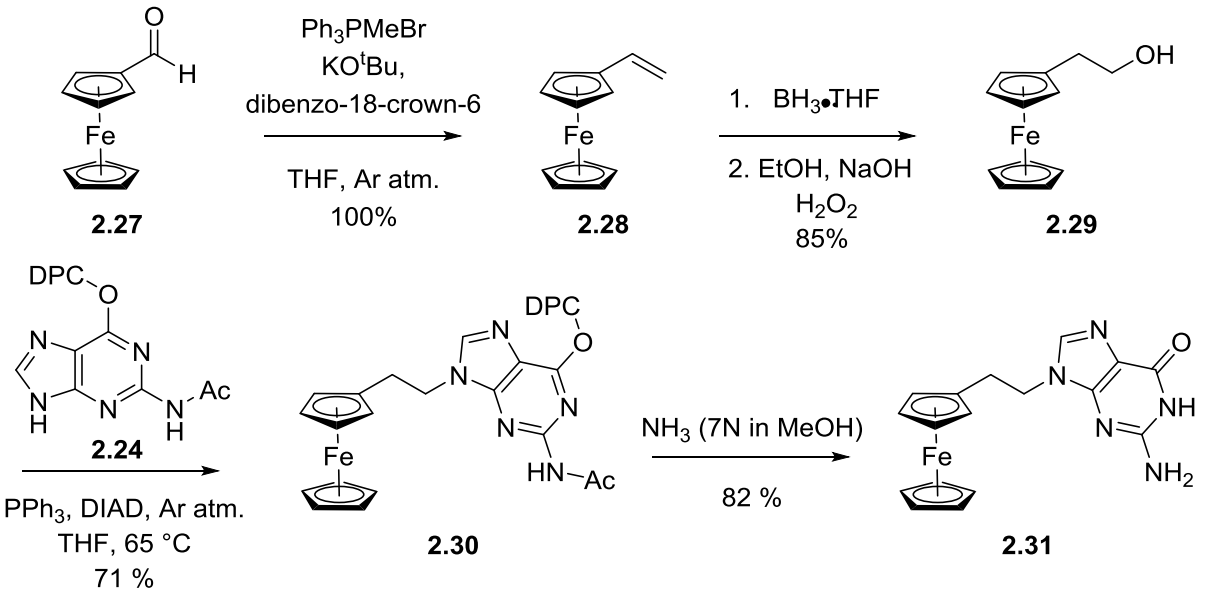
It was therefore proposed that the utility of protected guanine **2.24** be investigated in the production of diguaninyl FcNA monomers and a stock of material was produced according to the method of Zou (**Scheme 2.18**).[49] Guanine **2.25** was first reacted with acetic anhydride, which protected both the *N9* and the exocyclic amine with acetyl groups to give **2.26**. Reaction with Ph_2NCOCl and DIPEA in Py then installed the bulky carbamate group on the oxygen while simultaneously removing the labile hydrogen at *N1*. The acetyl group at *N9* was then selectively removed, by heating at 70 ºC for 1.5 hours in equal parts EtOH and H_2O to give protected guanine **2.24**.



2.25 **2.26** **2.24**

Scheme 2.18 Protection of guanine **2.25** to give **2.24** according to the method of Zou[49]

Before attempting to employ this protected nucleobase within the challenging synthesis of a full tetrasubstituted FcNA monomer, protected guanine **2.24** was first coupled to a simple ferrocenyl alcohol **2.29**, which was produced in two steps from the commercially available ferrocenecarboxaldehyde **2.27** (**Scheme 2.19**). Firstly, a Wittig reaction with methyltriphenylphosphonium bromide was used to extend the carbon chain by one producing vinylferrocene **2.28**. Hydroboration/oxidation of the resulting alkene proceeded with high regioselectivity to give the anti-Markovnikov ferrocenyl ethanol product **2.29**. The small amount of Markovnikov byproduct was easily removed by column chromatography but was not characterised.



Scheme 2.19 Synthesis of the guanine ferrocene conjugate **2.31**

The Mitsunobu conditions favoured by Zou employ an excess of the alcohol reagent, thus favouring a high turnover of the protected guanine material. Conversely, in the tetrasubstituted ferrocene systems which comprise the FcNA monomers, the preceding ferrocene diol is the most precious material and therefore an excess of the protected nucleobase is typically employed to ensure a high turnover. As an added benefit, this modification reduces the likelihood of an undesired intramolecular reaction between the two

alcohol groups, again increasing the turnover of the precious material. With this in mind, using an excess of the protected guanine **2.24**, the Mitsunobu reaction was successfully completed, coupling selectively at the *N*9 position to produce the protected guaninyl ferrocene conjugate **2.30**. The PPh_3O generated during the reaction was difficult to fully remove and a small amount remained following repeated flash column chromatography. The final compound **2.31** was delivered using NH_3 in MeOH. Fortuitously, the product precipitated out of solution and was collected by filtration; the yellow crystals were washed with MeOH but required no further purification.

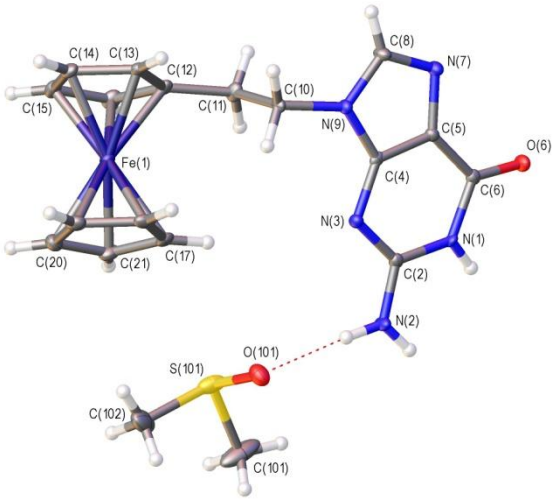


Fig. 2.27 Crystal structure of **2.31** with ellipsoids drawn at the 50% probability level. Hydrogen bonding is shown using dotted lines

Single crystals of the guaninyl ferrocene conjugate **2.31** were grown from a concentrated solution in DMSO and analysed by X-ray diffraction; the structure, and specifically the *N9* regioselectivity of the Mitsunobu coupling, was thus confirmed (**Fig. 2.27**). An extended, chain-like structure was also revealed which coincides with previous reports of small molecule guaninyl conjugates such as that of Gottarelli (**Fig 2.28**).[50] In this structure, each guanine residue forms four hydrogen bonds with its two nearest neighbours; in addition, a single DMSO molecule accompanies each ferrocene unit, hydrogen bonding to the exocyclic

amine N(2) to complete the lattice. The chains are aligned in a parallel orientation, off-set so that the nucleobases lie sandwiched between layers of ferrocene units; hence there is no π-stacking between the chains.

An interesting interaction also occurs between the hydrogen at C(8) and the oxygen O(6); although not a hydrogen bond in the classical sense, the geometry and interatomic distances are, nonetheless very similar and possibly provides some stabilisation to the supramolecular structure (**Table 2.2**). Previously classified as a "weak hydrogen bond", the proton is rendered unusually labile due to the sp^2 carbon C(8) being flanked by two electron withdrawing nitrogens N(7) and N(9).[51, 52] Full crystal data for compound **2.31** can be found in the appendix (**Chapter 6.11**).

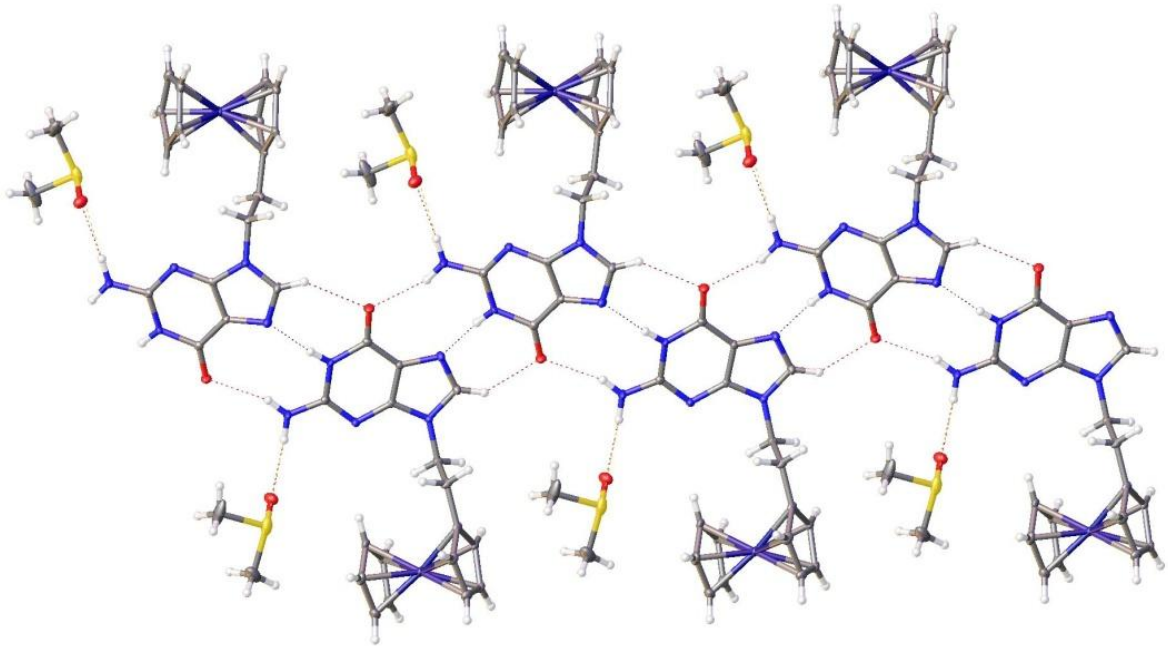


Fig. 2.28 One of the hydrogen-bonded chains in the crystal structure of **2.31** with ellipsoids drawn at the 50% probability level. Hydrogen bonding is shown using dotted lines. Chains of guanine molecules are formed in the direction of the *b* axis via hydrogen bonding. There is no hydrogen bonding or π-stacking between the chains.

Table 2.2 Hydrogen bond lengths and angles in the extended structure of ferrocene guanine conjugate **2.31**

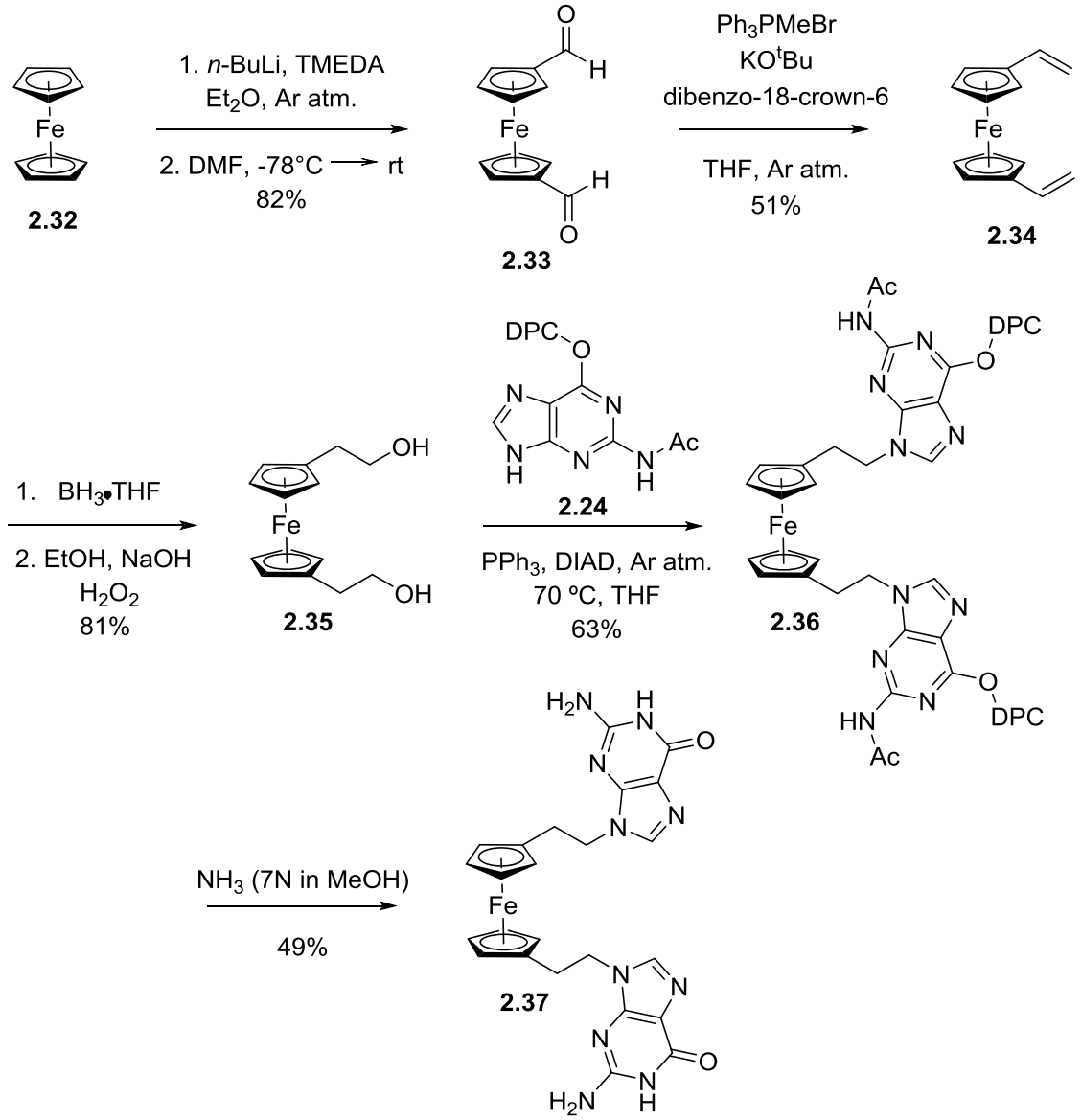
Donor	Hydrogen	Acceptor	Bond Lengths			Bond Angle
D	H	A	D–H / Å	H–A / Å	D–A / Å	D–H–A / º
N(1)	H(1)	N(7)	0.83 (3)	1.95 (3)	2.780 (3)	174 (3)
N(2)	H(2A)	O(101)	0.88 (3)	2.05 (3)	2.920 (3)	172 (2)
N(2)	H(2B)	O(6)	0.84 (3)	2.18 (3)	2.982 (3)	161 (2)
C(8)	H(8)	O(6)	0.93	2.71	3.304 (3)	122.7

*Highlighted entry may qualify as a "weak hydrogen bond"[51, 52]

The strategy was then adapted to produce the corresponding diguaninyl ferrocene conjugate **2.37** (**Scheme 2.20**). Ferrocene **2.32** was first reacted with *n*-BuLi in the presence of TMEDA to produce the dilithiated species which was then reacted with DMF to produce ferrocene dicarboxaldehyde **2.33**. This was then reacted with methyltriphenylphosphonium bromide in a Wittig reaction extending the carbon linkers by one and producing the divinyl species **2.34**. A hydroboration/oxidation reaction produced the ferrocene diol **2.35**, which was then coupled to two protected guanine residues **2.24** under Mitsunobu conditions to produce the disubstituted guaninyl ferrocene conjugate **2.36**.

Although deprotection using ammonia in methanol was very effective, purification of the highly polar, poorly soluble final compound **2.37** proved difficult. Column chromatography was soon abandoned as the highly polar guanine residues stuck irretrievably to the silica gel and no combination of polar solvents could be found to release them. A separate sample was purified however by the slow addition of water to a solution in hot methanol and DCM which gradually precipitated a relatively pure form of the product. It is worth noting that both the dialdehyde **2.33** and divinyl **2.34** species are quite unstable, rapidly degrading during column chromatography making purification difficult and yield analysis somewhat questionable. Further degradation of the dialdehyde **2.33** was observed following just one night of cold

storage in the freezer, timing is therefore important to ensure that this reagent is freshly prepared and reacted on in quick succession.



Scheme 2.20 Synthesis of the diguaninyl ferrocene conjugate **2.37**

2.3.1.3 Synthesis of Tetrasubstituted Diguaninyl Ferrocene Diol 2.38-(*RR*,S_pS_p)

Recent binding studies in the group had demonstrated that FcNA monomers with backbone linkers of three carbon atoms and nucleobase linkers of two carbon atoms produced the most stable duplex. Thus, having established a viable strategy for the coupling of ferrocene and

guanine, the synthesis of the tetrasubstituted diguaninyl ferrocene diol **2.38-(*RR,S*$_p$*S*$_p$)**, the precursor to the **Fcn3c2GG**$_{(RR,SpSp)}$ monomer was then attempted (**Fig. 2.29**).

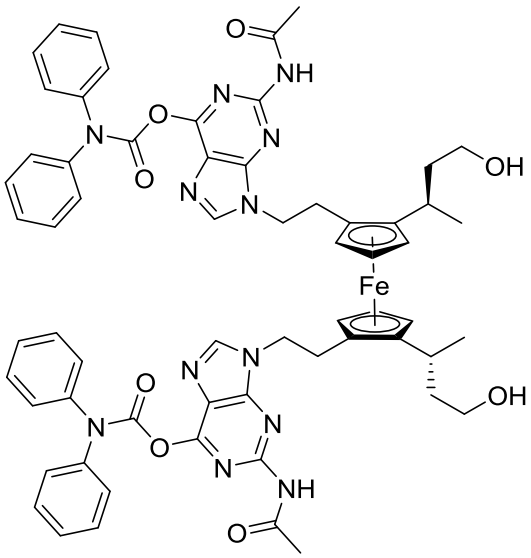
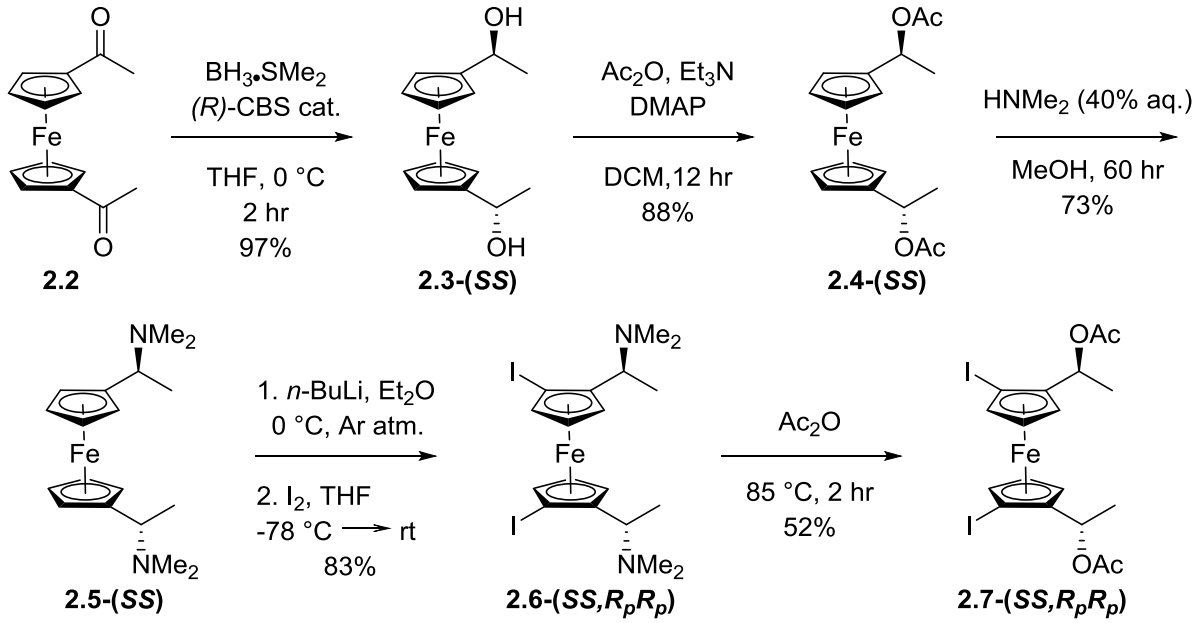


Fig. 2.29 Tetrasubstituted diguaninyl ferrocene diol target **2.38-(*RR,S*$_p$*S*$_p$)**



Scheme 2.21 Synthesis of tetrasubstituted diguaninyl ferrocene diol **2.38-(*RR,S*$_p$*S*$_p$)**

The first five steps of the synthesis (**Scheme 2.21**) were identical to that of the tetrasubstituted dithyminyl ferrocene diol **2.1-(*RR,S*$_p$*S*$_p$)** discussed previously. Diacetylferrocene **2.2** was reduced using the (*R*)-CBS catalyst to give diol **2.3-(*SS*)**, which

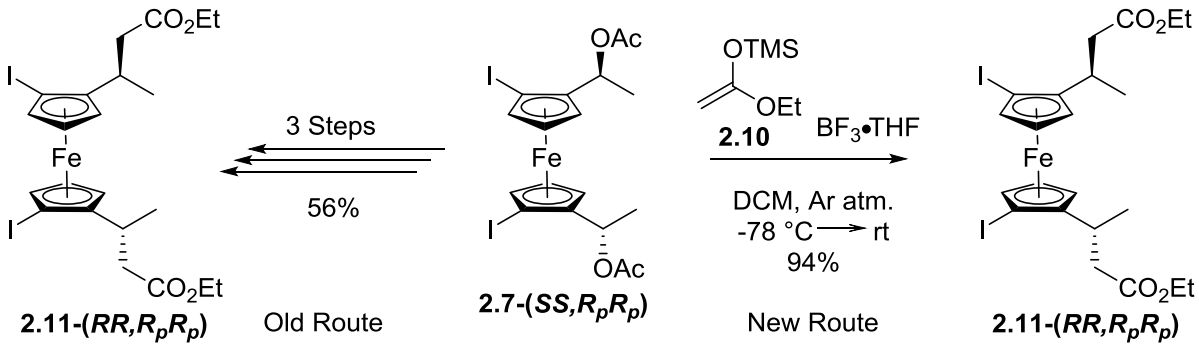
was then converted with stereoretention through the diacetoxy **2.4-(*SS*)**, to the 'Ugi' diamine **2.5-(*SS*)**. Ortho-lithiation followed by iodonation established the planar chirality of **2.6-(*SS*,R_pR_p)**, before the amines were reverted to acetoxy leaving groups **2.7-(*SS*,R_pR_p)**.

In the previous syntheses the next two steps converted the two acetoxy groups of **2.7-(*SS*,R_pR_p)** to methoxy groups via the corresponding alcohols, before substitution with the enolate nucleophile was used to extend the carbon skeleton. Further consideration of this process however led to the efficacy of this method being questioned and possible alternatives sought. Upon leaving, the acetoxy group produces the resonance stabilised acetate anion, the conjugate base of acetic acid, which has a pK_a of 4.76. In comparison, the methoxy leaving group produces the methoxide anion, the conjugate base of methanol, with a pK_a of 15.5 (**Fig. 2.30**). Producing a weaker conjugate base, the acetoxy is expected to be a better leaving group than the methoxy. It was therefore proposed that the two interconversion steps were unnecessary and that a direct substitution of the acetoxy **2.7-(*SS*,R_pR_p)** by enolate **2.10** was feasible.



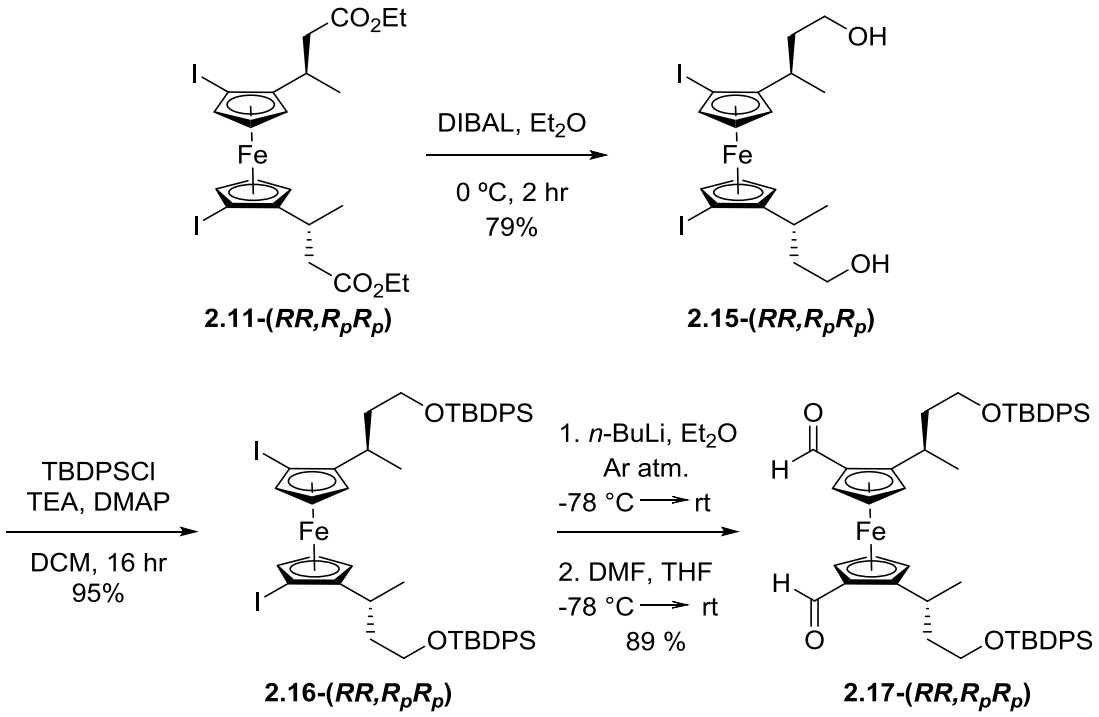
Fig. 2.30 Comparison of the pK_a's of the conjugate acids of the acetate and methoxy leaving groups

A small scale test reaction proved successful and upon scaling up, the ferrocene diester **2.11-(*RR*,R_pR_p)** was produced in a single step with a much improved yield of 94% (**Scheme 2.22**). In comparison, the previous route gave an overall percentage yield of about 56% with the three steps taking almost a week to complete (see also **Scheme 2.5 p39**).

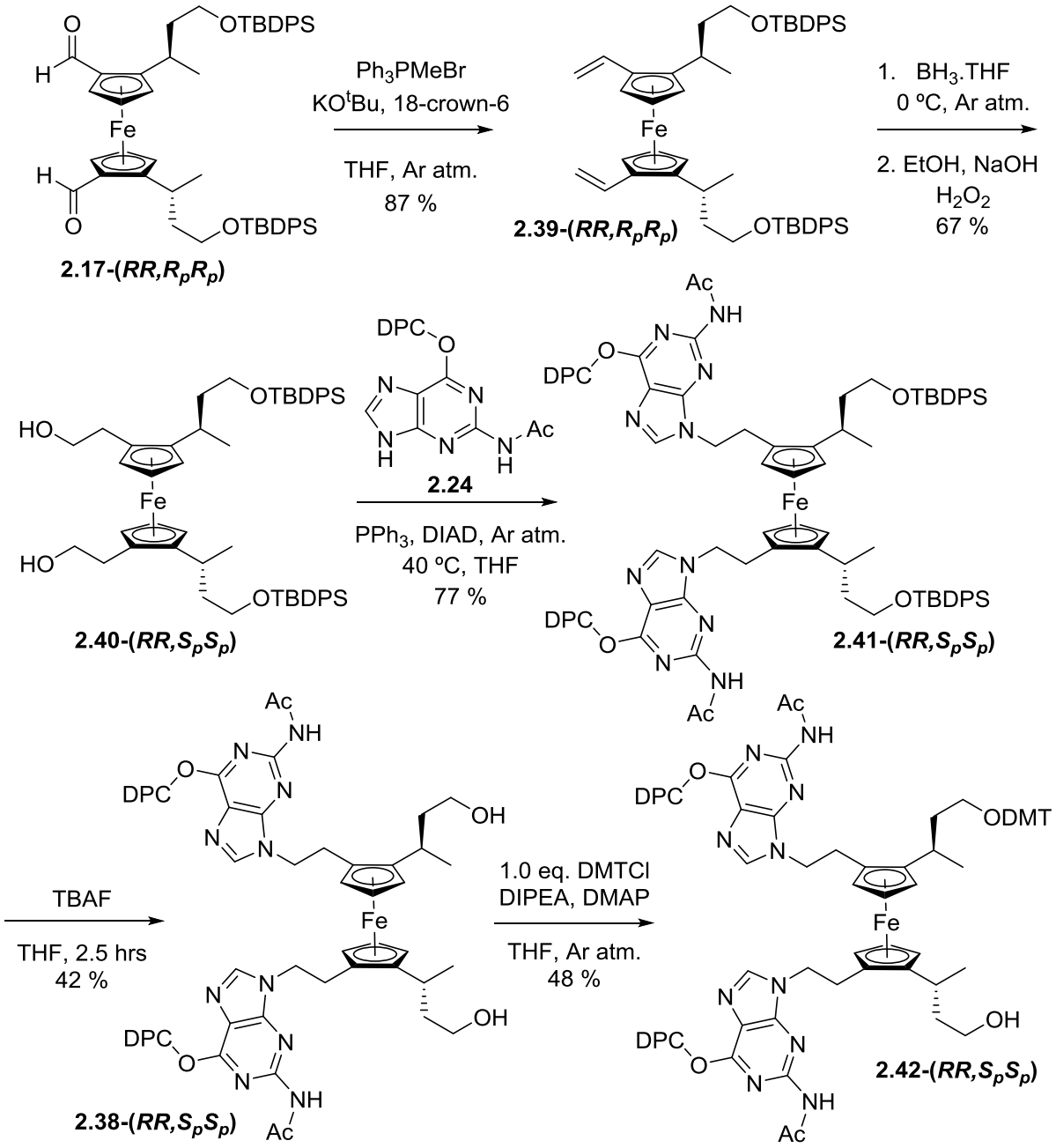


Scheme 2.22 Transformation from diacetoxy **2.7-(*SS*,R_pR_p)** to diester **2.11-(*RR*,R_pR_p)** comparing the new and old routes

The synthesis continued and diester **2.11-(*RR*,R_pR_p)** was reduced to diol **2.15-(*RR*,R_pR_p)** using DIBAL, before the resulting hydroxyls were protected with TBDPS groups to give **2.16-(*RR*,R_pR_p)** (**Scheme 2.23**). A lithiation/formylation reaction then installed aldehydes in place of the iodo groups to give **2.17-(*RR*,R_pR_p)** as described in the previous synthesis.



Scheme 2.23 Continued synthesis of tetrasubstituted diguaninyl ferrocene diol **2.38-(*RR*,S_pS_p)**



Scheme 2.24 Continued synthesis of the target tetrasubstituted diguaninyl ferrocene diol **2.38-(*RR,S*$_p$*S*$_p$)**, plus the mono-protection with a DMT group to give **2.42-(*RR,S*$_p$*S*$_p$)**

At this point, the synthesis for the two carbon linker to the base (c = 2), diverges from that which gives the three carbon linker (c = 3) such as the dithyminyl diol **2.1-(*RR,S*$_p$*S*$_p$)** discussed previously (see **Scheme 2.9 p44**). A Wittig reaction, employing

methyltriphenylphosphonium bromide, is therefore used extend the carbon skeleton by one, transforming the aldehyde groups of **2.17-(*RR*,R_pR_p)** to the corresponding vinyl groups of **2.39-(*RR*,R_pR_p)** (**Scheme 2.24**). A hydroboration/oxidation reaction was then used to produce diol **2.40-(*RR*,S_pS_p)**, before a Mitsunobu coupling with protected guanine **2.24** gave the protected diguaninyl ferrocene conjugate **2.41-(*RR*,S_pS_p)**. The two TPDPS protecting groups were removed with TBAF to yield the the target tetrasubstituted diguaninyl ferrocene diol **2.38-(*RR*,S_pS_p)** which was then mono-protected with a DMT group to give **2.42-(*RR*,S_pS_p)**.

As in the previous synthesis, the enantiomeric purity was assessed by HPLC examination of the precursor diol **2.40-(*RR*,S_pS_p)**. Using a cellulose column with isocratic eluent system of 10% H_2O in MeCN and a flow rate of 1.0 ml min^{-1}, following a 10.0 µl injection, the diol **2.40-(*RR*,S_pS_p)** eluted to produce a large sharp peak with area of 99.23% at 7.104 mins and a small peak of area 0.77% at 7.872 mins retention time (**Fig. 2.31**). The composition of diol **2.40-(*RR*,S_pS_p)** was thus found to be 99% desired enantiomer and 1% opposite enantiomer (e.e. = 98%).

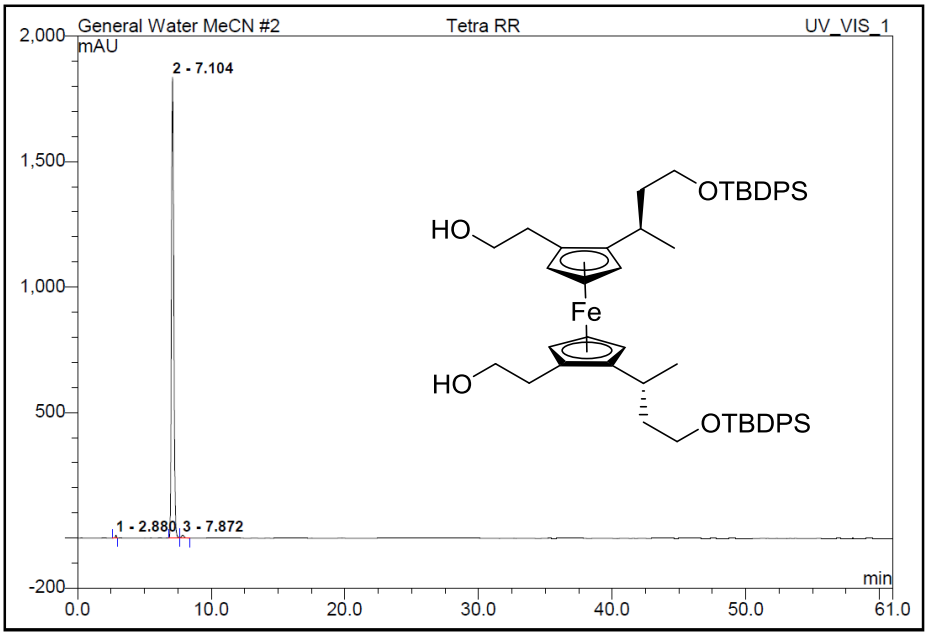


Fig. 2.31 Chiral HPLC trace of diol **2.40-(*RR*,S_pS_p)**

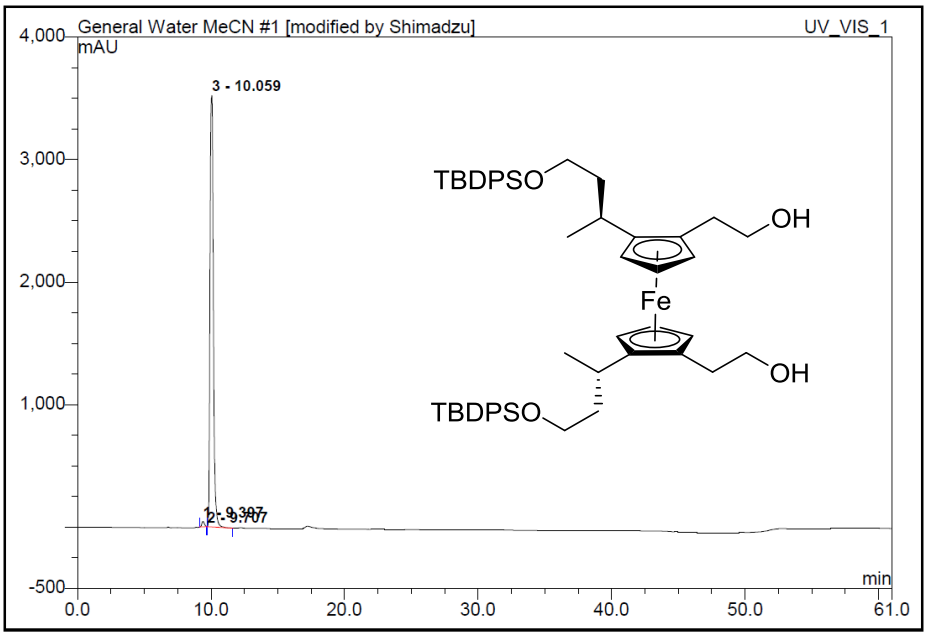


Fig. 2.32 Chiral HPLC trace of the opposite enantiomer, diol **2.40-(*SS,R*$_p$*R*$_p$)**

Under identical conditions, following a 10.0 µl injection, the opposite enantiomer (kindly donated by another member of the group) eluted to produce a small peak of area 0.92% at 9.397 mins and a large sharp peak of area 99.08% at 10.059 mins retention time (**Fig. 2.32**). The composition of the **2.40-(*SS,R*$_p$*R*$_p$)** was thus found to be 99% desired enantiomer and 1% opposite enantiomer (e.e. = 98%).

Finally, to confirm the presence of only the two compounds of interest, a sample was prepared containing both **2.40-(*SS,R*$_p$*R*$_p$)** and the opposite enantiomer **2.40-(*RR,S*$_p$*S*$_p$)**. As expected, under identical conditions the mixture eluted to produce two large sharp peaks at 7.061 and 7.819 mins retention time respectively (**Fig. 2.33**).

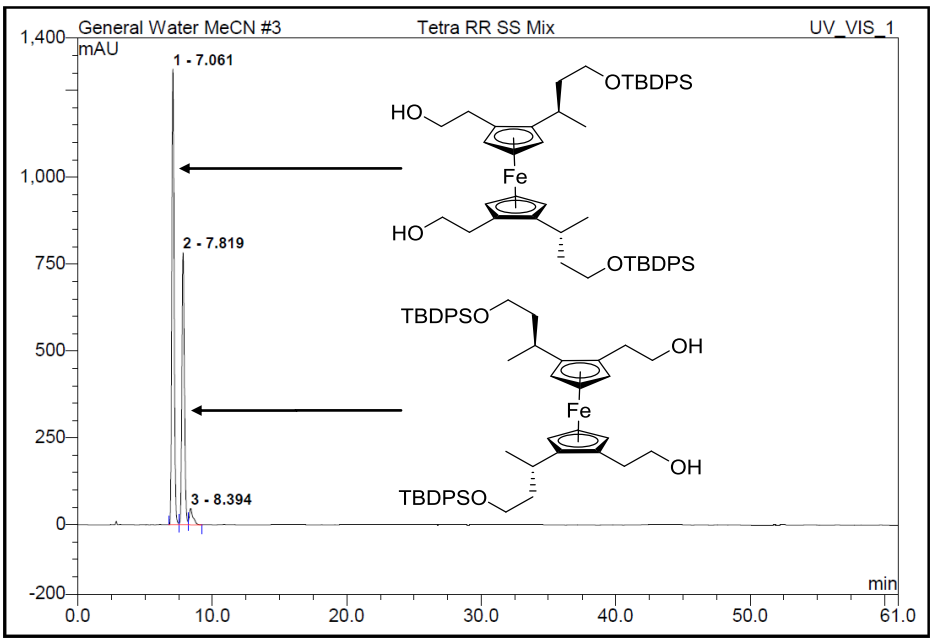
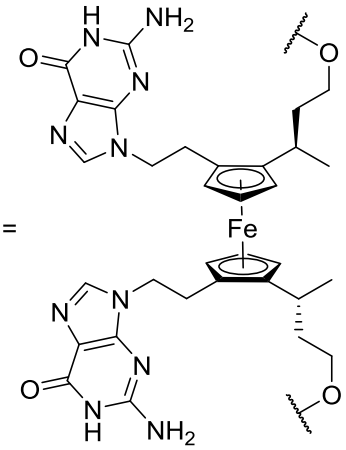


Fig. 2.33 Chiral HPLC trace of a mixture of diol **2.40-(*RR*,S_pS_p)** and its opposite enantiomer **2.40-(*SS*,R_pR_p)**

2.3.2 Attempted Oligomerisation of Tetrasubstituted Diguaninyl FcNA monomer Fcn3c2GG(*RRpSpS*)

a) **XX** =



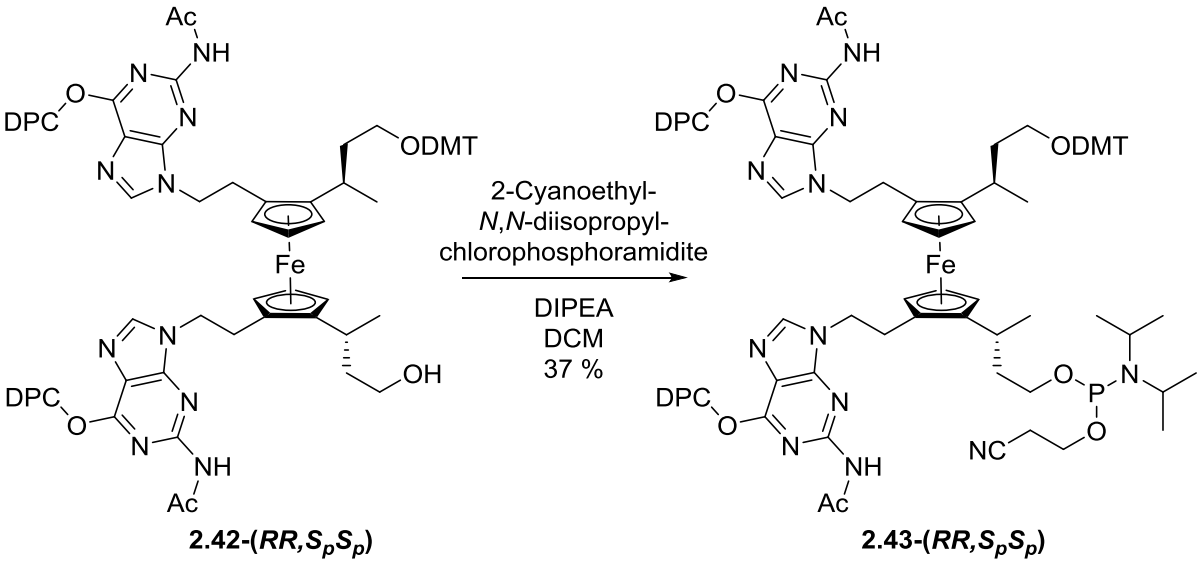
b) 5'-TGGACTC-**XX**-CTCAATG-3'

Fig. 2.34 a) the guaninyl FcNA dinucleotide, and **b**) the well-characterised hybrid **S1** strand used to interrogate the binding characteristics of the FcNA monomer **XX**

As discussed in more detail in the following section on thermal melting studies, the binding characteristics of each FcNA monomer are typically studied by incorporation into the centre

of a well characterised, otherwise natural DNA oligomer denoted **S1** in which **XX** represents the FcNA dinucleotide (**Fig. 2.34**).

In preparation for automated solid-phase oligonucleotide synthesis, the mono-DMT protected diguaninyl FcNA monomer **2.42-(*RR,S*$_p$*S*$_p$)** was freshly phosphitylated with 2-cyanoethyl *N*,*N*-diisopropyl-chlorophosphoramidite to give **2.43-(*RR,S*$_p$*S*$_p$)** (**Scheme 2.25**).



Scheme 2.25 Phosphitylation of DMT mono-protected tetrasubstituted diguaninyl ferrocene alcohol **2.42-(*RR,SpSp*)**, producing **2.43-(*RR,S*$_p$*S*$_p$)** in preparation for automated solid-phase synthesis

As expected, the ^{31}P NMR revealed two major singlet peaks at 147.3 and 147.0 ppm corresponding to each of the two P(III) stereoisomers. Other much smaller peaks were also observed at 13.9, 10.8, 8.3 and 8.2 ppm corresponding to common P(V) contaminants such as phosphoric acids, esters and amides (**Fig. 2.35**).

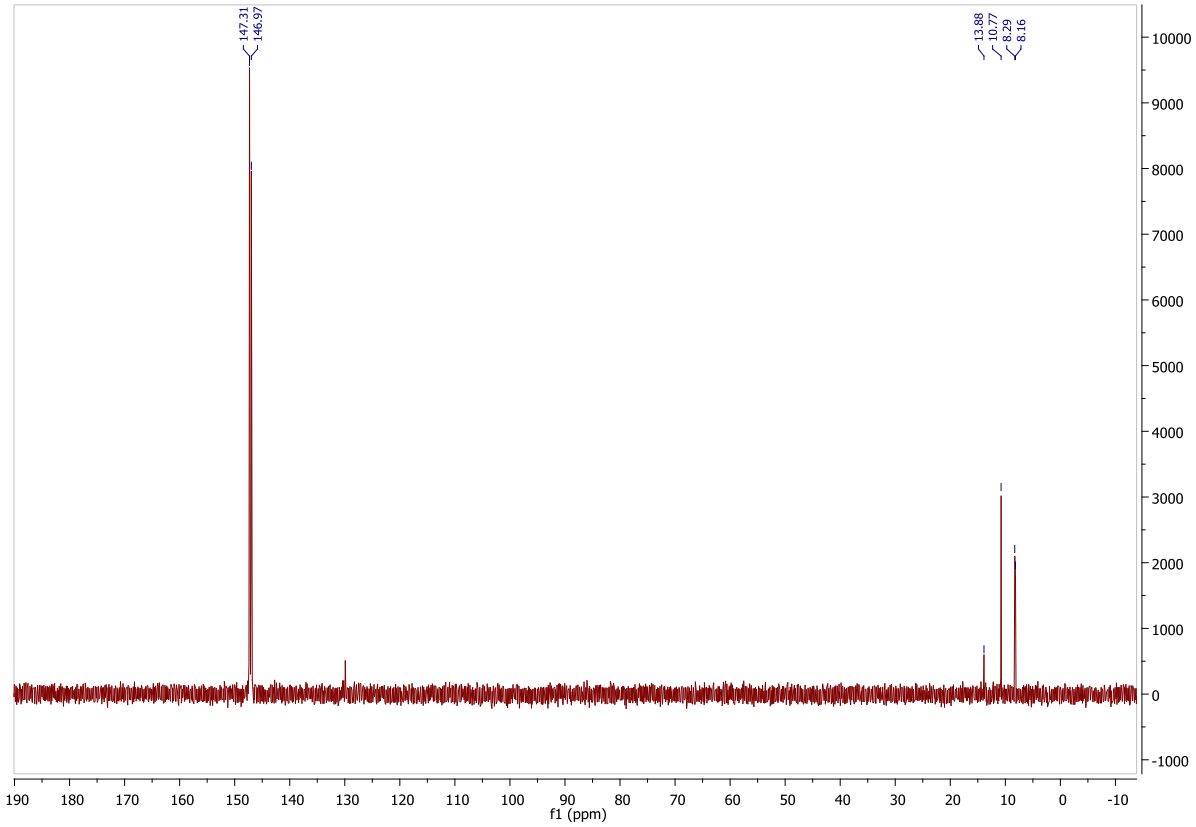


Fig. 2.35 ^{31}P NMR spectra of **2.43-(*RR*,S_pS_p)** showing two major peaks at 147.3 and 147.0 ppm corresponding to the two P(III) stereoisomers and minor P(V) impurities at 13.9, 10.8, 8.3 and 8.2 ppm

Although not totally pure, due to the somewhat unstable nature of the molecule it was decided to proceed with the oligomerisation. With precious little material, the concentration of the diguaninyl FcNA phosphoramidite had to be reduced to half of what is normally used. To compensate for this, the coupling time was extended from the usual 30 seconds to 10 mins.

To confirm the success or failure of the coupling, the crude mixture was first analysed by mass spectrometry. The mass of the desired strand is 4824.0 g mol^{-1}, we would therefore expect the molecular ion peak $[M]^{-1}$ at 4824.0 m/z, the $[M]^{-2}$ ion at 2412.0 m/z and the $[M]^{-3}$ ion at 1608.0 m/z. Unfortunately, using ES mass spectrometry none of these species were

detected. Three peaks were observed, the largest at 1038.7 m/z, a smaller one at 692.1 m/z and a very small signal at 2078.4 m/z corresponding to the first three negative ions of an oligomer approximately half the desired length. Hoping that the oligonucleotide had simply fragmented during ionisation, the softer technique of MALDI was employed. The molecular ion $[M]^{-1}$ peak was again observed at 2078 m/z accompanied by a peak at 653.1 m/z. No peaks were observed at any of the three values we would expect for the desired modified oligonucleotide.

It seems that the coupling of the FcNA monomer failed, the major peak observed by both ES and MALDI mass spectrometry corresponds to the first part of the target sequence CTCAATG-3′ which has a molecular mass of 2079.4 g mol^{-1}. Following the unsuccessful coupling of the FcNA dinucleotide, this portion of oligomer simply would have been capped and no more nucleotides added to it thus constituting the major portion of the crude material.

There are a few obvious possibilities which may account for the failed coupling. Firstly, it is possible that the diguaninyl phosphoramidite was simply not sufficiently pure or that the use of below-optimal concentration adversely affected the coupling. Another consideration is that the tetrasubstituted guaninyl FcNA dinucleotide bearing two, heavily protected guanine bases is much more bulky and sterically demanding than the corresponding thymine dinucleotides which had been previously studied in the group and which are deprotected prior to use on the synthesizer.

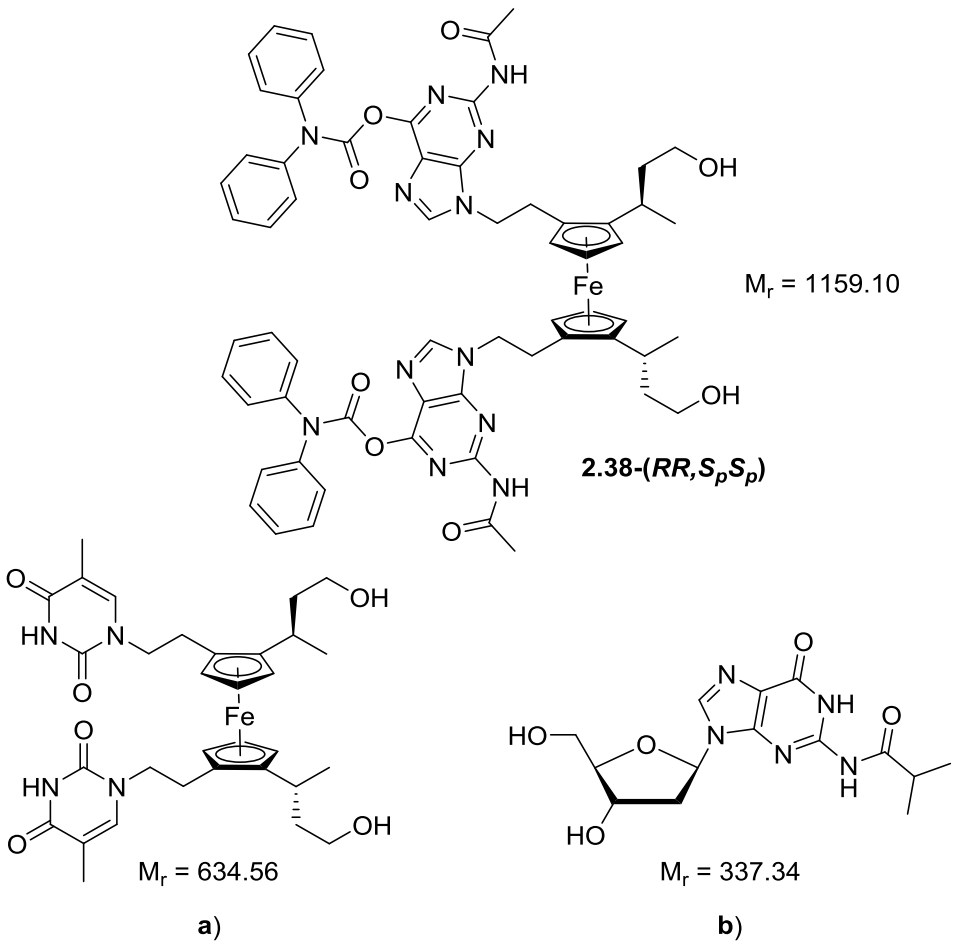


Fig. 2.36 Size comparison (by mass) of the tetrasubstituted diguaninyl FcNA diol precursor **2.38-(*RR,S$_p$S$_p$*)** with **a**) the tetrasubstituted dithyminyl FcNA diol equivalent and **b**) the standard protected guanine nucleotide employed in automated oligonucleotide synthesis

Consideration of the respective molecular masses gives a good indication of the sizes of these different monomers (**Fig. 2.36**). If we discount the DMT and phosphoramidite groups which are common to all, the protected guanine nucleotide typically employed in automated synthesis has a molecular mass of 337.34 g mol^{-1}. The dithyminyl FcNA diol is about twice as large with a molecular mass of 634.56 g mol^{-1}. The protected diguaninyl FcNA diol **2.38-(*RR,S$_p$S$_p$*)** however is almost four times as large as the unmodified guanine nucleotide, with a molecular mass of 1159.10 g mol^{-1}. It is possible that the monomer was simply too hindered to couple effectively. In addition, these large planar groups may have resulted in the molecule

intercalating into the growing DNA strands, again increasing the steric hindrance and reducing the availability of the reactive moieties.

2.3.3 Thermal Melting Studies

Now known as the hyperchromic effect, in 1951 René Thomas was the first to notice that the UV absorptivity of DNA greatly increased upon heating.[53] It has been demonstrated that at elevated temperatures, the hydrogen bonding network between complementary base-pairs becomes disrupted, the duplex becomes denatured and the two strands separate.[54] The nucleobases therefore experience a change of chemical environment, from a closely stacked sandwich, held rigidly in place by strong hydrogen bonds to a more random, fluid system. The π-electrons, which are largely responsible for the UV absorption, also therefore become less constrained both in terms of physical distribution and energy and hence interact more spontaneously with the incoming radiation. The absorption of UV light is therefore a function of duplex formation and can be used to monitor the extent of hybridisation within a sample.[53]

Using a temperature-controlled UV-spectrometer, the melting temperature (T_m), at which half the duplexes in the sample are denatured, can be therefore be determined and gives a good indication of their relative stability. In the first step, the sample is annealed through a process of repeated heating and cooling, thus the duplex is cycled through a state of denaturisation and renaturisation to ensure consistency. UV absorbance is monitored (typically at 280 nm) throughout the cycle and plotted against the temperature; the T_m is found opposite the maximum first derivative (**Fig. 2.37**).[55]

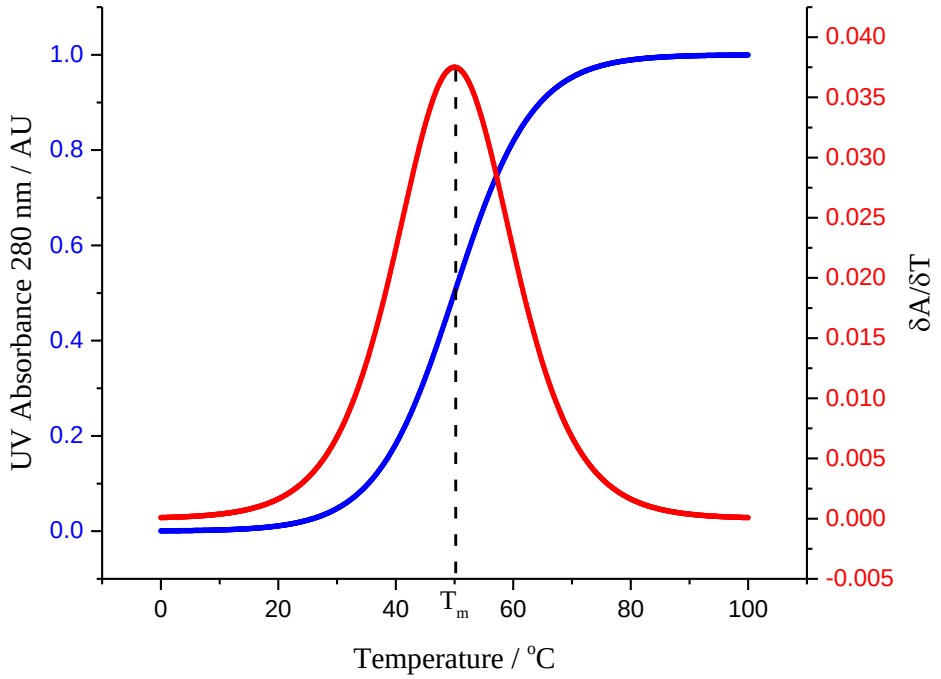


Fig. 2.37 Generic thermal melting curve for duplex DNA showing how the UV absorbance changes with temperature (blue line). The T_m is calculated from the maxima of the 1st derivative (red line).

Assuming total complementarity, the melting temperature of a particular duplex is mostly determined by two major factors. Firstly, the length of the sequence: as the number of complementary base-pairing units increases, the number of stabilising hydrogen-bonds and base-stacking interactions increases accordingly. Secondly, the ratio of C–G to T–A base-pairs: with three hydrogen-bonds between C and G compared to only two between T and A, as the ratio increases so does the total number of stabilising hydrogen-bonds. On the contrary, the presence of mismatching base-pairs will destabilise the duplex, the magnitude is governed by both the type and position in the strand.[55]

Hoping to identify the most promising FcNA candidate, initial studies were conducted to investigate the binding characteristics against native DNA. In these studies a single FcNA

monomer is incorporated into the middle of an otherwise natural DNA strand which has been well characterised in previous work by the group. The **S1** sequence thus consists of the respective FcNA (or control) dinucleotide (**XX**) flanked on either side by seven DNA nucleotides, giving a strand of sixteen nucleotides (16-mer) in total. Crucially, previous work in the group had showed that the closely related 15-mer, consisting of these two DNA sections linked through a single thymine nucleotide, displayed no evidence of self-complimentarity. When hybridised with a complementary strand, the FcNA monomer, at the centre of this system is forced to participate as part of the duplex and thus its binding characteristics are revealed. Each experiment therefore consists of the hybridisation of two, otherwise fully complementary strands: **S1** in which the FcNA (or control) monomer (**XX**) is expressed and **S2** in which the two central nucleobases (**YY**) are selected to interrogate the interactions with the FcNA unit (**Table 2.3**).

Table 2.3 S1XX and **S2YY** sequences, where **XX** and **YY** are variable FcNA or DNA dinucleotides

Strand	Sequence (5′– 3′)
S1**XX**	TGGACTC–**XX**–CTCAATG
S2**YY**	CATTGAG–**YY**–GAGTCCA

The following thermal melting studies were performed by James Carr-Smith of the Tucker group. Following automated synthesis, each oligomer was purified by reverse-phase HPLC and the structure confirmed by mass spectrometry prior to use. These studies are accompanied by molecular dynamic (MD) simulations (min. 5 ns) which were performed by Dr Jean-Louis Duprey of the Tucker group.

Although the attempted production of a diguaninyl FcNA monomer had proven unsuccessful, another member of the group produced a dicytosyl FcNA monomer **Fcn3c2CC**$_{(RR,SpSp)}$ which

could provide important information regarding the H-bonding in these systems. This monomer, along with the two enantiomeric abasic FcNA monomers (**Fcn3HH**$_{(RR)}$ and **Fcn3HH**$_{(SS)}$) and two sets of enantiomeric dithyminyl FcNA monomers, bearing two (**Fcn3c3TT**$_{(RR,SpSp)}$ and **Fcn3c3TT**$_{(SS,RpRp)}$) and three (**Fcn3c3TT**$_{(RR,SpSp)}$ and **Fcn3c3TT**$_{(SS,RpRp)}$) carbon linkers to the nucleobase, were all oligomerised into S1 strands and hybridised with various S2 strands bearing both purine (**YY** = AA and GG) and pyrimidine (**YY** = TT) residues at the opposite position. The stabilities of the resulting duplexes were determined by T_m studies and compared to the corresponding abasic, dithyminyl, and dicytidyl DNA equivalents (**DNAHH**, **DNATT** and **DNACC**) (**Table 2.4**).

Table 2.4 T_m values for S1**XX**•S2**YY** when **XX** = **Fcn3HH**$_{(RR)}$, **Fcn3c2TT**$_{(RR,SpSp)}$, **Fcn3c3TT**$_{(RR,SpSp)}$, **Fcn3c2CC**$_{(RR,SpSp)}$, **Fcn3HH**$_{(SS)}$, **Fcn3c2TT**$_{(SS,RpRp)}$, **Fcn3c3TT**$_{(SS,RpRp)}$, **DNAHH**, **DNATT** and **DNACC**; and **YY** = AA, GG, TT

	Thermal Melting Temperature (T_m) (± 0.25) / °C		
	S2 (**YY**)		
S1 (**XX**)	AA	GG	TT
Fcn3HH$_{(RR)}$	37.5	36.5	36.5
Fcn3c2TT$_{(RR,SpSp)}$	43.0	41.0	40.5
Fcn3c3TT$_{(RR,SpSp)}$	41.5	40.5	40.5
Fcn3HH$_{(SS)}$	37.5	36.5	36.0
Fcn3c2TT$_{(SS,RpRp)}$	41.0	39.5	39.5
Fcn3c3TT$_{(SS,RpRp)}$	43.0	40.5	40.5
Fcn3c2CC$_{(RR,SpSp)}$	39.5	48.0	37.5
DNAHH	37.0	37.0	34.0
DNATT	56.0	44.5	41.5
DNACC	38.0	60.0	38.0

*Highlighted Values Represent the Fully Complementary Sequences

2.3.3.1 Abasic FcNA Monomers

Only very small changes in T_m were observed between the two abasic ferrocene units **Fcn3HH**$_{(RR)}$ and **Fcn3HH**$_{(SS)}$ (**Fig. 2.38**) (**Table 2.4**). This was to be expected, the very slight change in structure producing a correspondingly small change in the stability of each duplex. Likewise, with no base discrimination on the S1 strand, changing the S2 nucleobases produced only small changes in stability. The presence of the larger purines AA and GG on the opposite strand stabilised the duplex slightly compared to the smaller pyrimidines TT. Most interestingly, neither abasic FcNA unit destabilises the duplex compared to the abasic DNA equivalent **DNAHH**, on the contrary, in most cases a slight stabilisation is observed. This may be due to the neutral charge of the FcNA monomer which, like PNA, and unlike DNA, experiences no electrostatic repulsion from its anionic neighbours.[30]

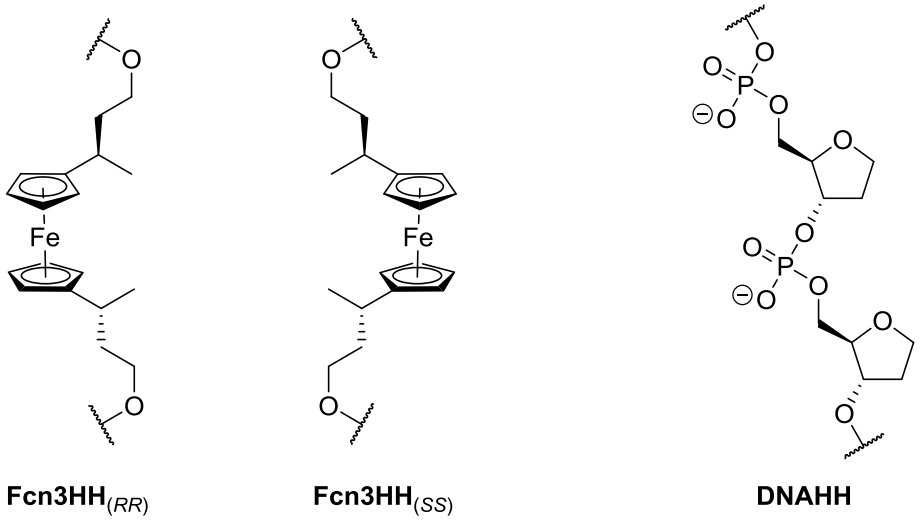
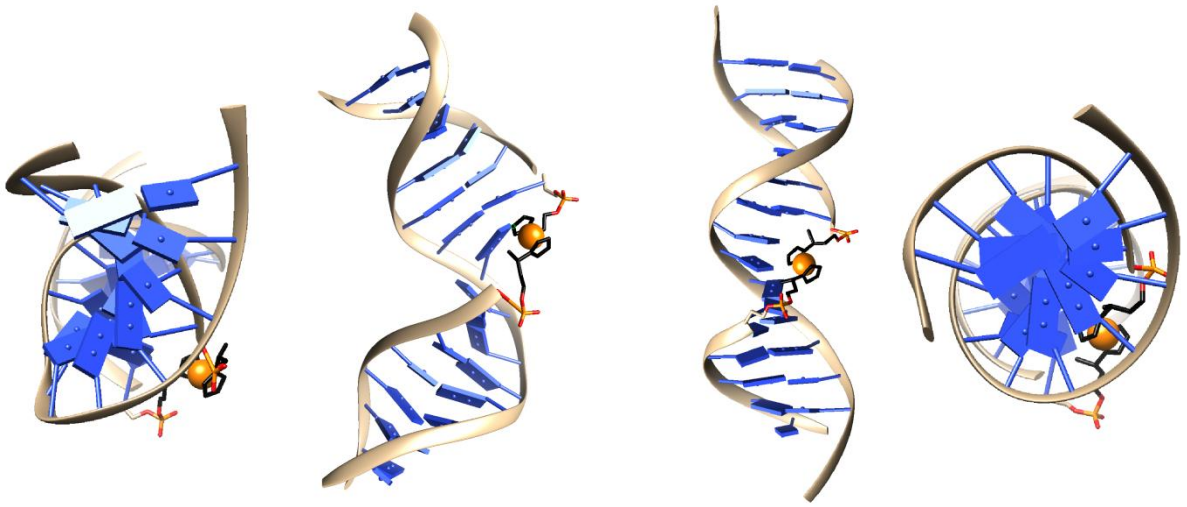


Fig. 2.38 The two enantiomeric abasic FcNA monomers **Fcn3HH**$_{(RR)}$ and **Fcn3HH**$_{(SS)}$, and the corresponding abasic DNA monomer **DNAHH**

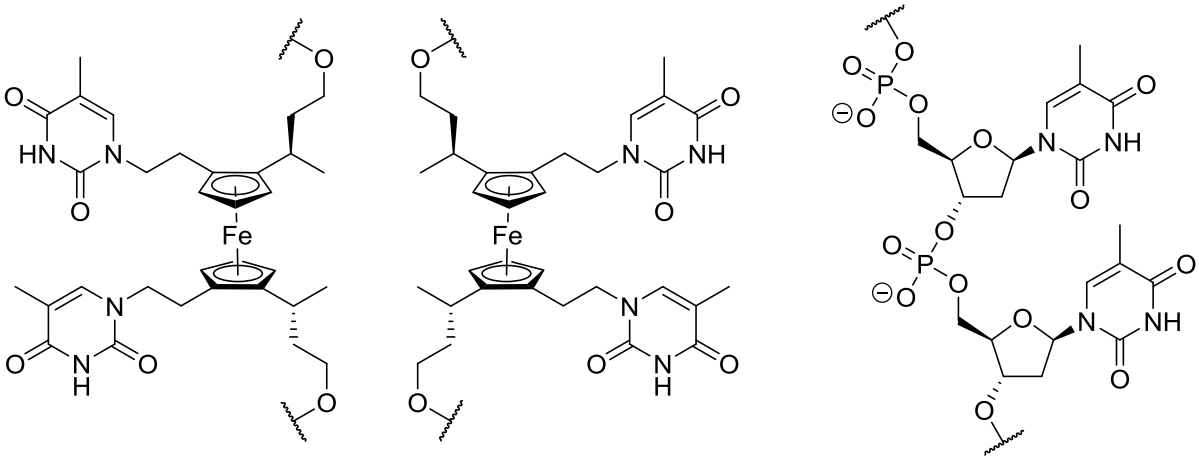
Molecular simulations revealed that helices containing the abasic FcNA units **Fcn3HH**$_{(RR)}$ and **Fcn3HH**$_{(SS)}$ were both very disordered. With no hydrogen-bonding nucleobases to anchor the unit, the ferrocene backbone was very free to move, resulting in distorted and even kinked duplexes which could assume a number of low-energy conformations (**Fig. 2.39**).



S1**Fcn3HH**$_{(RR)}$•S2**AA** S1**Fcn3HH**$_{(SS)}$•S2**AA**

Fig. 2.39 Molecular dynamic simulations (5 ns) of duplexes S1**Fcn3HH**$_{(RR)}$•S2**AA** and S1**Fcn3HH**$_{(SS)}$•S2**AA**

2.3.3.2 Dithyminyl FcNA Monomers with Two Carbon Nucleobase Linkers



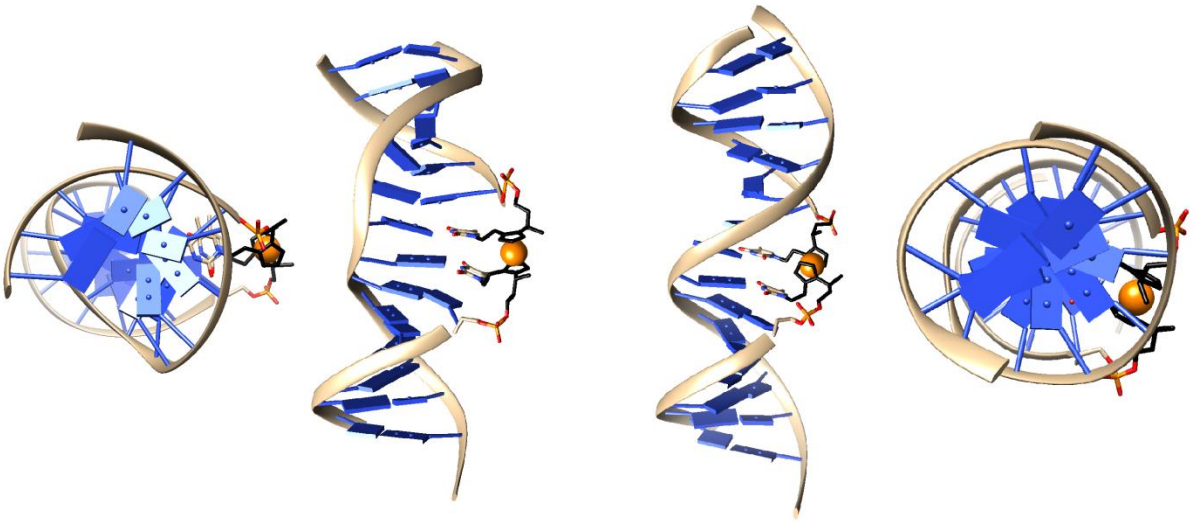
Fcn3c2TT$_{(RR,SpSp)}$ **Fcn3c2TT**$_{(SS,RpRp)}$ **DNATT**

Fig. 2.40 The two enantiomeric dithyminyl FcNA dinucleotides with two carbon linkers to the nucleobase **Fcn3c2TT**$_{(RR,SpSp)}$ and **Fcn3c2TT**$_{(SS,RpRp)}$, and the corresponding DNA dinucleotide **DNATT**

The incorporation of two thymine nucleobases confers the FcNA monomer with both hydrogen-bonding and π-stacking capabilities, and therefore offers the possibility of a far

greater range of potentially stabilising interactions compared to the abasic variety. This is clearly demonstrated by enantiomers **Fcn3c2TT**$_{(RRSpSp)}$ and **Fcn3c2TT**$_{(SSRpRp)}$ (**Fig. 2.40**) the presence of which stabilises the respective duplex compared to the corresponding abasic FcNA systems (**Table 2.4**). The effect is greatest with the matching AA pair on the opposite S2 strand which suggests that complementary H-bonding may be conferring additional stability upon the duplex.

Fcn3c2TT$_{(RR,SpSp)}$ stabilises the duplex slightly more than the **Fcn3c2TT**$_{(SS,RpRp)}$ monomer, increasing the T_m by 5.5 °C and 3.5 °C respectively when compared to the corresponding abasic monomers **Fcn3HH**$_{(RR)}$ and **Fcn3HH**$_{(SS)}$. The DNA equivalent **DNATT** however, is stabilised much more by the incorporation of the thymine residues, producing a T_m 19.0 °C higher than the abasic DNA unit **DNAHH** and 13.0 °C higher than the best FcNA monomer **Fcn3c2TT**$_{(RR,SpSp)}$.



S1**Fcn3c2TT**$_{(RR,SpSp)}$•S2**AA** S1**Fcn3c2TT**$_{(SS,RpRp)}$•S2**AA**

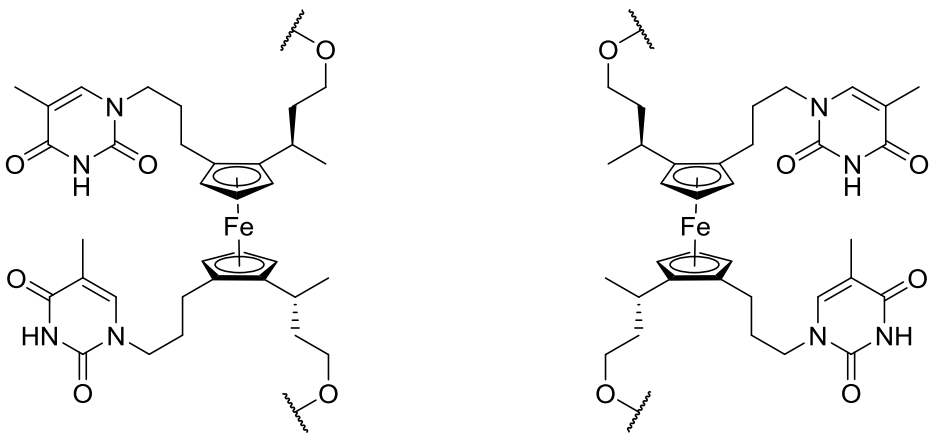
Fig. 2.41 Molecular dynamic simulation (5 ns) of duplexes S1**Fcn3c2TT**$_{(RR,SpSp)}$•S2**AA** and S1**Fcn3c2TT**$_{(SS,RpRp)}$•S2**AA**

The molecular modelling also provides evidence that **Fcn3c2TT**$_{(RRSpSp)}$ and **Fcn3c2TT**$_{(SSRpRp)}$ participate in H-bonding; in both cases the FcNA nucleobases are located within the duplex

and lie fairly co-planer with respect to those of the opposite strand (**Fig. 2.41**). In the case of S1**Fcn3c2TT**$_{(SS,RpRp)}$•S2**AA**, in which the natural curvature of the duplex is better maintained, the vertical alignment of the nucleobases may also indicate stabilisation through π-stacking interactions.

2.3.3.3 Dithyminyl FcNA Monomers with Three Carbon Nucleobase Linkers

It was hypothesised that increasing the nucleobase linker length from two to three carbon atoms may confer extra conformational flexibility to the base-pairing system, thus granting more freedom of movement for the alignment of stabilising H-bonds. Comparison of the T_m values suggests a more complex relationship however (**Table 2.4**). Intriguingly, with complementary **AA** bases on the S2 strand, the S1**Fcn3c3TT**$_{(RRpSpS)}$ duplex was less stable than the S1**Fcn3c2TT**$_{(RRpSpS)}$, whereas the opposite trend was observed for the other pair of enantiomers, with S1**Fcn3c3TT**$_{(SSpRpR)}$ producing a higher T_m than S1**Fcn3c2TT**$_{(SSpRpR)}$.

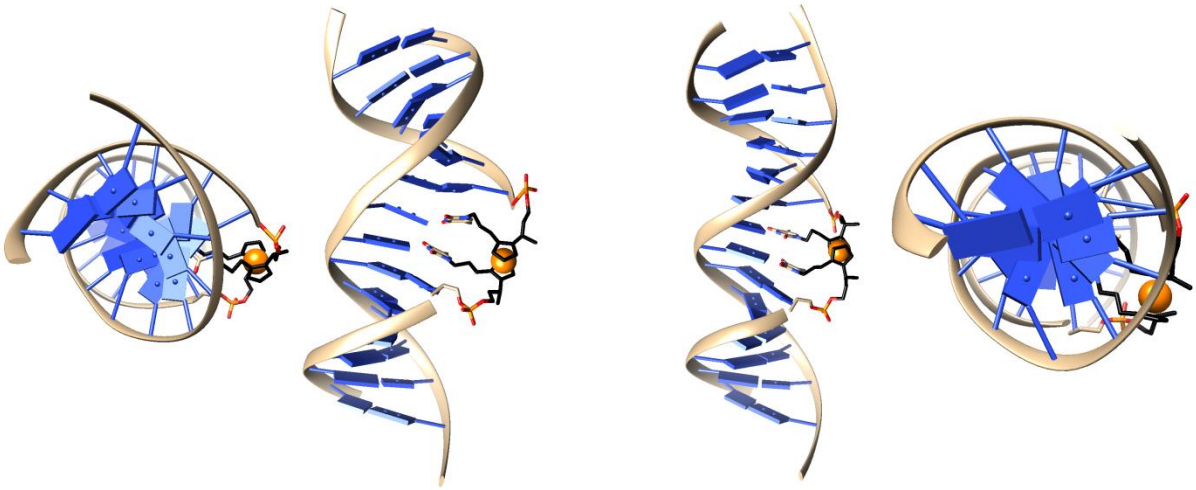


Fcn3c3TT$_{(RR,SpSp)}$ **Fcn3c3TT**$_{(SS,RpRp)}$

Fig. 2.42 The two enantiomeric dithyminyl FcNA dinucleotides with three carbon linkers to the nucleobase **Fcn3c3TT**$_{(RR,SpSp)}$ and **Fcn3c3TT**$_{(SS,RpRp)}$

For both S1**Fcn3c3TT**$_{(RR,SpSp)}$•S2**AA** and S1**Fcn3c3TT**$_{(SS,RpRp)}$•S2**AA**, molecular modelling locates the FcNA nucleobases within the duplex, in a fairly co-planar alignment with the

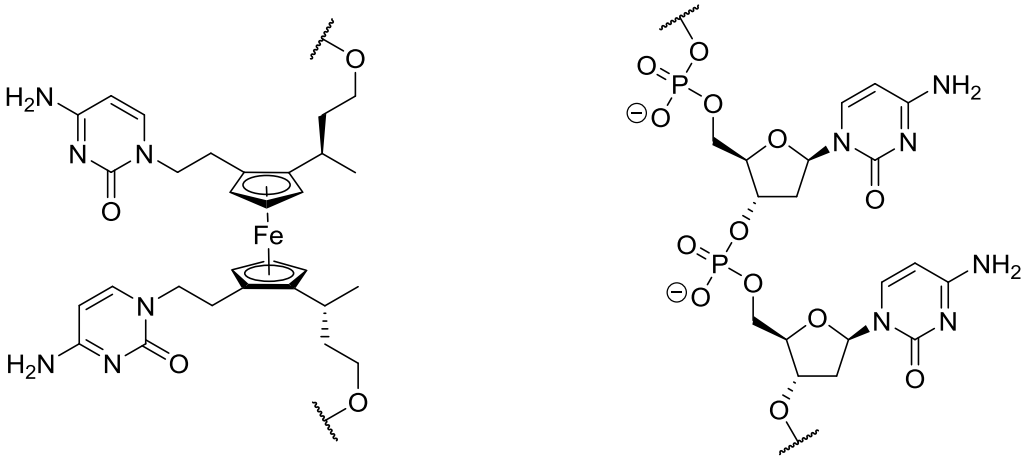
complementary bases opposite (**Fig. 2.44**). In both cases the planarity and vertical alignment of the nucleobases would also suggest stabilisation through π-stacking interactions.



S1**Fcn3c3TT**$_{(RR,SpSp)}$•S2**AA** S1**Fcn3c3TT**$_{(SS,RpRp)}$•S2**AA**

Fig. 2.43 Molecular dynamic simulations (5 ns) of S1**Fcn3c3TT**$_{(RR,SpSp)}$•S2**AA** and S1**Fcn3c3TT**$_{(SS,RpRp)}$•S2**AA**

2.3.3.4 A Dicytidyl FcNA monomer with a Two Carbon Nucleobase Linker


H2N
N
N
O
Fe
O
O
O

increase in T_m shown going from the S1**DNATT**•S2**AA** to the S1**DNACC**•S2**GG** duplex. Interestingly, this effect is slightly more pronounced in the FcNA system, the S1**Fcn3c2CC**$_{(RRpSpS)}$•S2**GG** duplex producing a T_m value 5 °C higher than the S1**Fcn3c2TT**$_{(RRpSpS)}$•S2**AA**. Nevertheless, the pure DNA system still produces a more stable duplex, with S1**DNACC**•S2**GG** producing a T_m value 12 °C higher than S1**Fcn3c2CC**$_{(RRpSpS)}$•S2**GG**.

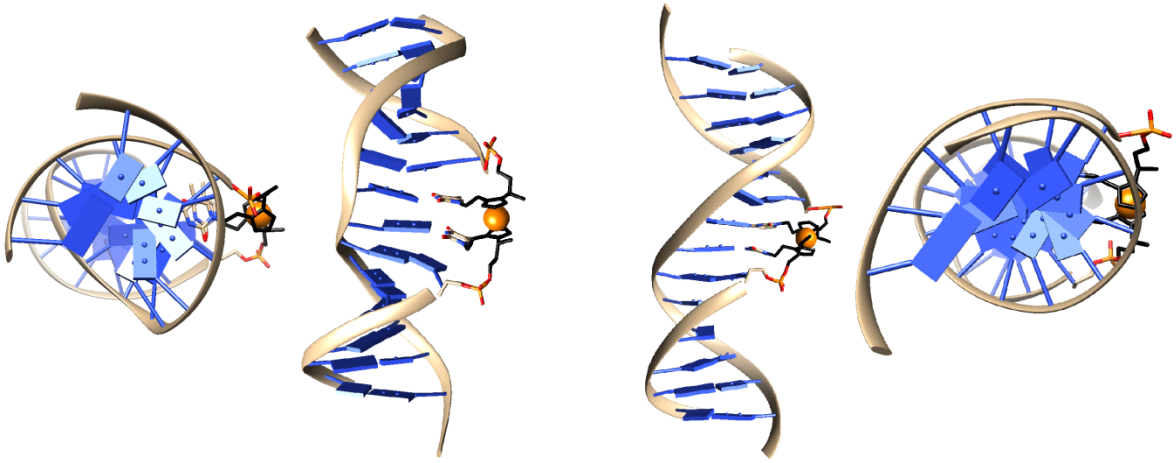


Fig. 2.1 Molecular Dynamic Simulation (5 ns) of S1**Fcn3c2TT**$_{(RRpSpS)}$•S2**AA** S1**Fcn3c2CC**$_{(RRpSpS)}$•S2**GG**

It is worth noting that the fully complementary duplex containing the dicytosinyl FcNA monomer seems to produce a more regular helix than corresponding dithyminyl FcNA duplex. In this case, the C–G base-pairs appear to be more co-planar than the corresponding T–A base-pairs, which would be expected given the extra hydrogen bond holding them together. The stabilisation may therefore be accentuated, the extra H-bond in turn facilitating greater π-stacking interactions between the nucleobase layers.

2.4 Conclusions

The bisubstituted FcNA **Fcc3HH**$_{(RR)}$ monomer was produced and, consisting of just the FcNA backbone, fulfilled the role of an 'abasic control'. Through comparison with this monomer, thermal melting studies showed that indeed, the nucleobase functionalities of the **Fcn3c2TT** and **Fcn3c3TT** monomers confer extra stability upon the resulting duplexes. Molecular modelling studies also provided additional evidence that this was due to the formation of complementary H-bonding and π-stacking interactions. The stabilising effect of the uncharged FcNA backbone was also demonstrated, producing a more stable duplex than the abasic DNA equivalent. In summary, we may therefore conclude that the strength of interaction between the two opposing dinucleotides on the S1 and S2 strands vary according to DNA:DNA > FcNA:DNA > FcNA:DNA (mismatch) > abasic FcNA:DNA.

The tetrasubstituted **Fcn3c3TT**$_{(RR,pSpS)}$ monomer was also successfully synthesised, complementing the **Fcn3c3TT**$_{(SS,pRpR)}$ which had been previously produced in the group. The effect of these monomers upon the T_m of an otherwise unmodified DNA duplex showed that planar chirality subtly influences the binding characteristics of the FcNA units. Though comparison with the corresponding **Fcn3c2TT** monomers it was demonstrated that the chirality and nucleobase linker length parameters combine in a complex fashion to produce the best fitting FcNA monomer.

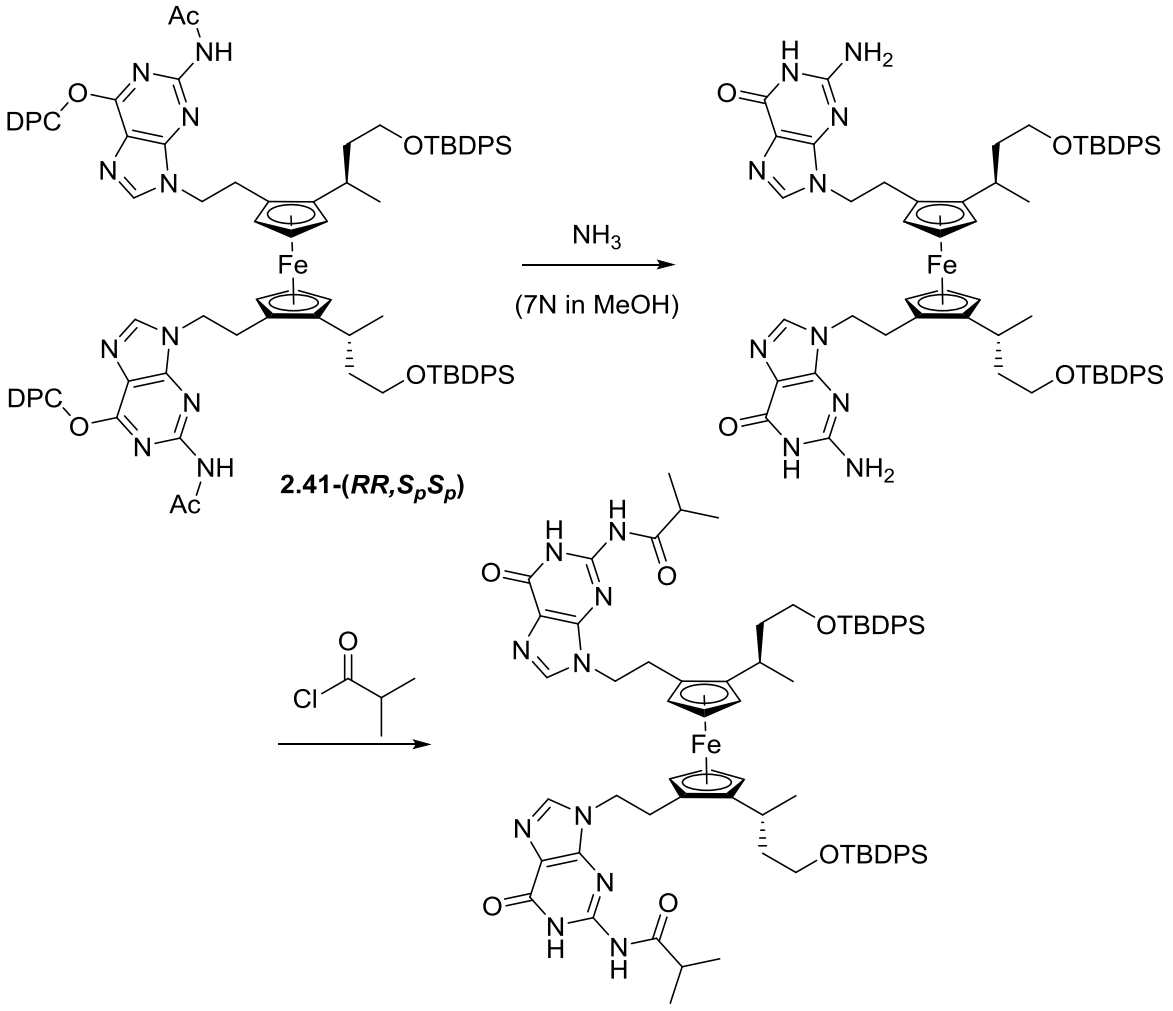
Although ultimately a question mark lies over the feasibility of oligomerisation, a synthetic route to produce the diguaninyl tetrasubstituted FcNA monomer precursor diol **Fcn3c2GG**$_{(RR,SpSp)}$ was also successfully established. Importantly, three steps, which hitherto had been used for the synthesis of all FcNA monomers, were replaced by a single step process, improving the efficiency in terms of both yield and time. In addition, simpler mono-

and diguaninyl ferrocene conjugates were produced during this process of development, the former displaying interesting properties relating to self-assembly in the solid state.

2.5 Future Work

2.5.1 Further investigation of Diguaninyl FcNA Monomer

Because only a small amount of the diguaninyl FcNA phosphoramidite was produced, only one coupling could be attempted, leaving some unanswered questions regarding the cause of the failed oligonucleotide synthesis. Further investigation of the diguaninyl FcNA monomer would therefore begin with the synthesis of another batch of the diol precursor **2.4-(*RR,S*$_p$*S*$_p$)** on a much larger scale. A large supply of this crucial compound would not only allow the re-investigation of the diguaninyl monomer **Fcn3c2GG**$_{(RR,SpSp)}$ but also enable the relatively rapid trialling of other guanine protecting strategies which may prove more successful.



Scheme 2.26 A possible solution for the removal of the bulky oxygen protecting group which involves re-protecting the exocyclic amine

It is quite possible that the sheer size of the guanine FcNA monomer was not compatible with the automated synthesis process. The first consideration should therefore be to reduce the size of the molecule prior to coupling. Unlike the protected exocyclic amine, the bulky oxygen protecting group, while crucial for the regioselectivity of the Mitsunobu reaction is not essential for automated synthesis. A strategy should therefore be implemented which removes this guanine protecting group following the Mitsunobu coupling. Although not elegant, one possible solution may be to deprotect at both oxygen and nitrogen, before selectively re-protecting the exocyclic amine (**Scheme 2.26**).

2.5.2 G-Quadruplex Formation

Although the tetrasubstituted guaninyl FcNA monomers were not successfully incorporated into oligonucleotides, a strategy for the coupling of ferrocene to guanine was demonstrated and small molecule guanine conjugates were produced. Given the current research interest in G-quadruplex formation, it would be very interesting to investigate the ability of these ferrocene guanine conjugates to form G-quartet or G-quadruplex structures.[56]

These tertiary structures are characteristic of guanine-rich sections of DNA such as that found in the telomeres, and are important structural features which help to secure the ends of the DNA strands so that the duplex does not unwind.[57] The structures are stabilised by the presence of a metal cation at the centre; sodium, caesium and potassium have all been found to perform this role. Four guanine nucleobases surround the metal cation, H-bonding via Hoogstein interactions to form a G-quartet. This repeated motif then forms stack to give an octet, which in turn, stack to produce the quadruplex structure (**Fig. 2.45**).

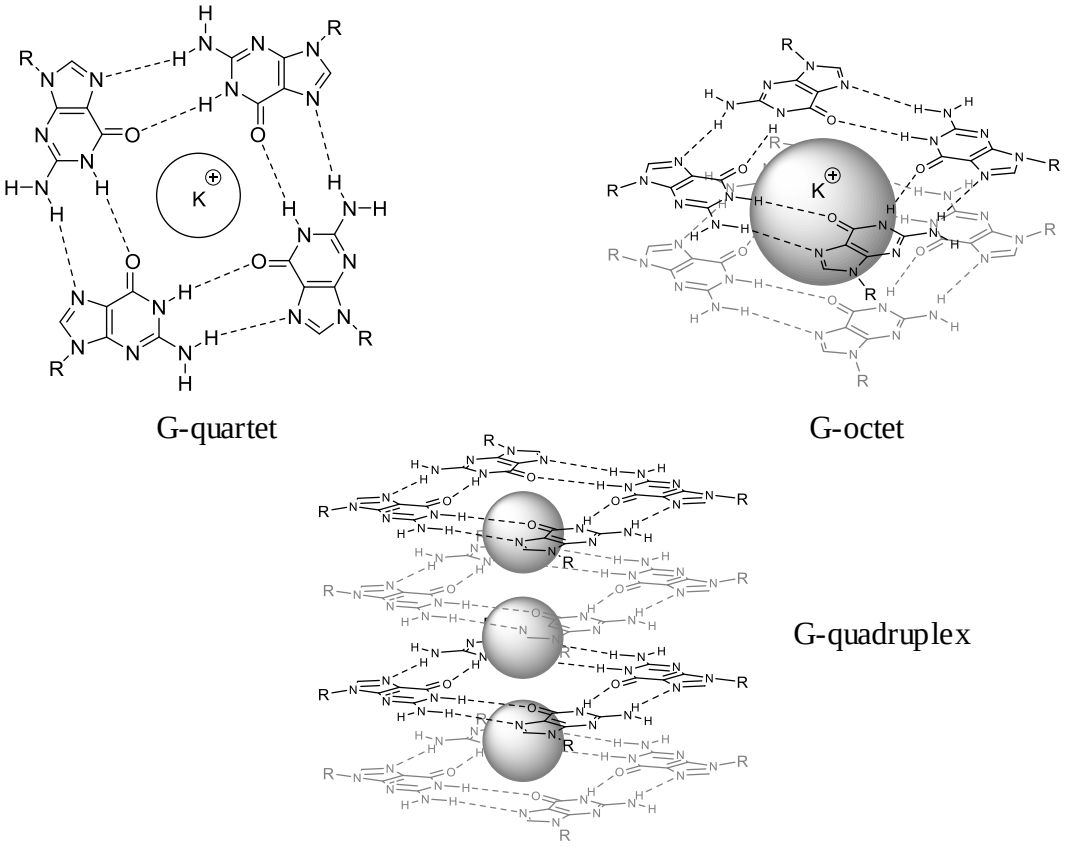


Fig. 2.45 The structures of a G-quartet, G-octet and G-quadruplex

Although predominantly found within guanine rich areas of DNA, small lipophilic, guanine containing molecules have also been shown to produce this motif. Investigating this self-assembly and with the hope of forming controllable ion channels, Jeffery Davis at the University of Maryland has produced these extended structures by adding potassium picrate to solutions of small molecule, modified lipophilic guanine nucleosides in organic solvents, thus disproving the dogma which had henceforth ascribed this behaviour to aqueous systems alone.[58,59,60]



Fig. 2.46 Small lipophilic guanine compounds which form G-quadruplexes in the presence of potassium picrate by Davis[58,59]

Future investigation into the G-quadruplex forming propensities of the guaninyl ferrocenes could prove very useful; it may be possible to harness the unique properties of ferrocene to produce electrochemical cation sensors or to induce novel G-quadruplex formation or dissociation through redox switched cation binding.[61]

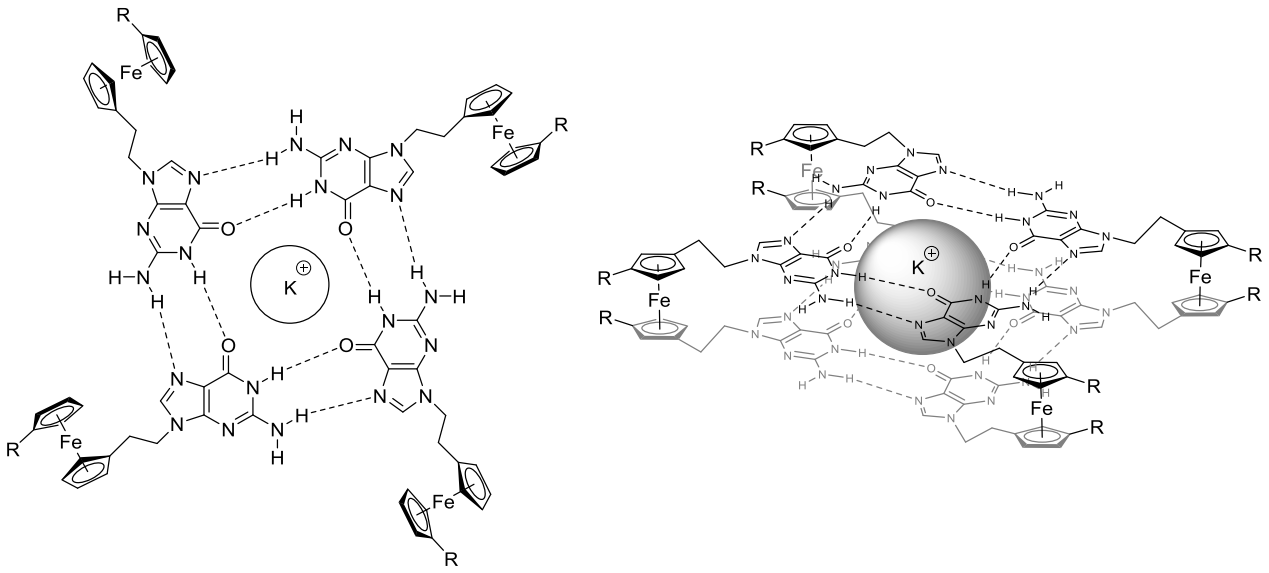


Fig. 2.47 Proposed ferrocene-containing G-quartet and G-quadruplexes in which R is a lipophilic group such as $–COC_9H_{19}$

Due to their lack of solubility in appropriate solvents, the mono- **2.31** and di-guaninyl **2.37** ferrocenes produced thus far are not suitable for this purpose. The simple attachment of extra lipophilic groups, such as the $–COC_9H_{19}$ however may improve their solubility and hence render the compounds more suitable for this purpose (**Fig. 2.47**).

2.6 References

[1] C. Darwin, *On the Origin of Species by Means of Natural Selection, Or, the Preservation of Favoured Races in the Struggle for Life*, **1859**, London J. Murray.

[2] J. D. Watson, F. H. C. Crick, *Nature*, **1953**, 171, 737 – 738.

[3] F. H. C. Crick, *Nature*, **1970**, 227, 561 – 563.

[4] E. S. Lander, *Nature*, **2011**, 470, 187 – 197.

[5] P. A. Limbach, P. F. Crain, J. A. McCloskey, *Nucleic Acids Res.*, **1994**, 22, 2183 – 2196.

[6] J. H. Gommers-Ampt, P. Borst, *FASEB J.*, **1995**, 9, 1034 – 1042.

[7] J. Jonsson, M. Sandberg, S. Wold, *J. Chemometrics*, **1996**, 10, 163 – 170.

[8] M. M. Suzuki, A. Bird, *Nature Reviews Genetics*, **2008**, 9, 465 – 476.

[9] M. D. Kirnos, I. Y. Khudyakov, N. I. Alexandrushkina, B. F. Vanyushin, *Nature*, **1977**, 270, 369 – 370.

[10] C. Bailly, M. J. Waring, *Nuc. Acids Res.*, **1998**, 26, 4309 – 4314.

[11] B. L. Gaffney, L. A. Marky, R. A. Jones, Tetrahedron, **1984**, 40, 3 – 13.

[12] M. Szekeres, A. V. Matveyev, *FEBS Lett.*, **1987**, 222, 89 – 94.

[13] Q. Wang, L. Chen, Y. Long, H. Tian, J. Wu, *Theranostics*, **2013**, 395 – 408.

[14] J. N. Wilson, E. T. Kool, *Org. Biomol. Chem.*, **2006**, 4, 4265 – 4274.

[15] M. J. Rist, J. P. Marino, *Curr. Org. Chem.*, **2002**, 6, 775 – 793.

[16] H. –B. Kraatz, *J. Inorg. Organomet. Polym. Mater.*, **2005**, 15, 83 – 106.

[17] S. L. Beaucage, M. H. Caruthers, *Tetrahedron Lett.*, **1981**, 22, 1859 – 1862.

[18] M. D. Matteucci, M. H. Caruthers, *J. Am. Chem. Soc.*, **1981**, 103, 3185 – 3191.

[19] G. H. Clever, C. Kaul, T. Carell, *Angew. Chem. Int. Ed.*, **2007**, 46, 6226 – 6236.

[20] G. H. Clever, M. Shionoya, *Coord. Chem. Rev.*, **2010**, 254, 2391 – 2402.

[21] S. Katz, *Biochim. Biophys. Acta.*, **1963**, 68, 240 – 253.

[22] A. Ono, S. Cao, H. Togashi, M. Tashiro, T. Fujimoto, T. Machinami, S. Oda, Y. Miyake, I. Okamoto, Y. Tanaka, *Chem. Commun.*, **2008**, 2825 – 2827.

[23] K. Tanaka, M. Shionoya, *J. Org. Chem.*, **1999**, 64, 5002 – 5003.

[24] K. Tanaka, Y. Yamada, M. Shionoya, *J. Am. Chem. Soc.*, **2002**, 124, 8802 – 8803.

[25] K. Tanaka, A. Tengeiji, T. Kato, N. Toyama, M. Shiro, M. Shionoya, *J. Am. Chem. Soc.*, **2002**, 124, 12494 – 12498.

[26] K. Tanaka, G. H. Clever, Y. Takezawa, Y. Yamada, C. Kaul, M. Shionoya, T. Carell, *Nat. Nanotechnol.*, **2006**, 1, 190 – 194.

[27] P. E. Nielsen, M. Egholm, R. H. Berg, O. Buchardt, *Science*, **1991**, 254, 1497 – 1500.

[28] S. Shakeel, S. Karim, A. Ali, *J. Chem. Technol. Biotechnol.*, **2006**, 81, 892 – 899.

[29] P. E. Nielsen, *Pure. Appl. Chem.*, **1998**, 70, 105 – 110.

[30] M. Egholm, O. Buchardt, L. Christensen, C. Behrens, S. M. Freier, D. A. Driver, R. H. Berg, S. K. Kims, B. Norden, P. E. Nielsen, *Nature*, **1993**, 365, 566 – 568.

[31] S. Shakeel, S. Karim, A. Ali, *J. Chem. Technol. Biotechnol.*, **2006**, 81, 892 – 899.

[32] V. N. Pandey, A. Upadhyay, B. Chaubey, *Expert Opin. Biol. Ther.*, **2009**, 9, 975 – 989.

[33] K. E. Nelson, M. Levy, S. L. Miller, *Proc. Natl. Acad. Sci. USA*, **2000**, 97, 3868 – 3871.

[34] P. G. Higgs, N. Lehmam, *Nature Reviews Genetics*, **2015**, 16, 7 – 17.

[35] A. Ono, H. Togashi, *Angew. Chem. Int. Ed.*, **2004**, 43, 4300 – 4302.

[36] J-L. H. A. Duprey, D. M. Bassani, E. I. Hyde, C. Ludwig, A. Rodger, J. S. Vyle, J. Wilkie, Z-Y. Zhao, J. H. R. Tucker, *Supramolecular Chemistry*, **2011**, 23, 273 – 277.

[37] S. Takenaka, Y. Uto, H. Kondo, T. Ihara, M. Takagi, *Anal. Biochem.*, **1994**, 218, 436 – 443.

[38] C. Fan, K. W. Plaxco, A. J. Heeger, *Proc. Natl. Acad. Sci. USA*, **2003**, 100, 9134 – 9137.

[39] M. Nakayama, T. Ihara, K. Nakano, M. Maeda, *Talanta*, **2002**, *56*, 857 – 866.

[40] H. V. Nguyen, Z. Zhao, A. Sallustrau, S. L. Horswell, L. Male, A. Mulas, J. H. R. Tucker, *Chem. Commun.*, **2012**, 48, 12165 – 12167.

[41] A. N. Patwa, S. Gupta, R. G. Gonnade, V. A. Kumar, M. M. Bhadbhade, K. N. Ganesh, *J. Org. Chem.*, **2008**, 73, 1508 – 1515.

[42] A. E. Navarro, N. Spinelli, C. Moustrou, C. Chaix, B. Mandrand, H. Brisset, *Nuc. Acids Res.*, **2004**, 32, 5310 – 5319.

[43] L. Schwink, P. Knochel, *Chem. Eur. J.*, **1998**, 4, 950 – 968.

[44] M. Edmonds, A. Abell, *Modern Carbonyl Olefination*, Wiley-VCH Verlag GmbH and Co., **2004**, 1 – 16.

[45] O. Mitsunobu, M. Yamada, *Bull. Chem. Soc. Jpn.*, **1967**, 40, 2380 – 2382.

[46] T. Y. S. But, P. H. Toy, *Chem. Asian J.*, **2007**, 2, 1340 – 1355.

[47] S. Schenk, J. Weston, E. Anders, *J. Am. Chem. Soc.*, **2005**, 127, 12566 – 12576.

[48] W. Lu, S. Sengupta, J. L. Petersen, N. G. Akhmedov, X. Shi, *J. Org. Chem.*, **2007**, 72, 5012 – 5015.

[49] R. Zou, M. J. Robins, *Can. J. Chem.*, **1987**, 65, 1436 – 1437.

[50] T. Giorgi, F. Grepioni, I. Manet, P. Mariani, S. Masiero, E. Mezzina, S. Pieraccini, L. Saturni, G. P. Spada, G. Gottarelli, *Chem. Eur. J.*, **2002**, 8, 2143 – 2152.

[51] A. Allerhand, P. V. R. Schleyer, *J. Am. Chem. Soc.*, **1963**, 85, 1715 – 1723.

[52] D. Bonchev, P. Cremaschi, *Theoret. Chim. Acta (Berl.)*, **1974**, 35, 69 – 80.

[53] R. Thomas, *Gene*, **1993**, 135, 77 – 79.

[54] R. Thomas, *Trans. Faraday Soc.*, **1954**, 50, 304.

[55] J. –L. Mergny, L. Lacroix, *Oligonucleotides*, **2003**, 13, 515 – 537.

[56] M. L. Bochman, K. Paeschke, V. A. Zakian, *Nature Rev. Genet.*, **2012**, 13, 770 – 780.

[57] H. J. Lipps, D. Rhodes, *Trends Cell Biol.*, **2009**, 19, 414 – 422.

[58] J. T. Davis, *Angew. Chem. Int. Ed.*, **2004**, 43, 668 – 698.

[59] S. L. Forman, J. C. Fettinger, S. Pieraccini, G. Gottarelli, J. T. Davis, *J. Am. Chem. Soc.*, **2000**, 122, 4060 – 4067.

[60] W. Guschlbauer, J. F. Chantot, D. J. Thiele, *J. Biomol. Struct. Dynam.*, **1990**, 8, 491 – 511.

[61] J. H. R. Tucker, S. R. Collinson, *Chem. Soc. Rev.*, **2002**, 31, 147 – 156.

3 Synthesis and Biological Activity of Novel Ferrocenyl Nucleoside Analogues

3.1 Introduction

Although predominantly watery, organic beings, humans also require a small but crucial supply of metallic micronutrients to maintain healthy functioning.[1] Among others, deficiencies of iron, zinc and copper can lead to serious illnesses including anaemia, growth defects and heart disease.[2] Conversely, the presence of metals of the wrong type or in the wrong concentration can also have a deleterious effect. Heavy metals such as mercury and lead are well known to damage vital organs and are often implicated, but lighter metals such as beryllium and lithium can also display toxic effects at high concentration.[3,4] Given their profound effects upon the body, it is no wonder that metals have been employed to both therapeutic and malicious effect throughout human history. Dating from 200 B.C., the *Shen Nong Ban Cao Jing* recommended various arsenic minerals including orpiment (As_2S_3), realgar (As_4S_4) and arsenolite (As_4O_6) for the treatment of diverse disorders such as cancer, syphilis, psoriasis and ulcers.[5] Similarly, the Ayurvedic practitioners of India pioneered metallo-herbal remedies, introducing compounds of gold, silver, copper, iron, zinc and even mercury in the preparation of their *rasa shastra* concoctions.[6] Although our modern ears may baulk at such apparent primitivism, the therapeutic use of poisonous metals has stood the test of time; the practice continues today, everyday across the world. Indeed, arsenic trioxide is now approved by western medicine to treat certain forms of leukemia, and radioactive implants of palladium and iridium are used in brachytherapy against prostate cancer.[7,8]

Predominantly however, our pharmacopeia consists of wholly organic molecules.[9] Hundreds of thousands of years of evolution have presented humankind with an abundance of

efficacious small molecules, biosynthesised and directed towards biochemical modulation. Naturally these molecules have formed the basis of our medicinal chemistry and have overwhelmingly preoccupied the research field.[10] It was only after the serendipitous discovery and subsequent development of the anticancer drug cisplatin that inorganic medicinal chemistry was seriously investigated. [11]

3.1.1 Cisplatin

Although known for years as "Peyrone's salt", the biological significance of the simple square-planar metal complex *cis*-$[Pt(NH_3)_2(Cl)_2]$ was only realised after it was inadvertently generated during an investigation into the effects of electric current upon *Escherichia coli* (E. coli) bacteria.[12,13] Having formed at the surface of the platinum electrode, it was concluded that this compound was responsible for inhibiting the proliferation of the bacteria. Subsequent studies demonstrated excellent activity against cancerous cells leading to the development of cisplatin, a very successful anti-tumour agent which transformed the world of chemotherapy (**Fig. 3.1**).[14] Effective against a range of sarcomas and carcinomas, its impact against testicular cancer is particularly noteworthy, improving the cure rate from 10 to 85%.[15]

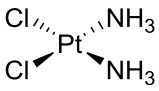


Fig. 3.1 The structure of cisplatin

While in the blood, the high concentration of chloride ions prevents aquation, and hence the chloride ligands remain bound to the complex. Once inside the cell however, the chloride ligands can be displaced by water and the complex binds to the nitrogenous nucleobases of DNA (most commonly at the *N7* position of guanine), causing irreversible interstrand cross-linkage and intrastrand kinking of the duplex. The major functions of the genetic material are thus severely impaired and apoptosis (programmed cell-death) is initiated.[16]

3.1.2 Medicinal Bioorganometallic Chemistry

Although for some time organometallic complexes were considered unlikely candidates for use in the biological setting, in 1979 Köpf-Maier and Köpf realised that d-electron deficient, *cis*-dihalide metallocenes could in fact be perfectly suited to the types of reactivity exhibited by cisplatin and soon confirmed titanocene dichloride as the first cytostatic metallocene (**Fig. 3.2**).[17] In subsequent years more dihalide metallocenes conforming to the general structure $M(\eta\text{-}C_5H_5)_2X_2$ and bearing metals such as vanadium, niobium and molybdenum at their centre were confirmed to exhibit tumor-inhibiting properties.[18]



a) **b**)

Fig. 3.2 a) Titanocene dichloride and **b**) the general structure of the bent metallocenes $M(\eta\text{-}C_5H_5)_2X_2$, where M = Ti, V, Nb and Mo; X = F, Cl, Br, I, NCS and N_3[18]

Although the actual mechanism of action of these 'bent' metallocenes is in some ways distinct from that of cisplatin, their medicinal potential had been realised and a new era of bioorganometallic chemistry had begun.[18,19] It is now recognised that, as well as offering far greater structural versatility and hence vastly more nuanced physicochemical properties, in contrast to other metal-complex containing pharmaceuticals such as cisplatin, organometallic compounds exhibit direct carbon-metal bonding which offers the possibility for novel modes of action.[20] Alongside the metallocenes, three other biologically relevant classes have so far been identified: the closely related M-arenes (also known as "half-sandwich" or "piano-stool" complexes), M-carbenes and M-carbonyls (**Fig. 3.3**).[20]

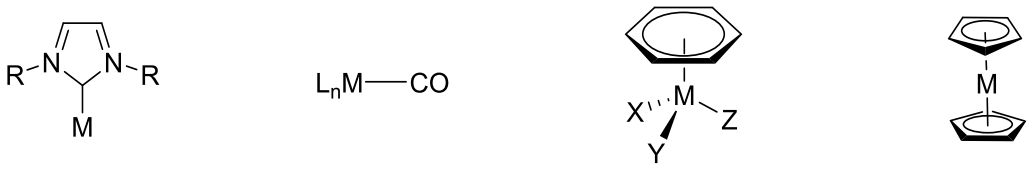


Fig. 3.3 The four main classess of organometallic compound with medicinal relevance **a**) M-carbene, **b**) M-carbonyl, **c**) M-arene and **d**) metallocene

3.1.3 Ferrocene and Ferrocenium Compounds

With no labile ligands, a full complement of d-electrons and with the central metal sandwiched tightly between the two Cp rings, ferrocene was certainly not expected to share the cytotoxic properties of other metallocenes. In 1984 however, to the surprise of Köpf-Maier and Köpf, the oxidised form of ferrocene was found to exert an antineoplastic effect upon Ehrlich ascites tumour cells implanted in mice.[21] It is believed that this type of cytotoxicity originates from the redox cycling between the neutral ferrocene (II) and the positively charged ferrocenium (III) forms according to a Fenton-type mechanism.[22] This catalyses the breakdown of cellular hydrogen peroxide into reactive oxygen species (ROS) such as the hydroxyl (**Eq. 3.1**) and hydroperoxide (**Eq. 3.2**) radicals which are very damaging to the cells.[23,24] It has been shown that cancer cells develop high concentrations of hydrogen peroxide and therefore may be more susceptible to these agents than normal healthy cells.[25]

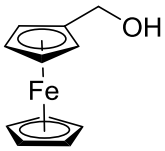
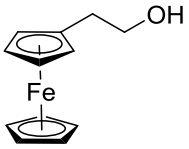
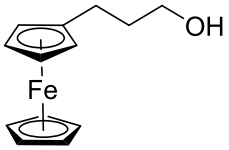
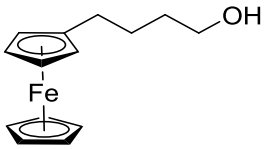
(**Eq. 3.1**) $Fe^{2+} + H_2O_2 \rightarrow Fe^{3+} + \bullet OH + OH^-$

(**Eq. 3.2**) $Fe^{3+}\ H_2O_2 \rightarrow Fe^{2+} + \bullet OOH + H^+$

To investigate the importance of these types of redox processes in the cytotoxicity of ferrocene compounds, Swarts evaluated a series of simple ferrocene-containing alcohols, relating the cytotoxicity to both the hydroxyl linker length and the formal reduction potential ($E^{o'}$).[26] Four compounds were investigated, with hydroxyl linker lengths of one, two, three and four carbon atoms respectively. The $E^{o'}$ values were measured versus an Ag/Ag^+

reference electrode in acetonitrile and the cytotoxicities given as mean IC_{50} values against HeLa cells over seven days (**Table 3.1**).

Table 3.1 The cytotoxicity (IC_{50})[a] and formal reduction potentials ($E^{o'}$)[b] of a series of ferrocenyl alcohols by Swarts[26]

Compound	Linker Length (C atoms)	$E^{o'}$[b] (V)	IC_{50}[a] (μM)
	1	0.111	>100
	2	0.029	35.0
	3	0.029	17.0
	4	0.026	5.7

[a] After 7 days incubation against HeLa cells. [b] Versus an Ag/Ag^+ electrode in MeCN

In general, the cytotoxicity increases as $E^{o'}$ decreases, however the correlation is not complete. Ferrocenyl propanol, for instance is twice as potent as ferrocenyl ethanol yet the $E^{o'}$ value is identical; clearly other factors must be contributing to the change in biological activity. A more direct correlation is observed between cytotoxicity and the hydroxyl linker length, with every additional methylene group conferring increased potency. The hydroxyl linker length and the $E^{o'}$ value are of course intimately connected; as the linker length increases, the Fc^+ ion gains additional stabilisation from the positive inductive effects of the

growing alkyl chain, the oxidised form therefore becomes more stable, reflected in a lower value of E^{o}'. Interestingly, the author concludes that the cytotoxicity is simply due to the ease of enzymatic oxidation of the ferrocenyl to the ferrocenium species. Although alluded to by the results, no consideration is given to the other possibly important factor, the lipophilicity; which is again directly related to the hydroxyl linker length and is largely responsible for a compounds membrane solubility and hence concentration within the cell.[27]

The biologically apposite properties of ferrocene as a stable, lipophilic, neutral compound also render the molecule a very suitable modification for existing medicinal agents. Early experimentation in the 1970s by Edwards led to the investigation of ferrocenyl-penicillin and ferrocenyl-cephalosporins as possible means to overcome the growing resistance to more conventional antibiotics.[28] In each case the core structure was maintained and the variable aromatic side groups substituted for ferrocene, the essential antibiotic activity of the β-lactamase parent compound was thus retained (**Fig. 3.4**).[28]

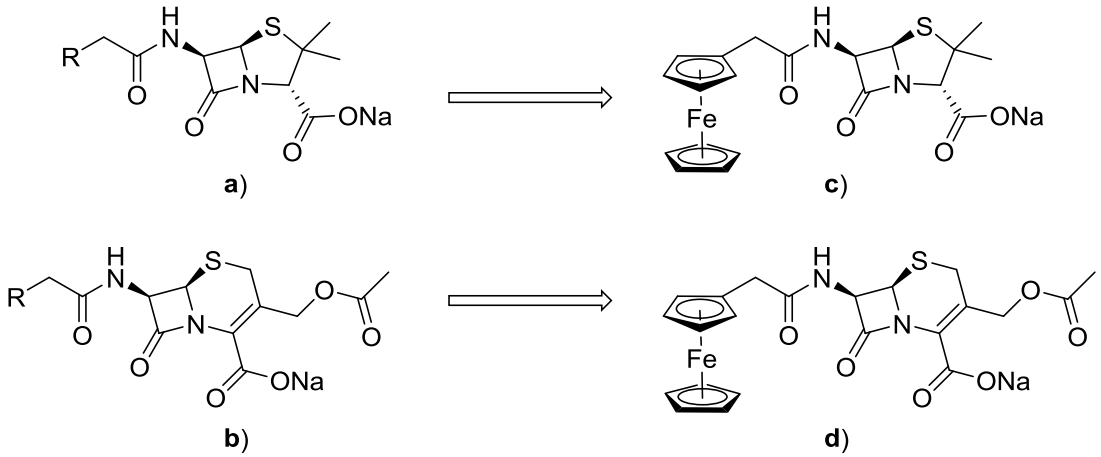


Fig. 3.4 The core structures of **a**) penicillin and **b**) cephalosporin, and the corresponding ferrocenyl derivatives **c**) and **d**) produced as sodium salts by Edwards[28]

More recently, this trend for incorporating ferrocene into established pharmaceutical architectures has led to the development of two particularly noteworthy drugs: ferrocifen (the

ferrocenyl analogue of Tamoxifen) and ferroquine (the ferrocenyl analogue of chloroquine) in which modification with ferrocene has enhanced the activity of the parent compound.[29,30]

3.1.3.1 Ferroquine

Reported by Biot in 1997, ferroquine is the ferrocenyl analogue of chloroquine, which has for many decades been a successful anti-malarial drug (**Fig. 3.5**).[30] Widespread use however has led to the parasite evolving resistance and these traditional quinoline-type agents are therefore increasingly ineffective in the tropics.[31,32]

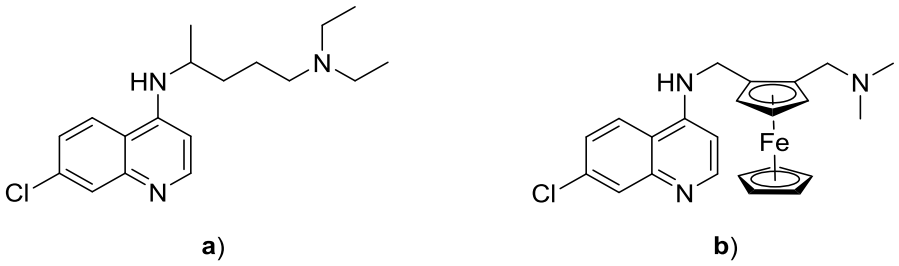


Fig. 3.5 a) the structure of the antimalarial drug chloroquine, and **b**) the ferrocenyl derivative ferroquine

Malarial trophozoites feast upon host haemoglobin, digesting the protein into its constituent amino acids and releasing haem. To avoid the accumulation of this toxic by-product, it is rendered inert by a process of biocrystallisation and stored safely in the food vacuole as innocuous haemozoin crystals.[33] There is much evidence that, alongside other deleterious biological effects, the weakly basic chloroquine concentrates in the acidic environment of the digestive vacuole and forms complexes with free haem; thus interfering with these important processes of storage and removal and effectively allowing the parasite to poison itself.[34,35,36,37] Resistance to chloroquine is thought to derive from the mutated Plasmodium falciparum Chloroquine Resistance Transporter (PfCRT) protein, which recognises and ejects chloroquine from the digestive vacuole, thus allowing the normal metabolic processes of detoxification to continue.[38] It has been shown that it is the aminoquinoline functionality of

chloroquine which crucially interrupts the formation of haemozoin and it is no surprise therefore that ferroquine, with the ferrocene moiety inserted into the side-chain, conforms to a similar mechanism of action.[39] Interestingly, it was found that reduction of the amine substituents from ethyl to methyl groups also actually boosted the activity of the ferrocene derivative. Most importantly however, ferroquine is active against chloroquine resistant strains; it is hypothesised that the bulky metallocene is not recognised by the mutated PfCRT protein and hence cannot be ejected from the site of action in the digestive vacuole. Ferroquine entered phase II clinical trials in 2007.[40]

3.1.3.2 Ferrocifen

First reported in 1996 by Jaouen, ferrocifen is an analogue of the successful breast cancer drug tamoxifen, in which ferrocene replaces one of the phenyl units of the active metabolite 4-hydroxytamoxifen (**Fig. 3.6**).[29] Tamoxifen acts as an antiproliferative, competitively binding to oestrogen receptor alpha (ERα), the activation of which is crucial to the growth of hormone dependent breast cancer cells.[41, 42]

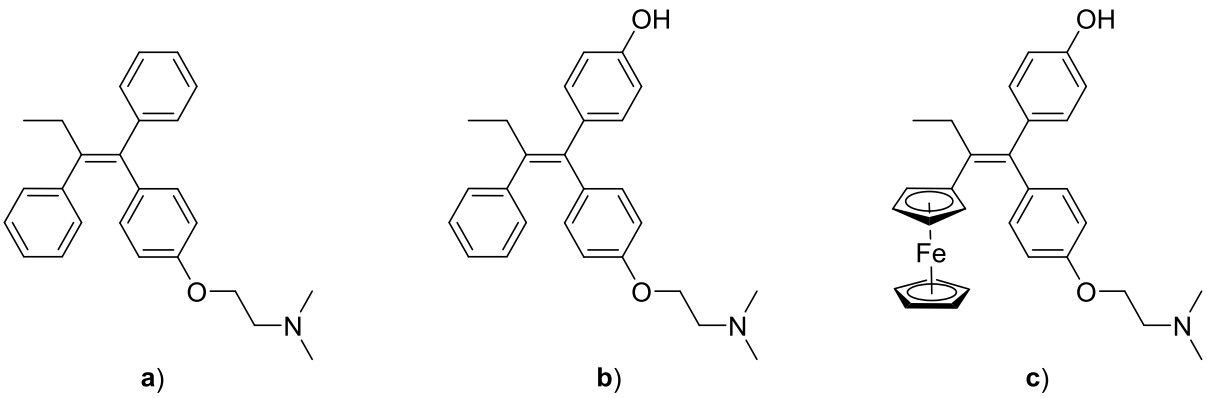
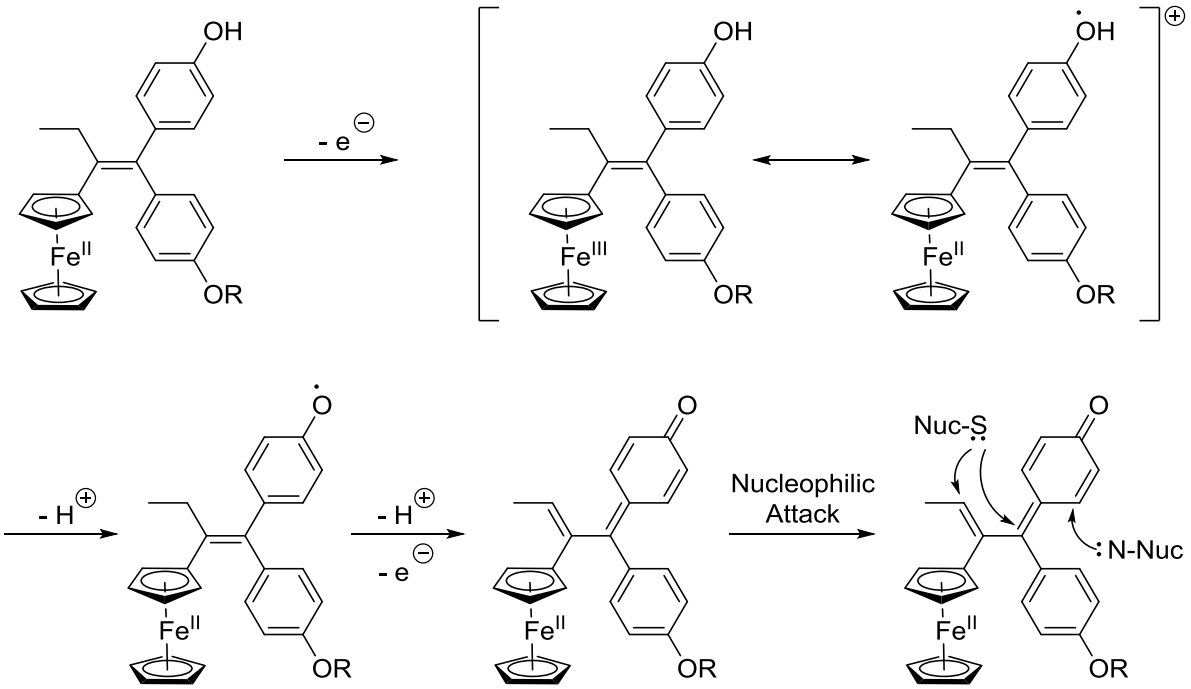


Fig. 3.6 a) the successful breast cancer drug tamoxifen, **b**) the active metabolite 4-hydroxytamoxifen, and **c**) the ferrocenyl derivative ferrocifen

Although the ERα binding affinity is somewhat reduced, the ferrocene derivative maintains the essential cytostatic mode of action of the parent compound, inhibiting the proliferation of

the tumours.[43] Cytotoxicity however is also observed, most surprisingly against both oestrogen-dependent and non-oestrogen-dependent breast cancer cells, thus indicating an entirely different mechanism of action. Evidence for the specific requirement of iron was also provided through investigations into the structurally similar ruthenocene derivatives, which although continuing to exhibit cytostatic activity, lacked the cytotoxicity of their iron-containing counterparts.[44] Having established that in the most cytotoxic compounds, the ferrocene unit is positioned *trans*- to a *para*- substituted phenol, with an ethyl group attached to the same carbon atom, a redox activation process, in which a highly reactive quinone methide is formed, was proposed to account for this striking difference in activity (**Scheme 3.1**).[45]



Scheme 3.1 Redox activation of ferrocifen to the reactive quinone methide proposed by Jaouen[46]

The ferrocene unit is first oxidised to the ferrocenium ion, which, through conjugation gives a resonance form with a radical on the phenol group. The acidic proton can then be abstracted to give the phenoxyl radical before a second oxidation, accompanied by loss of a proton,

gives the quinine methide. Nucleophilic attack by biological sulfur (such as glutathione) and nitrogen (such as the nucleobases) is then expected to give the 1,6- and 1,8- or 1,4- Michael additions respectively forming adducts which could account for the cytotoxicity of the compound.[45,46]

Clearly, in comparison with ferroquine, in which the ferrocene unit seems to assume a fairly passive, albeit very important role in subtly modulating the physicochemical parameters of the parent compound, ferrocifen demonstrates the powerful potential of ferrocene to open up new modes of action which are fairly specific to its unique set of physical, chemical and redox properties.

3.1.4 Nucleoside Analogues

The idea of slowing the growth of rapidly dividing cells through the inhibition of their nucleic acid synthesis was first proposed in the late 1940's by Hitchings, who later, alongside Sir James Black and Gertrude Elion, won the Nobel Prize for Physiology or Medicine for his pioneering work on chemotherapy.[47,48] Hitchings originally developed a number of compounds such as 2,6-diaminopurine and mercaptopurine which showed great promise as inhibitors of nucleic acid synthesis in leukemia.[49] Since then numerous nucleoside analogues and closely related nucleobase analogues have been developed to treat a wide range of cancers, blood disorders and as antiretroviral agents.[50]

In general, these agents closely mimic the endogenous nucleosides and as such comprise of a hydroxyl group, a sugar and a nucleobase (**Fig. 3.7**). While modifications are often applied to the nucleobase moiety, it remains, alongside the hydroxyl group a crucial structural feature necessary for recognition by the cellular machinery. Conversely, the sugar unit can be far

more varied and in some cases completely dispensed with. This is clearly demonstrated by abacavir, in which the sugar is replaced by a carbocycle; acyclovir, which features an ether linkage; and penciclovir, in which two pseudo-5′-hydroxy groups are attached to the nucleobase by a simple alkyl linker.[51,52,53] The simplest generic nucleoside analogue can therefore be conceived as a hydroxy group attached to a nucleobase moiety through an appropriate linker unit.[54]

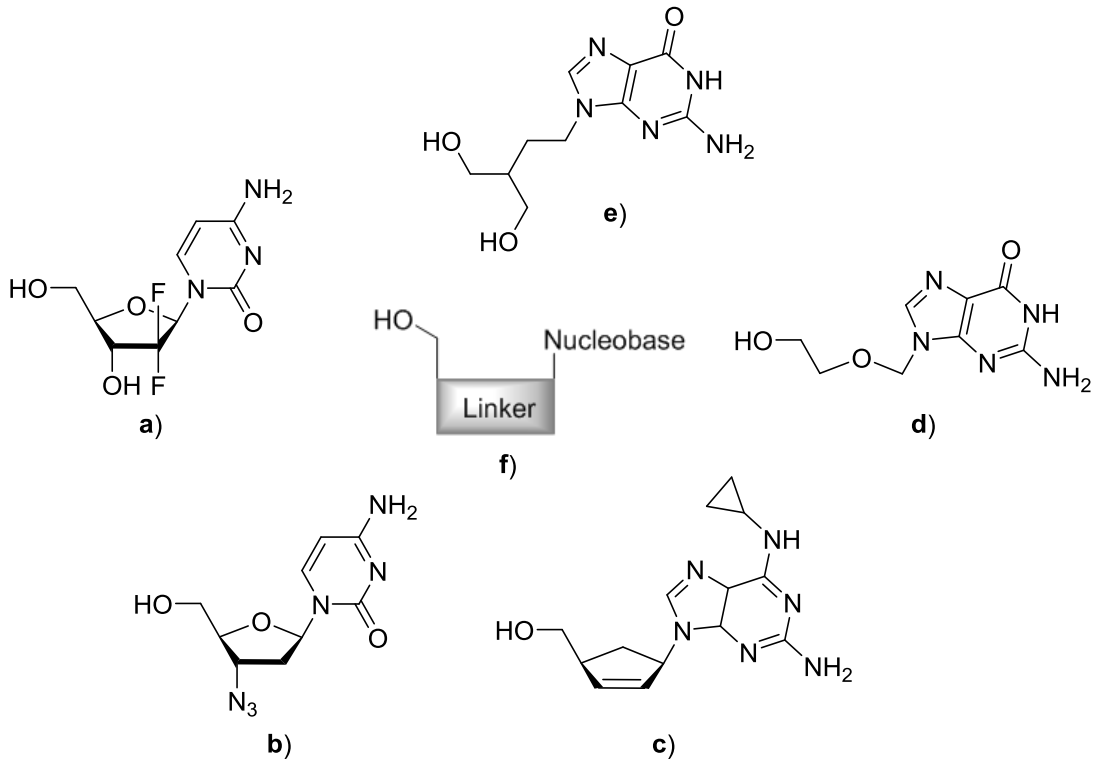


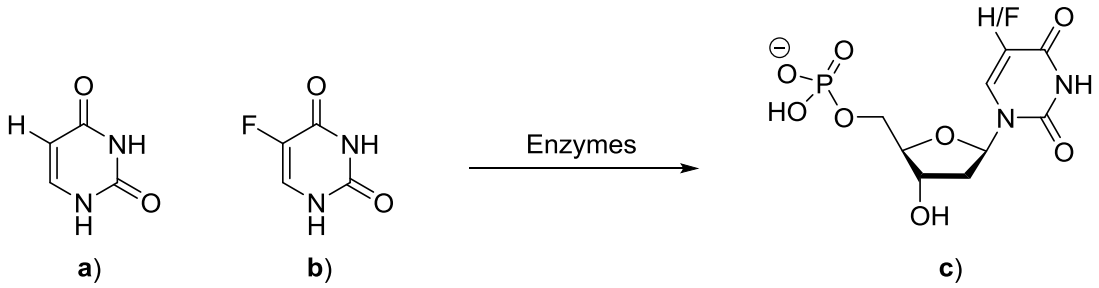
Fig. 3.7 Five successful nucleoside analogues **a**) gemcitabine, **b**) AZT, **c**) abacavir, **d**) acyclovir and **e**) penciclovir; and **f**) a simplified, generic structural representation

As discussed in more detail below, although the details are specific to each agent, all nucleoside analogues act as antimetabolites, mimicking the endogenous substrates of nucleic acid synthesis and as such typically require activation within the cell to the triphosphate form.[50] Cytotoxic or antiviral action is then achieved either through blocking the output of essential enzymes (e.g. 5-fluorouracil) or by being incorporated into and thus denaturing the oligonucleotide product itself (e.g. gemcitabine and azidothymidine).[55,56,57] The rapidly

proliferating cells which typify cancer are more susceptible to these agents due to the high turnover of nucleosidic substrates required for cell division.[58]

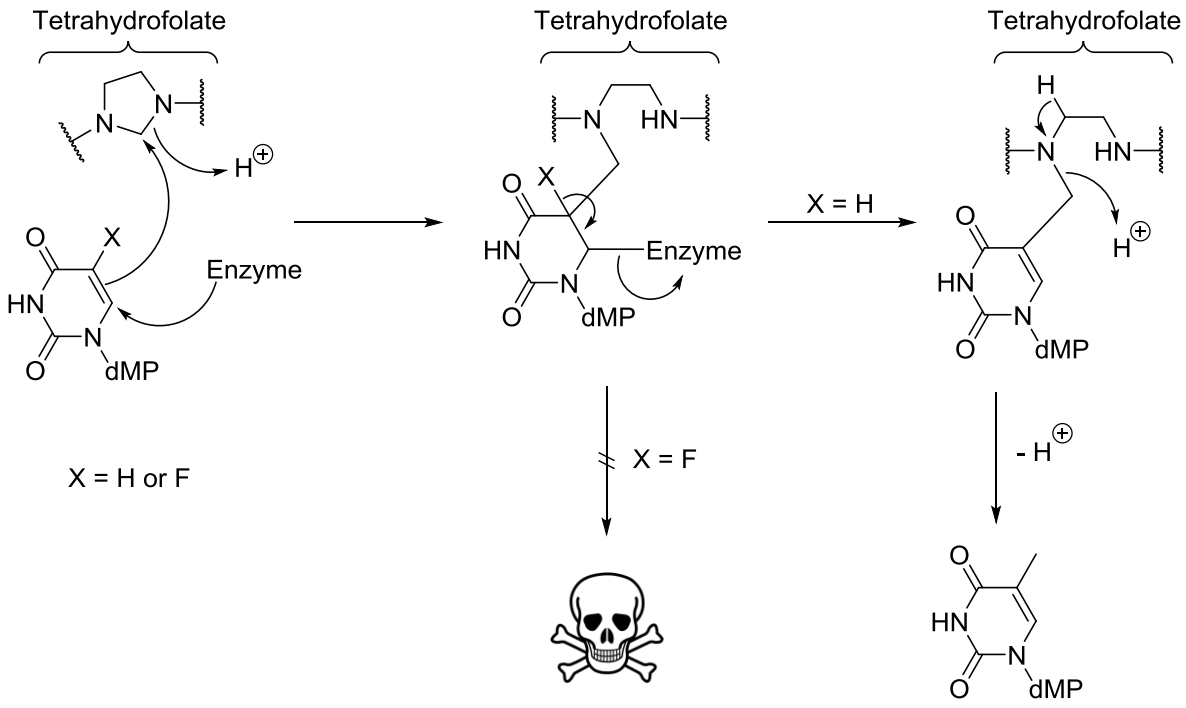
3.1.4.1 5-Fluorouracil

Discovered in 1957 by Dushinsky, Pleven and Heidelberger, 5-fluorouracil (5-FU) is a potent anticancer drug effective against a range of malignant tumours including colorectal and breast cancers.[59,60] Targeting *thymidilate synthase*, a ubiquitous enzyme crucial to the biosynthesis of thymidine, 5-FU shuts down fundamental metabolism pathways resulting in a state known as "thymineless death".[61] A fluorinated pyrimidine, 5-FU is otherwise identical to the endogenous nucleobase uracil, and is metabolised as such to the corresponding nucleotide monophosphate inside the cell (**Scheme 3.2**).[60]



Scheme 3.2 a) uracil, **b**) 5-FU and **c**) the respective monophosphate nucleotides dUMP or d(5-FU)MP following enzymatic metabolism

The activated substrate is then recognised by thymidilate synthase which, under normal conditions methylates the deoxyuridine monophosphate (dUMP), transforming it to the deoxythymidine monophosphate (dTMP) required for DNA synthesis. In the presence of tetrahydrofolate, the nucleotide forms covalent bonds to both the enzyme and the cofactor via the alkene functionality of the nucleobase. Loss of a proton from the 5-position allows release from the enzyme, before a second proton transfer breaks the bond to the cofactor to give the methylated product (**Scheme. 3.3**).[62]



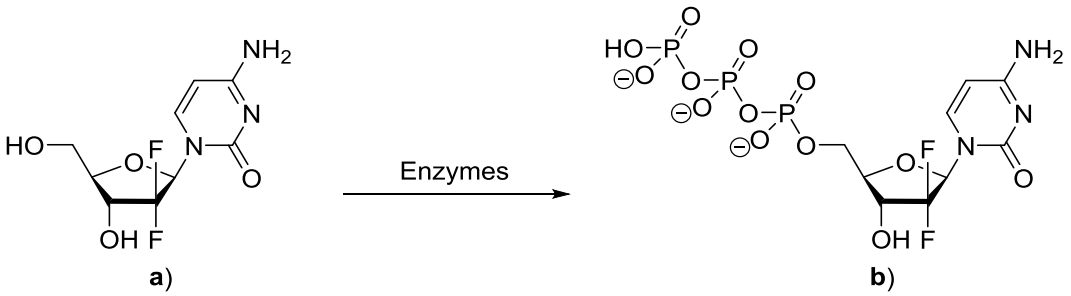
Scheme 3.3 The normal metabolism of dUMP (X = H) to dTMP by thymidilate synthase, and the suicide inhibition of the enzyme by d(5-FU)MP (X = F)

Fluorinated at the 5-position, 5-FU does not facilitate this process of release. The nucleotide becomes irreversibly bound to the active site of the enzyme thus precluding any further activity. Unable to produce dTMP, DNA synthesis effectively ceases and the cell triggers apoptosis. The major benefit of this type of inhibition is the selective and irreversible alkylation of a specific target. Termed "suicide inhibition", it is the very action of metabolism that brings about the destruction of the enzyme.[60,62]

3.1.4.2 Gemcitabine

Offering nano-molar activity, gemcitabine has become the "gold standard" treatment for pancreatic cancer since its discovery in 1990 by Hertel.[63,64] Like the active form of 5-FU, gemcitabine is a fluorinated analogue of cytidine and is activated by phosphorylation within the cell to the triphosphate (**Scheme 3.4**). The modified nucleotide then associates with DNA polymerase and is incorporated into a growing oligonucleotide. Crucially, one more natural

nucleotide is then successfully attached before chain termination occurs. This terminal nucleotide masks the presence of the disruptive agent, thus preventing recognition and repair by cellular enzymes; synthesis is arrested and junk DNA accumulates in the cell leading to apoptosis.[65] The activity of gemcitabine is also enhanced by a process of self-potentiation; cellular enzymes, crucial for the production of cytidine are down-regulated resulting in a dearth of natural substrate; the probability of gemcitabine incorporation is therefore increased.[66]



a) b)

Scheme 3.4 Enzymatic phosphorylation of **a)** gemcitabine to the active metabolite **b)** gemcitabine triphosphate

3.1.4.3 Azidothymidine

Following the AIDS (acquired immunodeficiency syndrome) epidemic of the 1980's, nucleoside analogues were also developed as antiretrovirals. Originally investigated in the 1960's as a potential anticancer agent, AZT came to prominence and gained government approval as the first effective, albeit highly toxic anti-retretroviral (**Fig. 3.8**).[67]

AIDS is the condition resulting from the deleterious effects of the human immunodeficiency virus (HIV).[68] Retroviruses, such as this, hijack the cellular machinery of the host and replicate inside the body by the process of reverse transcription. Once inside the cell, the viral enzyme, *reverse transcriptase*, produces cDNA from the viral RNA, which is then incorporated into the host genome by the viral enzyme integrase. The viral genes are then

unwittingly expressed by the host, releasing the various protein products required to assemble more virus particles.[69] Nucleoside analogue reverse-transcriptase inhibitors (NRTIs) such as AZT disrupt this crucial process thus preventing replication of the virus.

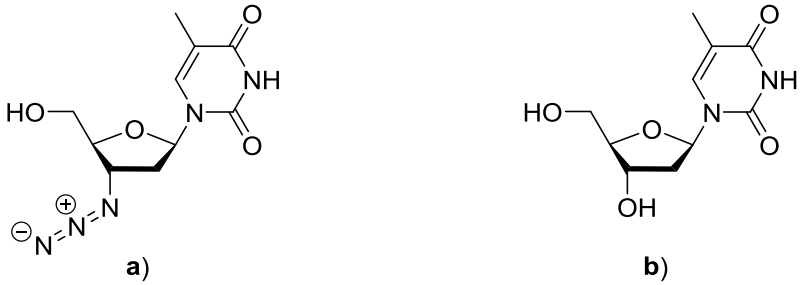


Fig. 3.8 a) the first approved antiretroviral drug AZT and **b**) the endogenous nucleoside thymidine from which it is derived

Once again the nucleoside analogue is first phosphorylated by physiological kinase enzymes to the triphosphate, which, as a derivative of the endogenous nucleotide thymidine competes with the natural substrate for oligomerisation by the viral enzyme reverse transciptase. Importantly, with affinity for the DNA polymerase 100-fold lower, AZT has been shown to be very selective for this viral enzyme.[70] Once incorporated into the growing viral cDNA chain, AZT, lacking the prerequisite 3′-hydroxy group, acts to terminate further chain extension and hence prevents successful transcription of the viral RNA. With this essential process of replication disrupted, the viral population is greatly diminished, its deleterious effects reduced and the progression to full blown AIDS greatly slowed.

3.1.4.4 Iron-Containing Nucleoside Analogues

Attempting to combine the cytotoxic effects of nucleoside analogues with the inherent toxicity of iron, Schmaltz developed some exotic organometallic nucleoside analogues. The first variety was reported in 2004, in which a furan-type ring appended with a η^4-butadiene-$Fe(CO)_3$ unit takes the place of the traditional sugar (**Fig. 3.9a**).[71] Although ineffective

against HIV, the agents proved quite cytotoxic, producing apoptosis in both human Burkitt lymphoma B (BJAB) cells and acute leukemic lymphoblasts (ALLs) at low micromolar concentrations. Attempting to elucidate the mechanism of action and identify the key structural features which bestowed activity, a number of structural variations were synthesised and their biological impact assessed. This lead to the development of two more candidates with comparable activity; firstly a simple carbocyclic variation (**Fig. 3.9b**) and a further development in which the iron is borne within a ferrocene unit appended to the ring (**Fig. 3.9c**).[72,73]

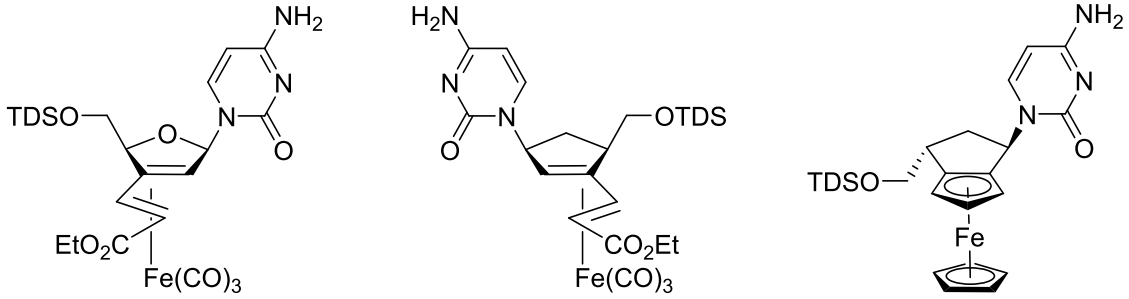


Fig. 3.9 Three iron-containing nucleoside analogues by Schmaltz, two of which contain a η^4-butadiene-$Fe(CO)_3$ unit appended to **a**) a furan-type ring, and **b**) a simple carbocycle, and a third **c**) in which the iron is contained within the ferrocene motif.

Cytosine was quickly identified as the most active nucleobase and in all cases a lipophilic (dimethyl)thexylsilane (TDS) protecting group on the 5′-oxygen was crucial to the activity. The first two varieties also favoured the presence of an ester substituent on the η^4-butadiene-$Fe(CO)_3$ unit. Interestingly the 'unnatural' enantiomer of the carbocyclic variation was more active than its 'natural' counterpart and the ring of the ferrocene containing compound was more active when unnaturally, *trans*-substituted. This, alongside the unavailability of the 5′-hydroxy, led the group to question the assumption that the compounds were acting as typical nucleoside analogues. The authors conclude that some unknown protein is the most likely target.[72]

3.1.5 Nucleoside Analogues with a Ferrocenyl Linker

Following the successful production of functional, tetrasubstituted FcNA monomers which, to a greater or lesser extent mimic native DNA, the Tucker group proposed the corresponding disubstituted systems as potential nucleoside analogues. It was hoped that incorporating the ferrocene unit into this established pharmaceutical motif will produce a synergistic effect of enhanced cytotoxicity, selectivity or novel mechanism(s) of action. In contrast to the iron-containing nucleoside analogues of Schmaltz, in which the iron unit is appended onto the sugar, these new compounds would feature the ferrocene unit taking its place entirely.

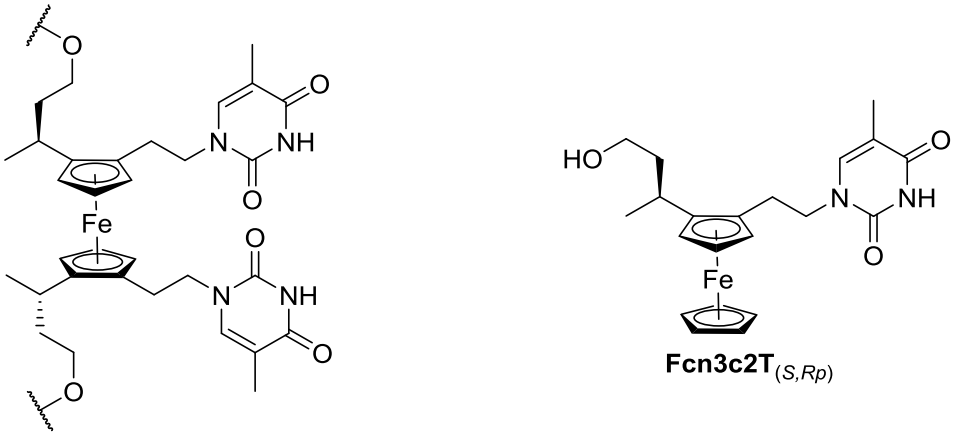
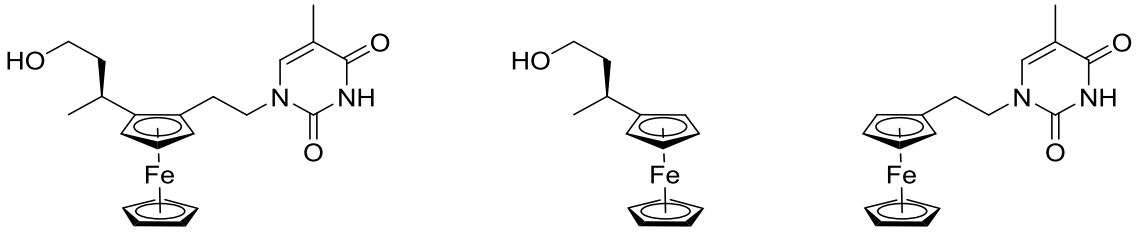


Fig. 3.10 The tetrasubstituted dithyminyl FcNA monomer **Fcn3c2TT**$_{(SS,RpRp)}$, the corresponding disubstituted ferrocenyl nucleoside analogue **Fcn3c2T**$_{(S,Rp)}$

Hitherto, binding studies had revealed **Fcn3c2TT**$_{(SS,RpRp)}$ as the FcNA monomer which formed the most stable duplex when incorporated into an otherwise natural DNA helix (**Fig. 3.10**). The corresponding disubstituted ferrocene **Fcn3c2T**$_{(S,Rp)}$ was therefore proposed as the logical starting point for the investigation into the potential of these compounds as nucleoside analogues. Looking at the wide variety of compounds which comprise this class of drugs, **Fcn3c2T**$_{(S,Rp)}$ conforms to the simple tripartite structure of hydroxyl, linker and nucleobase which loosely defines this class of compound. In 2014 the Tucker group

published the synthesis of **Fcn3c2T**$_{(S,Rp)}$ and its biological activity against various cancer cells.[74]

Cytotoxicity assays were performed against three tumor cell lines: murine leukemia (L1210), human T-lyphocyte (CEM) and HeLa (**Table 3.2**). Two control compounds based on the corresponding ferrocenyl alcohol **Fcn3**$_{(S)}$ and the ferrocenyl nucleobase **Fcc2T** structural fragments of **Fcn3c2T**$_{(S,Rp)}$ were also tested (**Fig. 3.11**) and compared to the established anti-cancer agents cisplatin and 5-FU.



Fcn3c2T$_{(S,Rp)}$ **Fcn3**$_{(S)}$ **Fcc2T**

Fig. 3.11 The disubstituted ferrocenyl nucleoside analogue **Fcn3c2T**$_{(S,Rp)}$ and the corresponding hydroxyl **Fcn3**$_{(S)}$ and nucleobase **Fcc2T** controls

Fcn3c2T$_{(S,Rp)}$ produced low micromolar activity against all three cell lines comparable to that of cisplatin and, although 5-FU was slightly more active against L1210 and HeLa cells, **Fcn3c2T**$_{(S,Rp)}$ was twenty times as potent against the CEM cell line. The hydroxyl control **Fcn3**$_{(S)}$ was about fifteen times less potent against L1210 and HeLa cells, and forty times less potent against CEM cells compared to **Fcn3c2T**$_{(S,Rp)}$. In all three cell lines the nucleobase control **Fcc2T** was hundreds of times less active than **Fcn3c2T**$_{(S,Rp)}$. Certainly, when these two structural fragments are combined, the resulting compound displays much greater cytostatic activity, supporting the notion that the hydroxy and nucleobase functionalities act, at least in some sense, synergistically.

Table 3.2 Cytotoxic activity of **Fcn3c2T**$_{(S,Rp)}$ compared to the hydroxyl **Fcn3**$_{(S)}$ and nucleobase **Fcc2T** controls, and two established anti-cancer agents cisplatin and 5-FU[74]

	IC_{50} (μM)		
Compound	L1210	CEM	HeLa
Fcn3c2T$_{(S,Rp)}$	0.78	0.9	2.68
Fcn3T$_{(S)}$	12	39	45
Fcc2T	417	592	509
Cisplatin	1.0	0.9	1.2
5-FU	0.33 ± 0.17	18 ± 5	0.5 ± 0.12

3.2 Objectives

The promising cytotoxic properties of **Fcn3c2T**$_{(S,Rp)}$ clearly warrant further investigation. It was hoped therefore, that through the biological investigation of a library of related compounds, structure-activity relationships would be revealed which may, in turn, suggest a mechanism of action. The possibility of honing the structure and improving the activity would then be realised. The four most salient structural features were identified as the nucleobase linker length, the hydroxyl linker length, the planar chirality and the nucleobase identity and a naming system concordant with that used for FcNA monomers was adopted (**Fig. 3.12**). In addition, the 1,2-substitution pattern, in which both substituents occupy adjacent positions on the same Cp ring could be easily modified to a 1,1'-arrangement in which the substitutents occupy opposing Cp rings. This particular variation would exhibit no planar chirality and would be identified by the lack of a descriptor in the naming system.

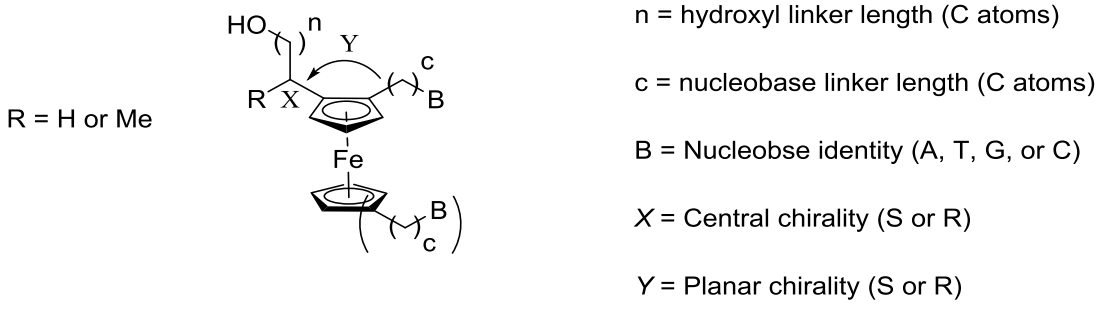


Fig. 3.12 Structural parameters and nomenclature of disubstituted ferrocenyl nucleoside analogues

Having initially proposed these molecules as potential nucleoside analogues, it was decided that the first structural variations would be designed to test this hypothesis. The structure would therefore be modified to better resemble an endogenous nucleoside which, it was hoped, may interact more efficiently with the relevant replication enzymes. Thus, two variations were proposed in which the hydroxyl linker length was reduced from three, to two

and one carbon atoms to give **Fcn2c2T**$_{(Rp)}$ and **Fcn1c2T**$_{(Rp)}$ respectively (**Fig. 3.13**). Through this stepwise truncation of the linker length (n = 3, 2 and 1), not only will the alcohol group approach a position (relative to ferrocene) similar to the 5′-hydroxyl group of a natural nucleoside (such as thymidine), but trends relating to the bulk physicochemical properties of the molecule may also be revealed.

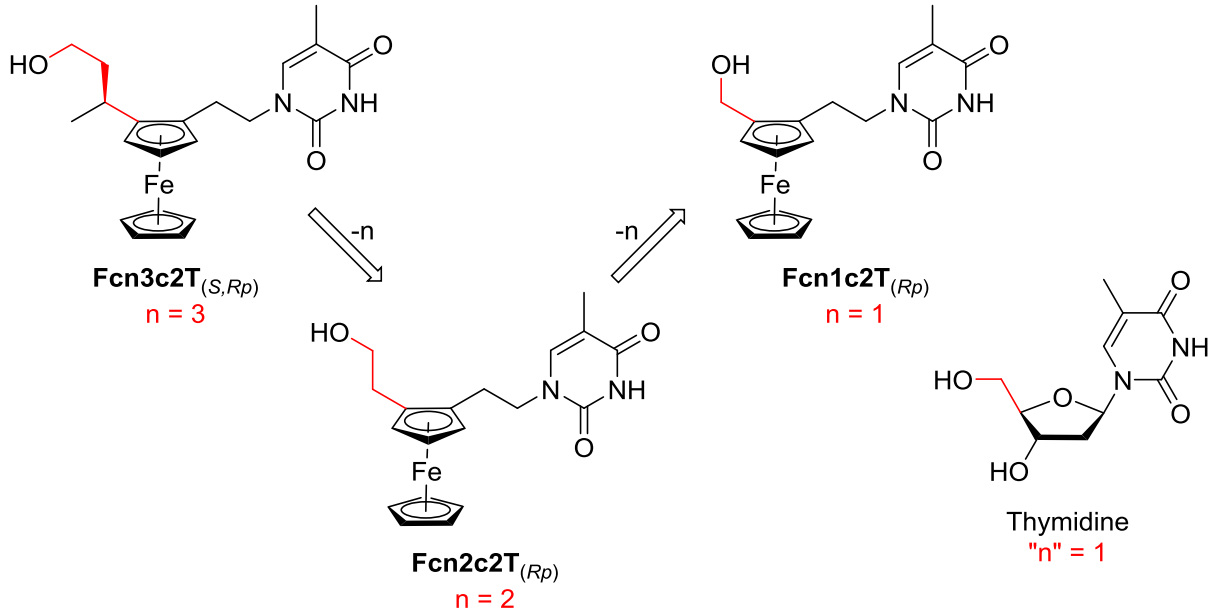
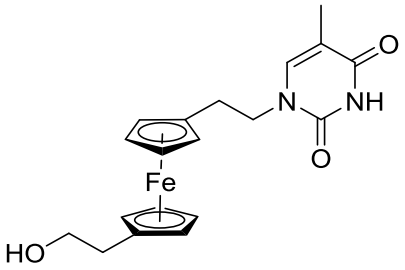


Fig. 3.13 Stepwise truncation of the hydroxyl linker length (n) of **Fcn3c2T**$_{(S,Rp)}$ to give **Fcn2c2T**$_{(S,Rp)}$ and **Fcn1c2T**$_{(S,Rp)}$ which more closely mimic a natural nucleoside such as thymidine

Given the chiral specificity of many enzymatic interactions, both enantiomers of each variation were to be investigated.[75] A significant difference in biological activity between a pair of enantiomers may suggest that a specific biological target is involved in the mechanism of action, and that the effect is less likely to result from just some non-specific bulk physicochemical property. The enantiomers of the β-blocker propranolol for example, although safely administered together as a racemic mixture, exhibit a hundred-fold difference in activity due to their chiral interactions with the target β-adrenergic receptors.[76]

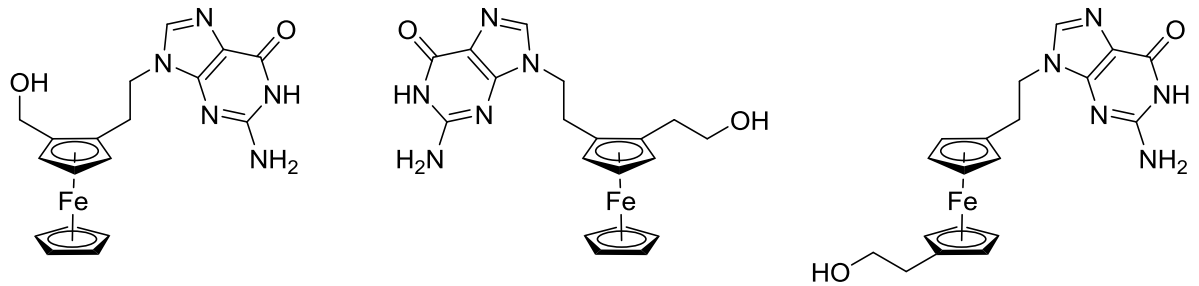
With the hydroxyl and the nucleobase moieties appended onto separate Cp rings, another variation **Fcn2c2T** would be made to explore the substitution pattern of the ferrocene itself (**Fig. 3.14**). This modification would allow the functional groups of the molecule far greater relative movement, facilitating entirely different modes of conformational flexibility.



Fcn2c2T

Fig. 3.14 The structure of the 1,1′-regioisomer **Fcn2c2T** in which the hydroxyl and nucleobase functionalities are separated onto opposite Cp rings of the ferrocene.

Using the recently developed methodology for the synthesis of guaninyl FcNA monomers, the respective guaninyl analogues **Fcn1c2G**$_{(Rp)}$, **Fcn2c2G**$_{(Sp)}$ and **Fcn2c2G** were also to be investigated to establish the importance of the nucleobase identity (**Fig. 3.15**). Not only would this modification provide a different H-bonding motif, which may offer insight into the importance of specific binding and recognition characteristics, but the physicochemical properties of the compounds will also be drastically altered, from which other structure-activity relationships may be revealed.



Fcn1c2G$_{(Rp)}$ **Fcn2c2G**$_{(Sp)}$ **Fcn2c2G**

Fig. 3.15 Three target ferrocenyl nucleoside analogues bearing guanine nucleobases **Fcn1c2G**$_{(Rp)}$, **Fcn2c2G**$_{(Sp)}$ and **Fcn2c2G**

These potential ferrocenyl nucleoside analogues were to be synthesised and tested for their cytotoxicity alongside the existing compounds **Fcn3c2T**$_{(S,Rp)}$ and its enantiomer **Fcn3c2T**$_{(R,Sp)}$ from which, it was hoped structure-activity relationships would be revealed. To investigate the relationship between redox activity and cytotoxicity, all of the compounds were to be be electrochemically characterised by cyclic voltammetry and their $E_{1/2}$ values determined. In addition, trends relating to the lipophilicities of the compounds would be considered through comparison of their respective ClogP values.

3.3 Results and Discussion

3.3.1 Synthesis of Ferrocene Containing Nucleoside Analogues

3.3.1.1 Synthesis of the Common Chiral Synthons 3.10-(R_p) and 3.10-(S_p)

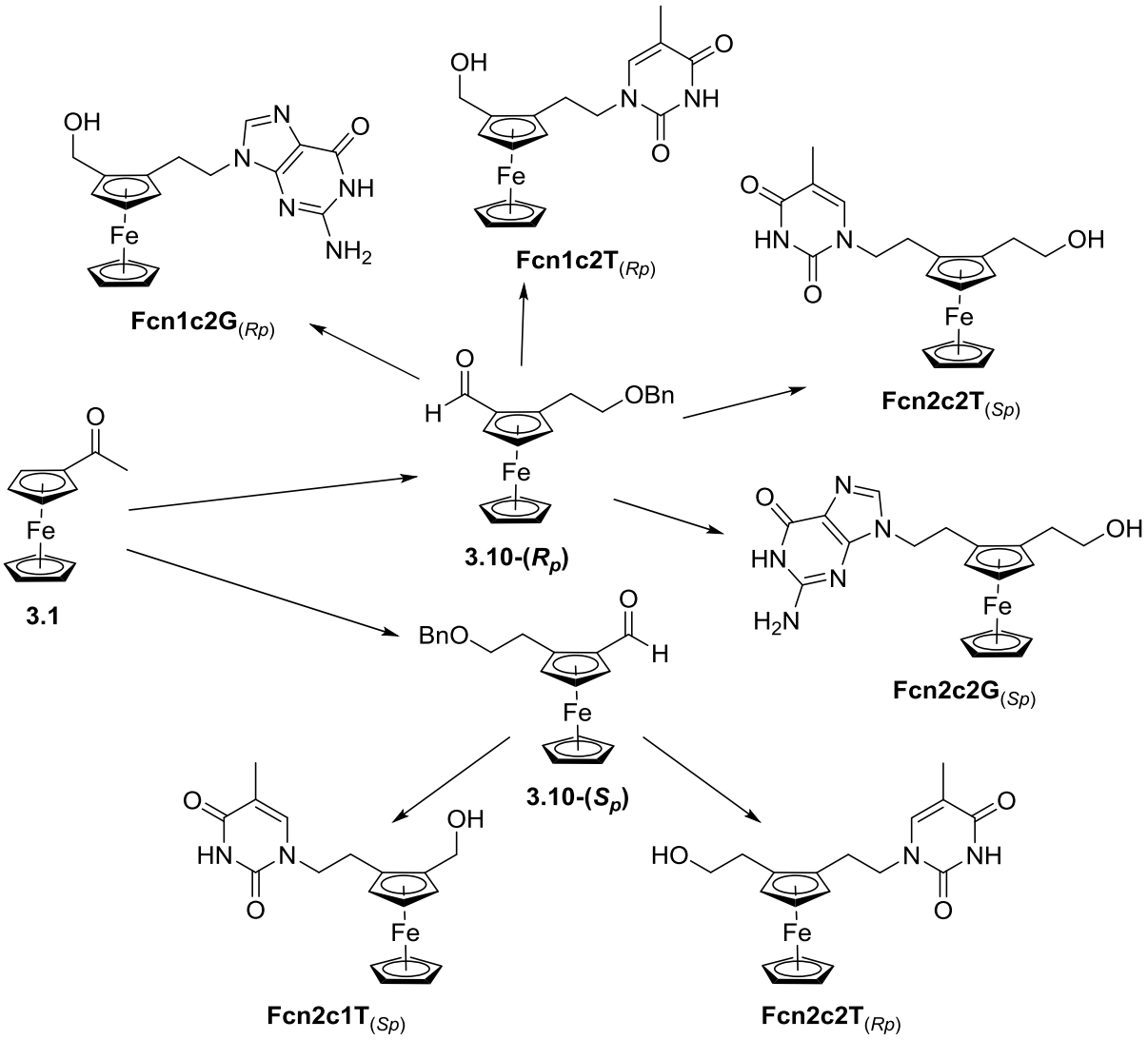
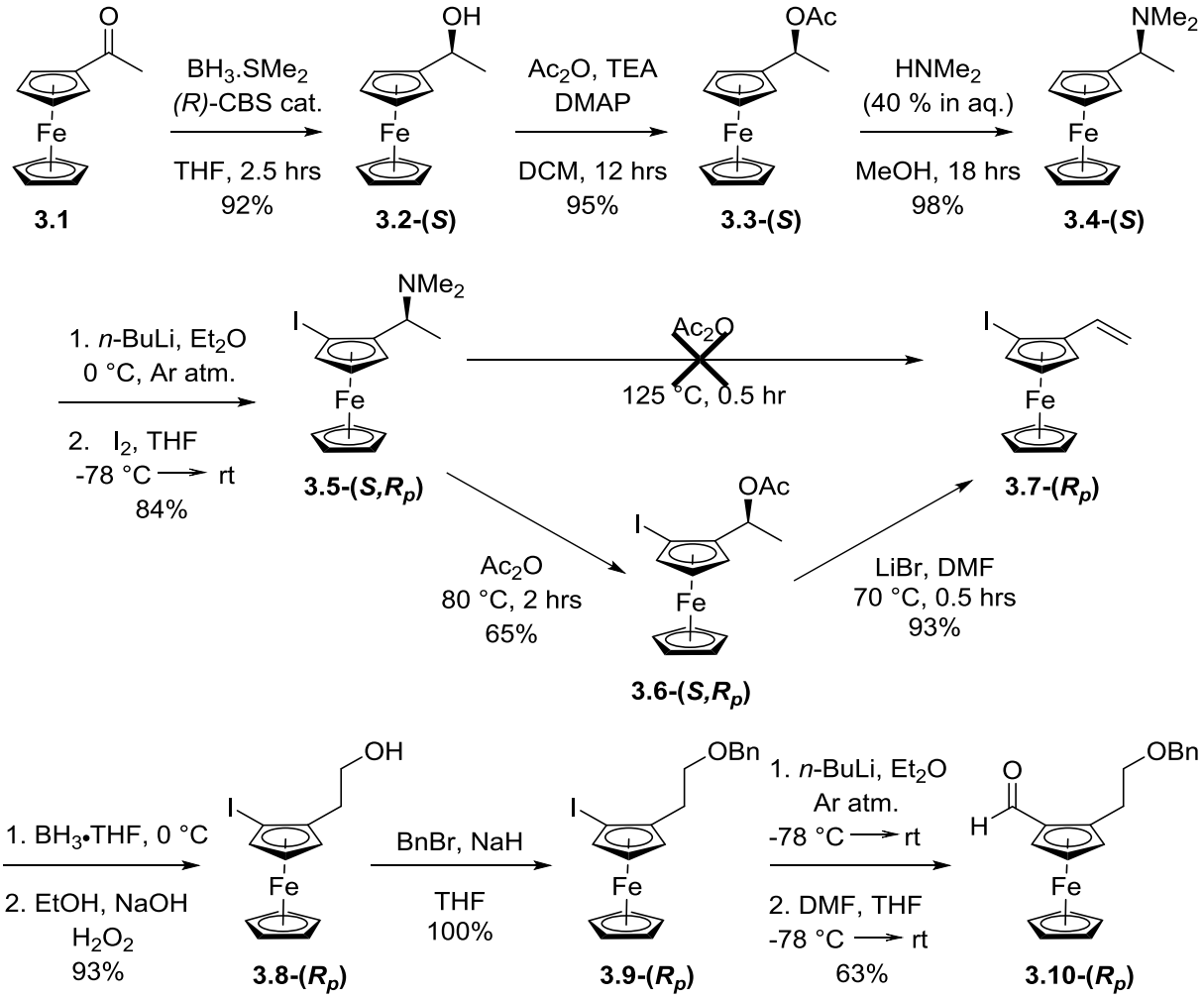


Fig. 3.16 The enantiomeric chiral synthons **3.10-(R_p)** and **3.10-(S_p)** and the target compounds which are produced from each

Conveniently, the planar chiral ferrocene nucleoside analogues **Fcn1c2T**$_{(Rp)}$, **Fcn2c2T**$_{(Sp)}$, **Fcn1c2G**$_{(Rp)}$ and **Fcn2c2G**$_{(Sp)}$, were all synthesised from the same chiral synthon **3.10-(R_p)** (**Fig. 3.16**). This synthon was produced following a sequence of nine linear steps from acetylferrocene **3.1**, which was procured from the undergraduate teaching laboratories and

purified by flash column chromatography on silica gel prior to use (**Scheme 3.5**). **Fcn1c2T**$_{(Sp)}$ and **Fcn2c2T**$_{(Rp)}$ were likewise both synthesised from the opposite chiral synthon **3.10-(S_p)** which was prepared according to the same method using the appropriate CBS chiral catalyst.



Scheme 3.5 Nine step synthesis of chiral synthon **3.10-(R_p)** from acetylferrocene **3.1**

To produce the chiral synthon **3.10-(R_p)**, the (*R*)-CBS catalyst was employed to introduce central chirality through the reduction of acetylferrocene **3.1** to the (*S*)-alcohol **3.2-(*S*)**. Reaction with acetic anhydride then prepared the acetoxy **3.3-(*S*)** which in turn was converted to the Ugi amine **3.4-(*S*)** with retention of stereochemistry as discussed in **Chapter 1**. In conjunction with *n*-BuLi, the Ugi amine was then used to direct a stereoselective ortho-lithiation which was reacted on in-situ to give the corresponding planar chiral iodo compound **3.5-(S,R_p)**.

Although producing a single spot by TLC, NMR analysis of **3.5-(*S*,*R*$_p$)** revealed the presence of a small amount of the minor diastereomer which could not be removed by standard column chromatography (**Fig. 3.17**).

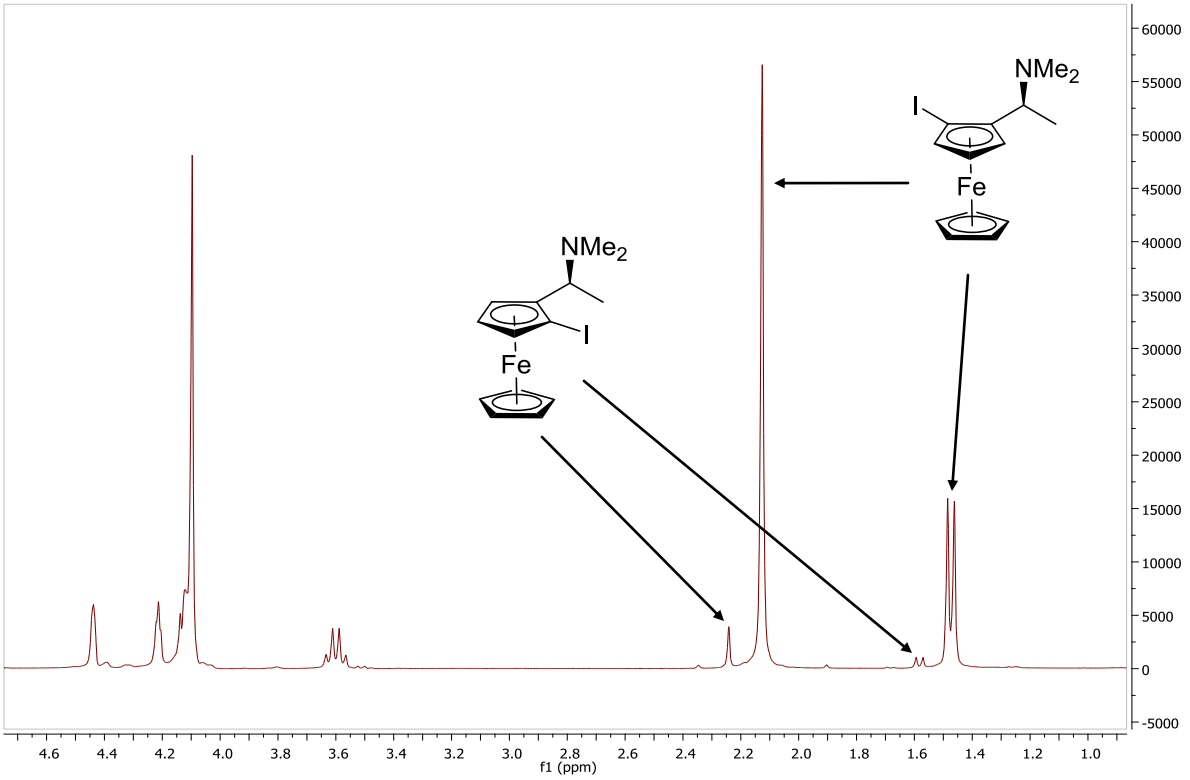


Fig. 3.17 ^{1}H NMR spectrum of amine **3.5-(*S*,*R*$_p$)** in $CDCl_3$ showing the major product and minor diastereomer impurity **3.5-(*S*,*Sp*)**

Although by performing the next step at higher temperature, it was possible to access the vinyl species **3.7-(*R*$_p$)** directly from the amine, in the interest of chiral purity it was necessary to proceed via the acetoxy **3.6-(*S*,*R*$_p$)**, since the diastereomers of of this compound can be separated. Column chromatography followed by repeated recrystalisation and filtration of the solid compound afforded a diasteromerically pure form of **3.6-(*S*,*R*$_p$)** which was confirmed by consideration of the ^{1}H NMR spectra (**Fig. 3.18** and **Fig. 3.19**).

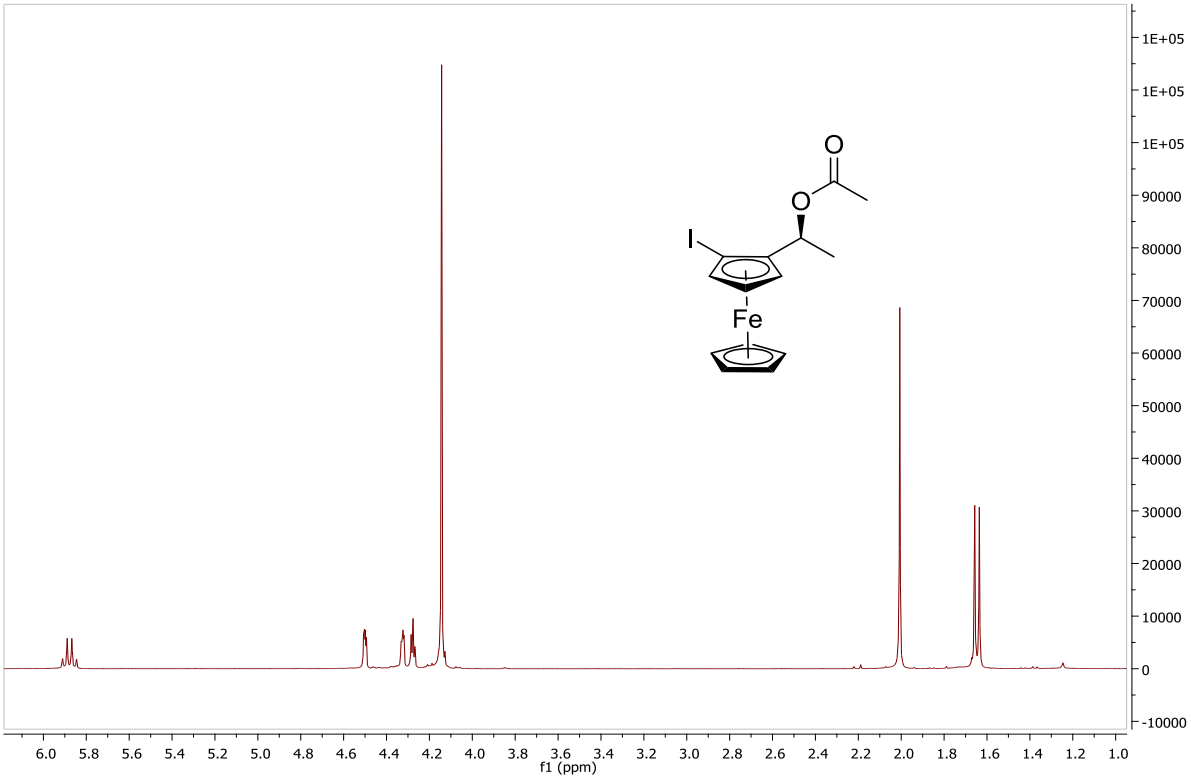


Fig. 3.18 ^{1}H NMR spectrum of the diastereomerically pure acetoxy **3.6-(*S*,*R*$_p$)** in $CDCl_3$

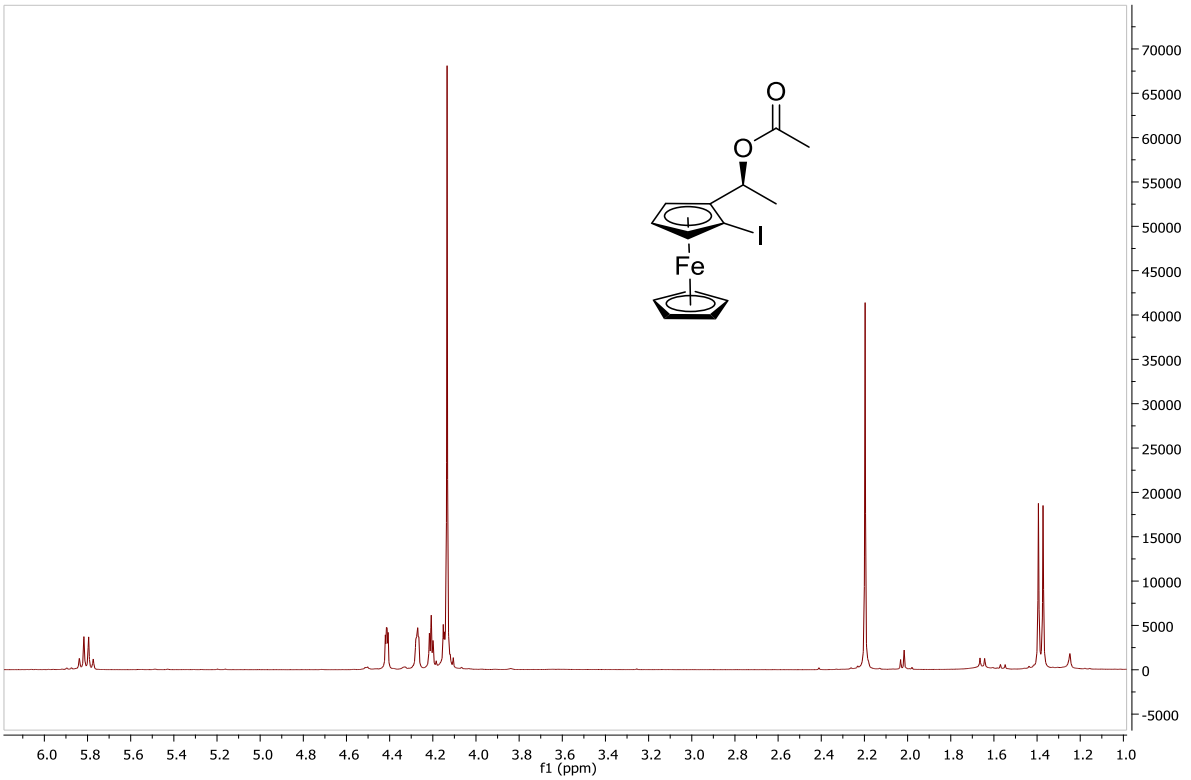
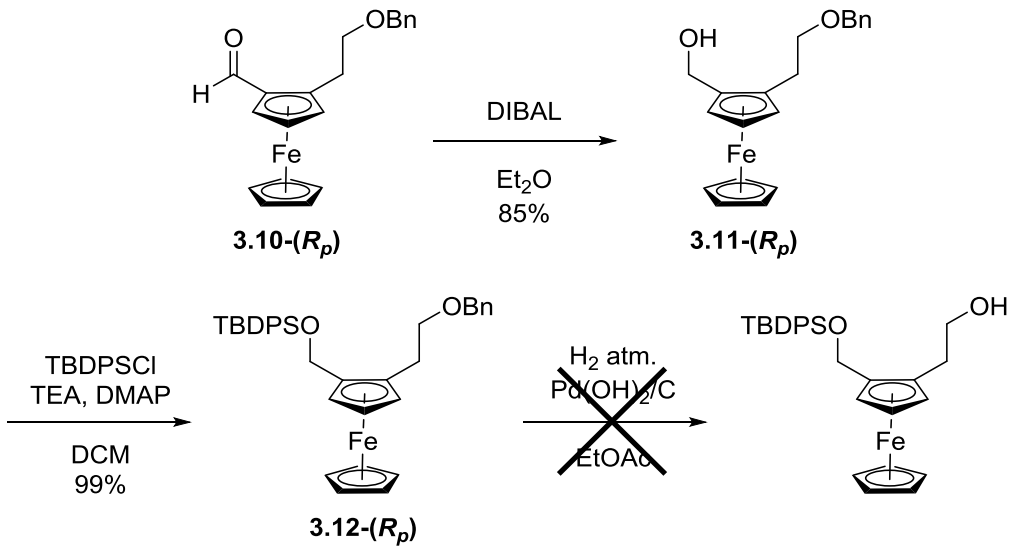


Fig. 3.19 ^{1}H NMR spectrum of the (mostly) isolated acetoxy impurity **3.6-(*S*,*S*$_p$)** in $CDCl_3$

Elimination of the diastereomerically pure acetoxy **3.6-(S,R_p)** was then effected using LiBr in DMF at 70 °C, simultaneously removing the element of central chirality and leaving the vinyl product **3.7-(R_p)**. A hydroboration/oxidation reaction then installed a hydroxyl group, and as expected, the anti-Markovnikov product predominated at 0 °C to give **3.8-(R_p)**. A small quantity of byproduct, assumed to be the Markovnikov regioisomer, was easily removed by column chromatography but was not characterised. The hydroxyl group was then protected to allow the opposing linker arm to be developed in relative freedom; the simple and fairly stable benzyl group was selected for this purpose knowing that an orthogonal protecting group could be used to protect the hydroxyl group which would be installed on the other linker arm. The benzyl ether **3.9-(R_p)** was successfully produced before *n*-BuLi was used to effect a lithium-halogen exchange which, upon quenching with DMF, yielded the chiral synthon **3.10-(R_p)** as a red oil.

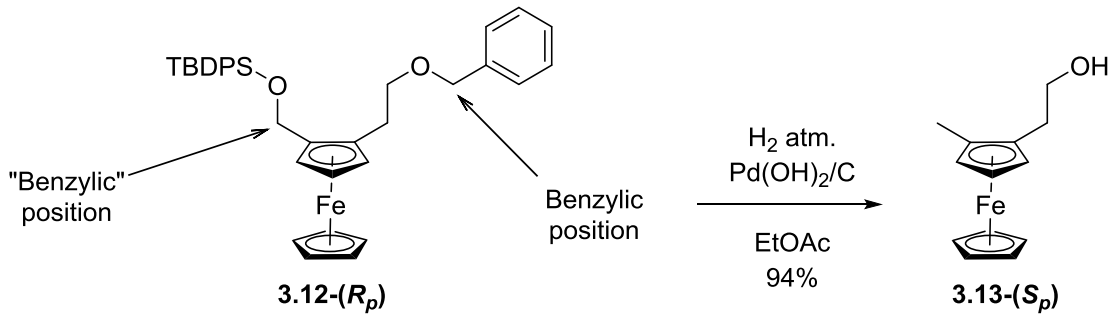
3.3.1.2 Synthesis of Fcn1c2T$_{(Rp)}$ and Fcn1c2T$_{(Sp)}$

With the important chiral synthon **3.10-(R_p)** in hand, synthesis continued towards the production of **Fcn1c2T**$_{(Rp)}$ (**Scheme 3.6**). Initially, DIBAL was employed to reduce the aldehyde **3.10-(R_p)** to the desired hydroxymethyl group **3.11-(R_p)** which was then protected with a TBDPS group **3.12-(R_p)**. Given the orthogonal nature of the TBDPS and benzyl protecting groups, it seemed facile to selectively reveal the nucleobase linker hydroxyl, couple, and then deprotect the nucleobase to give the final compound. A crucial oversight in the protecting group strategy quickly became clear however; the benzylic character of the ferrocene unit thwarting these otherwise simple plans.



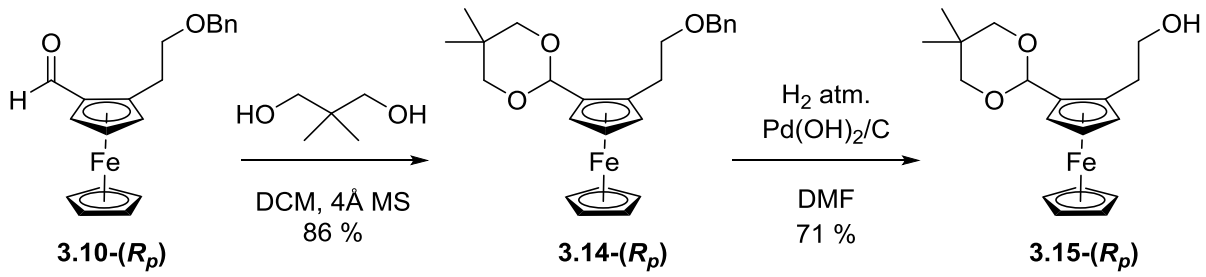
Scheme 3.6 First attempted synthesis of **Fcn1c2T**$_{(Rp)}$ from chiral synthon **3.10-(R_p)**

Although, using typical hydrogenation conditions of hydrogen over Pearlman's catalyst, the target alcohol was released, the "benzylic" character of the position α- to ferrocene resulted in a concomitant cleavage of the ferrocenyl ether, leaving a useless methyl group **3.13-(S_p)** (**Scheme 3.7**).



Scheme 3.7 Debenzylation of **3.12-(R_p)** resulted in concomitant cleavage of the ferrocenyl ether producing **3.13-(S_p)**

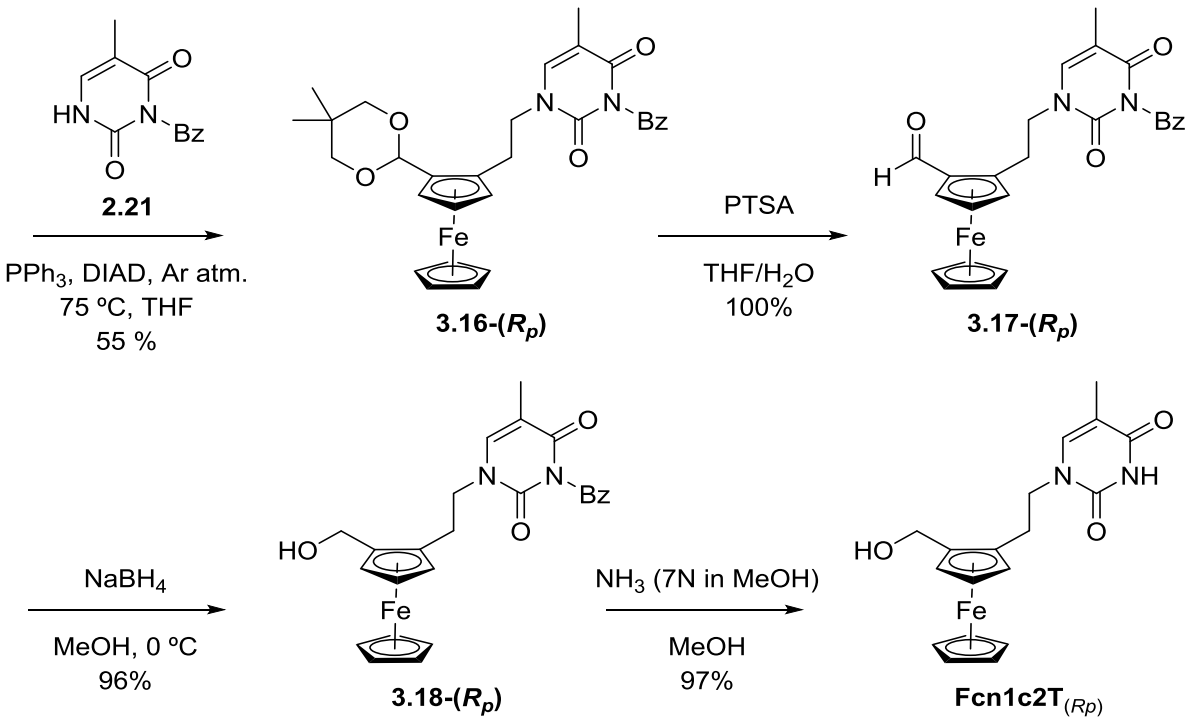
An alternative strategy was therefore devised in which the aldehyde of **3.10-(R_p)** was disguised as an acetal. The chiral synthon **3.10-(R_p)** was thus reacted with 1,3-dimethylpropanediol in the presence of 4 Å molecular sieves to give the stable, six-membered cyclic acetal **3.14-(R_p)** (**Scheme 3.8**).



Scheme 3.8 Continued synthesis of **Fcn1c2T**$_{(Rp)}$

On small scale, the benzyl protecting group of **3.14-(R_p)** was successfully removed by hydrogenolysis in the next step to give **3.15-(R_p)** in 77% yield, again using hydrogen over Pearlman's catalyst in EtOAc. Upon scaling up however, undesired hydrolysis of the acetal was also observed and it was proposed that acid production was the cause. Performing the reaction in dry DMF (which is slightly basic), with careful monitoring and gentle stirring remedied the situation; the benzylic ether was selectively cleaved to give the alcohol **3.15-(R_p)** while leaving the acetal intact. Although the desired transformation was achieved, subsequent investigation of the literature suggested that the reasoning was perhaps flawed. A more realistic explanation, invokes the palladium centre as a Lewis acid catalyst, activating the acetal towards cleavage by a suitable nucleophile such as water.[77] It may therefore be the use of more anhydrous conditions, not the identity of the solvent itself, which has resulted in the fortuitous shift of reactivity.

Alcohol **3.15-(R_p)** was then coupled to *N3* benzoyl protected thymine **2.21** under Mitsunobu conditions to give the ferrocene conjugate **3.16-(R_p)**, and the acetal protecting group removed with PTSA in wet THF to return the aldehyde **3.17-(R_p)** (**Scheme 3.9**). Leaving the imide/amide functionalities of the protected thymine unaffected, $NaBH_4$ was then used to selectively reduce the aldehyde to the corresponding alcohol **3.15-(R_p)**. Finally, NH_3 in methanol was used to cleave the benzoyl amide to give the target compound **Fcn1c2T**$_{(Rp)}$.



Scheme 3.9 Continued synthesis of disubstituted ferrocenyl nucleoside analogue **Fcn1c2T**$_{(Rp)}$

Single crystals of **Fcn1c2T**$_{(Rp)}$ were grown by the slow evaporation of a concentrated chloroform solution and the absolute structure was confirmed by XRD (**Fig. 3.20**). A very low Flack parameter of 0.003(5) suggests the presence of just one enantiomer in the sample crystal.[78] Full crystal data for compound **Fcn1c2T**$_{(Rp)}$ can be found in the appendix (**Chapter 6.12**).

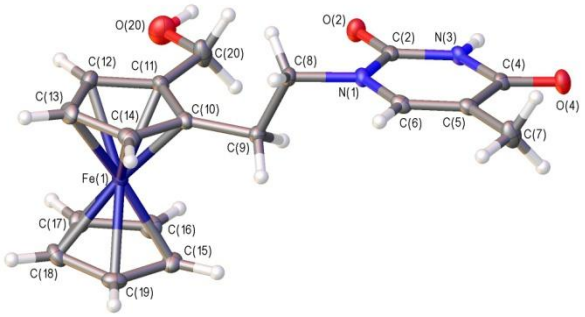


Fig. 3.20 Crystal structure of of **Fcn1c2T**$_{(Rp)}$ with ellipsoids drawn at the 50% probability level. The structure contains two crystallographically-independent crystallographically-independent molecules of which only one is shown.

The opposite enantiomer **Fcn1c2T**$_{(Sp)}$ was produced using the same method, from the corresponding chiral synthon **3.10-(S_p)**. Again, single crystals of **Fcn1c2T**$_{(Sp)}$ were grown by the slow evaporation of a concentrated chloroform solution and the absolute structure was confirmed by XRD (**Fig. 3.21**). A low Flack parameter of 0.018(7) suggests the presence of just one enantiomer in the sample crystal. Full crystal data for compound **Fcn1c2T**$_{(Sp)}$ can be found in the appendix (**Chapter 6.13**).

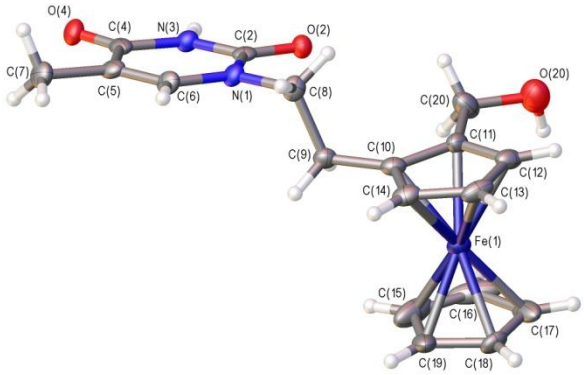


Fig. 3.21 Crystal structure of **Fcn1c2T**$_{(Sp)}$ with ellipsoids drawn at the 50% probability level. The structure contains two crystallographically-independent molecules of which only one is shown.

With both enantiomers in hand, the chiral purity was assessed by HPLC. Using a cellulose column, an isocratic eluent system of 30% acetonitrile in water, and a flow rate of 1.0 ml min^{-1}, the enantiomers were effectively separated. Following a 10.0 µl injection, **Fcn1c2T**$_{(Rp)}$ eluted to produce a large sharp peak (94.66%) at 16.351 min and a small (5.44%) peak at 17.480 min. The composition of **Fcn1c2T**$_{(Rp)}$ was thus found to be 95% desired enantiomer and 5% opposite enantiomer (e.e. = 90%) (**Fig. 3.22**).

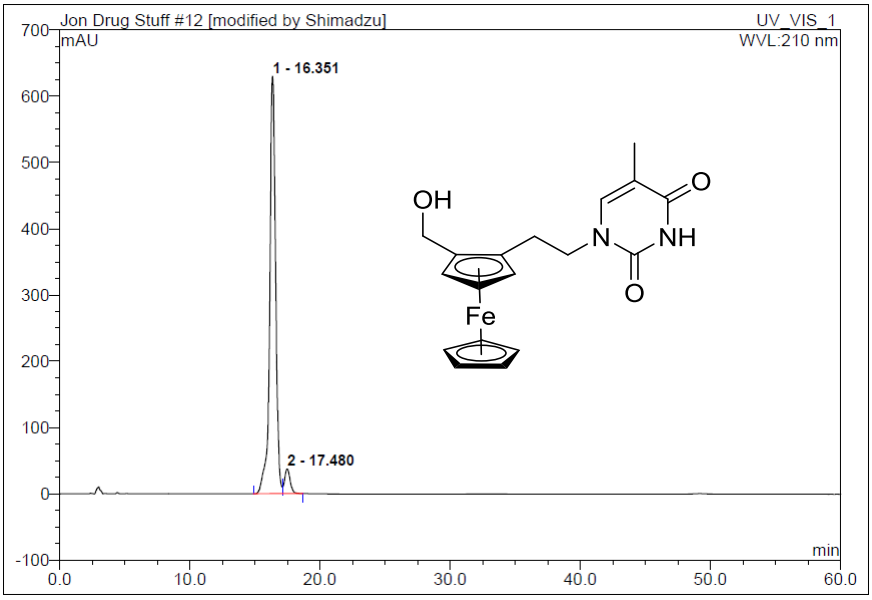


Fig. 3.22 Chiral HPLC trace of **Fcn1c2T**$_{(Rp)}$

Under identical conditions **Fcn1c2T**$_{(Sp)}$ eluted to produce a small peak (8.33%) at 16.544 min and a large sharp peak (91.67%) at 17.473 min (**Fig. 3.23**). The composition of **Fcn1c2T-(S_p)** was thus found to be 92% desired enantiomer and 8% opposite enantiomer (e.e. = 84%).

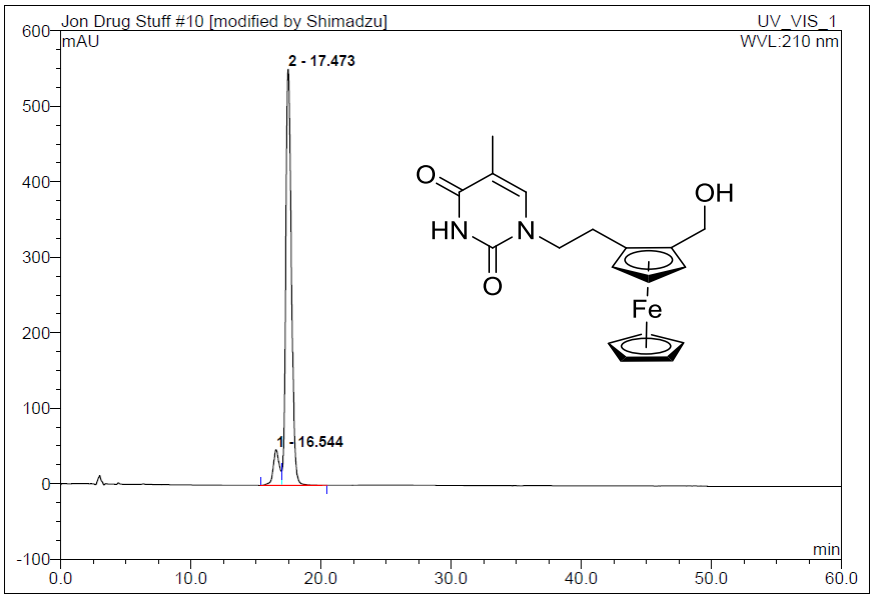


Fig. 3.23 Chiral HPLC trace of **Fcn1c2T**$_{(Sp)}$

Finally, to confirm the presence of only the two enantiomers of interest, a sample was prepared containing both **Fcn1c2T**$_{(Rp)}$ and **Fcn1c2T**$_{(Sp)}$. As expected, under identical

conditions the mixture eluted to produce just two sharp peaks with 16.414 min and 17.457 min retention time respectively (**Fig. 3.24**).

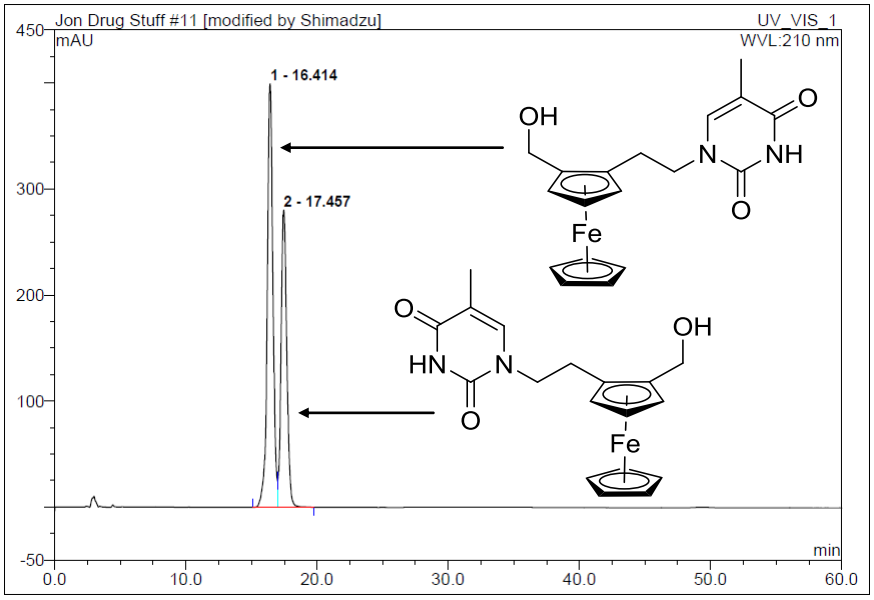
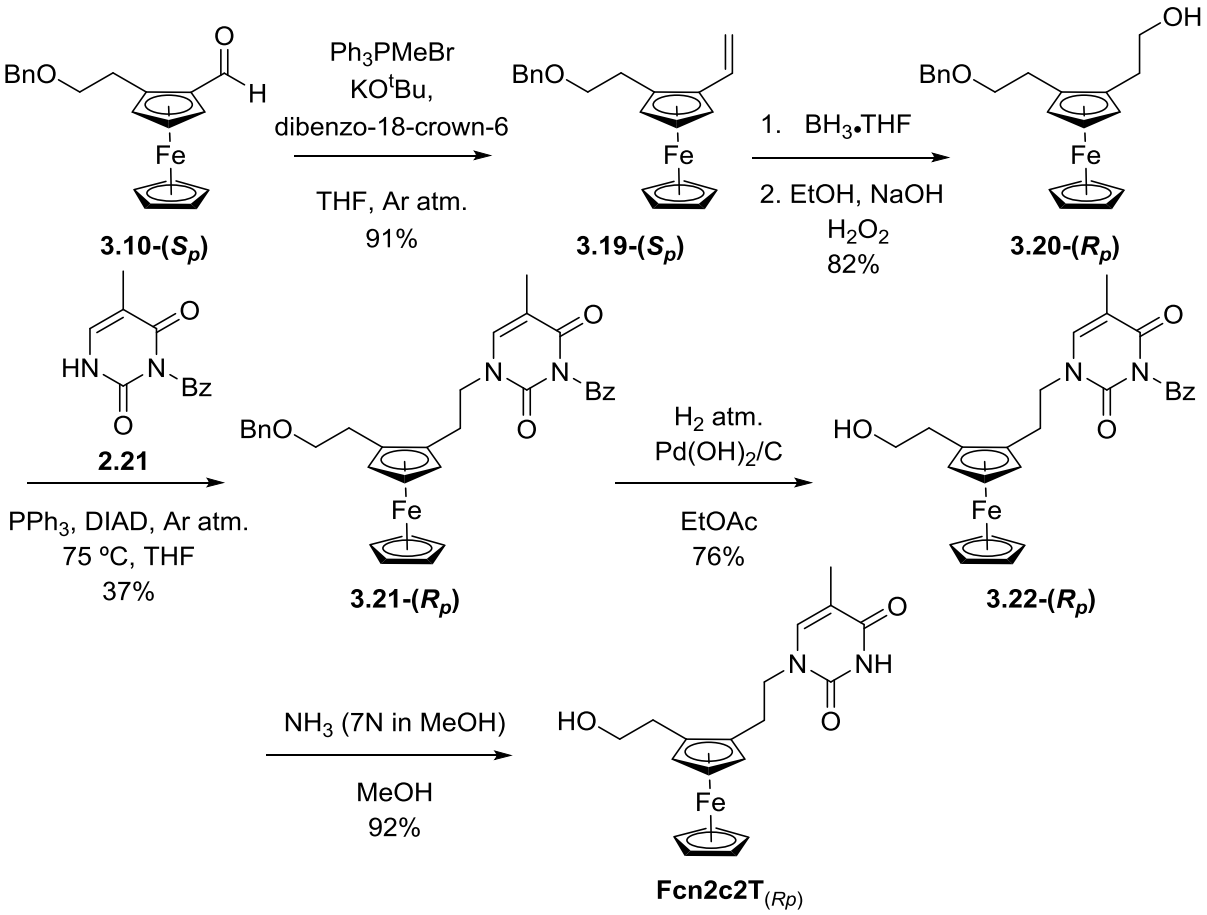


Fig. 3.24 Chiral HPLC trace of a mixture of **Fcn1c2T**$_{(Rp)}$ and **Fcn1c2T**$_{(Sp)}$

3.3.1.3 Synthesis of Fcn2c2T$_{(Rp)}$ and Fcn2c2T$_{(Sp)}$

Fcn2c2T$_{(Rp)}$ was synthesised in five steps from chiral synthon **3.10-(S_p)** (**Scheme. 3.10**). A Wittig reaction was first used to extend the carbon skeleton by one before the resulting alkene **3.19-(S_p)** was converted to alcohol **3.20-(R_p)** by a simple hydroboration/oxidation reaction. Once again, the small amount of minor Markovnikov product was easily removed by column chromatography. Alcohol **3.20-(R_p)** was then coupled to *N3* benzoyl protected thymine under Mitsunobu conditions to give the ferrocene conjugate **3.21-(R_p)**. The poor yield of this reaction (37%) was due to the erroneous addition of DIAD before the the addition of the protected nucleobase. It is suspected that some of the **3.20-(R_p)** substrate therefore underwent an intermolecular coupling to form a diferrocenyl ether, but this was not confirmed. Fortunately, enough material was successfully reacted and the synthesis continued. The benzyl group was removed by hydrogenolysis, using hydrogen over Pearlman's catalyst in

EtOAc, to reveal alcohol **3.22-(R_p)**. In the last step, ammonia in methanol was used to cleave the benzoyl protecting group from the nucleobase to give the target compound **Fcn2c2T**$_{(Rp)}$.



Scheme 3.10 Synthesis of **Fcn2c2T**$_{(Rp)}$ in five steps from chiral synthon **3.10-(S_p)**

Single crystals of **Fcn2c2T**$_{(Rp)}$ were grown by the slow evaporation of a concentrated solution in EtOAc allowing the absolute structure to be confirmed by XRD (**Fig. 3.25**). A very low Flack parameter of – 0.003(5) suggests the presence of just one enantiomer in the sample crystal. Full crystal data for compound **Fcn2c2T**$_{(Rp)}$ can be found in the appendix (**Chapter 6.14**).

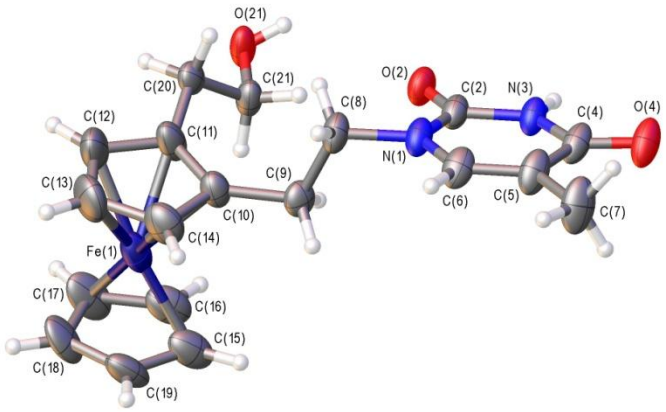
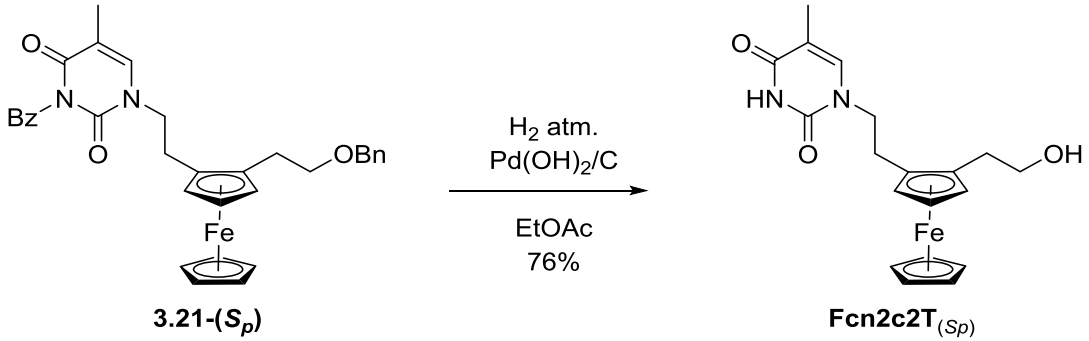


Fig. 3.25 Crystal structure of **Fcn2c2T**$_{(Rp)}$ with ellipsoids drawn at the 50% probability level. The Cp ring C(15)-C(19) / C(15')-C(19') and the group C(20), C(21), O(21) / C(20'), C(21'), O(21') are both disordered over two positions, with only the major positions shown for clarity.

The opposite enantiomer **Fcn2c2T**$_{(Sp)}$ was prepared according to an almost identical method from the corresponding chiral synthon **3.10-(R_p)**. It is worth noting however that in this case both the benzyl and the benzoyl protecting groups were removed from **3.21-(S_p)** to give the target compound **Fcn2c2T**$_{(Sp)}$ in one step by the action of hydrogen gas and Pearlman's catalyst (**Scheme 3.11**).



Scheme 3.11 Removal of the Bn and Bz protecting groups to give the target compound **Fcn2c2T**$_{(Sp)}$ in one step from **3.21-(S_p)**

Single crystals of **Fcn2c2T**$_{(Sp)}$ were grown by the slow evaporation of a concentrated solution in EtOAc allowing the absolute structure to be confirmed by XRD (**Fig. 3.26**). A low Flack

parameter of 0.018(6) suggests the presence of just one enantiomer in the sample crystal. Full crystal data for compound **Fcn1c2T**$_{(Sp)}$ can be found in the appendix (**Chapter 6.15**).

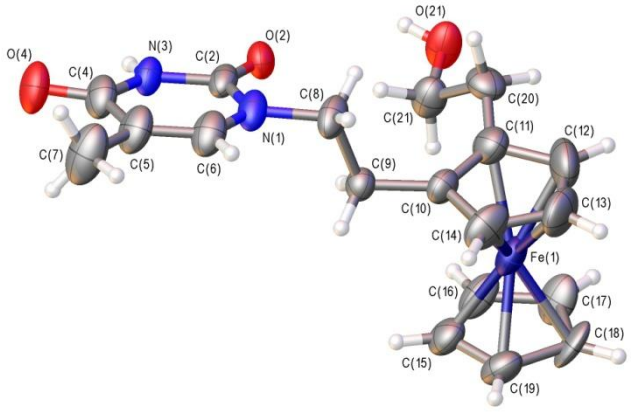


Fig. 3.26 Crystal structure of **Fcn2c2T**$_{(Sp)}$ with ellipsoids drawn at the 50% probability level. The Cp ring C(15)-C(19) / C(15')-C(19') is disordered over two positions with the refined occupancy ratio being 0.58(3):0.42(3). The group C(20), C(21), O(21) / C(0'), C(1'), O(1') is disordered over two positions with the refined occupancy ratio being 0.581(14):0.419(14). The minor positions have been omitted for clarity.

With both enantiomers in hand, the chiral purity of **Fcn2c2T**$_{(Rp)}$ and **Fcn2c2T**$_{(Sp)}$ were assessed by HPLC. Using a cellulose column and an isocratic eluent system of 30% acetonitrile in water with a flow rate of 1.0 ml min^{-1} the two enantiomers were successfully separated. Following a 10.0 µl injection, **Fcn2c2T**$_{(Rp)}$ eluted to produce a small (2.85%) peak at 20.249 min and large sharp peak (97.15%) at 22.885 min (**Fig. 3.27**). The composition of **Fcn2c2T**$_{(Rp)}$ was thus found to be 97% desired enantiomer and 3% opposite enantiomer (e.e. = 94%).

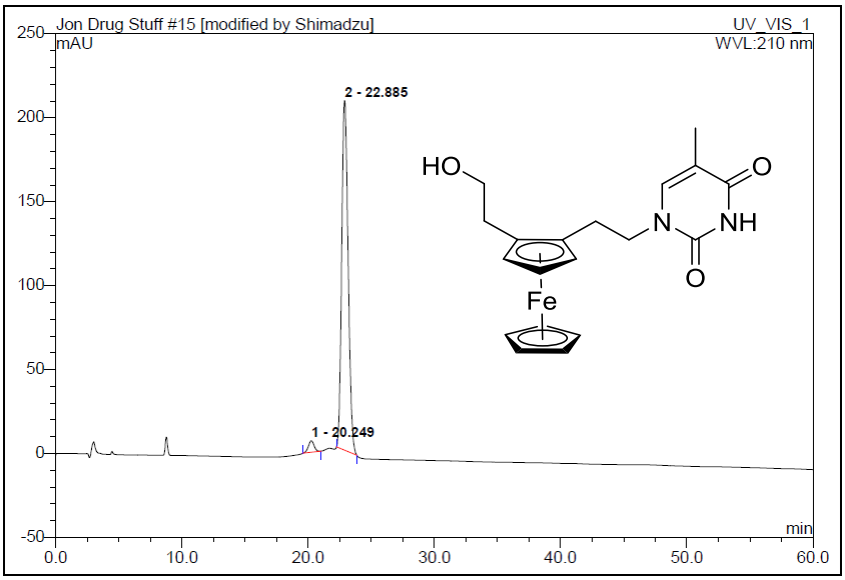


Fig. 3.27 Chiral HPLC trace of **Fcn2c2T**$_{(Rp)}$

Under identical conditions **Fcn2c2T-(S_p)** eluted to produce a large sharp peak (97.02%) at 20.012 min and a small peak (2.98%) at 22.730 min (**Fig. 3.28**). The composition of **Fcn2c2T**$_{(Sp)}$ was thus found to be 92% desired enantiomer and 8% opposite enantiomer (e.e. = 84%).

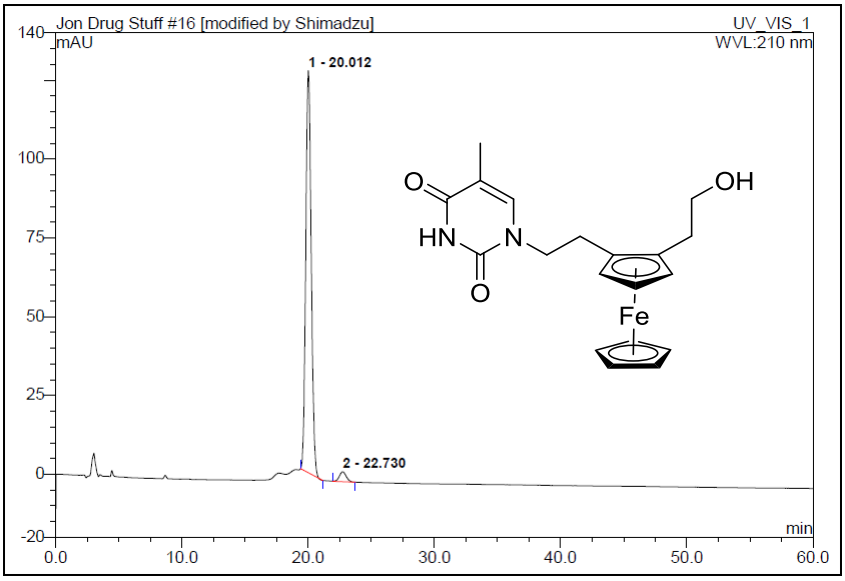


Fig. 3.28 Chiral HPLC trace of **Fcn2c2T**$_{(Rp)}$

Finally, to confirm the presence of only the two enantiomers of interest, a sample was prepared containing both **Fcn2c2T**$_{(Rp)}$ and **Fcn2c2T**$_{(Sp)}$. As expected, under identical

conditions the mixture eluted to produce just two sharp peaks with 19.979 min and 22.620 min retention time respectively (**Fig. 3.29**).

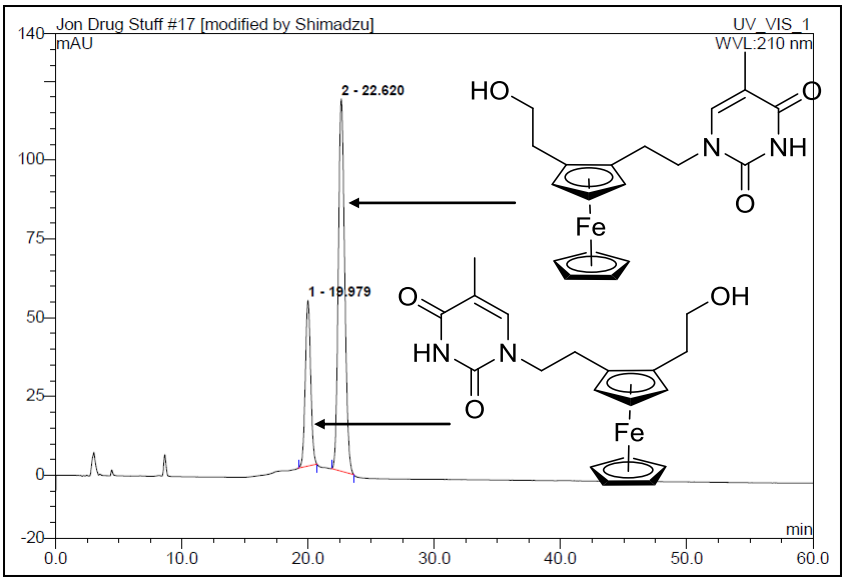
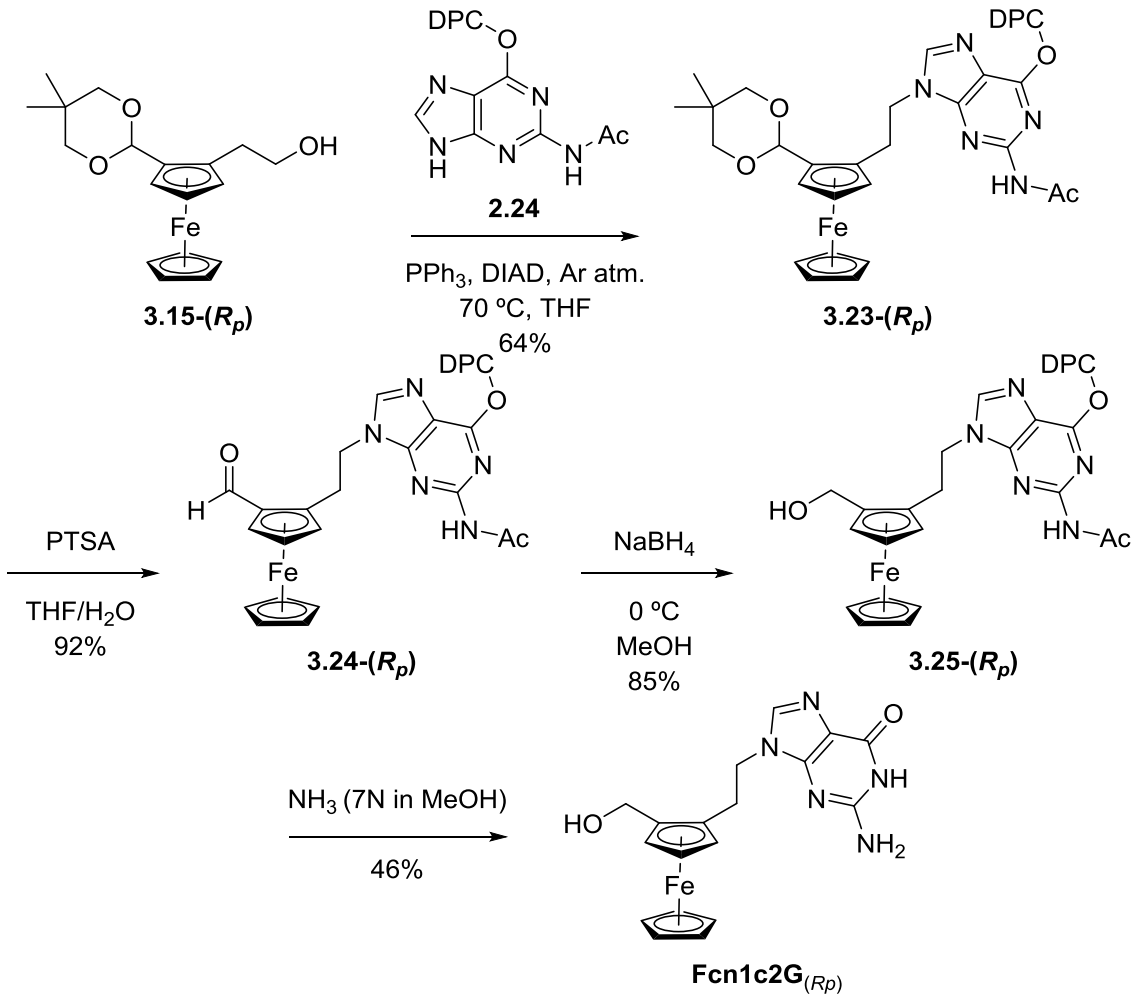


Fig. 3.29 Chiral HPLC trace of a mixture of **Fcn2c2T**$_{(Rp)}$ and **Fcn2c2T**$_{(Sp)}$

3.3.1.4 Synthesis of Fcn1c2G$_{(Rp)}$ and Fcn2c2G$_{(Sp)}$

Using a portion of alcohol **3.15-(R_p)** produced in the synthesis of **Fcn1c2T**$_{(Rp)}$, the guaninyl equivalent **Fcn1c2G**$_{(Rp)}$ was produced according to a very similar synthetic strategy (**Scheme 3.12**). The alcohol **3.15-(R_p)** was selectively coupled under Mitsunobu conditions to *N9* of protected guanine **2.24** to give the ferrocene conjugate **3.23-(R_p)** before PTSA in wet THF was used to remove the acetal group giving **3.24-(R_p)**. The aldehyde of **3.24-(R_p)** was then selectively reduced using $NaBH_4$ to give the alcohol **3.25-(R_p)**, before ammonia in methanol was used to effect removal of the carbamate and acetyl protecting groups from the guanine residue delivering the target compound **Fcn1c2G**$_{(Rp)}$.



Scheme 3.12 Synthesis of **Fcn1c2G**$_{(Rp)}$ in four steps from **3.15-(R_p)**

Single crystals of **Fcn1c2G**$_{(Rp)}$ were grown in a concentrated solution of DMSO and the absolute structure, including the *N9* regioselectivity of the Mitsunobu coupling, was confirmed by XRD; a low Flack parameter of 0.011(6) suggests the presence of just one enantiomer in the sample crystal (**Fig. 3.30 and Fig. 3.32**). Two crystallographically-independant molecules were identified, which form H-bonded chains with others of the same type (**Fig. 3.31**, **Fig. 3.33** and **Table 3.3**). The two chains then alternate in a parallel alignment with π-stacking interactions between guanine moieties and H-bonding through the presence of additional water molecules. Interestingly, the distance between the planes of guanine nucleobases is 3.2 Å, very close to the 3.4 Å distance obsereved in DNA (**Fig. 3.34**). Full crystal data for compound **Fcn1c2G**$_{(Rp)}$ can be found in the appendix (**Chapter 6.16**).

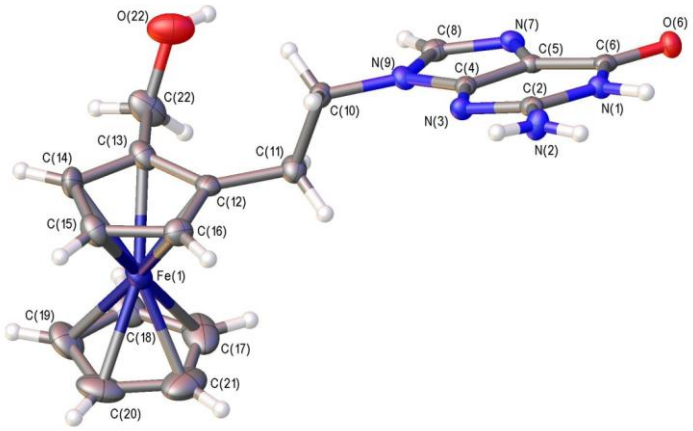


Fig. 3.30 Crystal structure of the first of two crystallographically-independent molecules in **Fcn1c2G**$_{(Rp)}$ with ellipsoids drawn at the 50% probability level. The structure contains four molecules of water which have been omitted for clarity.

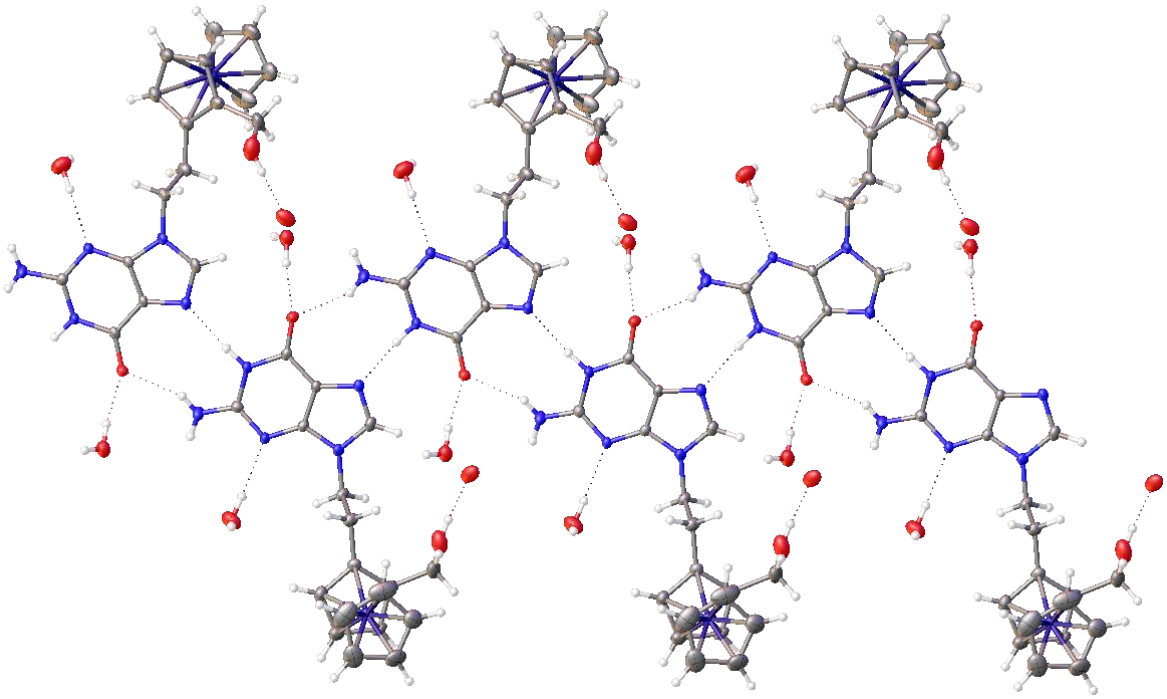


Fig. 3.31 The first of two hydrogen-bonded chains in the crystal structure of **Fcn1c2G**$_{(Rp)}$ with ellipsoids drawn at the 50 % probability level. Hydrogen bonding is shown using dotted lines. Three water molecules are shown which provide H-bonding between the alternating parallel chains.

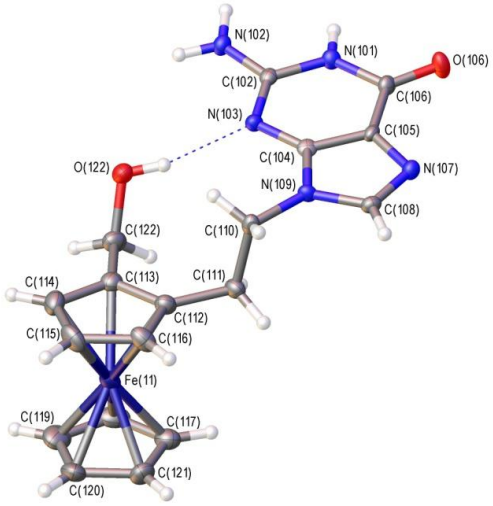


Fig. 3.32 Crystal structure of the second of two crystallographically-independent molecules in **Fcn1c2G**$_{(Rp)}$ with ellipsoids drawn at the 50 % probability level. The structure contains four molecules of water which have been omitted for clarity.

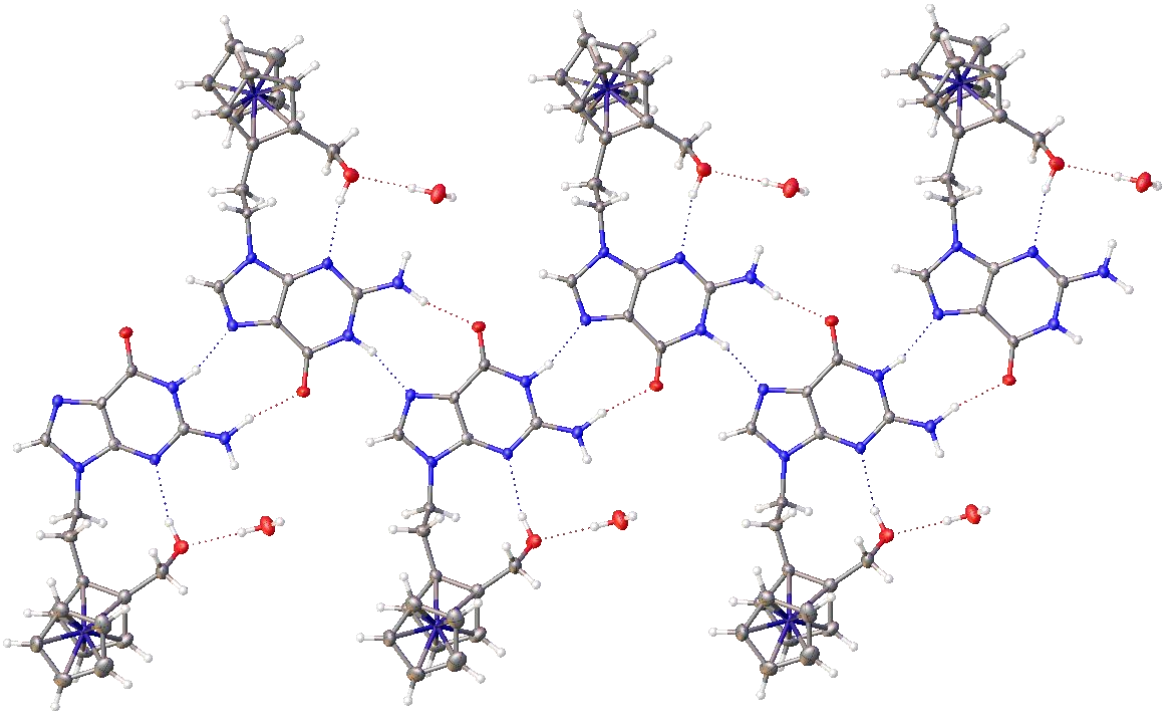


Fig. 3.33 The second of two hydrogen-bonded chains in the crystal structure of **Fcn1c2G**$_{(Rp)}$ with ellipsoids drawn at the 50 % probability level. Hydrogen bonding is shown using dotted lines. One molecule of water sits close to the plane and provides H-bonding between the alternating parallel chains.

Table 3.3 Hydrogen-bond lengths and angles in the extended structure of ferrocene guanine conjugate **Fcn1c2G**$_{(Rp)}$

Donor	Hydrogen	Acceptor	Bond Lengths			Bond Angle
D	H	A	D–H / Å	H–A / Å	D–A / Å	D–H–A / º
N(1)	H(1)	N(7)	0.92 (6)	1.96 (6)	2.872 (6)	174 (5)
N(2)	H(2A)	O(501)	0.85 (6)	2.17 (6)	2.971 (8)	158 (6)
N(2)	H(2A)	O(51′)	0.85 (6)	2.49 (7)	3.189 (18)	140 (5)
N(2)	H(2B)	O(6)	0.79 (6)	2.09 (6)	2.821 (6)	153 (6)
O(22)	H(22)	O(501)	0.82 (3)	2.2 (3)	2.782 (8)	134 (41)
O(22)	H(22)	O(51′)	0.82 (3)	1.69 (6)	2.509 (16)	175 (61)
C(8)	H(8)	O(6)	0.93	2.98	3.548	120.8
C(8)	H(8)	O(401)	0.93	2.56	3.272 (6)	134.1
C(8)	H(8)	O(51′)	0.93	2.75	3.634 (16)	159.4
N(101)	H(101)	N(107)	0.92 (9)	1.86 (9)	2.758 (6)	165 (8)
N(102)	H(10C)	O(301)	0.91 (6)	2.20 (6)	3.090 (6)	167 (5)
N(102)	H(10D)	O(106)	0.99 (8)	1.94 (8)	2.918 (6)	168 (6)
O(122)	H(122)	N(103)	0.86 (6)	2.06 (6)	2.910 (5)	166 (6)
C(108)	H(108)	O(106)	0.93	2.69	3.313 (6)	125.4
O(201)	H(20B)	N(3)	0.85	2.03	2.875 (5)	176.1
O(301)	H(30A)	O(22)	0.85	1.90	2.748 (6)	176.0
O(301)	H(30B)	O(122)	0.85	1.98	2.818 (6)	168.6
O(401)	H(40A)	O(6)	0.85	1.96	2.800 (5)	169.4
O(401)	H(40B)	O(301)	0.85	1.97	2.781 (6)	159.3
O(501)	H(50A)	O(401)	0.85	1.98	2.803 (8)	162.1
O(501)	H(50B)	O(201)	0.85	2.00	2.833 (9)	165.3

*Highlighted entries may qualify as “weak hydrogen-bonds”

Similar to the simple guanine conjugate **2.31** discussed in **Chapter 2** (**Fig. 2.28, p55**), the extended structure of **Fcn1c2G**$_{(Rp)}$ possibly gains some stabilisation from the presence of ‘weak H-bonds’, between both C(108) and O(106); and between C(8), O(6) and the accompanying water molecules (**Table 3.3**).

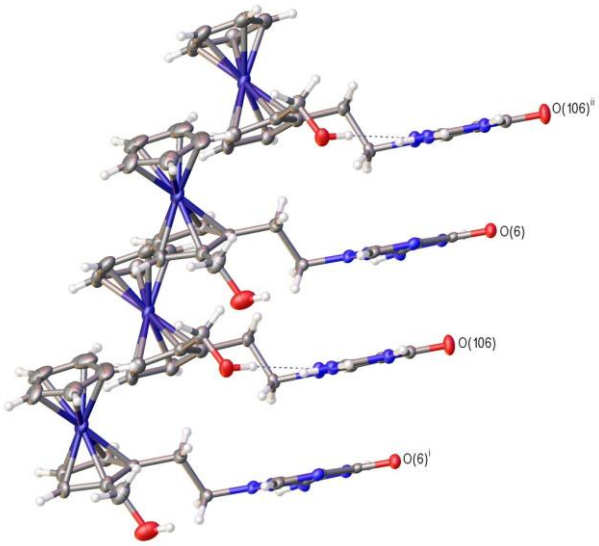
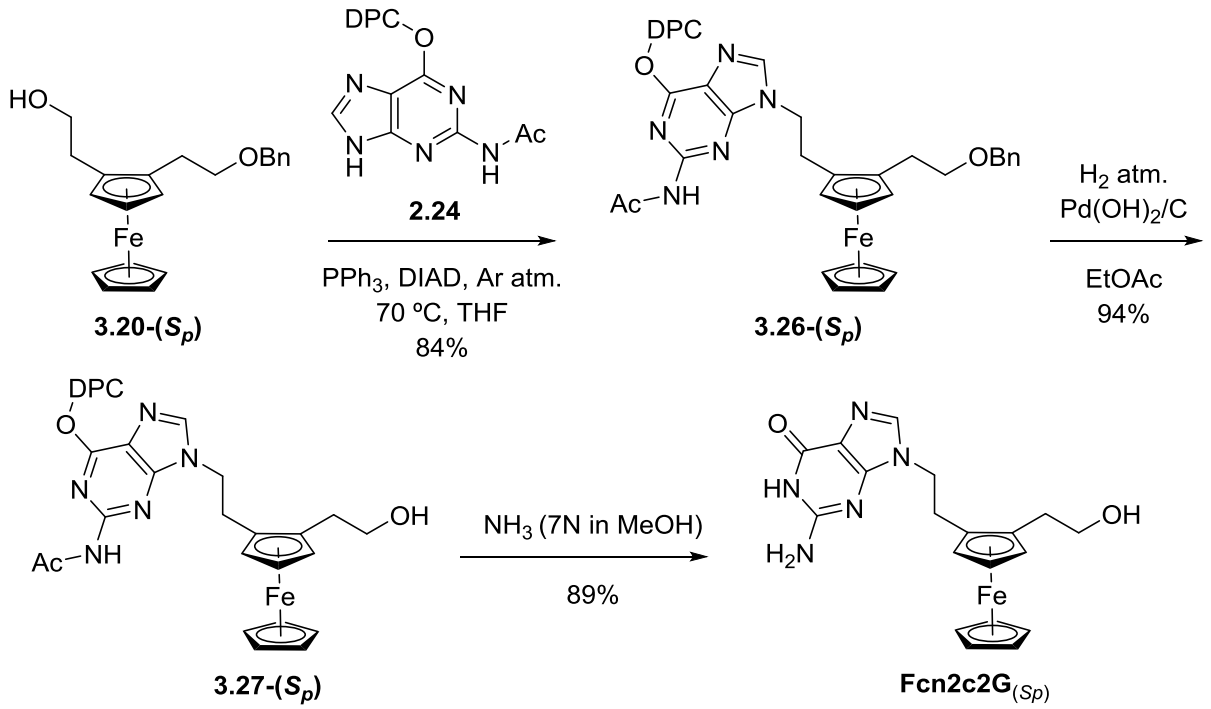


Fig. 3.34 The π-π stacking interactions in **Fcn1c2G**$_{(Rp)}$ with ellipsoids drawn at the 50% probability level. Hydrogen bonding is shown using dotted lines. The structure contains two crystallographically-independent ferrocene molecules and four molecules of water, which have been omitted for clarity. The mean planes through the guanine rings are virtually parallel (less than 0.5° twist) and the perpendicular distance between the planes is 3.2 Å in both cases. A chain of molecules are formed through π-π stacking interactions along the *c* axis. Symmetry codes for generation of equivalent atoms: \$1; x, y, 1+z, \$2; x, y, -1+z

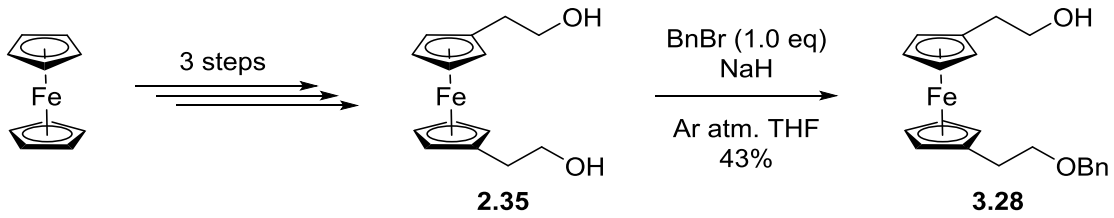
In a similar manner, the guaninyl equivalent **Fcn2c2G**$_{(Sp)}$ was synthesised using a portion of compound **3.20-(S_p)** produced in the synthesis of **Fcn2c2T**$_{(Sp)}$ (**Scheme 3.13**). Alcohol **3.20-(S_p)** was successfully coupled under Mitsunobu conditions to protected guanine **2.24** at the *N9* position producing the ferrocene conjugate **3.26-(S_p).** The benzyl group was then removed by hydrogenolysis using hydrogen over Pearlman's catalyst in EtOAc to give alcohol **3.27-(S_p)**. In the final step, the carbamate and acetyl protecting groups of the guanine residue were removed using ammonia in methanol to give the target compound **Fcn2c2G**$_{(Sp)}$.



Scheme 3.13 Synthesis of **Fcn2c2G**$_{(Sp)}$ in three steps from alcohol **3.20-(S_p)**

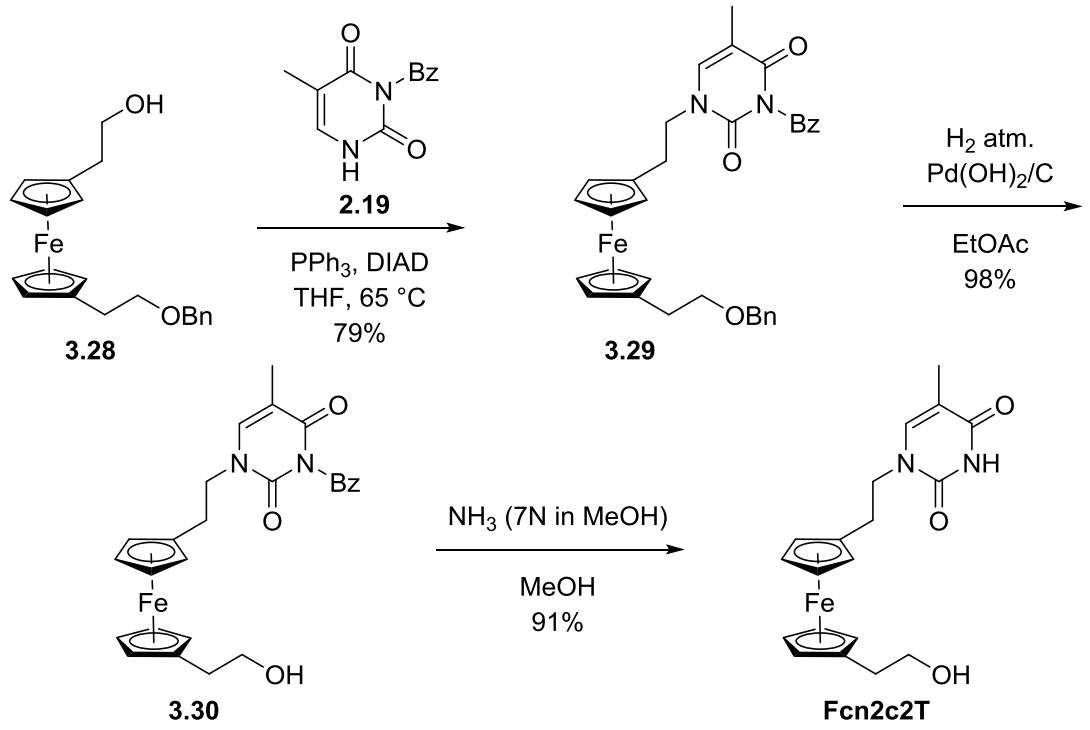
3.3.1.5 Synthesis of the 1,1'-Substituted Isomers Fcn2c2T and Fcn2c2G

Both **Fcn2c2T** and **Fcn2c2G**, in which the nucleobase and hydroxyl linkers are separated onto the separate Cp rings of ferrocene, were synthesised from a linear sequence of seven steps starting from ferrocene. Again the two compounds share a common synthon **3.28** which was synthesised in one step from the ferrocenyl diol **2.35**, the preparation of which is described in **Chapter 2**. Mono-protection of diol **2.35** was achieved using 1.0 equivalent of benzyl bromide to give compound alcohol **3.28** (**Scheme 3.14**). It is worth noting that, given the statistical nature of this reaction, significant quantities of starting diol and di-benzylated material were also recovered following a straightforward purification by flash column chromatography.



Scheme 3.14 Mono benzyl protection of diol **2.35** to give **3.28**

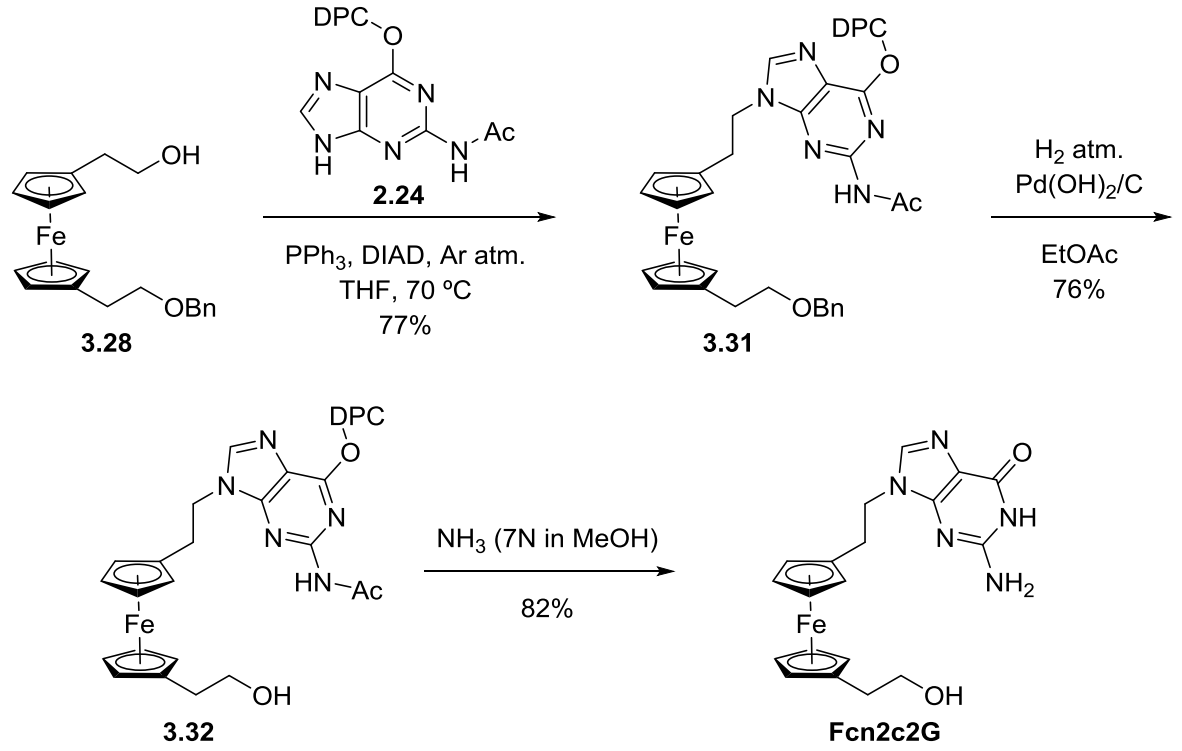
Fcn2c2T was produced from alcohol **3.28** in three steps (**Scheme 3.15**). *N3*-benzoyl thymine **2.19** was first coupled under Mitsunobu conditions to give the corresponding ferrocene conjugate **3.29**, before removal of the benzyl group was effected by hydrogenolysis releasing the hydroxyl group **3.30**. Finally, ammonia in methanol was used to deprotect the nucleobase to yield the target compound **Fcn2c2T**.



Scheme 3.15 Synthesis of **Fcn2c2T** in three steps from alcohol **3.28**

Fcn2c2G was produced from alcohol **3.28** in an analogous three step sequence (**Scheme 3.16**). Mitsunobu coupling of the protected guanine **2.24** gave the corresponding ferrocene conjugate **3.31**, before hydrogenolysis was used to selectively remove the benzyl

protecting group **3.32**. Ammonia in methanol was then used to deprotect the nucleobase yielding the target compound **Fcn2c2G**.



Scheme 3.16 Synthesis of **Fcn2c2G** in three steps from alcohol **3.28**

3.3.2 Electrochemistry and Lipophilicity

As discussed earlier, there is increasing evidence in the literature that ferrocene compounds in their native (II) state are not cytotoxic, but are instead activated inside the cell through oxidation to the ferrocenium (III) species.[22] It is postulated that in this state the iron centre undergoes a redox cycling process, generating hydroxyl, superoxide or other free radicals which in turn damage the genetic material leading to apoptosis; the ease with which oxidation occurs may therefore be a crucial factor in the cytotoxicity of these compounds.[79,80] It is however very important to take account of other parameters which may change alongside the redox behaviour. The series of ferrocenyl alcohols studied by Swarts for instance sees an increase in lipophilicity, concomitant with the ease of oxidation, as the length of the hydroxyalkyl linker is varied.[26] Therefore, alongside the electrochemical characterisation of

new compounds, it was decided that the lipophilicities of each should also be estimated using an in silico method.

3.3.2.1 Electrochemistry

Corresponding to the half-way point between the oxidation and reduction potential, the half-wave potential ($E_{1/2}$) provides a good indication of the relative ease of oxidation. Compounds with higher $E_{1/2}$ values require larger voltages before electron transfer processes are induced. Including ferrocene (Fc) and the previously published compound **Fcn3c2T**$_{(S,Rp)}$, the new compounds: **Fcn2c2T**$_{(Rp)}$, **Fcn1c2T**$_{(Rp)}$, **Fcn2c2G**$_{(Sp)}$, **Fcn1c2G**$_{(Rp)}$, **Fcn2c2T** and **Fcn2c2G** were therefore electrochemically characterised by cyclic voltammetry (CV) and their half-wave potential ($E_{1/2}$) values determined with respect to an internal reference of decamethylferrocene (dmfc). A three-electrode system consisting of a 3.0 mm diameter glassy carbon disc W.E., a platinum wire C.E. and an Ag/AgCl/3 M KCl R.E. was used in a solution of each of the ferrocenyl analytes (1.0 mM), in dry acetonitrile with dmfc (1.0 mM) and a supporting electrolyte of tetrabutylammonium hexafluorophosphate ($TBAPF_6$) (0.1 M). Using this set-up, the $E_{1/2}$ value for Fc was found to be + 509 mV compared to dmfc, which is in close agreement with the literature value of + 507 mV.[81] As an example, the cyclic voltammogram and plot of *peak current vs. the square root of the scan rate* for **Fcn3c2T**$_{(Rp)}$ are shown in **Fig. 3.35** and **Fig. 3.36** respectively. The corresponding figures for compounds **Fcn2c2T**$_{(Rp)}$, **Fcn1c2T**$_{(Rp)}$, **Fcn2c2G**$_{(Sp)}$, **Fcn1c2G**$_{(Rp)}$, **Fcn2c2T** and **Fcn2c2G** are provided in the appendix (**Chapter 6.2.2** – **6.2.7**). Although only one enantiomer of each of the chiral pairs was electrochemically characterised, it is reasonable to assume no difference in the electrochemistry.

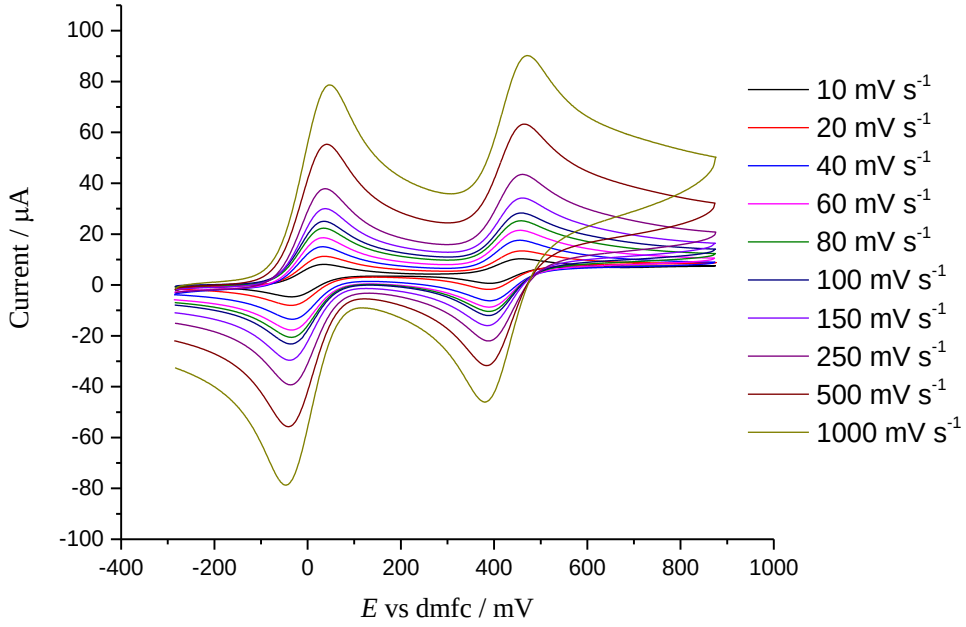


Fig. 3.35 Cyclic voltammograms of **Fcn3c2T**$_{(S,Rp)}$ (1.0 mM) at various scan rates wrt dmfc (1.0 mM) in dry acetonitrile with an electrolyte of $TBAPF_6$ (0.1 M)

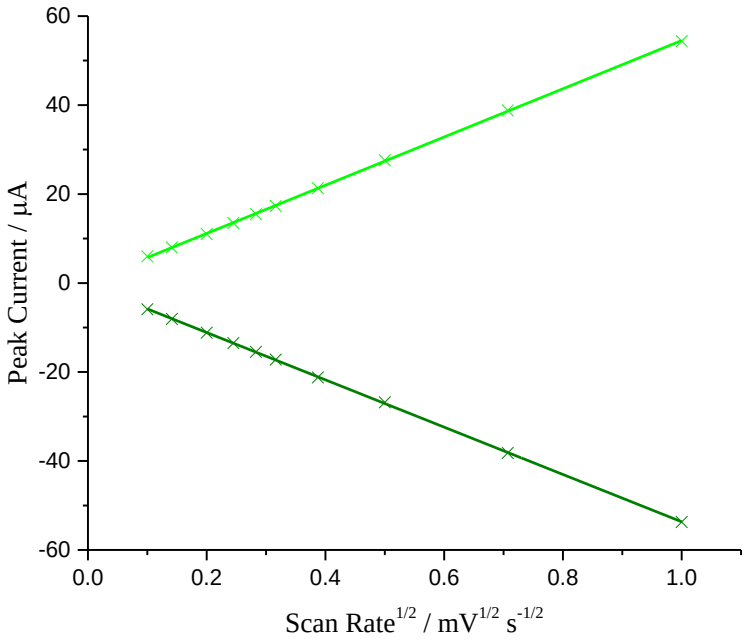


Fig. 3.36 Scan rate dependence of anodic (light green) and cathodic (dark green) peak currents for **Fcn2c3T**$_{(Rp)}$. The linear relationship between the current and square root of the scan rate indicates a reversible process.

All of the thymine compounds **Fcn3c2T**$_{(S,Rp)}$, **Fcn2c2T**$_{(Rp)}$, **Fcn1c2T**$_{(Rp)}$, and **Fcn2c2T** clearly displayed reversible, single-electron redox behaviour, evidenced by linear plots of peak current vs. the square root of the scan rate (see appendix); oxidation and reduction peak current ratios close to unity; and peak separations (mean for scan rates 10 – 100 mV s^{-1}) very similar to that observed for dmfc (ca. 65 – 70 mV) (**Table 3.3**). Interestingly the guanine containing compounds **Fcn2c2G**$_{(Sp)}$, **Fcn1c2G**$_{(Rp)}$ and **Fcn2c2G** all deviated slightly from this ideal behaviour, most noticeably in the ratio between the oxidation and reduction peak currents in which all three compounds produced values of approximately 1.20.

Table 3.4 Electrochemical characterisation of compounds **Fcn3c2T**$_{(S,Rp)}$, **Fcn2c2T**$_{(Rp)}$, **Fcn1c2T**$_{(Rp)}$, **Fcn2c2G**$_{(Sp)}$, **Fcn1c2G**$_{(Rp)}$, **Fcn2c2T** and **Fcn2c2G** showing the half-wave potential ($E_{1/2}$) values wrt dmfc, the ratios of the anodic and cathodic peak currents (i_{pa} / i_{pc}) and the mean separation between the peaks ($E_{pa} - E_{pc}$) (10 – 100 mV s^{-1}).

Compound	$E_{1/2}$ (mV) ± 5 wrt dmfc	i_{pa} / i_{pc}	Mean $E_{pa} - E_{pc}$ (mV) (10 – 100 mV s^{-1})
dmFc	0	1.00	69
Fcn3c2T$_{(S,Rp)}$	424	1.01	67.8
Fcn2c2T	460	0.95	66.8
Fcn2c2G	462	1.19	69.7
Fcn2c2T$_{(Rp)}$	467	0.95	67.7
Fcn2c2G$_{(Sp)}$	468	1.22	65.8
Fc	509	1.03	73.5
Fcn1c2T$_{(Rp)}$	518	0.98	66.3
Fcn1c2G$_{(Rp)}$	519	1.19	67.2

In agreement with previous researchers such as Swarts and Houlton, there is a clear inverse correlation between the hydroxyalkyl linker length and the corresponding $E_{1/2}$ value of the ferrocene compounds.[26,82] This trend can be rationalised in terms of the progressive stabilisation of the ferrocenium ion through positive inductive effects; longer alkyl chains donate more electron density to the metallocene, allowing oxidation to occur at a lower potential.

In agreement with the literature, the different nucleobases have only a slight effect upon the ease of oxidation.[82] Although the guanine compounds consistently produced $E_{1/2}$ values 1 or 2 mV higher than the corresponding thymine compounds these differences are within the error limits for this experiment. The substitution pattern of the ferrocene has a slightly greater effect upon the ease of oxidation. Comparing **Fcn2c2T**$_{(Rp)}$ and **Fcn2c2G**$_{(Sp)}$ (in which the hydroxyl and nucleobase groups are appended onto the same Cp ring) with their structural isomers **Fcn2c2T** and **Fcn2c2G** (in which the substituents occupy opposing rings), we see the former produce $E_{1/2}$ values 6 and 7 mV higher respectively, than the corresponding latter. This result is not surprising; with electron releasing groups on both Cp rings, the donated electron density is more evenly spread around the central metal, better stabilising the positive charge.

3.3.2.2 Lipophilicity

The important relationship between a compound's lipophilicity and its biological activity was identified over a century ago by Meyer and Overton while investigating the action of anaesthetics.[83] The effect is twofold; alongside other stronger forces such as hydrogen bonding and dipole interactions, the lipophilic character of a molecule can make an important contribution to the binding of a biological ligand to its target. Indeed, the hydrophobic

cavities which enclose the binding sites of many enzymes favour lipophilic guests which can gain extra stabilisation through London forces.[84] A second, more general effect is that of membrane permeability which influences the distribution and transport of the agent around the organism.[85] Lipid bilayers are essential to living organisms allowing the compartmentalisation and control of nuanced microenvironments. They are impermeable to ions, proteins and other water soluble species and regulate the movement of these items through the use of specialised channels and pumps. Lipophilic molecules however diffuse relatively easily across these membranes and are in general not so tightly controlled by the organism. It can be seen therefore that the absorption and distribution of a xenobiotic within an organism is largely dictated by its lipophilicity.[85]

Control of lipophilicity is therefore a major consideration in drug design and discovery.[86] Small increases in the lipophilicity of a lead candidate are often accompanied by a corresponding increase in activity, as more of the agent successfully reaches its target. Unfortunately however, in itself, this modification will not improve the selectivity, and therefore off-target interactions such as with the hERG (human Ether-à-g-go-Related Gene) channel (which contributes to the coordination of the heartbeat) are also likely to increase resulting in higher toxicity.[87] This misguided approach, in which potency is achieved through the inappropriate use of lipophilicity was termed 'molecular obesity' by Hann in 2011.[88] Lipophilicity is therefore an important physicochemical property which must be taken into account when comparing the activities of different compounds. Ideally it is measured experimentally; a known quantity of the compound of interest is partitioned between an organic (typically octanol) and an aqueous phase and the concentration of each determined. The *partition coefficient* (P) is defined as the ratio of the concentration in organic solvent to the concentration in the aqueous with lipophilicities typically expressed as the corresponding

logarithm (log P).[89] Although this is the best method for reliably determining the lipophilicity of a compound, it does rely on the synthesis of the compound of interest and with sufficient yield to accurately measure the concentrations. As an alternative, *in silico* methods have been developed which assess the constituent fragments of a molecule and piece them together to estimate the lipophilicity.[90,91,92] Reliable ClogP values can therefore be quickly determined for whole libraries of compounds without the need to synthesise them first.

Table 3.5 ClogP values for **Fcn3c2T**$_{(S,Rp)/(R,Sp)}$, **Fcn2c2T**$_{(Rp)/(Sp)}$, **Fcn1c2T**$_{(Rp)/(Sp)}$, **Fcn2c2G**$_{(Sp)}$ and **Fcn1c2G**$_{(Rp)}$ predicted by *ChemBioDraw Ultra 13.0*.

Compound	ClogP
Fcn3c2T$_{(S,Rp)/(R,Sp)}$	0.958
Fcn2c2T	– [a]
Fcn2c2T$_{(Rp)/(Sp)}$	0.030
Fcn1c2T$_{(Rp)/(Sp)}$	– 0.049
Fcn2c2G	– [a]
Fcn2c2G$_{(Sp)}$	– 0.653
Fcn2c1G$_{(Rp)}$	– 0.732

[a] Compounds **Fcn2c2T** and **Fcn2c2G** are expected to have slightly greater ClogP values than their respective regioisomers **Fcn2c2T**$_{(Rp)/(Sp)}$ and **Fcn2c2G**$_{(Sp)}$

The lipophilicities of the putative ferrocenyl nucleoside analogues **Fcn3c2T**$_{(S,Rp)}$, **Fcn2c2T**$_{(Rp)}$, **Fcn1c2T**$_{(Rp)}$, **Fcn2c2G**$_{(Sp)}$ and **Fcn1c2G**$_{(Rp)}$ were therefore investigated, as has been demonstrated by other researchers using *ChemBioDraw Ultra 13.0* to calculate their ClogP values (**Table 3.5**).[93,94] With substituents on both Cp rings, due to the limitations of the software, ClogP values could not be generated for the ferrocene compounds **Fcn2c2T** and **Fcn2c2G**. Due to the increased linearlity and hence surface area of these molecules, one

might expect the lipophilicity of these compounds to be similar, yet somewhat greater than their more branched structural isomers **Fcn2c2T**$_{(Rp)}$ and **Fcn2c2G**$_{(Sp)}$. Although these in silico estimations may not correlate to the absolute values one may obtain experimentally, they do, nonetheless, provide a rough indication of the relative lipophilicities of the agents. Indeed, the general trend is self-evident; lipophilicity increases with the length of the hydroxyalkyl linker and decreases upon replacement of the thymine nucleobase with the relatively polar guanine. The additional methyl group belonging to **Fcn3c2T**$_{(S,Rp)}$ and **Fcn3c2T**$_{(R,Sp)}$ increases the lipophilicity of these particular compounds still further.

Table 3.6 Half-wave potential ($E_{1/2}$) values (wrt dmfc) and ClogP values predicted by *ChemBioDraw Ultra 13.0*. for compounds **Fcn3c2T**$_{(S,Rp)/(R,Sp)}$, **Fcn2c2T**, **Fcn2c2G**, **Fcn2c2T**$_{(Rp)/(Sp)}$, **Fcn2c2G**$_{(Sp)}$, **Fcn1c2T**$_{(Rp)/(Sp)}$, and **Fcn1c2G**$_{(Rp)}$.

Compound	$E_{1/2}$ (mV) ± 5 wrt dmfc	ClogP
Fcn3c2T$_{(S,Rp)/(R,Sp)}$	424	0.958
Fcn2c2T	460	–
Fcn2c2G	462	–
Fcn2c2T$_{(Rp)/(Sp)}$	467	0.030
Fcn2c2G$_{(Sp)}$	468	– 0.653
Fcn1c2T$_{(Rp)/(Sp)}$	518	– 0.049
Fcn1c2G$_{(Rp)}$	519	– 0.732

As expected, the lipophilicities and the $E_{1/2}$ values for the series of compounds **Fcn3c2T**$_{(S,Rp)/(R,Sp)}$, **Fcn2c2T**$_{(Rp)/(Sp)}$ and **Fcn3c1T**$_{(Rp)/(Sp)}$, vary with the length of the hydroxyalkyl linker in a co-dependent fashion (**Table 3.6**). **Fcn2c2T** also seems to fit this

trend, having a somewhat lower $E_{1/2}$ value and being probably a little more lipophilic than **Fcn2c2T**$_{(Rp)/(Sp)}$. Changing the nucleobase however has a much greater effect upon the lipophilicity of the compounds than on the $E_{1/2}$ value. Comparing **Fcn1c2T**$_{(Rp)}$ and **Fcn2c2T**$_{(Sp)}$ with the corresponding guanine compounds **Fcn1c2G**$_{(Rp)}$ and **Fcn1c2G**$_{(Sp)}$, we see effectively no difference in the $E_{1/2}$ values but a relatively large difference in ClogP value of 0.683.

3.3.3 Biological Activity

The library of putative ferrocenyl nucleoside analogues were assessed for their anti-proliferative activity in cancer cell-lines by Dr. Nikolas Hodges and Dr. Zahra Khan in the School of Biosciences. Anti-viral studies were conducted by Prof. Jan Balzarini from the Laboratory of Virology and Chemotherapy at the Rega Institute.

3.3.3.1 Anticancer Activity

A cytotoxicity assay typically consists of exposing cell lines to increasing concentrations of a putative cytotoxic agent and quantifying the cell number over time. A widely employed protocol is the crystal violet cell viability assay which utilises a distinctive histological stain and photospectrometry to quantify the number of cells in a sample.[95,96] A 96 well-plate is seeded with a known number of cells and cultured overnight. Different concentrations of the inocula of interest are then introduced by pipette and the cultures incubated, typically for a period of 24 – 72 hours. After this time, the growth media is removed and any dead cells washed from the plate; the healthy cells remain adhered to the surface and are fixed using paraformaldehyde. A solution of crystal violet dye is then introduced which intercalates into the nuclear DNA, any excess dye is then washed away to leave a quantitative stain. The cells are lysed with acetic acid which releases the dye back into solution and spectrophotometry is

used to determine the absorbance of each well. The absorbance is proportional to the quantity of dye present which, in turn, corresponds to the quantity of DNA and hence the number of cells. By comparison with a control sample, which remains untreated and is allowed to freely proliferate, IC_{50} values (concentration at which proliferation is half that of the untreated control) can be determined.[95]

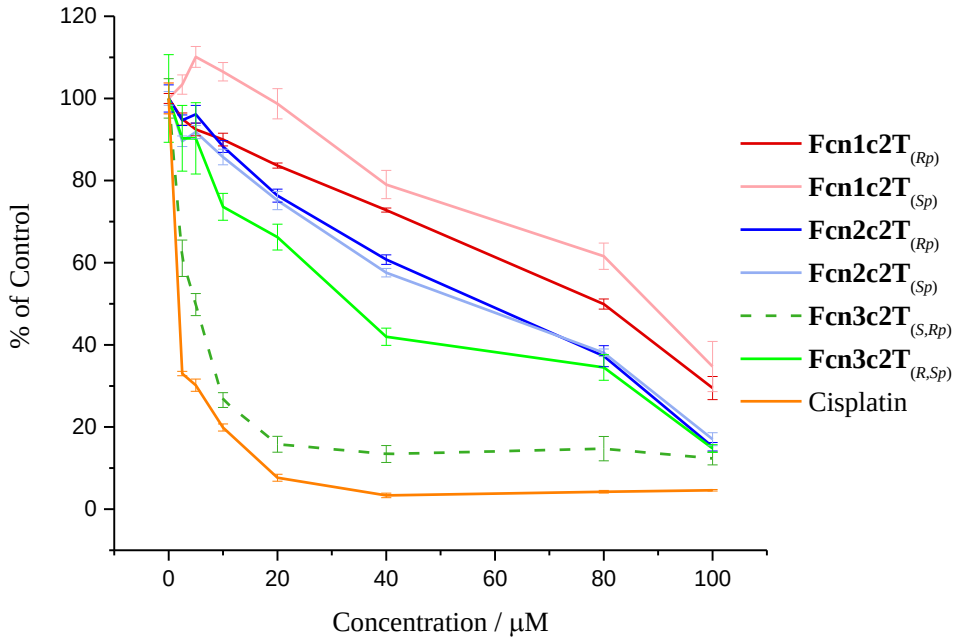


Fig. 3.37 Inhibition of HOS cell proliferation as a percentage of an untreated control after four days treatment with compounds **Fcn3c2T**$_{(S,Rp)}$, **Fcn3c2T**$_{(R,Sp)}$, **Fcn2c2T**$_{(Rp)}$, **Fcn2c2T**$_{(Sp)}$, **Fcn1c2T**$_{(Rp)}$, **Fcn1c2T**$_{(Sp)}$ and cisplatin. Error bars = SEM of at least three values.

The cytotoxicities of the series of compounds **Fcn3c2T**$_{(S,Rp)}$, **Fcn3c2T**$_{(R,Sp)}$, **Fcn2c2T**$_{(Rp)}$, **Fcn2c2T**$_{(Sp)}$, **Fcn1c2T**$_{(Rp)}$, and **Fcn1c2T**$_{(Sp)}$ were thus investigated at various concentrations in HOS osteosarcoma cells over 4 days and their activity compared to that of cisplatin. Absorbance (which corresponds to cell number) was plotted as a percentage of the untreated control against the concentration of test agent (**Fig. 3.37**). *Sigmaplot* was then used to fit the curves and the respective IC_{50} values (the concentration at which 50% inhibition is effected)

were calculated (**Table 3.7**). Giving IC_{50} values of 4.41 μM and 1.99 μM respectively, as in previous studies, **Fcn3c2T**$_{(S,Rp)}$ exhibits cytotoxicity comparable to that of cisplatin. Interestingly, the opposite enantiomer **Fcn3c2T**$_{(R,Sp)}$ is an order of magnitude less active, with an IC_{50} value of 34.3 μM. This striking effect is not however observed for the other pairs of enantiomers; **Fcn1c2T**$_{(Sp)}$ is approximately 15% less active than **Fcn1c2T**$_{(Rp)}$ and there is no significant difference in cytotoxicity between **Fcn2c2T**$_{(Rp)}$ and **Fcn2c2T**$_{(Sp)}$. A more general structure-activity relationship is however demonstrated, with clear correlation between the length of the hydroxyalkyl linker and the cytotoxicity. **Fcn1c2T**$_{(Rp)}$ and **Fcn1c2T**$_{(Sp)}$ are less active than **Fcn2c2T**$_{(Rp)}$ and **Fcn2c2T**$_{(Sp)}$ which are, in turn less active than **Fcn3c2T**$_{(S,Rp)}$ and **Fcn3c2T**$_{(R,Sp)}$.

Table 3.7 IC_{50} values for compounds **Fcn3c2T**$_{(S,Rp)}$, **Fcn3c2T**$_{(R,Sp)}$, **Fcn2c2T**$_{(Rp)}$, **Fcn2c2T**$_{(Sp)}$, **Fcn1c2T**$_{(Rp)}$, **Fcn1c2T**$_{(Sp)}$ and cisplatin against HOS cells

Compound	IC_{50} (μM)
Fcn3c2T$_{(S,Rp)}$	4.41
Fcn3c2T$_{(R,Sp)}$	34.3
Fcn2c2T$_{(Rp)}$	52.4
Fcn2c2T$_{(Sp)}$	50.7
Fcn1c2T$_{(Rp)}$	73.1
Fcn1c2T$_{(Sp)}$	85.7
Cisplatin	1.99

Fcn2c2G$_{(Sp)}$, **Fcn2c2G** and **Fcn2c2T** were also tested alongside **Fcn3c2T**$_{(S,Rp)}$ against HOS cells, under similar conditions but only up to a maximum concentration of 50 μM. Again, the absorbance was plotted as a percentage of an untreated control against concentration (**Fig. 3.38**). Although providing a rough indication of the activity of the compounds, the

concentrations used in this preliminary study were too low to calculate IC_{50} values. Instead, the % of an untreated control following four days of exposure at a concentration of 50 μM serves as the best indicator of activity available for these compounds (**Table 3.8**).

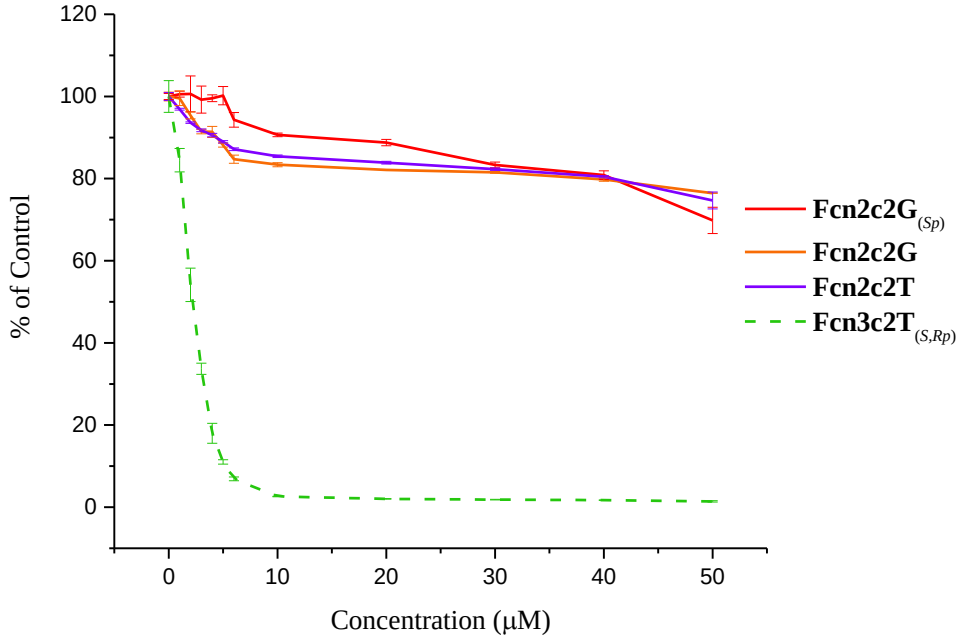


Fig. 3.38 Inhibition of HOS cell proliferation as a percentage of the untreated control after four days treatment with compounds **Fcn3c2T**$_{(S,Rp)}$, **Fcn2c2G**$_{(Sp)}$, **Fcn2c2G** and **Fcn2c2T**. Error bars = SEM of at least three values

Table 3.8 Percentage of the untreated control after four days treatment with compounds **Fcn3c2T**$_{(S,Rp)}$, **Fcn2c2G**$_{(Sp)}$, **Fcn2c2T** and **Fcn2c2G** at 50 μM in HOS cells

Compound	% of Control
Fcn3c2T$_{(S,Rp)}$	1
Fcn2c2G$_{(Sp)}$	73
Fcn2c2T	74
Fcn2c2G	76

Fcn2c2G$_{(Sp)}$, **Fcn2c2G** and **Fcn2c2T** displayed little difference in activity against HOS cells. All three inhibited the culture by approximately 25% compared to an untreated control. **Fcn3c2T**$_{(S,Rp)}$ is once again considerably more active than any of the other compounds, producing 99% inhibition of HOS cells after four days treatment at 50 µM.

Fcn1c2G$_{(Rp)}$ was not tested against HOS cells and therefore a direct comparison with the other compounds is not possible. An initial study, alongside **Fcn1c2T**$_{(Rp)}$ and **Fcn3c2T**$_{(S,Rp)}$ in oesophageal cancer cells (OE21), gives some indication of its relative cytotoxicity however. The cells were exposed to three concentrations of test agent (6.25 µM, 12.5 µM and 25.0 µM) and their growth assessed using the crystal violet assay over the course of four days. In this study all three concentrations of **Fcn3c2T**$_{(S,Rp)}$ inhibited the growth of the cells compared to the untreated control and displayed good dose-response (**Fig. 3.39**). Conversely, **Fcn1c2G**$_{(Rp)}$ and **Fcn1c2T**$_{(Rp)}$ showed very poor activity; neither compound produced any significant growth inhibition when compared to the untreated control sample (**Fig. 3.40** and **Fig. 3.41**).

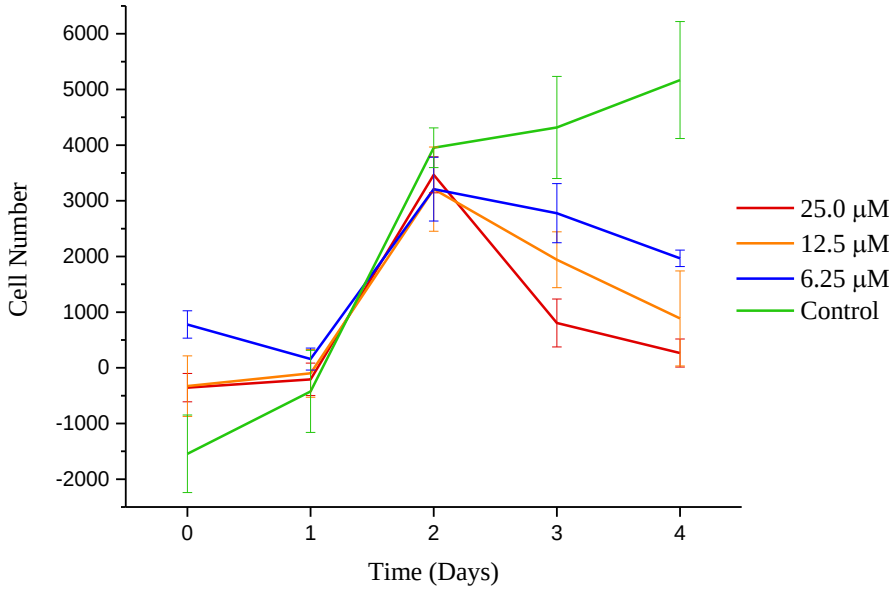


Fig. 3.39 Growth curves for **Fcn3c2T**$_{(S,Rp)}$ at 25.0 µM, 12.5 µM and 6.25 µM compared to an untreated control over four days against oesophageal cancer cells OE21

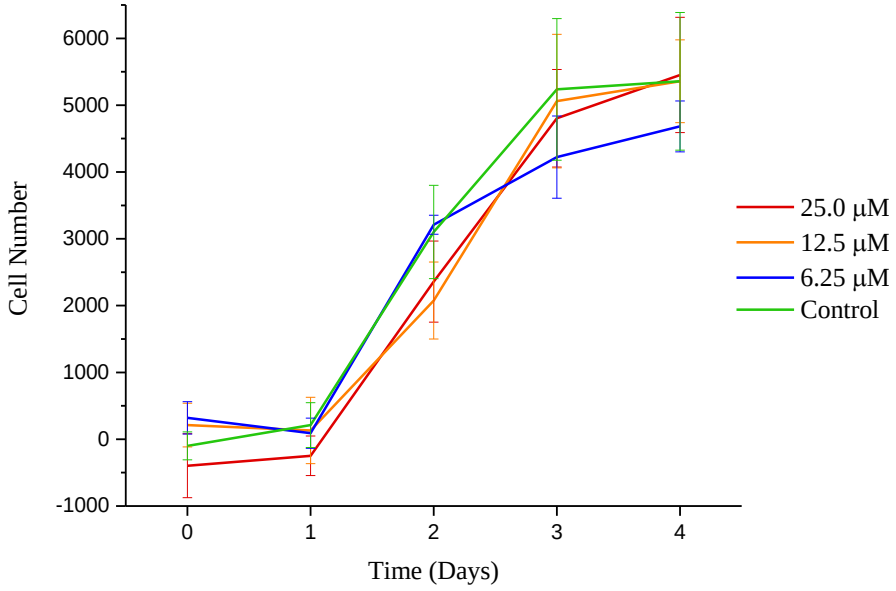


Fig. 3.40 Growth curves for **Fcn1c2G**$_{(Rp)}$ at 25.0 µM, 12.5 µM and 6.25 µM compared to an untreated control over four days against oesophageal cancer cells OE21

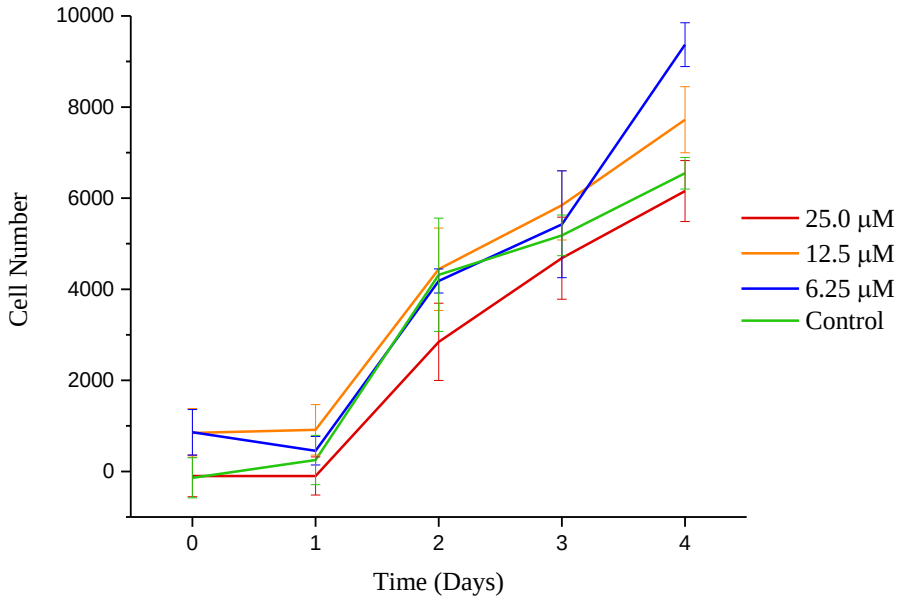


Fig. 3.41 Growth curves for **Fcn1c2T**$_{(Rp)}$ at 25.0 µM, 12.5 µM and 6.25 µM compared to an untreated control over four days against oesophageal cancer cells OE21

Table 3.9 IC_{50} values for compounds **Fcn3c2T**$_{(S,Rp)}$, **Fcn3c2T**$_{(R,Sp)}$, **Fcn1c2T**$_{(Rp)}$ and **Fcn1c2G**$_{(Rp)}$ in murine leukemia (L1210), human T-lymphocyte (CEM) and Hela cells.

	IC_{50} (μM)		
Compound	L1210	CEM	HeLa
Fcn3c2T$_{(S,Rp)}$	0.32 ± 0.06	0.37 ± 0.00	1.1 ± 0.5
Fcn3c2T$_{(R,Sp)}$	4.2 ± 0.6	3.6 ± 0.8	13 ± 6
Fcn1c2T$_{(Rp)}$	101 ± 16	87 ± 31	182 ± 11
Fcn1c2G$_{(Rp)}$	> 250	> 250	> 250

A collaborator, Prof. Jan Balzarini also undertook cytotoxicity studies of **Fcn3c2T**$_{(S,Rp)}$ **Fcn3c2T**$_{(R,Sp)}$, **Fcn1c2T**$_{(Rp)}$ and **Fcn1c2G**$_{(Rp)}$ in murine leukemia (L1210), human T-lyphocyte (CEM) and HeLa cells (**Table 3.9**) using the MTS assay for cell viability.[97] In agreement with the previous findings, the cytotoxicity of **Fcn3c2T**$_{(S,Rp)}$ is an order of magnitude greater than **Fcn3c2T**$_{(R,Sp)}$ in all three cell types. Once again **Fcn1c2T**$_{(Rp)}$ and **Fcn3c2G**$_{(Rp)}$ produced much lower levels of cytotoxicity.

3.3.3.2 Antiviral Activity

The antiviral activities of **Fcn3c2T**$_{(S,Rp)}$, **Fcn3c2T**$_{(R,Sp)}$, **Fcn1c2T**$_{(Rp)}$ and **Fcn1c2G**$_{(Rp)}$ were compared with the established antiviral agents brivudin, cidofovir, acyclovir and ganciclovir against herpes simplex virus 1 (HSV1) and 2 (HSV2) varicella virus (VV) and varicella zoster virus (VZV) in erythroleukemia (HEL) cells using a visual, cytopathic effect (CPE) assay (**Table 3.10**). This type of assay uses a confluent layer of cells which are not rapidly dividing. Under these conditions, **Fcn3c2T**$_{(S,Rp)}$ and **Fcn3c2T**$_{(R,Sp)}$ display much lower cytotoxicity allowing the investigation of their antiviral effects.[98]

Producing EC_{50} values of 1, 2, 0.4 and 0.03 mg ml^{-1} respectively, **Fcn3c2T**$_{(S,Rp)}$ displays antiviral activity against HSV1 and HSV2 comparable with cidofovir and acyclovir but somewhat less activity than gangciclovir. Against VV the most potent compounds are **Fcn3c2T**$_{(S,Rp)}$, brivudin and cidofovir with all three producing very similar EC_{50} values of 9, 10 and 17 mg ml^{-1} respectively. **Fcn3c2T**$_{(S,Rp)}$ does however display the most potent antiviral activity against VZV, producing an EC_{50} value at least ten times smaller than the established antiviral agents. **Fcn3c2T**$_{(R,Sp)}$ displays five to twenty times lower antiviral activity than **Fcn3c2T**$_{(S,Rp)}$, producing EC_{50} values of 20, 20, 45 and > 100 mg ml^{-1} against HSV1, HSV2, VV and VZV respectively. Both **Fcn1c2T**$_{(Rp)}$ and **Fcn3c2G**$_{(Rp)}$ displayed very poor antiviral activity, producing EC_{50} values of > 100 mg ml^{-1} in all instances.

Table 3.10 Antiviral activity of **Fcn3c2T**$_{(S,Rp)}$, **Fcn3c2T**$_{(R,Sp)}$, **Fcn1c2T**$_{(Rp)}$ and **Fcn3c2T**$_{(Rp)}$ against herpes simplex virus 1 (HSV1) and 2 (HSV2), varicella virus (VV), and varicella zoster virus (VZV) compared with the established antiviral drugs brivudin, cidofovir, acyclovir and ganciclovir.

		EC_{50} (μg ml^{-1})			
Compound	Min. cytotoxic conc. (μg ml^{-1})	HSV1 (KOS)	HSV2 (G)	VV	VZV
Fcn3c2T$_{(S,Rp)}$	100	1	1	9	> 20
Fcn3c2T$_{(R,Sp)}$	> 100	20	20	45	> 100
Fcn1c2T$_{(Rp)}$	> 100	> 100	> 100	> 100	> 100
Fcn1c2G$_{(Rp)}$	> 100	> 100	> 100	> 100	> 100
Brivudin	> 250	0.02	183	10	> 250
Cidofovir	> 250	2	2	17	> 250
Acyclovir	> 250	0.4	0.4	> 250	> 250
Ganciclovir	> 100	0.03	0.03	> 100	> 100

3.3.4 Discussion

Although superficially, the new thymine bearing compounds **Fcn1c2T**$_{(Rp)}$ and **Fcn2c2T**$_{(Rp)}$ more closely resemble an endogenous nucleoside, each progressive shortening of the hydroxyl linker length clearly reduces the cytotoxic activity of these compounds compared to **Fcn3c2T**$_{(S,Rp)}$ (**Table 3.11**). If, as is hypothesised, **Fcn3c2T**$_{(S,Rp)}$ is acting as a nucleoside analogue, it is possible that by moving the ferrocene unit into closer proximity with the pseudo-5′-hydroxyl group, these compounds appear progressively more foreign to the cellular machinery and therefore fail some crucial recognition or activation event such as phosphorylation, resulting in their reduced potency.

Table 3.11 Summary of $E_{1/2}$, ClogP and available IC_{50} values for compounds **Fcn3c2T**$_{(S,Rp)}$, **Fcn3c2T**$_{(R,Sp)}$, **Fcn2c2T**$_{(Rp)}$, **Fcn2c2T**$_{(Sp)}$, **Fcn1c2T**$_{(Rp)}$ and **Fcn1c2T**$_{(Sp)}$

Compound	$E_{1/2}$ (mV) ± 5	ClogP	IC_{50} (μM) HOS	L1210	CEM	Hela
Fcn3c2T$_{(S,Rp)}$	425	0.958	4.41	0.32 ± 0.06	0.37 ± 0.00	1.1 ± 0.5
Fcn3c2T$_{(R,Sp)}$	(425)	0.958	34.3	4.2 ± 0.6	3.6 ± 0.8	13 ± 6
Fcn2c2T$_{Rp)}$	468	0.030	50.7	-	-	-
Fcn2c2T$_{(Sp)}$	(468)	0.030	52.4	-	-	-
Fcn1c2T$_{(Rp)}$	518	– 0.049	73.1	101 ± 16	87 ± 31	182 ± 11
Fcn1c2T$_{(Sp)}$	(518)	– 0.049	85.7	-	-	-

Alternatively however, the cytotoxicity of these compounds may be much less specific, and may derive, as has been suggested for other ferrocene compounds, from their redox properties and/or lipophilicity, and both these scenarios fit the general trend observed for the thymine series of compounds. Firstly, the ease of oxidation of the compounds, as indicated by their respective $E_{1/2}$ values, correlates with their cytotoxicity. The most potent compound **Fcn3c2T**$_{(S,Rp)}$ is also the most easily oxidised; the ferrocenium form benefitting from the

stabilising, positive inductive effects of a three carbon hydroxyalkyl linker which also bears an additional α-methyl group. As the hydroxyalkyl linker is truncated, the ferrocenium form become less stable, disfavouring oxidation and thus rendering **Fcn2c2T**$_{(Rp)}$ and **Fcn1c2T**$_{(Rp)}$ successively less potent. For this series of compounds however, the $E_{1/2}$ value changes in tandem with ClogP, and therefore it is impossible to meaningfully attribute the potency to one, other, or a combination of both of these influences.

Of most interest is the order of magnitude difference in potency between the enantiomers **Fcn3c2T**$_{(S,Rp)}$ and **Fcn3c2T**$_{(R,Sp)}$. As a mirror-image pair, the bulk properties of these molecules are identical with no difference in lipophilicity or electrochemistry. This would suggest that some specific interaction with one or other chiral entity within the biological system, be it enzyme, protein or nucleic acid, may be responsible for this profound difference in cytotoxicity. A similar difference was observed in the antiviral activities of the two compounds against HSV1, HSV2, VV and VZV, providing more evidence of the unusual difference in biological interaction. However, given the widespread cytotoxicity of these compounds, they are unlikely to make useful antiviral agents.

Table 3.12 Summary of cytotoxicity (given as% of untreated control), $E_{1/2}$ and ClogP values for compounds **Fcn3c2T**$_{(S,Rp)}$, **Fcn3c2G**$_{(Sp)}$, **Fcn2c2T** and **Fcn2c2G**

Compound	% of Control	$E_{1/2}$ (mV) ± 5	ClogP
Fcn3c2T$_{(S,Rp)}$	1	425	0.958
Fcn2c2G$_{(Sp)}$	73	468	– 0.653
Fcn2c2T	74	460	-
Fcn2c2G	76	462	-

Little difference in cytotoxicity is exhibited by the compounds **Fcn2c2G**$_{(Sp)}$, **Fcn2c2T** and **Fcn2c2G**; after four days treatment at 50 μM, all three compounds inhibited HOS cell proliferation by approximately 25% compared to the untreated control (**Table 3.12**). This result would suggest that neither the change in nucleobase nor the ferrocene substitution pattern radically affects the activity of these compounds. This is interesting given the difference in physicochemical properties of the molecules. Although the ClogP values are not very reliable, we would certainly expect the guanine compounds to be less lipophilic than their thymine equivalents and therefore, with other considerations being equal, probably less biologically active. The $E_{1/2}$ values of these compounds are quite similar, neither the nucleobase nor the ferrocene substitution pattern affecting the ease of oxidation very much. This can be correlated with the similar levels of cytotoxicity exhibited, and therefore may be evidence for linking the redox chemistry, rather than lipophilicity with the biological activity.

Cytotoxicity studies involving the guanine compound **Fcn1c2G**$_{(Rp)}$ showed it to be certainly no more active than the thymine equivalent **Fcn1c2T**$_{(Rp)}$ (**Table 3.13**). Although at the concentrations used, neither compound inhibited the proliferation of OE21 cells, some discrimination was found at higher concentrations against L1210, CEM and HeLa cells, with **Fcn1c2T**$_{(Rp)}$ displaying one-and-a-half to three times the cytotoxicity of **Fcn1c2G**$_{(Rp)}$. Both compounds exhibited poor antiviral activity against HSV1, HSV2, VV and VZV. Once again, replacement of the thymine nucleobase with guanine renders the molecule less lipophilic and does not significantly alter the $E_{1/2}$ value. The fact that the guanine compound was, in some studies considerably less active than the thymine could suggest that the lipophilicity may play an important role in the activity of the compounds.

Table 3.13 Summary of the $E_{1/2}$, ClogP and the IC_{50} values for compounds **Fcn3c2T**$_{(S,Rp)}$, **Fcn1c2T**$_{(Rp)}$ and **Fcn1c2G**$_{(Rp)}$

Compound	$E_{1/2}$ (mV) ± 5	ClogP	IC_{50} (μM)		
			L1210	CEM	HeLa
Fcn1c2T$_{(S,Rp)}$	425	0.958	0.32 ± 0.06	0.37 ± 0.00	1.1 ± 0.5
Fcn1c2T$_{(Rp)}$	518	– 0.049	101 ± 16	87 ± 31	182 ± 11
Fcn1c2G$_{(Rp)}$	519	– 0.732	> 250	> 250	> 250

3.4 Conclusions

In conclusion, eight new structural variations based on the putative ferrocenyl nucleoside analogue **Fcn3c2T**$_{(S,Rp)}$ were successfully synthesised. Sharing the same planar chirality, and thymine nucleobase, the structures of **Fcn2c2T**$_{(Rp)}$ and **Fcn1c2T**$_{(Rp)}$ have the hydroxyalkyl linker length reduced to two and one carbon atoms respectively compared to the corresponding three carbons of **Fcn3c2T**$_{(S,Rp)}$. The opposite enantiomers **Fcn2c2T**$_{(Sp)}$ and **Fcn2c2T**$_{(Sp)}$ were also prepared. A second variation explored the ferrocene substitution pattern. **Fcn2c2T**, a structural isomer of **Fcn2c2T**$_{(Rp)}$ and **Fcn2c2T**$_{(Sp)}$ replaced the 1,2-arrangement, in which the nucleobase and hydroxyalkyl moieties are attached to the same Cp ring, with a 1,1'-arrangement in which they are attached to opposite rings. To explore the influence of the nucleobase identity, the guanine equivalents **Fcn2c2G**$_{(Sp)}$, **Fcn1c2G**$_{(Rp)}$ and **Fcn2c2G** were also prepared.

Single crystals of compounds **Fcn1c2T**$_{(Rp)}$, **Fcn1c2T**$_{(Sp)}$, **Fcn2c2T**$_{(Rp)}$, **Fcn2c2T**$_{(Sp)}$ and **Fcn1c2G**$_{(Rp)}$ were grown and XRD analysis used to confirm their absolute structures; the low Flack parameters obtained in these analyses suggested the sample crystals were of high enantiopurity. **Fcn1c2T**$_{(Rp)}$, **Fcn1c2T**$_{(Sp)}$, **Fcn2c2T**$_{(Rp)}$ and **Fcn2c2T**$_{(Sp)}$ were also assessed by chiral HPLC, which confirmed the chiral purities as 95%, 92%, 97% and 92% respectively.

Alongside the previously reported compound **Fcn3c2T**$_{(S,Rp)}$ and its opposite enantiomer **Fcn3c2T**$_{(S,Rp)}$, the electrochemisty of the eight new compounds was assessed by cyclic voltammetry, from which their respective half-wave potential ($E_{1/2}$) values were determined. In accordance with the work of other researchers, a negative correlation was demonstrated between the length of the hydroxyalkyl linker and the corresponding $E_{1/2}$ value. This was attributed to the increasing positive inductive effects progressively stabilising the ferrocenium

form of the compound and thus rendering oxidation more favourable. Changing the nucleobase from thymine to guanine produced a slight increase in the $E_{1/2}$ values of the compounds, again in accordance with the work of others. Changing the ferrocene substitution from a 1,2- arrangement to a 1,1'- arrangement produced a slight decrease in the $E_{1/2}$ value, corresponding to the positive inductive effects being spread more evenly around the molecule and thus once again providing better stabilisation of the ferrocenium ion.

The lipophilicities of the compounds were calculated as ClogP values using *ChemBioDraw Ultra 13.*. Although values could not be obtained for compounds **Fcn2c2T** and **Fcn2c2G**, for comparison it was assumed that they would follow the general trend of increasing lipophilicity with the length of the hydroxyalkyl linker and that the thymine compound would be more lipophilic than the guanine equivalent.

The cytotoxic activity of the compounds was assessed in osteosarcoma (HOS), oesophageal cancer (OE21), murine leukemia (L1210), human T-lyphocyte (CEM) and HeLa cells. These studies showed that, although compounds **Fcn1c2T**$_{(Rp)}$ and **Fcn2c2T**$_{(Rp)}$, and their opposite enantiomers **Fcn1c2T**$_{(Sp)}$ and **Fcn2c2T**$_{(Sp)}$, better resemble an endogenous nucleoside analogue than **Fcn3c2T**$_{(S,Rp)}$ and **Fcn3c2T**$_{(R,Sp)}$, their cytotoxicity is in fact reduced. Given that these modifications did not have the desired effect, and instead having demonstrated that the cytotoxicity of this series of compounds is more closely related to both the ease of oxidation and the lipophilicity, we might conclude that these non-specific physicochemical and electrochemical properties are solely responsible for the activity of the compounds. This explanation however cannot explain the striking difference in cytotoxicity between **Fcn3c2T**$_{(S,Rp)}$ and its enantiomer **Fcn3c2T**$_{(R,Sp)}$ which must surely share identical ClogP and

$E_{1/2}$ values. On the contrary, this result clearly suggests a specific mechanism of action based upon the chiral recognition of one or more biological targets.

3.5 Future Work

Exchanging the thymine nucleobase of **Fcn1c2T**$_{(Rp)}$, **Fcn2c2T**$_{(Sp)}$ and **Fcn2c2T** with guanine, to give **Fcn1c2G**$_{(Rp)}$ and **Fcn2c2G**$_{(Sp)}$ and **Fcn2c2G**, did not increase the cytotoxicity of these compounds, however the guanine equivalent of the most active structure **Fcn3c2T**$_{(S,Rp)}$ was not investigated. To confirm that this behaviour is consistent across the library of compounds, future work would therefore be to synthesise and investigate the biological activity of **Fcn3c2G**$_{(S,Rp)}$ (**Fig. 3.42**).

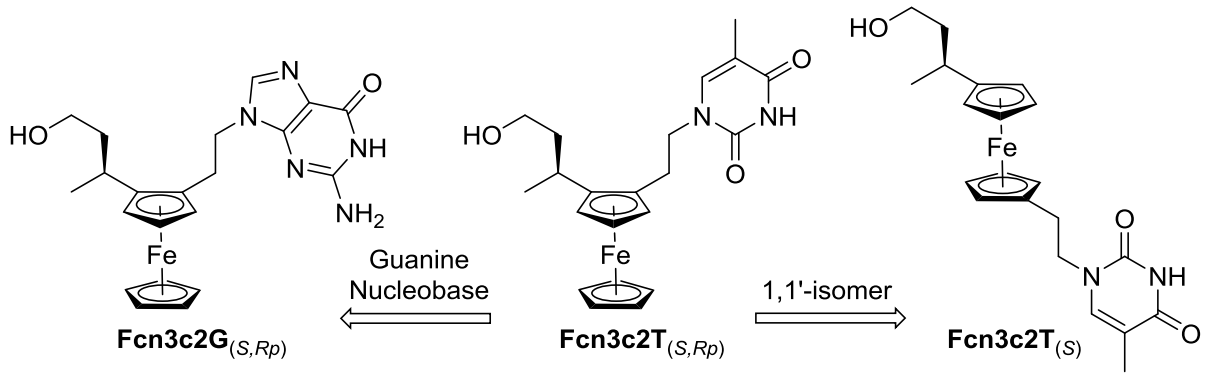


Fig. 3.42 Fcn3c2T$_{(S,Rp)}$ the guanine equivalent **Fcn3c2G**$_{(S,Rp)}$ and the 1,1′-regioisomer **Fcn3c2T**$_{(S)}$

Similarly, only the 1,1′-regioisomers of **Fcn2c2T**$_{(Rp)/(Sp)}$ and **Fcn2c2G**$_{(Rp)}$ have been examined for their biological activity. Future work should therefore focus upon the synthesis of the 1,1′-regioisomer **Fcn3c2T**$_{(S)}$ of the most potent compound **Fcn3c2T**$_{(S,Rp)}$ to confirm whether or not the substitution pattern is an important structural feature (**Fig. 3.42**).

It is interesting that Schmalz found that the presence of a lipophilic protecting group (typically TDS) at the pseudo 5′-hydroxyl was crucial to the cytotoxicity of his compounds.[72] Given the structural similarities between these two sets of "iron-containing nucleoside analogues", and that mechanistically neither seem to operate as typical nucleoside analogues, but instead, interact with some unknown biological target, it would be very interesting to

protect the less potent compounds **Fcn1c2T**$_{(Rp)}$ and **Fcn2c2T**$_{(Rp)}$ in this manner to give 5′-TDS-**Fcn1c2T**$_{(Rp)}$ and 5′-TDS-**Fcn2c2T**$_{(Rp)}$ respectively, and investigate the effect of this modification upon their cytotoxicity (**Fig. 3.43**).

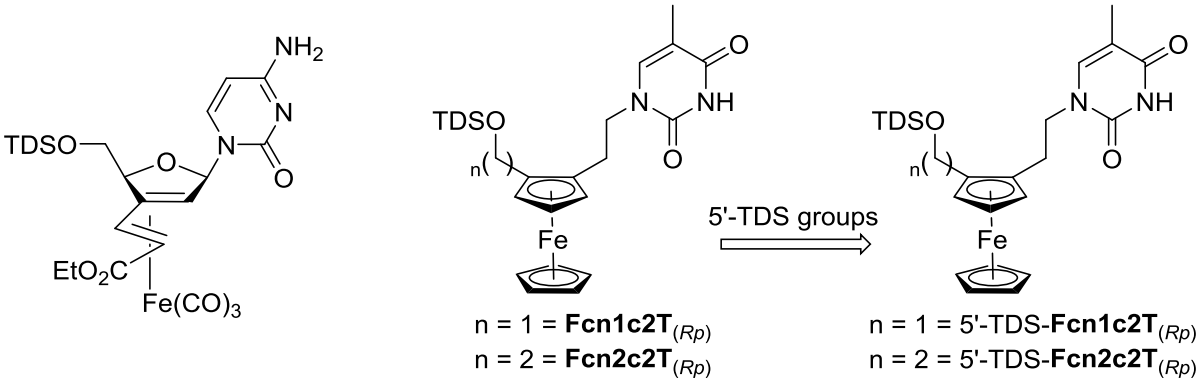


Fig. 3.43 TDS-protected variations based upon the work of Schmaltz, 5′-TDS-**Fcn1c2T**$_{(Rp)}$ and 5′-TDS-**Fcn2c2T**$_{(Rp)}$

3.6 References

[1] O. Wada, *Japan Med. Assoc. J.*, **2004**, 47, 351 – 358.

[2] S. J. Lippard, *Bioinorganic Chemistry*, University Science Books, **1994**, 505 – 583.

[3] R. F. McKnight, M. Adida, K. Budge, S. Stockton, G.M. Goodwin, J. R. Geddes, *Lancet*, **2012**, 379, 721 – 728.

[4] A. W. Stange, D. E. Hilmas, F. J. Furman, *Toxicology*, **1996**, 111, 213 – 224.

[5] J. Liu, Y. Lu, Q. Wu, R. A. Goyer, M. P. Waalkes, *J. Pharmacol. Exp. Ther.*, **2008**, 326, 363 – 368.

[6] A. Kumar, A. G. C. Nair, A. V. R. Reddy, A. N. Garg, *Biological Trace Element Research*, **2006**, 109, 231 – 254.

[7] W. H. Miller, H. M. Schipper, J. S. Lee, J. Singer, S. Waxman, *Cancer Res.*, **2002**, 62, 3893 – 3903.

[8] G. Koukourakis, N. Kelekis, V. Armonis, V. Kouloulias, *Adv. Urol.*, **2009**, 9.

[9] M. Frezza, S. Hindo, D. Chen, A. Davenport, S. Schmitt, D. Tomco, Q. P. Dou, *Curr. Pharm. Des.*, **2010**, 16, 1813 – 1825.

[10] T. W. Hambley, *Science*, **2007**, 318, 1392 – 1393.

[11] K. D. Mjos, C. Orvig, *Chem. Rev.*, **2014**, 114, 4540 – 4563.

[12] M. Peyrone, *Ann Chem Pharm*, **1844**, 51, 1 – 29.

[13] B. Rosenberg, L. Van Camp, T. Krigas, *Nature*, **1965**, 205, 698 – 699.

[14] B. Rosenberg, L. Van Camp, J. E. Trosko, V. H. Mansour, *Nature*, **1969**, 222, 385 – 386.

[15] L. H. Einhorn, *J. Clin. Oncol.*, **1990**, 8, 1777 – 81.

[16] S. Dasari, P. B. Tchounwou, *Eur. J. Pharmacol.*, **2014**, 740, 364 – 478.

[17] H. Köpf, P. Köpf-Maier, *Angew. Chem. Int. Ed. Engl.*, **1979**, 18, 477 – 478.

[18] H. Köpf, P. Köpf-Maier, *Chem. Rev.*, **1987**, 87, 1137 – 1152.

[19] E. Meléndez, *Inorg. Chim. Acta.*, **2012**, 393, 36 – 52.

[20] G. Gasser, I. Ott, N. Metzler-Nolte, *J. Med. Chem.*, **2011**, 54, 3 – 25.

[21] P. Köpf-Maier, H. Köpf, E. W. Neuse, *Angew. Chem. Int. Ed. Engl.*, **1984**, 23, 456 – 457.

[22] D. Osella, M. Ferrali, P. Zanello, F. Laschi, M. Fontani, C. Nervi, G. Cavigiolio, *Inorg. Chim. Acta.*, **2000**, 306, 42 – 48.

[23] S. Goldstein, D. Meyerstein, G. Czapski, *Free Radic. Biol. Med.*, **1993**, 15, 435 – 445.

[24] K. Barbusinski, *Ecol. Chem. Eng.*, **2009**, 16, 347 – 358.

[25] T. P. Szatrowski, C. F. Nathan, *Cancer Res.*, **1991**, 51, 794 – 798.

[26] R. F. Shago, J. C. Swarts, E. Kreft, C. E. J. Van Rensburg, *Anticancer Research*, **2007**, 27, 3431 – 3434.

[27] J. A. Arnott, R. Kumar, S. L. Planey, *J. Appl. Biopharm. Pharm.*, **2013**, 1, 31 – 36.

[28] E. I. Edwards, R. Epton, G. Marr, *J. Organomet. Chem.*, **1975**, 85, C23 – C25.

[29] S. Top, J. Tang, A. Vessières, D. Carrez, C. Provote, G. Jaouen, *Chem. Commun.*, **1996**, 8, 955 – 956.

[30] C. Biot, G. Glorian, L. A. Maciejewski, J. S. Brocard, *J. Med. Chem.*, **1997**, 40, 3715 – 3718.

[31] R. W. Snow, J.-F. Trape, K. Marsh, *Trends Parasitol*, **2001**, 17, 593 – 597.

[32] T. E. Wellems, C. V. Plowe, *J. Infect. Dis.*, **2001**, 184, 770 – 776.

[33] E. Hempelmann, H. M. Marques, *J. Pharmacol. Toxicol. Methods*, **1994**, 32, 25 – 30.

[34] A. F. G. Slater, *Pharmac. Ther.*, **1993**, 57, 203 – 235.

[35] R. G. Ridley, A. Dorn, S. R. Vippagunta, J. L. Vennerstrom, *Ann. Trop. Med. Parasitol.*, **1997**, 5, 559 – 566.

[36] A. Dorn, S. R. Vippagunta, H. Matile, A. Budendorf, J. L. Vennerstrom, R. G. Ridley, *Biochem. Pharmacol.*, **1998**, 55, 727 – 736.

[37] A. V. Pandey, H. Bisht, V. K. Babbarwal, J. Srivastava, K. C. Pandey, V. S. Chauhan, *Biochem. J.*, **2001**, 355, 333 – 338.

[38] A. Ecker, A. M. Lehane, J. Clain, D. A. Fidock, *Trends Parasitol*, **2012**, 28, 504 – 514.

[39] O. Domarle, G. Blampain, H. Agnaniet, T. Nzadiyabi, J. Lebibi, J. Brocard, L. Maciejewski, C. Biot, A. J. Georges, P. Millet, *Antimicrob. Agents*, **1998**, 42, 540 – 544.

[40] C. Biot, F. Nosten, L. Fraisse, D. Ter-Minassian, J. Khalife, D. Dive, *Parasite*, **2011**, 18, 207 – 214.

[41] A. K. Shiau, D. Barstad, P. M. Loria, L. Cheng, P. J. Kushner, D. A. Agard, G. L. Greene, *Cell*, **1998**, 95, 927 – 937.

[42] J. I. Macgregor, V. C. Jordan, *Pharmacol. Rev*., **1998**, 50, 151 – 196.

[43] G. Jaouen, S. Top, A. Vessières, G. Leclerq, J. Quivy, L. Jin, A. Croisy, *C. R. Acad. Sci. Paris Série IIc*, **2000**, 89 – 93.

[44] P. Pigeon, S. Top, A. Vessières, M. Huché, E. A. Hillard, E. Salomon, G. Jaouen, *J. Med. Chem.*, **2005**, 48, 2814 – 2821.

[45] E. Hillard, A. Vessières, L. Thouin, G. Jaouen, C. Amatore, *Angew. Chem.*, **2006**, 118, 291 – 296.

[46] U. Schatzschneider, N. Metzler-Nolte, *Angew. Chem. Int. Ed.*, **2006**, 45, 1504 – 1507.

[47] G. H. Hitchings, G. B. Elion, E. A. Falco, P. B. Russell, M. B. Sherwood, H. Vanderwerff, *J. Biol. Chem.*, **1950**, 183, 1 – 9.

[48] T. N. Raju, *Lancet*, **2000**, 355, 1022.

[49] G. B. Elion, G. H. Hitchings, H. Vanderwerff, *J. Biol. Chem.*, **1951**, 192, 505 – 518.

[50] C. M. Galmarini, J. R. Mackey, C. Dumontet, *Lancet Oncology*, **2002**, 3, 415 – 424.

[51] S. M. Daluge, S. S. Good, M. B. Faletto, W. H. Miller, M. H. St Clair, L. R. Boone, M. Tisdale, N. R. Parry, J. E. Reardon, R. E. Dornsife, D. R. Averett, T. A. Krenitsky, *Antimicrob. Agents Chemother.*, **1997**, 1082 – 1093.

[52] H. J. Schaffer, S. Gurwara, R. Vince, S. Bitner, *J. Med. Chem.*, **1971**, 14, 367 – 369.

[53] M. R. Boyd, T. H. Bacon, D. Sutton, M. Cole, *Antimicrob. Agents Chemother.*, **1987**, 31, 1238 – 1242.

[54] G. Romeo, U. Chiacchio, A. Corsano, P. Merino, *Chem. Rev.*, **2010**, 110, 3337 – 3370.

[55] D. B. Longley, D. P. Harkin, P. G. Johnston, *Nat. Rev. Cancer*, **2003**, 3, 330 – 338.

[56] E. Mini, S. Nobili, B. Caciagli, I. Landini, T. Mazzei, *Ann. Oncol.*, **2006**, 17, 7 – 12.

[57] J. W. Beach, *Clin. Ther.*, **1998**, 20, 2 – 25.

[58] T. J. Mitchison, *Mol. Biol. Cell*, **2012**, 23, 1 – 6.

[59] R. Duschinsky, C. Heidelberger, E. Pleven, *J. Am. Chem. Soc.*, **1957**, 79, 4559 – 4560.

[60] D. B. Longley, D. P. Harkin, P. G. Johnston, *Nature Rev.*, **2003**, 3, 330 – 338.

[61] S. I. Ahmad, S. H. Kirk, A. Eisenstark, *Annu. Rev. Microbiol.*, **1998**, 52, 591 – 625.

[62] G. L. Patrick, *An Introduction to Medicinal Chemistry*, Oxford University Press, **2001**, 52 – 53.

[63] L. W. Hertel, J. S. Kroin, J. W. Misner, J. M. Tustin, *J. Org. Chem.*, **1988**, 53, 2406 – 2409.

[64] M. Cantore, G. Fiorentini, G. Luppi, G. Rosati, R. Caudana, E. Piazza, G. Comella, C. Ceravolo, L. Miserocchi, A. Mambrini, A. Del Freo, D. Zamagni, C. Rabbi, M. Marangolo, *J. Chemother.*, **2004**, 16, 589 – 594.

[65] V. Gandhi, J. Legha, Chen F, L. W. Hertel, W. Plunkett, *Cancer. Res.*, **1996**, 56, 4453 – 4459.

[66] V. Heinemann, Y. Z. Xu, S. Chubb, A. Sen, L. W. Hertel, G. B. Grindey, W. Plunkett, *Mol. Pharmacol.*, **1990**, 38, 567 – 572.

[67] H. Mitsuya, K. J. Weinhold, P. A. Furman, M. H. St. Clair, S. N. Lehrman, R. C. Gallo, D. Bolognesi, D. W. Barry, S. Broder, *Proc. Natl. Acad. Sci. U.S.A.*, **1985**, 82, 7096 – 7100.

[68] H. Mitsuya, R. Yarchoan, S. Broder, *Science*, **1990**, 249, 1533 – 1544.

[69] Y. H. Zheng, N. Lovsin, B, M, Peterlin, *Immunol. Lett.*, **2005**, 97, 225 – 234.

[70] P. A. Furman, J. A. Fyfe, M. H. St. Clair, K. Weinhold, J. L. Rideout, G. A. Freeman, S. N. Lehrman, D. P. Bolognesis, S. Broder, H. Mitsuya, D. W. Barry, *Proc. Natl. Acad. Sci. USA*, **1986**, 83, 8333 – 8337.

[71] D. Schlawe, A. Majdalani, J. Velcicky, E. Heßler, T. Wieder, A. Prokop, H. G. Schmalz, *Angew. Chem. Int. Ed.*, **2004**, 43, 1731 – 1734.

[72] C. Hirschhäuser, J. Velcicky, D. Schlawe, E. Hessler, A. Majdalani, J-. M. Neudörfl, A. Prokop, T. Wieder, H.-G. Schmalz, *Chem. Eur. J.*, **2013**, 19, 13017 – 13029.

[73] P. James, J. Neudörfl, M. Eissmann, P. Jesse, A. Prokop, H-. G. Schmalz, *Org. Lett.*, **2006**, 8, 2763 – 2766.

[74] H. V. Nguyen, A. Sallastrau, J. Balzarini, M. R. Bedford, J. C. Eden, N. Georgousi, N. J. Hodges, J. Kedge, Y. Mehellou, C. Tselepis, J. H. R. Tucker, *J. Med. Chem.*, **2014**, 57, 5817 – 5822.

[75] S. W. Smith, *Toxicol. Sci.*, **2009**, 110, 4 – 30.

[76] R. Howe, R. G. Shanks, *Nature*, **1966**, 210, 1336 – 1338.

[77] C. Murali, S. S. Mysore, G. S. Chinnakonda, *Tetrahedron.*, **2007**, 63. 4149 – 4155.

[78] H. D. Flack, *Acta. Cryst.*, **1983**, A39, 876 – 881.

[79] D. Osella, M. Ferrali, P. Zanello, F. Laschi, M. Fontani, C. Nervi, G. Caviglio, *Inorganica. Chimica. Acta.*, **2000**, 306, 42 – 48.

[80] H. Hagen, P. Marzenell, E. Jentzsch, F. Wenz, M. R. Veldwijk, A. Mokhir, *J. Med. Chem.*, **2012**, 55, 924 – 934.

[81] F. Barrière, W. E. Geiger, *J. Am. Chem. Soc.*, **2006**, 128, 3980 – 3989.

[82] A. Houlton, C. J. Isaac, A E. Gibson, B. R. Horrocks, W. Clegg, M. R. J. Elsegood, *J. Chem. Soc., Dalton Trans.*, **1999**, 3229 – 3234.

[83] H. H. Meyer, *Arch. Exp. Pathol. Pharmakol.*, **1899**, 42, 109 – 118.

[84] S. Miyamoto, P. A. Kollman, *Proc. Natl. Acad. Sci. USA*, **1993**, 90, 8402 – 8406.

[85] S. Oie, *J. Clin. Pharmacol.*, **1986**, 26, 583 – 6.

[86] K. D. Freeman-Cook, R. L. Hoffman, T. W. Johnson, *Future Med. Chem.*, **2013**, 5, 113 – 115.

[87] P. D. Leeson, B. Springthorpe, *Nat. Rev. Drug Descov.*, **2007**, 6, 881 – 890.

[88] M. M. Hann, *Med. Chem. Commun.*, **2011**, 2, 349 – 355.

[89] A. Leo, C. Hansch, D. Elkins, *Chem. Rev.*, **1971**, 71, 525 – 616.

[90] A. K. Ghose, G. M. Crippen, *J. Chem. Inf. Comput. Sci.*, **1987**, 27, 21 – 35.

[91] V. N. Viswanadhan, A. K. Ghose, G. R. Revankar, R. K. Robins, *J. Chem. Inf. Comput. Sci.*, **1989**, 29, 163 – 172.

[92] P. Broto, G. Moreau, C. Van Dycke, *Eur. J. Med. Chem.*, **1984**, 19, 71 – 78.

[93] B. J. Marsh, L. Hampton, S. Goggins, C. G. Frost, *New J. Chem.*, **2014**, 38 5260 – 5263.

[94] ChemBioDraw Ultra 13.0, CambridgeSoft, **1986 – 2013**.

[95] K. Saotome, H. Morita, M. Umeda, *Toxic. in Vitro*, **1989**, 3, 317 – 321.

[96] D. A. Flick, G. E. Gifford, *J. Immunol. Methods.*, **1984**, 68, 167 – 175.

[97] T. Mosmann, *J. Immunol. Methods.*, **1983**, 65, 55 – 63.

[98] G. D. Hsiung, *Yale J. Biol. Med.*, **1984**, 57, 727 – 733.

4 Synthesis and Biological Activity of Novel Ferrocenyl β-Blockers

4.1 Introduction

β-blockers are a class of drug primarily used to control cardiac workload and hence the oxygen requirements of the heart. They selectively block β-adrenergic receptors (βARs), thus preventing activation by the natural catecholamine ligands norepinephrine and epinephrine, thereby suppressing the associated fight-or-flight response.[1] Although originally developed for the treatment of myocardial infarction and ischemia, β-blockers have been widely used for the treatment of many other cardiac disorders such as cardiac arrhythmias and hypertension, alongside less obviously related conditions including glaucoma, migraine and anxiety.[2,3,4,5,6] More recently, propranolol has become the best treatment available for infantile haemangioma, and research has demonstrated the use of β-blockers to inhibit cancer metastasis and as a host targeted antimalarial agent.[7,8,9]

4.1.1 Adrenergic Receptors

Populating the cell membranes of certain key tissues and organs, adrenergnic receptors (ARs) are primarily activated by the neurotransmitter norepinephrine, which is released from the terminal adrenergic neurons of the sympathetic nervous system to engender various physiological responses.[10] These transmembrane proteins are coupled to an intracellular, hetereotrimeric guanine nucleotide-binding protein (G-protein) which, through a conformational shift, transduces the signal produced by the binding of an activator ligand to trigger a cascade reaction of intracellular secondary messengers.[11] Two distinct types were identified in 1948 by Ahlquist, which were differentiated based upon their response to three different agonist ligands (**Fig. 4.1**).[12] While the αARs are most strongly activated by epinephrine, with norepinephrine and isoproterenol producing progressively weaker effects,

the trend is reversed for the βARs. Since then, further investigation of their respective small molecule binding characteristics has delineated two main α-subtypes (α_1 and α_2) and three β-subtypes (β_1, β_2 and β_3) among other more refined, but currently less clinically significant categorisations.[10,13,14]

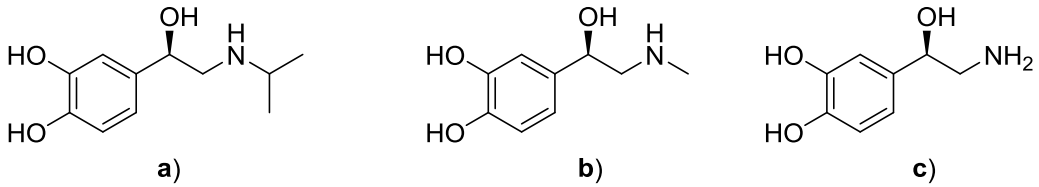


Fig. 4.1 Three AR agonists **a**) isoproteronol, **b**) epinephrine and **c**) norepinephrine

The different types of adrenergic receptor are distributed variously about the tissues of the body and are coordinated by the sympathetic nervous system to control important physiological processes. α_1 and α_2 are largely concentrated in the arterioles and control vasodilation and vasoconstriction; β_1 primarily control the force and rate of heart contraction alongside renin release from the kidneys; β_2 the bronchiodilation of the lungs; the liver contains both α_1 and β_2 which together control glycogenolysis and glucogenolysis.[10]

4.1.2 Propranolol, the Prototypical β-blocker

Located in the heart, β_2ARs are of particular clinical significance and were therefore the object of early research into ligand-receptor interactions in cell-signalling. In the early 1960s James Black made great contributions to this growing body of knowledge for which he was later awarded a Nobel prize.[15] He developed the first β-blockers, competitive inhibitors, which bind to, but do not activate the β-receptors and thus compete with the natural agonist ligands moderating their stimulatory effect; the workload and hence oxygen requirement of the heart is reduced and the likelihood of myocardial infarction and ischemia diminished.[16] Following the effective, but toxic forerunner pronethalol (**Fig. 4.2h**), propranolol (**Fig. 4.2g**) became the world's first truly clinically useful β-blocker and hence a blockbuster drug.[17,18]

Based on this prototype many other β-blockers have been developed with pharmacodynamic and pharmacokinetic properties tailored to treat a range of cardiovascular disorders. Discrimination of the three β-receptor sub-types (β_1-, β_2- and β_3-) is now possible and agents displaying intrinsic sympathomimetic (partial agonist) activity, alongside other potentially useful secondary effects such as membrane-stabilisation, ion channel blocking and anti-oxidant properties are also available.[8,19,20,21]

4.1.3 β-blocker Structure-Activity Relationships

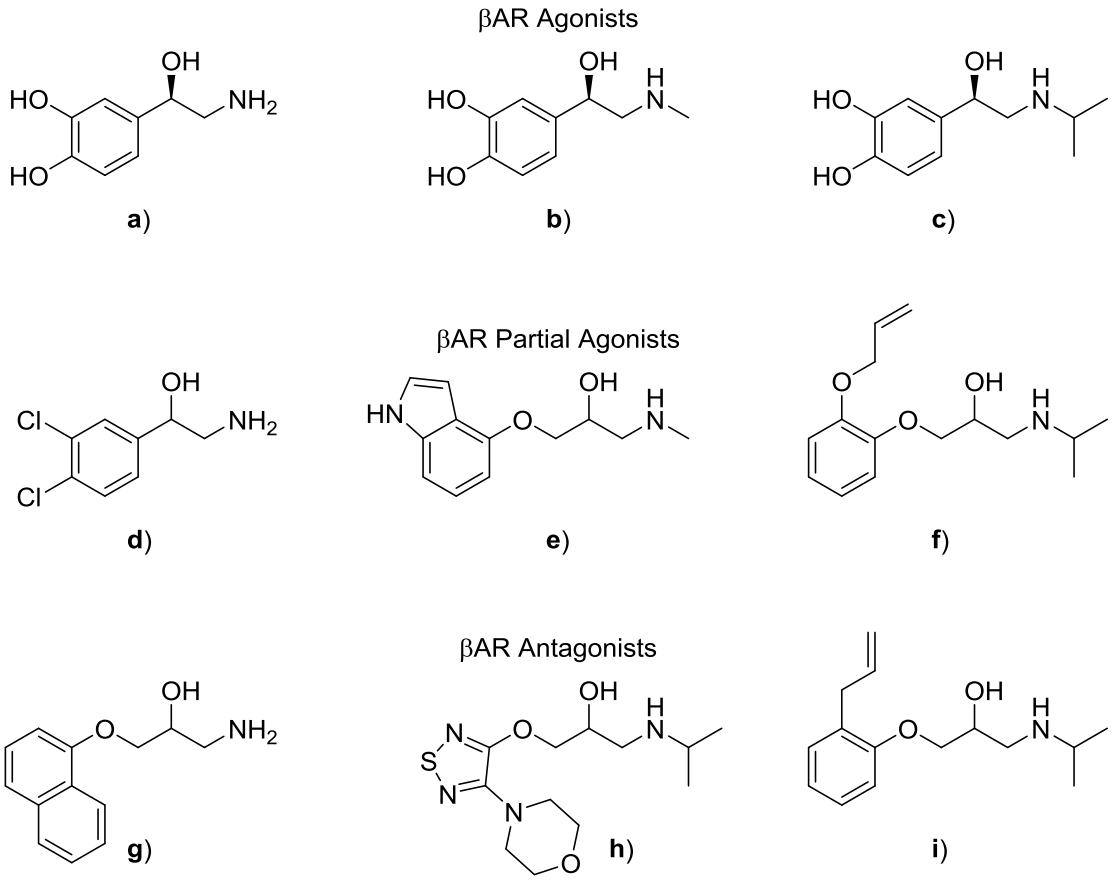


Fig. 4.2 Examples of βAR agonists **a**) norepinephrine, **b**) epinephrine and **c**) isoproterenol; partial agonists **d**) dichloroisoproterenol, **e**) pindolol and **f**) oxprenolol; and antagonists **g**) propranolol, **h**) pronethalol and **i**) alprenolol

Consisting of a hydroxy group vicinal to both a substututed amine and an ether linked aryl unit, propranolol shares a common structural motif with most other successful β-blockers, derived from the endogenous catecholamines which they mimic.[22] Central to the structure is an asymmetric carbon, and, although the (*S*-) form is orders of magnitude more potent than the (*R*-), propranolol, like the overwhelming majority of β-blockers is usually synthesised and administered as a racemic mixture.[23,24,25]

Extensive studies have revealed other structure-activity relationships related to these β-receptor ligands (**Fig. 4.3**).[10,26,27] Firstly, for both agonists and antagonists, it is the ethanolamine region that is crucial to the binding affinity which can be modulated through the use of different substituents on the secondary amine (R^3). Small, branched or cyclic alkyl groups, such as isopropyl, *t*-butyl and cyclopentyl tend to give the highest binding affinities. For antagonists, the presence of an ether linkage (O) between the ethanolamine and aryl group also increases the binding affinity.

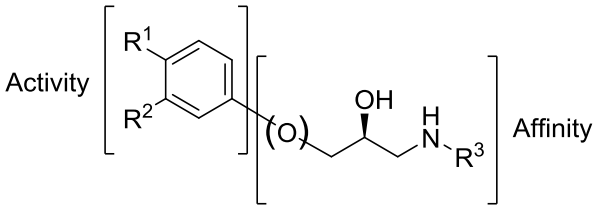


Fig. 4.3 Essential structure of βAR ligands showing the functional regions related to both binding affinity and agonist or antagonist activity

Conversely and quite independently, once the ligand is bound, activation or inhibition of the receptor is determined through the interactions of the aryl group. As exhibited by the catecholamine agonists epinephrine and norepinephrine, two hydroxy groups at the meta (R^2) and para (R^1) positions are required to activate the receptor. While substitution with phenolic equivalent groups such as $-CH_2OH$, $-NHCONH_2$ and $-NHSO_2CH_3$ can maintain activity,

complete removal or replacement with less similar substituents results in partial agonist or fully antagonist behaviour.[28,29]

4.1.4 β-blockers for Treatment of Infantile Haemangioma

Although predominantly used to modulate cardiac function, β-blockers have also proved useful for the treatment of other, ostensibly unrelated disorders. Propranolol for instance, is receiving increasing interest due to its apoptosis inducing properties, and has become the best treatment available for infantile haemangioma, a disease which, although usually benign, can lead to severe disfigurement, blindness and potentially life-threatening complications.[30,31] Previous treatment usually employed corticosteroids to halt proliferation in the early stages of development, however this does not reduce the size of the existing tumours.[30] It has been shown that propranolol not only rapidly arrests the progression of the tumours but also radically reduces their size often leading to complete involution.[31,32] The exact mechanisms of action are not known, but possible contributing factors are thought to include vasoconstriction, down-regulation of growth factor genes, angiogenesis inhibition and the instigation of apoptosis.[31,33,34,35] Indeed, in vitro studies by Li demonstrated that 24 hours exposure to 100 μM propranolol reduced the proliferation of hemangioma-derived endothelial cells before inducing apoptosis and similar findings have been made with other cancers such as von Hippel-Lindau hemangioblastoma and Hela cells.[30,36]

4.1.5 β-blockers for Treatment of Malaria

Propranolol has also demonstrated potential use as a host-targeted therapy against malaria. In vitro studies have shown that βAR signalling of the erythrocyte guanine nucleotide regulatory protein is crucial for recognition and entry into the cell by the parasite.[37] Propranolol was used to down-regulate this pathway thereby slowing the maturation and proliferation rate of

the parasite, trapping it in the blood-stage of development in which it is more vulnerable.[38] Although β-blockers alone would not be expected to eradicate the parasite, they have been shown to produce synergistic effects in combination with established anti-malarials. In a mouse model, a 2:1 propranolol:chloroquine mixture reduced the IC_{50} of the antimalarial from 1.64 to 0.66 mg kg^{-1} day^{-1} effectively doubling the activity. In this manner, otherwise resistant strains were also rendered more susceptible to the schizonticide.[38]

4.2 Objectives

Following the success of ferrocifen (discussed in **Chapter 3**), in which the incorporation of ferrocene bestowed complementary secondary effects upon the parent compound, it was proposed that the same approach be applied to the β-blocker pharmacophore. Although within their primary role as a treatment of cardiac related disorders, β-blockers are well established, with little scope, or need for improvement, their full biological relevance is not yet fully understood. Clearly the influence of these molecules is far-reaching with implications for multiple disease states; it is within these more unusual applications that further investigation may prove fruitful. In particular, the promising anti-cancer properties increasingly associated with this class of compound may be enhanced through the possible ROS generation the ferrocene modification may afford.

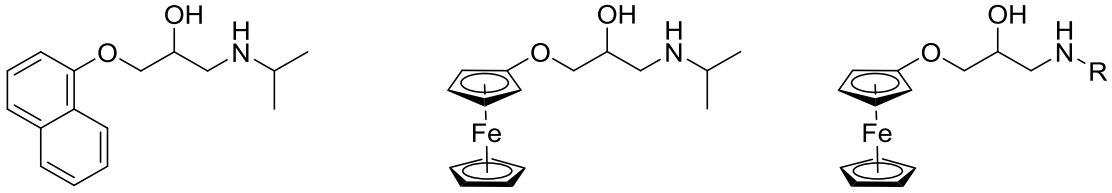
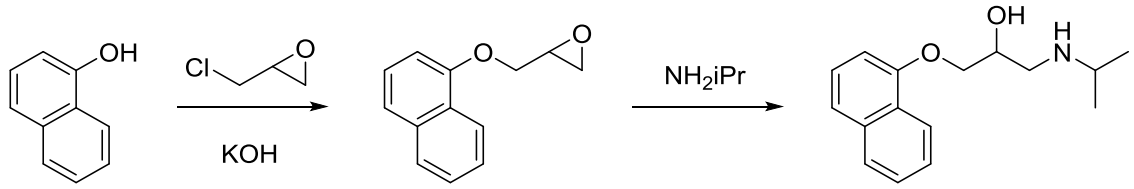


Fig. 4.4 a) the prototypical β-blocker propranolol, **b**) the ferrocenyl propranolol analogue and **c**) a ferrocenyl β-blocker with variable amine side-chain

The aim of this project therefore was the synthesis of ferrocene containing β-blockers in which the aryl unit is substituted for the metallocene (**Fig. 4.4b**). A small library of compounds would then be produced through variation of the amine substituent (**Fig. 4.4c**). Preliminary biological testing would focus upon the βAR interactions of these compounds to establish whether or not the primary mode of action is retained.

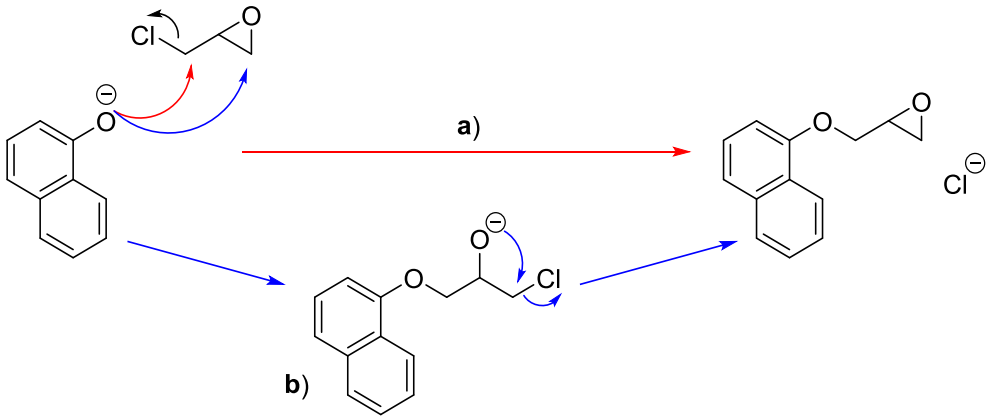
4.3 Results

4.3.1 Synthesis of Novel Ferrocenyl β-Blockers



Scheme 4.1 Synthesis of propranolol from naphthol using (±)epichlorohydrin

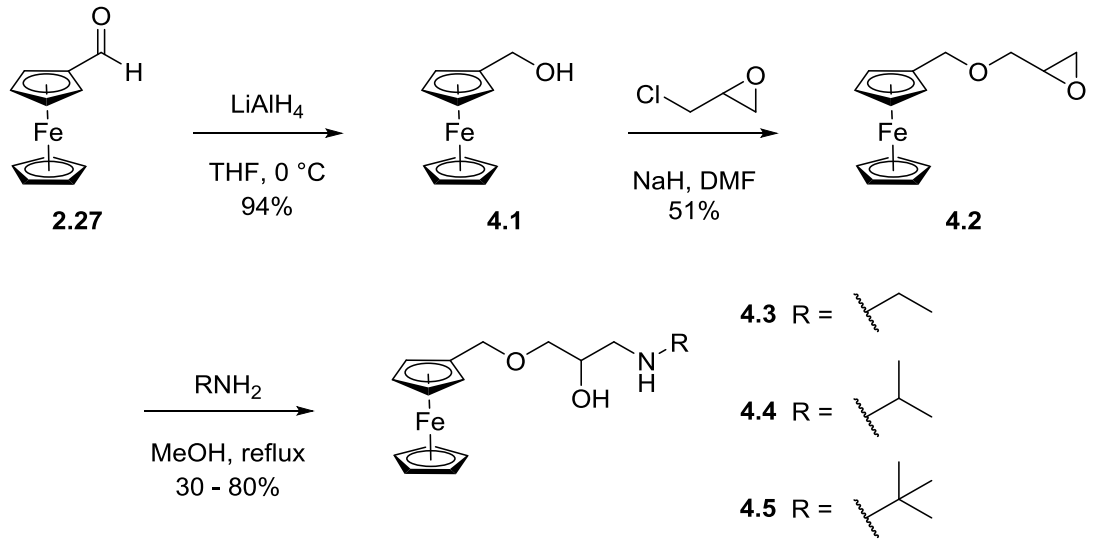
Propranolol is typically synthesised as a racemic mixture from naphthol in just two steps (**Scheme 4.1**).[39] Deprotonation with KOH yields the naphthoxide anion which then couples to (±)epichlorohydrin by a nucleophilic substitution mechanism. This reaction can proceed via two routes, reacting at either the chloro or the epoxide functionalities (**Scheme. 4.2**). Whereas substitution at the chloro-group proceeds directly to the product in a single step, the napthoxide ion can also momentarily open the epoxide which then reforms in a second step kicking out the chloride leaving group. In each case, because of the racemic nature of the substrate, the end product is identical. The final step involves opening the epoxide with isopropylamine to give the desired compound.



Scheme 4.2 Two pathways to the naphthyl ether oxirane **a**) a single-step substitution of the chloro-substituent and **b**) a two-step opening and re-forming of the epoxide[39]

4.3.1.1 Synthesis of Type-1 Ferrocenyl β-Blockers

Using the synthesis of propranolol as a guide, it was proposed that ferrocene could be incorporated into the structure by replacing the naphthol reagent with a ferrocenyl alcohol. Due to synthetic considerations, the first set of ferrocenyl β-blockers (type-1) were synthesised using ferrocenyl methanol resulting in the presence of extra carbon atom between the metallocene and the ether linkage (**Scheme 4.3**).



Scheme 4.3 The synthesis of the type-1 ferrocenyl β-blockers **4.3**, **4.4** and **4.5**

Ferrocene carboxaldehyde **2.27** was first reduced to the corresponding alcohol **4.1** using lithium aluminium hydride in ether. Ferrocenyl methanol **4.1** was then deprotonated using sodium hydride and the resulting methoxide coupled to (±)-epichlorohydrin in a typical Williamson ether formation to give **4.2**. Portions of the resulting epoxide **4.2** were then reacted under reflux with a range of amines to give the corresponding target compounds. This methodology was used by a Master's student, Matthew Rowbottom, who, by varying the amine nucleophile in the final step, produced the ethyl **4.3** and isopropyl **4.4** compounds for the group. A further *t*-butyl variation **4.5** was then synthesised to complete the mini-series of increasingly bulky alkyl groups. Single crystals of **4.5** were obtained by the slow evaporation of a concentrated solution in chloroform and XRD used to confirm the structure (**Fig. 4.5**).

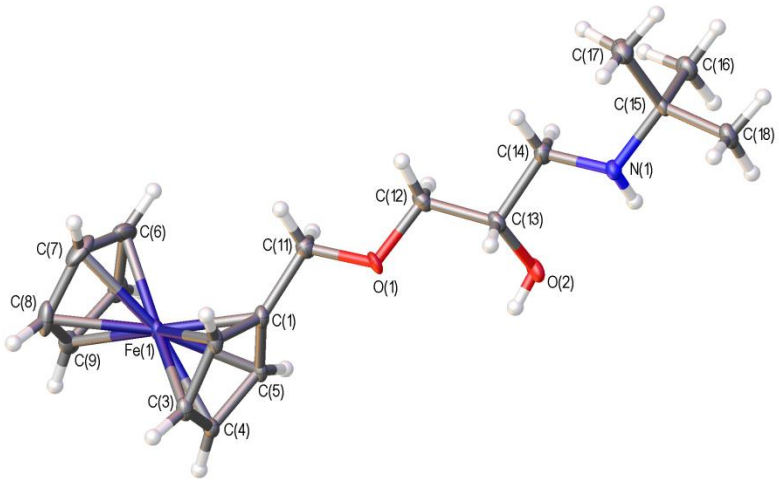
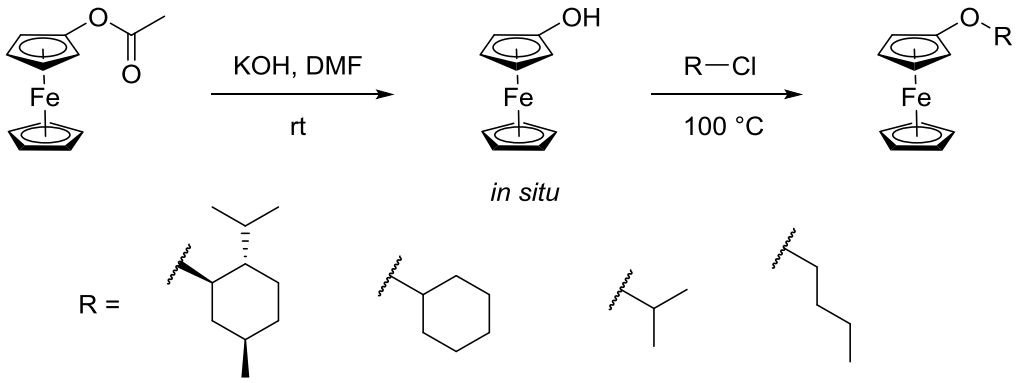


Fig. 4.5 Crystal structure of **4.5** with ellipsoids drawn at the 50% probability level. The space group is centrosymmetric which means that the structure is a racemic mixture. For clarity only the *S* enantiomer is shown.

4.3.1.2 Synthesis of Type-2 Ferrocenyl B-Blockers.



Scheme 4.4 Synthesis of ferrocenyl ethers via the Williamson-type reaction of in situ hydroxyferrocene and alkyl halides by Lang[40]

The second set of ferrocenyl β-blockers were more synthetically challenging and employed hydroxyferrocene to produce the direct ether linkage to the metallocene. This approach was based on a paper by Lang, in which hydroxyferrocene is generated in situ from ferrocenyl acetate before being reacted on with a range of halogenated substrates to give the corresponding Williamson-type ethers (**Scheme 4.4**).[40]

The ferrocenyl acetate is first produced through the Ullmann-type reaction of iodoferrocene and acetic acid. Although this type of copper-catalysed coupling was originally developed to link aryl halides, its scope and application has since been extended so that a range of reagents and catalysts can now be successfully employed following a very similar mechanism (**Fig. 4.6**).

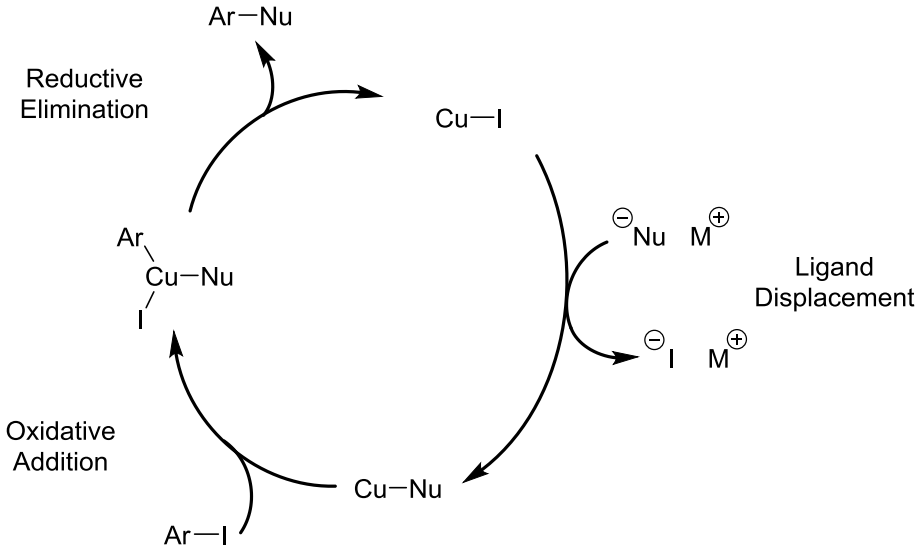
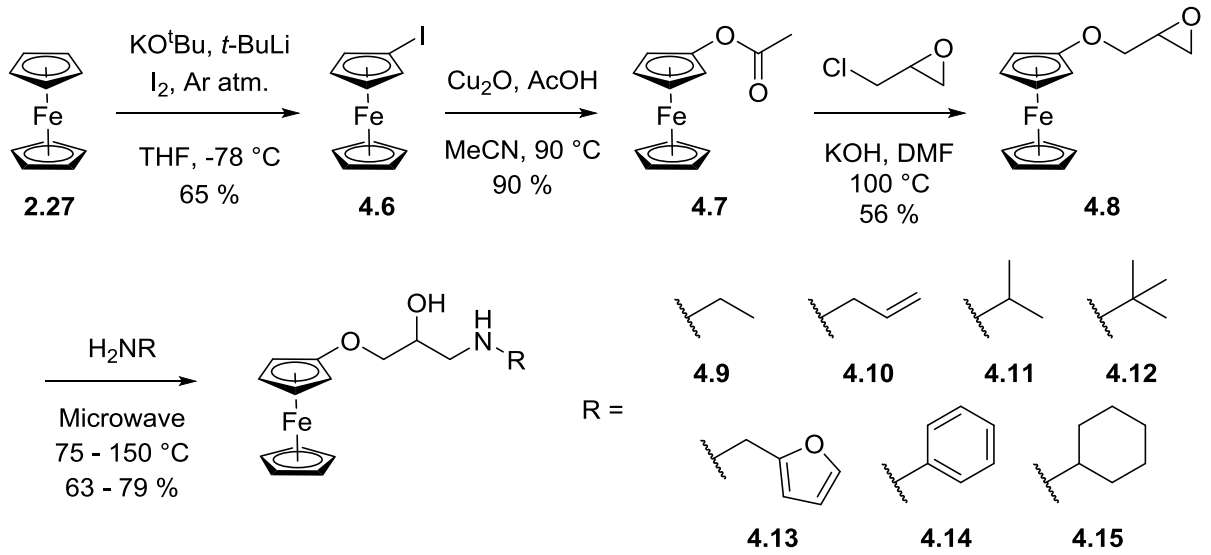


Fig. 4.6 Catalytic cycle of Ullmann-type coupling reactions

The nucleophile is first deprotonated and attaches to the surface of the copper (I) catalyst through a ligand displacement reaction, the aryl halide then adds to the metal by oxidative addition transforming the copper to the (III) state. The two units are then joined, leaving the metal by reductive elimination and returning the copper to the (I) state.

Using this chemistry the type-2 ferrocenyl β-blockers were synthesised from ferrocene in four steps (**Scheme 4.5**). Mono-iodonation was achieved using a superbasic mixture of potassium *t*-butoxide and *t*-BuLi (Schlosser's base) to deprotonate the ferrocene **2.32** followed by the addition of iodine according to the method of Roemer.[41] After filtration through a short plug of silica, unreacted ferrocene was removed by sublimation leaving pure mono-iodoferrocene **4.6** which was then coupled through the Ullmann-type reaction with acetic acid to yield

ferrocenyl acetate **4.7**. This was reacted with potassium hydroxide to release hydroxyferrocene in situ, which reacted with the (±)-epichlorohydrin in a Williamson-type ether formation to give the epoxide **4.8**. Portions of **4.8** were then microwave heated in a sealed tube with various amines which opened the epoxide to give the corresponding target compounds **4.9** to **4.15**.



Scheme 4.5 The four step synthesis of seven type-2 ferrocenyl β-blockers **4.9**, **4.10**, **4.11**, **4.12**, **4.13**, **4.14** and **4.15**

The microwave allowed the use of higher temperatures which, in conjunction with a pressurised reaction vessel, sped up the reaction and while preventing loss of the volatile amines. All of the final compounds (except for **4.11** which forms a waxy residue) were purified by recrystallisation from a mixture of hot hexane and DCM. Using this method, single crystals suitable for X-ray analysis were grown of compounds **4.10**, **4.12**, **4.13** and **4.15**, alongside the epoxide precursor **4.8** (single crystals of which were grown by the slow evaporation of a concentrated solution in chloroform) and the structures confirmed by XRD (**Fig. 4.7 – 4.11**).

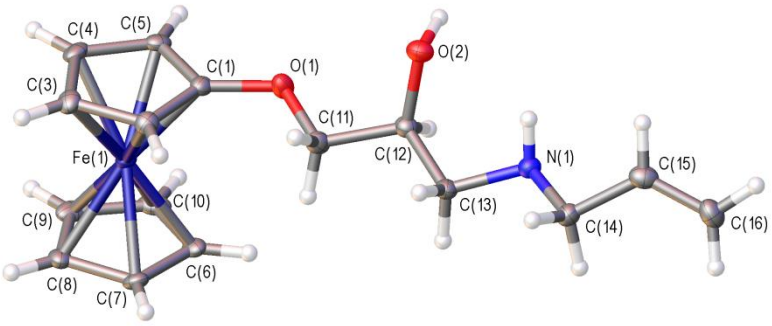


Fig. 4.7 Crystal structure of **4.10** with ellipsoids drawn at the 50% probability level. The structure is in a centrosymmetric space group such that in two of the molecules in the unit cell the chirality of C(12) is *S* and in the other two molecules the chirality of C(12) is *R*. For clarity only the *S* enantiomer is shown.

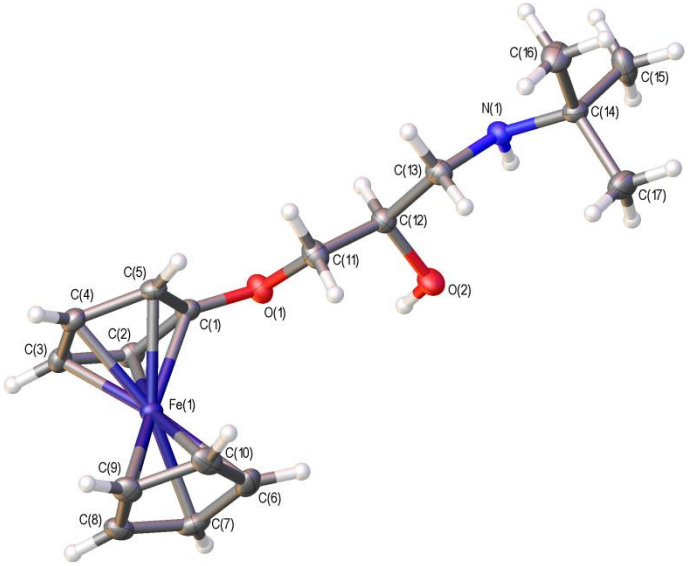


Fig. 4.8 Crystal structure of **4.12** with ellipsoids drawn at the 50% probability level. The structure is in a centrosymmetric space group such that in eight of the molecules in the unit cell the chirality of C(12) is *R* and in the other eight molecules the chirality of C(12) is *S*. For clarity only the *R* enantiomer is shown.

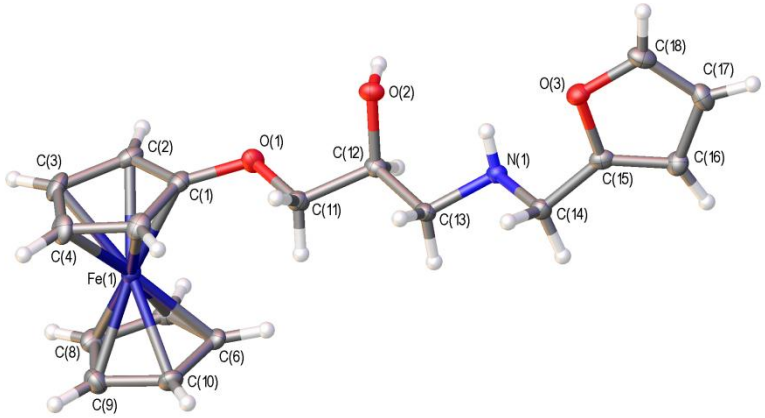


Fig. 4.9 Crystal structure of **4.13** with ellipsoids drawn at the 50% probability level. The structure is in a centrosymmetric space group such that in two of the molecules in the unit cell the chirality of C(12) is *S* and in the other two molecules the chirality of C(12) is *R*. For clarity only the *S* enantiomer is shown.

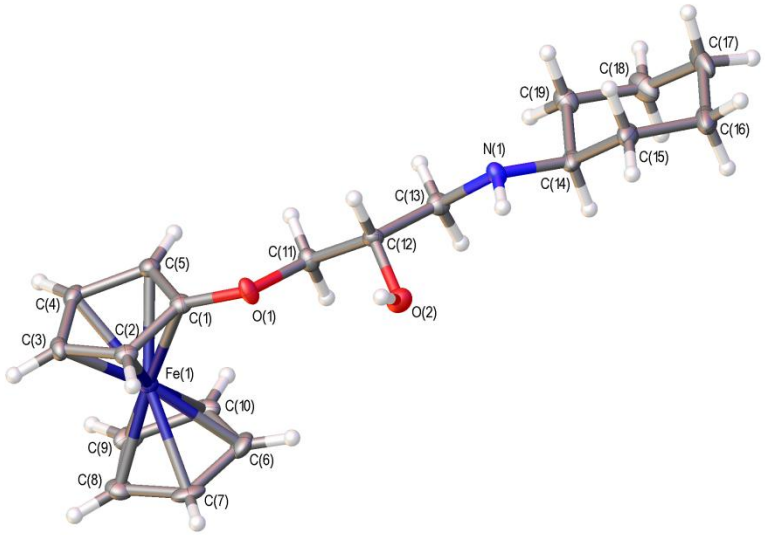


Fig. 4.10 Crystal structure of **4.15** with ellipsoids drawn at the 50% probability level. The structure is in a chiral space group and has been refined as an inversion twin with the refined ratio of domains being 0.75 (2) : 025 (2). This in 75% of cases the chirality of C(12) is *S* and in 25% of cases the chirality of C(12) is *R*. For clarity only the *S* enantiomer is shown.

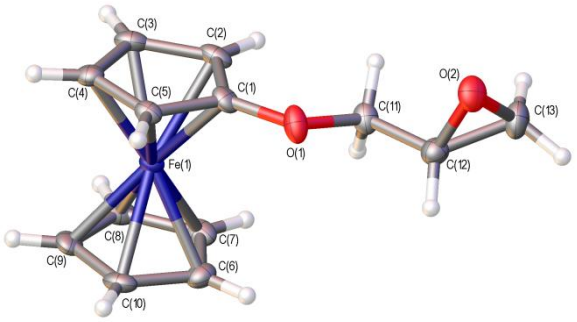


Fig. 4.11 Crystal structure of **4.8** with ellipsoids drawn at the 50% probability level. The group C(11)-C(12)/C(11')-C(12') is disordered over two positions with a refined percentage occupancy ratio of 85.8 (4): 14.2(4). Only the major component has been shown for clarity.

4.3.2 Biological Activity of Novel Ferrocenyl β-Blockers

As mentioned previously, ARs span the cell membrane and are linked to a larger, intracellular effector system through the coupling of a G-protein (**Fig. 4.12**). In the case of βARs, following the binding of an agonist such as isoproterenol, the G-protein undergoes a conformational shift and associates with the adenylyl cyclase enzyme stimulating the production of cyclic adenosine monophosphate (cAMP) from adenosine triphosphate (ATP). This secondary messenger in turn elicits response from various other intracellular enzymes which govern the metabolic state of the cell.[11] In particular, the cAMP-dependent protein kinase A (PKA) is activated, which phosphorylates specific serine residues such as (S428) on the LKB1 protein thus producing P-LKB1.

β-blockers are βAR antagonists, and as such bind to the receptor but do not elicit a response. Initial biological investigation therefore sought to establish the βAR activity of these potential ferrocenyl β-blockers by monitoring the downstream response of the G-

protein/cAMP pathway on the phosphorylation of the LKB1 protein in kidney (HEK293) cells.

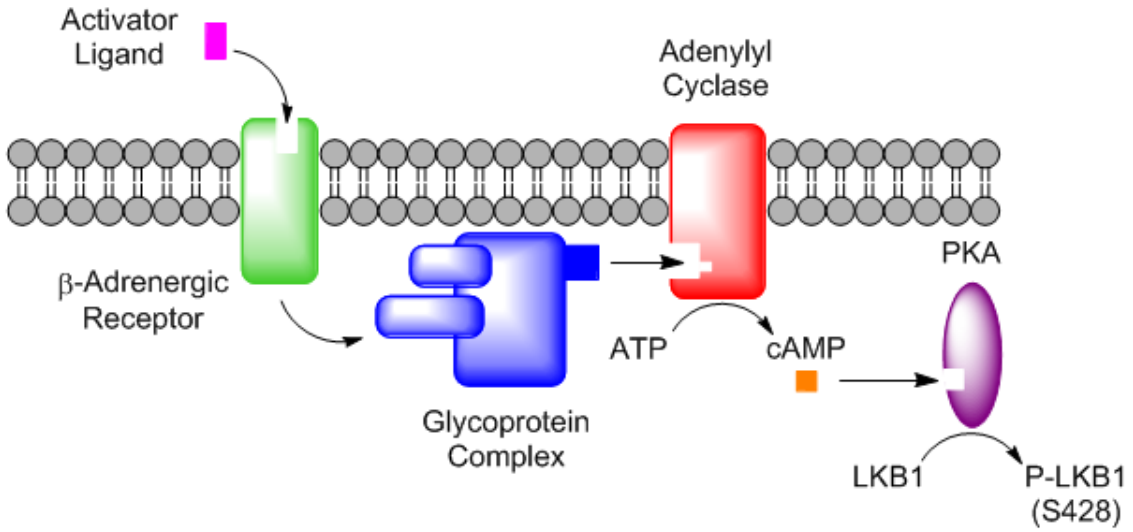
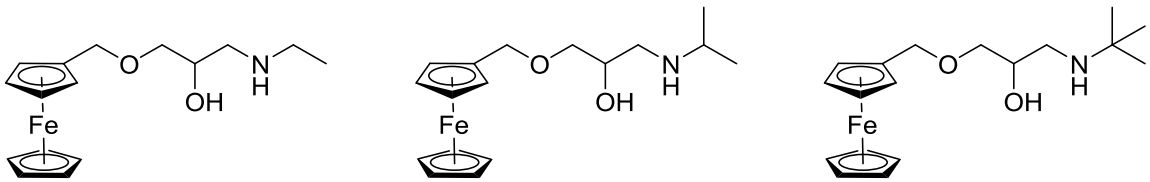


Fig. 4.12 Activation of βARs triggers a cascade reaction of secondary messengers resulting in the phosphorylation of LKB1 to P-LKB1 by the PKA kinase

The two types of ferrocenyl β-blocker were tested for their βAR activity on separate occasions by Dr. Youcef Mehellou, Migena Tushe and Lily Cao in the School of Medicine. A freshly cultured batch of HEK293 cells were treated simultaneously with isoproterenol (Isop), a known βAR agonist, and each of the type-1 ferrocenyl β-blockers **4.3**, **4.4** and **4.5** at 10 and 50 μg ml^{-1} (**Fig. 4.13**). Controls were treated with isoproterenol, in addition, positive controls were treated with the established β-blocker propranolol (prop) and negative controls (N.C.) were treated with **Fcn3c2T**$_{(S,Rp)}$ which is not expected to display any βAR activity. After five minutes incubation time, a western blot was used to assess the β-catenin and P-LKB1 (S428) protein output from each of the sets of cells (**Fig. 4.14**).



4.3 **4.4** **4.5**

Fig. 4.13 Type-1 ferrocenyl β-blockers **4.3**, **4.4** and **4.5**

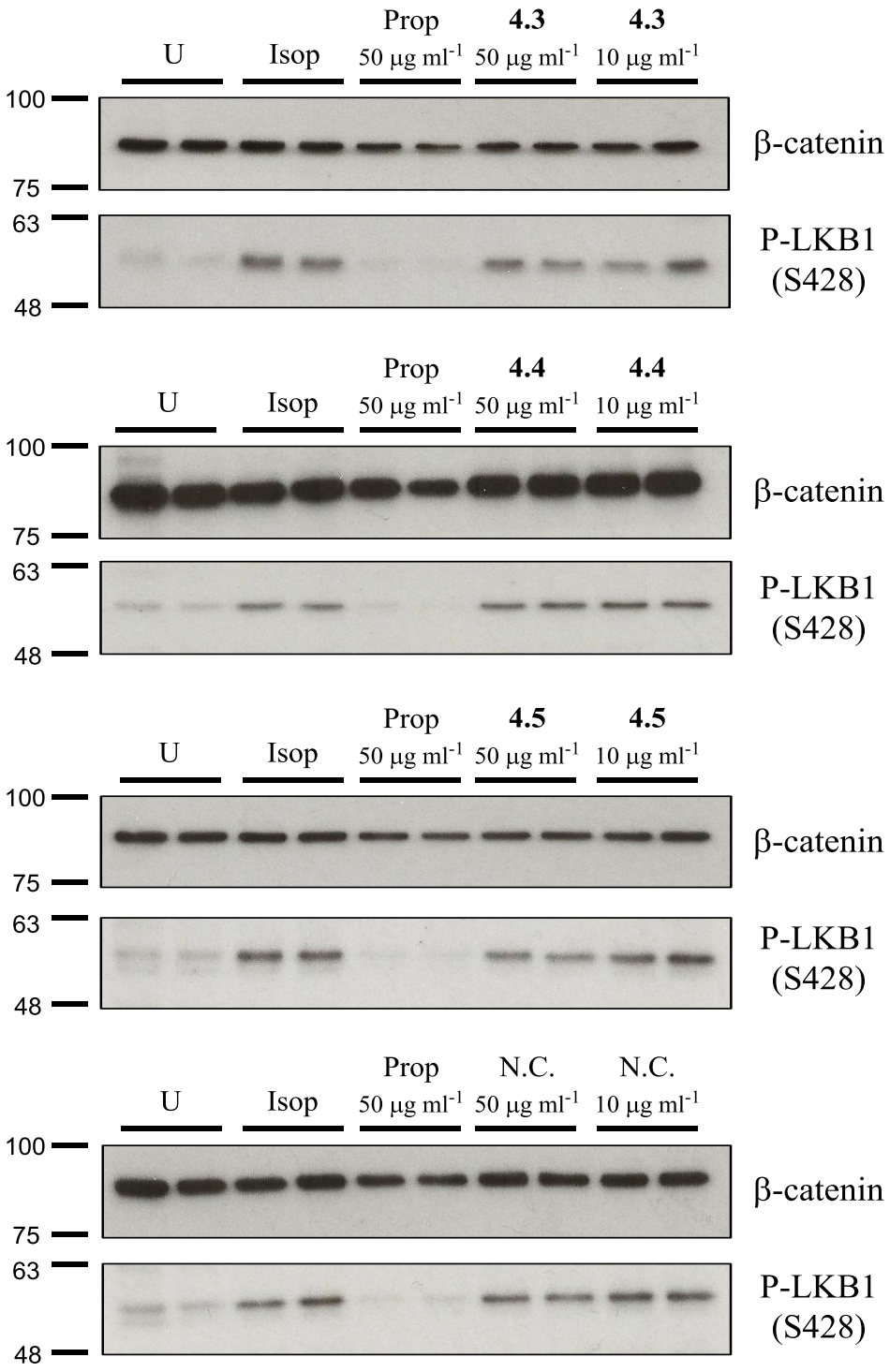


Fig. 4.14 Western blots for P-LKB1 (S428) (M_r: ~ 48 kDa) in HEK 293 cells after 5 minutes incubation with the respective agents. U – untreated, Isop – isoproterenol alone, Prop – propranolol, N.C. – the negative control compound **Fcn3c2T**$_{(S,Rp)}$ and the type-1 ferrocenyl β-blockers **4.3**, **4.4**, **4.5** at 10 and 50 μg ml^{-1}. β-catenin was used as a protein loading control.

The untreated cells (U) showed a single intense band corresponding to the loading control protein β-catenin. A second band was produced by those treated with isoproterenol (Isop) corresponding to the downstream phosphorylation of the LKB1 protein at serine 428 (S 428). As expected, cells treated with both isoproterenol and propranolol (Prop) showed a marked decrease in the intensity of this P-LKB1 (S428) band, due to the inhibitory effects of the β-blocker, whereas those treated with the negative control compound **Fcn3c2T**$_{(S,Rp)}$ displayed very little change. The cells treated with **4.5** showed a slight reduction in the intensity of the P-LKB1 (S428) band with some dose dependence. The cells treated with the other type-1 ferrocenyl β-blockers **4.3** and **4.4** displayed little change in the intensity of the P-LKB1 (S428) bands, at 10 or 50 μg ml^{-1} compared to the cells treated with isoproterenol alone.

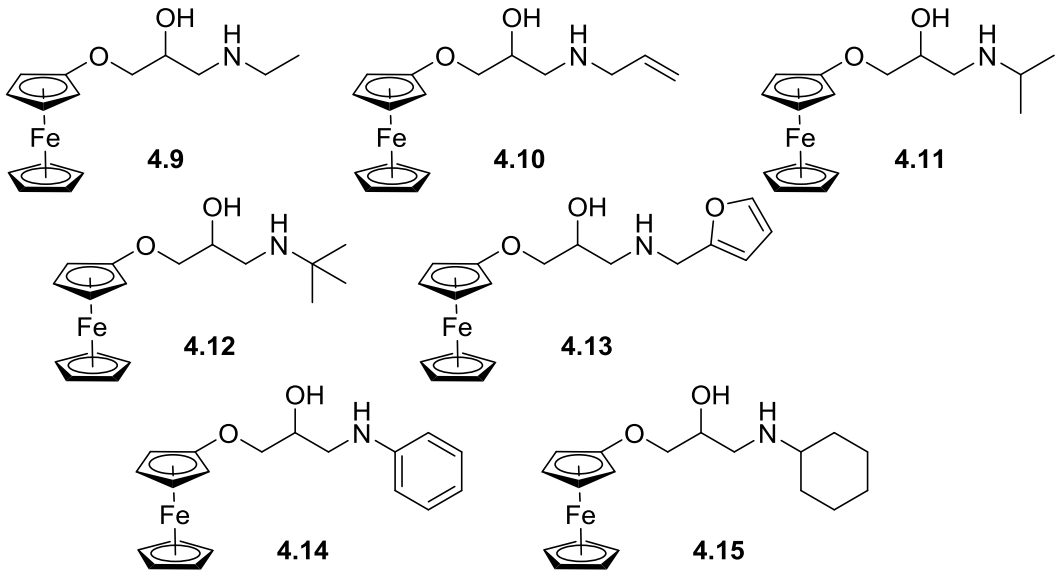


Fig. 4.15 Type-2 ferrocenyl β-blockers **4.9**, **4.10**, **4.11**, **4.12**, **4.13**, **4.14** and **4.15**

The same assay was used to investigate the βAR activity of the type-2 ferrocenyl β-blockers **4.9**, **4.10**, **4.11**, **4.12**, **4.13**, **4.14** and **4.15** at 50 μM concentration (**Fig. 4.15**). In this study, data analysis was used to quantify the activities of the compounds as shown in the corresponding bar charts. Band intensities were normalised with respect to the quantity of cells and background P-LKB1 presence (**Fig. 4.16** to **Fig. 4.19**).

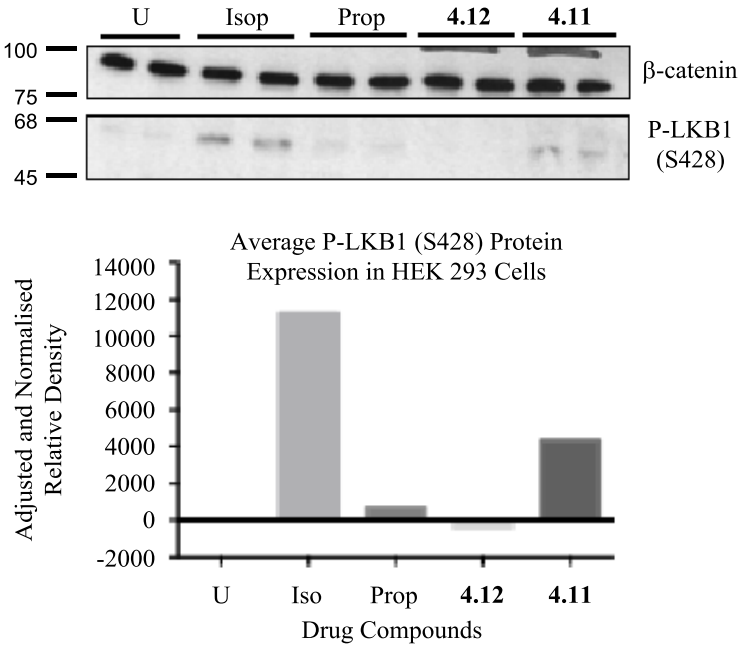


Fig. 4.16 Western blot banding intensity for P-LKB1 (S428) in HEK293 cells after 5 minutes incubation. U – untreated, Isop – isoproterenol alone, Prop – propranolol and compounds **4.11** and **4.12**. β-catenin was used as a protein loading control.

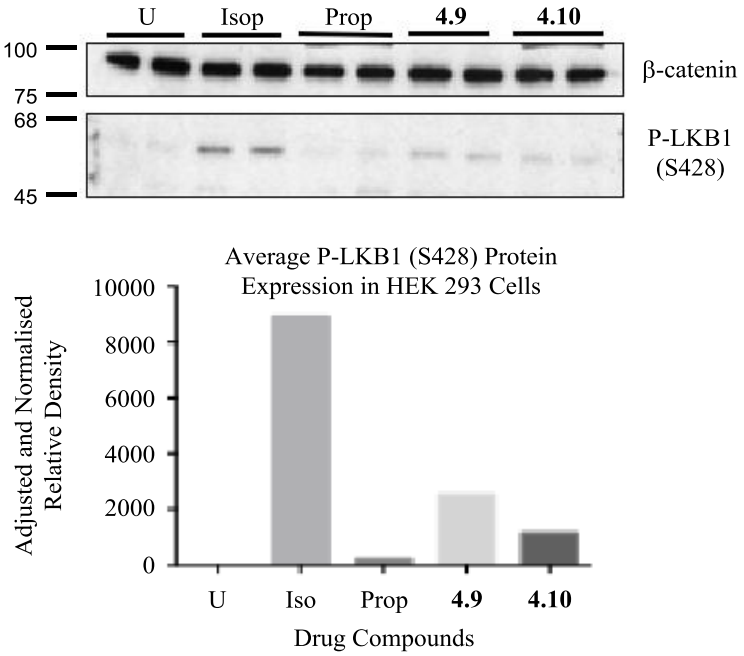


Fig. 4.17 Western blot banding intensity for P-LKB1 (S428) in HEK293 cells after 5 minutes incubation. U – untreated, Isop – isoproterenol alone, Prop – propranolol and compounds **4.9** and **4.10**. β-catenin was used as a protein loading control.

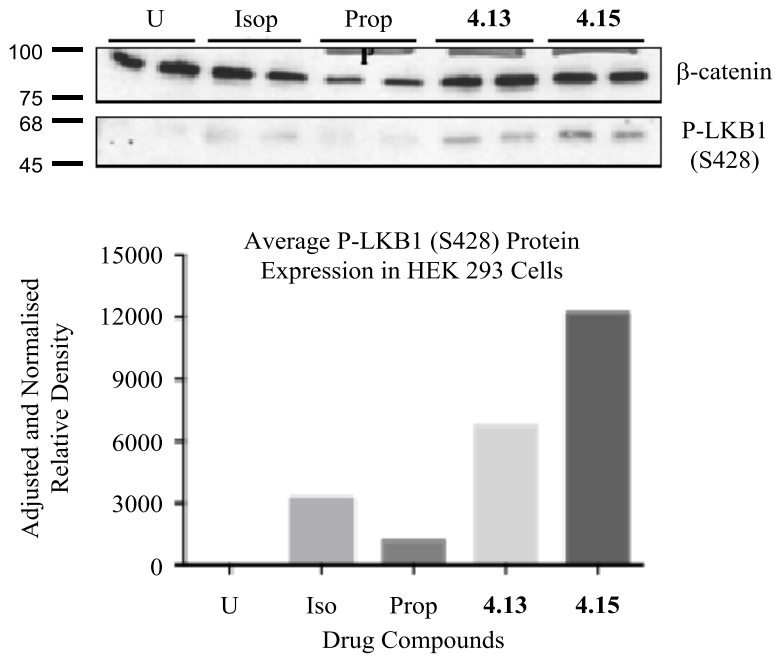


Fig. 4.18 Western blot banding intensity for P-LKB1 (S428) in HEK293 cells after 5 minutes incubation. U – untreated, Isop – isoproterenol alone, Prop – propranolol and compounds **4.13** and **4.15**. β-catenin was used as a protein loading control.

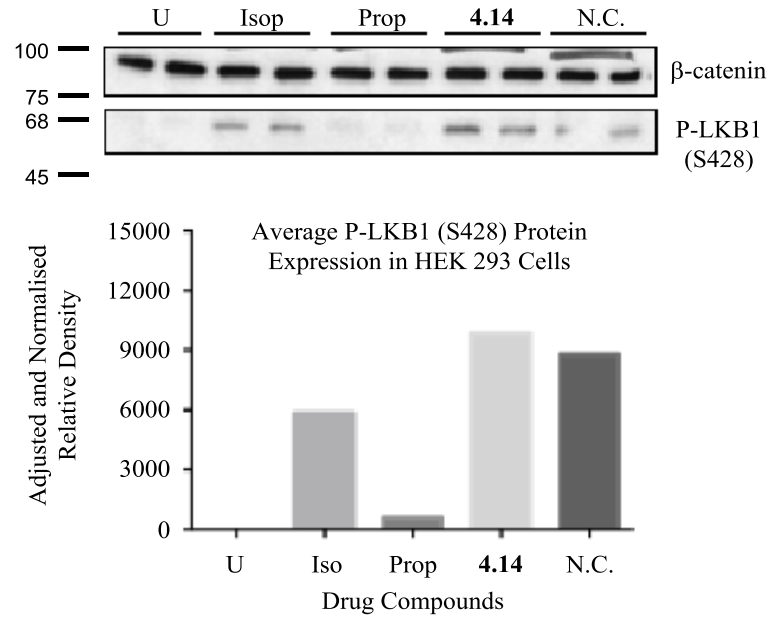


Fig. 4.19 Western blot banding intensity for P-LKB1 (S428) in HEK293 cells after 5 minutes incubation. U – untreated, Isop – isoproterenol alone, Prop – propranolol, compound **4.14** and the N.C. **Fcn3c2T**$_{(S,Rp)}$. β-catenin was used as a protein loading control.

Table 4.1 % inhibition of the isoproterenol response of HEK293 cells by propranolol, compounds **4.9** – **4.15** and the N.C. compound **Fcn3c2T**$_{(S,Rp)}$

Compound	Avg. wrt U	% inhibition
Isop	11245.2	0.0
Prop	718.9	93.6
4.12	-415.0	103.7
4.11	4323.6	61.6

Compound	Avg. wrt U	% inhibition
Isop	8916.3	0.0
Prop	213.3	97.6
4.9	2524.7	71.7
4.10	1136.2	87.3

Compound	Avg. wrt U	% inhibition
Isop	3195.6	0.0
Prop	1172.9	63.3
4.13	6718.2	-110.2
4.15	12176.4	-281.0

Compound	Avg. wrt U	% inhibition
Isop	5843.8	0.0
Prop	581.1	90.1
4.14	9836.5	-68.3
N.C.	8807.8	-50.7

In this study, compounds **4.9**, **4.10**, **4.11** and **4.12** exhibited promising βAR antagonist activity, inhibiting the isoproteronol response of HEK293 cells. Compound **4.12** was particularly effective, producing a more pronounced effect than the positive control compound propranolol and completely negating the stimulatory effects of isoproterenol. Interestingly, the remaining compounds **4.13**, **4.14** and **4.15** all enhanced the isoproterenol response, suggesting βAR agonist activity. In particular, compound **4.15** increased the P-LKB1 (S428) band intensity four-fold compared to that produced by isoproterenol alone. Unexpectedly, the negative control (N.C.) compound **Fcn3c2T**$_{(S,Rp)}$ also exhibited some βAR agonist activity, increasing the intensity of the P-LKB1 (S428) band by approximately 50% compared to that produced by isoproterenol alone.

4.4 Discussion

Clearly, in the first study, all of the type-1 ferrocenyl β-blockers displayed much reduced βAR antagonist activity compared to propranolol. Given that compound **4.4** bears the same isopropyl amine substituent as propranolol, this loss of activity must be attributed to the presence of the ferrocene unit and/or the extra carbon atom inserted adjacent to the ether linkage. It is worth noting that the only type-1 ferrocene compound which seems to produce any βAR blockade is **4.5**. It is possible that this compound, bearing the bulkiest, most branched amine substituent, binds more strongly to the receptor than the other compounds and hence produces a small antagonist effect.

The type-2 ferrocene compounds show much more βAR activity than the corresponding type-1 compounds. Compounds **4.9**, **4.11** and **4.12** form a series of increasingly branched alkanes, which in accordance with established β-blocker structure-activity relationships, correlates with their increasing antagonist activity. The presence of a *t*-butyl amine substituent again produces the greatest βAR activity; however in this case, compound **4.12** completely inhibits the receptor, nullifying the effect of the activator ligand isoproterenol even more strongly than propranolol.

It is also very interesting that we see both βAR activation and inhibition from members of the type-2 library. Dividing them according to this behaviour, it is worth noting the structural similarities in the amine substituents of each set (**Fig. 4.20**). The antagonists **4.9**, **4.11**, and **4.12** form a series of increasingly branched alkanes, with **4.10** bearing a comparably sized alkene group. Conversely, the agonists **4.13**, **4.14** and **4.15** all bear cyclic substituents on the nitrogen. Nevertheless, as discussed previously, it is widely accepted that the catechol unit is crucial to the activation of βARs and it is therefore very unusual that any of these

compounds, which have all undergone the identical substitution of the catechol ring by ferrocene exhibit agonist behaviour.

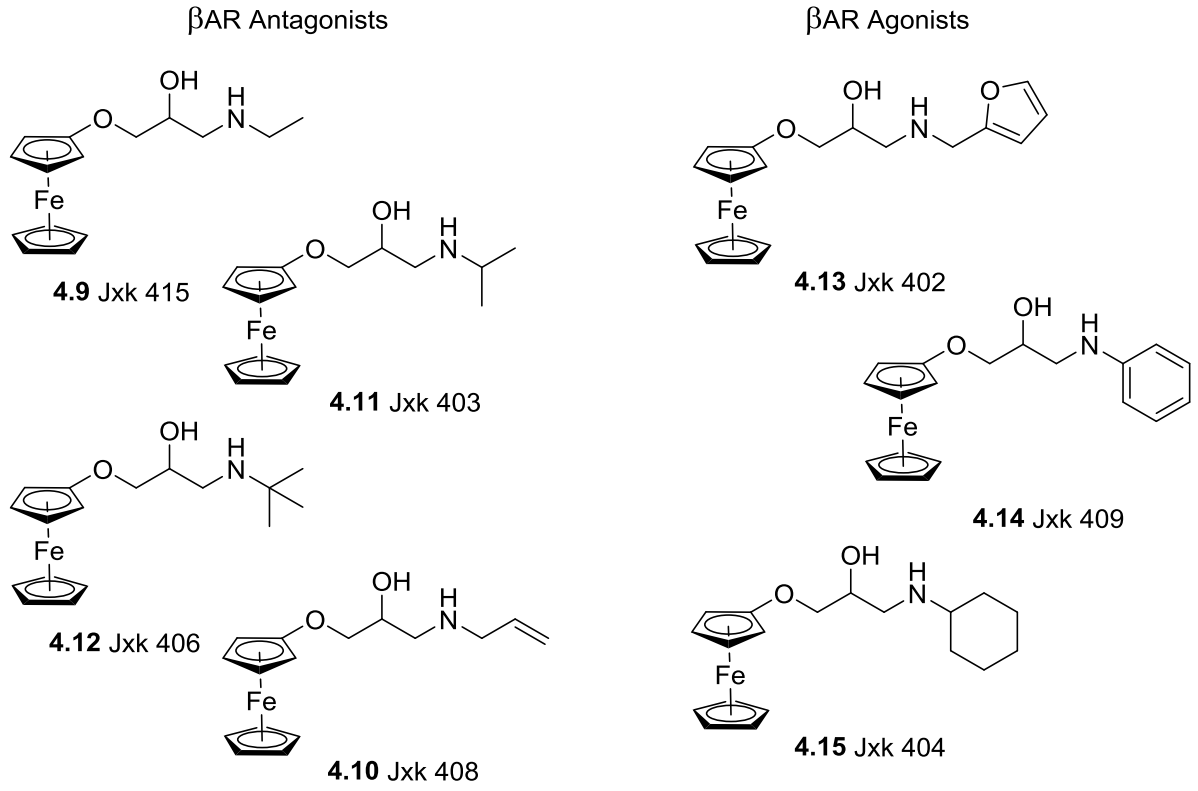


Fig. 4.20 Type-2 ferrocenyl β-blockers **4.9**, **4.10**, **4.11**, **4.12**, **4.13**, **4.14** and **4.15** grouped according to their βAR agonist or antagonist behaviour

4.5 Conclusion

Two synthetic strategies for the incorporation of ferrocene into the β-blocker pharmacophore were successfully developed. In both instances the metallocene is substituted for the catechol ring of the endogenous activator ligands and is attached via an ether linkage as exhibited by the majority of efficacious β-blockers. An additional carbon atom is present between the metallocene and the ether linkage in the type-1 set of compounds, but is not present in the type-2 compounds which therefore better resemble the prototypical β-blocker propranolol. In each synthesis the final step involves the opening of an epoxide with a primary amine, which allows for convenient production of a library of compounds. In this manner, three type-1 compounds; **4.3**, **4.4** and **4.5**, and seven type-2 compounds **4.9**, **4.10**, **4.11**, **4.12**, **4.13**, **4.14** and **4.15** were successfully synthesised. In many cases the final structures were confirmed by XRD as was the type-2 epoxide precursor **4.8**.

Biological testing sought to investigate the βAR interactions of these new compounds and, while very preliminary, produced very interesting and unexpected results. The type-1 compounds displayed very little βAR activity compared to propranolol, with only compound **4.5** producing any observable effect. Conversely the type-2 compounds retain far more βAR activity which would suggest that the extra carbon atom in the type-1 compounds is not tolerated by the receptor. Compound **4.12** was particularly active, producing more effective inhibition of the βAR than the positive control compound propranolol. Strangely, some of the type-2 ferrocenyl β-blockers seemed to exhibit agonist behaviour, which is very unusual given the absence of the catechol ring considered crucial for activation of βARs. Given that the negative control compound **Fcn3c2T**$_{(S,Rp)}$ also exhibited some agonist activity further studies are required to confirm these results.

4.6 References

[1] W. H. Frishman, A. Cheng-Lai, J. Nawarskas, **2005**, *Current Cardiovascular Drugs*, Current Science Group, 152 – 186.

[2] C. Venkata, S. Ram, *A. J. Cardiol*, **2010**, 1819 – 1825.

[3] J. A. van der Vring, M.C. Daniëls, N.J. Holwerda, P.J. Withagen, A. Schelling, T. J. Cleophas, M. G. Hendriks, *Angiology*, **1999**, 50, 447 – 54.

[4] S. J. Sorensen, S. R Abel, *Ann. Pharmacother.*, **1996**, 30, 43 – 54.

[5] V. Limmroth, M. C. Michel, *Br. J. Clin. Pharmacol.*, **2001**, 52, 237 – 243.

[6] S. A. Steenen, A. J. van Wijk, G. J. M. G. van der Heijden, R. van Westrhenen, J. de Lange, A. de Jongh, *J. Psychopharmacol.*, **2016**, 30, 128 – 139.

[7] P. McGee, S. Miller, C. Black, S. Hoey, *Ulster Med. J.*, **2013**, 82, 16 – 20.

[8] S. W. Cole, A. K. Sood, *Clin. Cancer Res.*, **2012**, 18, 1201 – 1206.

[9] J. G. Baker, S. J. Hill, R. J. Summers, *Trends Pharmacol. Sci.*, **2011**, 32, 227 – 234.

[10] T. L. Lemke, D. A. Williams, V. F. Roche, S. W. Zito, *Foyes Principles of Medicinal Chemistry 6th Edition*, **2008**, Lippincott Williams & Wilkins, 392 – 416.

[11] H. Lodish, A. Berk, S. L. Zipursky, P. Matsudaira, D. Baltimore, J. Darnell, *Molecular Cell Biology*, **2000**, *W. H, Freeman and Co.*, 862 – 871.

[12] R. P. Ahlquist, *Am. J. Physiol.*, **1948**, 153, 586 – 600.

[13] A. M. Lands, A. Arnold, J. B. McAuliff, A. P. Luduena, T. G. Brown, *Nature*, **1967**, 214, 597 – 598.

[14] B. Ablad, B. Carlsson, C. Dahlöf, L. Ek, E. Hultberg, *Adv. Cardiol.*, **1974**, 12, 290 – 302.

[15] M. P. Stapleton, *Tex. Heart Inst. J.*, **1997**, 24, 336 – 342.

[16] J. W. Black, *Postgrad. Med. J.*, **1976**, 52.

[17] J. W. Black, W. A. M. Duncan, R. G. Shanks, *Brit. J. Pharmacol.*, **1965**, 25, 577 – 591.

[18] V. Quirke, *Med. Hist.*, **2006**, 50, 69 – 92.

[19] W. H. Aellig, *Br. J. Clin. Pharmacol.*, **1982**, 13, 187 – 192.

[20] J. Kassotis, R. B. Sauberman, C. Candido, A. L. Wit, J. Coromilas, *J. Cardiovasc. Electrophysiol.*, **2003**, 14, 1233 – 1244.

[21] A. Gomes, D. Costa, J. L. F. C. Lima, E. Fernandes, *Bioorg. Med. Chem.*, **2006**, 14, 4568 – 4577.

[22] J. V. Okopski, *J. Clin. Pharm. Ther.*, **1987**, 12, 369 – 388.

[23] R. Howe, R. G. Shanks, *Nature*, **1966**, 210, 1336 – 1338.

[24] K. H. Rahn, *Eur. Heart. J.*, **1983**, 4, 27 – 30.

[25] K. Stoschitzky, G. Zernig, W. Lindner, *J. Clin. Bas. Cardiol.*, **1998**, 1, 14 – 8.

[26] R. J. Lefkowitz, L. E. Limbaud, C. Mukherjee, M. G. Caron, *Biochem. Biophys. Acta.*, **1976**, 457, 1 – 39.

[27] E. J. Ariëns, *Ann. N. Y. Acad. Sci.*, **1967**, 139, 606 – 631.

[28] C.Labrid, I. Rocher, O. Guery, *Am. J. Hypertens*, **1989**, 2, 245S – 251S.

[29] J. R. Jasper, P. A. Insel, *Biochem. Pharmacol.*, **1992**, 43, 119 – 130.

[30] Y. Ji, K. Li, X. Xiao, S, Zheng, T. Xu, S. Chen, *J. Pediatr. Surg.*, **2012**, 47, 2216 – 2223.

[31] C. Léauté-Labrèze, E. D. de la Roque, T. Hubiche, F. Boralevi, J.-B. Thambo, A. Taïeb, *N. Engl. J. Med.*, **2008**, 358, 2649 – 2651.

[32] V. Sans, E. D. de la Roque, J. Berge, N. Grenier, F. Boralevi, J. Mazereeuw-Hautier, D. Lipsker, E. Dupuis, K. Ezzedine, P. Vergnes, A Taïeb, C. Léauté-Labrèze, *Pediatrics,* **2009**, 124, 423 – 431.

[33] E. Pasquier, J. Ciccolini, M. Carre, S. Giacometti, R. Fanciullino, C. Pouchy, M.-P. Montero, C. Serdjebi, M. Kavallaris N. André, *Oncotarget*, **2011**, 2, 797 – 809.

[34] S. K. Sommers Smith, D. M. Smith, *In Vitro Cell Dev Biol Anim*, **2002**, 38, 298 – 304.

[35] C. H. Storch, P. H. Hoeger, *Br. J. Dermatol.*, **2010**, 163, 269 – 274.

[36] V. Albiñana, K. V. G. de las Heras, G. Serrano-Heras, T. Segura, A. B. Perona-Moratalla, M. Mota-Pérez, J. M. de Campos, L. M. Botella, *Orphanet. J. Rare Dis.*, **2015**, 10, 118.

[37] T. Harrison, B. U. Samuel, T. Akompong, H. Hamm, N. Mohandas, J. W. Lomasney, K. Haldar, *Science*, **2003**, 1734 – 1736.

[38] S. C. Murphy, T. Harrison, H. E. Hamm, J. W. Lomasney, N. Mohandas, K. Haldar, *PLos Med.*, **2006**, 3, 2403 – 2415.

[39] D. Lednicer, *Strategies for Organic Drug Synthesis and Design*, **1998**, John Wiley & Sons, 37 – 41.

[40] D. Schaarschmidt, H. Lang, *Organometallics*, **2010**, 29, 4196 – 4198.

[41] M. Roemer, C. A. Nijhuis, *Dalton. Trans.*, **2014**, 43, 11815 – 11818.

5 Experimental

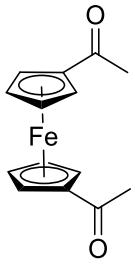
5.1 Synthesis

Except for acetylferrocene **3.1** and diacetylferrocene **2.2**, which were obtained from the undergraduate teaching laboratories and purified by flash column chromatography prior to use, all reagents and solvents were purchased from Sigma-Aldrich, Acros, Alfa Aesar and Fisher Scientific and used as received. Dry solvents were either purchased as such or obtained from a Pure Solv-MD solvent purification system and transported under an atmosphere of argon. Reactions using anhydrous solvents were performed in oven-dried glassware under an atmosphere of argon. Thin-layer chromatography (TLC) was performed on Merck 60 silica gel plates and visualised using short-wave UV light. Flash column chromatography was performed using Merck silica 60. Both were neutralised using TEA prior to use where specified. Melting points were determined using Stuart digital melting point apparatus and open glass capillary tubes. ^{1}H NMR and ^{13}C NMR spectroscopic data was recorded on either a Bruker AVIII300 (300 MHz ^{1}H, T = 293 K) or a Bruker AVIII400 (400 MHz ^{1}H, 101 MHz ^{13}C, T = 293 K) spectrometer while ^{31}P NMR spectroscopic data was recorded on a Bruker AV300. Spectra were recorded in either $CDCl_3$, CD_2Cl_2, DMSO-d6 or CD_3OD and chemical shifts (δ) given as parts per million (ppm) relative to residual $CHCl_3$ (^{1}H, 7.26 ppm; ^{13}C, 77.16 ppm), CH_2Cl_2 (^{1}H, 5.32 ppm; ^{13}C, 54.00 ppm), DMSO (^{1}H, 2.50 ppm; ^{13}C, 39.52 ppm) and MeOH (^{1}H, 4.87 ppm; ^{13}C, 49.00 ppm) respectively. Coupling constants (*J*) are given in hertz (Hz) and are averaged when close in value. Data was processed using Bruker Topspin v2.1 and MestReNova v10.0.2-15465. IR spectroscopy was performed on a Perkin–Elmer 100 FT-IR spectrometer using neat samples. Mass spectrometry (MS) and high resolution mass spectrometry (HRMS) was performed on either a Waters (Xevo, G2-XS TOF) a Waters Synapt G2-S or a Waters GCT using electrospray ionisation (ESI) or electron impact ionisation (EI).

5.1.1 Experimental Procedures for the Synthesis of Ferrocene Nucleic Acid (FcNA) Monomers

5.1.1.1 1,1'-Diacetylferrocene 2.2

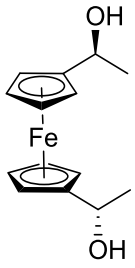
Known compound. Characterisation matches literature values[1]



1,1'-Diacetylferrocene **2.2** was obtained from the undergraduate teaching laboratory and purified by column chromatography using an eluent of 25% EtOAc in hexane. The solvent was removed to give the title compound as a red solid. ^{1}H NMR (300 MHz, $CDCl_3$) δ 4.76 (dd, *J* = 2.2, 1.8 Hz, 4H (Fc C***H***)), 4.52 – 4.47 (dd, *J* = 2.2, 1.8 Hz, 4H (Fc C***H***)), 2.34 (s, 6H (C***H***$_3$)). ^{13}C NMR (101 MHz, $CDCl_3$) δ 201.2 (***C***O), 80.8 (Fc ***C***–CO), 73.7 (Fc ***C***H), 71.1 (Fc ***C***H), 27.8 (***C***H_3).

5.1.1.2 (*S,S'*)-1,1'-Bis(α-hydroxyethyl)ferrocene 2.3-(*SS*)

Known compound. Characterisation matches literature values[1]

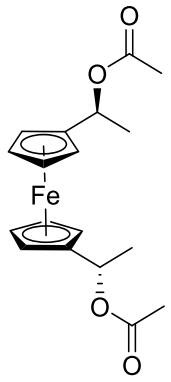


(*R*)-(+)-2-Methyl-CBS-oxazaborolidine (3.30 g, 12.0 mmol, 0.6 eq) was dissolved in dry THF (40 ml) under an atmosphere of argon and cooled to 0 ºC in an ice bath, BH_3•SMe_2 (2 M in THF) (4 ml) was added and the resultant mixture stirred for 15 min. 1,1'-diacetylferrocene **2.2** (5.40 g, 20.0 mmol, 1.0 eq) was dissolved in dry THF (200 ml) and added slowly, along

with the remaining BH_3•SMe_2 (2 M in THF) (16 ml). The mixture was then stirred at 0 ºC for 2 hrs. The reaction was quenched by dropwise addition of MeOH (50 ml), then poured into a solution of sat. NH_4Cl (300 ml) and extracted with DCM. The organic layer was washed with brine (100 ml), then water (2 x 100 ml) and dried over $MgSO_4$. The solvent was removed in vacuo and the crude product purified by flash column chromatography on silica gel using a gradient eluent system of 0 → 10% EtOAc in hexane. The solvent was removed in vacuo to give the title compound as a yellow solid (5.34 g, 19.5 mmol, 97%). ^{1}H NMR (300 MHz, $CDCl_3$) δ 4.66 (q, *J* = 6.3 Hz, 2H (C***H***CH_3)), 4.39 (s, 2H (O***H***)), 4.28 – 4.10 (m, 8H (Fc C***H***)), 1.39 (d, *J* = 6.3 Hz, 6H (C***H***$_3$)). ^{13}C NMR (101 MHz, $CDCl_3$) δ 95.3 (Fc ***C***–CH), 67.8 (Fc ***C***H), 67.7 (Fc ***C***H), 66.3 (Fc ***C***H), 66.1 (Fc ***C***H), 65.8 (***C***HCH_3), 25.7 (***C***H_3).

5.1.1.3 (*S*,*S'*)-1,1'-Bis(α-acetoxyethyl)ferrocene 2.4-(*SS*)

Known compound. Characterisation matches literature values[1]

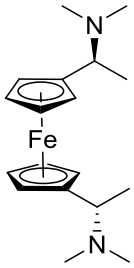


(*S*,*S*)-1,1'-Bis(α-hydroxyethyl)ferrocene **2.3-(*SS*)** (5.34 g, 19.5 mmol, 1.0 eq) was dissolved in dry DCM (60 ml) and stirred for 5 minutes under an atmosphere of argon. Acetic anhydride (4.56 ml, 48.75 mmol, 2.5 eq), TEA (6.80 ml, 48.75 mmol, 2.5 eq) and DMAP (0.12 g, 0.98 mmol, 0.05 eq.) were added successively and the resultant mixture stirred for 22 hrs. The reaction was quenched with sat. NH_4Cl (100 ml), extracted with DCM and the organic layers washed with brine (100 ml), then water (2 x 100 ml) and dried over $MgSO_4$. The solvent was removed in vacuo and the crude product purified by flash column

chromatography on silica gel using 20% EtOAc and 3% TEA in hexane. The solvent was removed in vacuo to give the title compound as a yellow solid (6.16 g, 17.2 mmol, 88%). ^{1}H NMR (300 MHz, $CDCl_3$) δ 5.80 (q, *J* = 6.4 Hz, 2H (C***H***CH_3)), 4.23 (dd, *J* = 3.3, 1.7 Hz, 2H (Fc C***H***)), 4.19 (dd, *J* = 3.3, 1.7 Hz, 2H (Fc C***H***)), 4.16 – 4.09 (m, 4H (Fc C***H***)), 2.04 (s, 6H (C***H***$_3$CO)), 1.53 (d, *J* = 6.4 Hz, 6H (C***H***$_3$CH)). ^{13}C NMR (101 MHz, $CDCl_3$) δ 170.6 (***C***O), 88.8 (Fc ***C***–CH), 69.3 (Fc ***C***H), 69.1 (Fc ***C***H), 69.0 (Fc ***C***H), 68.7 (Fc ***C***H), 66.7 (***C***HCH_3), 21.5 (***C***H_3CO), 20.4 (***C***H_3CH).

5.1.1.4 (*S*,*S'*)-1,1'-Bis(α-*N*,*N*-dimethylaminoethyl)ferrocene 2.5-(*SS*)

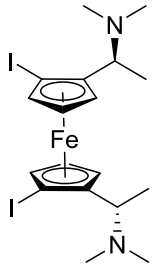
Known compound. Characterisation matches literature values[1]



(S,S)-1,1'-Bis(α-acetoxyethyl)ferrocene **2.4-(*SS*)** (6.16 g, 17.18 mmol) was dissolved in MeOH (10 ml) and $HNMe_2$ (40% in H_2O) added, the resulting solution was then stirred for 60 hrs. The reaction was quenched with water, extracted with DCM and the organic layers washed with brine (100 ml), then water (2 x 100 ml) and dried over $MgSO_4$. The solvent was removed in vacuo and the crude product purified by flash column chromatography on silica gel using 5% MeOH and 5% TEA in EtOAc. The solvent was removed in vacuo to give the title compound as a yellow solid (4.12 g, 12.56 mmol, 73%). ^{1}H NMR (300 MHz, $CDCl_3$) δ 4.25 – 3.89 (m, 8H (Fc C***H***)), 3.61 (q, *J* = 6.8 Hz, 2H (C***H***CH_3)), 2.07 (s, 12H (C***H***$_3$N)), 1.44 (d, *J* = 6.8 Hz, 6H (C***H***$_3$CH)). ^{13}C NMR (101 MHz, $CDCl_3$) δ 86.8 (Fc ***C***–CH), 70.5 (Fc ***C***H), 68.8 (Fc ***C***H), 68.5 (Fc ***C***H), 67.3 (Fc ***C***H), 58.9 (***C***HCH_3), 40.6 (***C***H_3N), 16.2 (***C***H_3CH).

5.1.1.5 (*S*,*S*)-2,2'-Bis(α-*N*,*N*-dimethylaminoethyl)-(R_p,R_p)-1,1'-bisiodoferrocene **2.6-(*SS*,R_pR_p)**

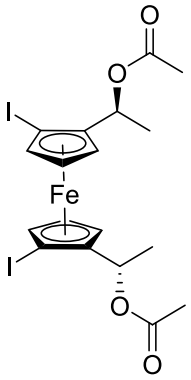
Known compound. Characterisation matches literature values[2]



(*S*,*S*)-1,1'-Bis(α-*N*,*N*-dimethylaminoethyl)ferrocene **2.5-(*SS*)** (4.10 g, 12.50 mmol, 1.0 eq) was dissolved in dry Et_2O (60 ml) and stirred under an atmosphere of argon at 0 ºC for 5 min. *n*-BuLi (2.5 M in hexane) (20.0 ml, 50.0 mmol, 4.0 eq) was added dropwise and the resulting solution was allowed to warm to rt, stirring for 18 hrs. Dry THF (10 ml) was added and the solution was cooled to -78 ºC using an acetone/dry ice bath. I_2 (14.28 g, 56.25 mmol, 4.5 eq) was dissolved in dry THF (20 ml) and added dropwise. The ice bath was removed and stirring continued for 3 hrs while warming to rt. The solution was cooled to 0 ºC using an ice bath, quenched with sat. $Na_2S_2O_3$ solution then extracted with Et_2O washed with water (2 x 100 ml) and dried over $MgSO_4$. The solvent was removed in vacuo and the crude product purified by flash column chromatography on neutralised silica gel using a gradient eluent system of 5% TEA in hexane → 5% TEA in EtOAc. The solvent was removed in vacuo to give the title compound as a yellow solid (5.99 g, 10.3 mmol, 83%). ^{1}H NMR (300 MHz, $CDCl_3$) δ 4.40 – 3.89 (m, 6H (Fc C***H***)), 3.52 (q, *J* = 6.8 Hz, 2H (C***H***CH_3)), 2.06 (s, 12H (C***H***$_3$N)), 1.37 (d, *J* = 6.8 Hz, 6H (C***H***$_3$CH)). ^{13}C NMR (101 MHz, $CDCl_3$) δ 90.6 (Fc ***C***–CH), 82.1 (Fc ***C***H), 72.1 (Fc ***C***H), 67.7 (Fc ***C***H), 56.9 (***C***HCH_3), 47.6 (Fc ***C***–I), 41.1 (***C***H_3N), 15.6 (***C***H_3CH).

5.1.1.6 (*S*,*S*)-2,2'-Bis(α-acetoxyethyl)-(R_p,R_p)-1,1'-bisiodoferrocene 2.7-(*SS*,R_pR_p)

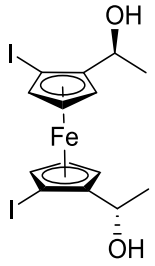
Known compound. Characterisation matches literature values[2]



(*S*,*S*)-2,2'-Bis(α-*N*,*N*-dimethylaminoethyl)-(R_p,R_p)-1,1'-bisiodoferrocene **2.6-(*SS*,R_pR_p)** (5.99 g, 10.3 mmol, 1.0 eq) was dissolved in Ac_2O (30 ml) and stirred for 2 hrs at 85 ºC. The reaction mixture was cooled to rt and quenched by the slow addition of sat. $NaHCO_3$ (200 ml). The crude product was then extracted with DCM washed with brine (100 ml), then water (2 x100 ml) and dried over $MgSO_4$. The solvent was removed in vacuo and the crude product purified by flash column chromatography on neutralised silica gel using an eluent of 20% EtOAc in hexane. The solvent was removed in vacuo to give the title compound as a yellow solid (3.27 g, 5.37 mmol, 52%). ^{1}H NMR (300 MHz, $CDCl_3$) δ 5.80 (q, *J* = 6.5 Hz, 2H (C***H***CH_3)), 4.35 (dd, *J* = 2.6, 1.4 Hz, 2H (Fc C***H***)), 4.30 (dd, *J* = 2.6, 1.4 Hz, 2H (Fc C***H***)), 4.21 (dd, *J* = 2.6, 2.6 Hz, 2H (Fc C***H***)), 2.01 (s, 6H (C***H***$_3$CO)), 1.60 (d, *J* = 6.5 Hz, 6H (C***H***$_3$CH)). ^{13}C NMR (101 MHz, $CDCl_3$) δ 170.3 (***C***O), 89.0 (Fc ***C***–CH), 82.4 (Fc ***C***H), 73.3 (Fc ***C***H), 68.7 (***C***HCH_3), 67.9 (Fc ***C***H), 45.7 (Fc ***C***–I), 21.2 (C***H***$_3$CH), 18.9 (C***H***$_3$CO).

5.1.1.7 (*S*,*S*)-2,2'-Bis(α-hydroxyethyl)-(R_p,R_p)-1,1'-bisiodoferrocene 2.8-(*SS*,R_pR_p)

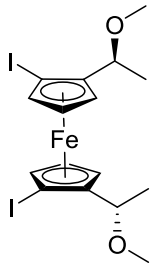
Known compound. Characterisation matches literature values[2]



(*S*,*S*)-2,2'-Bis(α-acetoxyethyl)-(R_p,R_p)-1,1'-bis(iodo)ferrocene **2.7-(*SS*,R_pR_p)** (3.27 g, 5.37 mmol) was dissolved in EtOH (100 ml) and stirred at 95 ºC. NaOH (10% in H_2O) (60 ml) was added and the resulting solution stirred for 30 mins. The reaction mixture was extracted with DCM, washed with H_2O (4 x 100 ml) and dried over $MgSO_4$. The solvent was removed in vacuo to give the title compound as a yellow solid (2.75 g, 5.22 mmol, 97%). ^{1}H NMR (300 MHz, $CDCl_3$) δ 4.79 (q, *J* = 6.6 Hz, 2H (C***H***CH_3)), 4.31 – 4.26 (m, 4H (Fc C***H***)), 4.20 (dd, *J* = 2.6, 2.6 Hz, 2H (Fc C***H***)), 2.03 (s, 2H O***H***)), 1.58 (d, *J* = 6.6 Hz, 6H (C***H***$_3$)). ^{13}C NMR (101 MHz, $CDCl_3$) δ 92.9 (Fc ***C***–CH), 80.7 (Fc ***C***H), 72.6 (Fc ***C***H), 67.3 (Fc ***C***H), 65.7 (***C***HCH_3), 45.1 (Fc ***C***–I), 21.8 (***C***H_3).

5.1.1.8 (*S*,*S*)-2,2'-Bis(α-methoxyethyl)-(*pR*,*pR*)-1,1'-bisiodoferrocene 2.9-(*SS*,R_pR_p)

Known compound. Characterisation matches literature values[2]

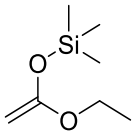


(*S*,*S*)-2,2'-Bis(α-hydroxyethyl)-(R_p,R_p)-1,1'-bis(iodo)ferrocene **2.8-(*SS*,R_pR_p)** (2.75 g, 5.22 mmol) was dissolved in MeOH (54 ml) and stirred for 5 mins. AcOH (6 ml) was then added and the mixture stirred for 48 hrs. The reaction was quenched by the slow addition of sat.

$NaHCO_3$ (50 ml) then extracted with DCM, washed with brine (100 ml) and water (2 x 100 ml) and dried over $MgSO_4$. The solvent was removed in vacuo and the crude product purified by flash column chromatography on silica gel using a gradient eluent system of 0 → 50% EtOAc in hexane. Unreacted starting material and mono-reacted species were collected and rereacted using the same procedure. The product was obtained as a yellow solid (2.50 g, 4.51 mmol, 86% in total). H NMR (300 MHz, $CDCl_3$) δ 4.33 – 4.26 (m, 4H (Fc C***H***, C***H***CH_3)), 4.24 (dd, *J* = 2.5, 1.4 Hz, 2H (Fc C***H***)), 4.18 (dd, *J* = 2.5, 2.5 Hz, 2H (Fc C***H***)), 3.26 (s, 6H (C***H***$_3$O)), 1.59 (d, *J* = 6.4 Hz, 6H (C***H***$_3$CH)). ^{13}C NMR (101 MHz, $CDCl_3$) δ 90.9 (Fc ***C***–CH), 81.6 (Fc ***C***H), 73.6 (***C***HCH_3), 72.9 (Fc ***C***H), 67.5 (Fc ***C***H), 56.3 (C***H***$_3$O), 47.3 (Fc ***C***–I), 19.6 (C***H***$_3$CH).

5.1.1.9 1-Ethoxy-1-trimethylsilyloxyethylene 2.10

Characterisation matches literature values[3]

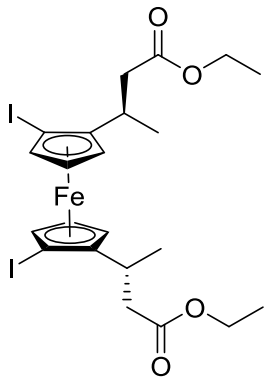


DIPA (4.18 ml, 29.6 mmol, 1.0 eq.) was added to dry THF (20 ml) and cooled to 0 ºC under an atmosphere of argon in a schlenk tube. *n*-BuLi (2.5 M in hexane) (11.85 ml, 29.6 mmol, 1.0 eq.) was added dropwise and stirring continued for 20 min. The resulting yellow solution was cooled to -78 ºC before EtOAc **2.12** (2.63 ml, 26.6 mmol, 0.9 eq.) was added. After 30 min stirring, TMSCl (4.13 ml, 32.6 mmol, 1.1 eq.) was added and stirring continued for a further 30 min. The mixture was then raised to rt and stirred for a further hr. THF was removed by gentle evaporation at 25 ºC on the rotovap and the remaining solution poured into a mixture of 9 hexane : 4 water (100 ml). The organic layer is collected and washed with brine (50 ml) and water (2 x 50 ml) and dried over $MgSO_4$. The majority of solvent was removed by gentle evaporation at 25 ºC on the rotovap before the remaining hexane and

excess EtOAc were removed by vacuum distillation at 43 ºC and 69 ºC respectively. The product distilled off at 80 ºC and NMR showed the composition to be ca. 70% in EtOAc. ^{1}H NMR (300 MHz, $CDCl_3$) δ 3.75 (q, *J* = 7.0 Hz, 2H, (C***H***$_2$CH$_3$)), 3.20 (d, *J* = 2.7 Hz, 1H (C***H***$_2$=CO)), 3.06 (d, *J* = 2.7 Hz, 1H (C***H***$_2$=CO)), 1.30 (t, J = 7.0 Hz, 3H (C***H***$_3$)), 0.23 (s, 9H SiC***H***$_3$).

5.1.1.10 (*R*,*R*)-2,2'-Bis(α-methyl-ethylpropanoate)-(*R*$_p$,*R*$_p$)-1,1'-bisiodoferrocene 2.11-(*RR*,*R*$_p$*R*$_p$)

Known compound. Characterisation matches literature values[2]



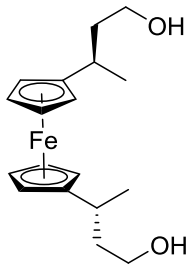
Method 1. (*S*,*S*)-2,2'-Bis(α-methoxyethyl)-(*R*$_p$,*R*$_p$)-1,1'-bisiodoferrocene **2.9-(*SS*,*R*$_p$*R*$_p$)** (2.50 g, 4.51 mmol, 1.0 eq) was dissolved in dry DCM (15 ml) and stirred at -78 ºC for 5 min under an atmosphere of argon. 1-ethoxy-1-trimethylsilyloxyethylene **2.10** (70% in EtOAc) (4.61 ml) was added and the mixture stirred for 5 mins before dropwise addition of BF_3•Et_2O (1.25 ml) and stirring continued for a further 20 min. The solution was allowed to warm to rt with stirring continued for 1 hr. The reaction was quenched with sat. $NaHCO_3$, extracted with DCM and dried over $MgSO_4$. The solvent was removed in vacuo and the crude product purified by flash column chromatography on silica gel using a gradiant eluent system of 0 → 20% EtOAc in hexane. The solvent was removed in vacuo to give the title compound as a yellow solid (2.01 g, 3.02 mmol, 67%). ^{1}H NMR (300 MHz, $CDCl_3$) δ 4.19 – 4.10 (m, 6H (Fc C***H***)), 4.10 (q, *J* = 7.1 Hz, 4H, C***H***$_2$O)), 3.03 (dqd, *J* = 10.2, 6.8, 3.7, 2H (C***H***CH$_3$)), 2.50

(dd, *J* = 15.0, 3.7 Hz, 2H (C***H***$_2$CH), 2.09 (dd, *J* = 15.0, 10.2 Hz, 2H (C***H***$_2$CH)), 1.36 (d, *J* = 6.8 Hz, 6H (C***H***$_3$CH)), 1.23 (t, *J* = 7.1 Hz, 6H (C***H***$_3$CH$_2$)). ^{13}C NMR (101 MHz, $CDCl_3$) δ 172.0 (***C***OO), 94.7 (Fc ***C***–CH), 81.2 (Fc ***C***H), 71.9 (Fc ***C***H), 66.5 (Fc ***C***H), 60.4 (***C***H$_2$O), 46.3 (Fc ***C***–I), 42.9 (***C***H$_2$CH), 30.0 (***C***HCH$_3$), 18.9 (***C***H$_3$CH), 14.4 (***C***H$_3$CH$_2$).

Method 2. (*S*,*S*)-2,2'-Bis(α-acetoxyethyl)-(*R*$_p$,*R*$_p$)-1,1'-bisiodoferrocene **2.7-(*SS*,*R*$_p$*R*$_p$)** (1.65 g, 2.71 mmol, 1.0 eq) was dissolved in dry DCM (20 ml) and cooled to -78 ºC in a schlenk tube under an atmosphere of argon with stirring. 1-ethoxy-1-trimethylsilyloxyethylene **2.10** (70% in EtOAc) (9.69 ml) was added and the mixture stirred for 30 mins before dropwise addition of BF_3•THF (0.74 ml, 5.96 mmol, 2.2 eq.) and stirring continued for a further 3 hrs at -78 ºC. The solution was allowed to warm to rt with stirring continued for 1 hr. The reaction was quenched with sat. $NaHCO_3$, extracted with DCM and dried over $MgSO_4$. The solvent was removed in vacuo and the crude product purified by flash column chromatography on silica gel using a gradient eluent system of 1 → 20% EtOAc in hexane. The solvent was removed in vacuo to give the title compound as a yellow solid (1.71 g, 2.56 mmol, 94%). ^{1}H and ^{13}C NMR spectra matched that obtained using **Method 1**, m/z Calcd for $C_{22}H_{28}FeO_4I_2Na$ $[M + Na]^+$: 688.9, found 688.9.

5.1.1.11 (*R*,*R*)-1,1'-Bis(α-methyl-γ-hydroxypropyl)ferrocene 2.13-(*RR*)

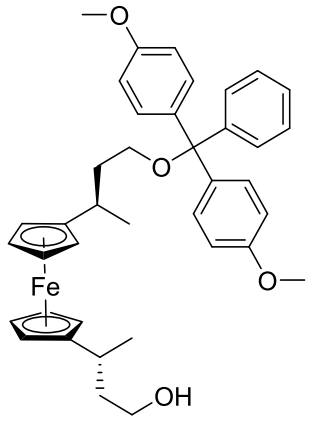
Known compound. Characterisation matches literature values[4]



(*R,R*)-2,2'-Bis(α-methyl-ethylpropanoate)-(R_p,R_p)-1,1'-bisiodoferrocene **2.11-(*RR*,R_pR_p)** (1.61 g, 2.42 mmol, 1.0 eq) was dissolved in dry THF (30 ml) and $LiAlH_4$ (1.46 g, 38.68 mmol, 16.0 eq.) added in small portions. The reaction was quenched by the slow addition of sat. Na^+/K^+ tartrate solution, extracted with DCM and dried over $MgSO_4$. The solvent was removed in vacuo and the crude product purified by flash column chromatography on silica gel using an eluent of 20% EtOAc → in hexane. The solvent was removed in vacuo to give the title compound as a yellow solid (0.571 g, 1.73 mmol, 71%). ^{1}H NMR (300 MHz, $CDCl_3$) δ 4.39 – 3.89 (m, 8H (Fc ***C***H)), 3.83 – 3.47 (m, 4H (C***H***$_2$O)), 2.89 – 2.45 (m, 2H (C***H***)), 1.83 – 1.58 (m, 4H (C***H***$_2$CH)), 1.85 (s, 2H (O***H***)), 1.25 (d, *J* = 6.9 Hz, 6H (C***H***$_3$)). ^{13}C NMR (101 MHz, $CDCl_3$) δ 95.5 (Fc ***C***–CH), 68.1 (Fc ***C***H), 68.0 (Fc ***C***H), 67.9 (Fc ***C***H), 66.1 (Fc ***C***H), 61.1 (***C***H$_2$O), 41.5 (***C***H$_2$CH), 29.6 (***C***H), 20.9 (***C***H$_3$). IR ν_{max}/cm^{-1} = 3311 (OH), 3089 (Fc CH), 2959 (CH), 2929 (CH), 2872 (CH). m/z: Calcd for $C_{18}H_{26}FeO_2$ $[M]^+$: 330.1, found 330.1.

5.1.1.12 (*R*)-1-(α-Methyl-γ-(dimethoxytrityl)oxypropyl),(*R*)-1'-(α-methyl-γ-hydroxypropyl)ferrocene 2.14-(*RR*)

Known compound. Characterisation matches literature values[4]

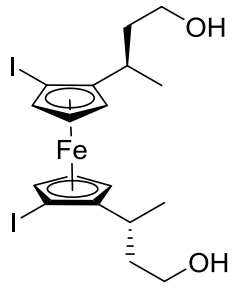


(*R,R*)-1,1'-Bis(α-methyl-γ-hydroxypropyl)ferrocene **2.13-(*RR*)** (0.478 g, 1.45 mmol, 1.0 eq.) and DMAP (0.035 g, 0.29 mmol, 0.2 eq.) were dissolved in dry THF (10 ml) in a schlenk

tube under an atmosphere of argon. 4,4-Dimethoxytrityl chloride (0.542 g, 1.60 mmol, 1.1 eq.) and *N*,*N*-diisopropylethylamine (0.25 ml, 1.45 mmol, 1.0 eq.) were added and the resulting mixture stirred for 16 hr. The reaction was quenched with MeOH (3 ml) and the solvent removed in vacuo before being redissolved in DCM, washed with water (2 x 20 ml) and dried over $MgSO_4$. The solvent was removed in vacuo and the crude product purified by flash column chromatography on neutralised silica gel using a gradient eluent system of 100% hexane → 100% EtOAc. The solvent was removed in vacuo to give the title compound as an orange oil (0.50 g, 0.79 mmol, 54%). ^{1}H NMR (300 MHz, $CDCl_3$) δ 7.46 (ddd, *J* = 12.3, 6.6, 4.5 Hz, 2H (Ph C***H***)), 7.42 – 7.18 (m, 7H (Ph C***H***)), 6.85 (d, *J* = 8.9 Hz, 4H (Ph C***H***)), 4.06 – 3.92 (m, 6H (Fc C***H***)), 3.96 (d, *J* = 13.9 Hz, 2H (Fc C***H***)), 3.80 (s, 6H ($C\boldsymbol{H}_3O$)), 3.66 (dd, *J* = 5.7, 5.7 Hz, 2H ($C\boldsymbol{H}_2OH$)), 3.12 (dd, *J* = 6.4, 6.4 Hz, 2H ($C\boldsymbol{H}_2$ODMT)), 2.76 – 2.57 (m, 2H (C***H***)), 1.89 (dtd, *J* = 12.4, 7.0, 5.7 Hz, 1H ($C\boldsymbol{H}_2CH_2OH$)), 1.82 – 1.57 (m, 3H ($C\boldsymbol{H}_2CH_2OH$, $C\boldsymbol{H}_2CH_2$ODMT)), 1.28 (s, 1H (OH)), 1.27 (d, *J* = 6.9 Hz, 3H ($C\boldsymbol{H}_3CH$)), 1.12 (d, *J* = 6.9 Hz, 3H ($C\boldsymbol{H}_3CH$)). ^{13}C NMR (101 MHz, $CDCl_3$) δ 158.4 (Ph ***C***–O), 145.5 (PhOMe ***C***–C), 136.8 (Ph C–C), 130.2 (Ph ***C***H), 128.3 (Ph ***C***H), 127.8 (Ph ***C***H), 126.7 (Ph ***C***H), 113.1 (Ph ***C***H), 95.9 (Fc ***C***–CH), 95.3 (Fc ***C***–CH), 85.9 (DMT ^{t}***C***–O), 68.0 (Fc ***C***–H), 67.9 (Fc ***C***–H), 67.9 (Fc ***C***–H), 67.8 (Fc ***C***–H), 67.7 (Fc ***C***–H), 66.3 (Fc ***C***–H), 66.0 (Fc ***C***–H), 61.6 ($OC\boldsymbol{H}_2CH_2$), 61.2 ($OC\boldsymbol{H}_2CH_2$), 55.3 ($\boldsymbol{C}H_3O$), 41.7 ($C\boldsymbol{H}_2CH$), 38.7 ($C\boldsymbol{H}_2CH$), 29.8 ($\boldsymbol{C}HCH_3$), 29.7 ($\boldsymbol{C}HCH_3$), 21.0 ($C\boldsymbol{H}_3CH$), 20.8 ($C\boldsymbol{H}_3CH$). IR ν_{max}/cm^{-1} = 3366 (OH), 3085 (Fc CH), 2957 (CH), 2930 (CH), 2872 (CH), 2835 (CH), 1607 (C=C). HRMS (ESI-TOF) m/z: $[M + Na]^+$ Calcd for $C_{39}H_{44}FeO_4Na$ 655.2487; Found 655.2471.

5.1.1.13 (*R*,*R*)-2,2'-Bis(α-methyl-γ-hydroxypropyl)-(R_p,R_p)-1,1'-bisiodoferrocene **2.15-(*RR*,R_pR_p)**

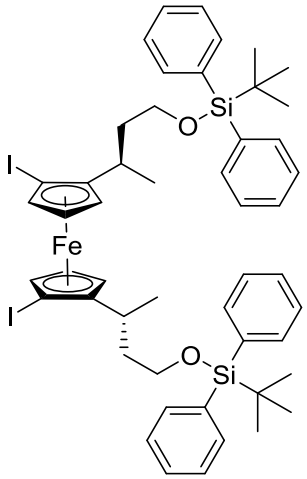
Known compound. Characterisation matches literature values[2]



(*R*,*R*)-2,2'-Bis(α-methyl-ethylpropanoate)-(R_p,R_p)-1,1'-bisiodoferrocene **2.11-(*RR*,R_pR_p)** (2.10 g, 3.15 mmol, 1.0 eq) was dissolved in Et_2O (15 ml) and cooled to 0 ºC under an atmosphere of argon. DIBAL (1 M in THF) (18.9 ml, 18.9 mmol, 6.0 eq) was added dropwise and the resulting solution stirred at 0 ºC for 1 hr. The reaction was quenched with sat. Na^+/K^+ tartrate solution, extracted with DCM and dried over $MgSO_4$. The crude product was then purified by flash column chromatography on silica gel using a gradient eluent system of 20 → 50% EtOAc in hexane. The solvent was removed in vacuo to give the title compound as a yellow solid (1.61 g, 2.77 mmol, 88%). ^{1}H NMR (300 MHz, $CDCl_3$) δ 4.17 – 4.09 (m, 6H (Fc C***H***)), 3.58 (dd, *J* = 6.9, 6.4 Hz, 4H (C***H***$_2$O)), 2.69 (dqd, *J* = 13.8, 6.9, 5.3 Hz, 2H (C***H***CH_3)), 1.66 (dtd, *J* = 12.4, 6.9, 5.3 2H (C***H***$_2$CH)), 1.53 (dtd, *J* = 13.8, 12.4, 6.4, 2H (C***H***$_2$CH)), 1.36 (d, *J* = 6.9 Hz, 6H (C***H***$_3$)), 1.32 (s, 2H (O***H***)). ^{13}C NMR (101 MHz, $CDCl_3$) δ 96.4 (Fc ***C***–CH), 80.9 (Fc ***C***H), 71.7 (Fc ***C***H), 66.2 (Fc ***C***H), 60.9 (***C***H_2O), 47.0 (Fc ***C***–I), 41.9 (***C***H_2CH), 29.2 (***C***HCH_3), 19.7 (***C***H_3).

5.1.1.14 (*R*,*R*)-2,2'-Bis(α-methyl-γ-(*tert*-butyldiphenylsilyl)oxypropyl)-(R_p,R_p)-1,1'-bisiodoferrocene 2.16-(*RR*,R_pR_p)

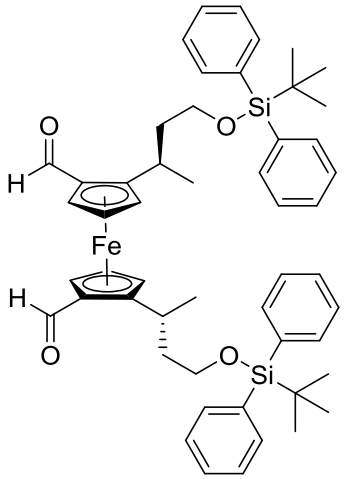
Known compound. Characterisation matches literature values[5]



(*R*,*R*)-2,2'-Bis(α-methyl-γ-hydroxypropyl)-(R_p,R_p)-1,1'-bisiodoferrocene **2.15-(*RR*,R_pR_p)** (1.60 g, 2.75 mmol, 1.0 eq) was dissolved in dry DCM (20 ml) under an atmosphere of argon. TEA (1.15 ml, 8.25 mmol, 3.0 eq), TBDPSCl (2.15 ml, 8.25 ml, 3.0 eq) and DMAP (10 crystals) were added sequentially and the resulting solution stirred for 64 hrs. The reaction was quenched with H_2O, extracted with DCM and dried over $MgSO_4$. The crude product was purified by flash column chromatography on silica gel using an eluent of 5% EtOAc in hexane. The solvent was removed in vacuo to give the title compound as a yellow oil (2.78 g, 2.63 mmol, 95%). ^{1}H NMR (300 MHz, $CDCl_3$) δ 7.75 – 7.65 (m, 8H (Ph C***H***)), 7.48 – 7.32 (m, 12H (Ph C***H***)), 4.15 (dd, J = 2.2, 1.6 Hz, 2H (Fc C***H***)), 4.07 – 4.03 (m, 4H (Fc C***H***)), 3.67 (dd, *J* = 7.8, 5.6 Hz, 4H (C***H***$_2$O), 2.74 (dqd, J = 13.6, 6.8, 3.8 Hz, 2H (C***H***CH_3)), 1.85 (dtd, *J* = 13.4, 7.8, 3.8 Hz, 2H (C***H***$_2$CH)), 1.42 – 1.30 (m, 2H (C***H***$_2$CH)), 1.28 (d, *J* = 6.8 Hz, 6H (C***H***$_3$CH)), 1.07 (s, 18H (tBu C***H***$_3$)). ^{13}C NMR (101 MHz, $CDCl_3$) δ 135.8 (Ph ***C***H), 135.8 (Ph ***C***H), 134.2 (Ph ***C***–Si), 134.1 (Ph ***C***–Si), 129.7 (Ph ***C***H), 129.6 (Ph ***C***H), 127.8 (Ph ***C***H), 127.7 (Ph ***C***H), 96.7 (Fc ***C***–CH), 80.4 (Fc ***C***H), 71.3 (Fc ***C***H), 66.2 (Fc ***C***H), 62.1 (***C***H_2O), 46.8 (Fc ***C***–I), 41.4 (***C***H_2CH), 29.2 (***C***HCH_3), 27.1 (tBu ***C***H_3), 19.4 (tBu ***C***), 18.8 (***C***H_3CH).

5.1.1.15 (*R*,*R*)-2,2'-Bis(α-methyl-γ-(*tert*-butyldiphenylsilyl)oxypropyl)-(R_p,R_p)-1,1'-bisformylferrocene 2.17-(*RR*,R_pR_p)

Known compound. Characterisation matches literature values[5]

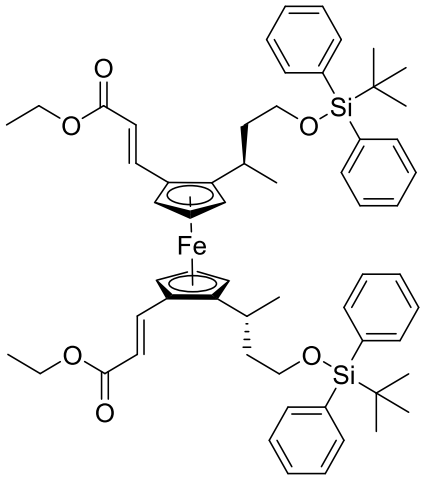


(*R*,*R*)-2,2'-Bis(α-methyl-γ-(*tert*-butyldiphenylsilyl)oxypropyl)-(R_p,R_p)-1,1'-bisiodoferrocene **2.16-(*RR*,R_pR_p)** (1.25 g, 1.18 mmol, 1.0 eq.) was dissolved in dry Et_2O (6 ml) and cooled to -78 ºC under an atmosphere of argon. *n*-BuLi (2.5 M in hexane) (1.66 ml, 4.15 mmol, 3.5 eq.) was added dropwise and the solution stirred for 10 mins before warming to rt with stirring continued for 1 hr. The reaction was again cooled to -78 ºC and DMF (0.37 ml, 4.74 mmol, 4.0 eq.) was added dropwise. Stirring was continued for 10 mins, before the ice bath was removed and the solution was allowed to warm to rt over 1 hr. The reaction was quenched with H_2O, extracted with DCM and dried over $MgSO_4$, the solvent was removed in vacuo and the crude product purified by flash column chromatography on silica gel using an eluent of 10% EtOAc in hexane. The solvent was removed in vacuo to give the title compound as a red oil (0.87 g, 1.01 mmol, 85%). ^{1}H NMR (300 MHz, $CDCl_3$) δ 10.08 (s, 2H (C***H***O)), 7.66 (ddd, *J* = 7.9, 3.5, 1.8 Hz, 8H (Ph C***H***)), 7.49 – 7.34 (m, 12H (Ph C***H***)), 4.82 (dd, *J* = 2.6, 1.5 Hz, 2H (Fc C***H***)), 4.50 – 4.40 (m, 4H (Fc C***H***)), 3.70 – 3.54 (m, 4H (C***H***$_2$O), 3.20 – 3.06 (m, 2H (C***H***CH_3)), 1.75 – 1.62 (m, 2H (C***H***$_2$CH), 1.61 – 1.45 (m, 2H (C***H***$_2$CH), 1.31 (d, *J* = 6.9 Hz,

6H (C***H***$_3$CH)), 1.07 (s, 18H (tBu C***H***$_3$)). ^{13}C NMR (101 MHz, $CDCl_3$) δ 193.0 (***C***O), 135.7 (Ph ***C***H), 135.6 (Ph ***C***H), 133.9 (Ph ***C***–Si), 133.8 (Ph ***C***–Si), 129.7 (Ph ***C***H), 129.7 (Ph ***C***H), 127.8 (Ph ***C***H), 127.7 (Ph ***C***H), 99.9 (Fc ***C***–CH), 77.5 (Fc ***C***–CHO), 72.5 (Fc ***C***H), 72.2 (Fc ***C***H), 71.6 (Fc ***C***H), 61.7 (***C***H_2O), 43.2 (C***H***$_2$CH), 27.5 (***C***HCH$_3$), 27.0 (tBu ***C***H$_3$), 19.2 (tBu ***C***), 18.8 (***C***H$_3$CH). IR ν_{max}/cm^{-1} = 3071 (Fc CH), 2929 (CH), 2856 (CH), 1674 (C=O). m/z: Calcd for $C_{52}H_{62}FeO_4Si_2Na$ $[M + Na]^+$: 885.4, found 885.3.

5.1.1.16 (*R*,*R*)-2,2'-Bis(α-methyl-γ-(*tert*-butyldiphenylsilyl)oxypropyl)-(R_p,R_p)-1,1'-bis(α-ene-ethylpropanoate)ferrocene 2.18-(*RR*,R_pR_p)

Novel compound

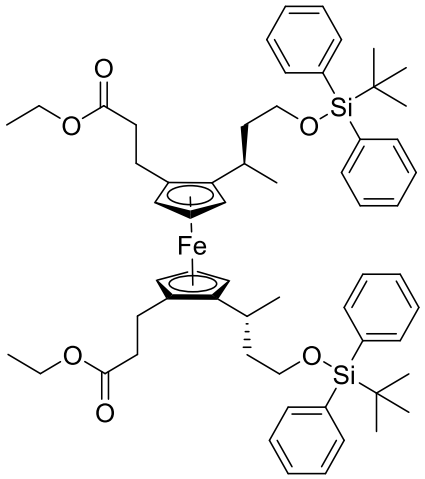


Triethyl phosphonoacetate (0.60 ml, 3.03 mmol, 3.0 eq) was dissolved in EtOH (2 ml) and stirred under an atmosphere of argon in a schlenk tube before NaH (0.08 g, 3.22 mmol, 3.2 eq.) was carefully added and the mixture stirred for 10 min. (*R*,*R*)-2,2'-Bis(α-methyl-γ-(*tert*-butyldiphenylsilyl)oxypropyl)-(R_p,R_p)-1,1'-bisformylferrocene **2.17-(*RR*,R_pR_p)** (0.87 g, 1.01 mmol, 1.0 eq.) was dissolved in EtOH (20 ml) and added slowly to the reaction mixture. The resulting solution was stirred at rt for 1.5 hrs. The reaction was quenched by the dropwise addition of H_2O, extracted with DCM and dried over $MgSO_4$. The solvent was removed in vacuo and the crude product purified by flash column chromatography on silica gel using an

eluent of 10% EtOAc in hexane. The solvent was removed in vacuo to give the title compound as a red oil (0.99 g, 0.99 mmol, 98%). ^{1}H NMR (300 MHz, $CDCl_3$) δ 7.70 – 7.56 (m, 8H (Ph C***H***)), 7.48 (d, *J* = 15.7 Hz, 2H (Fc C–C***H***=CH), 7.45 – 7.30 (m, 12H (Ph C***H***)), 5.94 (d, *J* = 15.7 Hz, 2H (Fc C–CH=C***H***), 4.33 (dd, *J* = 2.6, 1.3 Hz, 2H (Fc C***H***)), 4.27 (dd, *J* = 2.6, 2.6 Hz, 2H (Fc C***H***)), 4.25 – 4.16 (m, 4H ($CH_3C\boldsymbol{H}_2$), 4.14 (dd, *J* = 2.6, 1.3 Hz, 2H (Fc C***H***)), 3.54 (m, 4H (m, 4H ($C\boldsymbol{H}_2$OSi)), 2.87 – 2.72 (m, 2H ($C\boldsymbol{H}CH_3$)), 1.70 – 1.56 (m, 2H ($C\boldsymbol{H}_2$CH), 1.53 – 1.37 (m, 2H ($C\boldsymbol{H}_2$CH), 1.29 (t, *J* = 7.1 Hz, 6H ($C\boldsymbol{H}_3CH_2$)), 1.28 (d, *J* = 6.8 Hz, 6H ($C\boldsymbol{H}_3$CH)), 1.04 (s, 18H (tBu C***H***$_3$)). ^{13}C NMR (101 MHz, $CDCl_3$) δ 166.8 (***C***OO), 142.3 (Fc C–***C***H=CH), 135.7 (Ph ***C***H), 135.6 (Ph ***C***H), 134.0 (Ph ***C***–Si), 134.0 (Ph ***C***–Si), 129.6 (Ph ***C***H), 129.6 (Ph ***C***H), 127.7 (Ph ***C***H), 127.7 (Ph ***C***H), 116.4 (Fc C–CH=***C***H), 97.8 (Fc ***C***–$CHCH_3$), 78.4 (Fc ***C***–CH=CH), 71.1 (Fc ***C***H), 69.2 (Fc ***C***H), 68.7 (Fc ***C***H), 61.8 (***C***H_2OSi), 60.2 (***C***H_2CH_3), 42.7 (***C***H_2CH), 27.7 (***C***HCH_3), 27.0 (tBu ***C***H_3), 19.4 (***C***H_3CH), 19.3 (tBu ***C***), 14.5 (***C***H_3CH_2). IR ν_{max}/cm^{-1} = 3071 (Fc CH), 2959 (CH), 2931 (CH), 2857 (CH), 1704 (C=O), 1627 (C=C). m/z Calcd for $C_{60}H_{74}FeO_6Si_2Na$ $[M + Na]^+$: 1025.4, found 1025.2.

5.1.1.17 (*R*,*R*)-1,1'-Bis(α-methyl-γ-(*tert*-butyldiphenylsilyl)oxypropyl)-(S_p,S_p)-2,2'-bis(ethylpropanoate)ferrocene 2.19-(*RR*,S_pS_p)

Novel compound

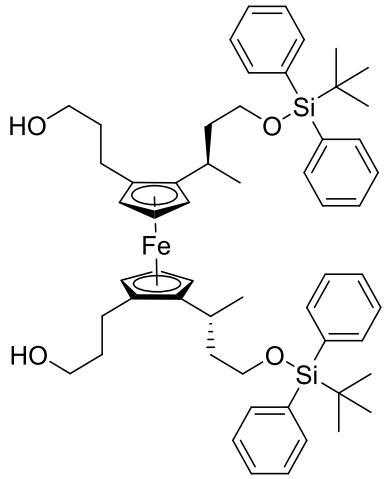


(*R*,*R*)-2,2'-Bis(α-methyl-γ-(*tert*-butyldiphenylsilyl)oxypropyl)-(R_p,R_p)-1,1'-bis(α-ene-ethylpropanoate)ferrocene **2.18-(*RR*,R_pR_p)** (0.99 g, 0.99 mmol, 1.0 eq) was dissolved in EtOAc (10 ml) and $Pd(OH)_2/C$ (0.70 g, 0.99 mmol, 1.0 eq) was added. The mixture was stirred for 16 hrs under an atmosphere of H_2. The reaction mixture was filtered through celite and the solvent removed in vacuo. The crude product was then purified by flash column chromatography using an eluent of 5% EtOAc in hexane. The solvent was removed in vacuo to give the product as an orange oil (0.79 g, 0.79 mmol, 80%). ^{1}H NMR (300 MHz, $CDCl_3$) δ 7.81 – 7.58 (ddd, *J* = 6.4, 3.5, 1.8 Hz, 8H (Ph C***H***)), 7.48 – 7.35 (m, 12H (Ph C***H***)), 4.15 (q, *J* = 7.2 Hz, 4H ($C\boldsymbol{H}_2CH_3$)), 3.90 (dd, *J* = 2.4, 1.5 Hz, 2H (Fc C***H***)), 3.85 (dd, *J* = 2.4, 1.5 Hz, 2H (Fc C***H***)), 3.81 (dd, *J* = 2.4, 2.4 Hz, 2H (Fc C***H***)), 3.65 (dd, *J* = 7.6, 5.3 Hz, 4H ($C\boldsymbol{H}_2$OSi)), 2.82 – 2.43 (m, 10H ($C\boldsymbol{H}_2$COO, Fc C–$C\boldsymbol{H}_2$, $C\boldsymbol{H}CH_3$)), 1.72 (dtd, *J* = 13.6, 7.6, 3.7 Hz, 2H ($C\boldsymbol{H}_2$CH)), 1.42 (m, 2H ($C\boldsymbol{H}_2$CH)), 1.26 (t, *J* = 7.2 Hz, ($C\boldsymbol{H}_3CH_2$)), 1.25 (d, *J* = 6.8 Hz, 6H ($C\boldsymbol{H}_3$CH)), 1.07 (s, 18H (tBu $C\boldsymbol{H}_3$)). ^{13}C NMR (101 MHz, $CDCl_3$) δ 173.2 (***C***OO), 135.7 (Ph ***C***H), 135.7 (Ph ***C***H), 134.1 (Ph ***C***–Si), 134.0 (Ph ***C***–Si), 129.7 (Ph ***C***H), 129.6 (Ph ***C***H), 127.7 (Ph ***C***H), 127.7 (Ph ***C***H), 94.2 (Fc ***C***–CH), 85.0 (Fc ***C***–CH_2), 69.7 (Fc

CH), 67.2 (Fc ***C***H), 66.1 (Fc ***C***H), 62.0 (***C***H_2OSi), 60.5 (***C***H_2CH_3), 42.5 (***C***H_2CH), 35.6 (***C***H_2COO), 27.5 (***C***HCH_3), 27.0 (tBu ***C***H_3), 23.0 (Fc C–***C***H_2), 19.7 (***C***H_3CH), 19.3 (tBu ***C***), 14.4 (***C***H_3CH_2). IR ν_{max}/cm^{-1} = 3072 (Fc CH), 2958 (CH), 2931 (CH), 2857 (CH), 1733 (C=O). HRMS (ESI-TOF) m/z: $[M + H]^+$ Calcd for $C_{60}H_{79}FeO_6Si_2$ 1007.4765; Found 1007.4625.

5.1.1.18 (*R,R*)-1,1'-Bis(α-methyl-γ-(*tert*-butyldiphenylsilyl)oxypropyl)-(S_p,S_p)-2,2'-bis(γ-hydroxypropyl)ferrocene 2.20-(*RR*,S_pS_p)

Novel compound

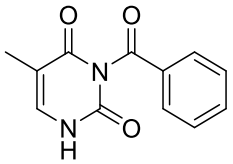


(*R,R*)-1,1'-Bis(α-methyl-γ-(*tert*-butyldiphenylsilyl)oxypropyl)-(S_p,S_p)-2,2'-bis(ethylpropanoate)ferrocene **2.19-(*RR*,S_pS_p)** (0.79 g, 0.79 mmol, 1.0 eq) was dissolved in dry Et_2O (20 ml) under an atmosphere of argon and cooled to 0 ºC in an ice bath. Diisobutylaluminium hydride (1 M in THF) (4.74 ml, 4.74 mmol, 6.0 eq) was added dropwise and the resulting solution stirred for 15 min. The reaction was quenched with sat. Na^+/K^+ tartrate, extracted with DCM and dried over $MgSO_4$. The solvent was removed in vacuo and the crude product purified by flash column chromatography on silica gel using an eluent of 25% EtOAc in hexane. The solvent was removed in vacuo to give the title compound as a yellow oil (0.56 g, 0.61 mmol, 77%). ^{1}H NMR (300 MHz, $CDCl_3$) δ 7.71

(ddd, *J* = 7.4, 4.3, 1.7 Hz, 8H (Ph C***H***)), 7.50 – 7.37 (m, 12H (Ph C***H***)), 3.94 (dd, *J* = 2.1, 1.6 Hz, 2H (Fc C***H***)), 3.88 – 3.83 (m, 4H (Fc C***H***)), 3.76 – 3.60 (m, 8H (C***H***$_2$OH, C***H***$_2$OSi)), 2.78 (dqd, *J* = 10.1, 6.8, 3.5 Hz, 2H (C***H***CH$_3$)), 2.57 – 2.45 (m, 2H (Fc C–C***H***$_2$)), 2.35 (dt, *J* = 21.3, 7.4 Hz, 2H (Fc C–C***H***$_2$)) 2.27 (s, 2H (O***H***)), 1.91 – 1.70 (m, 6H (Fc C–CH$_2$C***H***$_2$, C***H***$_2$CH)), 1.51 – 1.33 (m, 2H C***H***$_2$CH), 1.27 (d, *J* = 6.8 Hz, 6H (C***H***$_3$CH)), 1.11 (s, 18H (tBu C***H***$_3$)). ^{13}C NMR (101 MHz, $CDCl_3$) δ 135.7 (Ph ***C***H), 135.6 (Ph ***C***H), 134.1 (Ph ***C***–Si), 134.1 (Ph ***C***–Si), 129.7 (Ph ***C***H), 129.7 (Ph ***C***H), 127.7 (Ph ***C***H), 127.7 (Ph ***C***H), 93.8 (Fc ***C***–CH), 86.1 (Fc ***C***–CH$_2$), 70.2 (Fc ***C***H), 66.9 (Fc ***C***H), 65.4 (Fc ***C***H), 62.9 (***C***H$_2$OH), 62.2 (***C***H$_2$OSi), 42.5 (***C***H$_2$CH), 33.6 (Fc C–CH$_2$***C***H$_2$), 27.5 (***C***HCH$_3$), 27.0 (tBu ***C***H$_3$), 23.7 (Fc C–***C***H$_2$), 19.5 (***C***H$_3$CH), 19.3 (tBu ***C***). IR ν_{max}/cm^{-1} = 3326 (OH), 3071 (Fc CH), 2930 (CH), 2857 (CH). m/z: Calcd for $C_{56}H_{74}FeO_4Si_2$ $[M]^+$: 922.5, found 922.2.

5.1.1.19 *N*3-Benzoylthymine 2.21

Known compound. Characterisation matches literature values[6]

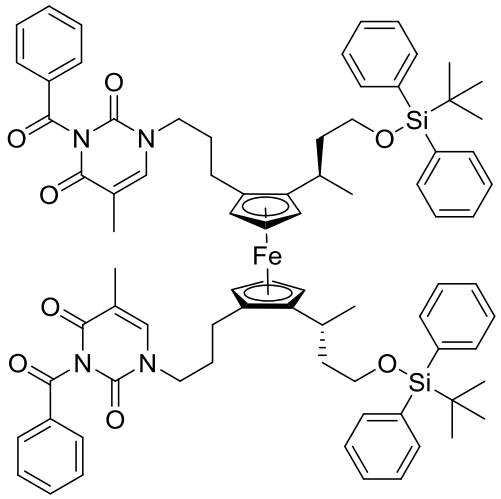


Thymine **2.23** (5.04 g, 40.0 mmol, 1.0 eq.) was added to a solution of 5 MeCN : 2 Py (56 ml) to form a white slurry. Benzoyl chloride (10.21 ml, 88.0 mmol, 2.2 eq.) was added and the resulting mixture stirred at rt for 48 hrs to produce a light orange solution. The solvent was removed in vacuo to reveal an off-white solid which was redissolved in a solution of 1 dioxane : 1 H_2O (120 ml). K_2CO_3 (8.33 g, 60.0 mmol, 3.0 eq.) was carefully added in small portions, producing a milky solution which was stirred for 16 hr. The solution was adjusted to pH ≈ 2 by the dropwise addition of HCl (1 M aq.) and the resulting white precipitate collected by vacuum filtration. Recrystallisation from minimal hot ethanol followed by

vacuum filtration and high vacuum drying gave the title compound as white crystals (6.14 g, 26.7 mmol, 68%). ^{1}H NMR (300 MHz, DMSO) δ 11.40 (s, 1H (N***H***)), 8.00 – 7.89 (m, 2H (Ph C***H***)), 7.84 – 7.73 (m, 1H (Ph C***H***)), 7.66 – 7.56 (m, 2H (Ph C***H***)), 7.55 (q, *J* = 1.1 Hz, 1H (C***H***)), 1.81 (d, *J* = 1.1 Hz, 3H (C$\boldsymbol{H}_3$)).

5.1.1.20 (*R*,*R*)-1,1'-Bis(α-methyl-γ-(*tert*-butyldiphenylsilyl)oxypropyl)-(S_p,S_p)-2,2'-bis(γ-(*N*3-benzoylthymine)propyl)ferrocene 2.22-(*RR*,S_pS_p)

Novel Compound

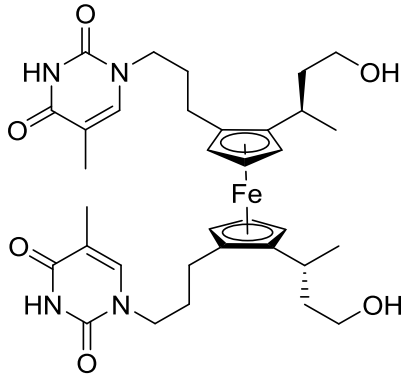


PPh_3 (0.48 g, 1.83 mmol, 3.0 eq) and *N*3-benzoylthymine **2.21** (0.37 g, 1.59 mmol, 2.6 eq) were dissolved in dry THF (10 ml) and stirred under an atmosphere of argon in a schlenk tube wrapped in foil. (*R*,*R*)-2,2'-Bis(α-methyl-γ-(*tert*-butyldiphenylsilyl)oxypropyl)-(S_p,S_p)-1,1'-bis(γ-hydroxypropyl)ferrocene **2.20-(*RR*,S_pS_p)** (0.56 g, 0.61 mmol, 1.0 eq.) dissolved in dry THF (10 ml) was added, followed by diethyl azodicarboxylate (0.36 ml, 1.83 mmol, 3.0 eq.) and the reaction mixture stirred at 65 ºC for 1.5 hrs. The solvent was removed in vacuo and the crude product purified by flash column chromatography on silica gel using an eluent of 40% EtOAc in hexane to give the title compound as a yellow oil (0.67 g, 0.50 mmol, 81%). ^{1}H NMR (300 MHz, $CDCl_3$) δ 7.91 (dd, *J* = 8.6, 1.1 Hz, 4H (Bz Ph C***H***)), 7.78 – 7.55 (m, 10H (TBDPS Ph C***H***, Bz Ph C***H***)), 7.55 – 7.29 (m, 16H (TBDPS Ph C***H***, Bz Ph

C***H***))), 6.88 (d, *J* = 1.1 Hz, 2H (C***H***=C)), 3.90 (s, 2H (Fc C***H***)), 3.79 (s, 4H (Fc C***H***)), 3.73 – 3.49 (m, 8H (C***H***$_2$OSi, (C***H***$_2$N)), 2.80 – 2.57 (m, 2H (C***H***CH$_3$)), 2.33 (m, 4H (C***H***$_2$CH$_2$N)), 2.00 – 1.84 (m, 4H (Fc C–C***H***$_2$)), 1.82 (d, *J* = 1.1 Hz, 6H (C***H***$_3$C=CH)), 1.77 – 1.55 (m, 2H (m, 2H (C***H***$_2$CH)), 1.49 – 1.30 (m, 2H (C***H***$_2$CH)), 1.25 (m, 6H, (C***H***$_3$CH)), 1.06 (s, 18H (tBu CH$_3$). ^{13}C NMR (101 MHz, $CDCl_3$) δ 169.4 (Bz C=O), 163.4 (N–***C***O–C), 149.9 (N–***C***O–N), 140.4 (***C***H=C), 135.6 (TBDPS Ph ***C***H), 135.6 (TBDPS Ph ***C***H), 135.1 (Bz Ph ***C***H), 134.2 (TBDPS Ph ***C***–Si), 134.0 (TBDPS Ph ***C***–Si), 131.8 (Bz Ph ***C***–CO), 130.5 (Bz Ph ***C***H), 129.8 (TBDPS Ph ***C***H), 129.8 (TBDPS Ph ***C***H), 129.3 (Bz Ph ***C***H), 127.8 (TBDPS Ph ***C***H), 127.8 (TBDPS Ph ***C***H), 110.7 (***C***=CH), 93.9 (Fc ***C***–CH), 84.9 (Fc ***C***–CH$_2$), 70.2 (Fc ***C***H), 67.5 (Fc ***C***H), 65.9 (Fc ***C***H), 62.0 (***C***H$_2$OSi), 49.2 (***C***H$_2$N), 42.6 (***C***H$_2$CH), 29.8 (Fc C–CH$_2$***C***H$_2$), 27.5 (***C***HCH$_3$), 27.1 (tBu ***C***H$_3$), 24.6 (Fc C–***C***H$_2$), 19.7 (***C***H$_3$CH), 19.4 (tBu ***C***), 12.4 (***C***H$_3$C=CH). IR ν_{max}/cm^{-1} = 3070 (Fc CH), 2931 (CH), 2857 (CH), 1747 (C=O), 1698 (C=O), 1650 (C=O), 1599 (C=C). HRMS (ESI-TOF) m/z: $[M + H]^+$ Calcd for $C_{80}H_{91}FeO_8N_4Si_2$ 1347.5725; Found 1347.5707.

5.1.1.21 (*R*,*R*)-1,1'-Bis(α-methyl-γ-hydroxypropyl)-(S_p,S_p)-2,2'-bis(γ-thymine-propyl)ferrocene 2.1-(*RR*,$S_p$$S_p$)

Novel Compound

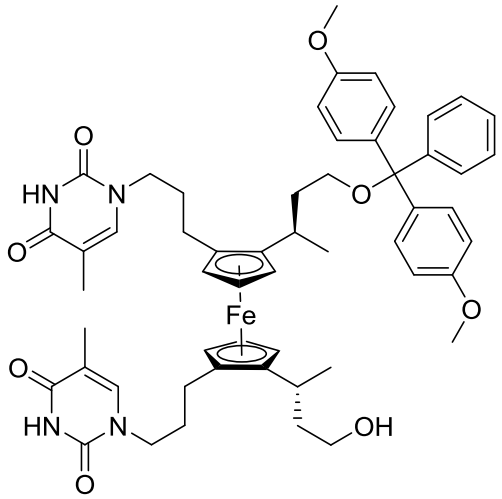


(*R*,*R*)-1,1'-Bis(α-methyl,γ-*tert*-butyldiphenylsilyloxy-propyl)-(S_p,S_p)-2,2'-bis(γ-*N*-3-benzoylthymine-propyl)ferrocene **2.22-(*RR*,$S_p$$S_p$)** (0.67 g, 0.50 mmol, 1.0 eq) was dissolved

in dry THF (3 ml), tetra-*n*-butylammonium fluoride (1 M in THF) (3 ml, 3.00 mmol, 6.0 eq) added and the resulting solution stirred for 2.5 hrs. The solvent was then removed in vacuo, methylamine (3 ml) added and the solution stirred for 15 mins. The solvent was removed in vacuo and the crude product dissolved in a solution of 5% MeOH in DCM which was then washed repeatedly with H_2O. Further purification was achieved by flash column chromatography on silica gel using a graduated eluent system of 0 → 5% MeOH in DCM. The solvent was removed in vacuo to give the title compound as an orange solid (0.27 g, 0.41 mmol, 81%).^{1}H NMR (300 MHz, $CDCl_3$) δ 7.22 (s, 2H (C***H***=C)), 4.16 (s, 4H (Fc C***H***)), 4.01 (s, 2H (Fc C***H***)), 3.87 (s, 4H (C***H***$_2$OH)), 3.75 (s, 4H (C***H***$_2$NH), 3.55 (s, 4H (C***H***$_2$CH$_2$OH), 3.38 (s, 2H, (O***H***)), 2.64 (s, 2H (C***H***CH$_3$)), 2.31 (s, 4H (C***H***$_2$CH$_2$N)), 1.91 (s, 10H (C***H***$_3$C=CH, Fc C–C***H***$_2$)), 1.63 (s, 2H (C***H***$_2$CH)), 1.46 (s, 2H (C***H***$_2$CH)), 1.28 (s, 6H (C***H***$_3$CH)). ^{13}C NMR (101 MHz, $CDCl_3$) δ 165.1 (N***C***OC), 151.3 (N***C***ON), 141.1 (***C***H=C), 110.5 (***C***=CH), 93.9 (Fc ***C***–CH), 85.2 (Fc ***C***–CH$_2$), 70.2 (Fc ***C***H), 67.1 (Fc ***C***H), 65.5 (Fc ***C***H), 59.9 (***C***H$_2$OH), 48.7 (***C***H$_2$N), 42.1 (***C***H$_2$CH), 30.1 (Fc C–CH$_2$***C***H$_2$), 27.2 (***C***HCH$_3$), 24.1 (Fc C–***C***H$_2$), 19.4 (***C***H$_3$CH), 11.8 (***C***H$_3$C=CH)). IR ν_{max}/cm^{-1} = 3452 (NH), 3421 (NH), 2951 (CH), 2912 (CH), 1698 (C=O), 1652 (C=C). HRMS (ESI-TOF) m/z: $[M + H]^+$ Calcd for $C_{34}H_{47}N_4FeO_6$ 663.2845; Found 663.2743.

5.1.1.22 (*R*,*R*)-1-(α-Methyl-γ-(dimethoxytrityl)oxy-propyl)-1'-(α-methyl-γ-hydroxypropyl)-(S_p,S_p)-2,2'-bis(γ-thymine-propyl)ferrocene 2.23-(*RR*,S_pS_p)

Novel Compound

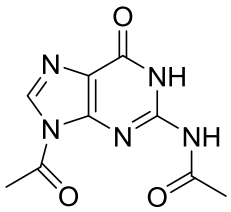


(*R*,*R*)-1,1'-Bis(α-methyl-γ-hydroxypropyl)-(S_p,S_p)-2,2'-bis(γ-thymine-propyl)ferrocene **2.1-(*RR*,S_pS_p)** (0.12 g, 0.18 mmol, 1.0 eq.) and DMAP (0.004 g, 0.036 mmol, 0.2 eq.) were dissolved in dry THF (20 ml) in a schlenk tube under an atmosphere of argon and sonicated for 5 min to aid dissolution. 4,4-Dimethoxytrityl chloride (0.067 g, 0.20 mmol, 1.1 eq.) and *N*,*N*-diisopropylethylamine (0.03 ml, 0.181 mmol, 1.0 eq.) were added and the resulting mixture stirred for 16 hr. The solvent was removed in vacuo before being redissolved in DCM, washed with water (2 x 20 ml) and dried over $MgSO_4$. The solvent was removed in vacuo and the crude product purified by flash column chromatography on neutralised silica gel using a gradient eluent system of 1 → 5% MeOH in DCM. The solvent was removed in vacuo to give the title compound as an orange oil (0.0597 g, 0.0619 mmol, 34%). ^{1}H NMR (300 MHz, $CDCl_3$) δ 9.45 (s, 2H (N***H***)), 7.41 (d, *J* = 7.1 Hz, 2H (Ph C***H***)), 7.36 – 7.13 (m, 8H (Ph C***H***)), 7.06 (d, *J* = 1.3 Hz, 1H (C***H***=C)), 6.82 (dd, *J* = 8.9, 2.2 Hz, 4H (Ph C***H***)), 6.66 (d, *J* = 1.2 Hz, 1H (C***H***=C)), 3.94 (s, 1H Fc C***H***), 3.90 (s, 1H Fc C***H***), 3.86 (s, 1H Fc C***H***), 383 (s, 1H Fc C***H***), 3.82 – 3.77 (m, 2H (Fc C***H***)) 3.79 (2s, 6H, (C***H***$_3$O)), 3.77 – 3.47 (m, 6H (C***H***$_2$OH, C***H***$_2$N)), 3.15 – 2.94 (m, 2H (C***H***$_2$ODMT)), 2.69 (s, 2H (C***H***CH_3, C***H***CH_3)), 2.35

(s, 4H Fc C–***C***H_2, Fc C–***C***H_2)), 2.01 – 1.79 (m, 4H, C***H***$_2$CH_2N, C***H***$_2$CH_2N) 1.79 – 1.52 (m, 2H) 1.89 (d, *J* = 1.2 Hz, 3H (C***H***$_3$C=CH)), 1.69 (d, J = 1.3 Hz, 3H (C***H***$_3$C=CH)), 1.51 – 1.24 (m, 4H, (C***H***$_2$CH, C***H***$_2$CH)), 1.28 (d, *J* = 6.4 Hz, 3H (C***H***$_3$CH)), 1.16 (d, *J* = 5.9 Hz, 3H (C***H***$_3$CH). ^{13}C NMR (101 MHz, $CDCl_3$) δ 164.7 (HN***C***OC), 158.5 (Ph ***C***–O), 151.4 (HN***C***ON), 151.3 (HN***C***ON), 145.5 (Ph ***C***–C), 140.8 (***C***H=C), 140.5 (***C***H=C), 136.7 (Ph ***C***–C), 136.5 (Ph ***C***–C), 130.1 (Ph ***C***H), 130.1 (Ph ***C***H), 128.3 (Ph ***C***H), 127.9 (Ph ***C***H), 126.9 (Ph ***C***H), 113.1 (Ph ***C***H), 113.1 (Ph ***C***H), 110.9 (***C***=CH), 110.8 (***C***=CH), 94.3 (Fc ***C***–CH), 93.9 (Fc ***C***–CH), 86.0 (DMT ^{t}***C***–O), 85.3 (Fc ***C***–CH_2), 85.1 (Fc ***C***–CH_2), 70.4 (Fc ***C***H), 67.2 (Fc ***C***H), 65.5 (Fc ***C***H), 65.4 (Fc ***C***H), 61.5 (***C***H_2ODMT), 60.5 (***C***H_2OH), 55.4 (***C***H_3O), 49.0 (***C***H_2N), 48.9 (***C***H_2N), 42.8 (***C***H_2CH), 40.5 (***C***H_2CH), 30.6 (Fc C–CH_2***C***H_2), 30.1 (Fc C–CH_2***C***H_2), 27.9 (***C***HCH_3), 27.4 (***C***HCH_3), 24.5 (Fc C–***C***H_2), 24.4 (Fc C–***C***H_2), 19.8 (***C***H_3CH), 19.7 (***C***H_3CH), 12.4 (***C***H_3C=CH), 12.3 (***C***H_3C=CH). IR ν_{max}/cm^{-1} = 3420 (NH), 2931 (CH), 1676 (C=O), 1608 (C=C). HRMS (ESI-TOF) m/z: $[M + Na]^+$ Calcd for $C_{55}H_{64}N_4FeO_8Na$ 987.3971; Found 987.3938.

5.1.1.23 2-*N*,9-Diacetylguanine 2.26

Known compound. Characterisation matches literature values[7]

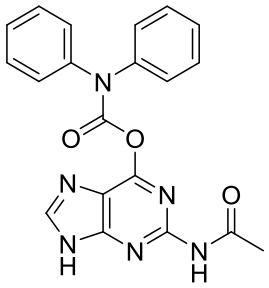


Guanine **2.25** (3.02 g, 20.0 mmol, 1.0 eq.) was suspended in dry DMAc (25 ml), Ac_2O (5 ml) was added and the mixture refluxed at 170 ºC for 7 hrs. The reaction mixture was cooled to rt and vacuum filtered to produce a white solid. The particles were crushed to a powder with a glass rod and washed repeatedly with EtOH then the solvent was removed in vacuo to give the title compound as an off-white solid (2.86 g, 12.2 mmol, 61%). ^{1}H NMR (300 MHz,

DMSO) δ 12.01 (s, 2H (N***H***)), 8.46 (s, 1H (NC***H***=N)), 2.81 (s, 3H (C$\boldsymbol{H}_3$)), 2.21 (s, 3H (C$\boldsymbol{H}_3$)).

5.1.1.24 2-*N*-Acetyl-6-*O*-diphenylcarbamoylguanine 2.24

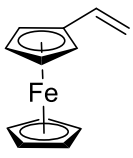
Known compound. Characterisation matches literature values[7]



2-*N*,9-Diacetylguanine **2.26** (2.86 g, 12.20 mmol, 1.0 eq.) was suspended in dry Py (100 ml) under an atmosphere of argon and DIPEA (4.24 ml, 24.3 mmol, 2.0 eq.) added with stirring. Ph_2NCOCl (3.10 g, 13.4 mmol, 1.1 eq.) was added and the mixture stirred for 16 hr. H_2O (10 ml) was added and stirring continued for 10 min. The solvent was removed before toluene (10 ml) was added and again removed in vacuo. The solid particles were crushed with a glass rod then heated in a solution of 1 EtOH : 1 H_2O at 70 ºC for 1.5 hrs. The solution was filtered and the resulting solid washed with EtOH then dried in vacuo to give the title compound as a blue-grey solid (3.83 g, 9.85 mmol, 81%). ^{1}H NMR (300 MHz, DMSO) δ 13.58 (s, 1H (N***H***)), 10.64 (s, 1H (N***H***), 8.45 (s, 1H (NC***H***=N)), 7.56 – 7.41 (m, 8H (Ph C***H***)), 7.32 (t, *J* = 6.9 Hz, 2H (Ph C***H***)), 2.15 (s, 3H (C$\boldsymbol{H}_3$)).

5.1.1.25 Vinylferrocene 2.28

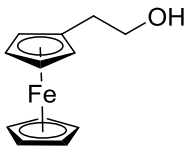
Known compound. Characterisation matches literature values[8]



Ph_3PMeBr (0.714 g, 2.0 mmol, 2.0 eq.), 18-crown-6 (0.002 g, 0.005 mmol, 0.005 eq.) and KO^tBu (0.224 g, 2.0 mmol, 2.0 eq.) were dissolved in dry THF (5 ml) under an atmosphere of argon and stirred for 1.5 hrs to produce a bright yellow solution. Formylferrocene **2.27** (0.214 g, 1.0 mmol, 1.0 eq.) was dissolved in dry THF (5 ml), added dropwise and the resulting orange solution stirred for 16 hr. The reaction was quenched with H_2O and stirring continued for 10 mins before being extracted with DCM and dried over $MgSO_4$. The solvent was removed in vacuo and the crude product purified by flash column chromatography on silica gel using a pure hexane eluent. The solvent was removed in vacuo to give the title product as an orange solid (0.211 g, 0.996 mmol, 100%). ^{1}H NMR (300 MHz, $CDCl_3$) δ 6.48 (dd, *J* = 17.5, 10.7 Hz, 1H (C***H***=CH_2), 5.37 (dd, *J* = 17.5, 1.6 Hz, 1H (CH=C***H***$_2$)), 5.06 (dd, *J* = 10.7, 1.6 Hz, 1H (CH=C***H***$_2$)), 4.38 (t, *J* = 1.8 Hz, 2H (Fc C***H***)), 4.24 (t, *J* = 1.8 Hz, 2H (Fc C***H***)), 4.14 (s, 5H (Cp C***H***)). ^{13}C NMR (101 MHz, $CDCl_3$) δ 134.8 (***C***H=CH_2), 111.2 (***C***H_2=CH), 83.7 (Fc ***C***–CH), 69.3 (Cp ***C***H), 68.8 (Fc ***C***H), 66.8 (Fc ***C***H). HRMS (ESI-TOF) m/z: $[M]^+$ Calcd for $C_{12}H_{12}Fe$ 212.0288; Found 212.0279.

5.1.1.26 Ferrocenyl ethanol 2.29

Known compound. Characterisation matches literature values[9]

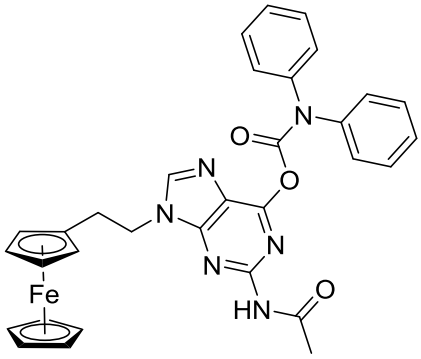


Vinylferrocene **2.28** (0.211 g, 0.996 mmol, 1.0 eq.) was dissolved in dry THF (5 ml) and cooled to 0 ºC with stirring in a schlenk tube under an atmosphere of argon. BH_3•THF (1M in THF) (1.49 ml, 1.49 mmol, 1.5 eq.) was added dropwise and stirring continued at 0 ºC for 1 hr. The reaction mixture was then allowed to warm to rt and stirring continued for a further 1.5 hrs. EtOH (1.49 ml) was carefully added and stirring continued for 5 mins, followed by the dropwise addition of NaOH (3M in H_2O) (1.49 ml) and a further 10 min of stirring. H_2O_2

(30% in H_2O) (3 ml) was then added slowly and stirring continued for 30 min. The reaction was extracted with Et_2O, washed with water (2 x 100 ml) and dried over $MgSO_4$. The crude product was then purified by flash column chromatography on silica gel using an eluent of 1 EtOAc : 1 hexane to give the title compound as an orange solid (0.194 g, 0.842 mmol, 85%). ^{1}H NMR (300 MHz, $CDCl_3$) δ 4.12 (s, 5H (Cp ***C***H)), 4.11 (t, *J* = 1.8 Hz, 2H (Fc ***C***H)), 4.09 (t, *J* = 1.7 Hz, 2H (Fc ***C***H)), 3.72 (t, *J* = 6.5 Hz, 2H (C***H***$_2$OH)), 2.59 (t, *J* = 6.5 Hz, 2H (Fc C–***C***H_2)), 2.05 (s, *J* = 25.6 Hz, 1H (O***H***)). ^{13}C NMR (101 MHz, $CDCl_3$) δ 84.9 (Fc ***C***–CH_2), 68.7 (Cp ***C***H), 68.5 (Fc ***C***H), 67.7 (Fc ***C***H), 63.5 (***C***H_2OH), 32.9 (Fc C–***C***H_2). m/z Calcd for $C_{12}H_{14}FeO$ $[M]^+$: 230.04, found 230.0.

5.1.1.27 β-(2-*N*-acetyl-6-*O*-diphenylcarbamoylguanine)ethyl)ferrocene 2.30

Novel Compound

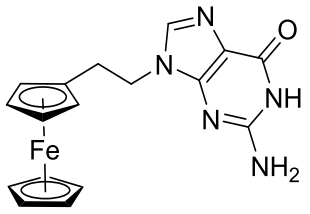


Ferrocenyl ethanol **2.29** (0.194 g, 0.842 mmol, 1.0 eq.), PPh_3 (0.442 g, 1.68 mmol, 2.0 eq.) and 2-*N*-acetyl-6-*O*-diphenylcarbamoylguanine **2.24** (0.491 g, 1.26 mmol, 1.5 eq.) were dissolved in dry THF (15 ml) and stirred in a schlenk tube under an atmosphere of argon. The tube was wrapped in foil and heated to 65 ºC before diethyl azodicarboxylate (0.33 ml, 1.68 mmol, 2.0 eq.) was added dropwise and stirring continued for 1.5 hr. The reaction was quenched with brine, extracted with Et_2O and dried over $MgSO_4$. The crude product was purified by repeated flash column chromatography on neutralised silica gel using an eluent of pure Et_2O. The product was a yellow solid but contained residual Ph_3PO as revealed by NMR

(0.349 g, 0.598 mmol, 71%). ^{1}H NMR (400 MHz, $CDCl_3$) δ 8.39 (s, 1H (N***H***)), 7.39 (m, 4H (Ph C***H***)), 7.35 – 7.29 (m, 4H (Ph C***H***)), 7.21 (t, *J* = 7.0 Hz, 2H (Ph C***H***)), 4.20 (t, *J* = 7.0 Hz, 2H (C***H***$_2$N)), 4.08 (s, 5H (Cp C***H***)), 4.05 (t, *J* = 1.8 Hz, 2H (Fc C***H***)), 3.89 (t, *J* = 1.8 Hz, 2H (Fc C***H***)), 2.82 (t, *J* = 7.0 Hz, 2H (Fc C–C***H***$_2$), 2.53 (s, 3H (C***H***$_3$CO)). ^{13}C NMR (101 MHz, $CDCl_3$) δ 170.9 (***C***OCH$_3$), 156.0 (***C***OO), 155.0 (N=***C***N$_2$), 152.1 (N$_2$***C***=CN), 150.5 (N=***C***O), 144.2 (N***C***H=N), 141.8 (Ph ***C***–N), 129.2 (Ph ***C***H), 128.6 (Ph ***C***H), 128.4 (Ph ***C***H), 126.9 (Ph ***C***H), 120.7 (N***C***=CN$_2$), 83.5 (Fc ***C***–CH$_2$), 68.7 (Cp ***C***H), 68.3 (Fc ***C***H), 68.1 (Fc ***C***H), 45.6 (***C***H$_2$N), 30.3 (Fc C–***C***H$_2$), 25.2 (C***H***$_3$CO). IR ν_{max}/cm^{-1} = 3057 (NH), 2927 (CH), 1738 (C=O), 1620 (C=C). HRMS (ESI-TOF) m/z: $[M + H]^+$ Calcd for $C_{32}H_{29}N_6FeO_3$ 601.1651; Found 601.1642.

5.1.1.28 β-Guaninylethylferrocene 2.31

Novel Compound

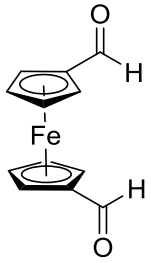


β-(2-*N*-Acetyl-6-*O*-diphenylcarbamoylguanine)ethyl)ferrocene **2.30** (0.349 g, 0.598 mmol) was dissolved in NH_3 (7N in MeOH) (10 ml) and stirred in a stoppered flask for 16 hrs at rt. Yellow crystals were precipitated by the addition of H_2O (5 ml), collected by vacuum filtration and washed with more H_2O (5ml). Drying in vacuo produced the title compound as yellow crystals (0.179 g, 0.491 mmol, 82%). Single crystals suitable for X-ray analysis were grown by the slow evaporation of a concentrated solution in DMSO. ^{1}H NMR (300 MHz, DMSO) δ 10.55 (s, 1H (N***H***)), 7.59 (s, 1H (NC***H***=N)), 6.43 (s, 2H (N***H***$_2$), 4.14 (s, 5H (Cp C***H***)), 4.11 – 4.01 (m, 6H, (Fc C***H***, C***H***$_2$N)), 2.75 (t, *J* = 7.5 Hz, 2H (C***H***$_2$CH$_2$N). ^{13}C NMR (101 MHz, DMSO) δ 156.8 (N=***C***N$_2$), 153.4 (N$_2$***C***=CN), 151.1 (N=***C***O), 137.4 (N***C***H=N),

116.6 (N***C***=CN_2), 84.4 (Fc ***C***–CH_2), 68.4 (Cp ***C***H), 67.8 (Fc ***C***H), 67.2 (Fc ***C***H), 43.5 (***C***H_2N), 29.4 (Fc C–***C***H_2). IR ν_{max}/cm^{-1} = 3335 (NH), 3169 (NH), 2655 (CH), 1686 (C=O), 1642 (C=C). HRMS (ESI-TOF) m/z: $[M + H]^+$ Calcd for $C_{17}H_{18}N_5FeO$ 364.0861; Found 364.0862.

5.1.1.29 1,1'-Diformylferrocene 2.33

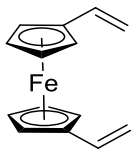
Known compound. Characterisation matches literature values[10]



Ferrocene **2.32** (4.00 g, 21.5 mmol, 1.0 eq) was dissolved in dry Et_2O (40 ml) in a schlenk tube under an atmosphere of argon before TMEDA (7.69 ml, 51.60 mmol, 2.4 eq) was added with stirring. *n*-BuLi (2.5 M in hexane) (22.36 ml, 55.90 mmol, 2.6 eq) was added dropwise and the reaction stirred for 16 hrs. The resulting red solution was cooled to -78 ºC before DMF (5.50 ml, 70.95 mmol, 3.3 eq) was added dropwise and the solution stirred for 10 mins. The solution was then warmed to rt and stirred for a further 2 hrs. The reaction was quenched with brine to produce a wine red solution, extracted with DCM and dried over $MgSO_4$. The solvent was removed in vacuo and the crude product purified by flash chromatography through a short column of neutralised silica gel using a gradient eluent system of 0 → 20% EtOAc in hexane. The solvent was removed in vacuo to give the title compound as a dark red solid (4.36 g, 17.7 mmol, 82%). ^{1}H NMR (300 MHz, $CDCl_3$) δ 9.95 (s, 2H (C***H***O)), 4.89 (dd, *J* = 1.8, 1.9 Hz, 4H (Fc ***C***H)), 4.68 (dd, *J* = 1.8, 1.9 Hz, 4H (Fc ***C***H)).

5.1.1.30 1,1'-Divinylferrocene 2.34

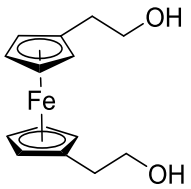
Known compound. Characterisation matches literature values[10]



Ph_3PMeBr (12.6 g, 35.4 mmol, 2.0 eq.), 18-crown-6 (0.032 g, 0.09 mmol, 0.005 eq.) and KO^tBu (3.97 g, 35.4 mmol, 2.0 eq.) were dissolved in dry THF (80 ml) in a schlenk tube under an atmosphere of argon and stirred for 30 min to produce a bright yellow solution. 1,1'-Diformylferrocene **2.33** (4.36 g, 17.7 mmol, 1.0 eq.) was dissolved in dry THF (40 ml), added slowly and the resulting orange solution stirred for 16 hr. The reaction was quenched with H_2O and the resulting dark brown solution stirred for 10 mins before being extracted with Et_2O and dried over $MgSO_4$. The solvent was removed in vacuo and the crude product purified by flash chromatography through a short column of neutralized (TEA) silica gel using a pure hexane eluent. The solvent was removed in vacuo to give the title product as an orange solid (2.13 g, 8.96 mmol, 51%). ^{1}H NMR (300 MHz, $CDCl_3$) δ 6.37 (dd, *J* = 17.5, 10.7 Hz, 2H (C***H***=CH_2), 5.29 (dd, *J* = 17.5, 1.5 Hz, 2H (C***H***$_2$=CH)), 5.06 (dd, *J* = 10.7, 1.5 Hz, 2H (C***H***$_2$=CH)), 4.25 (t, *J* = 1.8 Hz, 4H (Fc C***H***)), 4.16 (t, *J* = 1.8 Hz, 4H (Fc C***H***)).

5.1.1.31 1,1'-Di(β-hydroxyethyl)ferrocene 2.35

Known compound. Characterisation matches literature values[11]

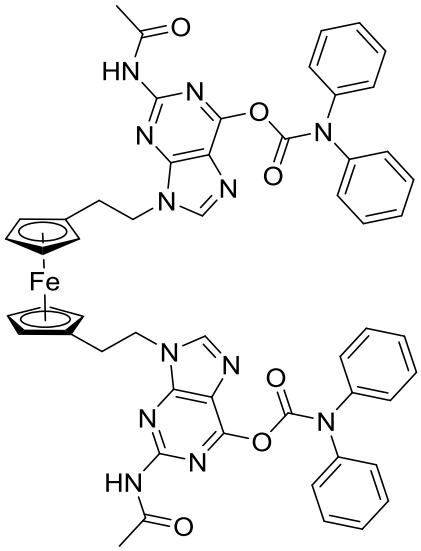


1,1'-Divinylferrocene **2.34** (2.13 g, 8.96 mmol, 1.0 eq.) was dissolved in dry THF (60 ml) in a schlenk tube under an atmosphere of argon. BH_3.THF (1M) (26.9 ml, 26.9 mmol, 3.0 eq.) was added dropwise and stirring continued at for 2 hr. EtOH (30 ml) was carefully added and

stirring continued for 5 min, followed by the slow addition of NaOH (3M in H_2O) (30 ml) and a further 10 min of stirring. H_2O_2 (30% in H_2O) (30 ml) was then added slowly and stirring continued for 2 hr. The reaction was extracted with Et_2O, washed with water (2 x 100 ml) and dried over $MgSO_4$, the crude product was then purified by flash column chromatography on silica gel using an eluent of 1 EtOAc : 1 hexane to give the title compound as an orange solid (2.00 g, 7.29 mmol, 81%). ^{1}H NMR (300 MHz, $CDCl_3$) δ 4.06 (s, 8H (Fc C***H***)), 3.71 (td, *J* = 6.4, 6.0 Hz, 4H (C***H***$_2$OH)), 2.59 (t, *J* = 6.4 Hz, 4H (Fc C–C***H***$_2$)), 1.57 (t, *J* = 6.0 Hz, 2H (O***H***)). ^{13}C NMR (101 MHz, $CDCl_3$) δ 85.1 (Fc ***C***–CH_2), 69.3 (Fc ***C***H), 68.6 (Fc ***C***H), 63.7 (***C***H_2OH), 32.8 (Fc C–***C***H_2). m/z Calcd for $C_{14}H_{18}FeO_2$: 274.1, found 275.1 $[M + H]^+$.

5.1.1.32 1,1'-Di(β-(2-*N*-acetyl-6-*O*-diphenylcarbamoylguanine)ethyl)ferrocene 2.36

Novel compound

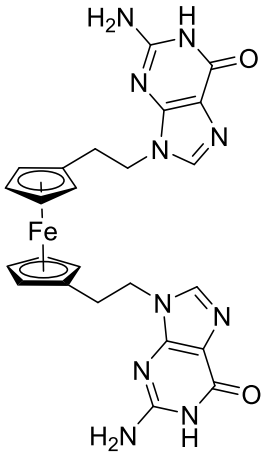


1,1'-Di(β-hydroxyethyl)ferrocene **2.35** (0.137 g, 0.50 mmol, 1.0 eq.), PPh_3 (0.393 g, 1.50 mmol, 2.6 eq.) and 2-*N*-acetyl-6-*O*-diphenylcarbamoylguanine **2.24** (0.504 g, 1.30 mmol, 2.6 eq.) were dissolved in dry THF (20 ml) and stirred in a schlenk tube under an atmosphere of argon. The tube was wrapped in foil and heated to 70 ºC before diethyl azodicarboxylate

(0.30 ml, 1.50 mmol, 3.0 eq.) was added dropwise and stirring continued for 1 hr. The reaction was quenched with water (20 ml) extracted with DCM, washed with water (2 x 20 ml) and dried over $MgSO_4$. The crude mixture was first purified by flash column chromatography on neutralised silica gel using a gradient eluent system of 0 → 5% MeOH in DCM. Further purification was achieved by the repeated precipitation of the product from a concentrated solution in DCM by the slow addition of hexane. This process delivered the title compound as a yellow solid (0.317 g, 0.312 mmol, 63%). m.p. = 136 °C. ^{1}H NMR (300 MHz, $CDCl_3$) δ 8.22 (s, 2H (N***H***)), 7.64 (s, 2H (NC***H***=N)), 7.55 – 7.13 (m, 20H (Ph C***H***)), 4.21 (t, *J* = 6.8 Hz, 4H (C***H***$_2$N)), 4.02 (s, 4H (Fc C***H***)), 3.84 (s, 4H (Fc C***H***)), 2.82 (t, *J* = 6.8 Hz, 4H (Fc C–C***H***2)), 2.48 (s, 6H (C***H***$_3$CO)). ^{13}C NMR (101 MHz, $CDCl_3$) δ 170.7 (***C***OCH_3), 156.1 (***C***OO), 155.1 (N=***C***N_2), 152.0 (N_2***C***=CN), 150.6 (N=***C***O), 144.3 (N***C***H=N), 141.9 (Ph ***C***–N), 129.3 (Ph ***C***H), 127.1 (Ph ***C***–N), 120.9 (N***C***=CN_2), 83.9 (Fc ***C***–CH_2), 69.2 (Fc ***C***H), 69.1 (Fc ***C***H), 45.8 (***C***H_2N), 30.0 (Fc C–***C***H_2), 25.2 (C***H***$_3$CO). IR ν_{max}/cm^{-1} = 3078 (NH), 1735 (C=O), 1619 (C=C). HRMS (ESI-TOF) m/z: $[M + H]^+$ Calcd for $C_{54}H_{47}N_{12}FeO_6$ 1015.3091; Found 1015.3016.

5.1.1.33 1,1'-Di(β-guaninylethyl)ferrocene 2.37

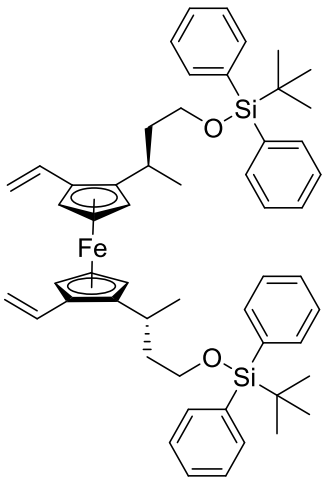
Novel compound



1,1'-Di(β-(2-*N*-acetyl-6-*O*-diphenylcarbamoylguanine)ethyl)ferrocene **2.36** (0.317 g, 0.312 mmol) was dissolved in NH_3 (7N in MeOH) (10 ml) and stirred in a stoppered flask for 16 hrs at rt. The precipitated product was collected by filtration and washed with MeOH. Drying in vacuo produced the title compound as a pale yellow powder (0.083 g, 0.154 mmol, 49%). Decomposed above 240 °C. ^{1}H NMR (300 MHz, DMSO-d_6) δ 8.52 (s, 2H, N***H***), 7.54 (s, 2H (NC***H***=N)), 6.45 (s, 4H (N***H***$_2$)), 4.03 (m, 8H (C***H***$_2$N, Fc C***H***)), 3.97 (t, *J* = 1.9 Hz, 4H (Fc C***H***)), 2.73 (t, *J* = 7.3 Hz, 4H (C***H***$_2$CH$_2$N)). ^{13}C NMR (101 MHz, DMSO) δ 157.2 (***C***O), 153.7 (N$_2$***C***=N), 151.1 (N$_2$***C***=CN), 137.4 (N***C***H=N), 116.5 (N***C***=CN$_2$), 84.5 (Fc ***C***–CH$_2$), 68.6 (Fc ***C***H), 68.2 (Fc ***C***H), 43.7 (***C***H$_2$N), 29.3 (***C***H$_2$CH$_2$N). IR ν_{max}/cm^{-1} = 3322 (NH), 3098 (NH), 2999 (CH), 1663 C=O), 1623 (C=C). HRMS (ESI-TOF) m/z: $[M + H]^+$ Calcd for $C_{24}H_{25}N_{10}FeO_2$ 541.1511; Found 541.1506.

5.1.1.34 (*R*,*R*)-1,1'-Bis(α-methyl-γ-(*tert*-butyldiphenylsilyl)oxypropyl)-(R_p,R_p)-2,2'-bisvinylferrocene 2.39-(*RR*,R_pR_p)

Known compound. Characterisation matches literature values[5]

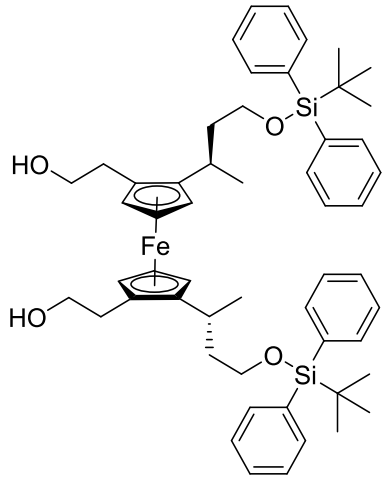


Ph_3PMeBr (3.53 g, 9.89 mmol, 6.0 eq.), 18-crown-6 (0.003 g, 0.008 mmol, 0.005 eq.) and KO^{t}Bu (1.11 g, 9.89 mmol, 6.0 eq.) were dissolved in dry THF (20 ml) in a schlenk tube

under an atmosphere of argon and stirred for 1 hr to produce a bright yellow solution. (*R*,*R*)-2,2'-Bis(α-methyl-γ-(*tert*-butyldiphenylsilyl)oxypropyl)-(R_p,R_p)-1,1'-bisformylferrocene **2.17-(*RR*,R_pR_p)** (1.42 g, 1.65 mmol, 1.0 eq.) was dissolved in dry THF (15 ml), added slowly and the resulting reddish-brown solution stirred for 16 hr. The reaction was quenched with H_2O and the resulting dark brown solution stirred for 10 mins before being extracted with Et_2O and dried over $MgSO_4$. The solvent was removed in vacuo and the crude product purified by flash chromatography through a short column of silica gel using a pure hexane eluent. The solvent was removed in vacuo to give the title product as a red oil (1.24 g, 1.44 mmol, 87%). ^{1}H NMR (300 MHz, $CDCl_3$) δ 7.78 – 7.70 (m, 8H (Ph C***H***)), 7.52 – 7.39 (m, 12H (Ph C***H***)), 6.57 (dd, *J* = 17.5, 10.9 Hz, 2H (C***H***=CH_2)), 5.34 (dd, *J* = 17.5, 1.8 Hz, 2H (C***H***$_2$=CH)), 5.17 (dd, *J* = 10.9, 1.8 Hz, 2H (C***H***$_2$=CH)), 4.27 (dd, *J* = 2.4, 1.5 Hz, 2H (Fc C***H***)), 4.12 – 4.07 (m, 4H (Fc C***H***)), 3.73 – 3.63 (m, 4H (C***H***$_2$OSi)), 2.94 (dtd, *J* = 10.9, 6.8, 4.2 Hz, 2H (C***H***CH_3)), 1.75 (dddd, *J* = 13.8, 8.0, 6.9, 4.2 Hz, 2H (C***H***$_2$CH)), 1.35 – 1.48 (m, 2H (C***H***$_2$CH)), 1.33 (d, *J* = 6.8 Hz, 6H (C***H***$_3$CH)), 1.14 (s, 18H (tBu C***H***$_3$). ^{13}C NMR (101 MHz, $CDCl_3$) δ 135.7 (Ph ***C***H), 135.7 (Ph ***C***H), 134.2 (Ph ***C***–Si), 134.1 (Ph ***C***–Si), 133.0 (***C***H=CH_2), 129.7 (Ph ***C***H), 129.6 (Ph ***C***H), 127.7 (Ph ***C***H), 127.7 (Ph ***C***H), 111.2 (***C***H_2=CH), 94.7 (Fc ***C***–CH=CH_2), 82.4 (Fc ***C***–$CHCH_3$), 68.0 (Fc ***C***H), 67.7 (Fc ***C***H), 66.5 (Fc ***C***H), 61.9 (***C***H_2OSi), 42.8 (***C***H_2CH), 27.0 (tBu ***C***H_3), 26.8 (***C***HCH_3), 19.4 (tBu ***C***), 18.6 (***C***H_3CH). IR ν_{max}/cm^{-1} = 3071 (ar CH), 2929 (CH), 2858 (CH), 1624 (C=C). HRMS (ESI-TOF) m/z: $[M]^+$ Calcd for $C_{54}H_{66}FeO_2Si_2$ 858.3951; Found 858.3973.

5.1.1.35 (*R*,*R*)-1,1'-Bis(α-methyl-γ-(*tert*-butyldiphenylsilyl)oxypropyl)-(R_p,R_p)-2,2'-bis(β-hydroxyethyl)ferrocene 2.40-(*RR*,S_pS_p)

Known compound. Characterisation matches literature values[5]

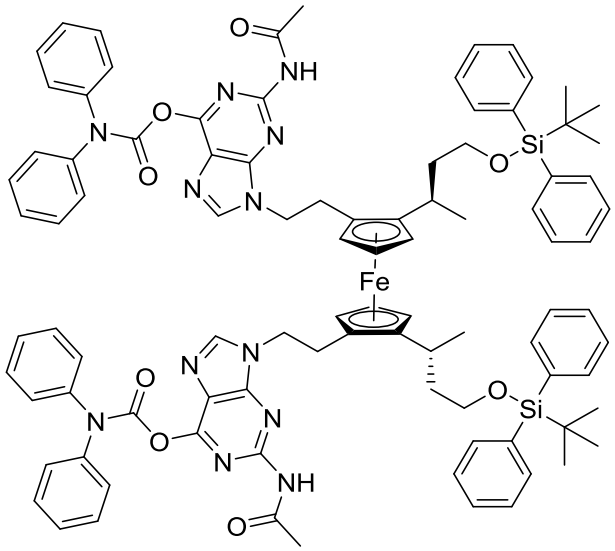


(*R*,*R*)-1,1'-Bis(α-methyl-γ-(*tert*-butyldiphenylsilyl)oxypropyl)-(R_p,R_p)-2,2'-bisvinylferrocene **2.39-(*RR*,R_pR_p)** (1.24 g, 1.44 mmol, 1.0 eq.) was dissolved in dry THF (15 ml) and cooled to 0 ºC in a schlenk tube under an atmosphere of argon. BH_3.THF (1M) (4.31 ml, 4.31 mmol, 3.0 eq.) was added dropwise and stirring continued at 0 ºC for 15 min. The solution was allowed to warm to rt and stirring continued for 2.5 hr. EtOH (5 ml) was carefully added and stirring continued for 5 min, followed by the slow addition of NaOH (3M in H_2O) (5 ml) and a further 10 min of stirring. H_2O_2 (30% in H_2O) (5 ml) was then added slowly and stirring continued for 2.5 hr. The reaction was extracted with DCM, washed with brine (50 ml), then water (2 x 50 ml) and dried over $MgSO_4$. The crude product was purified by flash column chromatography on silica gel using a gradient eluent system of 15 → 30% EtOAc in hexane to give the title compound as an orange oil (0.866 g, 0.967 mmol, 67%). ^{1}H NMR (300 MHz, $CDCl_3$) δ 7.76 – 7.56 (m, 8H (Ph C***H***)), 7.50 – 7.30 (m, 12H (Ph C***H***)), 3.98 (s, 2H (Fc C***H***)), 3.93 (s, 4H (Fc C***H***)), 3.79 – 3.52 (m, 8H (C***H***$_2$OH, C***H***$_2$–OSi)), 2.77 – 2.59 (m, 2H (C***H***CH_3)), 2.51 (t, *J* = 6.6 Hz, 4H (Fc C–C***H***$_2$)), 1.72 (dtd, *J* = 10.8, 7.5, 3.4 Hz, 2H (C***H***$_2$CH)), 1.52 – 1.30 (m, 4H (C***H***$_2$CH, OH), 1.19 (d, *J* = 6.6 Hz, 6H (C***H***$_3$CH)), 1.06 (s,

18H (tBu C***H***$_3$)). ^{13}C NMR (101 MHz, $CDCl_3$) δ 135.7 (Ph ***C***H), 135.7 (Ph ***C***H), 134.1 (Ph ***C***–Si), 134.0 (Ph ***C***–Si), 129.8 (Ph ***C***H), 129.7 (Ph ***C***H), 127.8 (Ph ***C***H), 127.8 (Ph ***C***H), 95.0 (Fc ***C***–CH_2), 82.8 (Fc ***C***–CH), 70.9 (Fc ***C***H), 67.7 (Fc ***C***H), 66.2 (Fc ***C***H), 63.2 (***C***H_2OH), 62.1 (***C***H_2OSi), 42.7 (***C***H_2CH), 30.8 (Fc C–***C***H_2), 27.4 (***C***H), 27.0 (tBu ***C***H_3), 19.6 (***C***H_3CH), 19.4 (tBu ***C***). IR ν_{max}/cm^{-1} = 3309 (OH) 3071 (ar CH), 2929 (CH), 2858 (CH), 1599 (C=C). HRMS (ESI-TOF) m/z: $[M]^+$ Calcd for $C_{54}H_{70}FeO_4Si_2$ 894.4162; Found 894.4155.

5.1.1.36 (*R*,*R*)-1,1'-Bis(α-methyl-γ-(*tert*-butyldiphenylsilyl)oxypropyl)-(R_p,R_p)-2,2'-bis(γ-(2-*N*-acetyl-6-*O*-diphenylcarbamoylguanine)ethyl)ferrocene 2.41-(*RR*,S_pS_p)

Novel Compound

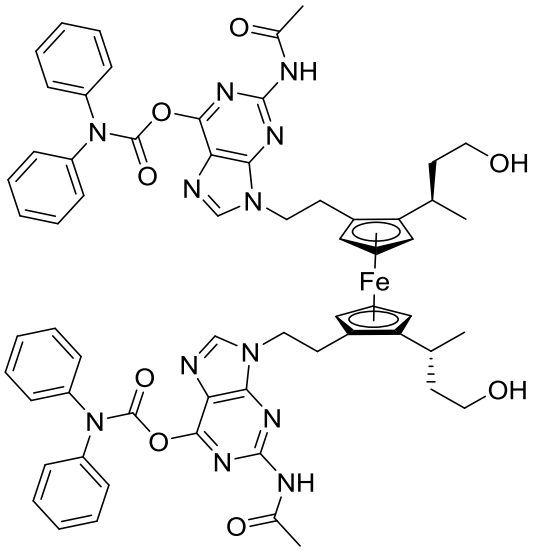


(*R*,*R*)-1,1'-Bis(α-methyl-γ-(*tert*-butyldiphenylsilyl)oxypropyl)-(R_p,R_p)-2,2'-bis(β-hydroxyethyl)ferrocene **2.40-(*RR*,S_pS_p)** (0.400 g, 0.447 mmol, 1.0 eq.), PPh_3 (0.469 g, 1.79 mmol, 4.0 eq.) and 2-*N*-acetyl-6-*O*-diphenylcarbamoylguanine **2.24** (0.521 g, 1.34 mmol, 3.0 eq.) were dissolved in dry THF (40 ml) and stirred in a schlenk tube under an atmosphere of argon. The tube was wrapped in foil and heated to 40 ºC before diethyl azodicarboxylate (0.35 ml, 1.79 mmol, 4.0 eq.) was added dropwise and stirring continued for 1.5 hr. The solvent was removed in vacuo, redissolved in DCM then washed with water (2 x 20 ml) and

dried over $MgSO_4$. The crude mixture was first purified by flash column chromatography on neutralised silica gel using a gradient eluent system of 30 → 0% hexane in EtOAc. The product was then dissolved in minimal, hot DCM and petroleum ether slowly added to precipitate out a white impurity, which was removed by filtration. This process was repeated to deliver the title compound as a yellow oil (0.559 g, 0.342 mmol, 77%). ^{1}H NMR (300 MHz, $CDCl_3$) δ 8.30 (s, 2H (N***H***)), 7.61 (dd, *J* = 1.6, 1.1 Hz, 2H (TBDPS Ph C***H***)), 7.61 – 7.59 (m, 2H (TBDPS Ph C***H***)), 7.59 (dd, *J* = 1.9, 1.1 Hz, 4H (TBDPS Ph C***H***)), 7.57 (s, 2H (NC***H***=N)), 7.50 – 7.45 (m, 4H (Ph C***H***)), 7.46 – 7.42 (m, 4H, (Ph C***H***)), 7.41 – 7.20 (m, 24H, (Ph C***H***)), 4.20 (ddd, *J* = 13.5, 8.7, 5.1 Hz, 2H (C***H***$_2$OSi)), 4.07 (ddd, *J* = 13.5, 7.8 Hz, 2H (C***H***$_2$OSi)), 3.94 (dd, *J* = 2.5, 1.3 Hz, 2H (Fc C***H***)), 3.81 (t, *J* = 2.5 Hz, 2H (Fc C***H***)), 3.64 (dd, *J* = 7.2, 5.6 Hz, 4H (C***H***$_2$N)), 3.59 (s, 2H (Fc C***H***)), 3.07 – 2.86 (m, 2H (C***H***$_2$CH$_2$N)), 2.80 – 2.70 (m, 2H (C***H***$_2$CH$_2$N)), 2.70 – 2.57 (m, 2H (C***H***CH$_3$)), 2.28 (s, 6H (C***H***$_3$CO), 1.69 – 1.54 (m, 2H (C***H***$_2$CH)), 1.51 – 1.35 (m, 2H (C***H***$_2$CH)), 1.22 (d, *J* = 6.8 Hz, 6H (C***H***$_3$CH)), 0.99 (s, 18H (tBu C***H***$_3$)). ^{13}C NMR (101 MHz, $CDCl_3$) δ 156.0 (***C***OO), 155.1 (N=***C***N$_2$), 152.0 (N$_2$***C***=CN), 150.8 (N=***C***O), 144.2 (N***C***H=N), 141.9 (carb Ph ***C***–N), 135.6 (TBDPS Ph ***C***H), 135.5 (TBDPS Ph ***C***H), 133.8 (TBDPS Ph ***C***–Si), 133.8 (TBDPS Ph ***C***–Si), 129.8 (carb Ph ***C***H), 129.3 (TBDPS Ph ***C***H), 129.3 (TBDPS Ph ***C***H), 127.8 (TBDPS Ph ***C***H), 127.8 (carb Ph ***C***H), 120.9 (N***C***=CN$_2$), 94.5 (Fc ***C***–CH), 81.3 (Fc ***C***–CH$_2$), 70.5 (Fc ***C***H), 68.5 (Fc ***C***H), 66.3 (Fc ***C***H), 62.0 (***C***H$_2$OSi), 45.0 (***C***H$_2$N), 43.1 (***C***H$_2$CH), 27.9 (Fc C–***C***H$_2$), 27.3 (***C***HCH$_3$), 27.0 (tBu ***C***H$_3$), 25.1 (***C***H$_3$CO), 19.9 (***C***H$_3$CH), 19.3 (tBu ***C***). IR ν_{max}/cm^{-1} = 3070 (ar CH), 2931 (CH), 2857 (CH), 1736 (C=O), 1619 (C=C). HRMS (ESI-TOF) m/z: $[M + H]^+$ Calcd for $C_{94}H_{99}N_{12}FeO_8Si_2$ 1635.6613; Found 1635.6597.

5.1.1.37 (*R*,*R*)-1,1'-Bis(α-methyl-γ-hydroxypropyl)-(S_p,S_p)-2,2'-bis(γ-(2-*N*-acetyl-6-*O*-diphenylcarbamoylguanine)ethyl)ferrocene 2.38-(*RR*,S_pS_p)

Novel Compound

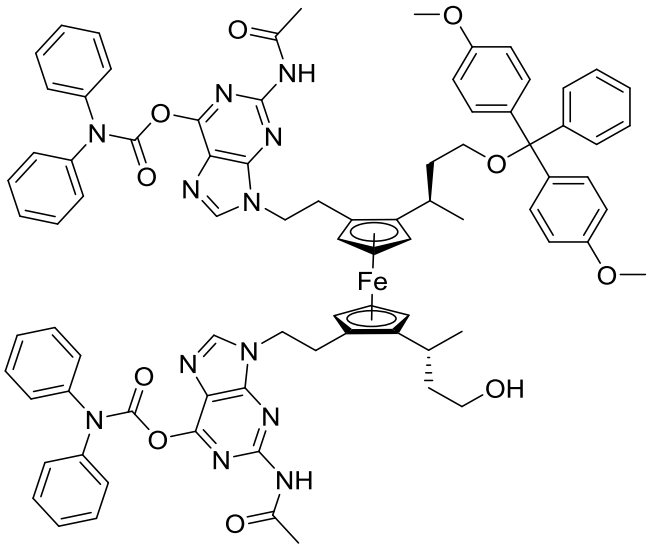


(*R*,*R*)-1,1'-Bis(α-methyl-γ-(*tert*-butyldiphenylsilyl)oxypropyl)-(R_p,R_p)-2,2'-bis(γ-(2-*N*-acetyl-6-*O*-diphenylcarbamoylguanine)ethyl)ferrocene **2.41-(*RR*,S_pS_p)** (0.559 g, 0.342 mmol, 1.0 eq) was dissolved in dry THF (15 ml) before TBAF (1 M in THF) (1.03 ml, 1.03 mmol, 3.0 eq) was added and the resulting mixture stirred for 2.5 hrs. H_2O (20 ml) was added and the crude product extracted with DCM before drying over $MgSO_4$. The solvent was removed in vacuo and the crude product purified by flash column chromatography on neutralised silica gel using a gradient eluent system of 0% MeOH and 5% TEA → 5% MeOH and 5% TEA in EtOAc. The solvent was removed in vacuo to give the title compound as a yellow oil (0.168 g, 0.145 mmol, 42%). ^{1}H NMR (400 MHz, CD_2Cl_2) δ 8.92 (s, 2H (N***H***)), 7.93 (s, 2H (NC***H***=N)), 7.53 – 7.40 (m, 8H (Ph C***H***)), 7.40 – 7.34 (m, 8H (Ph C***H***)), 7.30 – 7.24 (m, 4H (Ph C***H***)), 4.26 (ddd, *J* = 13.7, 10.9, 4.9 Hz, 2H (C***H***$_2$OH)), 4.14 (ddd, *J* = 12.4, 4.3 Hz, 2H (C***H***$_2$OH)), 4.01 (dd, *J* = 2.4, 1.3 Hz, 2H (Fc C***H***)), 3.95 (dd, *J* = 2.4, 2.3 Hz, 2H (Fc C***H***)), 3.81 (dd, *J* = 2.3, 1.3 Hz, 2H (Fc C***H***)), 3.64 – 3.50 (m, 4H C***H***$_2$N)), 3.02 – 2.92 (m, 2H (C***H***$_2$CH$_2$N)), 2.87 – 2.73 (m, 4H ((C***H***$_2$CH$_2$N, C***H***CH$_3$)), 2.25 (s, 6H (C***H***$_3$CO)), 1.72 – 1.54

(m, 2H (C***H***$_2$CH)), 1.48 – 1.36 (m, 2H (C***H***$_2$CH)), 1.33 (d, *J* = 6.8 Hz, 6H (C***H***$_3$CH)). ^{13}C NMR (101 MHz, CD_2Cl_2) δ 170.3 (***C***OCH$_3$), 156.2 (***C***OO), 155.7 (N=***C***N$_2$), 152.5 (N$_2$***C***=CN), 151.2 (N=***C***O), 144.8 (N***C***H=N), 142.4 (Ph ***C***–N), 129.8 (Ph ***C***H), 127.7 (Ph ***C***H), 121.2 (N***C***=CN$_2$), 95.5 (Fc ***C***–CH$_2$), 81.8 (Fc ***C***–CH), 70.9 (Fc ***C***H), 68.0 (Fc ***C***H), 66.2 (Fc ***C***H), 60.6 (***C***H$_2$OH), 45.6 (***C***H$_2$N), 43.9 (***C***H$_2$CH), 28.4 (Fc C–***C***H$_2$), 27.4 (***C***HCH$_3$), 25.4 (***C***H$_3$CO), 20.0 (***C***H$_3$CH). IR ν_{max}/cm^{-1} = 3267 (OH), 3067 (ar CH), 2933 (CH), 1737 (C=O), 1620 (C=C). HRMS (ESI-TOF) m/z: [M]$^+$ Calcd for $C_{62}H_{62}N_{12}FeO_8$ 1158.4163; Found 1158.4174.

5.1.1.38 (*R,R*)-1-(α-Methyl-γ-(dimethoxytrityl)oxy-propyl)-1'-(α-methyl-γ-hydroxypropyl)-(*S$_p$,S$_p$*)-2,2'-bis(γ-(2-*N*-acetyl-6-*O*-diphenylcarbamoylguanine)ethyl)ferrocene 2.42-(***RR,S$_p$S$_p$***)

Novel Compound



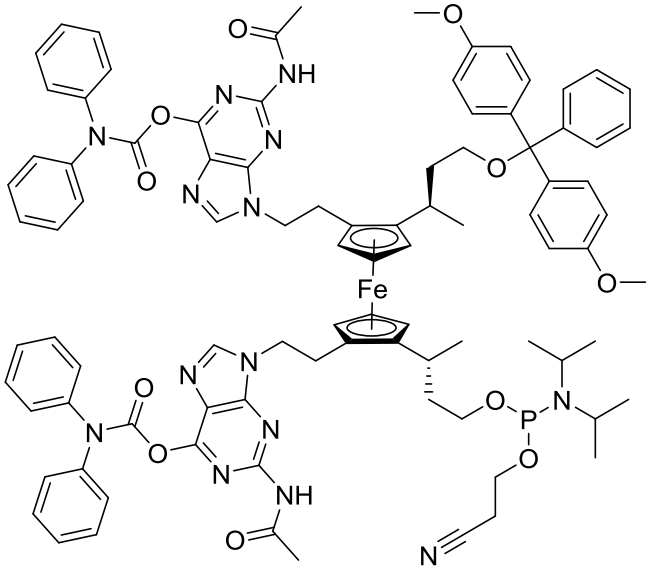
(*R,R*)-1,1'-Bis(α-methyl-γ-hydroxypropyl)-(*S$_p$,S$_p$*)-2,2'-bis(γ-(2-*N*-acetyl-6-*O*-diphenylcarbamoylguanine)ethyl)ferrocene **2.38-(*RR,S$_p$S$_p$*)** (0.168 g, 0.145 mmol, 1.0 eq.) was dissolved in dry THF (10 ml) in a Schlenk tube under an atmosphere of argon before DMTCl (0.049 g, 0.145 mmol, 1.0 eq.), DIPEA (0.028 ml, 0.159 mmol, 1.1 eq.) and DMAP

(0.001 g, 0.007 mmol, 0.05 eq.) was added and the resulting mixture stirred at rt for 3 hrs. The reaction was quenched with brine, extracted with DCM, washed with water (2 x 5 ml) before being dried over $MgSO_4$ and the solvent removed in vacuo. The crude product was purified by flash column chromatography on neutralised silica gel using a gradient eluent system of 0 → 5% MeOH with 5% TEA in EtOAc. The solvent was removed in vacuo to give the title compound as a yellow oil (0.101 g, 0.069 mmol, 48%). 1^1H NMR (400 MHz, $CDCl_3$) δ 8.85 (s, 1H (N***H***)), 8.37 (s, 1H, (N***H***)), 7.94 (s, 1H (NC***H***=N)), 7.64 (s, 1H (NC***H***=N)), 7.49 – 7.39 (m, 8H (Ph C***H***)), 7.39 – 7.29 (m, 12H (Ph C***H***)), 7.29 – 7.09 (m, 9H (Ph C***H***)), 6.80 – 6.71 (m, 4H (DMT Ph C***H***)), 4.35 – 4.08 (m, 4H (C***H***$_2$OH, C***H***$_2$ODMT)), 3.99 (dd, *J* = 2.3, 1.3 Hz, 1H (Fc C***H***)), 3.96 (dd, *J* = 2.3, 1.3 Hz, 1H (Fc C***H***)), 3.91 (dd, *J* = 2.5, 2.4 Hz, 1H (Fc C***H***)), 3.86 (t, *J* = 2.5, 2.4 Hz, 1H (Fc C***H***)), 3.79 (dd, *J* = 2.4, 1.3 Hz, 1H (Fc C***H***)), 3.71 (s, 6H (OC***H***$_3$)), 3.65 – 3.53 (m, 3H (Fc C***H***, C***H***$_2$N)), 3.32 – 316 (m, 2H (C***H***$_2$N)), 3.14 (s, 1H, O***H***), 3.12 – 3.00 (m, 2H (C***H***$_2$CH2OH)), 3.00 – 2.71 (m, 6H, C***H***$_2$CH$_2$N, C***H***$_2$CH$_2$N, C***H***CH$_3$, C***H***CH$_3$)), 2.35 (s, 3H, (C***H***$_3$CO)), 2.33 (s, 3H (C***H***$_3$CO)), 1.70 – 1.46 (m, 4H, (C***H***$_2$CH)) 1.31 (d, *J* = 6.8 Hz, 3H (C***H***$_3$CH)), 1.22 (d, *J* = 6.8 Hz, 3H, (C***H***$_3$CH)). ^{13}C NMR (101 MHz, $CDCl_3$) δ 158.4 (DMT Ph ***C***–OMe), 158.4 (DMT Ph ***C***–OMe), 156.0 (***C***OO), 155.9 (***C***OO), 155.1 (N=***C***N$_2$), 155.1 (N=***C***N$_2$), 152.0 (N$_2$***C***=CN), 151.9 (N$_2$***C***=CN), 150.7 (N=***C***O), 150.7 (N=***C***O), 145.2 (DMT Ph ***C***–C), 144.4 (N***C***H=N), 144.1 (N***C***H=N), 141.8 (carb Ph ***C***–N), 141.8 (carb Ph ***C***–N), 136.5 (DMT Ph ***C***–C), 136.4 (DMT Ph ***C***–C), 130.0 (DMT Ph ***C***H), 130.0 (DMT Ph ***C***H), 129.3 (carb Ph ***C***H), 128.1 (DMT Ph ***C***H), 127.8 (DMT Ph ***C***H), 126.8 (DMT Ph ***C***H), 120.9 (N***C***=CN$_2$), 120.8 (N***C***=CN$_2$), 113.1 (DMT Ph ***C***H), 113.1 (DMT Ph ***C***H), 86.1 (Fc ***C***–CH$_2$), 81.1 (Fc ***C***–CH), 70.5 (Fc C***H***), 68.2 (Fc C***H***), 66.4 (Fc C***H***), 61.5 (***C***H$_2$ODMT), 60.1 (***C***H$_2$OH), 55.3 (***C***H$_3$O), 46.0 (***C***H$_2$N), 44.7 (***C***H$_2$N), 29.8 (***C***H$_2$CH), 29.7 (***C***H$_2$CH$_2$N), 29.4 (***C***H$_2$CH), 28.0 (C***H***CH$_3$), 27.9 (***C***H$_2$CH$_2$N), 27.8 (***C***HCH$_3$), 26.9 (C***H***CH$_3$), 25.1 (***C***H$_3$CO), 25.1 (***C***H$_3$CO), 20.3 (C***H***$_3$CH), 20.0 (C***H***$_3$CH).

IR ν_{max}/cm^{-1} = 3270 (OH), 2931 (CH), 1737 (C=O), 1619 (C=C). HRMS (ESI-TOF) m/z: [M + Na]$^+$ Calcd for $C_{83}H_{80}N_{12}FeO_{10}Na$ 1483.5367; Found 1483.5310.

5.1.1.39 (*R,R*)-1-(α-Methyl-γ-(dimethoxytrityl)oxy-propyl)-1'-(α-methyl-γ-(2-cyanoethyl-*N,N*-diisopropylphosphoramidityl)oxy-propyl)-(S_p,S_p)-2,2'-bis(γ-(2-*N*-acetyl-6-*O*-diphenylcarbamoylguanine)ethyl)ferrocene 2.43-(*RR*,S_pS_p)

Novel Compound



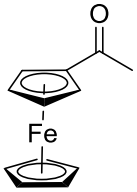
(*R,R*)-1-(α-Methyl-γ-(dimethoxytrityl)oxy-propyl)-1'-(α-methyl-γ-hydroxypropyl)-(S_p,S_p)-2,2'-bis(γ-(2-*N*-acetyl-6-*O*-diphenylcarbamoylguanine)ethyl)ferrocene **2.42-(*RR*,S_pS_p)** (0.101 g, 0.069 mmol, 1.0 eq.) was dissolved in dry DCM (5 ml) in a Schlenk tube under an atmosphere of argon before DIPEA (0.120 ml, 0.344 mmol, 5.0 eq.) was added with stirring. 2-Cyanoethyl-*N,N*-diisopropyl-chlorophosphoramidite (0.018 ml, 0.083 mmol, 1.2 eq.) was added dropwise and the resulting mixture stirred at rt for 0.5 hrs. More DIPEA (0.120 ml, 0.344 mmol, 5.0 eq.) was then added and stirring continued for a further 0.5 hrs. The solvent was removed in vacuo and the crude product purified by flash column chromatography on neutralised silica gel using an eluent of 1% TEA and 20% hexane in EtOAc. The solvent was removed in vacuo to give the title compound as a yellow oil (0.042 g, 0.025 mmol, 37 %). ^{1}H

NMR (300 MHz, CD_2Cl_2) δ 8.40 (s, 1H (N***H***)), 8.29 (s, 1H (N***H***)), 7.89 (2x s, 1H (NC***H***=N)), 7.69 (s, 1H (NC***H***=N)), 7.29 (m, 31H (Ph C***H***)), 6.76 (m, 4H (DMT Ph C***H***)), 4.43 – 4.13 (m, 4H (C***H***$_2$OP, C***H***$_2$ODMT)), 4.08 (2x dd, *J* = 14.3, 7.2, 2H (C***H***$_2$CH$_2$CN)) 4.04 – 4.00 (m, 1H (Fc C***H***)), 4.00 – 3.95 (s, 1H (Fc C***H***)), 3.90 – 3.81 (m, 2H (Fc C***H***)), 3.79 – 3.67 (m, 2H (Fc CH)), 3.72 (s, 6H (C***H***$_3$O)), 3.66 – 3.45 (m, 4H (C***H***$_2$N)), 3.64 – 3.59 (m, 2H (C***H***$_2$CH$_2$N)), 3.01 – 2.76 (m, 4H (2 x *i*Pr CH, (C***H***$_2$CH$_2$N))), 2.76 – 2.62 (m, 2H (C***H***CH$_3$)), 2.58 (2x t, *J* = 6.2 Hz, 2H (C***H***$_2$CN)), 2.38 (2x s, 3H C***H***$_3$CO)), 2.35 (s, 3H C***H***$_3$CO)), 2.11 – 1.92 (m, 2H), 1.85 – 1.59 (m, 4H (C***H***$_2$CH)), 1.25 – 1.18 (m, 6H (C***H***$_3$CH)), 1.17 – 1.06 (m, 12H, (iPr C***H***$_3$)). ^{31}P NMR (300 MHz, CD_2Cl_2) δ 147.3, 147.0 (P(III) two stereoisomers). HRMS (ESI-TOF) m/z: $[M + Na]^+$ Calcd for $C_{92}H_{97}N_{14}FeO_{11}PNa$ 1683.6446; Found 1683.6278.

5.1.2 Experimental Procedures for the Synthesis of Ferrocenyl Nucleoside Analogues

5.1.2.1 Acetylferrocene 3.1

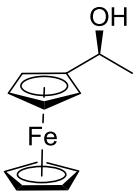
Known compound. Characterisation matches literature values[12]



Acetylferrocene **3.1** was obtained from the undergraduate teaching laboratory and purified by column chromatography using a gradient eluent system of 10 → 20% EtOAc in hexane. The solvent was removed to give the title compound as an orange solid. ^{1}H NMR (300 MHz, $CDCl_3$) δ 4.77 (dd, *J* = 1.8, 1.7 Hz, 2H (Fc C***H***)), 4.50 (dd, *J* = 1.8, 1.7 Hz, 2H (Fc C***H***)), 4.20 (s, 5H (Cp C***H***)), 2.39 (s, 3H (C***H***$_3$)). ^{13}C NMR (400 MHz, $CDCl_3$) δ 202.2 (***C***O), 79.4 (Fc ***C***–CO), 72.5 (Fc ***C***H), 70.0 (Cp ***C***H), 69.7 (Fc ***C***H), 27.6 (***C***H$_3$).

5.1.2.2 (*S*)-α-Hydroxyethylferrocene 3.2-(*S*)

Known compound. Characterisation matches literature values[13]



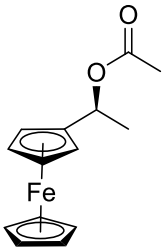
(*R*)-(+)-2-Methyl-CBS-oxazaborolidine (1.90 g, 6.91 mmol, 0.3 eq) was dissolved in dry THF (40 ml) under an atmosphere of argon and cooled to 0 °C using an ice bath with stirring. BH_3•SMe_2 (2M in THF) (12.0 ml) was added and stirring continued for 0.5 hrs at 0 °C. Acetylferrocene **3.1** (5.24 g, 23.0 mmol, 1.0 eq.) was separately dissolved in dry THF (200 ml) under an atmosphere of argon and cooled to 0 °C. The (*R*)-(+)-2-methyl-CBS-oxazaborolidine/BH_3•SMe_2 mixture was then added slowly to the acetylferrocene solution and stirring continued for 2.5 hrs at 0 °C. The reaction was quenched by the slow addition of MeOH (12 ml), before sat. NH_4Cl solution (50 ml) was added, the reaction mixture extracted with Et_2O and dried over $MgSO_4$. The solvent was removed in vacuo and the crude product purified by flash column chromatography on neutralised silica gel using a gradient eluent system of 0 → 30% EtOAc in hexane. The solvent was removed in vacuo to give the title compound as a yellow solid (5.17 g, 21.2 mmol, 92%). ^{1}H NMR (300 MHz, $CDCl_3$) δ 4.55 (qd, *J* = 6.4, 4.7 Hz, 1H (C***H***)), 4.24 – 4.20 (m, 2H (Fc C***H***)), 4.20 (s, 5H, (Cp C**H**)), 4.17 (dd, *J* = 1.9, 1.9 Hz, 2H (Fc C***H***)), 1.85 (d, *J* = 4.7 Hz, 1H (O***H***)), 1.44 (d, *J* = 6.4 Hz, 3H (C$\boldsymbol{H}_3$)). ^{13}C NMR (400 MHz, $CDCl_3$) δ 95.0 (Fc ***C***–CH), 68.4 (Cp ***C***H), 68.1 (Fc ***C***H), 68.0 (Fc ***C***H), 66.3 (Fc ***C***H), 66.2 (Fc ***C***H), 65.7 (***C***H), 23.9 (***C***H_3).

With identical ^{1}H and ^{13}C NMR spectra, the opposite enantiomer (*R*)-α-hydroxyethylferrocene **3.2-(*R*)** (5.24 g, 22.77 mmol 99%) was produced according to the

same method from acetylferrocene **3.1** (5.40 g, 23.00 mmol), using the (*S*)-(–)-2-methyl-CBS-oxazaborolidine catalyst.

5.1.2.3 (*S*)-α-Acetoxyethylferrocene 3.3-(*S*)

Known compound. Chracterisation matches literature values[14]

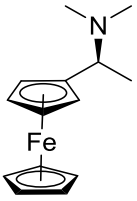


(*S*)-α-Hydroxyethylferrocene **3.2-(*S*)** (5.17 g, 21.2 mmol, 1.0 eq.) was dissolved in dry DCM (60 ml) before Ac_2O (3.15 ml, 33.7 mmol, 1.5 eq.), TEA (4.70 ml, 33.7 mmol, 1.5 eq.) and DMAP (0.065 g, 0.53 mmol, 0.025 eq.) were added. The resulting solution was stirred at rt for 16 hrs. The reaction was then quenched by the careful addition of sat. $NaHCO_3$ solution (50 ml), extracted with DCM, washed with water (2 x100 ml) and dried over $MgSO_4$. The solvent was removed in vacuo and the crude product purified by flash column chromatography on neutralised silica gel using a gradient eluent system of 0 → 10% EtOAc in hexane. The solvent was removed in vacuo to give the title compound as a yellow/orange solid (5.19 g, 20.19 mmol, 95%). ^{1}H NMR (300 MHz, $CDCl_3$) δ 5.83 (q, *J* = 6.5 Hz, 1H (C***H***)), 4.27 (ddd, *J* = 2.5, 1.4, 1.4 Hz, 1H (Fc C***H***)), 4.23 (ddd, *J* = 2.5, 1.4, 1.4 Hz, 1H (Fc C***H***)), 4.19 – 4.15 (m, 2H (Fc C***H***)), 4.15 (s, 5H (Cp C***H***)), 2.03 (s, 3H (C***H***$_3$CO)), 1.56 (d, *J* = 6.5 Hz, 3H (C***H***$_3$CH)). ^{13}C NMR (400 MHz, $CDCl_3$) δ 170.7 (***C***O), 88.1 (Fc ***C***–CH), 69.1 (***C***H), 68.9 (Cp ***C***H), 68.5 (Fc ***C***H), 68.5 (Fc ***C***H), 68.1 (Fc ***C***H), 66.1 (Fc ***C***H), 21.6 (***C***H$_3$CH), 20.1 (***C***H$_3$CO).

With identical ^{1}H and ^{13}C NMR spectra, the opposite enantiomer (*R*)-α-acetoxyethylferrocene **3.3-(*R*)** (4.61 g, 16.93 mmol, 74%) was produced according to the same method from (*R*)-α-hydroxyethylferrocene **3.2-(*R*)** (5.24 g, 22.77 mmol).

5.1.2.4 (*S*)-α-*N*-*N*-Dimethylaminoethylferrocene 3.4-(*S*)

Known compound. Chracterisation matches literature values[14]

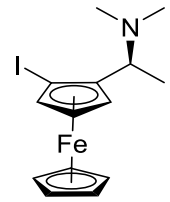


(*S*)-α-Acetoxyethylferrocene **3.3-(*S*)** (5.19 g, 20.2 mmol, 1.0 eq.) was dissolved in a mixture of MeOH (30 ml), DCM (3 ml) and HNMe2 (40% in H_2O) (150 ml) and stirred at rt for 16 hrs. The reaction mixture was extracted with DCM, washed with water (2 x 100 ml) and dried over $MgSO_4$. The solvent was removed in vacuo and the crude product purified by flash column chromatography using an eluent of 3% TEA in hexane. The solvent was removed in vacuo to give the title compound as a dark orange solid (5.10 g, 19.83 mmol, 98%). ^{1}H NMR (300 MHz, $CDCl_3$) δ 4.16 – 4.07 (m, 4H (Fc C***H***)), 4.11 (s, 5H (Cp C***H***)), 3.59 (q, *J* = 6.9 Hz, 1H (C***H***)), 2.08 (s, 6H (C***H***$_3$N), 1.44 (d, *J* = 6.9 Hz, 3H (C***H***$_3$CH)). ^{13}C NMR (101 MHz, $CDCl_3$) δ 87.4 (Fc ***C***–CH), 69.5 (Fc ***C***H), 68.7 (Cp ***C***H), 67.5 (Fc ***C***H), 67.3 (Fc ***C***H), 67.0 (Fc ***C***H), 58.8 (***C***H), 40.8 (***C***H$_3$N), 16.2 (***C***H$_3$CH).

With identical ^{1}H and ^{13}C NMR spectra, the opposite enantiomer (*S*)-α-*N*-*N*-dimethylaminoethylferrocene **3.4-(*R*)** (4.07 g, 15.84 mmol, 94%) was produced according to the same method from (*R*)-α-acetoxyethylferrocene **3.3-(*R*)** (4.61 g, 16.93 mmol).

5.1.2.5 2-(*S*)-α-*N*,*N*-Dimethylaminoethyl-(R_p)-1-iodoferrocene 3.5-(S,R_p)

Known compound. Chracterisation matches literature values[15]



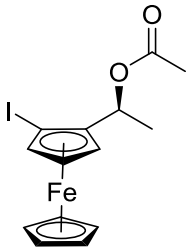
(*S*)-α-*N*-*N*-Dimethylaminoethylferrocene **3.4-(*S*)** (5.10 g, 19.8 mmol, 1.0 eq.) was dissolved in dry Et_2O (50 ml) in a Schlenk tube under an atmosphere of argon and cooled to 0 °C with stirring. *n*-BuLi (2.5 M in hexane) (8.46 ml, 21.1 mmol, 2.0 eq) was added dropwise, the resulting solution was allowed to warm to rt and stirring continued for 16 hrs. Dry THF (10 ml) was added and the reaction mixture cooled to -78 °C using an acetone/dry ice bath. I_2 (15.1 g, 59.5 mmol, 3.0 eq.) was dissolved in dry THF (30 ml) under an atmosphere of argon and transferred slowly to the reaction vessel via needle and syringe. The ice bath was removed and stirring continued for 3 hrs while warming to rt. The solution was cooled to 0 ºC using an ice bath, quenched with sat. $Na_2S_2O_3$ solution then extracted with DCM, washed with water (2 x 100 ml) and dried over $MgSO_4$. The solvent was removed in vacuo and the crude product purified by flash column chromatography on neutralised silica gel using an eluent system of 3% TEA in hexane. The solvent was removed in vacuo to give the title compound an orange oil (6.38 g, 16.66 mmol, 84%). ^{1}H NMR (300 MHz, $CDCl_3$) δ 4.46 – 4.42 (m, 1H (Fc C***H***)), 4.21 (dd, *J* = 2.4, 2.4 Hz, 1H (Fc C***H***)), 4.18 – 4.12 (m, 1H (Fc C***H***)), 4.10 (s, 5H (Cp C***H***)), 3.60 (q, *J* = 6.8 Hz, 1H (C***H***)), 2.13 (s, 6H (C$\boldsymbol{H}_3$N)), 1.47 (d, *J* = 6.8 Hz, 3H (C$\boldsymbol{H}_3$CH)). ^{13}C NMR (400 MHz, $CDCl_3$) δ 90.2 (Fc ***C***–CH), 74.3 (Fc ***C***H), 71.7 (Cp ***C***H), 68.2 (Fc ***C***H), 65.6 (Fc ***C***H), 57.6 (***C***H), 41.3 (***C***H_3N), 16.0 (***C***H_3CH).

With identical ^{1}H and ^{13}C NMR spectra, the opposite enantiomer 2-(*R*)-α-*N*,*N*-dimethylaminoethyl-(S_p)-1-iodoferrocene **3.5-($\boldsymbol{R,S_p}$)** (0.86 g, 2.24 mmol, 57 %) was produced

according to the same method from (*S*)-α-*N*-*N*-dimethylaminoethylferrocene **3.4-(*R*)** (1.02 g, 3.96 mmol).

5.1.2.6 2-(*S*)-α-Acetoxyethyl-(R_p)-1-iodoferrocene 3.6-(*S*,R_p)

Known compound. Chracterisation matches literature values[15]

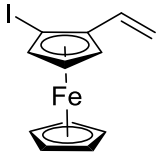


2-(*S*)-α-*N*,*N*-Dimethylaminoethyl-(R_p)-1-iodoferrocene **3.5-(*S*,R_p)** (6.38 g, 16.66 mmol, 1.0 eq.) was dissolved in Ac_2O (50 ml) and the resulting solution heated at 60 °C for 2 hrs. The reaction was cooled to rt and quenched by the careful addition of sat. $NaHCO_3$ (100 ml). The reaction mixture was extracted with DCM, washed with water (2 x 100 ml), dried over $MgSO_4$ and the solvent removed in vacuo. The crude product was purified by flash column chromatography on neutralised silica gel using a gradient eluent system of 0 → 10% EtOAc in hexane. Further enantioenrichment was achieved following repeated recrystalisation from hot petroleum ether and collection of the brown/orange crystalline product by filtration. The solvent was removed in vacuo to give the title compound as brown/orange crystals (4.30 g, 10.81 mmol, 65%). ^{1}H NMR (300 MHz, $CDCl_3$) δ 5.87 (q, *J* = 6.5 Hz, 1H (C***H***)), 4.49 (dd, *J* = 2.5, 1.4 Hz, 1H (Fc C***H***)), 4.32 (dd, *J* = 2.7, 1.4 Hz, 1H (Fc C***H***)), 4.27 (dd, *J* = 2.7, 2.5 Hz, 1H (Fc C***H***)), 4.14 (s, 5H), 2.00 (s, 3H (C$\boldsymbol{H}_3$CO)), 1.64 (d, *J* = 6.5 Hz, 3H (C$\boldsymbol{H}_3$CH)). ^{13}C NMR (400 MHz, $CDCl_3$) δ 170.4 (***C***O), 87.6 (Fc ***C***–CH), 75.7 (Fc ***C***H), 71.9 (Cp ***C***H), 69.8 (***C***H), 69.0 (Fc ***C***H), 65.9 (Fc ***C***H), 44.2 (Fc ***C***–I), 21.3 (***C***H_3CH), 18.8 (C$\boldsymbol{H}_3$CO).

With identical ^{1}H and ^{13}C NMR spectra, the opposite enantiomer (*R*)-2-α-*O*-acetoxyethyl-(S_p)-1-iodo-ferrocene **3.6-(*R*,S_p)** (3.09 g, 7.77 mmol, 73%) was produced according to the same method from 2-(*R*)-α-*N*,*N*-dimethylaminoethyl-(S_p)-1-iodoferrocene **3.5-(*R*,S_p)** (4.10 g, 10.71 mmol).

5.1.2.7 (R_p)-1-Iodo-2-vinyl-ferrocene 3.7-(R_p)

Novel compound

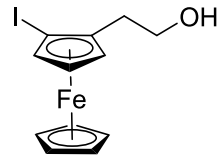


(*S*)-2-α-*O*-Acetoxyethyl-(R_p)-1-iodo-ferrocene **3.6-(*S*,R_p)** (4.30 g, 10.81 mmol, 1.0 eq.) was dissolved in dry DMF (20 ml), LiBr (14.0 g, 162 mmol, 15.0 eq.) was added and the resulting mixture heated with stirring at 85 °C for 1 hr. The reaction was quenched by addition of sat. $Na_2S_2O_3$ solution, extracted with DCM, washed with water (2 x 100 ml), dried over $MgSO_4$ and the solvent removed in vacuo. The crude product was purified by flash column chromatography on neutralised silica gel using an eluent of hexane. The solvent was removed in vacuo to give the title compound as a brown orange oil (3.40 g, 10.09 mmol, 93%). ^{1}H NMR (300 MHz, $CDCl_3$) δ 6.58 (dd, *J* = 17.5, 10.9 Hz, 1H (C***H***=CH_2)), 5.50 (dd, *J* = 17.5, 1.4 Hz, 1H (C***H***$_2$=CH)), 5.22 (dd, *J* = 10.9, 1.4 Hz, 1H (C***H***$_2$=CH)), 4.55 (dd, *J* = 2.6, 1.4 Hz, 1H (Fc C***H***)), 4.53 (dd, *J* = 2.6, 1.4 Hz, 1H (Fc C***H***)), 4.34 (dd, *J* = 2.6, 2.6 Hz, 1H (Fc C***H***)), 4.14 (s, 5H (Cp C***H***)). ^{13}C NMR (400 MHz, $CDCl_3$) δ 134.2 (***C***H=CH_2), 113.3 (***C***H_2=CH), 84.2 (Fc ***C***–CH), 75.3 (Fc ***C***H), 72.4 (Cp ***C***H), 69.5 (Fc ***C***H), 63.8 (Fc ***C***H), 45.0 (Fc ***C***–I). IR ν_{max}/cm^{-1} = 3087 (Fc CH), 1628 (C=C). HRMS (ESI-TOF) m/z: $[M]^+$ Calcd for $C_{12}H_{11}FeI$ 337.9255; Found 337.9258.

With identical ^{1}H and ^{13}C NMR spectra, the opposite enantiomer (S_p)-1-iodo-2-vinyl-ferrocene **3.7-(S_p)** (2.32 g, 6.85 mmol, 88%) was produced according to the same method from (*R*)-2-α-*O*-acetoxyethyl-(S_p)-1-iodo-ferrocene **3.6-(R,S_p)** (3.09 g, 7.77 mmol).

5.1.2.8 (R_p)-2-β-Hydroxyethyl-1-iodo-ferrocene 3.8-(R_p)

Novel compound



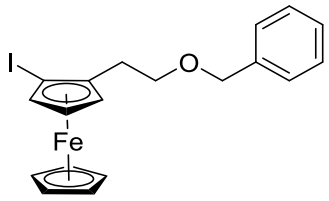
(R_p)-1-Iodo-2-vinyl-ferrocene **3.7-(R_p)** (3.40 g, 10.09 mmol, 1.0 eq) was dissolved in dry THF (30 ml) in a Schlenk tube under an atmosphere of argon and cooled to 0 °C in an ice bath. BH_3•THF (1M in THF) (8.87 ml, 8.87 mmol, 1.5 eq.) was added dropwise and stirring continued at 0 °C for 1 hr then the solution was warmed to rt and stirring continued for another 1.5 hrs. EtOH (8.87 ml) was carefully added and stirring continued for 5 min, followed by the dropwise addition of NaOH (3M in H_2O) (8.87 ml) and a further 10 min of stirring. H_2O_2 (30% in H_2O) (16 ml) was then added slowly and stirring continued for 30 min. The reaction was extracted with Et_2O, washed with water (2 x 100 ml) and dried over $MgSO_4$. The solvent was removed in vacuo and the crude product purified by flash column chromatography on silica gel using a gradient eluent system of 5 → 10% EtOAc in hexane. The solvent was removed in vacuo to give the title compound as a yellow oil (3.34 g, 9.38 mmol, 93%). ^{1}H NMR (300 MHz, $CDCl_3$) δ 4.41 (dd, *J* = 2.5, 1.4 Hz, 1H (Fc C***H***)), 4.21 (dd, *J* = 2.5, 1.4 Hz, 1H (Fc C***H***)), 4.18 (dd, *J* = 2.5, 2.5 Hz, 1H (Fc C***H***)), 4.12 (s, 5H (Cp C***H***)), 3.85 – 3.62 (m, 2H (C***H***$_2$OH)), 2.83 – 2.55 (m, 2H (C***H***$_2$CH$_2$OH)), 1.61 (s, 2H (O***H***)). ^{13}C NMR (400 MHz, $CDCl_3$) δ 86.2 (Fc ***C***–CH$_2$), 74.5 (Fc ***C***H), 71.7 (Cp ***C***H), 68.6 (Fc ***C***H), 67.7 (Fc ***C***H), 63.0 (***C***H$_2$OH), 45.5 (Fc ***C***–I), 33.5 (***C***H$_2$CH$_2$OH). IR ν_{max}/cm^{-1} = 3303 (OH),

3092 (Fc CH), 2923 (CH), 2873 (CH). HRMS (ESI-TOF) m/z: $[M]^+$ Calcd for $C_{12}H_{13}FeIO$ 355.9360; Found 355.9361.

With identical ^1H and ^{13}C NMR spectra, the opposite enantiomer (S_p)-2-β-hydroxyethyl-1-iodo-ferrocene **3.8-(S_p)**. (1.37 g, 3.85 mmol, 89%) was produced according to the same method from (S_p)-1-iodo-2-vinyl-ferrocene **3.7-(S_p)** (1.55 g, 4.34 mmol).

5.1.2.9 (R_p)-2-β-Benzyloxyethyl-1-iodo-ferrocene 3.9-(R_p)

Novel compound



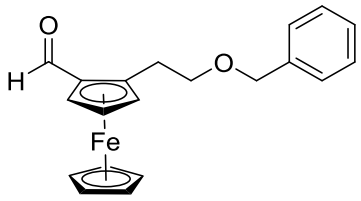
(R_p)-2-β-Benzyloxyethyl-1-iodo-ferrocene **3.8-(R_p)** (1.11 g, 3.13 mmol, 1.0 eq.) was dissolved in dry DMF (25 ml) and stirred in a Schlenk tube under an atmosphere of argon. NaH (0.188 g, 7.83 mmol, 2.5 eq.) was added in small portions, the solution turned from orange to yellow and stirring was continued for 1 hr. BnBr (0.74 ml, 6.26 mmol, 2.0 eq.) was added and stirring continued for 16 hrs. The reaction was quenched by the dropwise addition of water, extracted with Et_2O and dried over $MgSO_4$. The solvent was removed in vacuo and the crude product was purified by flash column chromatography on silica gel using an eluent of hexane. The solvent was removed in vacuo to give the title compound as a yellow oil (1.40 g, 3.13 mmol, 100%). ^1H NMR (300 MHz, $CDCl_3$) δ 7.34 – 7.12 (m, 5H (Ph C***H***)), 4.43 (s, 2H (Ph C–C***H***$_2$)), 4.28 (dd, *J* = 2.6, 1.3 Hz, 1H (Fc C***H***)), 4.11 (dd, *J* = 2.6, 1.3 Hz, 1H (Fc C***H***)), 4.03 (dd, *J* = 2.6, 2.6 Hz, 1H (Fc C***H***)), 3.99 (s, 5H (Cp C***H***)), 3.62 – 3.36 (m, 2H (CH_2C***H***$_2$O), 2.73 – 2.53 (m, 2H (C***H***$_2$$CH_2$O)). ^{13}C NMR (400 MHz, $CDCl_3$) δ 138.4 (Ph ***C***–CH_2), 128.4 (Ph ***C***H), 127.7 (Ph ***C***H), 127.6 (Ph ***C***H), 86.6 (Fc ***C***–CH_2), 74.0 (Fc ***C***H), 72.9

(Ph C–***C***H_2), 71.6 (Cp ***C***H), 70.2 (CH_2***C***H_2O), 68.3 (Fc ***C***H), 67.6 (Fc ***C***H), 45.8 (Fc ***C***–I), 30.6 (***C***H_2CH_2O). IR ν_{max}/cm^{-1} = 3088 (Fc CH), 3029 (Ph CH), 2921 (CH), 2853 (CH). HRMS (ESI-TOF) m/z: $[M]^+$ Calcd for $C_{19}H_{19}FeIO$ 455.9830; Found 455.9827.

With identical ^1H and ^{13}C NMR spectra, the opposite enantiomer (S_p)-2-β-Benzyloxyethyl-1-iodo-ferrocene **3.9-(S_p)** (1.47 g, 3.30 mmol, 86%) was produced according to the same method from (S_p)-2-β-Hydroxyethyl-1-iodo-ferrocene **3.8-(S_p)**. (1.37 g, 3.85 mmol).

5.1.2.10 (R_p)-2-β-Benzyloxyethyl-1-formyl-ferrocene 3.10-(R_p)

Novel compound



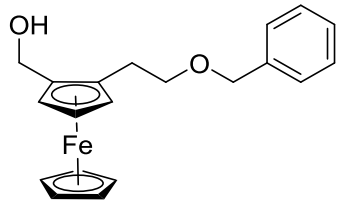
(R_p)-2-β-Benzyloxyethyl-1-iodo-ferrocene **3.9-(R_p)** (1.47 g, 3.28 mmol, 1.0 eq.) was dissolved in dry Et_2O (20 ml) with stirring and cooled to -78 °C in a Schlenk tube under argon. *n*-BuLi (2.5 M in hexane) (2.30 ml, 5.74 mmol, 1.75 eq.) was added slowly and stirring continued at -78 °C for 0.5 hrs before the reaction mixture was warmed to rt over 0.5 hrs. After cooling again to -78 °C, DMF (0.76 ml, 9.84 mmol, 3.0 eq.) was added slowly and stirring continued for 0.5 hrs, the mixture was then allowed to warm to rt and stirring continued for 0.5 hrs. The reaction was quenched by the slow addition of water (10 ml), extracted with Et_2O and dried over $MgSO_4$. The solvent was removed in vacuo and the crude product purified by flash column chromatography on silica gel using a gradient eluent system of 0 → 30% EtOAc in hexane. The solvent was removed in vacuo to give the title compound as a red oil (0.720 g, 2.07 mmol, 63%). ^1H NMR (300 MHz, $CDCl_3$) δ 10.01 (s, 1H (C***H***O)), 7.33 – 7.18 (m, 6H (Ph C***H***)), 4.67 (dd, *J* = 2.7, 1.5 Hz, 1H (Fc C***H***)), 4.53 (dd, *J* = 2.6, 1.5

Hz, 1H (Fc C***H***)), 4.47 (d, *J* = 11.9 Hz, 2H, (Bn C$\boldsymbol{H}_2$)), 4.43 (d, *J* = 11.9 Hz, 2H, (Bn C$\boldsymbol{H}_2$)), 4.44 (dd, *J* = 2.7, 2.6 Hz, 1H (Fc C***H***)), 4.14 (s, 5H (Cp C***H***)), 3.63 – 3.47 (m, 2H ($CH_2C\boldsymbol{H}_2O$)), 3.04 (ddd, *J* = 14.5, 6.5, 6.5 Hz, 1H (Fc C–C$\boldsymbol{H}_2$)), 2.80 (ddd, *J* = 14.5, 6.8, 6.8 Hz, 1H (Fc C–C$\boldsymbol{H}_2$)). ^{13}C NMR (400 MHz, $CDCl_3$) δ 193.8 (***C***HO), 138.4 (Ph ***C***–CH_2), 128.4 (Ph ***C***H), 127.7 (Ph ***C***H), 127.6 (Ph ***C***H), 88.4 (Fc ***C***–CH_2), 77.1 (Fc ***C***–CHO), 74.7 (Fc ***C***H), 73.0 (Ph C–***C***H_2), 71.5 (Fc ***C***H), 70.8 ($CH_2\boldsymbol{C}H_2O$), 70.2 (Cp ***C***H), 70.2 (Fc ***C***H), 28.9 (***C***H_2CH_2O). IR ν_{max}/cm^{-1} = 3088 (Fc CH), 3030 (Ph CH), 2925 (CH), 2856 (CH), 2723 (OC–H), 1669 (C=O). HRMS (ESI-TOF) m/z: $[M + Na]^+$ Calcd for $C_{20}H_{20}FeO_2Na$ 371.0710; Found 371.0707.

With identical ^{1}H and ^{13}C NMR spectra, the opposite enantiomer (*S*$_p$)-2-β-Benzyloxyethyl-1-formyl-ferrocene **3.10-(*S*$_p$)** (1.05 g, 3.02 mmol, 91%) was produced according to the same method from (*S*$_p$)-2-β-Benzyloxyethyl-1-iodo-ferrocene **3.9-(*S*$_p$)** (1.47 g, 3.30 mmol).

5.1.2.11 (*R*$_p$)-2-β-Benzyloxyethyl-1-hydroxymethyl-ferrocene 3.11-(*R*$_p$)

Novel compound

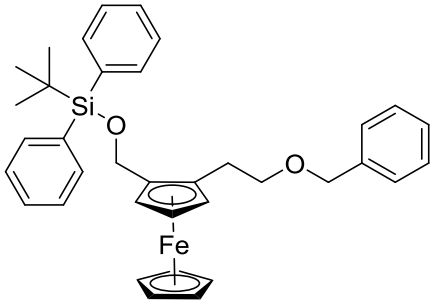


(*R*$_p$)-2-β-Benzyloxyethyl-1-formyl-ferrocene **3.10-(*R*$_p$)** (0.24 g, 0.68 mmol, 1.0 eq) was dissolved in dry Et_2O (5 ml) under an atmosphere of argon and cooled to 0 °C in an ice bath. DIBAL (1M in hexane) (1.0 ml, 1.0 mmol, 1.5 eq.) was added dropwise and the resulting solution stirred at 0 °C for 30 mins. H_2O (5 ml) was carefully added and the reaction mixture was extracted with DCM, dried over $MgSO_4$ and the solvent removed in vacuo. The crude product was then purified by flash column chromatography on silica gel using an eluent of

20% EtOAc in hexane. The solvent was removed in vacuo to give the title compound as an orange solid (0.20 g, 0.58 mmol, 85%). m.p. = 92 °C, ^{1}H NMR (300 MHz, $CDCl_3$) δ 7.49 – 7.09 (m, 5H (Ph C***H***)), 4.52 (dd, *J* = 12.1, 2.6 Hz, 1H (C***H***$_2$OH)), 4.45 (d, *J* = 12.0 Hz, 1H (Bn C***H***$_2$)), 4.39 (d, *J* = 12.0 Hz, 1H (Bn C***H***$_2$)), 4.20 – 4.16 (m, 1H (Fc C***H***)), 4.14 (dd, *J* = 12.1, 9.8 Hz, 1H (C***H***$_2$OH)), 4.09 – 4.06 (m, 1H (Fc C***H***)), 4.06 – 4.04 (m, 1H (Fc C***H***)), 4.03 (s, 5H (Cp C***H***)), 3.64 (ddd, *J* = 8.7, 4.5, 3.6 Hz, 1H), 3.40 (dd, *J* = 9.8, 2.6 Hz, 1H (O***H***)), 3.32 (ddd, *J* = 10.8, 8.7, 3.4 Hz, 1H (CH$_2$C***H***$_2$O)), 2.77 (ddd, *J* = 14.8, 10.8, 4.5 Hz, 1H (Fc C–C***H***$_2$)), 2.54 (ddd, *J* = 14.8, 3.6, 3.4 Hz, 1H (Fc C–C***H***$_2$)). ^{13}C NMR (101 MHz, $CDCl_3$) δ 137.3 (Ph ***C***–CH$_2$), 128.5 (Ph ***C***H), 128.0 (Ph ***C***H), 127.9 (Ph ***C***H), 86.5 (Fc ***C***–CH$_2$OH), 85.4 (Fc ***C***–CH$_2$CH$_2$), 73.3 (Bn ***C***H$_2$), 71.5 (CH$_2$***C***H$_2$O), 69.3 (Fc ***C***H), 69.2 (Fc ***C***H), 68.8 (Cp ***C***H), 66.7 (Fc ***C***H), 59.2 (***C***H$_2$OH), 29.0 (***C***H$_2$CH$_2$O). HRMS (ESI-TOF) m/z: $[M]^+$ Calcd for $C_{20}H_{22}FeO_2$ 350.0969; Found 350.0968.

5.1.2.12 (*R*$_p$)-2-β-Benzyloxyethyl-1-(*tert*-butyldiphenylsilyl)oxymethyl-ferrocene 3.12-(*R*$_p$)

Novel compound

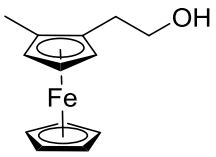


(*R*$_p$)-2-β-Benzyloxyethyl-1-hydroxymethyl-ferrocene **3.11-(*R*$_p$)** (0.20 g, 0.58 mmol, 1.0 eq) was dissolved in dry DCM (10 ml) and stirred under an atmosphere of argon. TEA (0.12 ml, 0.87 mmol, 1.5 eq.), TBDPSCl (0.23 ml, 0.87 mmol, 1.5 eq.) and DMAP (0.0007 g, 0.006 mmol 0.01 eq.) were added sequencially and the resulting solution stirred for 16 hrs at rt. The reaction was quenched with water (10 ml) extracted with DCM and dried over $MgSO_4$ before

the solvent was removed invacuo. The crude product was then purified by flash column chromatography on silica gel using an eluent of 5% EtOAc in hexane. The solvent was removed in vacuo to give the title compound as a yellow oil (0.32 g, 0.58 mmol, 99%). ^{1}H NMR (300 MHz, $CDCl_3$) δ 7.86 – 7.72 (m, 4H (TBDPS Ph C***H***)), 7.58 – 7.42 (m, 6H (TBDPS Ph C***H***)), 7.42 – 7.37 (m, 4H (Bn C***H***)), 7.37 – 7.29 (m, 1H (Bn C***H***)), 4.70 (d, *J* = 11.7 Hz, 1H (C***H***$_2$OSi)), 4.57 (d, *J* = 11.8 Hz, 1H (Bn C***H***$_2$)), 4.53 (d, *J* = 11.8 Hz, 1H (Bn C***H***$_2$)), 4.47 (d, *J* = 11.7 Hz, 1H (C***H***$_2$OSi)), 4.20 (dd, *J* = 2.4, 1.5 Hz, 1H (Fc C***H***)), 4.10 (t, *J* = 2.5, 1.5 Hz, 1H (Fc C***H***)), 4.07 (dd, *J* = 2.5, 2.4 Hz, 1H (Fc C***H***)), 4.04 (s, 5H (Cp C***H***)), 3.75 (td, *J* = 8.7, 6.0 Hz, 1H (CH_2C***H***$_2$O)), 3.62 (td, *J* = 8.7, 6.5 Hz, 1H (CH_2C***H***$_2$O)), 2.91 – 2.61 (m, 2H (C***H***$_2$$CH_2$O)), 1.12 (s, 9H (C***H***$_3$)). ^{13}C NMR (101 MHz, $CDCl_3$) δ 138.6 (Ph ***C***–CH_2), 135.9 (TBDPS ***C***H), 135.7 (TBDPS ***C***H), 133.9 (Ph ***C***–Si), 133.8 (Ph ***C***–Si), 129.8 (TBDPS ***C***H), 129.7 (TBDPS ***C***H), 128.5 (Bn ***C***H), 127.8 (Bn ***C***H), 127.8 (Bn ***C***H), 127.7 (TBDPS ***C***H), 127.6 (TBDPS ***C***H), 85.7 (Fc ***C***–CH_2O), 84.4 (Fc ***C***–CH_2CH_2), 73.1 (Ph C–***C***H_2), 71.4 (CH_2***C***H_2O), 69.3 (Fc ***C***H), 69.0 (Cp ***C***H), 68.8 (Fc ***C***H), 66.1 (Fc ***C***H), 61.1 (***C***H_2CH_2O), 28.8 (***C***H_2), 27.0 (***C***H_3), 19.3 (tBu ***C***). HRMS (ESI-TOF) m/z: $[M]^+$ Calcd for $C_{36}H_{40}FeO_2Si$ 588.2147; Found 588.2145.

5.1.2.13 (S_p)-1-β-Benzyloxyethyl-2-methyl-ferrocene 3.13-(S_p)

Novel compound

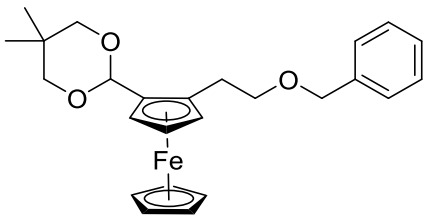


(R_p)-2-β-Benzyloxyethyl-1-(*tert*-butyldiphenylsilyl)oxymethyl-ferrocene **3.12-(R_p)** (0.32 g, 0.58 mmol, 1.0 eq.) was dissolved in EtOAc (5 ml) and $Pd(OH)_2$/C (0.08 g, 0.58 mmol, 1.0 eq.) added. A balloon containing hydrogen was attached to the top of the flask and the mixture stirred for 24 hrs. The crude mixture was then filtered through a short pad of celite

and the solvent removed in vacuo before being purified by flash column chromatography on silica gel using an eluent of 20% EtOAc in hexane. The solvent was removed in vacuo to give the title compound as an orange oil (0.13 g, 0.54 mmol, 94%). ^{1}H NMR (300 MHz, $CDCl_3$) δ 4.18 – 4.04 (m, 2H, (Fc C***H***)), 4.02 (s, 5H (Cp C***H***)), 3.96 (t, *J* = 2.4 Hz, 1H (Fc C***H***)), 3.87 – 3.45 (m, 2H (C***H***$_2$OH)), 2.75 – 2.49 (m, 2H (C***H***$_2$CH$_2$OH)), 2.18 (s, 1H (O***H***)), 1.97 (s, 3H (C***H***$_3$)). ^{13}C NMR (101 MHz, $CDCl_3$) δ 83.4 (Fc ***C***–CH$_2$), 83.0 (Fc ***C***–CH$_3$), 69.3 (Fc ***C***H), 69.2 (Cp ***C***H), 67.9 (Fc ***C***H), 65.3 (Fc ***C***H), 63.1 (***C***H$_2$OH), 31.3 (***C***H$_2$CH$_2$OH), 13.3 (***C***H$_3$). HRMS (ESI-TOF) m/z: $[M]^+$ Calcd for $C_{13}H_{16}FeO_3Na$ 267.0448; Found 267.0449.

5.1.2.14 (R_p)-2-β-Benzyloxyethyl-1-formyl-(3,3-dimethyl-1,5-pentanediol-acetal)-ferrocene 3.14-(R_p)

Novel compound



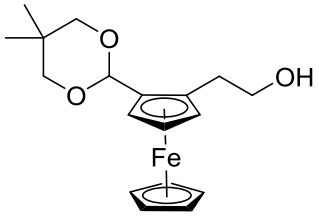
(R_p)-2-β-Benzyloxyethyl-1-formyl-ferrocene **3.10-(R_p)** (0.720 g, 2.07 mmol, 1.0 eq.) was dissolved in dry DCM (20 ml) in a Schlenk tube under an atmosphere of argon and 4 Å molecular sieves (ca. 0.1 g) were added with stirring. 3,3-dimethylpentane-1,5-diol (0.431 g, 4.14 mmol, 2.0 eq.) was added, followed by PTSA (0.040 g, 0.21 mmol, 0.10 eq.) and the reaction mixture stirred under argon for 4 hrs. The reaction was quenched by the addition of anhydrous K_2CO_3 (0.25 g) and stirring continued for 10 mins. The mixture was filtered through a small pad of celite, dried over $MgSO_4$ and the solvent removed in vacuo. The crude product was purified by flash column chromatography on neutralised silica gel using an eluent of 10% EtOAc in hexane. The solvent was removed in vacuo to give the title compound as an orange oil (0.772 g, 1.78 mmol, 86%). ^{1}H NMR (400 MHz, $CDCl_3$) δ 7.42 –

7.23 (m, 5H Ph C***H***)), 5.27 (s, 1H (C***H***OO)), 4.53 (d, *J* = 12 Hz, 2H (Bn–C***H***$_2$)), 4.49 (d, *J* = 12 Hz, 2H (Bn–C***H***$_2$)), 4.31 (dd, *J* = 2.5, 1.5 Hz, 1H (Fc C***H***)), 4.09 (s, 6H (Cp C***H***, Fc C***H***)), 4.03 (dd, *J* = 2.5 Hz, 2.4 Hz 1H (Fc C***H***)), 3.77 – 3.44 (m, 6H (CH_2C***H***$_2O$, OC***H***$_2C(CH_3)_2$)), 2.85 (ddd, *J* = 14.0, 9.1, 5.7 Hz, 1H (Fc C–C***H***$_2$)), 2.71 (ddd, *J* = 14.0, 9.4, 6.2 Hz, 1H (Fc C–C***H***$_2$)), 1.23 (s, 3H (C***H***$_3$)), 0.76 (s, 3H (C***H***$_3$)). ^{13}C NMR (101 MHz, $CDCl_3$) δ 138.7 (Ph ***C***–CH_2), 128.5 (Ph ***C***H), 127.9 (Ph ***C***H), 127.6 (Ph ***C***H), 100.7 (***C***HOO), 84.3 (Fc ***C***–CHOO), 83.3 (Fc ***C***–CH_2), 77.9 (O***C***$H_2C(CH_3)_2$), 77.8 (O***C***$H_2C(CH_3)_2$), 73.1 (Ph C–***C***H_2), 71.2 (CH_2***C***H_2O), 69.5 (Fc ***C***H), 69.5 (Cp ***C***H), 66.8 (Fc ***C***H), 66.5 (Fc ***C***H), 30.2 (***C***$(CH3)_2$), 28.9 (***C***H_2CH_2O), 23.2 (***C***H_3), 22.1 (***C***H_3). IR ν_{max}/cm^{-1} = 3090 (Fc CH), 3031 (Ph CH), 2954 (CH), 2918 (CH), 2849 (CH). HRMS (ESI-TOF) m/z: $[M]^+$ Calcd for $C_{25}H_{30}FeO_3$ 434.1544; Found 434.1545.

With identical ^{1}H and ^{13}C NMR spectra, the opposite enantiomer (*S*$_p$)-2-β-Benzyloxyethyl-1-formyl-(3,3-dimethyl-1,5-pentanediol-acetal)-ferrocene **3.14-(*S*$_p$)** (0.59 g, 1.35 mmol 89%) was produced according to the same method from (*S*$_p$)-2-β-Benzyloxyethyl-1-formyl-ferrocene **3.10-(*S*$_p$)** (0.53 g, 1.51 mmol).

5.1.2.15 (*R*$_p$)-1-Formyl-(3,3-dimethyl-1,5-pentanediol-acetal)-2-β-hydroxyethyl-ferrocene 3.15-(*R*$_p$)

Novel compound



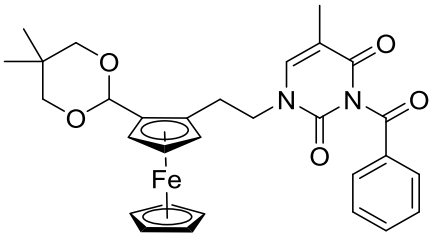
(*R*$_p$)-2-β-Benzyloxyethyl-1-formyl-(3,3-dimethyl-1,5-pentanediol-acetal)-ferrocene **3.14-(*R*$_p$)** (0.538 g, 1.24 mmol) was dissolved in dry DMF (10 ml) in a round bottomed flask fitted with

a rubber septum. A balloon of hydrogen was fitted with a long needle and the gas bubbled through the solution; a second needle through the septum allowed the pressure to equalise. $Pd(OH)_2/C$ (0.30 g) was added and the solution carefully stirred with continued bubbling of hydrogen gas. The reaction was carefully monitored by TLC until, after 20 mins all starting material was consumed. The hydrogen balloon was removed and the reaction mixture filtered through a small pad of celite. Brine (20 ml) was added, the crude product extracted with Et_2O and dried over $MgSO_4$. The crude product was then purified by flash column chromatography on neutralised silica gel using an eluent of 30% EtOAc in hexane. The solvent was removed in vacuo to give the title compound as an orange oil (0.305 g, 0.885 mmol, 71%). ^{1}H NMR (400 MHz, $CDCl_3$) δ 5.31 (s, 1H (C***H***)), 4.37 (dd, *J* = 2.0, 2.0 Hz, 1H (Fc C***H***)), 4.11 (s, 5H (Cp C***H***)), 4.10 – 4.07 (m, 2H (Fc C***H***)), 3.80 – 3.69 (m, 1H (C***H***$_2$OH)), 3.75 (dd, *J* = 11.1, 2.5 Hz, 1H (C***H***$_2$OCH)), 3.67 (dd, *J* = 11.0, 2.6 Hz, 1H (C***H***$_2$OCH)), 3.61 (dd, *J* = 11.1, 0.9 Hz, 1H (C***H***$_2$OCH)), 3.60 (dd, *J* = 11.0, 0.9 Hz, 1H (C***H***$_2$OCH)) 3.59 – 3.51 (m, 1H (C***H***$_2$OH)), 2.76 (ddd, *J* = 14.5, 8.7, 4.7 Hz, 1H (C***H***$_2$CH$_2$OH)), 2.75 (s, 1H (O***H***)) 2.63 (ddd, *J* = 14.5, 5.5, 4.2 Hz, 1H (C***H***$_2$CH$_2$OH)), 1.23 (s, 3H (C***H***$_3$), 0.77 (s, 3H (C***H***$_3$)). ^{13}C NMR (101 MHz, $CDCl_3$) δ 100.6 (***C***H), 84.4 (Fc ***C***–CH), 84.1 (Fc ***C***–CH$_2$), 77.9 (***C***H$_2$OCH), 77.7 (***C***H$_2$OCH), 69.7 (Fc ***C***H), 69.6 (Cp ***C***H), 67.1 (Fc ***C***H), 66.9 (Fc ***C***H), 64.1 (***C***H$_2$OH), 32.1 (***C***H$_2$CH$_2$OH), 30.2 (***C***(CH$_3$)$_2$), 23.2 (***C***H$_3$), 22.0 (***C***H$_3$). IR ν_{max}/cm^{-1} = 3420 (OH), 3095 (Fc CH), 2953 (CH), 2847 (CH). HRMS (ESI-TOF) m/z: $[M]^+$ Calcd for $C_{18}H_{24}FeO_3$ 344.1075; Found 344.1084.

With identical ^{1}H and ^{13}C NMR spectra, the opposite enantiomer (S_p)-1-Formyl-(3,3-dimethyl-1,5-pentanediol-acetal)-2-β-hydroxyethyl-ferrocene **3.15-(S_p)** (0.37 g, 1.07 mmol, 79%) was produced according to the same method from (S_p)-2-β-Benzyloxyethyl-1-formyl-(3,3-dimethyl-1,5-pentanediol-acetal)-ferrocene **3.14-(S_p)** (0.58 g, 1.34 mmol).

5.1.2.16 (R_p)-2-β-(*N*3-Benzoylthyminyl)ethyl-1-formyl-(3,3-dimethyl-1,5-pentanediol-acetal)ferrocene 3.16-(R_p)

Novel compound



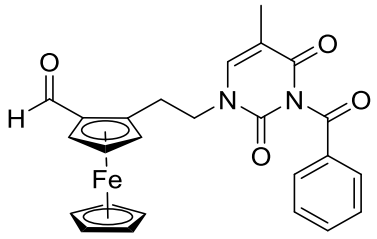
PPh_3 (0.596 g, 2.27 mmol, 1.5 eq.) and *N*3-benzoylthymine **2.21** (0.454 g, 1.97 mmol, 1.3 eq.) were dissolved in dry THF (10 ml) and stirred under an atmosphere of argon in a schlenk tube wrapped in foil. (R_p)-1-Formyl-(3,3-dimethyl-1,5-pentanediol-acetal)-2-β-hydroxyethyl-ferrocene **3.15-(R_p)** (0.522 g, 1.52 mmol, 1.0 eq.) dissolved in dry THF (10 ml) was added, followed by diethyl azodicarboxylate (0.45 ml, 2.27 mmol, 1.5 eq.) and the reaction mixture stirred at 75 °C for 2 hrs. The reaction was quenched with brine (10 ml), extracted with Et_2O and dried over $MgSO_4$. The solvent was removed in vacuo and the crude product purified by flash column chromatography on neutralised silica gel using a gradient eluent system of 10 → 40% EtOAc in hexane. The solvent was removed in vacuo to give the title compound as an orange/yellow solid (0.465 g, 0.836 mmol, 55%) m.p. = 87 °C. ^{1}H NMR (400 MHz, $CDCl_3$) δ 7.91 (dd, *J* = 8.1, 1.2 Hz, 2H (Ph C***H***)), 7.63 (tt, *J* = 7.4, 1.2 Hz, 1H (Ph C***H***)), 7.48 (dd, *J* = 8.1, 7.4 Hz, 2H (Ph C***H***)), 6.78 (q, *J* = 1.0 Hz, 1H (C***H***=C)), 5.30 (s, 1H (C***H***OO)), 4.34 (dd, *J* = 2.4, 1.5 Hz, 1H (Fc C***H***)), 4.11 (s, 5H (Cp C***H***)), 4.06 (dd, *J* = 2.4, 2.2 Hz, 1H (Fc C***H***)), 4.05 – 3.96 (m, 1H (C***H***$_2$N)), 3.95 (dd, *J* = 2.2, 1.5 Hz, 1H (Fc C***H***)), 3.76 – 3.67 (m, 3H (C***H***$_2$N, C***H***$_2$O)), 3.61 (d, *J* = 10.7 Hz, 2H (C***H***$_2$O), 2.94 (ddd, *J* = 14.0, 6.8, 4.4 Hz, 1H (OC***H***$_2$C(CH$_3$)$_2$)), 2.77 (ddd, *J* = 14.0, 8.4, 7.6 Hz, 1H (OC***H***$_2$C(CH$_3$)$_2$)), 1.79 (d, *J* = 1.0 Hz, 3H (C***H***$_3$C=CH)), 1.24 (s, 3H (C***H***$_3$CCH$_3$)), 0.78 (s, 3H (C***H***$_3$CCH$_3$)). ^{13}C NMR (101 MHz, $CDCl_3$) δ 169.4 (Bz ***C***O), 163.5 (C–***C***O–N), 149.8 (N–***C***O–N), 141.5 (***C***H=C), 134.9 (Ph ***C***H), 131.8 (Ph ***C***–CO), 130.5 (Ph ***C***H), 129.2 (Ph ***C***H), 109.4 (***C***=CH), 101.0 (***C***HOO),

84.1 (Fc ***C***–CH), 82.0 (Fc ***C***–CH_2), 77.9 (***C***H_2O), 77.8 (***C***H_2O), 70.0 (Fc ***C***H), 69.6 (Cp ***C***H), 67.8 (Fc ***C***H), 66.9 (Fc ***C***H), 50.1 (***C***H_2N), 30.2 (***C***$(CH_3)_2$), 27.9 (***C***H_2CH_2N), 23.3 (***C***H_3CCH_3), 22.0 (***C***H_3CCH_3), 12.2 (***C***H_3C=CH). IR ν_{max}/cm^{-1} = 3088 (Fc CH), 2955 (CH), 2850 (CH), 1745 (C=O), 1697 (C=O), 1647 (C=O), 1599 (C=C). HRMS (ESI-TOF) m/z: $[M]^+$ Calcd for $C_{30}H_{32}FeN_2O_5$ 556.1661; Found 556.1669.

With identical ^1H and ^{13}C NMR spectra, the opposite enantiomer (S_p)-2-β-(*N*3-Benzoylthyminyl)ethyl-1-formyl-(3,3-dimethyl-1,5-pentanediol-acetal)ferrocene **3.16-(S_p)** (0.46 g, 0.82 mmol, 77%) was produced according to the same method from (S_p)-1-Formyl-(3,3-dimethyl-1,5-pentanediol-acetal)-2-β-hydroxyethyl-ferrocene **3.15-(S_p)**.

5.1.2.17 (R_p)-2-β-(*N*3-Benzoylthyminyl)ethyl-1-formyl-ferrocene 3.17-(R_p)

Novel compound



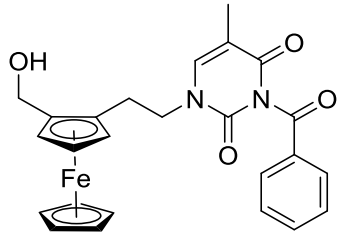
(R_p)-2-β-(*N*3-Benzoylthyminyl)ethyl-1-formyl-(3,3-dimethyl-1,5-pentanediol-acetal)ferrocene **3.16-(R_p)** (0.329 g, 0.591 mmol, 1.0 eq.) was dissolved in a mixture of THF (8 ml) and water (2ml) to produce a yellow solution. PTSA (0.056 g, 0.296 mmol, 0.5 eq.) was added and the resulting mixture stirred at rt for 45 min to produce a red solution. The reaction was quenched by the slow addition of sat. $NaHCO_3$ solution, extracted with EtO_2, dried over $MgSO_4$ and the solvent removed in vacuo. The crude product was purified by flash column chromatography using an eluent of 50% EtOAc in hexane and the solvent was removed in vacuo to give the title compound as an orange/red solid (0.277 g, 0.589 mmol, 100%) m.p. = 69 °C. ^1H NMR (300 MHz, $CDCl_3$) δ 10.01 (s, 1H (C***H***O)), 7.94 (dd, *J* = 8.4,

1.3 Hz, 2H (Ph C***H***)), 7.64 (tt, *J* = 7.4, 1.3 Hz, 1H (Ph C***H***))), 7.50 (dd, *J* = 8.4, 7.4 Hz, 2H (Ph C***H***))), 7.02 (q, *J* = 1.2 Hz, 1H (C***H***=C)), 4.70 (dd, *J* = 2.6, 1.4 Hz, 1H (Fc C***H***)), 4.53 (dd, *J* = 2.6, 1.4 Hz, 1H (Fc C***H***)), 4.50 (dd, *J* = 2.6, 2.6 Hz, 1H (Fc C***H***)), 4.24 (s, *J* = 4.0 Hz, 5H (Cp C***H***)), 3.98 (ddd, *J* = 13.5, 8.4, 7.0 Hz, 1H (C***H***$_2$N)), 3.69 (ddd, *J* = 13.5, 8.7, 5.1 Hz, 1H (C***H***$_2$N)), 3.21 (ddd, *J* = 13.5, 8.4, 5.1 Hz, 1H (C***H***$_2$)), 2.93 (ddd, *J* = 13.5, 8.7, 7.0 Hz, 1H (C***H***$_2$)), 1.89 (d, *J* = 1.2 Hz, 3H (C***H***$_3$)). ^{13}C NMR (101 MHz, $CDCl_3$) δ 194.5 (***C***HO), 169.3 (Bz ***C***O), 163.4 (C–***C***O–N), 149.9 (N–***C***O–N), 140.8 (***C***H=C), 135.0 (Ph ***C***H), 131.8 (Ph ***C***–CO), 130.6 (Ph ***C***H), 129.2 (Ph ***C***H), 110.4 (***C***=CH), 85.2 (Fc ***C***–CH_2), 77.1 (Fc ***C***–CO), 75.5 (Fc ***C***H), 73.0 (Fc ***C***H), 72.0 (Fc ***C***H), 70.5 (Cp ***C***H), 50.0 (***C***H_2N), 28.6 (***C***H_2CH_2N), 12.4 (***C***H_3). IR ν_{max}/cm^{-1} = 3068 (Ph CH), 2930 (CH), 2217 (CH), 1741 (C=O), 1694 (C=O), 1642 (C=O), 1598 (C=C). HRMS (ESI-TOF) m/z: $[M + Na]^+$ Calcd for $C_{25}H_{22}FeN_2O_4Na$ 493.0827; Found 493.0825.

With identical ^{1}H and ^{13}C NMR spectra, the opposite enantiomer (S_p)-2-β-(*N*3-benzoylthyminyl)ethyl-1-formyl-ferrocene **3.17-(S_p)** (0.33 g, 0.71 mmol, 86%) was produced according to the same method from (S_p)-2-β-(*N*3-benzoylthyminyl)ethyl-1-formyl-(3,3-dimethyl-1,5-pentanediol-acetal)ferrocene **3.16-(S_p)** (0.45 g, 0.82 mmol).

5.1.2.18 (R_p)-2-β-(*N*3-Benzoylthyminyl)ethyl-1-hydroxymethyl-ferrocene 3.18-(R_p)

Novel compound



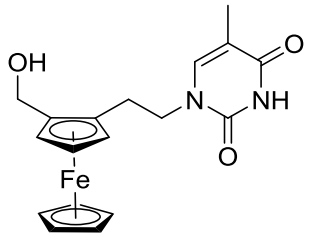
(R_p)-2-β-(*N*3-Benzoylthyminyl)ethyl-1-formyl-ferrocene **3.17-(R_p)** (0.055 g, 0.117 mmol, 1.0 eq.) was dissolved in MeOH (5 ml) and cooled to 0 °C with stirring. $NaBH_4$ (0.008 g,

0.233 mmol, 2.0 eq.) was added to the red solution and stirring continued for 15 min at 0 °C. The resulting yellow solution was quenched with brine, extracted with DCM and dried over $MgSO_4$. The crude product was purified by flash column chromatography using an eluent of 40% hexane in EtOAc, the solvent was removed in vacuo to give the title compound as an orange oil (0.053 g, 0.113 mmol, 96%). ^{1}H NMR (400 MHz, $CDCl_3$) δ 7.87 (dd, *J* = 8.3, 1.3 Hz, 2H (Ph C***H***)), 7.64 (tt, *J* = 7.5, 1.3 Hz, 1H (Ph C***H***)), 7.48 (dd, *J* = 8.3, 7.5 Hz, 2H (Ph C***H***)), 6.93 (q, *J* = 1.2 Hz, 1H (C***H***=C)), 4.47 (d, *J* = 11.9 Hz, 1H (C***H***$_2$OH)), 4.31 (d, *J* = 11.9 Hz, 1H (C***H***$_2$OH)), 4.19 (s, 1H (Fc C***H***)), 4.11 (t, *J* = 2.1 Hz, 1H (Fc C***H***)), 4.08 (s, 5H (Cp C***H***)), 4.04 (s, 1H (Fc C***H***)), 3.91 (ddd, *J* = 13.6, 8.4, 7.3 Hz, 1H (CH_2C***H***$_2$N)), 3.76 (ddd, *J* = 13.6, 7.8, 4.4 Hz, 1H (CH_2C***H***$_2$N)), 2.85 (ddd, *J* = 14.2, 7.3, 4.4 Hz, 1H (C***H***$_2$$CH_2$N)), 2.74 (ddd, *J* = 14.2, 8.4, 7.8 Hz, 1H (C***H***$_2$$CH_2$N)), 2.40 (s, 1H (O***H***)), 1.86 (d, *J* = 1.2 Hz, 3H (C***H***$_3$)). ^{13}C NMR (101 MHz, $CDCl_3$) δ 169.3 (Bz ***C***O), 163.3 (C–***C***O–N), 150.1 (N–***C***O–N), 140.7 (***C***H=C), 135.1 (Ph ***C***H), 131.7 (Ph ***C***–CO), 130.6 (Ph ***C***H), 129.2 (Ph ***C***H), 110.4 (***C***=CH), 85.6 (Fc ***C***–CH_2CH_2), 83.0 (Fc ***C***–CH_2OH), 70.0 (Fc ***C***H), 69.9 (Fc ***C***H), 69.2 (Cp ***C***H), 67.2 (Fc ***C***H), 59.5 (***C***H_2OH), 49.9 (***C***H_2N), 27.9 (***C***$H_2$$CH_2$N), 12.3 (***C***$H_3$). IR ν_{max}/cm^{-1} = 3474 (OH), 3072 (Ph CH). 2928 (CH), 2251 (CH), 1743 (C=O), 1693 (C=O), 1639 (C=O), 1599 (C=C). HRMS (ESI-TOF) m/z: $[M + Na]^+$ Calcd for $C_{25}H_{24}FeN_2O_4Na$ 495.0983; Found 495.0972.

With identical ^{1}H and ^{13}C NMR spectra, the opposite enantiomer (S_p)-2-β-(*N*3-Benzoylthyminyl)ethyl-1-hydroxymethyl-ferrocene **3.18-(S_p)** (0.33 g, 0.70 mmol, 99%) was produced according to the same method from (S_p)-2-β-(*N*3-Benzoylthyminyl)ethyl-1-formyl-ferrocene **3.17-(S_p)** (0.33 g, 0.71 mmol).

5.1.2.19 (R_p)-1-Hydroxymethyl-2-β-thyminylethyl-ferrocene Fcn1c2T$_{(Rp)}$

Novel compound

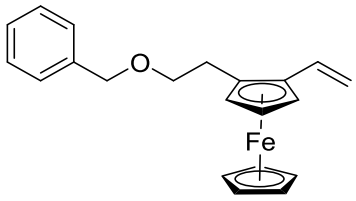


(R_p)-2-β-(*N*3-Benzoylthyminyl)ethyl-1-hydroxymethyl-ferrocene **3.18-(R_p)** (0.0327 g, 0.069 mmol) was dissolved in MeOH (2 ml) before excess $MeNH_2$ (30% in MeOH) (0.2 ml) was added and the resulting mixture was stirred at rt for 5 min. Brine (5 ml) was added, the crude product extracted with DCM, dried over $MgSO_4$ and the solvent removed in vacuo. The crude product was purified by flash column chromatography on silica gel using an eluent of 20% hexane in EtOAc. Recrystallisation by the slow evaporation of a concentrated solution in chloroform produced orange crystals and the solvent was removed in vacuo to give the title compound as a yellow solid (0.025 g, 0.067 mmol, 97%) Decomposes above 160 °C. ^{1}H NMR (300 MHz, $CDCl_3$) δ 8.68 (s, 1H (N***H***)), 6.82 (q, *J* = 1.2 Hz, 1H (C***H***=C)), 4.52 (d, *J* = 12.0 Hz, 1H (C***H***$_2$OH)), 4.37 (d, *J* = 12.0 Hz, 1H (C***H***$_2$OH)), 4.20 (dd, *J* = 2.5, 1.4 Hz, 1H (Fc C***H***)), 4.17 – 4.10 (m, 1H (Fc C***H***)), 4.08 (s, 5H (Cp C***H***)) 4.00 (dd, *J* = 2.3, 1.4 Hz, 1H (Fc C***H***)), 3.81 (dd, *J* = 8.3, 1.3 Hz, 1H (C***H***$_2$N)), 3.79 (d, *J* = 8.3 Hz, 1H (C***H***$_2$N)), 2.89 – 2.66 (m, 2H (C***H***$_2$CH$_2$N)), 2.17 (s, 1H (O***H***)), 1.85 (d, *J* = 1.2 Hz, 3H (C***H***$_3$)). ^{13}C NMR (101 MHz, $CDCl_3$) δ 164.1 (C–***C***O–N), 151.0 (N–***C***O–N), 140.9 (***C***H=C), 110.5 (***C***=CH), 85.7 (Fc ***C***–CH$_2$CH$_2$), 83.1 (Fc ***C***–CH$_2$OH), 70.0 (Fc ***C***H), 69.7 (Fc ***C***H), 69.1 (Cp ***C***H), 67.1 (Fc ***C***H), 59.6 (***C***H$_2$OH), 50.0 (***C***H$_2$N), 28.1 (***C***H$_2$CH$_2$N), 12.3 (***C***H$_3$). IR ν_{max}/cm^{-1} = 3411 (OH), 2926 (CH), 2853 (CH), 2818 (CH), 2250 (CH), 1658 (C=O), 1627 (C=C). HRMS (ESI-TOF) m/z: [M]$^+$ Calcd for $C_{18}H_{20}FeN_2O_3$ 368.0823; Found 368.0811. Anal. Calcd for $C_{18}H_{20}FeN_2O_3$: C, 58.72; H, 5.48; N, 7.61. Found: C, 58.91; H, 5.45; N, 7.74.

With identical ^{1}H and ^{13}C NMR spectra, the opposite enantiomer (S_p)-1-Hydroxymethyl-2-β-thyminylethyl-ferrocene **Fcn1c2T**$_{(Sp)}$ (0.24 g, 0.67 mmol 95%) was produced according to the same method from (S_p)-2-β-(*N*3-Benzoylthyminyl)ethyl-1-hydroxymethyl-ferrocene **3.18-(S_p)** (0.33 g, 0.70 mmol). Decomposes above 160 °C. Anal. Found: C, 58.80; H, 5.55; N, 7.47.

5.1.2.20 (S_p)-2-β-Benzyloxyethyl-1-vinyl-ferrocene 3.19-(S_p)

Novel compound



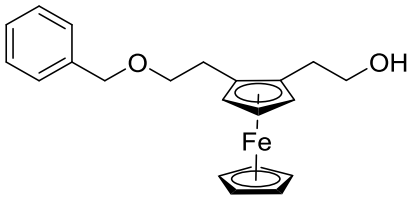
Methyltriphenylphosphonium bromide (1.62 g, 4.53 mmol, 3.0 eq.), KO^{t}Bu (0.51 g, 4.53 mmol, 3.0 eq.) and dibenzo-18-crown-6 (0.003 g, 0.008 mmol, 0.005 eq.) were dissolved in dry THF (15 ml) in a Schlenk tube under an atmosphere of argon and stirred for 30 mins at rt to produce a bright yellow solution. (S_p)-2-β-Benzyloxyethyl-1-formyl-ferrocene **3.10-(S_p)** (0.526 g, 1.51 mmol, 1.0 eq.) was dissolved in dry THF (15 ml) and added slowly, the resulting orange solution was stirred at rt for 1 hr. The reaction was quenched by the careful addition of water (15 ml), extracted with Et_2O, dried over MgSO4 and the solvent removed in vacuo. The crude product was purified by flash column chromatography on neutralised silica gel using an eluent of 10% EtOAc in hexane. The solvent was removed in vacuo to give the title compound as an orange oil (0.476 g, 1.37 mmol, 91%). ^{1}H NMR (300 MHz, $CDCl_3$) δ 7.51 – 7.22 (m, 5H (Ph C***H***)), 6.58 (dd, *J* = 17.4, 10.9 Hz, 1H (C***H***=CH_2)), 5.37 (dd, *J* = 17.4, 1.6 Hz, 1H (C***H***$_2$=CH)), 5.09 (dd, *J* = 10.9, 1.6 Hz, 1H (C***H***$_2$=CH)), 4.53 (s, 2H (Ph C–C***H***$_2$), 4.43 (dd, *J* = 2.6, 1.4 Hz, 1H (Fc C***H***)), 4.20 (dd, *J* = 2.6, 1.4 Hz, 1H (Fc C***H***)), 4.15 (dd, *J* = 2.6 Hz, 1H (Fc C***H***)), 4.03 (s, 5H (Cp C***H***)), 3.58 (m, 2H (CH_2C***H***$_2$O)), 2.81 (m, 2H

(C***H***$_2$CH$_2$O)). ^{13}C NMR (400 MHz, $CDCl_3$) δ 138.5 (Ph ***C***–C), 133.2 (***C***H=CH_2), 128.5 (Ph ***C***H), 127.8 (Ph ***C***H), 127.7 (Ph ***C***H), 111.8 (***C***H_2=CH), 84.1 (Fc ***C***–CH_2), 82.4 (Fc ***C***–CH), 73.1 (Ph C–***C***H_2), 71.1 (CH_2***C***H_2O), 69.9 (Cp ***C***H), 69.8 (Fc ***C***H), 67.2 (Fc ***C***H), 64.8 (Fc ***C***H), 28.8 (***C***H_2CH_2O). IR ν_{max}/cm^{-1} = 3085 (Fc CH), 3029 (Ph CH), 3005 (CH), 2924 (CH), 2853 (CH), 1626 (C=C). HRMS (ESI-TOF) m/z: $[M + Na]^+$ Calcd for $C_{21}H_{22}FeONa$ 369.0918; Found 369.0905.

With identical ^{1}H and ^{13}C NMR spectra, the opposite enantiomer (R_p)-2-β-benzyloxyethyl-1-vinyl-ferrocene **3.19-(*R*$_p$)** (0.87 g, 2.51 mmol, 98%) was produced according to the same method from (R_p)-2-β-Benzyloxyethyl-1-formyl-ferrocene **3.10-(*R*$_p$)** (0.89 g, 2.56 mmol).

5.1.2.21 (*R*$_p$)-1-β-Benzyloxyethyl-2-β-hydroxyethyl-ferrocene 3.20-(*R*$_p$)

Novel compound



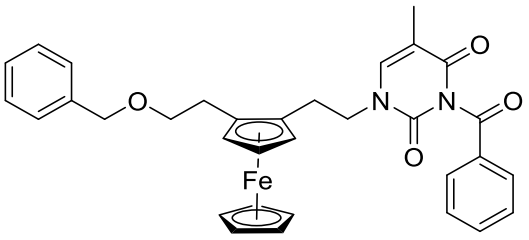
(S_p)-2-β-Benzyloxyethyl-1-vinyl-ferrocene **3.19-(*S*$_p$)** (0.476 g, 1.37 mmol, 1.0 eq) was dissolved in dry THF (7 ml) in a Schlenk tube under an atmosphere of argon and cooled to 0 °C in an ice bath. BH_3•THF (1M in THF) (2.06 ml, 2.06 mmol, 1.5 eq.) was added dropwise and stirring continued at 0 °C for 15 mins before the solution was warmed to rt and stirring continued for another 1.5 hrs. The solution was cooled to 0 °C before EtOH (2.0 ml) was carefully added and stirring continued for 5 min, followed by the dropwise addition of NaOH (3M in H_2O) (2.0 ml) and a further 10 min of stirring. H_2O_2 (30% in H_2O) (4.0 ml) was then added slowly and stirring continued for 30 min and the solution allowed to warm to rt. The reaction was extracted with Et_2O, washed with water (2 x 50 ml) and dried over $MgSO_4$. The

solvent was removed in vacuo and the crude product purified by flash column chromatography through a short column of neutralised silica gel using an eluent of 10% EtOAc in hexane. The solvent was removed in vacuo to give the title compound as an orange oil (0.413 g, 1.13 mmol, 82%). ^{1}H NMR (300 MHz, $CDCl_3$) δ 7.38 – 7.24 (m, 5H (Ph C***H***)), 4.49 (s, 2H (Ph C–C***H***$_2$)), 4.14 – 4.07 (m, 2H (Fc C***H***)), 4.06 – 4.03 (m, 1H (Fc C***H***)), 4.02 (s, 5H (Cp C***H***)) 3.76 – 3.45 (m, 4H (CH_2C***H***$_2OCH_2$, C***H***$_2$OH)), 2.79 – 2.54 (m, 4H (C***H***$_2CH_2OCH_2$, C***H***$_2CH_2$OH)), 2.18 (t, *J* = 5.9 Hz, 1H (O***H***)). ^{13}C NMR (400 MHz, $CDCl_3$) δ 138.2 (Ph ***C***–CH_2), 128.5 (Ph ***C***H), 127.9 (Ph ***C***H), 127.8 (Ph ***C***H), 84.7 (Fc ***C***–$CH_2CH_2OCH_2$), 84.4 (Fc ***C***–CH_2CH_2OH), 73.1 (Ph C–***C***H_2), 71.0 (CH_2***C***H_2OCH_2), 69.4 (Cp ***C***H), 68.3 (Fc ***C***H), 68.2 (Fc ***C***H), 66.3 (Fc ***C***H), 63.7 (CH_2***C***H_2OH), 31.7 (***C***H_2CH_2OH), 28.7 (***C***$H_2CH_2OCH_2$). IR ν_{max}/cm^{-1} = 3381 (OH), 3089 (Fc CH), 3030 (Ph CH), 2933 (CH), 2858 (CH). HRMS (ESI-TOF) m/z: $[M]^+$ Calcd for $C_{21}H_{24}FeO_2$ 364.1126; Found 364.1120.

With identical ^{1}H and ^{13}C NMR spectra, the opposite enantiomer (S_p)-1-β-benzyloxyethyl-2-β-hydroxyethyl-ferrocene **3.20-(*S*$_p$)** (0.80 g, 2.20 mmol, 88%) was produced according to the same method from (R_p)-2-β-benzyloxyethyl-1-vinyl-ferrocene **3.19-(*R*$_p$)** (0.87 g, 2.51 mmol).

5.1.2.22 (*R*$_p$)-2-β-(*N*3-Benzoylthyminyl)ethyl-1-β-benzyloxyethyl-ferrocene 3.21-(*R*$_p$)

Novel compound



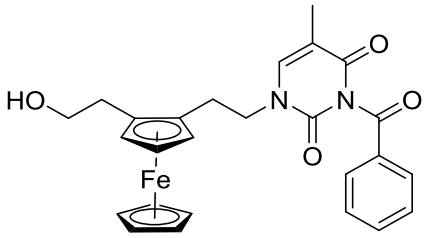
PPh_3 (0.595 g, 2.27 mmol, 2.0 eq.) and (R_p)-1-β-Benzyloxyethyl-2-β-hydroxyethyl-ferrocene **3.20-(*R*$_p$)** (0.413 g, 1.13 mmol, 1.0 eq.) were dissolved in dry THF (20 ml) and stirred under an atmosphere of argon in a schlenk tube wrapped in foil. Diethyl azodicarboxylate (0.45 ml,

2.27 mmol, 2.0 eq.) was added slowly followed by *N*3-benzoylthymine **2.21** (0.392 g, 1.70 mmol, 1.5 eq.) and the reaction mixture stirred at 75 °C for 1 hr. The reaction was quenched with brine (5 ml), extracted with Et_2O and dried over $MgSO_4$. The solvent was removed in vacuo and the crude product purified by flash column chromatography on neutralised silica gel using a gradient eluent system of 30 → 50% EtOAc in hexane. The solvent was removed in vacuo to give the title compound as an orange solid (0.241 g, 0.417 mmol, 37%). m.p. = 57 °C. ^{1}H NMR (400 MHz, $CDCl_3$) δ 7.92 (dd, *J* = 8.3, 1.3 Hz, 2H (Bz C***H***)), 7.63 (tt, *J* = 7.5, 1.3 Hz, 1H ((Bz C***H***)), 7.48 (dd, *J* = 8.3, 7.5 Hz, 2H (Bz C***H***)), 7.36 – 7.25 (m, 5H (Bn C***H***)), 6.67 (q, *J* = 1.2 Hz, 1H (C***H***=C)), 4.49 (d, *J* = 11.6 Hz, 1H (Bn C***H***$_2$O)), 4.48 (d, *J* = 11.6 Hz, 1H (Bn C***H***$_2$O)), 4.15 (dd, *J* = 2.5, 1.3 Hz, 1H (Fc C***H***)), 4.04 (dd, *J* = 2.5, 2.5 Hz, 1H (Fc C***H***)), 4.03 (s, 5H (Cp C***H***)), 3.96 (dd, *J* = 2.5, 1.3 Hz, 1H (Fc C***H***)), 3.76 (dd, *J* = 8.0, 6.6 Hz, 2H (C***H***$_2$N)), 3.70 (ddd, *J* = 8.9, 5.6, 5.5 Hz, 1H (CH$_2$C***H***$_2$O)), 3.57 (ddd, *J* = 8.9, 7.1, 7.1 Hz, 1H (CH$_2$***C***H$_2$O)), 2.88 – 2.58 (m, 4H (C***H***$_2$CH$_2$O, C***H***$_2$CH$_2$N)), 1.78 (d, *J* = 1.2 Hz, 3H (C***H***$_3$)). ^{13}C NMR (400 MHz, $CDCl_3$) δ 169.3 (Bz ***C***O), 163.3 (C–***C***O–N), 149.7 (N–***C***O–N), 141.0 (***C***H=C), 138.1 (Bn ***C***–CH$_2$), 135.0 (Bz ***C***H), 131.7 (Bz ***C***–CO), 130.5 (Bz ***C***H), 129.2 (Bz ***C***H), 128.5 (Bn ***C***H), 128.0 (Bn ***C***H), 127.8 (Bn ***C***H), 109.6 (***C***=CH), 84.8 (Fc ***C***–CH$_2$CH$_2$O), 82.6 (Fc ***C***–CH$_2$CH$_2$N), 73.3 (Bn C–***C***H$_2$), 71.4 (CH$_2$***C***H$_2$O), 69.3 (Cp ***C***H), 68.5 (Fc ***C***H), 68.4 (Fc ***C***H), 66.4 (Fc ***C***H), 49.5 (***C***H$_2$N), 28.6 (***C***H$_2$CH$_2$O), 27.7 (***C***H$_2$CH$_2$N), 12.3 (***C***H$_3$). IR ν_{max}/cm^{-1} = 3075 (Fc CH), 1744 (C=O), 1696 (C=O), 1646 (C=O), 1599 (C=C). HRMS (ESI-TOF) m/z: [M]$^+$ Calcd for $C_{33}H_{32}FeN_2O_4$ 576.1711; Found 576.1715.

With identical ^{1}H and ^{13}C NMR spectra, the opposite enantiomer (S_p)-2-β-(*N*3-benzoylthyminyl)ethyl-1-β-benzyloxyethyl-ferrocene **3.21-(S_p)** (0.21 g, 0.37 mmol, 74%) was produced according to the same method from (S_p)-1-β-benzyloxyethyl-2-β-hydroxyethyl-ferrocene **3.20-(S_p)** (0.18 g, 0.50 mmol).

5.1.2.23 (R_p)-2-β-(*N*3-Benzoylthyminyl)ethyl-1-β-hydroxyethyl-ferrocene 3.22-(R_p)

Novel compound

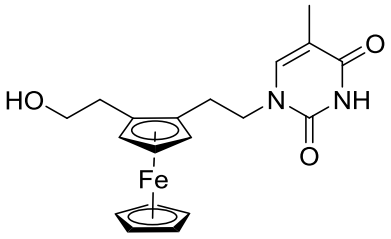


(R_p)-2-β-(*N*3-Benzoylthyminyl)ethyl-1-β-benzyloxyethyl-ferrocene **3.21-(R_p)** (0.240 g, 0.417 mmol) was dissolved in EtOAc (5 ml) and hydrogen gas bubbled through the solution using a balloon and needle with stirring. $Pd(OH)_2/C$ (0.30 g) was added and the resulting mixture stirred at rt with gentle bubbling and stirring for 30 mins. The mixture was filtered through a short pad of celite, washed with water (2 x 5 ml) and dried over $MgSO_4$. The solvent was removed in vacuo and the crude product was purified by flash column chromatography on silica gel using an eluent of EtOAc. The solvent was removed in vacuo to give the title compound as a yellow solid (0.15 g, 0.317 mmol, 76%) m.p. = 68 °C. ^{1}H NMR (400 MHz, $CDCl_3$) δ 7.88 (dd, *J* = 8.3, 1.3 Hz, 2H (Bz C***H***)), 7.66 (tt, *J* = 7.5, 1.3 Hz, 1H (Bz C***H***)), 7.49 (dd, *J* = 8.3, 7.5 Hz, 2H (Bz C***H***)), 6.99 (q, *J* = 1.1 Hz, 1H (C***H***=C)), 4.11 (dd, *J* = 2.4, 1.4 Hz, 1H (Fc C***H***)), 4.06 (dd, *J* = 2.4, 2.4 Hz, 1H (Fc C***H***)), 4.04 (s, 5H (Cp C***H***)), 3.97 (dd, *J* = 2.4, 1.4 Hz, 1H (Fc C***H***)), 3.90 (ddd, *J* = 13.6, 8.1 Hz, 1H (C***H***$_2$N)), 3.80 – 3.66 (m, 2H (C***H***$_2$N, C***H***$_2$OH)), 3.58 (ddd, *J* = 10.6, 7.7, 5.9 Hz, 1H (C***H***$_2$OH)), 2.85 – 2.66 (m, 2H (C***H***$_2$CH$_2$N), 2.66 – 2.49 (m, 2H (C***H***$_2$CH$_2$OH), 2.36 (s, 1H (O***H***)), 1.90 (d, *J* = 1.1 Hz, 3H (C***H***$_3$). ^{13}C NMR (101 MHz, $CDCl_3$) δ 169.3 (Bz ***C***O), 163.3 (C–***C***O–N), 150.0 (N–***C***O–N), 140.6 (***C***H=C), 135.1 (Bz ***C***H), 131.6 (Bz ***C***–CO), 130.6 (Bz ***C***H), 129.2 (Bz ***C***H), 110.6 (***C***=CH), 84.6 (Fc ***C***–CH$_2$CH$_2$OH), 82.6 (Fc ***C***–CH$_2$CH$_2$N), 69.4 (Cp ***C***H), 68.7 (Fc ***C***H), 68.4 (Fc ***C***H), 66.7 (Fc ***C***H), 63.5 (***C***H$_2$OH), 49.7 (***C***H$_2$N), 31.4 (***C***H$_2$CH$_2$OH), 27.9 (***C***H$_2$CH$_2$N), 12.4 (***C***H$_3$). IR ν_{max}/cm^{-1} = 3377 (OH), 3081 (Fc CH), 2928 (CH), 1742 (C=O), 1692 (C=O),

1640 (C=C). HRMS (ESI-TOF) m/z: $[M]^+$ Calcd for $C_{26}H_{26}FeN_2O_4$ 486.1242; Found 486.1244.

5.1.2.24 (R_p)-1-β-Hydroxyethyl-2-β-thyminylethyl-ferrocene Fcn2c2T$_{(Rp)}$

Novel compound



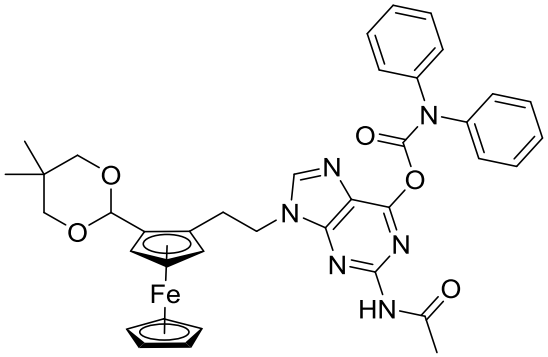
(R_p)-2-β-(*N*3-Benzoylthyminyl)ethyl-1-β-hydroxyethyl-ferrocene **3.22-(R_p)** (0.154 g, 0.317 mmol) was dissolved in NH_3 (7N in MeOH) (5 ml) and stirred at rt for 1 hr before the solvent was removed in vacuo. The crude product purified by flash column chromatography on silica gel using an eluent of EtOAc and the solvent was removed in vacuo. Recrystalisation from hot EtOAc produced orange crystals which were collected by filtration and dried in vacuo to give the title compound as an orange solid (0.111 g, 0.290 mmol, 92%) m.p. = 197 °C, ^{1}H NMR (400 MHz, $CDCl_3$) δ 10.02 (s, 1H, N***H***), 6.93 (q, *J* = 1.1 Hz, 1H (C***H***=C)), 4.13 (dd, *J* = 2.4, 1.3 Hz, 1H (Fc C***H***)), 4.04 (s, 5H (Cp C***H***)), 4.03 (dd, *J* = 2.4, 2.4 Hz, 1H (Fc C***H***), 3.95 (dd, *J* = 2.4, 1.3 Hz, 1H (Fc C***H***)), 3.85 – 3.60 (m, 4H (C***H***$_2$N, C***H***$_2$OH)), 3.20 (t, *J* = 5.3 Hz, 1H (O***H***)), 2.81 (ddd, *J* = 13.6, 9.1, 4.3 Hz, 1H (C***H***$_2$CH$_2$N)), 2.71 – 2.61 (m, 3H, (C***H***$_2$CH$_2$OH, C***H***$_2$CH$_2$N)), 1.90 (d, *J* = 1.1 Hz, 3H (C***H***$_3$)). ^{13}C NMR (101 MHz, $CDCl_3$) δ 164.6 (C–***C***O–N), 151.6 (N–***C***O–N), 140.6 (***C***H=C), 111.0 (***C***=CH), 84.4 (Fc ***C***–CH$_2$CH$_2$OH), 82.5 (Fc ***C***–CH$_2$CH$_2$N), 69.4 (Cp ***C***H), 68.9 (Fc ***C***H), 68.3 (Fc ***C***H), 66.7 (Fc ***C***H), 63.7 (***C***H$_2$OH), 50.1 (***C***H$_2$N), 31.7 (***C***H$_2$CH$_2$OH), 28.2 (***C***H$_2$CH$_2$N), 12.4 (***C***H$_3$). IR ν_{max}/cm^{-1} = 3477 (OH), 3149 (NH), 3019 (NH), 2921 (CH), 2851 (CH), 1736 (C=O), 1664 (C=C). HRMS (ESI-TOF) m/z: $[M + Na]^+$ Calcd for $C_{19}H_{22}FeN_2O_3Na$ 405.0878; Found

405.0874. Anal. Calcd for $C_{19}H_{22}FeN_2O_3$: C, 59.70; H, 5.80; N, 7.33. Found: C, 59.81; H, 5.99; N, 7.14.

With identical ^{1}H and ^{13}C NMR spectra, (S_p)-1-β-hydroxyethyl-2-β-thyminylethyl-ferrocene **Fcn2c2T**$_{(Sp)}$ was produced in one step from (R_p)-2-β-(*N*3-benzoylthyminyl)ethyl-1-β-benzyloxyethyl-ferrocene **3.21-(R_p)**. (R_p)-2-β-(*N*3-benzoylthyminyl)ethyl-1-β-benzyloxyethyl-ferrocene **3.21-(R_p)** (0.213 g, 0.370 mmol) was dissolved in EtOAc (5 ml) and hydrogen gas bubbled through the solution with stirring using a balloon and needle. $Pd(OH)_2/C$ (0.30 g) was added and the resulting mixture stirred at rt with bubbling and stirring for 1 hr. The mixture was filtered through a short pad of celite, washed with water (2 x 5 ml) and dried over $MgSO_4$. The crude product was dissolved in minimal hot EtOAc and allowed to cool, the title compound precipitated out as orange crystals which were collected by filtration and dried in vacuo (0.108 g, 0.283 mmol, 76 %). m.p. = 198 – 200 °C. Anal. Found C, 59.67; H, 5.75; N, 7.52.

5.1.2.25 (R_p)-2-β-*N*9-(2-*N*-Acetyl-*O*-6-diphenylcarbamoylguaninyl)ethyl-1-formyl-(3,3-dimethyl-1,5-pentanediol-acetal)ferrocene 3.23-(R_p)

Novel compound

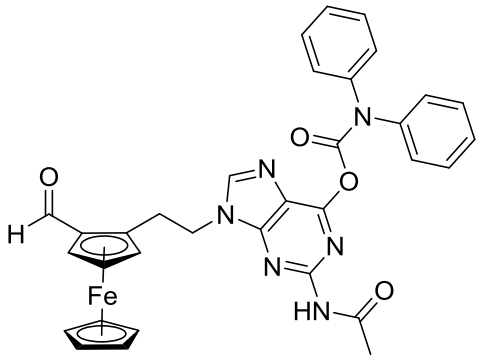


(R_p)-1-Formyl-(3,3-dimethyl-1,5-pentanediol-acetal)-2-β-hydroxyethyl-ferrocene **3.15-(R_p)** (0.36 g, 1.04 mmol, 1.0 eq.), PPh_3 (0.55 g, 2.08 mmol, 2.0 eq.) and 2-*N*-acetyl-6-*O*-

diphenylcarbamoylguanine **2.24** (0.61 g, 1.56 mmol, 1.5 eq.) were dissolved in dry THF (20 ml) in Schlenk tube, under an atmosphere of argon with stirring. The tube was wrapped in foil and heated to 70 °C, before DIAD (0.41 ml, 2.08 mmol, 2.0 eq.) was added dropwise and the resulting solution stirred at 70 °C for 1.5 hrs. The reaction mixture was quenched with brine, extracted with Et_2O and washed with water (2x 5 ml). The organic extracts were then dried over $MgSO_4$ and the solvent removed in vacuo. The crude product was then purified by flash column chromatography on neutralised silica gel using an eluent of 30% hexane in EtOAc. The solvent was removed in vacuo and the PPh_3 oxide impurity removed by repeated filtration through a short plug of neutralised silica gel, using an eluent of Et_2O. The solvent was removed in vacuo to give the title compound as an orange solid (0.48 g, 0.67 mmol, 64%) m.p. = 86 °C. ^{1}H NMR (300 MHz, $CDCl_3$) δ 8.14 (s, 1H (N***H***)), 7.59 (s, 1H (NC***H***=N)), 7.51 – 7.13 (m, 10 H (Ph C***H***)), 5.20 (s, 1H (C***H***OO)), 4.42 – 4.17 (m, 2H (C***H***$_2$N)), 4.30 (dd, *J* = 2.5, 1.4 Hz, 1H (Fc C***H***)), 4.09 (s, 5H (Cp C***H***)), 4.01 (dd, *J* = 2.5, 2.5 Hz, 1H (Fc C***H***)), 3.70 (dd, *J* = 2.5, 1.4 Hz, 1H (Fc C***H***)), 3.65 (m, 2H (C***H***$_2$O)), 3.53 (m, 2H (C***H***$_2$O)), 3.15 (ddd, *J* = 14.0, 6.7, 5.1 Hz, 1H (C***H***$_2$CH$_2$N)), 2.82 (ddd, *J* = 14.0, 8.3, 7.3 Hz, 1H (C***H***$_2$CH$_2$N)), 2.58 (s, 3H (C***H***$_3$CO)), 1.21 (s, 3H (C***H***$_3$CCH$_3$)), 0.75 (s, 3H (C***H***$_3$CCH$_3$)). ^{13}C NMR (101 MHz, $CDCl_3$) δ 171.2 (***C***OCH$_3$), 156.0 (***C***OO), 155.1 (N=***C***N$_2$), 152.0 (N$_2$***C***=CN), 150.5 (N=***C***O), 144.7 (N***C***H=N), 141.9 (Ph ***C***–N), 129.2 (Ph ***C***H), 127.1 (Ph ***C***H), 120.9 (N***C***=CN$_2$), 101.0 (***C***HOO), 84.2 (Fc ***C***–CHOO), 81.9 (Fc ***C***–CH$_2$), 77.8 (***C***H$_2$O), 77.8 (***C***H$_2$O), 69.7 (Fc ***C***H), 69.6 (Cp ***C***H), 68.0 (Fc ***C***H), 67.0 (Fc ***C***H), 45.4 (***C***H$_2$N), 30.1 (***C***(CH$_3$)$_2$), 29.2 (***C***H$_2$CH$_2$N), 25.3 (***C***H$_3$CO), 23.3 (***C***H$_3$CCH$_3$), 22.0 (***C***H$_3$CCH$_3$). IR ν_{max}/cm^{-1} = 3101 (Fc CH), 2954 (CH), 2847 (CH), 1744 (C=O), 1700 (C=O), 1621 (C=C). HRMS (ESI-TOF) m/z: $[M + H]^+$ Calcd for $C_{38}H_{39}FeN_6O_5$ 715.2331; Found 715.2328.

5.1.2.26 (R_p)-2-β-*N*9-(2-*N*-Acetyl-*O*6-diphenylcarbamoylguaninyl)ethyl-1-formyl-ferrocene 3.24-(R_p)

Novel compound

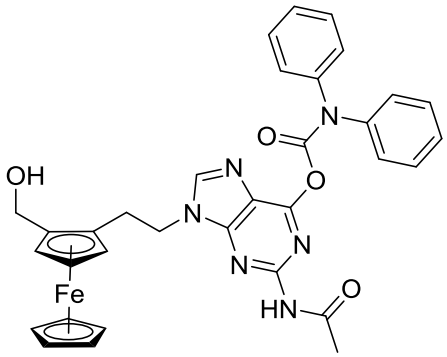


(R_p)-2-β-*N*9-(2-*N*-Acetyl-*O*-6-diphenylcarbamoylguaninyl)ethyl-1-formyl-(3,3-dimethyl-1,5-pentanediol-acetal)ferrocene **3.23-(R_p)** (0.48 g, 0.67 mmol, 1.0 eq.) was dissolved in a mixture of THF (4.5 ml) and water (0.5 ml), before PTSA (0.25 g, 1.34 mmol, 2.0 eq.) was added and the resulting yellow solution stirred for 10 mins. The resulting red solution was neutralised with sat. $NaHCO_3$ (10 ml), extracted with Et_2O, washed with water (2x 5ml) and dried over $MgsO_4$. The solvent was removed in vacuo and the crude product purified by flash column chromatography on neutralised silica gel using an eluent of 20% hexane in EtOAc. The solvent was removed in vacuo to give the title compound as a red solid (0.39 g, 0.62 mmol, 92%) m.p. = 70 °C. ^{1}H NMR (400 MHz, $CDCl_3$) δ 9.97 (s, 1H (C***H***O)), 8.31 (s, 1H (N***H***)), 7.69 (s, 1H (NC***H***=N)), 7.40 (d, *J* = 7.5 Hz, 4H (Ph C***H***)), 7.34 (dd, *J* = 7.5, 7.4 Hz, 4H (Ph C***H***)), 7.22 (t, *J* = 7.4 Hz, 2H (Ph C***H***)), 4.65 (dd, *J* = 2.7, 1.4 Hz, 1H (Fc C***H***)), 4.39 (dd, *J* = 2.7, 2.7 Hz, 1H (Fc C***H***)), 4.36 (dd, *J* = 13.6, 5.0, 2.6 Hz, 1H (C***H***$_2$N)), 4.33 (dd, *J* = 7.6, 4.9 Hz, 1H (C***H***$_2$N)), 4.26 – 4.20 (m, 2H (Fc C***H***, C***H***$_2$N)), 4.18 (s, 5H (Cp)), 3.39 (ddd, *J* = 13.9, 6.9, 4.9 Hz, 1H (C***H***$_2$CH$_2$N)), 2.97 (ddd, *J* = 13.9, 7.9, 7.8 Hz, 1H (C***H***$_2$CH$_2$N)), 2.53 (s, 3H (C***H***$_3$)). ^{13}C NMR (101 MHz, $CDCl_3$) δ 194.1 (***C***HO), 171.0 (***C***OCH$_3$), 156.0 (***C***OO), 155.1 (N=***C***N$_2$), 152.0 (N$_2$***C***=CN), 150.5 (N=***C***O), 144.3 (N***C***H=N), 141.8 (Ph ***C***–N), 129.2 (Ph ***C***H), 127.1 (Ph ***C***H), 120.7 (N***C***=CN$_2$), 85.1 (Fc ***C***–CH$_2$CH$_2$), 75.2 (Fc ***C***H), 72.9 (Fc

CH), 72.0 (Fc ***C***H), 71.3 (Fc ***C***–CHO), 70.4 (Cp ***C***H), 45.2 (***C***H_2N), 29.6 (***C***H_2CH_2N), 25.2 (***C***H_3). IR ν_{max}/cm^{-1} = 3098 (Fc CH), 3010 (Ph CH), 2929 (CH), 1736 (C=O), 1667 (C=O), 1620 (C=C). HRMS (ESI-TOF) m/z: $[M + H]^+$ Calcd for $C_{33}H_{29}FeN_6O_4$ 629.1600; Found 629.1587.

5.1.2.27 (R_p)-2-β-*N*9-(2-*N*-Acetyl-*O*-6-diphenylcarbamoylguaninyl)ethyl-1-hydroxymethyl-ferrocene 3.25-(R_p)

Novel compound

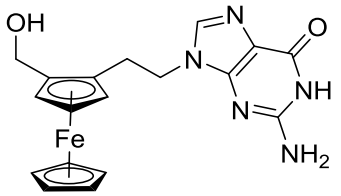


(R_p)-2-β-*N*9-(2-*N*-Acetyl-*O*6-diphenylcarbamoylguaninyl)ethyl-1-formyl-ferrocene **3.24-(R_p)** was dissolved in MeOH (5 ml) and the red solution cooled to 0 °C with stirring. $NaBH_4$ was added in small portions and the solution stirred at 0 °C for 15 mins. The resulting yellow solution was quenched by the dropwise addition of water (3 ml), extracted with DCM and dried over $MgSO_4$. The solvent was removed in vacuo and the crude product purified by flash column chromatography using an eluent of 100% EtOAc. The solvent was removed in vacuo to give the title compound as a yellow solid (0.33 g, 0.52 mmol, 85%) m.p. = 112 – 115 °C. ^{1}H NMR (400 MHz, $CDCl_3$) δ 8.80 (s, 1H (N***H***)), 7.78 (s, 1H (NC***H***=N)), 7.40 (d, *J* = 7.6 Hz, 4H (Ph C***H***)), 7.36 – 7.28 (m, 4H (Ph C***H***)), 7.21 (t, *J* = 7.3 Hz, 2H (Ph C***H***)), 4.53 (d, *J* = 11.9 Hz, 1H), 4.34 *J* = 11.9 Hz, 1H), (d, 4.35 – 4.19 (m, 2H (C***H***$_2$N)), 4.09 (dd, *J* = 2.5, 1.4 Hz, 1H (Fc C***H***)), 3.98 (s, 5H (Cp C***H***)), 3.87 (dd, *J* = 2.5, 2.4 Hz, 1H (Fc C***H***)), 3.68 (dd, *J* = 2.4, 1.4 Hz, 1H (Fc C***H***)), 2.97 (ddd, *J* = 13.9, 7.4, 4.4 Hz, 1H (C***H***$_2$CH$_2$N)), 2.68 (ddd, *J* =

13.9, 8.5 Hz, 1H (C***H***$_2$CH$_2$N)), 2.34 (s, 3H (C***H***$_3$)). ^{13}C NMR (101 MHz, $CDCl_3$) δ 170.1 (***C***OCH$_3$), 155.7 (***C***OO), 155.2 (N=***C***N$_2$), 151.7 (N$_2$***C***=CN), 150.5 (N=***C***O), 144.5 (N***C***H=N), 141.7 (Ph ***C***–N), 129.2 (Ph ***C***H), 127.0 (Ph ***C***H), 120.7 (N***C***=CN$_2$), 85.5 (Fc ***C***–CH$_2$OH), 83.0 (Fc ***C***–CH$_2$CH$_2$), 70.0 (Fc ***C***H), 69.5 (Fc ***C***H), 68.9 (Cp ***C***H), 66.6 (Fc ***C***H), 59.2 (***C***H$_2$OH), 45.2 (***C***H$_2$N), 29.5 (***C***H$_2$CH$_2$N), 25.0 (***C***H$_3$). IR ν_{max}/cm^{-1} = 3309 (OH), 3096 (Fc CH), 2924 (CH), 1736 (C=O), 1620 (C=C). HRMS (ESI-TOF) m/z: $[M + H]^+$ Calcd for $C_{33}H_{31}FeN_6O_4$ 631.1756; Found 631.1759.

5.1.2.28 (***R$_p$***)-2-β-*N*9-Guaninylethyl-1-hydroxymethyl-ferrocene Fcn1c2G$_{(Rp)}$

Novel compound

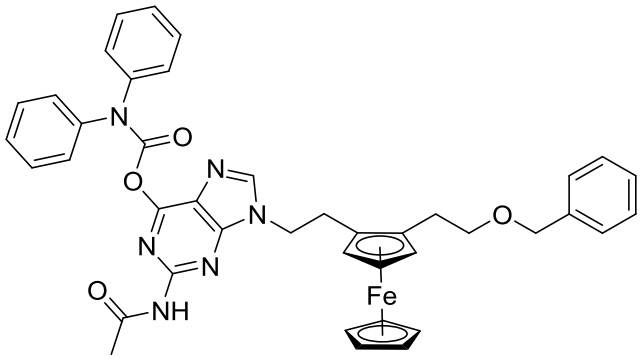


(*R$_p$*)-2-β-*N*9-(2-*N*-Acetyl-*O*-6-diphenylcarbamoylguaninyl)ethyl-1-hydroxymethyl-ferrocene **3.25-(*R$_p$*)** (0.10 g, 0.16 mmol, 1.0 eq.) was dissolved in NH_3 (7N in MeOH) (5 ml) and stirred at rt for 4 hrs. Brine was added and the solution left standing for 16 hrs producing yellow crystals of the title compound, which were collected by filtration and dried in vacuo (0.029 g, 0.075 mmol, 46%) Degraded above 100 °C. ^{1}H NMR (400 MHz, DMSO) δ 10.57 (s, 1H (N***H***)), 7.48 (s, 1H (NC***H***=N)), 6.43 (s, 2H (N***H***$_2$), 4.76 (dd, *J* = 6.1, 4.4 Hz, 1H (O***H***)), 4.31 (dd, *J* = 12.2, 6.1 Hz, 1H (C***H***$_2$OH)), 4.18 (dd, *J* = 12.2, 4.4 Hz, 1H (C***H***$_2$OH)), 4.14 (dd, *J* = 2.5, 1.5 Hz, 1H (Fc C***H***)), 4.12 – 3.99 (m, 2H (CH$_2$C***H***$_2$N)), 4.07 (s, 5H (Cp C***H***)), 3.96 (dd, *J* = 2.5, 2.4 Hz, 1H (Fc C***H***)), 3.88 (dd, J = 2.4, 1.5 Hz, 1H (Fc C***H***)), 2.88 – 2.69 (m, 2H (C***H***$_2$CH$_2$N)). ^{13}C NMR (101 MHz, DMSO) δ 156.9 (***C***O), 153.5 (N=***C***N$_2$), 151.0 (N$_2$***C***=CN), 137.4 (N***C***H=N), 116.6 (N***C***=CN$_2$), 86.3 (Fc ***C***–CH$_2$OH), 83.5 (Fc ***C***–CH$_2$CH$_2$), 68.8 (Fc ***C***H), 68.8 (Cp ***C***H), 68.2 (Fc ***C***H), 65.6 (Fc ***C***H), 57.7 (***C***H$_2$OH), 43.5 (***C***H$_2$N), 28.1

(***C***H_2CH_2N). IR ν_{max}/cm^{-1} = 3600 (OH), 3313 (NH), 3180 (NH), 2855 (CH), 2717 (CH), 1702 (C=O), 1634 (C=N), 1605 (C=C). HRMS (ESI-TOF) m/z: $[M + H]^+$ Calcd for $C_{18}H_{20}FeN_5O_2$ 394.0966; Found 394.0954.

5.1.2.29 (S_p)-2-β-*N*9-(*N*2-Acetyl-*O*6-diphenylcarbamoylguaninyl)ethyl-1-β-benzyloxyethyl-ferrocene 3.26-(S_p)

Novel compound

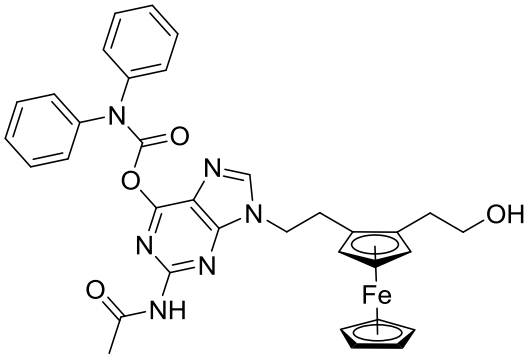


(S_p)-1-β-Benzyloxyethyl-2-β-hydroxyethyl-ferrocene **3.20-(S_p)** (0.182 g, 0.50 mmol, 1.0 eq.), PPh_3 (0.26 g, 1.00 mmol, 2.0 eq.) and 2-*N*-acetyl-6-*O*-diphenylcarbamoylguanine **2.24** (0.29 g, 0.75 mmol, 1.5 eq.) were dissolved in dry THF (10 ml) in Schlenk tube, under an atmosphere of argon with stirring. The tube was wrapped in foil and heated to 70 °C, before DIAD (0.20 ml, 1.00 mmol, 2.0 eq.) was added dropwise and the resulting solution stirred at 70 °C for 0.5 hrs. The reaction mixture was quenched with brine, extracted with Et_2O and dried over $MgSO_4$ before the solvent removed in vacuo. The crude product was then purified by flash column chromatography on neutralised silica gel using an gradient eluent of 40 → 20% hexane in EtOAc. The solvent was removed in vacuo and the PPh_3 oxide impurity removed by repeated filtration through a short plug of neutralised silca gel, using an eluent of Et_2O. The solvent was removed in vacuo to give the title compound as a yellow solid (0.31 g, 0.42 mmol, 84%). m.p. = 84 °C. ^{1}H NMR (400 MHz, $CDCl_3$) δ 8.44 (s, 1H (N***H***)), 7.51 (s, 1H (NC***H***=N)), 7.45 – 7.17 (m, 15H (Ph C***H***)), 4.47 (d, *J* = 11.8 Hz, 1H (Bn C$\boldsymbol{H}_2$O)), 4.43 (d,

J = 11.8 Hz, 1H (Bn C***H***$_2$O)), 4.25 – 4.02 (m, 2H (C***H***$_2$N)), 4.10 (dd, *J* = 2.5, 1.4 Hz, 1H (Fc C***H***)), 3.98 (s, 5H (Cp C***H***)), 3.97 (dd, *J* = 2.5, 2.3 Hz, 1H (Fc C***H***)), 3.74 (dd, *J* = 2.5, 1.4 Hz, 1H (Fc C***H***)), 3.61 (dt, *J* = 8.9, 6.0 Hz, 1H (CH$_2$***C***H$_2$O)), 3.48 (dt, *J* = 8.9, 7.3 Hz, 1H (CH$_2$***C***H$_2$O)), 2.91 – 2.74 (m, 2H (C***H***$_2$CH$_2$O)), 2.63 (dd, *J* = 6.9, 5.3 Hz, 2H (C***H***$_2$CH$_2$N)), 2.54 (s, 3H (C***H***$_3$)). ^{13}C NMR (101 MHz, $CDCl_3$) δ 171.0 (***C***OCH$_3$), 155.9 (***C***OO), 154.9 (N=***C***N$_2$), 152.0 (N$_2$***C***=CN), 150.4 (N=***C***O), 144.3 (N***C***H=N), 141.8 (Carb Ph ***C***–N), 138.0 (Bn ***C***–CH$_2$), 129.1 (Carb Ph ***C***H), 128.4 (Bn ***C***H), 127.8 (Bn ***C***H), 127.7 (Bn ***C***H), 120.7 (N***C***=CN$_2$), 84.5 (Fc ***C***–CH$_2$CH$_2$O), 82.5 (Fc ***C***–CH$_2$CH$_2$N), 73.1 (Bn ***C***H$_2$O), 71.1 (CH$_2$***C***H$_2$O), 69.2 (Cp ***C***H), 68.6 (Fc ***C***H), 68.0 (Fc ***C***H), 66.5 (Fc ***C***H), 45.0 (***C***H$_2$N), 28.7 (***C***H$_2$CH$_2$O), 28.6 (***C***H$_2$CH$_2$N), 25.2 (***C***H$_3$). IR ν_{max}/cm^{-1} = 2857 (CH), 1738 (C=O), 1619 (C=C). HRMS (ESI-TOF) m/z: $[M + Na]^+$ Calcd for $C_{41}H_{38}FeN_6O_4Na$ 757.2202; Found 757.2201.

5.1.2.30 (*S*$_p$)-2-β-*N*9-(*N*2-Acetyl-*O*6-diphenylcarbamoylguaninyl)ethyl-1-β-hydroxyethyl-ferrocene 3.27-(*S*$_p$)

Novel compound

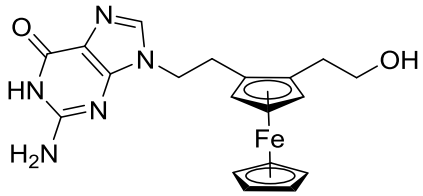


(*S*$_p$)-2-β-*N*9-(*N*2-Acetyl-*O*6-diphenylcarbamoylguaninyl)ethyl-1-β-benzyloxyethyl-ferrocene **3.26-(*S*$_p$)** (0.31 g, 0.42 mmol) was dissolved in EtOAc (10 ml) and $Pd(OH)_2/C$ (0.30 g) added. A balloon containg H_2 gas was attached to the top of the flask and the mixture stirred at rt for 3 hrs. The crude mixture was filtered by flushing through a plug of celite using

EtOAc and the solvent removed in vacuo. The crude product was then purified by flash column chromatography on silica gel using an gradient eluent of 0 → 5% MeOH in EtOAc. The solvent was removed in vacuo to give the title compound as a yellow solid (0.25 g, 0.39 mmol, 94%). m.p = 103 – 104 °C. ^{1}H NMR (400 MHz, $CDCl_3$) δ 8.70 (s, 1H (N***H***)), 7.78 (s, 1H (NC***H***=N)), 7.15 – 7.49 (m, 10H (Ph C***H***)), 4.42 (m, 1H (C***H***$_2$N)), 4.01 – 4.10 (m, 1H (C***H***$_2$N)), 4.08 (dd, *J* = 2.5, 1.4 Hz, 1H (Fc C***H***)), 3.98 – 4.00 (m, 1H (Fc C***H***)), 3.98 (s, 5H (Cp C***H***)), 3.83 – 3.93 (m, 1H (C***H***$_2$O)), 3.75 (s, 1H (O***H***)), 3.60 – 3.43 (m, 1H (C***H***$_2$O)), 2.98 (ddd, *J* = 13.9, 9.7, 4.8 Hz, 1H (C***H***$_2$CH$_2$N)), 2.69 (ddd, *J* = 13.9, 10.0, 7.0 Hz, 1H (C***H***$_2$CH$_2$N)), 2.52 – 2.64 (m, 2H (C***H***$_2$CH$_2$O)), 2.32 (s, 3H C***H***$_3$)). ^{13}C NMR (101 MHz, $CDCl_3$) δ 169.6 (***C***OCH$_3$), 155.8 (***C***OO), 155.1 (N=***C***N$_2$), 151.7 (N$_2$***C***=CN), 150.6 (N=***C***O), 144.4 (N***C***H=N), 141.8 (Ph ***C***–N), 129.3 (Ph ***C***H), 127.4 (Ph ***C***H), 121.1 (N***C***=CN$_2$), 85.3 (Fc ***C***–CH$_2$CH$_2$O), 82.7 (Fc ***C***–CH$_2$CH$_2$N), 69.3 (Cp ***C***H), 68.8 (Fc ***C***H), 68.2 (Fc ***C***H), 66.6 (Fc ***C***H), 63.8 (***C***H$_2$OH), 45.7 (***C***H$_2$N), 32.1 (***C***H$_2$CH$_2$OH), 29.5 (***C***H$_2$CH$_2$N), 25.1 (***C***H$_3$). IR ν_{max}/cm^{-1} = 3257 (NH), 3096 (Ph CH), 3014 (Ph CH), 2855 (CH), 1736 (C=O), 1620 (C=C). HRMS (ESI-TOF) m/z: [M + Na]$^+$ Calcd for $C_{34}H_{32}FeN_6O_4Na$ 667.1732; Found 667.1724.

5.1.2.31 (*S*$_p$)-2-β-*N*9-guaninylethyl-1-β-hydroxyethyl-ferrocene Fcn2c2G$_{(Sp)}$

Novel compound

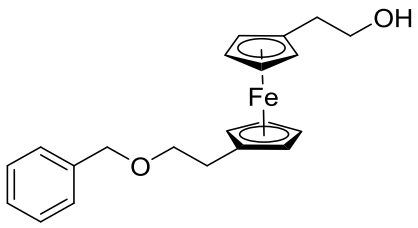


(*S*$_p$)-2-β-*N*9-(*N*2-Acetyl-*O*6-diphenylcarbamoylguaninyl)ethyl-1-β-hydroxyethyl-ferrocene **3.27-(*S*$_p$)** (0.25 g, 0.39 mmol) was dissolved in NH_3 (7N in MeOH) (10 ml) and stirred at rt for 3 hrs. Small, yellow needle-like crystals were formed which were collected by filtration and dried in vacuo to give the title compound (0.14 g, 0.35 mmol, 89 %). Decomposed above

180 °C. ^{1}H NMR (400 MHz, DMSO-d_6) δ 10.55 (s, 1H (N***H***)), 7.54 (s, 1H (NC***H***=N)), 6.40 (s, 2H (N***H***$_2$)), 4.60 (dd, *J* = 5.2, 5.2 Hz, 1H (C***H***$_2$N)), 4.08 (dd, *J* = 2.5, 1.4 Hz, 1H (Fc C***H***)), 4.06 (s, 1H (C***H***$_2$N))), 4.04 (s, 5H (Cp C***H***)), 3.94 (dd, *J* = 2.5, 2.5 Hz, 1H (Fc C***H***)), 3.90 (dd, *J* = 2.5, 1.4 Hz, 1H (Fc C***H***)), 3.55 – 3.38 (m, 2H (C***H***$_2$OH)), 2.86 – 2.69 (m, 2H (C***H***$_2$-CH2N)), 2.42 (tt, *J* = 14.4, 6.8 Hz, 2H (C***H***$_2$CH$_2$O)). ^{13}C NMR (101 MHz, DMSO) δ 156.8 (***C***O), 153.4 (N=***C***N$_2$), 151.0 (N$_2$***C***=CN), 137.5 (N***C***H=N), 116.6 (N***C***=CN$_2$), 84.5 (Fc ***C***–CH$_2$CH$_2$O), 83.2 (Fc ***C***–CH$_2$CH$_2$N), 69.0 (Cp ***C***H), 68.0 (Fc ***C***H), 67.1 (Fc ***C***H), 65.4 (Fc ***C***H), 61.7 (***C***H$_2$OH), 43.4 (***C***H$_2$N), 31.0 (***C***H$_2$CH$_2$OH), 28.1 (***C***H$_2$CH$_2$N). IR ν_{max}/cm^{-1} = 3294 (NH), 3168 (NH), 1696 (C=O), 1632 (C=C). HRMS (ESI-TOF) m/z: [M]$^{+}$ Calcd for $C_{19}H_{21}FeN_5O_2$ 407.1045; Found 407.1039.

5.1.2.32 1-β-Benzyloxyethyl-1′-β-hydroxyethyl-ferrocene 3.28

Novel compound

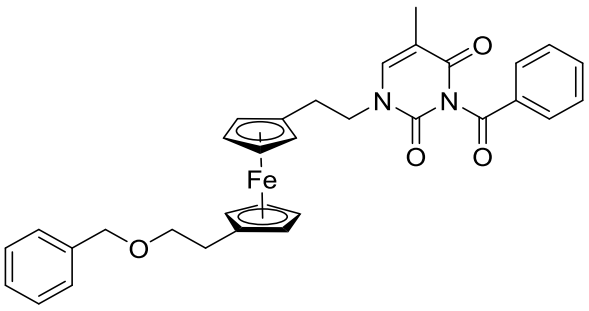


1,1'-Di(β-hydroxyethyl)ferrocene **2.35** (0.50 g, 1.82 mmol, 1.0 eq.) was dissolved in dry DMF (25 ml) in a Schlenk tube under an atmsphere of argon and cooled to 0 °C in an ice bath with stirring. NaH (0.044 g, 1.82 mmol, 1.0 eq.) was added slowly, in small portions and the resulting solution stirred at 0 °C for 15 mins before being slowly warmed to rt and stirring continued for a further 16 hrs. The reaction was quenched by the dropwise addition of brine and the reaction mixture extracted with DCM. The extracts were washed with brine (10 ml), then water (10 ml) before being dried over MgSO4 and the solvent removed in vacuo. The crude product was purified by flash column chromatography on silica gel using an eluent of 10 → 90% EtOAc in hexane. The solvent was removed to give the title compound as a

yellow oil (0.28 g, 0.78 mmol, 43 %). ^{1}H NMR (400 MHz, $CDCl_3$) δ 7.39 – 7.27 (m, 5H (Ph C***H***)), 4.53 (s, 2H (Bn C***H***$_2$)), 4.08 – 4.01 (m, 8H (Fc C***H***)), 3.68 (t, *J* = 6.6 Hz, 2H (C***H***$_2$OBn)), 3.60 (t, *J* = 7.2 Hz, 2H (C***H***$_2$OH)), 2.66 (t, *J* = 7.2 Hz, 2H (C***H***$_2$CH$_2$OH)), 2.56 (t, *J* = 6.6 Hz, 2H (C***H***$_2$CH$_2$OBn)) 1.89 (s, 1H (O***H***)). ^{13}C NMR (101 MHz, $CDCl_3$) δ 138.4 (Ph ***C***–CH$_2$), 128.4 (Ph ***C***H), 127.8 (Ph ***C***H), 127.6 (Ph ***C***H), 85.5 (Fc ***C***–CH$_2$CH$_2$OBn), 84.8 (Fc ***C***–CH$_2$CH$_2$OH), 73.0 (Bn ***C***H$_2$), 71.2 (***C***H$_2$OBn), 69.2 (Fc ***C***H), 69.1 (Fc ***C***H), 68.4 (Fc ***C***H), 68.2 (Fc ***C***H), 63.6 (***C***H$_2$OH), 32.7 (***C***H$_2$CH$_2$OBn), 29.9 (***C***H$_2$CH$_2$OH). IR ν_{max}/cm^{-1} = 3380 (OH), 3085 (Fc CH), 3031 (Ph CH), 2934 (CH), 2858 (CH). HRMS (ESI-TOF) m/z: [M]$^+$ Calcd for $C_{21}H_{24}FeNO_2$ 364.1126; Found 364.1114.

5.1.2.33 1-β-Benzyloxyethyl-1′-β-(*N*3-benzoylthyminyl)ethyl-ferrocene 3.29

Novel compound

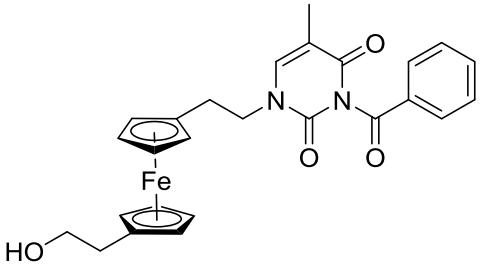


1-β-Benzyloxyethyl-1′-β-hydroxyethyl-ferrocene **3.28** (0.12 g, 0.32 mmol, 1.0 eq.) was dissolved in dry THF (6 ml), with PPh_3 (0.17 g, 0.64 mmol, 2.0 eq.) and *N*3-benzoyl thymine **2.21** (0.11 g, 0.48 mmol, 1.5 eq.) in Schlenk tube under an atmosphere of argon. The tube was wrapped in foil and heated to 45 °C before DIAD (0.13 ml, 0.64 mmol, 2.0 eq.) was added dropwise and the resulting solution stirred at 45 °C for 1 hr. The reaction was quenched with brine and extracted with DCM, dried over $MgSO_4$ and the solvent removed in vacuo. The crude product was purified by column chromatography on silica gel using a gradient eluent of 10 → 50% EtOAc in hexane. The solvent was removed in vacuo to give the title compound as an orange oil (0.14 g, 0.25 mmol, 79%). ^{1}H NMR (400 MHz, $CDCl_3$) δ

7.91 (dd, *J* = 8.4, 1.3 Hz, 2H (Bz C***H***)), 7.64 (tt, *J* = 7.4, 1.3 Hz, 1H (Bz C***H***)), 7.50 (dd, *J* = 8.4, 7.4 Hz, 2H (Bz C***H***)), 7.39 – 7.26 (m, 5H (Bn C***H***)), 6.79 (q, *J* = 1.1 Hz, 1H (C***H***=C)), 4.51 (s, 2H (Bn C$\boldsymbol{H}_2$)), 4.07 (dd, *J* = 2.7, 1.1 Hz, 2H (Fc C***H***)), 4.06 – 4.02 (m, 4H (Fc CH)), 3.95 (dd, *J* = 2.7, 1.1 Hz, 2H), 3.78 (t, *J* = 7.1 Hz, 2H (C$\boldsymbol{H}_2$N)), 3.57 (t, *J* = 7.1 Hz, 2H (C$\boldsymbol{H}_2$OBn)), 2.70 (t, *J* = 7.1 Hz, 2H (C$\boldsymbol{H}_2$CH$_2$N)), 2.63 (t, *J* = 7.1 Hz, 2H (C$\boldsymbol{H}_2$CH$_2$O)), 1.86 (d, *J* = 1.1 Hz, 3H (C$\boldsymbol{H}_3$)). ^{13}C NMR (101 MHz, CDCl$_3$) δ 169.2 (Bz ***C***O), 163.3 (CH=C***C***ON), 149.7 (N***C***ON), 140.8 (***C***H=C), 138.5 (Bn ***C***–CH$_2$), 135.0 (Bz ***C***H), 131.7 (Bz ***C***–CO), 130.5 (Bz ***C***H), 129.2 (Bz ***C***H), 128.5 (Bn ***C***H), 127.8 (Bn ***C***H), 127.6 (Bn ***C***H), 110.0 (CH=**C**), 85.8 (Fc ***C***–CH$_2$CH$_2$O), 83.5 (Fc ***C***–CH$_2$CH$_2$N), 73.0 (Bn ***C***H$_2$), 71.2 (***C***H$_2$OBn), 69.4 (Fc ***C***H), 69.1 (Fc ***C***H), 68.8 (Fc ***C***H), 68.3 (Fc ***C***H), 50.4 (***C***H$_2$N), 29.9 (***C***H$_2$CH$_2$O), 29.0 (***C***H$_2$CH$_2$N), 12.3 (***C***H$_3$). IR ν_{max}/cm^{-1} = 3074 (Fc CH), 2924 (CH), 2854 (CH), 1744 (C=O), 1696 (C=O), 1647 (C=O) 1598 (C=C). HRMS (ESI-TOF) m/z: [M + Na]$^+$ Calcd for $C_{33}H_{32}FeN_2O_4Na$ 599.1609; Found 599.1608.

5.1.2.34 1′-β-(*N*3-benzoylthyminyl)ethyl-1-β-hydroxyethyl-ferrocene 3.30

Novel compound

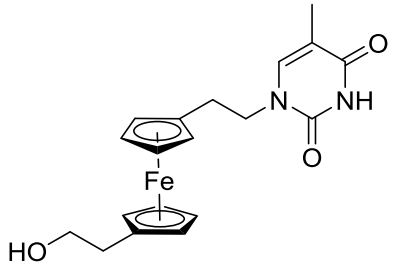


1-β-Benzyloxyethyl-1′-β-(*N*3-benzoylthyminyl)ethyl-ferrocene **3.29** (0.14 g, 0.25 mmol) was dissolved in EtOAc with stirring and H_2 gas bubbled through the solution using a balloon and needle. Pd(OH)$_2$/C (0.15 g) was added with stirring and the bubbling of H_2 gas continued for 15 mins. The reaction mixture was filtered through celite and washed through with EtOAc before the solvent was removed in vacuo. The crude product was purified by flash column

chromatography using an eluent of 20 → 10% hexane in EtOAc. The solvent was removed in vacuo to give the title compound as a yellow oil (0.12 g, 0.25 mmol, 98 %). ^{1}H NMR (400 MHz, $CDCl_3$) δ 7.90 (dd, *J* = 8.3, 1.4 Hz, 2H (Bz C***H***)), 7.65 (tt, *J* = 7.5, 1.4 Hz, 1H (Bz C***H***)), 7.50 (dd, *J* = 8.3, 7.5 Hz, 2H (Bz C***H***)), 6.80 (q, *J* = 1.2 Hz, 1H (C***H***=C)), 4.09 – 4.07 (m, 2H (Fc C***H***)), 4.07 – 4.04 (m, 4H (Fc C***H***)), 3.98 – 3.97 (m, 2H (Fc C***H***)), 3.80 (t, *J* = 7.1 Hz, 2H ($C\boldsymbol{H}_2$N)), 3.68 (dd, *J* = 11.9, 6.4 Hz, 2H ($C\boldsymbol{H}_2$OH)), 2.72 (t, *J* = 7.1 Hz, 2H ($C\boldsymbol{H}_2CH_2$N)), 2.55 (t, *J* = 6.4 Hz, 2H ($C\boldsymbol{H}_2CH_2$OH)), 1.86 (d, *J* = 1.2 Hz, 3H ($C\boldsymbol{H}_3$)), 1.65 (s, 1H (O***H***)). ^{13}C NMR (101 MHz, $CDCl_3$) δ 169.2 (Bz ***C***O), 163.3 (CH=C***C***ON), 149.8 (N***C***ON), 140.7 (***C***H=C), 135.1 (Bz ***C***H), 131.7 (Bz ***C***–CO), 130.6 (Bz ***C***H), 129.3 (Bz ***C***H), 110.2 (CH=**C**), 85.4 (Fc ***C***–CH_2CH_2O), 83.6 (Fc ***C***–CH_2CH_2N), 69.4 (Fc ***C***H), 69.2 (Fc ***C***H), 69.0 (Fc ***C***H), 68.7 (Fc ***C***H), 63.6 (***C***H_2OH), 50.5 (***C***H_2N), 32.8 (***C***H_2CH_2O), 29.0 (***C***H_2CH_2N), 12.4 (***C***H_3). IR ν_{max}/cm^{-1} = 3478 (OH), 3075 (Fc CH), 3010 (ar CH), 2929 (CH), 1742 (C=O), 1693 (C=O), 1639 (C=O), 1598 (C=C). HRMS (ESI-TOF) m/z: $[M + Na]^+$ Calcd for $C_{26}H_{26}FeN_2O_4Na$ 509.1140; Found 509.1138.

5.1.2.35 1′-β-thyminylethyl-1-β-hydroxyethyl-ferrocene Fcn2c2T

Novel compound

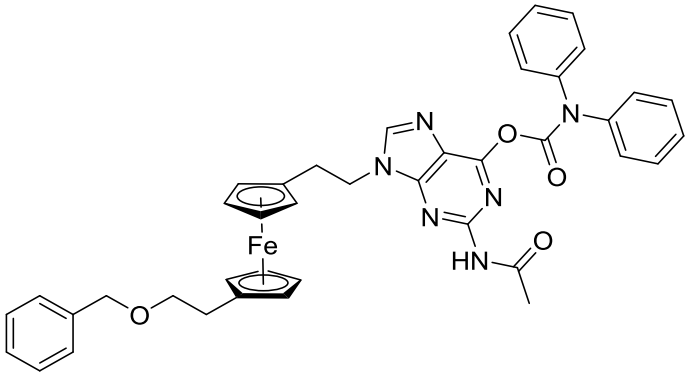


1′-β-(*N*3-benzoylthyminyl)ethyl-1-β-hydroxyethyl-ferrocene **3.30** (0.12 g, 0.25 mmol) was dissolved in $MeNH_2$ (33% in EtOH) (15 ml) and stirred at rt for 30 mins. Water was then added and the reaction mixture extracted with DCM before drying over $MgSO_4$ and the solvent removed in vacuo. The crude product was then purified by flash column

chromatography on silica gel using an eluent of EtOAc. The solvent was removed in vacuo to give the title compound as a yellow solid (0.085 g, 0.22 mmol, 91%). m.p. = 206 – 209 °C. ^{1}H NMR (400 MHz, $CDCl_3$) δ 9.49 (s, 1H (N***H***)), 6.67 (q, *J* = 1.1 Hz, 1H (C***H***=C)), 4.08 – 4.04 (m, 6H (Fc C***H***)), 3.96 – 3.95 (m, 2H (Fc C***H***)), 3.77 (t, *J* = 7.1 Hz, 2H (C***H***$_2$N)), 3.69 (t, *J* = 6.2 Hz, 2H (C***H***$_2$OH)), 2.69 (t, *J* = 7.1 Hz, 2H (C***H***$_2$CH$_2$N)), 2.56 (t, *J* = 6.6 Hz, 2H (C***H***$_2$CH$_2$OH)), 2.03 (s, *J* = 1.3 Hz, 1H (O***H***)), 1.82 (d, *J* = 1.1 Hz, 3H (C***H***$_3$)). ^{13}C NMR (101 MHz, $CDCl_3$) δ 164.6 (C***C***ON), 151.1 (N***C***ON), 141.2 (***C***H=C), 110.1 (CH=**C**), 85.4 (Fc ***C***–CH$_2$CH$_2$O), 83.9 (Fc ***C***–CH$_2$CH$_2$N), 69.4 (Fc ***C***H), 69.2 (Fc ***C***H), 68.8 (Fc ***C***H), 68.6 (Fc ***C***H), 63.6 (***C***H$_2$OH), 50.4 (***C***H$_2$N), 32.8 (***C***H$_2$CH$_2$OH), 29.0 (***C***H$_2$CH$_2$N), 12.3 (***C***H$_3$). IR ν_{max}/cm^{-1} = 3396 (OH), 3169 (NH), 3025 (Fc CH), 2926 (CH), 1660 (C=O), 1652 (C=C). HRMS (ESI-TOF) m/z: [M + Na]$^+$ Calcd for $C_{19}H_{22}FeN_2O_3$ 405.0878; Found 405.0880.

5.1.2.36 1′-β-(2-*N*-Acetyl-6-*O*-diphenylcarbamoylguaninyl)ethyl-1-β-benzyloxyethyl-ferrocene 3.31

Novel compound

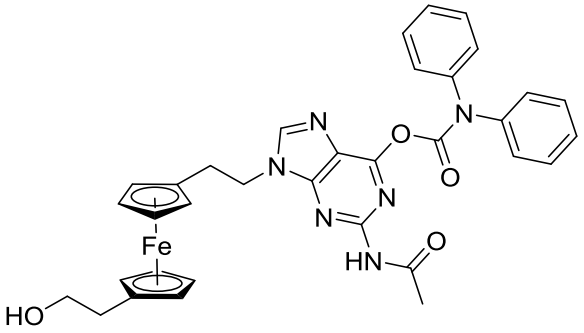


1-β-Benzyloxyethyl-1′-β-hydroxyethyl-ferrocene **3.28** (0.28 g, 0.78 mmol, 1.0 eq.) was dissolved in dry THF, in a Schlenk tube under an atmosphere of argon. PPh_3 (0.41 g, 1.53 mmol, 2.0 eq.) and 2-*N*,9-diacetylguanine (0.45 g, 1.17 mmol, 1.5 eq.) were then added with stirring. The tube was wrapped in foil before DIAD (0.31 ml, 1.53 mmol, 2.0 eq.) was added dropwise and stirring continued for 1.5 hrs. The reaction was quenched by the slow addition

of water, extracted with DCM, dried over $MgSO_4$ and the solvent removed in vacuo. The crude product was purified by flash column chromatography on silica gel using an eluent of 50 → 80% EtOAc in hexane. The solvent was removed in vacuo to give the title compound as a yellow foam (0.44 g, 0.60 mmol, 77%). m.p. = 64 – 65 °C. ^{1}H NMR (400 MHz, $CDCl_3$) δ 8.25 (s, 1H (N***H***)), 7.62 (s, 1H (NC***H***=N)), 7.52 – 7.15 (m, 15H (Ph C***H***)), 4.50 (s, 2H (Bn C***H***$_2$O)), 4.20 (t, *J* = 6.9 Hz, 2H (C***H***$_2$OBn)), 4.04 (dd, *J* = 1.8, 1.8 Hz, 2H (Fc C***H***)), 4.00 (d, *J* = 1.9 Hz, 2H (Fc C***H***)), 3.99 (d, *J* = 1.9 Hz, 2H (Fc C***H***), 3.81 (dd, *J* = 1.8, 1.8 Hz, 2H (Fc C***H***)), 3.55 (t, *J* = 7.1 Hz, 2H (C***H***$_2$N)), 2.80 (t, *J* = 6.9 Hz, 2H (C***H***$_2$CH$_2$O)), 2.61 (t, *J* = 7.1 Hz, 2H (C***H***$_2$CH$_2$N)), 2.56 (s, 3H (C***H***$_3$)). ^{13}C NMR (101 MHz, $CDCl_3$) δ 171.1 (***C***OCH$_3$), 156.0 (***C***OO), 155.0 (N=***C***N$_2$), 152.1 (N$_2$***C***=CN), 150.5 (N=***C***O), 144.2 (N***C***H=N), 141.8 (Carb Ph ***C***–N), 138.4 (Bn ***C***–CH$_2$), 129.2 (Carb Ph ***C***H), 128.4 (Bn ***C***H), 127.7 (Bn ***C***H), 120.7 (N***C***=CN$_2$), 85.7 (Fc ***C***–CH$_2$CH$_2$O), 83.5 (Fc ***C***–CH$_2$CH$_2$N), 73.0 (Bn ***C***H$_2$O), 71.1 (***C***H$_2$OBn), 69.3 (Fc ***C***H), 68.9 (Fc ***C***H), 68.9 (Fc ***C***H), 68.2 (Fc ***C***H), 45.7 (***C***H$_2$N), 30.2 (***C***H$_2$CH$_2$O), 29.9 (***C***H$_2$CH$_2$N), 25.3 (***C***H$_3$). IR ν_{max}/cm^{-1} = 3087 (Fc CH), 3035 (ar CH), 2933 (CH), 2856 (CH), 1737 (C=O), 1618 (C=C). HRMS (ESI-TOF) m/z: $[M + Na]^+$ Calcd for $C_{41}H_{38}FeN_6O_4Na$ 757.2202; Found 757.2216.

5.1.2.37 1′-β-(2-*N*-Acetyl-6-*O*-diphenylcarbamoylguaninyl)ethyl-1-β-hydroxyethyl-ferrocene 3.32

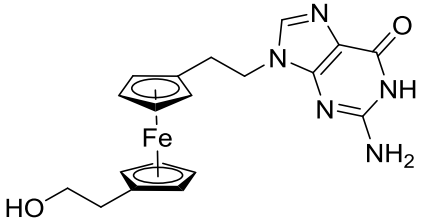
Novel compound



1′-β-(2-*N*-Acetyl-6-*O*-diphenylcarbamoylguaninyl)ethyl-1-β-benzyloxyethyl-ferrocene **3.31** (0.44 g, 0.60 mmol) was dissolved in EtOAc (15 ml) and H_2 gas bubbled through the solution using a balloon and needle for 5 mins. $Pd(OH)_2/C$ (0.15 g) was added and stirring continued with bubbling of H_2 gas for 1 hr. The crude mixture was filtered through a pad of celite and washed through with additional EtOAc before the solvent was removed in vacuo. The crude product was purified by flash column chromatography on silica gel using an eluent of EtOAc. The solvent was removed in vacuo to give the title compound as a yellow foam (0.29 g, 0.46 mmol, 76%). m.p. = 107 – 109 °C ^{1}H NMR (300 MHz, $CDCl_3$) δ 8.51 (s, 1H (N***H***)), 7.66 (s, 1H (NC***H***=N)), 7.53 – 7.14 (m, 10H (Ph C***H***)), 4.22 (t, *J* = 6.6 Hz, 2H (C***H***$_2$O)), 4.09 (s, 2H (Fc CH)), 4.06 (s, 4H, (Fc C***H***)) 3.88 (s, 2H), 3.66 (t, *J* = 6.6 Hz, 2H (C***H***$_2$O)), 2.79 (t, *J* = 6.8 Hz, 2H (C***H***$_2$CH$_2$N)), 2.54 (t, *J* = 6.6 Hz, 2H (C***H***$_2$CH$_2$O)), 2.50 (s, 3H (C***H***$_3$)), 2.33 (s, 1H (O***H***)). ^{13}C NMR (101 MHz, $CDCl_3$) δ 171.1 (***C***OCH$_3$), 155.9 (***C***OO), 155.0 (N=***C***N$_2$), 152.0 (N$_2$***C***=CN), 150.5 (N=***C***O), 144.3 (N***C***H=N), 141.7 (Ph ***C***–N), 129.2 (Ph ***C***H), 127.0 (Ph ***C***H), 120.7 (N***C***=CN$_2$), 86.0 (Fc ***C***–CH$_2$CH$_2$O), 84.0 (Fc ***C***–CH$_2$CH$_2$N), 69.6 (Fc ***C***H), 69.2 (Fc ***C***H), 69.0 (Fc ***C***H), 68.6 (Fc ***C***H), 63.3 (***C***H$_2$OH), 45.4 (***C***H$_2$N), 32.6 (***C***H$_2$CH$_2$OH), 29.7 (***C***H$_2$CH$_2$N), 25.2 (***C***H$_3$). IR ν_{max}/cm^{-1} = 3260, 3096, 2924, 2852, 1736, 1620. HRMS (ESI-TOF) m/z: $[M + Na]^+$ Calcd for $C_{34}H_{32}FeN_6O_4Na$ 667.1732; Found 667.1755.

5.1.2.38 1′-β-(Guaninyl)ethyl-1-β-hydroxyethyl-ferrocene Fcn2c2G

Novel compound



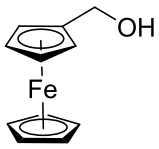
1′-β-(2-*N*-Acetyl-6-*O*-diphenylcarbamoylguaninyl)ethyl-1-β-hydroxyethyl-ferrocene **3.32** (0.29 g, 0.46 mmol) was dissolved in NH_3 (7N in MeOH) (10 ml) and stirred at rt for 16 hrs.

The resulting yellow crystals were collected by filtration and washed with water and DCM before being dried in vacuo to give the title compound as a yellow solid (.15 g, 0.37 mmol, 82%). Decomposed above 160 °C. ^{1}H NMR (300 MHz, DMSO) δ 10.53 (s, 1H (N***H***)), 7.55 (s, 1H (NC***H***=N)), 6.42 (s, 2H (N***H***$_2$)), 4.54 (t, *J* = 5.2 Hz, 1H (O***H***)), 4.06 (t, *J* = 1.8 Hz, 2H (Fc C***H***)), 4.01 (d, *J* = 1.8 Hz, 2H (Fc C***H***)), 4.00 (d, *J* = 1.8 Hz, 2H (Fc C***H***)), 3.93 (t, *J* = 1.8 Hz, 2H (Fc C***H***)), 3.48 (td, *J* = 7.2, 5.3 Hz, 2H (C***H***$_2$OH)), 2.74 (dd, *J* = 7.2, 7.2 Hz, 2H (C***H***$_2$CH2N)), 2.43 (t, *J* = 7.2 Hz, 2H (C***H***$_2$CH$_2$O)). ^{13}C NMR (101 MHz, DMSO) δ 156.8 (***C***O), 153.4 (N=***C***N$_2$), 151.0 (N$_2$***C***=CN), 137.4 (N***C***H=N), 116.6 (N***C***=CN$_2$), 85.7 (Fc ***C***–CH$_2$CH$_2$O), 84.2 (Fc ***C***–CH$_2$CH$_2$N), 68.9 (Fc ***C***H), 68.4 (Fc ***C***H), 67.9 (Fc ***C***H), 67.7 (Fc ***C***H), 62.0 (***C***H$_2$OH), 43.7 (***C***H$_2$N), 32.6 (***C***H$_2$CH$_2$OH), 29.4 (***C***H$_2$CH$_2$N). IR ν_{max}/cm^{-1} = 3388, 3190, 2851, 2710, 1699, 1633, 1607. HRMS (ESI-TOF) m/z: [M + Na]$^{+}$ Calcd for $C_{19}H_{21}FeN_5O_2$ 430.0942; Found 430.0943.

5.1.3 Experimental Procedures for the Synthesis of Ferrocenyl β-Blockers

5.1.3.1 Ferrocene methanol 4.1

Known compound. Characterisation matches literature values[16]

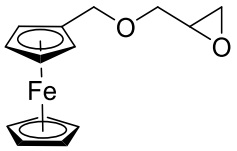


Ferrocenecarboxaldehyde **2.27** (0.26 g 1.21 mmol, 1.0 eq.) was dissolved in dry THF (10 ml), with stirring, in a Schlenk tube under an atmosphere of argon and cooled to 0 ºC in an ice bath. LiAlH (0.096 g, 2.54 mmol, 2.1 eq.) was added in small portions to the red solution and stirring continued for 1hr while the temperature raised to rt. Water was added slowly to quench the reaction and the resulting yellow solution was extracted with DCM, washed with water and dried over $MgSO_4$ before the solvent was removed in vacuo. The mixture was purified by column chromatography on silica gel using an eluent of 40% EtOAc in hexane to

give the title compound as yellow solid (0.25 g, 1.14 mmol, 94%). ^{1}H NMR (300 MHz, $CDCl_3$) δ 4.33 (s, 2H (C***H***$_2$)), 4.24 (dd, *J* = 1.9, 1.9 Hz, 2H (Fc C***H***)), 4.21 – 4.13 (m, 7H (Cp C***H***, Fc C***H***)), 1.73 (s, 1H (O***H***)). ^{13}C NMR (101 MHz, $CDCl_3$) δ 88.6 (Fc ***C***–CH_2), 68.5 (Fc ***C***H), 68.4 (Cp ***C***H), 68.0 (Fc ***C***H), 60.9 (***C***H_2). m/z Calcd for $C_{12}H_{14}FeO$ $[M]^+$: 216.0; Found 216.0.

5.1.3.2 (±)-(Ferrocenmethoxymethyl)oxirane 4.2

Known compound. Characterisation matches literature values[17]

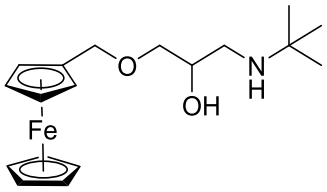


Ferrocene methanol **4.1** (0.59 g, 2.72 mmol, 1.0 eq.) was dissolved in dry DMF (5 ml), with stirring, in an Schlenk tube under an atmosphere of argon. NaH (0.13 g 5.43 mmol, 2.0 eq) was added in small portions resulting in bubbling and formation of a yellow precipitate. More dry DMF (10 ml) was added and stirring continued for 5 mins. (±)-Epichlorohydrin (1.70 ml, 21.74 mmol, 8.0 eq.) was added slowly producing effervescence and the resulting reddish brown solution was stirred at rt for 30 mins. More (±)-epichlorohydrin (1.70 ml, 21.74 mmol, 8.0 eq.) was added, followed by further small portions of NaH (0.39 g 16.32 mmol, 6.0 eq) and stirring continued for a further 30 mins. The reaction was quenched by the slow addition of water, extracted with Et_2O and dried over $MgSO_4$. The solvent was removed in vacuo and the product purified by flash column chromatography on silica gel a gradient eluent system of 0 → 10% EtOAc in hexane. The solvent was removed in vacuo to give the title compound as an orange solid (0.37 g, 1.37 mmol, 51%). m.p. = 58 – 59 °C. ^{1}H NMR (300 MHz, $CDCl_3$) δ 4.37 (d, *J* = 11.3 Hz, 1H (Fc C–C***H***$_2$)), 4.30 (d, *J* = 11.3 Hz, 1H (Fc C–C***H***$_2$)), 4.25 – 4.20 (m, 2H (Fc C***H***)), 4.17 – 4.13 (m, 2H (Fc C***H***)), 4.12 (s, 5H (Cp C***H***)), 3.68 (dd, *J* = 11.4, 3.1 Hz, 1H (CHC***H***$_2$OCH$_2$)), 3.35 (dd, *J* = 11.4, 5.8 Hz, 1H (CHC***H***$_2$OCH$_2$)), 3.10 (dddd, *J* = 5.8, 4.2,

3.1, 2.7 Hz, 1H (ep C***H***)), 2.75 (dd, *J* = 5.0, 4.2 Hz, 1H (ep C***H***$_2$)), 2.56 (dd, *J* = 5.0, 2.7 Hz, 1H (ep C***H***$_2$)). ^{13}C NMR (101 MHz, $CDCl_3$) δ 83.0 (Fc ***C***–CH_2), 70.5 (Fc C–***C***H_2), 69.7 (CH***C***H_2OCH_2), 69.6 (Fc ***C***H), 69.6 (Fc ***C***H), 68.7 (Fc ***C***H), 68.7 (Fc ***C***H), 68.6 (Cp ***C***H), 51.1 (ep ***C***H), 44.4 (ep ***C***H_2). m/z Calcd for $C_{12}H_{14}FeO$ $[M]^+$: 272.1; Found 272.1.

5.1.3.3 (±)-1-(*tert*-Butylamino)-3-ferrocenmethoxypropan-2-ol 4.5

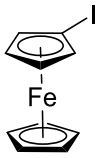
Novel compound



(±)-(Ferrocenmethoxymethyl)oxirane **4.2** was dissolved in MeOH (5 ml) with stirring before $tBuNH_2$ (7 ml) was added. The resulting solution was refluxed at 65 ºC for 1 hr. Water (5 ml) was added, the reaction mixture extracted with Et_2O, dried over $MgSO_4$ and the solvent removed in vacuo. The crude product was then purified by flash column chromatography on silica gel using a gradient eluent system of 0 → 5% TEA in EtOAc. The solvent was removed in vacuo to give the title compound as a yellow solid (0.376 g, 1.09 mmol, 80%) m.p. = 102 ºC. ^{1}H NMR (400 MHz, $CDCl_3$) δ 4.29 (s, 2H (Fc C–C***H***$_2$)), 4.21 – 4.18 (m, 2H (Fc C***H***)), 4.14 – 4.11 (m, 2H (Fc C***H***)), 4.10 (s, 5H (Cp C***H***)), 3.69 (ddd, *J* = 7.8, 5.6, 4.9, 3.9 Hz, 1H (C***H***OH)), 3.41 (dd, *J* = 9.7, 4.9 Hz, 1H (CHC***H***$_2$O)), 3.38 (dd, *J* = 9.7, 5.6 Hz, 1H (CHC***H***$_2$O)), 2.61 (dd, *J* = 11.6, 3.9 Hz, 1H (C***H***$_2$N)), 2.48 (dd, *J* = 11.6, 7.8 Hz, 1H (C***H***$_2$N)), 1.04 (s, 9H (C***H***$_3$)). ^{13}C NMR (101 MHz, $CDCl_3$) δ 83.3 (Fc ***C***–CH_2), 72.6 (CH***C***H_2O), 69.6 (Fc C–***C***H_2), 69.4 (Fc ***C***H), 69.4 (Fc ***C***H), 69.3 (C***H***OH), 68.5 (Fc ***C***H), 68.5 (Fc ***C***H), 68.4 (Cp ***C***H), 50.1 (*t*-Bu ***C***), 45.0 (***C***H_2N), 29.1 (***C***H_3). IR ν_{max}/cm^{-1} = 3290 (NH), 3173 (OH), 3104 (ar CH) , 2964 (CH), 2949 (CH), 2882 (CH), 2839 (CH). HRMS (ESI-TOF) m/z: $[M + H]^+$ Calcd for $C_{18}H_{28}FeNO_2$ 346.1469; Found 346.1460.

5.1.3.4 Iodoferrocene 4.6

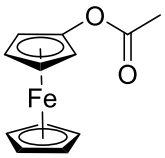
Characterisation matches literature values[18]



Ferrocene **2.27** (3.00 g, 16.1 mmol, 1.0 eq) and KO^{t}Bu (0.225 g, 2.0 mmol, 0.125 eq) was dissolved in dry THF (150 ml) with stirring, under an atmosphere of argon and cooled to -78 ºC. *t*-BuLi (1.7 M in pentane) (23.7 ml, 40.33 mmol, 2.5 eq) was added dropwise and stirring continued for 2 hrs at -78 ºC. I_2 (19.0 g, 80.7 mmol 5.0 eq) was added and the resulting mixture stirred at -78 ºC for 15 min. The mixture was allowed to warm to rt after which stirring was continued for 30 min. The reaction was quenched by the dropwise addition of $Na_2S_2O_3$ sat. solution (100 ml), extracted with hexane and dried over $MgSO_4$. The solvent was removed in vacuo and the crude product purified by flash column chromatography on silica gel using an eluent of hexane. Further purification was achieved by sublimation at 95 – 100 ºC, the unreacted ferrocene forming crystals on the cold finger. The title compound was cooled to rt forming dark orange crystals (3.28 g, 10.5 mmol, 65%). ^{1}H NMR (300 MHz, $CDCl_3$) δ 4.47 – 4.42 (dd, *J* = 1.9, 1.8 Hz, 2H, (Fc C***H***)), 4.25 (s, 5H (Cp C***H***)), 4.19 – 4.17 (dd, *J* = 1.9, 1.8 Hz, 2H (Fc C***H***)). ^{13}C NMR (101 MHz, $CDCl_3$) δ 74.5 (Fc ***C***H), 71.1 (Cp ***C***H), 68.9 (Fc ***C***H), 39.9 (Fc ***C***–I). m/z Calcd for $C_{10}H_9FeI$: 312; Found 312 $[M]^+$ and 313 $[M + H]^+$.

5.1.3.5 Ferrocenyl acetate 4.7

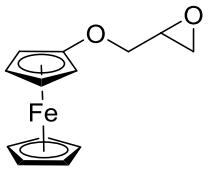
Known compound. Characterisation matches literature values[19]



Iodoferrocene **4.6** (1.35 g, 4.32 mmol, 1.0 eq) was dissolved in dry MeCN (30 ml) under an atmosphere of argon and heated to 90 ºC with stirring. Cu_2O (0.37 g, 2.59 mmol, 0.6 eq) was added and stirring continued at 90 ºC for 1 min. AcOH (0.30 ml, 5.18 mmol, 1.2 eq) was added dropwise and stirring continued for 1 hr before more Cu_2O (0.04 g, 0.3 mmol, 0.06) was added and stirring continued for an additional 1 hr. The reaction was quenched by the slow addition of $NaHCO_3$ sat. solution (30 ml), extracted with Et_2O and dried over $MgSO_4$. The solvent was removed in vacuo and the crude product purified by column chromatography on silica gel using a gradient eluent of 0 → 10% EtOAc in hexane. The solvent was removed in vacuo to give the title copmpound as an orange crystalline solid (0.95 g, 3.87 mmol, 90%). ^{1}H NMR (300 MHz, $CDCl_3$) δ 4.42 (t, *J* = 1.9 Hz, 2H (Fc C***H***)), 4.23 (s, 5H (Cp C***H***)), 3.96 (t, J = 1.9 Hz, 2H (Fc C***H***)), 2.17 (s, 3H (C$\boldsymbol{H}_3$). ^{13}C NMR (400 MHz, $CDCl_3$) δ 169.3 (***C***=O), 115.7 (Fc ***C***–O), 69.4 (Cp ***C***H), 63.3 (Fc ***C***H), 60.9 (Fc ***C***H), 21.3 (***C***H_3). m/z Calcd for $C_{12}H_{12}FeO_2$: 244, Found 244 $[M]^+$ and 245 $[M + H]^+$.

5.1.3.6 (±)-(Ferrocenoxymethyl)oxirane 4.8

Novel compound

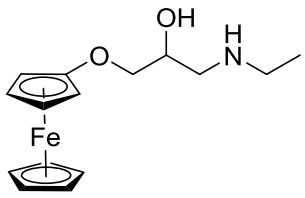


Ferrocenyl acetate **4.7** (1.0 g, 4.10 mmol, 1.0 eq) was dissolved in dry DMF (28 ml) under an atmosphere of argon, KOH (0.51 g, 9.01 mmol, 2.2 eq) added and the resulting mixture stirred at 40 °C for 0.5 hr. (±)-epichlorohydrin (1.28 ml, 16.4 mmol, 4.0 eq) was added, the temperature raised to 100 °C and stirred for 0.5 hr. The reaction was quenched by the addition of brine (50 ml), extracted with Et_2O (50 ml), washed with H_2O (5 x 20 ml) and dried over $MgSO_4$. The solvent was removed in vacuo and the crude product purified by flash

column chromatography on silica gel using 0 → 5% EtOAc in hexane. The solvent was removed in vacuo and the product redissolved in minimal $CHCl_3$. Slow evaporation of the concentrated solution produced single yellow crystals of the title compound which were suitable for X-ray analysis (0.60 g, 2.31 mmol, 56%). m.p. = 72 °C. ^{1}H NMR (400 MHz, $CDCl_3$) δ 4.20 (s, 5H (Cp C***H***)), 4.11 (m, 2H (Fc C***H***)), 4.04 (dd, *J* = 11.0, 3.2 Hz, 1H (Fc C–O–C***H***$_2$)), 3.84 (dd, *J* = 2.0, 2.0 Hz, 2H (Fc C***H***)), 3.77 (dd, *J* = 11.0, 5.8 Hz, 1H (Fc C–O–C***H***$_2$)), 3.29 (dddd, *J* = 5.8, 4.1, 3.2, 2.7 Hz, 1H (ep C***H***)), 2.89 (dd, *J* = 5.0, 4.1 Hz, 1H (ep C***H***$_2$)), 2.72 (dd, *J* = 5.0, 2.7 Hz, 1H (ep C***H***$_2$)). ^{13}C NMR (400 MHz, $CDCl_3$) δ 126.3 (Fc ***C***–O), 71.4 (Fc–O–***C***H_2), 68.7 (Cp ***C***H), 62.2 (Fc ***C***H), 62.2 (Fc ***C***H), 55.8 (Fc ***C***H), 55.8 (Fc ***C***H), 50.2 (ep ***C***H), 44.9 (ep ***C***H_2). IR ν_{max}/cm^{-1} = 3078 (Fc CH), 3012 (Fc CH), 2927 (CH), 2875 (CH). HRMS (ESI-TOF) m/z: $[M + H]^+$ Calcd for $C_{13}H_{15}FeNO_2$ 259.0421; Found 259.0425.

5.1.3.7 (±)-1-(Ethylamino)-3-ferrocenoxypropan-2-ol 4.9

Novel compound

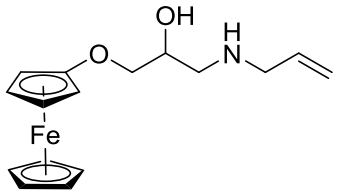


(±)-(Ferrocenoxymethyl)oxirane **4.8** (0.050 g, 0.194 mmol) was dissolved in ethylamine (70% in H_2O) (4 ml) in a sealed tube and heated in the microwave reactor at 100 °C for 1 hr. The reaction mixture was cooled to rt, extracted with hexane then washed with brine (3 x 5 ml) then water (3 x 5 ml), dried over MgSO4 and the solvent removed in vacuo. The crude product was then dissolved in a mixture of DCM and hexane with gentle heating and the solvent slowly cooled to precipitate yellow crystals. The solvent was removed by filtration and the crystals washed with hexane before drying in vacuo to give the title compound as

single yellow crystals which were suitable for X-ray analysis (0.037 g, 0.122 mmol, 63%). m.p. = 84 °C. ^{1}H NMR (400 MHz, $CDCl_3$) δ 4.20 (s, 5H (Cp C***H***)), 4.10 (dq, *J* = 5.2, 1.7 Hz, 2H (Fc C***H***)), 3.98 (m, 1H (C***H***OH)), 3.85 – 3.79 (m, 4H (Fc C***H***, C***H***$_2$)), 2.85 (dd, *J* = 12.0, 3.0 Hz, 1H (CHC***H***$_2$N)), 2.71 (m, 5H (CHC***H***$_2$N, NC***H***$_2$CH$_3$, O***H***, N***H***), 1.15 (t, *J* = 7.0 Hz, 3H (C***H***$_3$)). ^{13}C NMR (101 MHz, $CDCl_3$) δ 126.4 (Fc ***C***–O), 72.9 (***C***H$_2$O), 68.6 (Cp ***C***H)), 68.3 (***C***HOH), 62.1 (Fc ***C***H), 62.1 (Fc ***C***H), 55.6 (Fc ***C***H), 55.5 (Fc ***C***H), 51.8 (CH***C***H$_2$N), 44.2 (N***C***H$_2$CH$_3$), 15.4 (***C***H$_3$). IR ν_{max}/cm^{-1} = 3100 (NH), 2924 (CH), 2852 (CH), 2824 (CH). HRMS (ESI-TOF) m/z: $[M + H]^+$ Calcd for $C_{15}H_{22}FeNO_2$ 304.1000; Found 304.1003. Anal. Calcd for $C_{15}H_{21}FeNO_2$: C, 59.42; H, 6.98; N, 4.62. Found: C, 59.16; H, 7.09; N, 4.68.

5.1.3.8 (±)-1-(Allylamino)-3-ferrocenoxypropan-2-ol 4.10

Novel compound

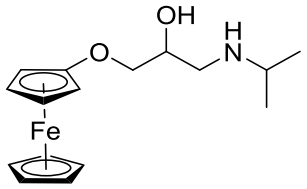


(±)-(Ferrocenoxymethyl)oxirane **4.8** (0.050 g, 0.194 mmol) was dissolved in allylamine (1 ml) in a sealed tube and heated in the microwave reactor at 150 °C for 1 hr. The reaction mixture was cooled to rt and the solvent was removed in vacuo. The crude product was dissolved in a mixture of DCM and hexane with gentle heating and the solvent slowly cooled to precipitate yellow crystals. The solvent was removed by filtration and the crystals washed with hexane before drying in vacuo to give the title compound as single yellow crystals which were suitable for X-ray analysis (0.048 g, 0.152 mmol, 79%). m.p. = 85 °C. ^{1}H NMR (400 MHz, $CDCl_3$) δ 5.91 (ddt, *J* = 17.2, 10.3, 6.0 Hz, 1H (C***H***=CH$_2$)), 5.21 (dd, *J* = 17.2, 1.6 Hz, 1H (C=C***H***$_2$)), 5.12 (dd, *J* = 10.2, 1.3 Hz, 1H (C=C***H***$_2$)), 4.20 (s, 5H (Cp C***H***)), 4.12 – 4.07 (m, 2H (Fc C***H***)), 4.01 – 3.94 (m, 1H (C***H***OH)), 3.87 – 3.76 (m, 4H (Fc C***H***, C***H***$_2$O)),

3.36 – 3.24 (m, 2H, (C***H***$_2$CH=CH$_2$)), 2.83 (dd, *J* = 12.1, 3.8 Hz, 1H (OCHC***H***$_2$N), 2.72 (dd, *J* = 12.1, 8.0 Hz, 1H (OCHC***H***$_2$N)), 2.42 (s, 2H, (O***H***, N***H***)). ^{13}C NMR (101 MHz, $CDCl_3$) δ 136.7 (***C***H=C), 126.4 (Fc ***C***–O), 116.4 (C=***C***H$_2$), 72.9 (***C***H$_2$O), 68.6 (Cp ***C***H), 68.6 (***C***HOH), 62.1 (Fc ***C***H), 62.1 (Fc ***C***H), 55.6 (Fc ***C***H), 55.5 (Fc ***C***H), 52.4 (***C***H$_2$CH=CH$_2$), 51.3 (OCH***C***H$_2$N). IR ν_{max}/cm^{-1} = 3284 (NH), 3086 (Fc CH), 2923 (CH), 2788 (CH), 1646 (C=C). HRMS (ESI-TOF) m/z: $[M + H]^+$ Calcd for $C_{16}H_{22}FeNO_2$ 316.1000; Found 316.1003. Anal. Calcd for $C_{16}H_{21}FeNO_2$: C, 60.97; H, 6.72; N, 4.44. Found: C, 61.15; H, 6.50; N, 4.43.

5.1.3.9 (±)-1-(Isopropylamino)-3-ferrocenoxypropan-2-ol 4.11

Novel compound

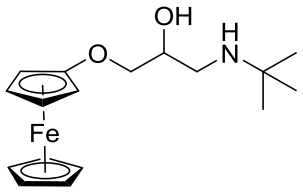


(±)-(Ferrocenoxymethyl)oxirane **4.8** (0.050 g, 0.194 mmol) was dissolved in isopropylamine (1 ml) in a sealed tube and heated in the microwave reactor at 115 °C for 3 hrs. The reaction mixture was cooled to rt and the solvent was removed in vacuo. The crude product was dissolved in a mixture of DCM and hexane with gentle heating and the solvent slowly cooled to precipitate a yellow film onto the side of the flask. The solvent was removed and the remaining yellow residue dried in vacuo to give the title compound as a waxy solid (0.044 g, 0.140 mmol, 71%). ^{1}H NMR (400 MHz, $CDCl_3$) δ 4.20 (s, 5H (Cp C***H***)), 4.12 – 4.08 (m, 2H (Fc C***H***), 3.99 – 3.90 (m, 1H (C***H***OH)), 3.83 (dd, *J* = 2.0, 2.0 Hz, 2H (Fc ***C***H), 3.81 (d, *J* = 4.9, Hz, 2H) 2.91 – 2.80 (m, 2H (C***H***N, C***H***$_2$N), 2.69 (dd, *J* = 12.0, 8.0 Hz, 1H (C***H***$_2$N)), 2.38 (s, 2H (N***H***, O***H***)), 1.11 (d, *J* = 6.2 Hz, 6H (C***H***$_3$)). ^{13}C NMR (101 MHz, $CDCl_3$) δ 126.4 (Fc ***C***–O), 72.9 (O***C***H$_2$), 68.6 (Cp ***C***H), 68.6 (***C***HOH), 62.1 (Fc ***C***H), 62.1 (Fc ***C***H), 55.7 (Fc ***C***H), 55.5 (Fc ***C***H), 49.4 (***C***H$_2$N), 49.1 (***C***HN), 23.2 (***C***H$_3$), 23.1 (***C***H$_3$). IR ν_{max}/cm^{-1} = 3094 (Fc

CH), 2963 (CH), 2921 (CH), 2851 (CH). HRMS (ESI-TOF) m/z: $[M + H]^+$ Calcd for $C_{16}H_{24}FeNO_2$ 318.1156; Found 318.1162.

5.1.3.10 (±)-1-(*tert*-Butylamino)-3-ferrocenoxypropan-2-ol 4.12

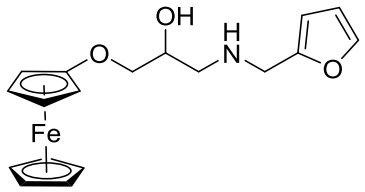
Novel compound



(±)-(Ferrocenoxymethyl)oxirane **4.8** (0.050 g, 0.194 mmol) was dissolved in *t*-butylamine (1 ml) in a sealed tube and heated in the microwave reactor at 150 °C for 4 hr. The reaction mixture was cooled to rt and the solvent was removed in vacuo. The crude product was dissolved in a mixture of DCM and hexane with gentle heating and the solvent slowly cooled to precipitate orange crystals. The solvent was removed by filtration and the crystals washed with hexane before drying in vacuo to give the title compound as single orange crystals which were suitable for X-ray analysis (0.047 g, 0.14 mmol, 73%). m.p. = 92 °C. ^{1}H NMR (400 MHz, $CDCl_3$) δ 4.20 (s, 5H (Cp C***H***)), 4.12 – 4.08 (m, 2H (Fc C***H***)), 3.91 (m, 1H (C***H***)), 3.86 – 3.76 (m, 4H (Fc C***H***, C***H***$_2$O)), 2.84 (dd, *J* = 11.9, 3.4 Hz, 1H (C***H***$_2$N)), 2.83 (s, 2H (O***H***, N***H***), 2.66 (dd, *J* = 11.9, 8.0 Hz, 1H (C***H***$_2$N)), 1.16 (s, 9H (C***H***$_3$)). ^{13}C NMR (101 MHz, $CDCl_3$) δ 126.5 (Fc ***C***–O), 72.9 (***C***H$_2$O), 68.6 (Cp ***C***H), 68.5 (***C***H), 62.1 (Fc ***C***H), 62.1 (Fc ***C***H), 55.7 (Fc ***C***H), 55.6 (Fc ***C***H), 51.1 (^{t}Bu ***C***), 45.0 (***C***H$_2$N), 29.0 (***C***H$_3$). IR ν_{max}/cm^{-1} = 3287 (NH), 3087 (Fc CH), 2963 (CH). HRMS (ESI-TOF) m/z: $[M + H]^+$ Calcd for $C_{17}H_{26}FeNO_2$ 332.1313; Found 332.1314. Anal. Calcd for $C_{17}H_{25}FeNO_2$: C, 61.64; H, 7.61; N, 4.23. Found: C, 61.78; H, 7.75; N, 4.40.

5.1.3.11 (±)-1-((Furan-2-ylmethyl)amino)-3-ferrocenoxypropan-2-ol 4.13

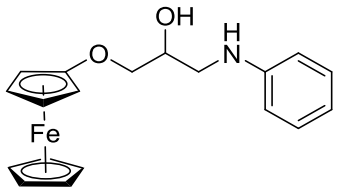
Novel compound



(±)-(Ferrocenoxymethyl)oxirane **4.8** (0.050 g, 0.194 mmol) was dissolved in furfurylamine (5 ml) and heated at 75 °C for 6 hrs with stirring. H_2O (10 ml) was added and the crude product extracted with DCM, washed with further H_2O (5 x 10 ml), dried over $MgSO_4$ and the solvent removed in vacuo. The crude product was dissolved in a mixture of DCM and hexane with gentle heating and the solvent slowly cooled to precipitate orange crystals. The solvent was removed by filtration and the crystals washed with hexane before drying in vacuo to give the title compound as single orange crystals which were suitable for X-ray analysis (0.045 g, 0.126 mmol, 65%). m.p. = 96 °C. ^{1}H NMR (400 MHz, $CDCl_3$) δ 7.37 (dd, *J* = 1.8, 0.6 Hz, 1H (OC***H***=CH)), 6.32 (dd, *J* = 3.1, 1.8 Hz, 1H (C***H***=CHO), 6.20 (dd, *J* = 3.1, 0.6 Hz, 1H (CHC***H***=C)), 4.19 (s, 5H (Cp C***H***)), 4.11 – 4.06 (m, 2H (Fc C***H***)), 3.97 (dddd, *J* = 12.6, 7.9, 4.2, 4.2 Hz, 1H (C***H***OH)), 3.89 – 3.75 (m, 6H (Fc C***H***, C***H***$_2$O, NC***H***$_2$C), 2.84 (dd, *J* = 12.1, 4.2 Hz, 1H (CHC***H***$_2$N)), 2.73 (dd, *J* = 12.1, 7.9 Hz, 1H (CHC***H***$_2$N)), 2.34 (s, 2H (N***H***, O***H***)). ^{13}C NMR (101 MHz, $CDCl_3$) δ 153.7 (O***C***=CH), 142.1 (O***C***H=CH), 126.4 (Fc ***C***–O), 110.3 (***C***H=CHO), 107.2 (CH***C***H=C), 72.8 (***C***H$_2$O), 68.6 (***C***HOH), 68.6 (Cp ***C***H), 62.1 (Fc ***C***H), 62.1 (Fc ***C***H), 55.6 (Fc ***C***H), 55.5 (Fc ***C***H), 51.1 (CH***C***H$_2$N), 46.2 (N***C***H$_2$C). IR ν_{max}/cm^{-1} = 3319 (NH), 3121 (CH), 3094 (Fc CH), 2924 (CH), 2825 (CH), 1667 (C=C). HRMS (ESI-TOF) m/z: $[M + H]^+$ Calcd for $C_{18}H_{22}FeNO_3$ 356.0949; Found 356.0947. Anal. Calcd for $C_{18}H_{21}FeNO_3$: C, 60.86; H, 5.96; N, 3.94. Found: C, 60.99; H, 5.85; N, 4.19.

5.1.3.12 (±)-1-(Phenylamino)-3-ferrocenoxypropan-2-ol 4.14

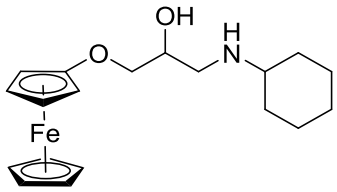
Novel compound



(±)-(Ferrocenoxymethyl)oxirane **4.8** (0.050 g, 0.194 mmol) was dissolved in phenylamine (2 ml) in a sealed tube and heated in the microwave reactor at 150 °C for 1 hr. The dark brown reaction mixture was cooled to rt and H_2O (5 ml) added. The crude product was extracted with Et_2O, washed with H_2O (5 x 5 ml), dried over MgSO4 and the solvent removed in vacuo. The crude product was dissolved in a mixture of DCM and hexane with gentle heating and the solvent slowly cooled to precipitate light-brown crystals. The solvent was removed by filtration and the crystals washed with hexane before drying in vacuo to give the title compound as light-brown coloured single crystals which were suitable for X-ray analysis (0.036 g, 0.104 mmol, 54%). m.p. = 95 °C. ^{1}H NMR (400 MHz, $CDCl_3$) δ 7.20 (dd, *J* = 7.9, 7.7 Hz, 2H (Ph C***H***)), 6.75 (t, *J* = 7.3 Hz, 1H (Ph C***H***)), 6.66 (d, *J* = 7.3 Hz, 2H (Ph C***H***)), 4.45 (s, 7H (Fc C***H***, Cp C***H***)), 4.25 (s, 2H (Fc C***H***, C***H***)), 4.07 (s, 1H (Fc ***C***H)), 3.99 (s, 1H (C***H***$_2$O)), 3.92 (s, 1H (C***H***$_2$O)), 3.33 (dd, *J* = 12.8, 3.4 Hz, 1H (C***H***$_2$N)), 3.19 (dd, *J* = 12.8, 6.8 Hz, 1H (C***H***$_2$N)), 1.26 (s, 2H (O***H***, N***H***)).^{13}C NMR (101 MHz, $CDCl_3$) δ 148.2 (Ph ***C***–N), 129.5 (Ph ***C***H), 118.2 (Ph ***C***H), 113.4 (Ph ***C***H), 72.5 (***C***H$_2$O), 70.7 (Cp ***C***H), 69.0 (Fc ***C***H), 63.4 (***C***H), 54.7 (Fc ***C***H), 46.7 (***C***H$_2$N). IR ν_{max}/cm^{-1} = 3451 (NH), 3356 (NH), 3097 (ar CH), 3084 (Fc CH), 3053 (ar CH), 3031 (ar CH), 2939 (CH), 2902 (CH), 2859 (CH), 1603 (C=C). HRMS (ESI-TOF) m/z: $[M + H]^+$ Calcd for $C_{19}H_{22}FeNO_2$ 352.1000; Found 352.1003. Anal. Calcd for $C_{19}H_{21}FeNO_2$: C, 64.97; H, 6.03; N, 3.99. Found: C, 65.09; H, 6.29; N, 4.08.

5.1.3.13 (±)-1-(Cyclohexlyamino)-3-ferrocenoxypropan-2-ol 4.15

Novel compound



(±)-(Ferrocenoxymethyl)oxirane **4.8** (0.050 g, 0.194 mmol) was dissolved in cyclohexylamine (1 ml) in a sealed tube and heated in the microwave reactor at 135 °C for 1 hr. The reaction mixture was cooled to rt and the solvent was removed in vacuo. The crude product was dissolved in a mixture of DCM and hexane with gentle heating and the solvent slowly cooled to precipitate orange crystals. The solvent was removed by filtration and the crystals washed with hexane before drying in vacuo to give the title compound as single orange crystals which were suitable for X-ray analysis (0.047 g, 0.13 mmol, 68%). m.p. = 96 °C. ^{1}H NMR (400 MHz, $CDCl_3$) δ 4.20 (s, 5H (Cp C***H***)), 4.12 – 4.07 (m, 2H (Fc C***H***)), 3.91 (dddd, *J* = 9.0, 5.2, 5.2, 3.9, 1H (C***H***OH)), 3.82 (dd, *J* = 2.0, 2.0 Hz, 2H (Fc C***H***)), 3.80 (dd, *J* = 5.2, 0.9 Hz, 2H (OC***H***$_2$)), 2.88 (dd, *J* = 12.1, 3.9 Hz, 1H (C***H***$_2$N)), 2.69 (dd, *J* = 12.1, 8.2 Hz, 1H (C***H***$_2$N))), 2.44 (tt, *J* = 10.4, 3.7 Hz, 1H (NC***H***)), 2.35 (s, 2H (O***H***, N***H***)), 1.92 (d, *J* = 11.4 Hz, 2H (cy C***H***$_2$)), 1.80 – 1.67 (m, 2H (cy C***H***$_2$)), 1.61 (ddd, *J* = 10.8, 7.1, 3.4 Hz, 1H (cy C***H***$_2$)), 1.38 – 0.97 (m, 5H (cy C***H***$_2$)). ^{13}C NMR (101 MHz, $CDCl_3$) δ 126.5 (Fc ***C***–O), 72.9 (O***C***H$_2$), 68.6 (Cp C***H***), 68.6 (***C***HOH), 62.1 (Fc ***C***H), 62.1 (Fc ***C***H), 56.9 (N***C***H), 55.6 (Fc ***C***H), 55.5 (Fc ***C***H), 49.0 (***C***H$_2$N), 34.0 (CHC***H***$_2$CH$_2$), 33.8 (CHC***H***$_2$CH$_2$), 26.2 (CHCH$_2$CH$_2$C***H***$_2$), 25.2 (CHCH$_2$C***H***$_2$). IR ν_{max}/cm^{-1} = 3240 (NH), 3092 (Fc CH), 2917 (CH), 2850 (CH). HRMS (ESI-TOF) m/z: $[M + H]^+$ Calcd for $C_{19}H_{28}FeNO_2$ 358.1469; Found 358.1474. Anal. Calcd for $C_{19}H_{27}FeNO_2$: C, 63.87; H, 7.62; N, 3.92. Found: C, 63.79; H, 7.43; N, 3.95.

5.2 High-Performance Liquid Chromatography

Analytical HPLC for compounds **2.13-(*RR*)** and **2.20-(*RR*,S_pS_p)** was performed using a Shimadzu system consisting of a DGU-20A_3 degasser, LC-20AD pump, SIL-2AC HT auto-sampler, CTO-20AC column oven and SPD-M20A diode array detector with a Phenomenex Luna 10µ C18(2) 100Å column (4.60 mm x 250 mm). For compound **2.13-(*RR*)** an isocratic eluent system of 5% H_2O in MeCN was used at a flow rate of 1.00 ml min^{-1}. For compound **2.20-(*RR*,S_pS_p)** an eluent system of 5% H_2O in MeCN was used at a flow rate of 0.75 ml min^{-1}.

Chiral HPLC for compounds **2.13-(*RR*)**, **2.13-(*SS*)**, **2.20-(*RR*,S_pS_p)** and **2.20-(*RR*,S_pS_p)** was performed using a Dionex P580 pump and a Polymer Laboratories PL-ELS 2100 detector with a Daicel Chemical Industries Chiralpak AD column (4.60 mm x 250 mm). Compounds **2.13-(*RR*)** and **2.13-(*SS*)** were separated using an isocratic eluent system of 5% IPA in hexane, at a flow rate of 1.00 ml min^{-1}. Compounds **2.20-(*RR*,S_pS_p)** and **2.20-(*RR*,S_pS_p)** were separated using an isocratic eluent system of 1.5% IPA in hexane, at a flow rate of 2.50 ml min^{-1}.

Chiral HPLC for compounds **2.40-(*RR*,S_pS_p)**, **2.40-(*SS*,R_pR_p)**, **Fcn1c2T**$_{(Rp)}$, **Fcn1c2T**$_{(Sp)}$, **Fcn2c2T**$_{(Rp)}$ and **Fcn2c2T**$_{(Sp)}$ was performed using a Shimadzu system consisting of a DGU-20A_3 degasser, LC-20AD pump, SIL-2AC HT auto-sampler, CTO-20AC column oven and SPD-M20A diode array detector with a Phenomenex Lux 5µ Cellulose-1 column (4.60 mm x 250 mm). Compounds **2.40-(*RR*,S_pS_p)** and **2.40-(*SS*,R_pR_p)** were separated using an isocratic eluent system of 10% H_2O in MeCN and a flow rate of 1.0 ml min^{-1}. **Fcn1c2T**$_{(Rp)}$ was separated from **Fcn1c2T**$_{(Sp)}$ and **Fcn2c2T**$_{(Rp)}$ was separated from **Fcn2c2T**$_{(Sp)}$ using an isocratic eluent system of 30% acetonitrile in water with a flow rate of 1.0 ml min^{-1}.

5.3 X-Ray Diffraction

An Agilent SuperNova diffractometer equipped with an Atlas detector was used for the measurement of all datasets. All data collections were driven and processed using CrysAlisPro, which also performed numerical absorption corrections based on gaussian integration over a multifaceted crystal model.[20] ShelXS was used to solve all the structures and refinement using a full matrix least-squares procedure on F2 was performed in ShelXL.[21] OLEX2 was used to generate all reports and figures.[22] In all cases the hydrogen atoms bonded to oxygen and nitrogen were located in the electron density and the positions freely refined while the remaining hydrogen atoms were fixed as riding models. The U_{iso} of the hydrogen atoms were based on the U_{eq} of the parent atoms in all cases.

5.4 Oligonucleotide Solid-Phase Synthesis

The incorporation of compound **2.43-(*RR*,S_pS_p)** into an oligonucleotide was attempted on an Applied Biosystems ABI 394 DNA/RNA synthesiser. All phosphoramadites and reagents were purchased from Link Technologies (Scotland, UK). DNA synthesis grade dichloromethane and trichloroacetic acid in dichloromethane were purchased from Life Technologies (Paisley, UK) and DNA grade aceontonitrile was purchased from Rathburn Chemicals Ltd (Scotland, UK). The synthesis was carried out on a 1.0 μM scale. 0.5 M ETT in acetonitrile was used as the activator and 0.02 M iodine in water solution was used as the oxidising agent. 10% acetic anhydride in THF and 10% methylimidazole in THF were used as capping agents. All standard phosphoramadites were diluted in DNA synthesis grade acetonitrile to a concentration of 0.1 M before use. Standard phosphoramadites were allowed 25 seconds coupling time and **2.43-(*RR*,S_pS_p)** was allowed 10 mins. 90 mins treatment with 30% ammonia hydroxide solution was used to remove the oligonucleotides from the solid support, before deprotection of the nucleobases was effected through heating in the same solution for 6 hrs at 55 ºC.

5.5 Thermal Melting Experimental

Thermal melting temperatures were measured on a Cary 5000 UV/vis spectrophotometer (Agilent Technologies Ltd, Cheshire, UK) in combination with with a peltier temperature controller. The absorbance was measured at 260 nm while the temperature was ramped between 15 °C and 85 °C at a rate of 0.5 °C per minute. Each experiment consisted one annealing ramp and two dissociation ramps and was repeated three times. The T_m corresponds to the average of the first derivatives of the dissociation curves and are given to the nearest 0.5 °C. Samples were prepared as 0.5 ml solutions consisting of 5 μM of each oligonucleotide (S1 and S2) with 0.1 M $NaClO_4$ and 10 mM NaH_2PO_4 buffer pH 7.0.

5.6 Electrochemistry

Cyclic voltammetry measurements were obtained for compounds Fc, **Fcn3c2T**$_{(S,Rp)}$, **Fcn2c2T**$_{(Rp)}$, **Fcn1c2T**$_{(Rp)}$, **Fcn2c2G**$_{(Sp)}$, **Fcn1c2G**$_{(Rp)}$, **Fcn2c2T** and **Fcn2c2G** using 1.0 mM solutions in dry and de-oxygenated acetonitrile with a base electrolyte of 0.1 M tetrabutylammonium hexafluorophosphate ($TBAPF_6$, ≥ 99%, Fluka) with an internal reference of dmfc also at 1.0 mM. Measurements were performed using a traditional 3-electrode set-up and a BioAnalytical Systems Inc. (West Lafayette, IN) EC Epsilon potentiostat using a C3 cell stand. All measurements were carried out at rt. A 3 mm diameter, glassy carbon electrode was used as a W.E and a platinum wire was used as a C.E. The R.E. was housed in a compartment, connected to the cell via a frit and consisted of a Ag|AgCl|3 M KCl electrode (BASi). All electrodes were supplied by IJ Cambria (Llanelli, Wales).

Before use, all glassware was cleaned by soaking overnight in a 1:1 mixture of hydrogen peroxide (30%) and ammonia (35%) before being rinsed with copious amounts of ultrapure water (purified with a Millipore tandem Elix-A10 system, resistivity > 18 MΩ cm, TOC < 5 ppb). The glassware was then immersed in ultrapure water overnight and carefully dried in an oven for several hrs before use. The platinum wire C.E was prepared by flame annealing and the R.E was cleaned with dry acetonitrile before each use. The W.E. was prepared by polishing with successively finer grades of alumina slurry (1.0 μm, 0.3 μm and 0.05 μm) before being rinsed with plenty of ultrapure water and then acetonitrile before being dried under a stream of argon and placed in the analyte solution. A blanket of argon was maintained throughout the experiment and molecular sieves were employed to maintain the dryness of the solvent.

5.7 Biological Methods

5.7.1 Crystal Violet Cell Viability Assay for HOS

HOS cells were seeded in 100 µL of media, at a density of 6250 cells per well, in a 96-well plate and incubated at 37 ºC for 24 hrs. The media was then replaced with that containing the appropriate concentration of test compound. Following four days incubation at 37 ºC, the media was removed and phosphate buffered saline (PBS) solution (100 µL) used to wash the wells, before a solution of paraformaldehyde (4%) (100 µL) was added and the plate incubated at rt for 15 mins to fix the remaining cells. The excess paraformaldehyde solution was removed, the cells stained with a crystal violet (0.5% w/v in 10% ethanol and distilled water) solution (100 µL) and the plate incubated at rt for 20 mins with gentle shaking. The excess crystal violet solution was carefully removed and the stained cells were washed with 100µl of distilled water three times before being left to air dry. After approximately 20 mins, a solution of acetic acid (10% v/v in distilled water) (100µL) was added to each well and the plate was left at rt for 20 mins with gentle shaking to redissolve the dye. The absorbance of each well was determined at 590 nm wavelength in a spectrophotometer and compared against a blank of acetic acid solution.

5.7.2 Crystal Violet Cell Viability Assay for OE21

A calibration curve was first generated to link the intensity of absorption to the cell number. Cells were seeded in a 96-well plate at densities of 100,000, 50,000, 25,000, 12,500, 6250 and 0 cells per well and incubated overnight at 37 ºC in an atmosphere of 5% CO_2. They were then fixed and stained with crystal violet according to the method provided below and the absorbance of each well measured using a spectrophotometer at 590 nm. This calibration curve allowed the absorbance at 590 nm to be translated directly into the corresponding cell number.

OE21 cells were seeded in 100 µL of media, at a density of 6250 cells per well, in 5 duplicate 96-well plates and incubated at 37 ºC for 24 hrs. The media of four of the plates was then replaced with that containing the appropriate concentration of test compound and incubation continued at 37 ºC. The media was removed from the fifth plate and phosphate buffered saline (PBS) solution (100 µL) used to wash the wells, before a solution of paraformaldehyde (4%) (100 µL) was added and the plate incubated at rt for 15 mins to fix the remaining cells. The excess paraformaldehyde solution was removed, the cells stained with a crystal violet (0.5% w/v in 10% ethanol and distilled water) solution (100 µL) and the plate incubated at rt for 20 mins with gentle shaking. The excess crystal violet solution was carefully removed and the stained cells were washed with 100µl of distilled water three times before being left to air dry. After approximately 20 mins, a solution of acetic acid (10% v/v in distilled water) (100µL) was added to each well and the plates were left at rt for 20 mins with gentle shaking to redissolve the dye. The absorbance of each well was determined at 590nm wavelength in a spectrophotometer and compared against a blank of acetic acid solution. This process was repeated on one plate each day for four more days.

5.7.3 MTS Cell Viability Assay for L1210, CEM and Hela Cells

To each well of a 96-well microtiter plate were added 5 to 7.5×10^4 cells and a given amount of the test compound. The cells were allowed to proliferate for 48 h to 96 h (depending on the nature of the tumor cell line) at 37 °C in a humidified CO_2-controlled atmosphere. At the end of the incubation period, the wells were washed phosphate buffered saline (PBS) solution the cells stained with MTS dye and counted in a Coulter Counter (Coulter Electronics Ltd, Harpenden Herts, United Kingdom). The IC_{50} (50% inhibitory concentration) was defined as the concentration of compound that reduced the number of viable cells by 50%.

5.7.4 CPE Reduction Assay for Antiviral Activity

Serial dilutions of the test compounds were added together with the virus of interest at a multiplicity of infection (M.O.I.) of 50 $CCID_{50}$, to a confluent monolayer of erythroleukemia (HEL) cells and incubated at 35 °C. At 4 days post-infection, microscopy was performed to evaluate the antiviral activity, expressed as the concentration producing 50% inhibition of virus-induced cytopathic effect (50% effective concentration; EC_{50}); and the cytotoxicity, expressed as the minimum compound concentration that causes a microscopically detectable alteration of normal cell morphology (MCC).

5.7.5 Western Blot Cells and Chemicals

Human embryonic kidney cells (HEK 293) were readily available at the School of Pharmacy, University of Birmingham, U.K. Cell culture reagents were obtained from Gibco BRL. Rabbit anti-β-catenin monoclonal antibody (D10A8), rabbit anti-LKB1 monoclonal antibody (D60C5), rabbit anti-P-LKB1 (Ser428) monoclonal antibody (C67A3), and anti-rabbit 2° horseradish peroxidase (HRP)-labelled IgG antibody were purchased from Cell Signalling Technology®. Isoproterenol and propranolol were obtained from the School of Pharmacy. Phosphodiesterase inhibitor 3-isobutyl-1-methylxanthine (IBMX 500 mM) was purchased from Sigma-Aldrich. The enhanced Amersham chemiluminescence (ECL) Western Blotting detecting reagent and Amersham Hyperfilm ECL was purchased from GE Healthcare Life Sciences.

5.7.6 Western Blot Cell Culture and Maintainance

HEK 293 cell isolates were maintained by constant growth to ~70 – 80% confluency in humidified 5% CO_2, 95% air in a tissue culture incubator at 37 °C. During the splitting process, old media was aspirated and the 75 cm^2 flask thoroughly washed with phosphate

buffered saline (Dulbecco's PBS). Followed by two or three mins of simultaneous trypsinisation incubation with 0.05% trypsin-ethylenediaminetetraacetic acid (EDTA) (1X, phenol red, Gibco) or Tryp™ Express (stable trypsin replacement, phenol red, Gibco), respectively, fresh full growth media warmed to 37 °C (Dulbecco's Modified Eagle Medium (DMEM); 200 mM L-glutamine, 10% foetal bovine serum, 1% Penstrep (5,000 units/ml penicillin, 5,000 µg/ml streptomycin)) was added to terminate the trypsinisation process with sufficient mixing by pipetting up and down to break up cell populations. Cell suspensions were added to new, clearly labelled flasks containing full DMEM in ratios suitable for appropriate cell confluency time constraints.

5.7.7 Compound Preparation for Western Blot

Stock solutions of isoproterenol, propranolol, the three type-1 (**4.3**, **4.4** and **4.5**), seven type-2 (**4.9**, **4.10**, **4.11**, **4.12**, **4.13**, **4.14** and **4.15**) ferrocenyl β-blockers and the negative control compound **Fcn3c2T**$_{(S,Rp)}$ were prepared in dimethyl sulfoxide (DMSO, ≥99.5%) at concentrations indicated for cell treatment and lysis for immunoblotting. Drugs were also prepared at certain fixed concentrations in clear media or Krebs Ringer Buffer (KRB) (deionised water, $MgCl_2$, KCl, NaCl, Na_2HPO_4, NaH_2PO_4, $NaHCO_3$; pH = 7.5) containing IBMX for the purpose of the cAMP-Glo™ bioluminescence assay. It should be noted that all drug concentrations mentioned in the text is the final concentration the cells are actually exposed to.

5.7.8 Cell Plating and Cell Lysate Preparation

Cell lines were plated into multiple six-well plates at a ratio of cell suspension and full DMEM of 1:2 and grown to ~70-80% confluency. A six-well plate was dedicated to each of the Isop only and Prop cells, whilst two wells each were assigned to each of the ferrocenyl β-

blockers. **Fcn3c2T**$_{(SS,RpRp)}$ was utilised as a negative control. To stimulate a response, all of the wells were treated with the non-selective βAR agonist isoproterenol at 50 nM concentration. Each of the treated wells were simultaneously treated with propranolol, one of the 3 type-1 ferrocenyl β-blockers, one of the 7 type-2 β-blockers or the negative control compound **Fcn3c2T**$_{(SS,RpRp)}$ at 10 or 50 µM concentration before being incubated in 5% CO_2, at 37 °C for 5 mins. Following incubation, the culture plates were cooled on ice and maintained at 0 °C.

After growth media aspiration, 150 µl of ice cold full cell lysis buffer (NP-40 lysis buffer for whole cell protein extraction: 5M NaCl/ 10% NP-40/ 1M Tris and H_2O; protease inhibitors: 0.25 M phenylmethanesulfonyl fluoride (PMSF); 1 M benzamidine; 2-mercaptoethanol ≥99.0%) was dispensed into the first well of each category of treated cells, scraped vigorously and transferred to the subsequent wells and scraped again prior to transferring cell lysate into labelled microtubes. Homogenate cell lysate was centrifuged and spun down at 4°C, 12,000 RPM for ten mins to pellet the large cell debris and nuclei. The supernatant was consequently collected and stored at -80 °C.

5.7.9 Measurement of Protein Concentration

Cell supernatant was then subjected to the Bradford Assay for protein concentration quantification by the FLUOstar® Omega (BMG LABTECH) spectrophotometer at 595 nm. 2 µl of each cell lysate sample was measured against a standard curve generated by 5 µl of 0.125 mg/ml, 0.25 mg/ml, 0.5 mg/ml and 1 mg/ml of bovine albumin serum (BSA) with the use of Bradford reagent for binding of Coomassie Brilliant Blue G-250 dye to proteins for quantification. The average of protein concentration reading was multiplied by 2.5 to upscale it to that seen with BSA. Protein samples were made to contain: 200 or 400 mg/ml protein,

4X- or 5X-sodium dodecyl sulphate (SDS) and water. The samples were heated to 95°C for four mins and stored under -20 °C conditions.

5.7.10 Sodium Dodecyl Sulphate Polyacrylamide Gel Electrophoresis (SDS-PAGE) and Transphoresis

For the immunoblotting for P-LKB1 (M_r*: 48 kDa*) and P-CREB (M_r*: 45 kDa*) to detect for βAR blockade, SDS samples previously prepared from the cell lysate of each category of treated cells were subjected to SDS electrophoresis in 10% polyacrylamide gel (1.5 M Tris (pH = 8.8), 30% bis-acrylamide, 20% SDS, 10% ammonium persulphate, *N,N,N',N'*-tetramethylethylenediamine (TMEDA, H_2O) in duplicate repeats of 20 µl, unless stated otherwise. For the complete set of immunoblotting for one target of phosphorylated protein, a total of four gels were used, with the controls in place for each set. 5 µl of Triple Coloured BlueStar PLUS prestrained protein ladder was injected into the first well of the 'untreated' doublet of each polyacrylamide gel. The Mini-PROTEAN® Tetra Cell tank (Bio-rad) was set to run for approximately 180V for one hr, or until the dye front reaches the bottom of the electrophorator.

Protein transfer was carried out briefly after SDS-PAGE whereby protein bandings were transferred to 0.45 µm nitrocellulose membrane papers (Bio-rad) electrophoretically at 85V for 1.5 hrs in a Trans-Blot® Cell apparatus (Bio-rad) containing transfer buffer with 20% methanol. The nitrocellulose membranes were cut to only contain protein of interest and loading control protein β-catenin (M_r*: ~100 kDa*) and were briefly stained with Ponceau S (0.1% w/v in 5% acetic acid) and washed with distilled water until clear.

5.7.11 Immunolocalisation of Proteins (Western Blot)

Membranes were blocked with 10% non-fat dry skim milk in Tris-buffered saline/0.25% detergent Tween20 (TBST) on an oscillating device and washed twice with TBST prior to incubation with rabbit anti-P-LKB1 (S428) (1:1000 dilution, 5% w/v BSA/TBST), rabbit anti-LKB1 (1:1000, 5% w/v BSA/TBST), primary antibodies. For each immunoblotting procedure, rabbit anti-β-catenin (1:1000, 5% w/v BSA/TBST) was used to detect for the housekeeping protein loading control. The incubation period with primary antibodies were either for 1.5 hrs at rt or overnight in 4 °C cold room on a rolling machine.

Membranes were washed four times of ten mins each on an oscillating machine with TBST and subjected to secondary antibody: horseradish peroxidase (HRP)-conjugated goat anti-rabbit IgG antibody, for 1 hr at rt on a rolling machine followed by four sets of washing with TBST. Finally, antibody complexes were visualised by an ECL Detection System whereby the membrane was developed by chemiluminescence by adding ECL reagents of 1:1 ratios and visualised by exposure to X-ray films.

5.7.12 Data Analysis and Statistics

The method of data analysis is to visually and numerically quantify the intensity of immunoblot bandings. The Image Processing and Analysis in Java software (ImageJ) developed at the National Institute of Health was used for the quantification process.

All data from immunoblotting were manipulated on Microsoft Excel 2016. Firstly, P-LKB1 bandings were normalised accordingly with the average intensity for β-catenin obtained from the duplicate of ‘untreated’ cells. This is to alter banding intensity based on standardised loading control. Secondly, given that conditions permit, i.e. fully functioning positive

controls, the average intensity of P-LKB1 for the ‘untreated’ group will be deducated from each reading to remove ‘background’ ßAR-AC-cAMP-PKA activity. The resulting numerical values will be used to determine the effect of drug compounds on the signalling pathway in accordance to their activity at the receptors. Graphs were generated on GraphPad PRISM commercial software.

5.8 References

[1] L. Schwink, P. Knochel, *Chem. Eur. J.*, **1998**, 4, 950 – 968.

[2] H. V. Nguyen, Z. -Y. Zhao, A. Sallastrau, S. L. Horswell, L. Male, A. Mulas, J. H. R. Tucker, *Chem. Commun.*, **2012**, 48, 12165 – 12167.

[3] K. Mikami, S. Matsumoto, A. Ishida, S. Takamuku, T. Suenobu, S. Fukuzumi, *J. Am. Chem. Soc.*, **1995**, 117, 11134 – 11141.

[4] J. C-. Smith, *Modified Nucleic Acids: Structural Studies and Applications in Biosensing*, PhD Thesis, University of Birmingham, **2015**.

[5] A. Sallustrau, *Synthesis of Ferrocenyl Derivatives as Novel Nucleic Analogue Monomers*, PhD Thesis, University of Birmingham, **2013**.

[6] K. A. Cruickshank, J. Jiricny, C. B. Reese, *Tetrahedron Lett.*, **1984**, 25, 681 – 684.

[7] R. Zou, M. J. Robins, *Can. J. Chem.*, **1987**, 65, 1436 – 1437

[8] M. I. Reyes Valderrama, R. A. Vázquez García, T. Klimova, E. Klimova, L. Ortiz-Frade, M. Martínez García, *Inorg. Chim. Acta.*, **2008**, 1597 – 1605.

[9] C. H. Mauldin, E. R. Biehl, P. C. Reeves, *Tetrahedron Lett.*, **1972**, 2955 – 2958.

[10] O. Nuyken, T. Pöhlmann, M. Heberhold, *Macromol. Chem. Phys.*, **1996**, 197, 3343 – 3354.

[11] K. P. Barry, C. Nataro, *Inorg. Chim. Acta.*, **2009**, 2068 – 2070.

[12] B. Lu, Q. Wang, M. Zhao, X. Xie, Z. Zhang, *J. Org. Chem.*, **2015**, 80, 9563 – 9569.

[13] Wright, L. Frambes, P. Reeves, *J. Organomet. Chem.*, **1994**, 476, 215 – 217.

[14] G. –F. Zha, W. –Y. Xu, P. Dai, X. –Y. Lai, W. Liu, Y. –C. Shen, *Chin. Chem. Lett.*, **2014**, 25, 1301 – 1304.

[15] H. V. Nguyen, A. Sallastrau, J. Balzarini, M. R. Bedford, J. C. Eden, N. Georgousi, N. J. Hodges, J. Kedge, Y. Mehellou, C. Tselepis, J. H. R. Tucker, *J. Med. Chem.*, **2014**, 57, 5817 – 5822.

[16] W. L. Davis, R. F. Shago, E. H. G. Langner, J. C. Swarts, *Polyhedron*, **2005**, 24, 1611 – 1616.

[17] C. Tonhauser, A. Alkan, M. Schömer, C. Dingels, S. Ritz, V. Mailänder, H. Frey, F. R. Wurm, *Macromolecules*, **2013**, 46, 647 – 655.

[18] M. Roemer, C. A. Nijhuis, *Dalton. Trans.*, **2014**, 43, 11815 – 11818.

[19] D. Schaarschmidt, H. Lang, *Organometallics*, **2010**, 29, 4196 – 4198.

[20] CryAlisPro, Agilent Technologies, Version 1.171.36.28, **2013**.

[21] G. M. Sheldrick, *Acta Cryst.*, **2008**, A64, 112 – 122.

[22] O. V. Dolomanov, L. J. Bourhis, R. J. Gildea, J. A. K. Howard, H. Puschmann, *J. Appl. Crystallogr.*, **2009**, 42, 339 – 341.

6 Appendix

6.1 Crystal Data

6.1.1 Crystal Data for 2.31

Identification code	**2.31**
Empirical formula	$C_{19}H_{23}FeN_5O_2S$
Formula weight	441.33
Temperature/K	99.98(13)
Crystal system	monoclinic
Space group	$P2_1/n$
a/Å	12.4764(3)
b/Å	11.0956(3)
c/Å	14.1311(4)
α/°	90
β/°	97.305(3)
γ/°	90
Volume/Å^3	1940.34(10)
Z	4
ρ_{calc}g/cm^3	1.511
μ/mm^{-1}	0.911
F(000)	920.0
Crystal size/mm^3	0.2584 × 0.1983 × 0.068
Radiation	MoKα (λ = 0.71073)
2Θ range for data collection/°	4.93 to 51.354
Index ranges	-15 ≤ h ≤ 15, -13 ≤ k ≤ 13, -13 ≤ l ≤ 17
Reflections collected	9682
Independent reflections	3681 [R_{int} = 0.0253, R_{sigma} = 0.0309]
Data/restraints/parameters	3681/0/267
Goodness-of-fit on F^2	1.069
Final R indexes [I>=2σ (I)]	R_1 = 0.0345, wR_2 = 0.0793
Final R indexes [all data]	R_1 = 0.0402, wR_2 = 0.0829
Largest diff. peak/hole / e Å^{-3}	1.10/-0.85

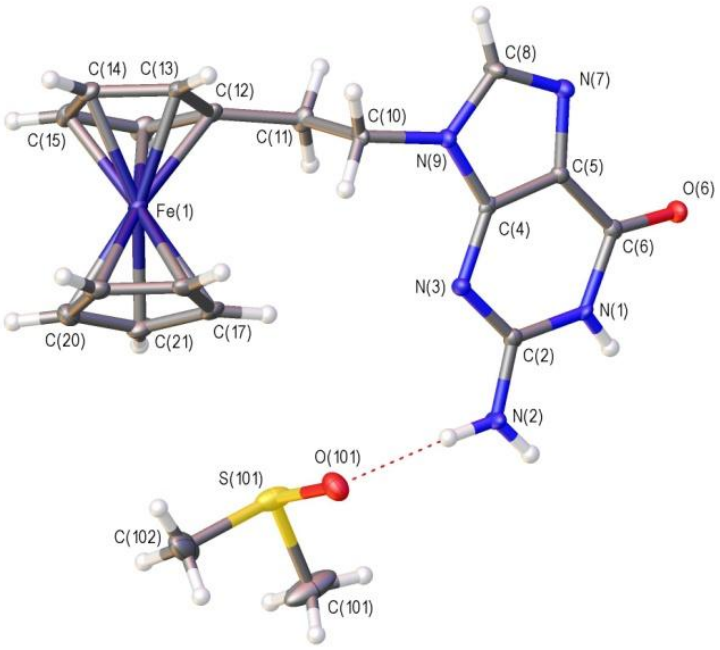


Fig. 6.1 Crystal structure of **2.31** with ellipsoids drawn at the 50% probability level. Hydrogen bonding is shown using dotted lines.

6.1.2 Crystal Data for Fcn1c2T$_{(Rp)}$

Identification code	**Fcn2c1T$_{(Rp)}$**
Empirical formula	$C_{18}H_{20}FeN_2O_3$
Formula weight	368.21
Temperature/K	99.98(12)
Crystal system	orthorhombic
Space group	$P2_12_12_1$
a/Å	11.3617(3)
b/Å	11.8847(3)
c/Å	23.7138(6)
α/°	90
β/°	90
γ/°	90
Volume/Å^3	3202.07(14)
Z	8
ρ_{calc}g/cm^3	1.528
μ/mm^{-1}	0.961
F(000)	1536.0
Crystal size/mm^3	0.1998 × 0.1946 × 0.1185
Radiation	MoKα (λ = 0.71073)
2Θ range for data collection/°	6.856 to 54.962
Index ranges	-14 ≤ h ≤ 14, -14 ≤ k ≤ 15, -30 ≤ l ≤ 30
Reflections collected	34740
Independent reflections	7237 [R_{int} = 0.0381, R_{sigma} = 0.0299]
Data/restraints/parameters	7237/2/447
Goodness-of-fit on F^2	1.097
Final R indexes [I>=2σ (I)]	R_1 = 0.0318, wR_2 = 0.0743
Final R indexes [all data]	R_1 = 0.0332, wR_2 = 0.0751
Largest diff. peak/hole / e Å^{-3}	1.11/-0.28
Flack parameter	0.003(5)

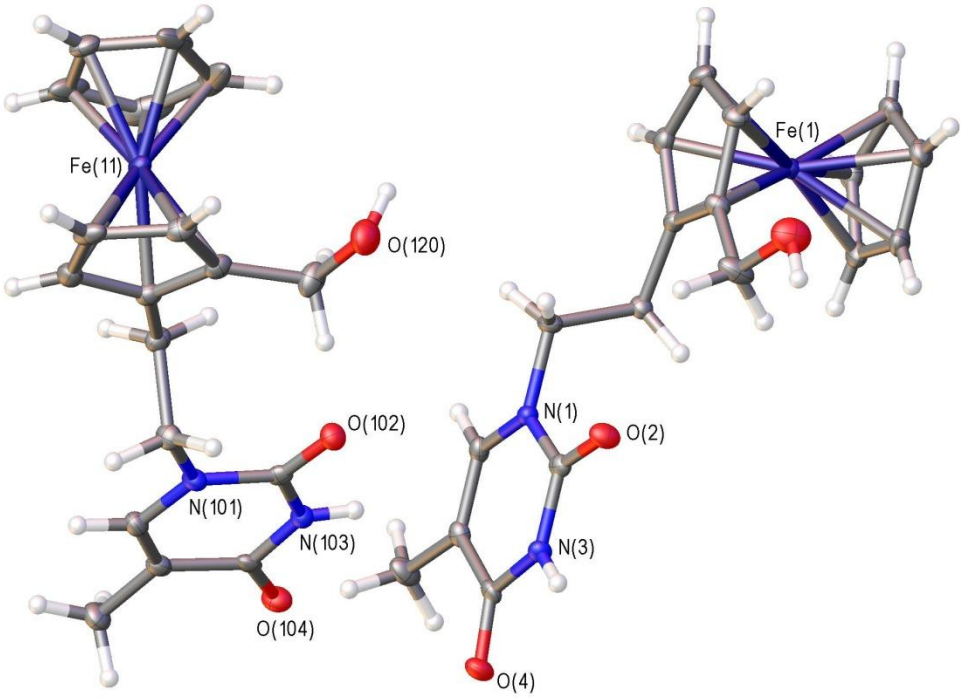


Fig. 6.2 Crystal structure of **Fcn2c1T**$_{(Rp)}$ with ellipsoids drawn at the 50% probability level. The structure contains two crystallographically-independent molecules.

6.1.3 Crystal Data for Fcn1c2T$_{(Sp)}$

Identification code	**Fcn1c2T$_{(Sp)}$**
Empirical formula	$C_{18}H_{20}FeN_2O_3$
Formula weight	368.21
Temperature/K	100.00(10)
Crystal system	orthorhombic
Space group	$P2_12_12_1$
a/Å	11.3958(6)
b/Å	11.8730(6)
c/Å	23.7314(10)
α/°	90
β/°	90
γ/°	90
Volume/Å^3	3210.9(3)
Z	8
ρ_{calc}g/cm^3	1.523
μ/mm^{-1}	0.958
F(000)	1536.0
Crystal size/mm^3	0.1379 × 0.1028 × 0.0737
Radiation	MoKα (λ = 0.71073)
2Θ range for data collection/°	4.954 to 56.56
Index ranges	-14 ≤ h ≤ 10, -14 ≤ k ≤ 15, -29 ≤ l ≤ 31
Reflections collected	24084
Independent reflections	7488 [R_{int} = 0.0481, R_{sigma} = 0.0485]
Data/restraints/parameters	7488/19/469
Goodness-of-fit on F^2	1.130
Final R indexes [I>=2σ (I)]	R_1 = 0.0496, wR_2 = 0.1094
Final R indexes [all data]	R_1 = 0.0544, wR_2 = 0.1115
Largest diff. peak/hole / e Å^{-3}	1.03/-0.40
Flack parameter	0.018(7)

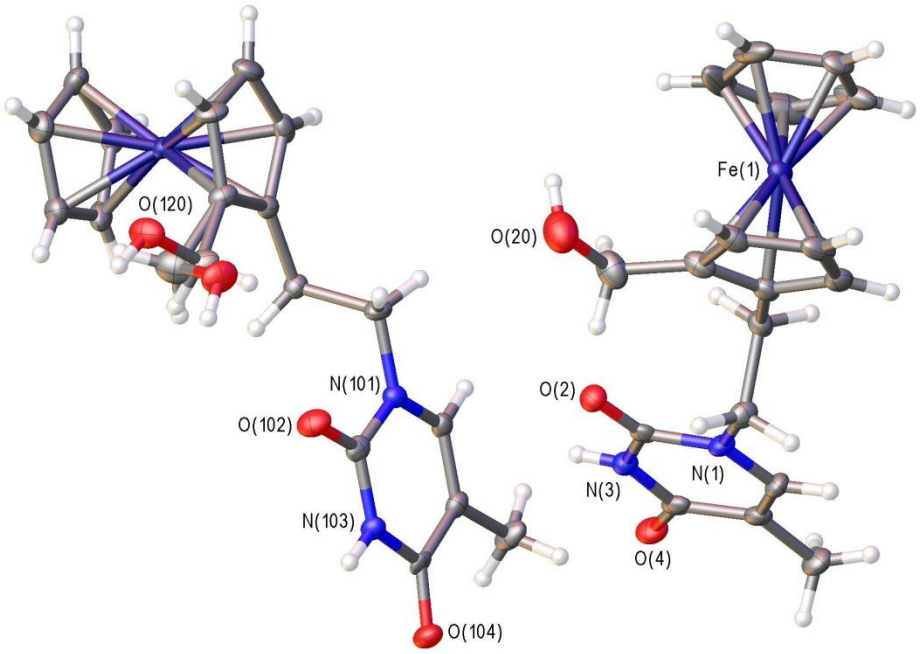


Fig. 6.3 Crystal structure of **Fcn1c2T**$_{(Sp)}$ with ellipsoids drawn at the 50% probability level. The structure contains two crystallographically-independent molecules. The group C(120)-O(120)/C(20')-O(20') is disordered over two positions with the refined percentage occupancy ratio being 73(1):27(1).

6.1.4 Crystal Data for Fcn2c2T$_{(Rp)}$

Identification code	**Fcn2c2T$_{(Rp)}$**
Empirical formula	$C_{19}H_{22}FeN_2O_3$
Formula weight	382.23
Temperature/K	100.01(10)
Crystal system	tetragonal
Space group	$P4_32_12$
a/Å	11.96948(10)
b/Å	11.96948(10)
c/Å	24.1571(3)
α/°	90
β/°	90
γ/°	90
Volume/Å^3	3460.95(7)
Z	8
ρ_{calc}g/cm^3	1.467
μ/mm^{-1}	0.892
F(000)	1600.0
Crystal size/mm^3	0.3796 × 0.2721 × 0.2025
Radiation	MoKα (λ = 0.71073)
2Θ range for data collection/°	4.792 to 58.954
Index ranges	-16 ≤ h ≤ 15, -15 ≤ k ≤ 16, -31 ≤ l ≤ 33
Reflections collected	71538
Independent reflections	4700 [R_{int} = 0.0401, R_{sigma} = 0.0162]
Data/restraints/parameters	4700/155/309
Goodness-of-fit on F^2	1.085
Final R indexes [I>=2σ (I)]	R_1 = 0.0410, wR_2 = 0.0948
Final R indexes [all data]	R_1 = 0.0542, wR_2 = 0.1030
Largest diff. peak/hole / e Å^{-3}	0.39/-0.40
Flack parameter	-0.003(5)

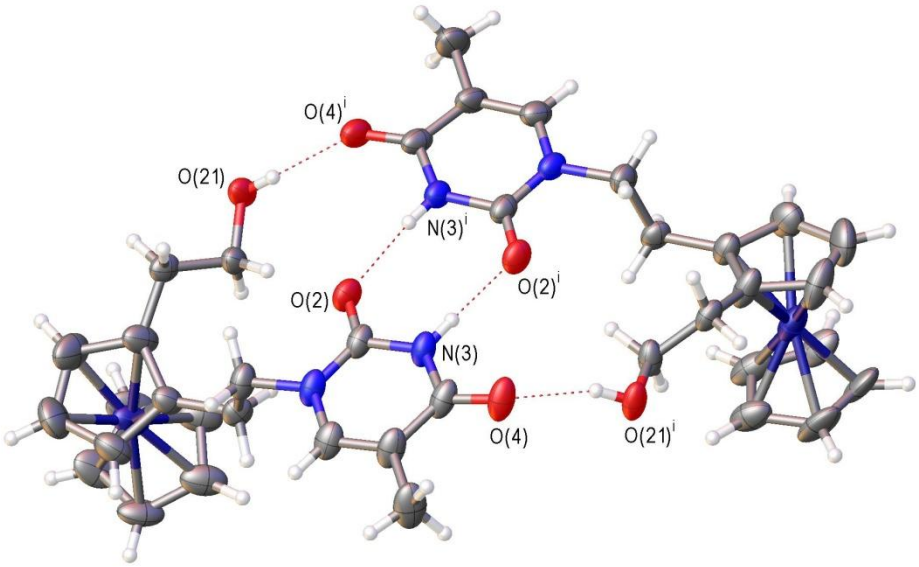


Fig. 6.4 Hydrogen bonded dimer formed by **Fcn2c2T**$_{(Rp)}$ with ellipsoids drawn at the 50% probability level. Hydrogen bonds are shown as dotted lines. The Cp ring C(15)-C(19) / C(15')-C(19') and the group C(20), C(21), O(21) / C(20'), C(21'), O(21') are both disordered over two positions, with only the major positions shown for clarity. Symmetry code for generation of equivalent atoms: i) y, x, -z.

6.1.5 Crystal Data for Fcn2c2T$_{(Sp)}$

Identification code	**Fcn2c2T$_{(Sp)}$**
Empirical formula	$C_{19}H_{22}FeN_2O_3$
Formula weight	382.23
Temperature/K	100.0(3)
Crystal system	orthorhombic
Space group	$P2_12_12_1$
a/Å	11.8672(3)
b/Å	12.1205(3)
c/Å	24.1747(5)
α/°	90
β/°	90
γ/°	90
Volume/Å^3	3477.19(13)
Z	8
ρ_{calc}g/cm^3	1.460
μ/mm^{-1}	0.888
F(000)	1600.0
Crystal size/mm^3	0.2717 × 0.2039 × 0.1759
Radiation	MoKα (λ = 0.71073)
2Θ range for data collection/°	4.76 to 52.74
Index ranges	-14 ≤ h ≤ 14, -15 ≤ k ≤ 15, -30 ≤ l ≤ 29
Reflections collected	35875
Independent reflections	7092 [R_{int} = 0.0418, R_{sigma} = 0.0241]
Data/restraints/parameters	7092/373/566
Goodness-of-fit on F^2	1.053
Final R indexes [I>=2σ (I)]	R_1 = 0.0571, wR_2 = 0.1389
Final R indexes [all data]	R_1 = 0.0632, wR_2 = 0.1442
Largest diff. peak/hole / e Å^{-3}	0.73/-0.69
Flack parameter	0.018(6)

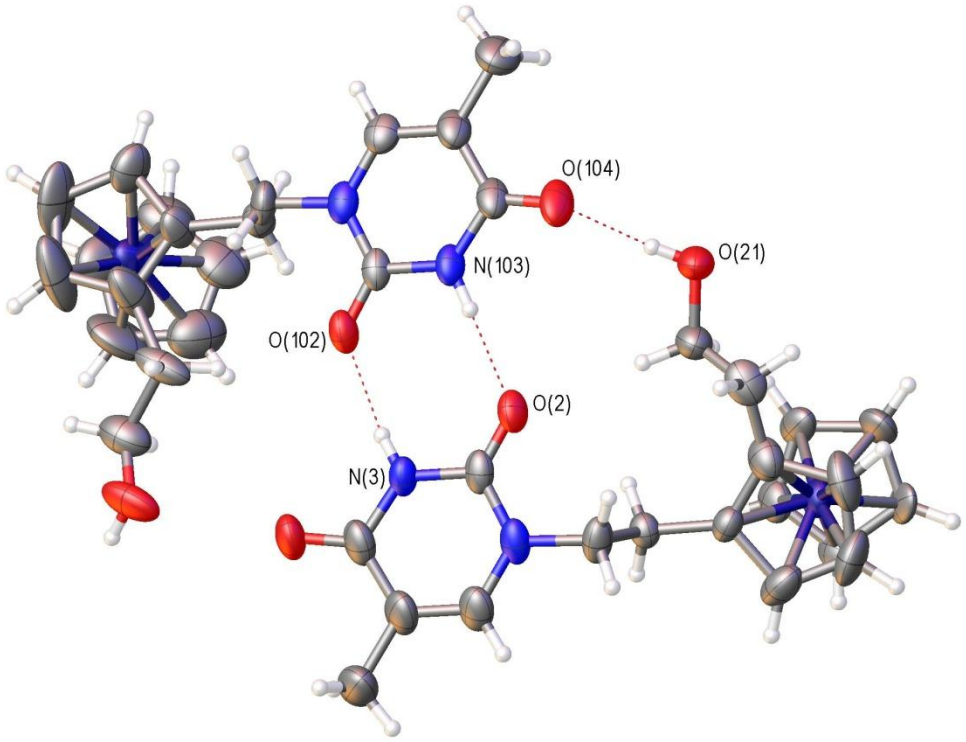


Fig. 6.5 Crystal structure of **Fcn2c2T**$_{(Sp)}$ with ellipsoids drawn at the 50% probability level. The Cp ring C(15)-C(19) / C(15')-C(19') is disordered over two positions with the refined occupancy ratio being 0.58(3):0.42(3). The group C(20), C(21), O(21) / C(0'), C(1'), O(1') is disordered over two positions with the refined occupancy ratio being 0.581(14):0.419(14). The group C(120), C(121), O(121) / C(20'), C(21'), O(21') is disordered over two positions with the refined occupancy ratio being 0.525(11):0.475(11).

6.1.6 Crystal Data for Fcn1c2G$_{(Rp)}$

Identification code	**Fcn1c2G$_{(Rp)}$**
Empirical formula	$C_{18}H_{23}FeN_5O_4$
Formula weight	429.26
Temperature/K	100.01(10)
Crystal system	orthorhombic
Space group	$P2_12_12$
a/Å	43.2453(8)
b/Å	11.1749(3)
c/Å	7.75582(18)
α/°	90
β/°	90
γ/°	90
Volume/Å^3	3748.10(16)
Z	8
ρ_{calc}g/cm^3	1.521
μ/mm^{-1}	0.841
F(000)	1792.0
Crystal size/mm^3	0.209 × 0.088 × 0.0393
Radiation	MoKα (λ = 0.71073)
2Θ range for data collection/°	4.612 to 53.454
Index ranges	$-54 \leq h \leq 52$, $-14 \leq k \leq 13$, $-9 \leq l \leq 9$
Reflections collected	19244
Independent reflections	7519 [R_{int} = 0.0277, R_{sigma} = 0.0388]
Data/restraints/parameters	7519/2/559
Goodness-of-fit on F^2	1.167
Final R indexes [I>=2σ (I)]	R_1 = 0.0501, wR_2 = 0.1075
Final R indexes [all data]	R_1 = 0.0544, wR_2 = 0.1095
Largest diff. peak/hole / e Å^{-3}	0.89/-0.50
Flack parameter	0.011(6)

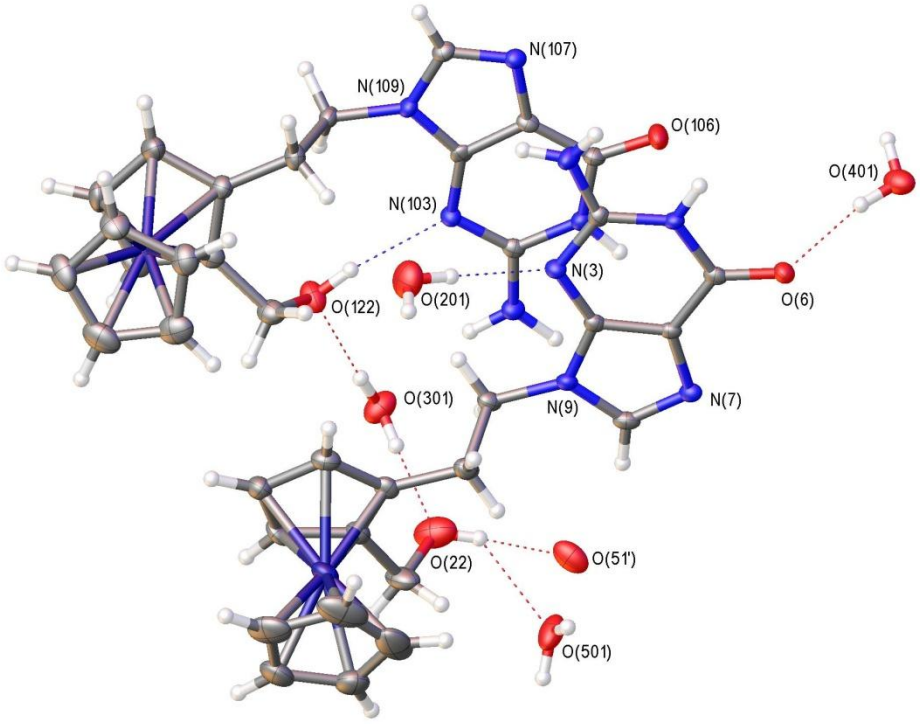


Fig. 6.6 Crystal structure of **Fcn1c2G**$_{(Rp)}$ with ellipsoids drawn at the 50% probability level. Hydrogen bonding is shown using dotted lines. The structure contains two crystallographically-independent ferrocene molecules and four molecules of water, one of which, O(501)/O(51') is disordered over two positions with a refined percentage occupancy ratio of 71.3(11):28.7(11). It was not possible to refine hydrogen atom positions on the minor component, O(51').

Note:

One of the hydrogen atoms belonging to water molecules O(201), H(20A) does not form a hydrogen bond. We are confident of its position as there is a peak of electron density in that location. H(20A) is pointing directly at the centre of the ring C(112)-C(116) with the distance between H(20A) and the ring centroid being 2.59 Å and the O(201)-H(20A)...centroid angle being 158°.

6.1.7 Crystal Data for 4.5

Identification code	**4.5**
Empirical formula	$C_{18}H_{27}FeNO_2$
Formula weight	345.25
Temperature/K	100.01(10)
Crystal system	monoclinic
Space group	$P2_1/n$
a/Å	14.4245(7)
b/Å	7.4031(3)
c/Å	17.2738(8)
α/°	90
β/°	105.391(5)
γ/°	90
Volume/Å^3	1778.43(15)
Z	4
ρ_{calc}g/cm^3	1.289
μ/mm^{-1}	0.854
F(000)	736.0
Crystal size/mm^3	0.323 × 0.119 × 0.067
Radiation	MoKα (λ = 0.71073)
2Θ range for data collection/°	5.858 to 52.744
Index ranges	$-17 \leq h \leq 18$, $-9 \leq k \leq 9$, $-21 \leq l \leq 21$
Reflections collected	8133
Independent reflections	8133 [R_{int} = N/A, R_{sigma} = 0.0524]
Data/restraints/parameters	8133/0/211
Goodness-of-fit on F^2	1.056
Final R indexes [I>=2σ (I)]	R_1 = 0.0575, wR_2 = 0.1659
Final R indexes [all data]	R_1 = 0.0745, wR_2 = 0.1725
Largest diff. peak/hole / e Å^{-3}	1.47/-0.69

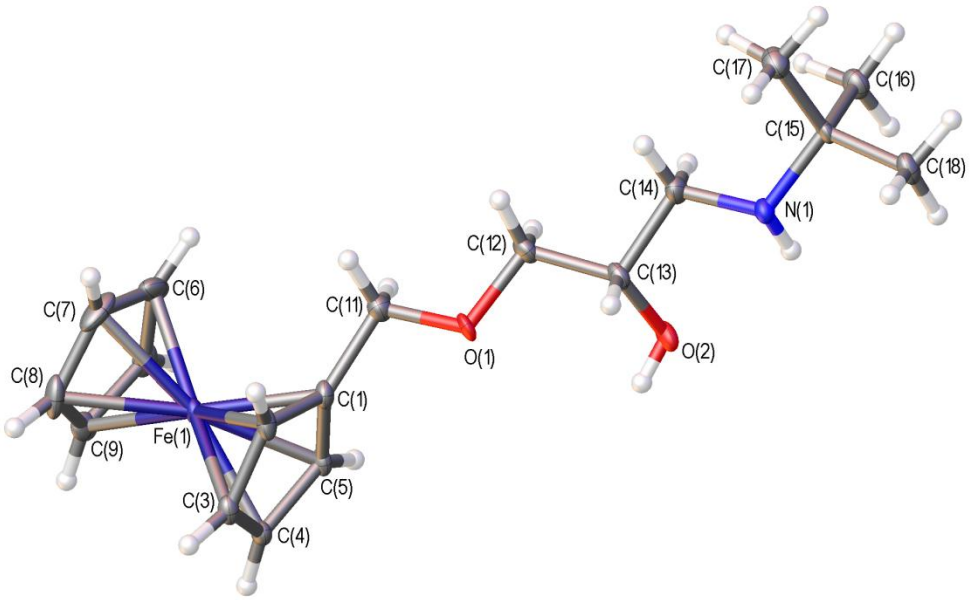


Fig. 6.7 Crystal structure of **4.5** with ellipsoids drawn at the 50% probability level. The crystal is a two-component twin, with the refined percentage ratio of domains being 69:31. The space group is centrosymmetric which means that the structure is a racemic mixture of enantiomers. The hydrogen atoms bonded to N(1) and O(2) were located in the electron density and the positions freely refined while the remaining hydrogen atoms were fixed as riding models.

6.1.8 Crystal Data for 4.8

Identification code	**4.8**
Empirical formula	$C_{13}H_{14}FeO_2$
Formula weight	258.09
Temperature/K	99.99(10)
Crystal system	monoclinic
Space group	$P2_1/c$
a/Å	13.8764(4)
b/Å	9.07141(19)
c/Å	9.1712(3)
α/°	90
β/°	106.676(3)
γ/°	90
Volume/Å^3	1105.91(6)
Z	4
ρ_{calc}g/cm^3	1.550
μ/mm^{-1}	1.343
F(000)	536.0
Crystal size/mm^3	0.3334 × 0.1614 × 0.1389
Radiation	MoKα (λ = 0.71073)
2Θ range for data collection/°	6.13 to 52.74
Index ranges	$-17 \leq h \leq 17$, $-11 \leq k \leq 11$, $-11 \leq l \leq 11$
Reflections collected	9631
Independent reflections	2262 [R_{int} = 0.0270, R_{sigma} = 0.0245]
Data/restraints/parameters	2262/19/158
Goodness-of-fit on F^2	1.061
Final R indexes [I>=2σ (I)]	R_1 = 0.0253, wR_2 = 0.0568
Final R indexes [all data]	R_1 = 0.0317, wR_2 = 0.0607
Largest diff. peak/hole / e Å^{-3}	0.38/-0.33

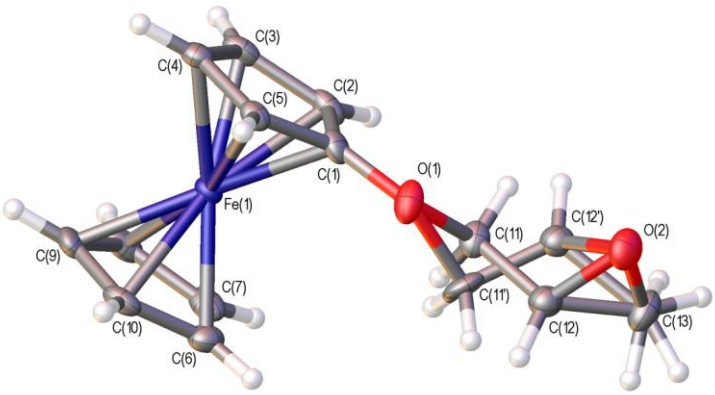


Fig. 6.8 Crystal structure of **4.8** with ellipsoids drawn at the 50% probability level. The group C(11)-C(12)/C(11')-C(12') is disordered over two positions with a refined percentage occupancy ratio of 85.8 (4): 14.2(4). All hydrogen atoms were fixed as riding models. The U_{iso} of the hydrogen atoms were based on the U_{eq} of the parent atoms in all cases.

6.1.9 Crystal Data for 4.10

Identification code	**4.10**
Empirical formula	$C_{16}H_{21}FeNO_2$
Formula weight	315.19
Temperature/K	99.9(3)
Crystal system	monoclinic
Space group	$P2_1/c$
a/Å	13.0469(4)
b/Å	15.9279(3)
c/Å	7.15908(16)
α/°	90
β/°	105.366(3)
γ/°	90
Volume/Å^3	1434.55(6)
Z	4
ρ_{calc}g/cm^3	1.459
μ/mm^{-1}	1.052
F(000)	664.0
Crystal size/mm^3	0.45 × 0.114 × 0.09
Radiation	MoKα (λ = 0.71073)
2Θ range for data collection/°	5.114 to 52.742
Index ranges	$-16 \leq h \leq 13$, $-19 \leq k \leq 19$, $-8 \leq l \leq 8$
Reflections collected	12219
Independent reflections	2924 [R_{int} = 0.0247, R_{sigma} = 0.0223]
Data/restraints/parameters	2924/0/189
Goodness-of-fit on F^2	1.036
Final R indexes [I>=2σ (I)]	R_1 = 0.0267, wR_2 = 0.0611
Final R indexes [all data]	R_1 = 0.0315, wR_2 = 0.0634
Largest diff. peak/hole / e Å^{-3}	0.61/-0.31

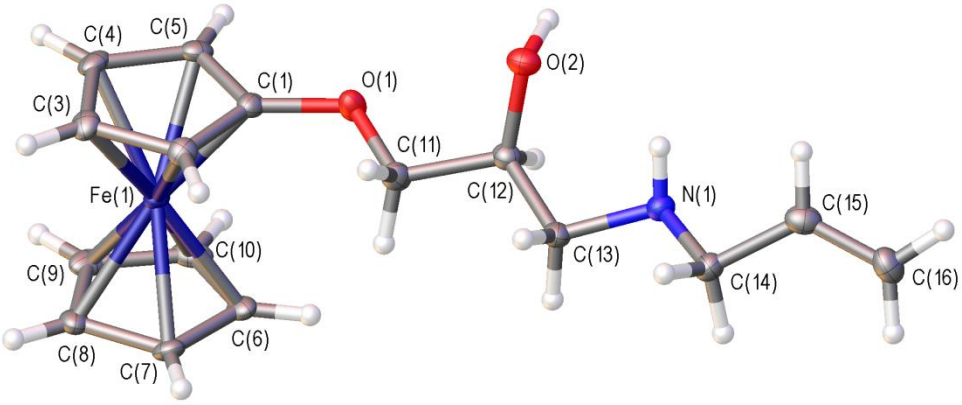


Fig. 6.9 Crystal structure of **4.10** with ellipsoids drawn at the 50% probability level. The structure is in a centrosymmetric space group such that in two of the molecules in the unit cell the chirality of C(12) is *S* and in the other two molecules the chirality of C(12) is *R*. The positions of the hydrogen atoms bonded to O(2) and N(1) were located in the electron density and refined freely. All remaining hydrogen atoms were fixed as riding models. The U_{iso} of all the hydrogen atoms were based on the U_{eq} of the parent atoms.

6.1.10 Crystal Data for 4.12

Identification code	**4.12**
Empirical formula	$C_{17}H_{25}FeNO_2$
Formula weight	331.23
Temperature/K	99.98(13)
Crystal system	tetragonal
Space group	$I4_1/a$
a/Å	23.5334(3)
b/Å	23.5334(3)
c/Å	11.6069(2)
α/°	90
β/°	90
γ/°	90
Volume/Å^3	6428.1(2)
Z	16
ρ_{calc}g/cm^3	1.369
μ/mm^{-1}	0.942
F(000)	2816.0
Crystal size/mm^3	0.3269 × 0.0865 × 0.0612
Radiation	MoKα (λ = 0.71073)
2Θ range for data collection/°	4.896 to 54.198
Index ranges	$-29 \leq h \leq 21$, $-30 \leq k \leq 25$, $-11 \leq l \leq 14$
Reflections collected	17216
Independent reflections	3533 [R_{int} = 0.0263, R_{sigma} = 0.0206]
Data/restraints/parameters	3533/0/199
Goodness-of-fit on F^2	1.045
Final R indexes [I>=2σ (I)]	R_1 = 0.0287, wR_2 = 0.0705
Final R indexes [all data]	R_1 = 0.0356, wR_2 = 0.0749
Largest diff. peak/hole / e Å^{-3}	0.46/-0.26

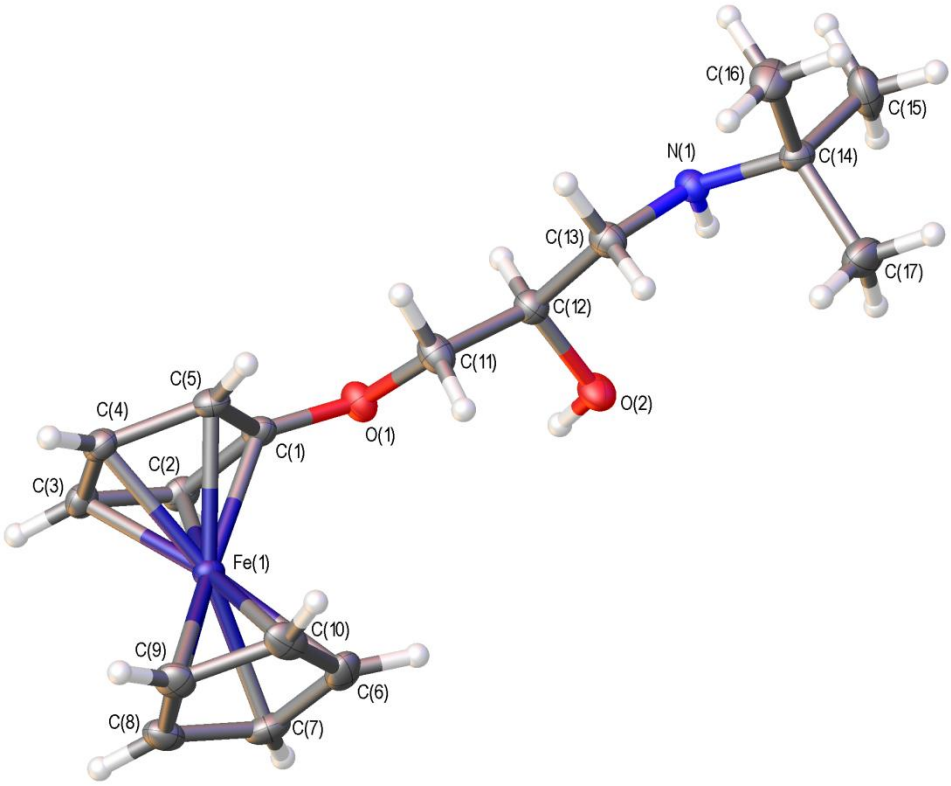


Fig. 6.10 Crystal structure of **4.12** with ellipsoids drawn at the 50% probability level. The structure is in a centrosymmetric space group such that in eight of the molecules in the unit cell the chirality of C(12) is *R* and in the other eight molecules the chirality of C(12) is *S*.The positions of the hydrogen atoms bonded to O(2) and N(1) were located in the electron density and refined freely. All remaining hydrogen atoms were fixed as riding models. The U_{iso} of all the hydrogen atoms were based on the U_{eq} of the parent atoms.

6.1.11 Crystal Data for 4.13

Identification code	**4.13**
Empirical formula	$C_{18}H_{21}FeNO_3$
Formula weight	355.21
Temperature/K	99.98(10)
Crystal system	monoclinic
Space group	$P2_1/c$
a/Å	14.4157(5)
b/Å	15.8275(5)
c/Å	7.1621(2)
α/°	90
β/°	101.753(3)
γ/°	90
Volume/Å^3	1599.88(9)
Z	4
ρ_{calc}g/cm^3	1.475
μ/mm^{-1}	0.957
F(000)	744.0
Crystal size/mm^3	0.3651 × 0.1803 × 0.0361
Radiation	MoKα (λ = 0.71073)
2Θ range for data collection/°	6.322 to 52.74
Index ranges	$-13 \leq h \leq 18$, $-14 \leq k \leq 19$, $-8 \leq l \leq 8$
Reflections collected	6334
Independent reflections	3250 [R_{int} = 0.0249, R_{sigma} = 0.0390]
Data/restraints/parameters	3250/0/216
Goodness-of-fit on F^2	1.087
Final R indexes [I>=2σ (I)]	R_1 = 0.0355, wR_2 = 0.0853
Final R indexes [all data]	R_1 = 0.0448, wR_2 = 0.0912
Largest diff. peak/hole / e Å^{-3}	0.50/-0.47

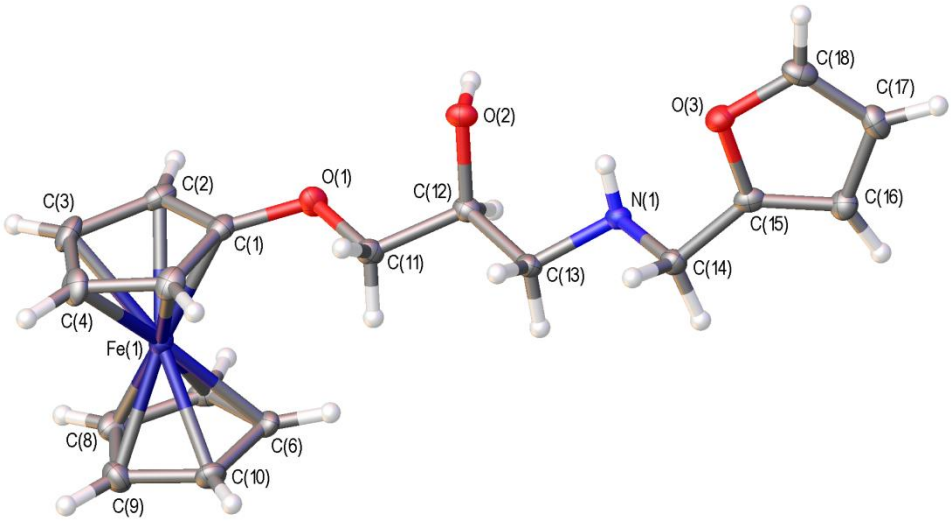


Fig. 6.11 Crystal structure of **4.13** with ellipsoids drawn at the 50% probability level. The structure is in a centrosymmetric space group such that in two of the molecules in the unit cell the chirality of C(12) is *S* and in the other two molecules the chirality of C(12) is *R*. All hydrogen atoms were fixed as riding models. The U_{iso} of the hydrogen atoms were based on the U_{eq} of the parent atoms in all cases.

6.1.12 Crystal Data for 4.15

Identification code	**4.15**
Empirical formula	$C_{19}H_{27}FeNO_2$
Formula weight	357.26
Temperature/K	99.97(16)
Crystal system	monoclinic
Space group	$P2_1$
a/Å	11.8112(3)
b/Å	5.59969(14)
c/Å	13.1257(4)
α/°	90
β/°	101.448(3)
γ/°	90
Volume/Å^3	850.85(4)
Z	2
ρ_{calc}g/cm^3	1.394
μ/mm^{-1}	0.896
F(000)	380.0
Crystal size/mm^3	0.1834 × 0.0336 × 0.0245
Radiation	MoKα (λ = 0.71073)
2Θ range for data collection/°	5.18 to 52.03
Index ranges	$-14 \leq h \leq 13$, $-6 \leq k \leq 6$, $-16 \leq l \leq 15$
Reflections collected	6395
Independent reflections	3317 [R_{int} = 0.0216, R_{sigma} = 0.0376]
Data/restraints/parameters	3317/1/215
Goodness-of-fit on F^2	1.068
Final R indexes [I>=2σ (I)]	R_1 = 0.0285, wR_2 = 0.0604
Final R indexes [all data]	R_1 = 0.0326, wR_2 = 0.0622
Largest diff. peak/hole / e Å^{-3}	0.53/-0.20

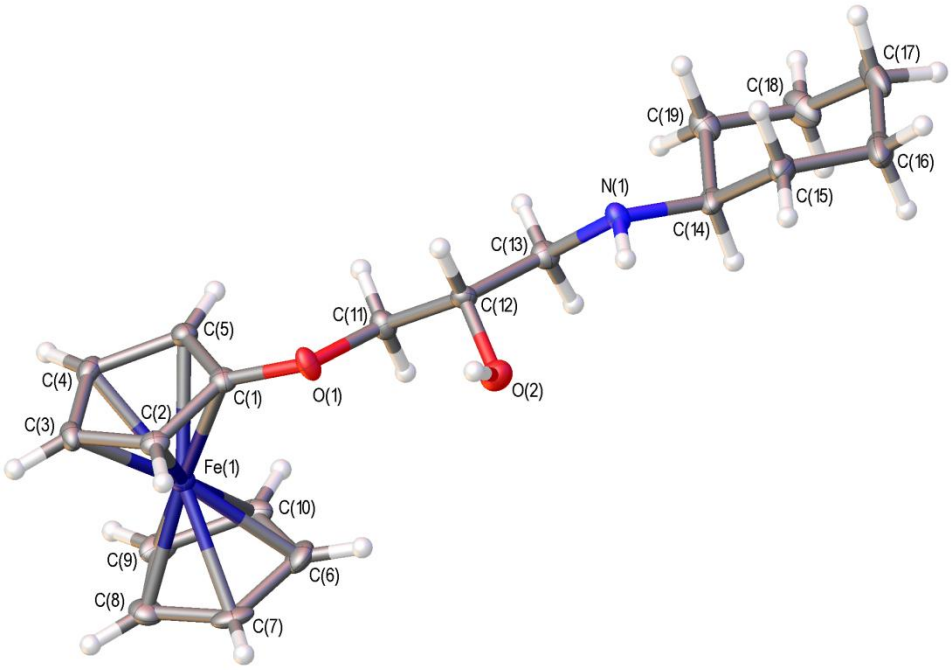


Fig. 6.12 Crystal structure of **4.15** with ellipsoids drawn at the 50% probability level. The structure is in a chiral space group and has been refined as an inversion twin with the refined ratio of domains being 0.75 (2) : 025 (2). This in 75% of cases the chirality of C(12) is *S* and in 25% of cases the chirality of C(12) is *R*. The positions of the hydrogen atoms bonded to N(1) and O(2) were located in the electron density and refined freely. All remaining hydrogen atoms were fixed as riding models. The U_{iso} of all the hydrogen atoms were based on the U_{eq} of the parent atoms.

6.2 Electrochemistry

6.2.1 Electrochemistry Plots for Fcn3c2T$_{(S,Rp)}$

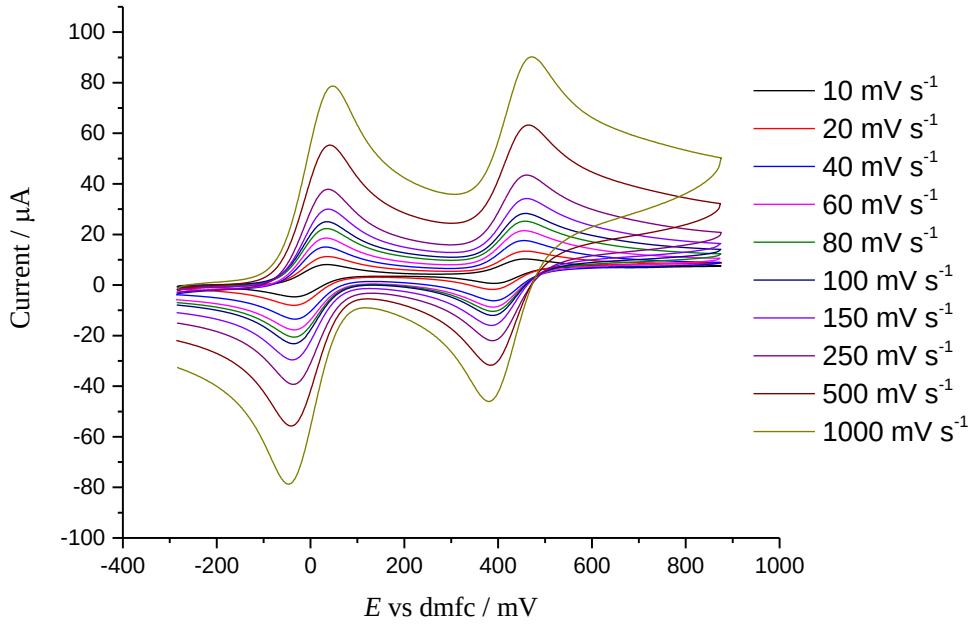


Fig. 6.13 CV of **Fcn3c2T**$_{(S,Rp)}$ vs dmfc at various scan rates

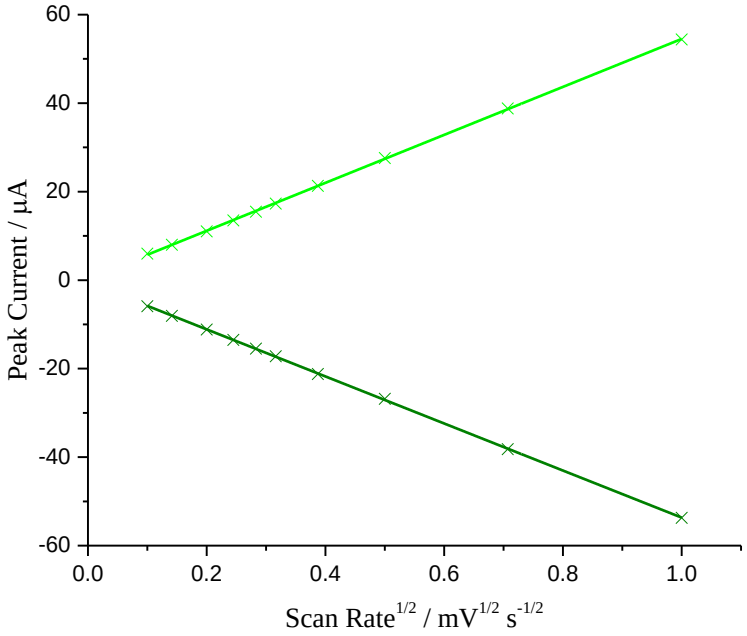


Fig. 6.14 Plot of peak current vs square root of the scan rate for **Fcn3c2T**$_{(S,Rp)}$

6.2.2 Electrochemistry Plots for Fcn2c2T$_{(Rp)}$

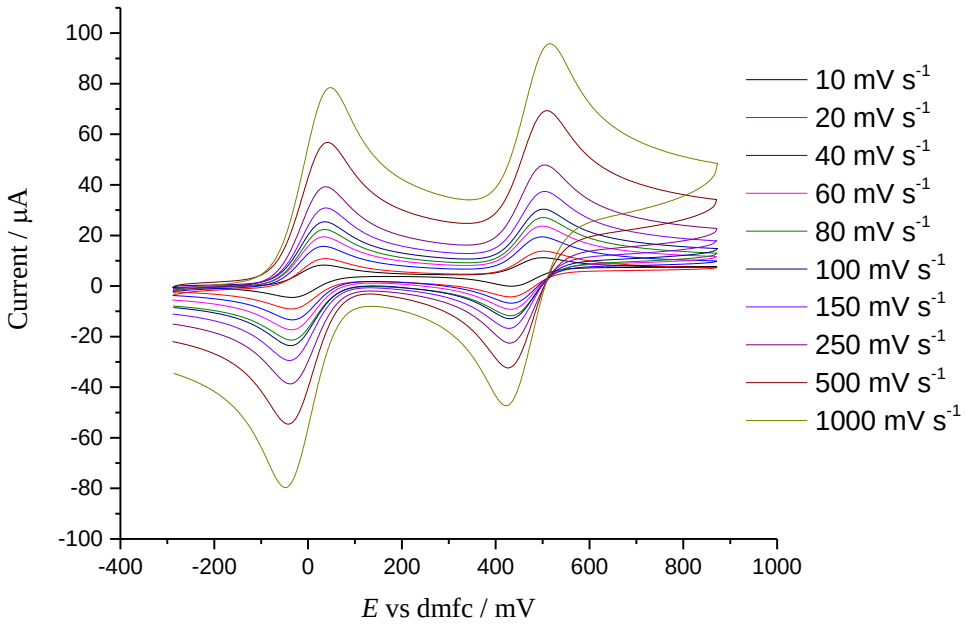


Fig. 6.15 CV of **Fcn2c2T**$_{(Rp)}$ vs dmfc at various scan rates

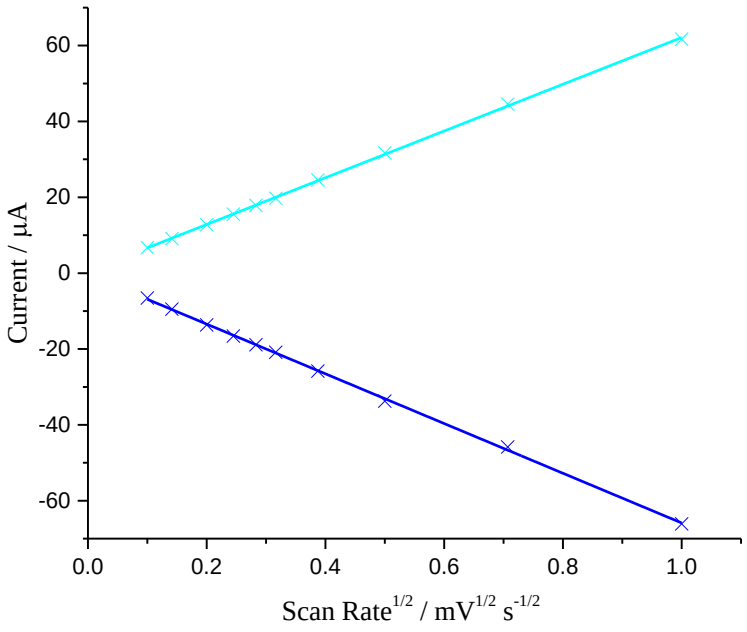


Fig. 6.16 Plot of peak current vs square root of the scan rate for **Fcn2c2T**$_{(Rp)}$

6.2.3 Electrochemistry Plots for Fcn1c2T$_{(Rp)}$

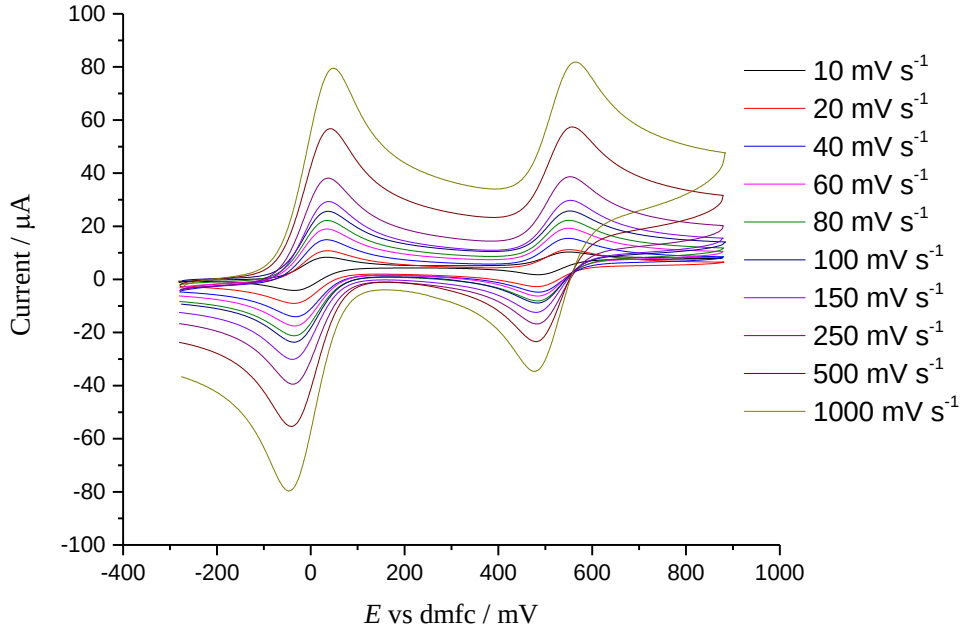


Fig. 6.17 CV of **Fcn1c2T**$_{(Rp)}$ vs dmfc at various scan rates

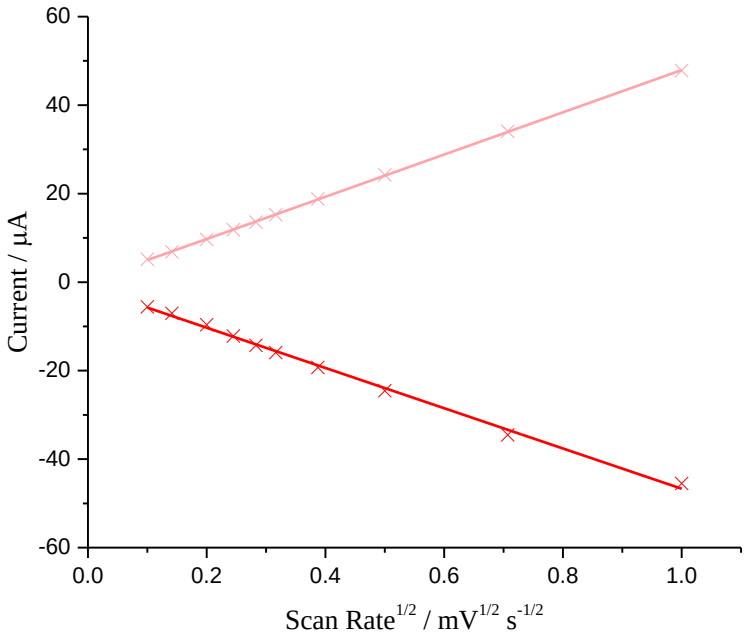


Fig. 6.18 Plot of peak current vs square root of the scan rate for **Fcn1c2T**$_{(Rp)}$

6.2.4 Electrochemistry Plots for Fcn2c2T

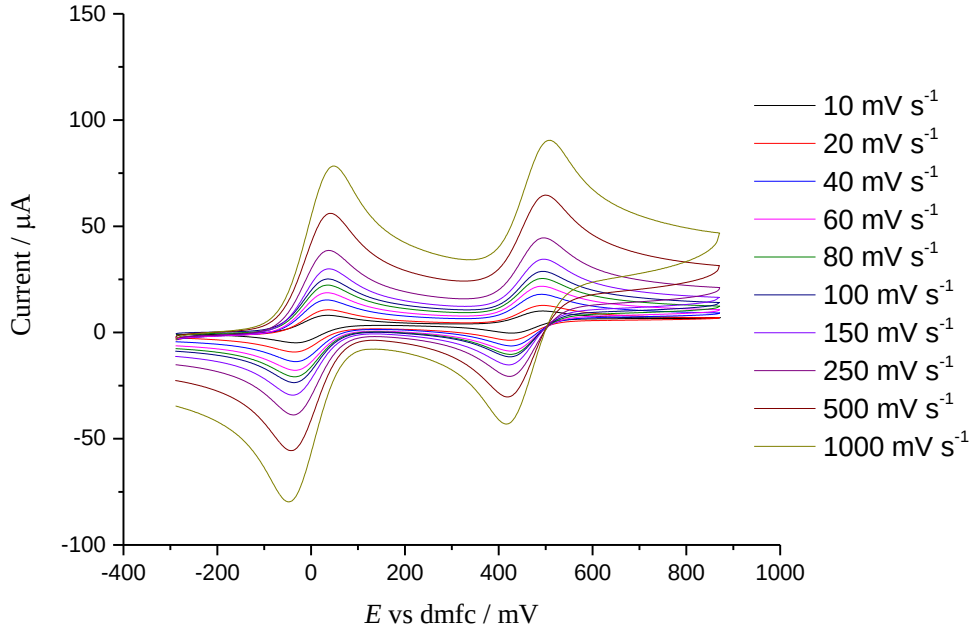


Fig. 6.19 CV of **Fcn2c2T** vs dmfc at various scan rates

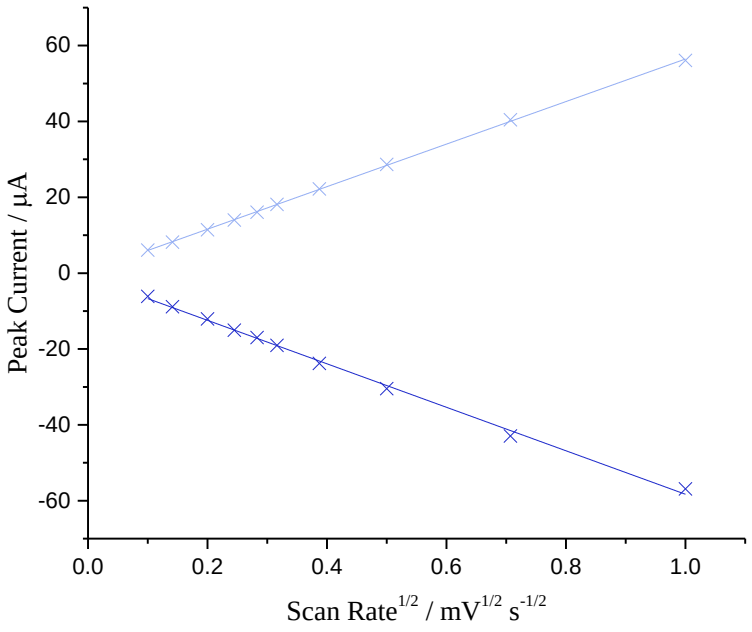


Fig. 6.20 Plot of peak current vs square root of the scan rate for **Fcn2c2T**

6.2.5 Electrochemistry Plots for Fcn2c2G$_{(Sp)}$

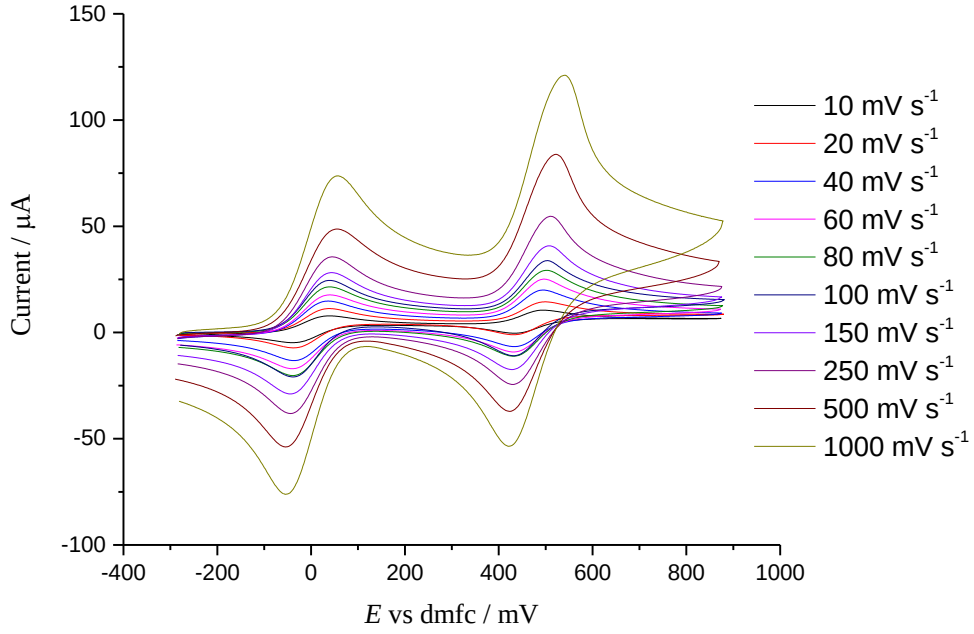


Fig. 6.21 CV of **Fcn2c2G**$_{(Sp)}$ vs dmfc at various scan rates

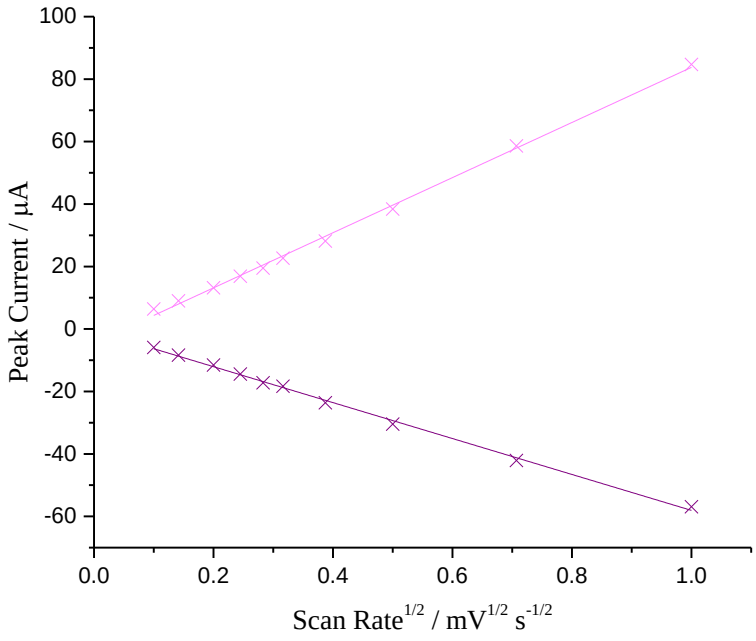


Fig. 6.22 Plot of peak current vs square root of the scan rate for **Fcn2c2G**$_{(Sp)}$

6.2.6 Electrochemistry Plots for Fcn1c2G$_{(Rp)}$

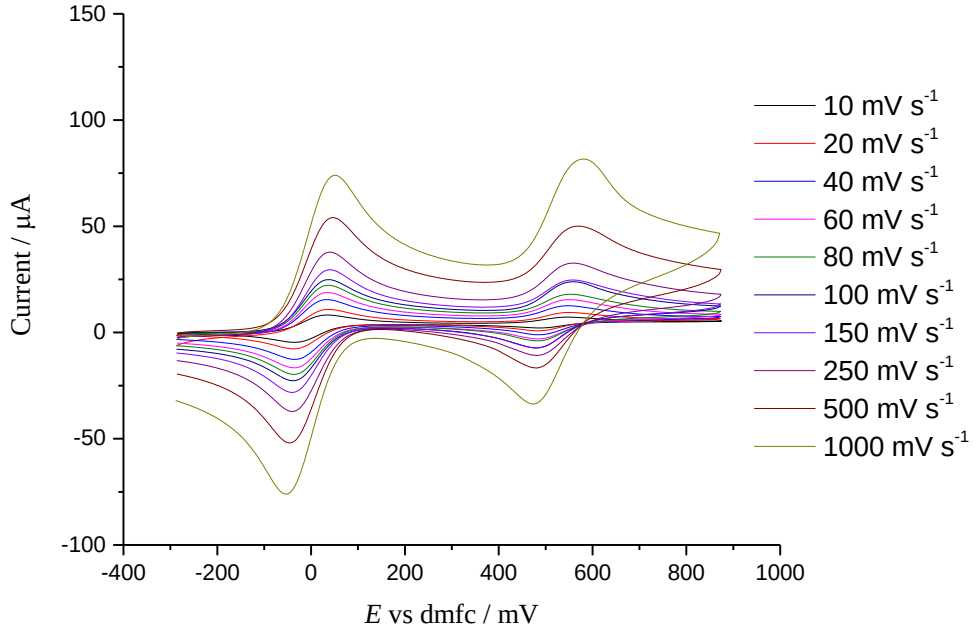


Fig. 6.23 CV of **Fcn1c2G**$_{(Rp)}$ vs dmfc at various scan rates

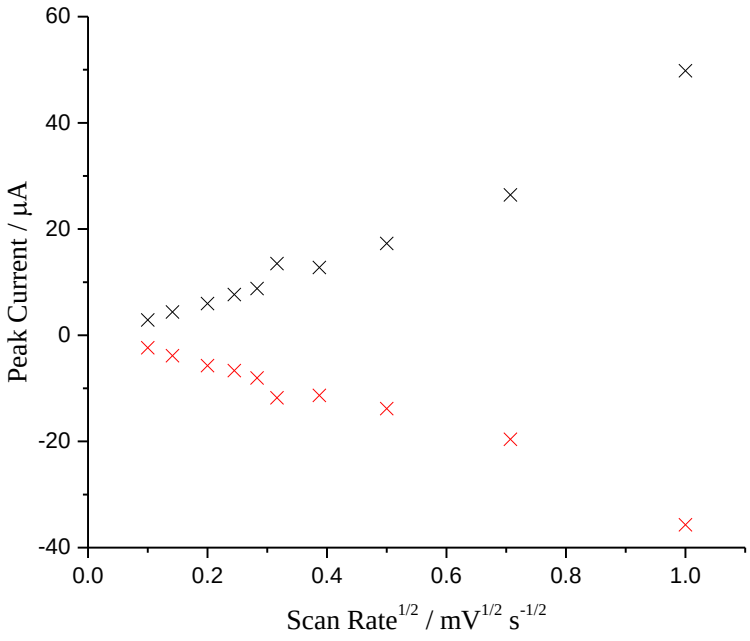


Fig. 6.24 Plot of peak current vs square root of the scan rate for **Fcn1c2G(R_p)**

6.2.7 Electrochemistry Plots for Fcn2c2G

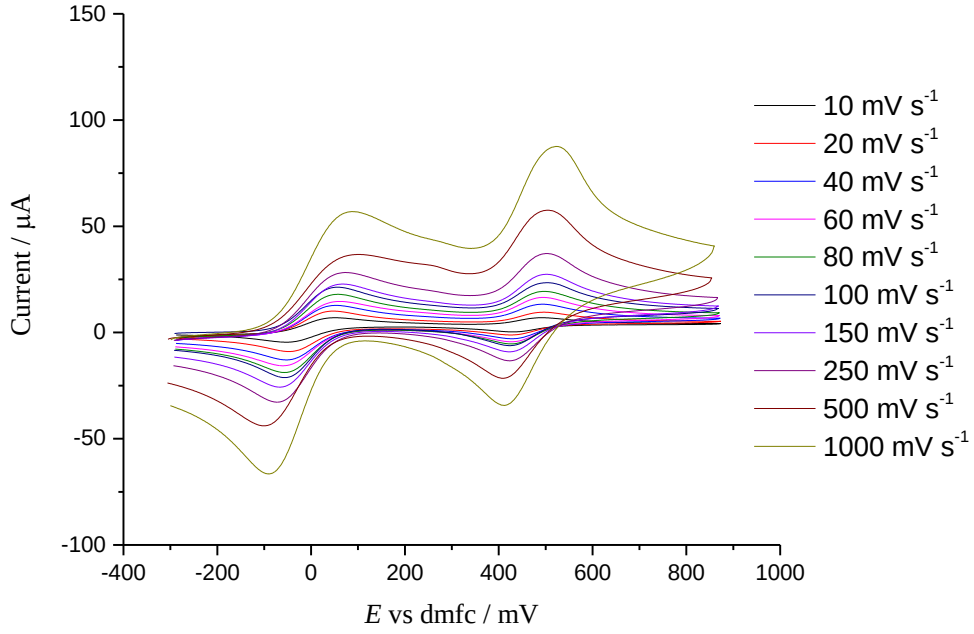


Fig. 6.25 CV of **Fcn2c2G** vs dmfc at various scan rates

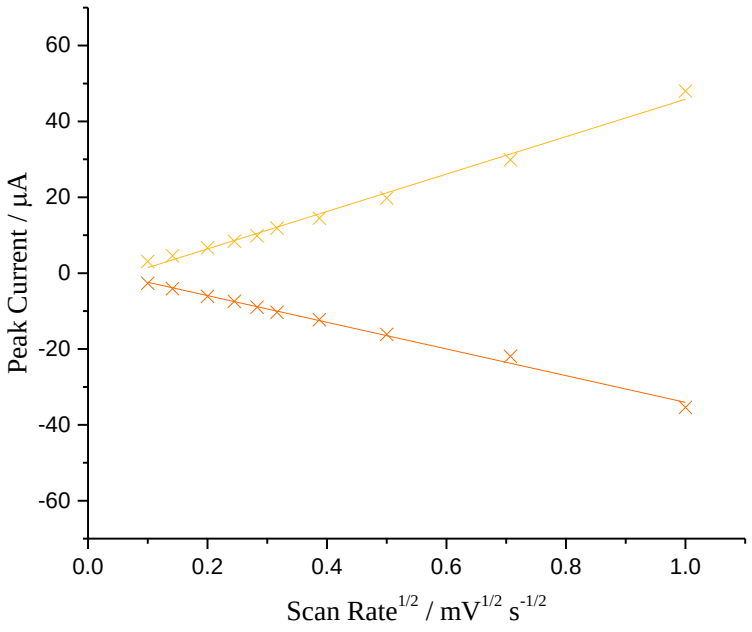


Fig. 6.26 Plot of peak current vs square root of the scan rate for **Fcn3c2G**

7 Publications, Presentations, Awards and Courses

Publications

1st Author - Organometallic Nucleoside Analogues: Effect of Hydroxylalkyl Linker Length on Cancer Cell Line Toxicity: **J. L. Kedge**, H. V. Nguyen, Z. Khan, L. Male, M. K. Ismail, N. J. Hodges, S. L. Horswell, Y. Mehellou, J. H. R. Tucker, *Eur. J. Inorg. Chem*. Accepted for publication.

Contributor - Organometallic Nucleoside Analogues with Ferrocenyl Linker Groups: Synthesis and Cancer Cell Line Studies: H. V. Nguyen, A. Sallustrau, J. Balzarini, M. R. Bedford, J. C. Eden, N. Georgousi, N. J. Hodges, **J. Kedge**, Y. Mehellou, C. Tselepis, J. H. Tucker, *J. Med. Chem.*, **2014**, 13, 5817 – 5822.

Presentations

2015 - Nucleotides and Nucleosides, Burlington House, London

2015 - University of Birmingham, School of Chemistry Symposium

2014 - Nucleic Acid Forum, Burlington House, London

Awards

2015 – Awarded the prize for 'Best Poster' at the 'Nucleosides and Nucleotides' conference.

Courses

2013 - Attended the five-day RSC Medicinal Chemistry Residential School at Loughborough University